In this book, a theoretical analysis is presented for estimating the 3-D large displacement elastic stability behavior including shear deformations of both ordinary and cable-frame interactions in their both suspended or stayed cases subjected to proportional increase in static vertical or horizontal concentrated or distributed loads or both. A new Bowing Functions has been established and checked; a new approach has been established and checked regarding the 3-D effect (SS effect). A new function called "twisting function" has been derived associated to the 3-D effect. A new tangent stiffness matrix in space including shear deformations and 3-D effect has been derived. The effect of axial force on bending, shear & torsional stiffness has been included. All other effects of temperature, lack of fit, initial imperfections, support yielding, pre- twisting members, pretension in cables & cable sag have been considered. A multi-purpose computer program (NASCFI) has been introduced. More than 30 study cases have been examined by (NASCFI) to verify its validity.

khalid sideek

PhD / Str. Eng. since 1997- Ass. Prof. since 2004- Lect. in many Eng. Depts. & Insts.- Cntrb. in many global confrncs.- Many papers & books published -Qualified in many softwares appls.- Unlimited str. Conslt./ Dubai Mncplty. since 2005- Certificated as Str. Eng. Expert in many worldwide companies during 26 yrs.- Membership in many Eng. Socts.

9 783844 333923 978-3-8443-3392-3

khalid sideek

3-D STABILITY FOR CABLE-STAYED TOWERS

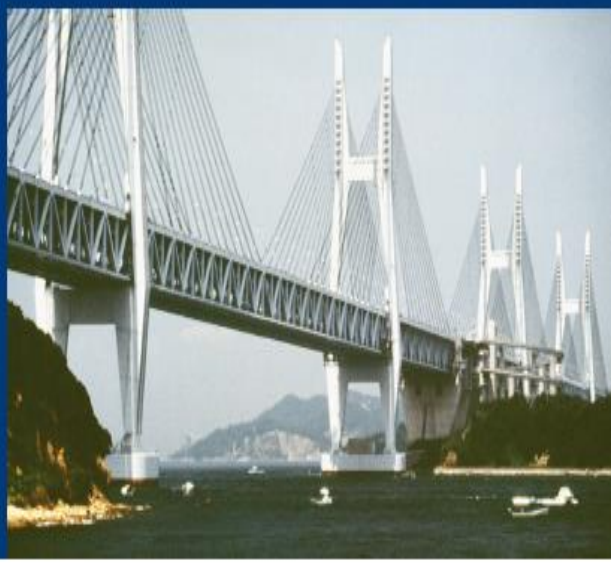

NEW 3-D STABILITY APPROACH FOR THE ELASTIC CABLE-STAYED TOWERS

SHEAR AND 3-D LARGE DEFORMATION EFFECTS ON THE STABILITY OF ELASTIC CABLE-STAYED TOWERS UNDER STATIC LOADS

LAP LAMBERT Academic Publishing

LIST OF CONTENTS

CHAPTER ONE

INTRODUCTION ***1***

1.1 General:- **1**

1.2 Exact and Approximate Theories (Small & Large Deflection Theories): **1**

1.3 Non-linear Analysis:- **9**

1.3.1 Geometrical Non-linearity **10**

1.3.2Material Non-linearity (the material σ-ε relation) **10**

1.3.1.1 Stability non-linearity:- 10

1.3.1.2 Change in geometry non-linearity:- 12

1.3.1.3 Special effect of non linearity:- 12

1.4 The cable element behavior:- **14**

1.5 The computational techniques and the numerical methods:- **15**

1.6 The multi-purpose computer program *NASCFI*:- **15**

1.7 Objective of the study:- **15**

1.7.1 Theoretical original contributions:- which are subdivided into:- 15

1.7.2 Application objective:- 16

1.7.3 Numerical objective:- 16

1.7.4 Computer program *NACSFI*:- 16

1.7.5 Parametric study:- 16

1.8 Scope of the study:- **16**

CHAPTER TWO

REVIEW OF LITERATURE ***18***

2.1 Introduction:- **18**

2.2 Historical Background:- **18**

2.3 Books Review:- **20**

2.4 More Recent Review of Literature:- **20**

2.4.1 Basic Theory Literature:- 20

2.4.2. Shear Deformations of Lattice, Batten, and Laced Elements:- 29
2.4.3 Cable-Frame interaction literature:- 32

CHAPTER THREE

Shear and 3-D effects of Beam-Column Element Basic Theory and Derivations 38

3.1 Introduction 38

3.2 The shear effect on the non-linearity:- 38

3.2.1 The effect of shearing force on the critical load:- 38
3.2.2 The equivalent shear parameter technique:- 41
3.2.3 Shear effect on the elastic stability of frames:- 43
3.2.3.1 Method -1- at $\rho > 0$ (compressive axial force) 44
3.2.3.2 Method -1- at $\rho < 0$ (tensile axial force) 44
3.2.3.3 Method-1- at $\rho=0$ (no axial force) 44
3.2.3.4 Method-2- at $\rho > 0$ (compressive axial force) 44
3.2.3.5 Method-2- at $\rho < 0$ (tensile axial force) 45
3.2.3.6 Method-2- at $\rho=0$ (no axial force) 45
3.2.4 The shear effect on the flexural bowing:- 48
3.2.4.1 Modified Bowing formula and functions using Method-1- 49
3.2.4.2 Modified bowing formula and functions using Meth.-2- 52
3.2.4.3 Checking and testing the new modified bowing functions 55
3.2.4.3.1 Checking the new function with **Saafan**:- 56
3.2.4.3.2 Check the convergence of the functions at $\bar{\rho} = 0$ and $\bar{\rho} > 4$ 56
3.2.4.3.3 Check the convergence of the functions with each other. 57
3.2.4.3.4 Check the validity of relations of the no shear stability bowing functions derived by **Saafan**: 57
3.2.4.3.5 Check the accuracy by using the finite difference method (F.D.M.) 58

3.3 The effect of transverse loading on the non-linearity (fixed end action F.E.A.):- 60

3.4 The 3-D effect on the non-linearity 64

3.4.1 Basic phenomenon:- 65
3.4.2 The basic differential equation 66
3.4.2.1 The constant torsion-no warping case (Closed and mono-symmetric sections with no warping stiffness) 69
3.4.2.1.1 The twisting functions of the B-C element. 70

3.4.2.1.2 Checking and testing the twisting functions: 72
3.4.2.1.2.1 Check the behavior near ρ=0 73
3.4.2.1.2.2 Check with the F.D.M. 73
3.4.2.1.2.3 Check the values of ($\bar{t}_1$ & $\bar{t}_2$) with each other for different values of (u). 75
3.4.2.2 The variable torsion-warping case (open skew or bi-symmetric sections) 77
3.4.2.3 The effect of torsion on bowing:- 80
3.5 The special effects on non-linearity 80
3.6 Full derivation of the new 3-D coupled T.S.M. 81

CHAPTER FOUR

Cable Element Basic Theory and Derivation 88
4.1 Introduction 88
4.2 Types, physical properties, and behavior of cables:- 88
4.2.1 Types, material and composition of cables:- 88
4.2.2 Pre-stretching 91
4.2.3 Modulus of elasticity of the cable 91
4.2.4 Permissible strength of the cables:- 95
4.2.5. Flexural and shear behavior of bent cable:- 95
4.3 Cable-structure interaction and methods of connecting:- 97
4.3.1 Idealized interaction:- 97
4.3.2 Actual interaction:- 99
4.4 The Guy Analysis:- 99
4.4.1 The exact catenary approach:- 99
4.4.2 The approximate parabolic approach:- 101
4.4.3 The preliminary analysis:- 101
4.4.4 The non-linear cable analysis:- 102
4.5 The T.S.M. of the cable element in space:- 109

CHAPTER FIVE

Computational Techniques and Numerical Solutions 112

5.1 Introduction 112

5.2 Tracing the equilibrium path in the non-linear stability problems 112

5.2.1 Linear incremental method (*LIM*):- 112

5.2.2 Non-Linear incremental method (*NLIM*):- 114

5.2.3 Direct or Secant method (*DM*):- 115

5.3 Iterative-Incremental methods of tracing equilibrium path 116

5.3.1 *Newton Raphson* Methods and Its Derivatives (*Tesar* Method) 116

5.3.2 Riks-Wempner Method (The modified constant Arc-Length method) 117

5.3.3 Wessels Modified Version of the Riks-Wempner Method 118

5.3.4 *Ramm* Method 119

5.3.5 *Crisfield* Method 121

5.4 Non-linear stability analysis and perturative methods to trace equilibrium paths 121

5.4.1 Buckling of a Discrete N-dimensional System 122

5.4.2 Linear Stability Analysis 124

5.4.3 Non-linear Stability Analysis 126

5.5 Newton-Raphson (N-R) Methods 128

5.5.1 **N-R** methods modification:- 129

5.5.1.1 Conventional **N-R** Method:- 129

5.5.1.2 Modified **N-R** Method: Constant Stiffness Iteration 129

5.5.1.3 Combined Conventional and Modified **N-R** Method:- 130

5.5.1.4 **N-R** Iteration in a single step without Equilibrium Correction (step by step without Equilibrium Correction):- 130

5.5.1.5 **N-R** Iteration in a single step with equilibrium correction (step by step with equilibrium correction):- 131

5.6 Convergence Criterion:- 131

5.6.1 Displacement Criterion:- 131

5.6.2 Force Criterion:- 132

5.6.3 Work Done Criterion:- 132

5.7 Detection of Instability:- 132

5.7.1 Detection of Convergence Criterion:- 135

5.7.2 Extrapolation Method 135

5.7.3 Fundamental Eigenvalue Criterion:- 137

5.8 Available procedures for non-linear analysis of cable stayed structures:- 138

5.8.1 The proposed method of analysis 138

5.9 The equilibrium equation solver techniques **141**

5.10 The multipurpose computer program NASCFI **142**

5.10.1 Program description and facilities:- 142

5.10.2 Program algorithm 143

CHAPTER SIX

CASE STUDIES AND COMPUTER PROGRAM TESTING *150*

6.1 Introduction:- **150**

6.2 Basic theory case studies:- **151**

6.2.1 Case study no. 1(cantilever beam):- 154

6.2.2 Case study no. 2(two-member cantilever):- 155

6.2.3. Case study no. 3(3-D angle cantilever beam-column):- 158

6.2.4 Case study no.4 3-D initial imperfect. circular ring pin-ended beam-column):- 160

6.2.5 Case study no.5 (3-D initial imperfection S.H.S. pin-ended beam-column):- 164

6.2.6 Case study no.6((3-D initial imperfect. circular ring fixed-ended beam-column):- 167

6.2.7 Case study no. 7 (Two bar shallow truss):- 169

6.2.8 Case study no. 8 (one storey bent frame):- 171

6.2.9 Case study no. 9 (William Toggle frame):- 175

6.2.10 Case study no.10 (rigid-ended portal frame):- 177

6.2.11 Case no. 11 (clamped hinged deep arch):- 179

6.2.12 Case no. 12(3-D cantilever horizontal bent joint):- 181

6.2.13 Case no. 13(Pre-tilted, & pre-twisted, pyramid-shaped frame):- 183

6.2.14 Case no.14 (Space arch frame):- 185

6.2.15 Case study no. 15 (Framed dome with vertical load):- 187

6.3 Shear effect case studies:- **190**

6.3.1 Case study no.16 (Simply-supported slender beam):- 190

6.3.2 Case study no.17 (Four storey frame):- 193

6.3.3 Case no. 18 (Truss cantilever):- 196

6.3.4 Case study no. 19 (3-D transmission tower):- 199

6.3.5 Case study no. 20 (2-bay lattice portal frame):- 204

6.4 Cable-frame interaction case studies: **208**

6.4.1 Case study no. 21(simple stayed column): 209

6.4.2 Case study no. 22 (Simple guy tower): 212

6.4.3 Case study no. 23 (3-D 2-Pretensioned single level guy tower): 215

6.4.4 Case study no. 24 (3-D, 3-Pretensioned multilevel guy tower): 219
6.4.5 Case study no. 25 (2-D bow-string girder): 224
6.4.6 Case study no. 26 (2-D single level single-sided lattice guy tower): 225
6.4.7 Case study no. 27 (Multi-span single-sided lattice guy tower): 230
6.4.8 Case study no. 28 (3-D R.C. Tower cable-stay bridge, Model -I-): 233
6.4.9 Case study no. 29 (3-D R.C. tower cable-stayed bridge, Model-II-): 241
6.4.10 Case study no. 30 (2-D, warren bracing tower, cable-suspended bridge): 243

CHAPTER SEVEN

PARAMETRIC STUDY AND APPLICATIONS 250

7.1 Introduction:- 250

7.2 Parametric study no.1(3-D, 3-legged, X-bracing, pin-ended 40-bay truss column): 252

7.3 Parametric study no. 2 (3-D, Full-scale Free standing Transmission Tower): 255

7.4 Parametric study no.3 (2-D lattice guyed tower): 258

7.5 Parametric study no.4 (3-D, Multilevel guyed tower): 267

7.6 Parametric study no.5(2-D, Cable-stayed bridge): 272

CHAPTER EIGHT

CONCLUSIONS AND RECOMMENDATIONS 276

8.1 Introduction: 276

8.2 Final Conclusions on the beam-column element: 276

8.3 Final Conclusions on the cautionary cable element: 277

8.4 Final Conclusions on the numerical techniques: 277

8.5 Final Conclusions on the multi-propose computer program (*NASCFI*): 278

8.6 Final conclusions on case and parametric study results: 278

8.7 Recommendations: 282

REFERENCES 284

APPENDIX A

Total shear and flexural shear methods ***A-1***

A-1 The total shear slope (Meth.-1-) **A-1**

A-2 The flexural shear slope (Meth.-2-) **A-3**

A-3 No axial force case (P=0): **A-4**

APPENDIX B

The conventional stability and bowing functions with their derivatives ***B-1***

B-1 Stability Functions **B-1**

B-2 Bowing Functions **B-1**

B-3 Derivatives with Respect to ρ **B-2**

B-4 Series Expressions **B-2**

APPENDIX C

The Conventional Beam-Column Linearized-Incremental Large-Deformation Analysis ***C-1***

C-1 The Large Deformation Analysis **C-1**

C-2 Original system equilibrium equation **C-1**

C-3 Joint rotation matrix **C-2**

C-4 Member geometry **C-4**

C-5 Basic Member Force-Deformation Relations **C-7**

C-6 Tangent Stiffness for Relative Deformations **C-9**

C-7 Local Transformation **C-10**

C-8 Tangent Stiffness in Global Coordinates **C-13**

APPENDIX D

The fixed end actions (F.E.A) _____ ***D-1***

APPENDIX E

"Program description and structure" _____ **E-1**

APPENDIX F

Shear Deflection In Beams _____ ***F-1***

F-1Nature Of Shear Deflection _____ **F-1**

F-2 Determining Shear Deflection _____ **F-2**

LIST OF FIGURES

CHAPTER ONE

Figure (1-1.a) Compressive member as part of inflectional elastic curve 3

Figure (1-1.b) Buckled compressive member 3

Figure (1-1.c) Buckled frame referred to tow inflectional elastic curve 5

Figure (1-2) the effect of non-linear 2-D beam-column equation. 6

Figure (1-3) 3-D beam-column in space (a). System Equilibrium (b). Forces and Moments (c). Non-Linear Torsional Effects 7

Figure (1-4) Bowing Effect 11

CHAPTER THREE

Figure (3-1) Shear force of beam-column element 39

Figure (3-2) (a) Shear contribution of flexural curvature; (b) First approach; (c) Second approach. 40

Figure (3-3) Types of lacing 42

Figure (3-4) P/P_e versus stability function curves including shear effect by both methods (u=0.1) 46

Figure (3-5) P/P_e versus stability function curves including shear effect by both methods (u=1.0) 46

Figure (3-6) P/P_e versus stability function curves including shear effect by both methods (u=5.0) 47

Figure (3-7) P/P_e versus stability function curves including shear effect by both methods (u=10.0) 47

Figure (3-8) P/P_e versus bowing function curves including shear effect by both methods (u=0.1) 54

Figure (3-9) P/P_e versus bowing function curves including shear effect by both methods (u=1.0) 54

Figure (3-10) P/P_e versus bowing function curves including shear effect by both methods (u=5.0) 55

Figure (3-11) P/P_e versus bowing function curves including shear effect by both methods (u=10.0) 55

Figure (3-12) Fixed End Action: Tow Sets of force systems acting on same structural member 61

Figure (3-13) U.D.L. over full length P/P_e versus fixed-end moment including shear effect for various shear parameter (u) using both methods 64

Figure (3-14) a: Actual twisted bar b: Idealized undeformed bar. c: Idealized twisted bar. d: Original dividing line. e: Line after twisting. 66

Figure (3-15) the twisted member 66

Figure (3-16) (a): Cross section behavior after twisting. Point -a- moves in a 3-D path to make a shear deformation $d\alpha$ in addition to the dx, dy, dz displacements. (b): The detailed section. (c): The approximate top view of the triangle (a-a'-b). 67

Figure (3-17) P/P_e versus twisting function curves without shear effect by both methods (u=0.0) 74

Figure (3-18) P/P_e versus twisting function curves including shear effect by both methods (u=0.1) 74

Figure (3-19) P/P_e versus twisting function curves including shear effect by both methods (u=1.0) 75

Figure (3-20) P/P_e versus twisting function curves including shear effect by both methods (u=5.0) 76

Figure (3-21) P/P_e versus twisting function curves including shear effect by both methods (u=10.0) 76

Figure (3-22): (a) B-C view. (b) B-C after lateral- buckling. "Notice the constraints at -A- and -B- ($\phi_A=\phi_B=0$)". (c) & (d) cross sections 77

CHAPTER FOUR

Figure (4-1) Strand of Twisted Wires 89

Figure (4-2) Robe of Twisted Strands 90

Figure (4-3) Typical Licked-coil wire rope 91

Figure (4-4.a) The Inclined Cable Arrangement 93

Figure (4-4.b) Uniformly Loaded Cable 94

Figure (4.5) Variation of Ideal Modulus With Span Length 94

Figure (4.6)Bending stress of wire .95

Fig. (4-7) Rope diameter and cable diameter 97

Figure (4-8): Inclined cable under its own weight 100

Figure (4-9): Non-linear stress-strain relationship for a cable stay 104

Figure (4-10): Geometrical non-linearity of cable element (a) imaginary forces "K" (b) the formed cable (c) total imaginary loads of cable (d) imaginary loads of tower 106

Figure (4-11): Method of finding correct root of cable equation 108

Figure (4-12): Principle of iterational technique in cable structure 108

Figure (4-13) Typical cable element in local co-ordinates (a) actual element with sag≠0,(b) idealization and D.O.F. 111

CHAPTER FIVE

Figure (5-1) Linear Incremental Method. 114

Figure.(5-2) Non-Linear Incremental Method. 114

Figure (5-3) Direct Method 116

Figure (5-4) Crisfield Method 121

Figure (5-5) 3-D Tracing Equilibrium Path 122
Figure (5-6) Conventional N-R Method 128
Figure (5-7) Modified N-R Method 129
Figure (5-8) Combined Conventional and Modified N-R Method 130
Figure (5-9) N-R in a Single Step Without Equilibrium Correction 130
Figure (5-10) N-R in a single step with equilibrium correction 131
Figure (5-11) Imperfect Structure 133
Figure (5-12) Imperfect Sensitive Structure in 2-D problems 133
Figure (5-13) Load Versus Displacement Plot Showing Limit Point at "A" 134
Figure (5-14) A Typical Load Displacement Plot With the Solution Obtained by Different Methods 135
Figure (5-15) Determinant Versus Load Factor Curve 136
Figure (5-16) Typical Limit Point 137
Figure (5-17) Typical Bifurcation Point 137
Figure (5-18) Mixed procedure used for non-linear structure analysis 140
Figure (5-19) The most widely known solver strategies 142

CHAPTER SIX

Figure (6-1) Load-Deflection Curve for cantilever Beam 155
Figure (6-2) Load-deflection curve for the two-member cantilever 158
Figure (6-3) Load-deflection curve for the 3-D angle cantilever beam-column 160
Figure (6-4.a) Load-deflection curve for the 3-D initial imperfection pin-ended circular ring for L/r=80 162
Figure (6-4.b) Load-Deflection curve for the 3-D initial imperfection pin-ended circular ring for L/r=120 163
Figure (6-4.c) Load-Deflection curve for the 3-D initial imperfection pin-ended circular ring for L/r=160 163
Figure (6-5.a) Load-deflection curve for the 3-D initial imperfection square hollow section S.H.S. (L/r=65.7, e_{imp}=5.271 mm.) 166
Figure (6-5.b) Load-deflection curve for the 3-D initial imperfection square hollow section S.H.S. (L/r=96.7, e_{imp}=7.685 mm.) 166
Figure (6-5.c) Load-Deflection curve for the 3-D initial imperfection square hollow section S.H.S.(L/r=62.5, e_{imp}=0 mm.) 167
Figure (6-6) Load-deflection curve for the 3-D initial imperfection fixed-ended circular ring for various L/r 169
Figure (6-7) Pre-buckling and post-buckling load-deflection curve for the two-bar truss 170
Figure (6-8) Load versus determinant curve for the two-bar truss 171
Figure (6-9.a) Load Deflection Curve for the one story bent frame (case 1 & 2) 173

FiFigure (6-9.b) Load Deflection Curve for the one story bent frame (case 3 & 4) 173
Figure (6-10) Load versus determinant curve of one-story bent frame (with n=1/1000) 174
Figure (6-11) Load-deflection curve for the William Toggel frame 176
Figure (6-12.a) Load-Deflection curve for the Rigid-Ended portal frame 178
Figure (6-12.b) Load-Deflection curve for the Rigid-Ended portal frame 178
Figure (6-12.c) Load-Deflection curve for the Rigid-Ended portal frame 179
Figure (6-13) Load-deflection curve for the clamped hinged arch 181
Figure (6-14) Load-Deflection curve for the 3-D Horizontal bent joint frame 183
Figure (6-15.a) The pre-tilted and pre-twisted pyramid-shaped frame. 183
Figure (6-15.b) Load-deflection curve for 3-D pre-tilted, pre-twisted pre-tensioned member pyramid-shaped 185
Figure (6-16) Load-Deflection curve for the 3-D arch frame 186
Figure (6-17.a) Frame dome with crown load details 188
Figure (6-17.b) Load-deflection curve for the 3-D crown vertical load dome 190
Figure (6-18) Load-Deflection Curve for the Simply Supported Slender Beam 193
Figure (6-19.a) Four-Storage Frame 194
Figure (6-19.b) Load-Deflection curve for the four story portal frame 196
Figure (6-20.a) Actual and Equivalent elements of truss cantilever 197
Figure (6-20.b) Load-Deflection curve for the truss cantilever 199
Figure (6-21.a) The actual and equivalent towers 200
Figure (6-21.b) Load-Deflection curve fir the 3-D Transmission 201
Figure (6-22) The actual and equivalent lattice frames 204
Figure (6-23.a) The Simple stay column tested by Temple et.al 210
Figure (6-23.b) Load-deflection curve for the simple stayed column 211
Figure (6-24.a) The simple guy column 213
Figure (6-24.b) Load-deflection curve for the simple guy column 215
Figure (6-25.a) 3-D, 2-Pretensioned single-level guy tower 216
Figure (6-25.b) Load-deflection curve for the 3-D single-level guy tower 218
Figure (6-26.a) 3-D, Multi-level Pretensioned guy tower 219
Figure (6-26.b) Load-deflection curve for the 3-D multi-level guy tower 221
Figure (6-27) The Bow-String Girder properties and loading 224
Figure (6-28) (a) Spring idealization of the single-span single-sided guy tower. (b)The present designed single-span single-sided tower. (c)Equivalent cable stayed tower 227
Figure (6-29) (a) Actual spring representation tower. (b.1) Designed cable stayed tower model -I- 230
Figure (6-29.b2) Designed cable stayed tower Model-II- 231
Figure (6-30.a) The two models of 3-D, R.C. tower deck cable-stayed bridge 235

Figure(6-30.b) Load-deflection for the 3-D R.C. tower cable-stayed bridge (Model -I-) 237
Figure (6-31) Load-deflection for the 3-D R.C. tower cable-stayed bridge (Model-II-) 243
Figure (6-32.a) Adige River cable-suspended bridge 244
Figure (6-32.b) Idealization of the suspended bridge 245
Figure (6-32.c) Continues suspension bridge-idealization and initial configuration 246
Figure (6-33) The effect of shear represented by Meth. -1 & 2- / Meth.-0- versus shear parameter (u) 247
Figure (6-34) The new twisting effect (SS effect) versus shear parameter (u) 248

CHAPTER SEVEN

Figure (7-1) 3-D, 3-Legged, X-bracing pin-ended truss column 252
Figure (7-2) Meth.-1- (e_{imp}-Δ) curve for the 3-D initial imperfection pin-ended lattice column for various "u" values 254
Figure (7-3) 3-D, Full scale, Free-standing, 220-kV Double-Circuit Tangent Transmission Tower 255
Figure (7-4) 3-D effect Meth.-1- load-deflection curve for the 3-D free standing full-scale transmission tower (case -1- with various eccentricities) 257
Figure (7-5) 3-D effect Meth.-1- load-deflection curve for the 3-D free standing full-scale transmission tower (case -2- with various eccentricities) 257
Figure (7-6) 3-D effect Meth.-1- load-deflection curve for the 3-D free standing full-scale transmission tower (case -3- with various eccentricities) 258
Figure (7-7) Lattice guyed transmission tower:- a:-Typical guyed tower, b:-Typical bar arrangements for space truss segment(X, Warren, & Vierendeel lacing), c:-Typical cable support arrangement(starmount, 120 radial, and 60 radial) 259
Figure (7-8) Height-bending moment curve for the 2-D, X-bracing type, constant and variable cross section cable stayed tower 262
Figure (7-9) Height-bending moment curve for the 2-D, Warren-bracing type, constant and variable cross section cable stayed tower 263
Figure (7-10) Height-bending moment curve for the 2-D, Vierendeel-bracing type, constant and variable cross section cable stayed tower 264
Figure (7-11) Height-deflection curve for the 2-D, various bracing, constant cross section cable stayed tower. 264
Figure (7-12) Height-deflection curve for the 2-D, various bracing, variable cross section cable stayed tower 265
Figure (7-13) Height-axial force curve for the 2-D, X-bracing type, constant and variable cross section cable stayed tower 266
Figure (7-14) Height-axial force curve for the 2-D, Warren-bracing type, constant and variable cross section cable stayed tower 266

Figure (7-15) Height-axial force curve for the 2-D, Vierendeel-bracing type, constant and variable cross section cable stayed tower ____ *267*
Figure (7-16) Multilevel solid mast guy tower:-a: Top plan with wind directions(g), b: Side view ____ *268*
Figure (7-17) Wind velocity versus cable tension curve of cable -3- for the 3-D solid section cable stayed tower ____ *268*
Figure (7-18) Wind velocity versus cable tension curve of cable -2- for the 3-D solid section cable stayed tower ____ *270*
Figure (7-19) wind velocity versus cable tension curve of cable -1- for the 3-D solid section cable stayed tower ____ *270*
Figure (7-20) wind velocity versus bending moment curve of cable -2- of node -9- for the 3-D solid section cable stayed tower ____ *271*
Figure (7-21) wind velocity versus axial force curve of cable -2- of bottom member for the 3-D solid section cable stayed tower ____ *271*
Figure (7-22: a-b) The 2-D cable stayed bridge : a: Geometry and sectional properties of bridge prototype. b: Dimensions and sectional properties of the bridge model. ____ *272*
Figure (7-22-c): The bridge model test set-up ____ *273*
Figure (7-23) Bridge node numbering and load positions ____ *273*
Figure (7-24) The influence lines for the cable tension ____ *274*
Figure (7-25) The influence lines for the nodal vertical displacement ____ *274*

APPENDIX A

Figure (A-1) Force system of elastic beam-column ____ *A-2*

APPENDIX B

Figure (B-1) No shear elastic stability functions (C_1 and C_2) ____ *B-3*
Figure (B-2) No shear elastic bowing functions (b_1 and b_2) ____ *B-3*

APPENDIX C

Figure (C-1) Member coordinates ____ *C-4*
Figure (C-2) Relative member deformations and corresponding forces ____ *C-5*
Figure (C-3) Member forces ____ *C-11*

APPENDIX D

Figure (D-1.a) The transverse load action for fixed ended elements. ____ *D-1*
Figure (D-1.b) The transverse load action for hinged elements. ____ *D-2*
Figure (D-2) The temperature action. ____ *D-3*
Figure (D-3) The pre-strains fixed end action ____ *D-4*
Figure (D-4) The end-displacement action:- Axial displacement, Sway displacement, Flexural displacement, Twist displacement. ____ *D-5*

APPENDIX E

Figure (E-1): Program flowchart _____ *E-4 to E-7*

APPENDIX F

Figure (F-1) Deflection in beam caused by bending moment, left, and by shear, right _____ *F-1*

Figure (F-2) Shear deflection and bending deflection of cantilever I-section _____ *F-2*

Figure (F-3) Shear stress-strain diagram _____ *F-2*

Figure (F-4) Form factor for shear deflection in built-up beams _____ *F-3*

Figure (F-5) Beam sections for which eq.(F-5) applies _____ *F-4*

LIST OF TABLES

CHAPTER THREE

Table (3-1): The Shape Factor Typical Values 39

Table (3-2): The shear parameter (u) governing equations 42

Table (3-3): Various methods for comparison of shear parameter (u) versus load parameter (P/P_e) 48

Table (3-4): validity of new functions at u=1. 60

CHAPTER FOUR

Table (4-1): Types of cable - tower interaction 98

CHAPTER SIX

Table (6-1.a): Basic Theory Case Studies 151

Table (6-1.b): Effect of Shear Case Studies 152

Table (6-1.c): Guy Towers Case Studies 153

Table (6-2.a): Cantilever Beam Properties 154

Table (6-2.b): Compression of Solutions for Cantilever Beam 156

Table (6-3.a): Two-Member Cantilever Beam Properties 156

Table (6-3.b): Compression of Solutions for Two-Member Cantilever Beam 157

Table (6-4.a):3-D Angle Cantilever Column Properties 158

Table (6-4.b):-Various Methods Compression for 3-D Angle Cantilever Deflections 159

Table (6-5.a):3-D Initial Imperfection Circular Ring Pin-Ended Beam-Column Properties 160

Table (6-5.b): Results & Comparison of 3-D Initial Imperfection Circular Ring Pin-Ended Beam-Column 161

Table (6-6.a): 3-D Cold-Formed Initial Imperfection S.H.S Pin-Ended Beam-Column Properties 164

Table (6-6.b):-Results & Comparison of 3-D Cold-Formed Initial Imperfection S.H.S Pin-Ended Beam-Column 165

Table (6-7.a): 3-D Circular Ring Fixed-Ended Beam-Column Properties 167

Table (6-7.b): Results & Comparison of 3-D Circular Ring Fixed-Ended Beam-Column 168

Table (6-8.a): Two-Bar Shallow Truss Properties 169

Table (6-8.b): Compression of Solutions for Two-Bar Shallow Truss 170

Table (6-9.a): One-Storey Bent Frame Properties 172

Table (6-9.b): Compression of Solutions for One-Story Bent Frame 172

Table (6-10.a): William-Toggle Frame Properties 175

Table (6-10.b): Compression of Solutions for William Toggle Frame 175
Table (6-11.a): Rigid-Ended Portal Frame Properties 177
Table (6-11.b): Compression of Solutions for Rigid-Ended Portal Frame 177
Table (6-12.a): Clamped Hinged Arch Properties 180
Table (6-12.b): Comparison of Solutions for Clamped-Hinged Arch 180
Table (6-13.a): Two-Member Bent-Joint Frame Properties 181
Table (6-13.b):-Comparison of Solutions for Two-Member Bent-Joint Frame 182
Table (6-14.a): Pretensioned, Pre-tilted, & Pre-twisted Pyramid-Shaped Four-Member with Crown Load Properties 184
Table (6-14 .b): Comparison of Solutions for Pre-tensioned, Pre-tilted & Pre-twisted Pyramid-Shaped Four- Member with Crown Load 184
Table (6-15.a): Space Arch Frame Properties 185
Table (6-15.b): Comparison of Solutions for Space Arch Frame 186
Table (6-16.a): Framed Dome with Crown Load Properties 187
Table (6-16.b): Comparison of Solutions for Framed Dome with Crown Load 189
Table (6-17.a): Properties of Simply-Supported Slender Beam 192
Table (6-17.b): Comparison of Simply-Supported Slender Beam Results 192
Table (6-18.a): Four-Storey Frame Properties 193
Table (6-18.b): Comparison of Solutions for Four-Storey Frame 195
Table (6-19.a): Truss Cantilever Actual Properties 197
Table (6-19.b): Truss Cantilever Equivalent Properties 197
Table (6-19.c): Comparison of Solutions for Truss Cantilever 198
Table (6-20.a): 3-D Transmission Tower Equivalent Properties 200
Table (6-20.b): Comparison of Solutions for 3-D Transmission Tower 201
Table (6-21.a): Geometric Arrangements and Elements Properties of Two-Bay Lattice Frame Structure 206
Table (6-21.b): Moments Calculated by Different Methods for The Two-Bay Lattice Frame Structure. 206
Table (6-22.a): Properties of Simple Stayed Column 209
Table (6-22.b): Results of Comparison of Mid-Height Lateral Deflections in Simple Stayed Columns 212
Table (6-23.a): Simple Guy Column Properties 213
Table (6-23.b): Deflections at Free End for The Simple Guy Column by Different Methods 214
Table (6-24.a): Two-Level Guy Tower Properties 217
Table (6-24.b): Comparison of Results of Two-Level Guyed Tower 217
Table (6-25.a): Multiple Guy Tower Properties 220
Table (6-25.b): Comparison of Results of Multilevel Guyed Tower 222

Table (6-26.a):2-D Bow-String Girder Properties _____ *225*
Table (6-26.b): In-Plane Bow-String Girder Results _____ *225*
Table (6-27.a): Single &Multi-Span Lattice Guyed Tower actual properties (Mast properties) _____ *227*
Table (6-27.b): Single-Span Lattice Guyed Tower actual properties (Cable properties) _____ *228*
Table (6-27.c): Comparison of Solutions for Single-Span Lattice Guyed Tower _____ *229*
Table (6-28.a): Multi-Span Lattice Guyed Tower actual properties (Cable properties) _____ *232*
Table (6-28.b): Multi-Span Lattice Guyed Tower Equivalent Properties _____ *232*
Table (6-28.c): Comparison of Results of Multi-Span Lattice Guyed Tower Model -I- _____ *233*
Table (6-29.b): Deflections at Mid-span & Top of Left Tower for Model "I" By Different Methods _____ *238*
Table (6-29.a): 3-D, R.C. Cable-Stayed Bridge Model-I- Properties _____ *239*
Table (6-30.a): 3-D, R.C. Cable-Stayed Bridge Model-II- Properties _____ *240*
Table (6-30.b): Deflections at Mid-span & Top of Left Tower for Model-II- By Different Methods _____ *241*
Table (6-31.a):2-D Continuous Cable-Suspension Bridge Properties _____ *244*
Table (6-31.b): 2-D Continuous Cable-Suspension Bridge Results _____ *246*

CHAPTER SEVEN

Table (7-1): Types of applications and parametric studies applied to (NASCFI) _____ *251*
Table (7-2): 3-Legged, X-Bracing Truss column Properties _____ *253*
Table (7-3): 3-Legged, X-Bracing Truss column design requirements _____ *254*
Table (7-4): Free-Standing Full-Scale X-Bracing Transmission Tower Equivalent Properties _____ *256*
Table (7-5.a): 3-D, 3-Legged, Constant & Variable Cross Sectional Area, Multi-Span Cable-Stayed Lattice Tower Actual Properties for Deferent Types of Bracing _____ *260*
Table (7-5.b): 3-D, 3-Legged, Constant & Variable Cross Sectional Area, Multi-Span Cable-Stayed Lattice Tower Loading Data for Deferent Types of Bracing _____ *261*
Table (7-5.c): 3-D, 3-Legged, Constant & Variable Cross Sectional Area, Multi-Span Cable-Stayed Lattice Tower equivalent Properties for Deferent Types of Bracing _____ *262*

APPENDIX E

Table E-1- _____ *E-1*

List of symbols

a, b, α, A_d, A_l, A_h, I_d, I_l, I_h	Laced section properties
A	Area of section
A_e	Effective area of laced section
A_f	Flange area
A_w	Web area
b_1	First bowing function for no shear effect
b_2	Second bowing function for no shear effect
C_1	First stability function for no shear effect
C_2	Second stability function for no shear effect
C_b	Bowing factor for no shear effect
C_t	Axial force effect on torsional rigidity
C_T	Twisting factor including shear effect
C_w	Warping effect coefficient
e	Overall axial shortening in the buckling element
E	Elastic modulus
E_e	Modulus of elasticity of straight cable
E_f	Apparent modulus of elasticity of cable
$e_{imp.}$	Imperfection
E_i	Modulus of elasticity of sagged cable
$E_{mod.}$	Modified modulus of elasticity of cable
f	Cable sag

F	Tensile axial force of cable
F_0	Initial tensile axial force of cable after first stage of loading
F_f	Final tensile axial force of cable
F_i	Initial tensile axial force of cable
G	Shear modulus
H	The horizontal component of the cable tensile force
I	Moment of inertia of section
I_e	Effective moment of inertia of laced section
J	Polar moment of inertia of section (indicated as KT elsewhere)
L	Original length
L_c	Updated length
L_h	The horizontal length
M	End moment
M_{f0}	Fixed End Action momets
n	Shape factor
N	Normal force to the section
P	Axial force
P_{cr}	Critical axial load
P_e	Euler load
r	Radius of gyration
R	Radius of curvature
s	Arc length

t_e	Effective thickness of laced section
u	Shear parameter
u, v, w	Deflections in the three directions of 3-D analysis
V	Shear force
Vel.	Wind velocity
w	Load intensity
W_e	Work done by external loads
W_i	Work done by internal forces
y	Deflection in 2-D analysis for no shear effect
$\bar{C}_1$	First stability function for shear effect
$\bar{C}_2$	Second stability function for shear effect
$\bar{b}_1$	First bowing function for shear effect
$\bar{b}_2$	Second bowing function for shear effect
$\bar{t}_1$	First new twisting function
$\bar{t}_2$	Second new twisting function
$\bar{K}$	Wagnor effect
$\bar{C}_b$	Bowing factor including shear effect
$\bar{\phi}$	Total potential energy
$[\bar{\gamma}]$	Rotational matrix in local coordinates
$[\Delta\bar{\gamma}]$	Incremental rotational matrix in local coordinates
$\bar{\omega}$	Angle between equilibrium path and it's normal in the control surface
$\bar{\rho}$	Axial force parameter including shear effect

$\bar{y}$	Deflection in 2-D analysis including shear effect
$\overline{\overline{bb}}_i$	Bowing functions obtained from Finite Different Method
$\overline{\overline{tt}}_i$	Twisting functions obtained from Finite Different Method
θ	Slope of the elastic curve
σ	Axial stress
ε	Axial strain
γ	Specific gravity of the material of the element
φ	Cable inclination
ψ	Flexural slope
β	Shear slope
ν	Poisson's ratio
ρ	Axial force parameter for no shear effect
ϕ	Angle of twist
μ	Elastic shortening due to axial force
φ_0	Initial cable inclination
δ_b	Axial shortening due to flexural bowing
λ_c	Critical load parameter
ε_x	Strain in X direction
ε_y	Strain in Y direction
ε_z	Strain in Z direction
$[\tau]$	Overall tangent stiffness matrix for the beam-column element in global coordinates

$[\Delta W]$	Incremental rotational matrix in global coordinates
$[K_0]$	Conventional linear elastic stiffness matrix
$[K_1]$ & $[K_2]$	Non-linear stiffness matrices
$[K_G]$	Geometrical non-linear stiffness matrix
$[K_p]$	Initial stress matrix
$[K_s]$	Secant stiffness matrix
$[K_T]$	Tangent stiffness matrix (indicated as "τ" elsewhere)
[r]	Transformation matrix
[t]	Tangent stiffness matrix for the beam-column element in local coordinates
[W]	Rotational matrix in global coordinates
$\{\Delta\lambda\}_i$	The incremental load parameter vector in the i^{th} cycle of loading
$\{\lambda\}_i$	The load parameter vector in the i^{th} cycle of loading
$\{\Delta P\}_i$	The incremental applied load vector in the i^{th} cycle of loading
$\{\Delta Q\}_i$	The incremental load equilibrium vector in the i^{th} cycle of loading
$\{\Delta X\}_i$	The incremental displacement vector in the i^{th} cycle of loading
$\{F\}_i$	The nodal force vector in the i^{th} cycle of loading
$\{P\}_i$	The applied load vector in the i^{th} cycle of loading
$\{Q\}_i$	The load equilibrium vector in the i^{th} cycle of loading
$\{X\}_i$	The displacement vector in the i^{th} cycle of loading

CHAPTER ONE

INTRODUCTION

1.1 General:-

The recent developments in television and telecommunication services have necessitated the amounting of antennae at great heights for transmission purposes, also the developments have taken place during the three decades in the cable-suspension and cable-stayed bridges which are very appealing aesthetically and are also very important lifeline structures. Slender masts and towers laterally supported by gays or stiff cables are usually adopted for this purpose as they provide economical solutions compared with free standing towers. The behavior of such structures is influenced by many factors and parameters making a highly complex problem. This highly non-linear problem is exhibited either by gays due to sags, low level of pretension or by masts or towers due to large displacements and beam-column effects, in addition to the effect of wind loading at various heights, initial geometry effects such as initial tension in cables, initial imperfection in tower members, lack of fit, etc., and also special effects due special causes such as temperature, support yielding. Thus, in an actual situation, such structures experience simultaneous increase in axial thrust and lateral loads in both directions, such a combination can actually introduce a highly non-linear problem that could be solved either by discrete field mechanics, finite element technique or by beam-column theory, in which we are concerned. Towers or masts in such structures could have a solid cross-section or a lattice, batten and open-web ones, where the effect of shear deformations is rather dominant. Therefore, the study of the shear effect on stability and bowing functions takes a major rule accordingly. So many considerable researches has been made during the last three decades into the non-linear behavior and the large deformation analysis of the structures. As a brief explanation for the subject, some major definitions must be settled in order to understand the issue

1.2 Exact and Approximate Theories (Small & Large Deflection Theories):-

The elastic body of a system usually consists of an aggregate of constitutive elements connected in some way so that kinematics freedom involving rigid-body motion of these elements is eliminated. A pin or rigid ended prismatic bar in plane or space frameworks loaded centrally at the joint of the member is one of the most widely used type of elements. Several non-linear equilibrium forms, determinate or indeterminate, may be realized in such systems under divers geometrical and conservative loading conditions. The geometrical continuity or discontinuity conditions play a major part in the realization of equilibrium states which follow non-linear paths. To analyze

unstable equilibrium states of system composed of slender elastic bars of finite deformations, exact and accurate laws governing the behavior of single members in equilibrium under arbitrary end-restraint conditions must be established, the general stress resultants at restraints and plane elastic deformation must be studied and the differential equations of equilibrium must be derived[14].

Briefly, if we follow the real path or shape of the elastic curve when found, then the exact differential equation established from it is called the ***Elastica,*** and such analysis is called ***the exact theory or large deflection theory*** of beam-column. On the other hand following the chord path or similarly making some assumptions on the exact theory, the ***approximate (simplified or linear) theory or the small deflection theory*** would be introduced. figure (1-1.b) shows a typical compressive member and its elastic curve, the elastic buckling of the member is conditioned by the end-restraints and the axial load ***(P)***. The initial length of the member is ***(L),*** and the overall contraction in the buckled form is ***(e)***, so the length of the chord ***(i,j)*** is ***(L-e)***. It may be assumed that the distorted form of the centroidal axis of the member equals the initial length ***L***, so the member is said to be inextensional or axially rigid, but otherwise flexurally perfectly elastic. In the buckled form the end couples M_i and M_j (+ pos. clockwise), and shearing forces V_i , V_j, normal to the chord ***(i,j)***, are set up. for overall equilibrium of the member[14]:-

$$V = V_i = V_j = \frac{\left(M_i + M_j\right)}{\left(L - e\right)} \quad \text{..... (1-1)}$$

If the member is axially rigid the moment (m) at any point at distance (s) along the centroidal axis is given by:-

$$\frac{1}{R} = \frac{d\theta}{ds} = -\frac{m}{EI} \quad \text{..... (1-2)}$$

where (R) is the radius of curvature and (θ) is the tangent rotation measured positive clockwise, from equilibrium:-

$$m = Pv - Vu + M_i = EI\frac{d\theta}{ds} \quad \text{.....(1-3)}$$

differentiating and putting:-

$$\frac{dv}{ds} = \sin\theta \;\; \& \;\; \frac{du}{ds} = \cos\theta \quad \text{.....(1-4)}$$

which reduces eq.(1-3) to:-

$$EI\frac{d^2\theta}{ds^2} + P\sin\theta - V\cos\theta = 0 \quad \text{.....(1-5)}$$

If considering the elastic extensibility of the centroidal axis, then:-

$$EI\frac{d^2\theta}{ds^2}+\left(P\sin\theta-V\cos\theta\right)\left(1-\left(\frac{P}{EA}\right)\cos\theta\right)=0 \quad \text{.....(1-6)}$$

from the figure we have:-

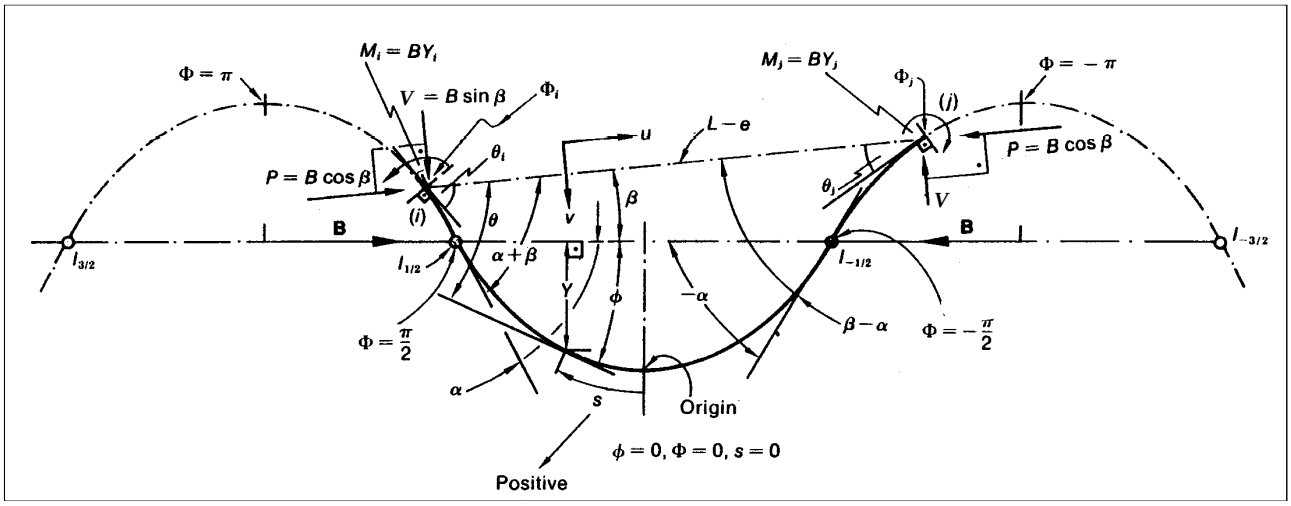

Figure (1-1.a) Compressive member as part of inflectional elastic curve

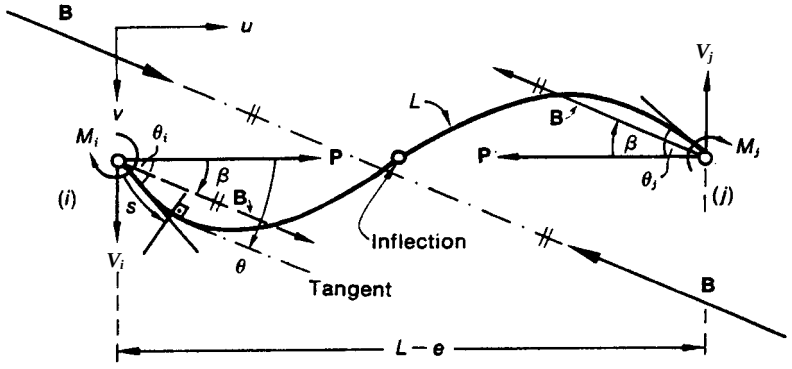

Figure (1-1.b) Buckled compressive member

$$\begin{aligned} P &= B\cos\beta \\ V &= B\sin\beta \end{aligned} \quad \text{.....(1-7)}$$

where *"B"* is the resultant of *"P & V"*, and *"β"* is the angle included by *"B & P"*, integrating and substituting:-

$$\frac{EI}{2}\left(\frac{d\theta}{ds}\right)^2-B\cos\phi=C \quad \text{..... (1-8)}$$
$$\phi=\theta-\beta$$

finally, after a long derivation we have:-

$$\sqrt{\frac{Bs^2}{EI}} = \int_0^{\phi} \frac{d\phi}{\sqrt{1 - K^2 \sin^2 \phi}} + C_1 \quad \text{..... (1-9)}$$

where:-

α= tangent rotation at inflection point for which $d\theta/ds = 0$

C_1=integration constant, k=sin ($\alpha/2$), & ϕ= end amplitudes ($a\pi$), a=0 to $\propto$

Equation (1-9) is the first elliptical integral, in extension of the solution we shall have **the complete** elliptical integral of the first kind:-

$$K = \frac{\pi}{2}\left(\frac{P}{P_e}\right)^{1/2} = \int_0^{\frac{\pi}{2}} \frac{d\phi}{\sqrt{1 - K^2 \sin^2 \phi}} \quad \text{..... (1-10)}$$

$$\frac{P}{P_e} = \frac{4}{\pi^2} K^2(\alpha) = \frac{4}{\pi^2} F(\phi, K)^2 \quad \text{..... (1-11)}$$

The function **K(α)** which depends only on **(α)** is tabulated numerically in many handbooks[14 & 94].

With case of frame buckling, the problem will have more difficulties as it is illustrated in Figure (1-1.c), since we have B_1, B_2 & elastica 1, elastica 2.

In 2-D analysis, the governing equation of beam-column is (1-5) or (1-6), which simply can be transformed to the most widely known form of:-

$$\phi = \frac{1}{R} = -\frac{w''}{\left(1 + (w')^2\right)^{3/2}} \quad \text{..... (1-12)}$$

which is shown in figure (1-2)**.**

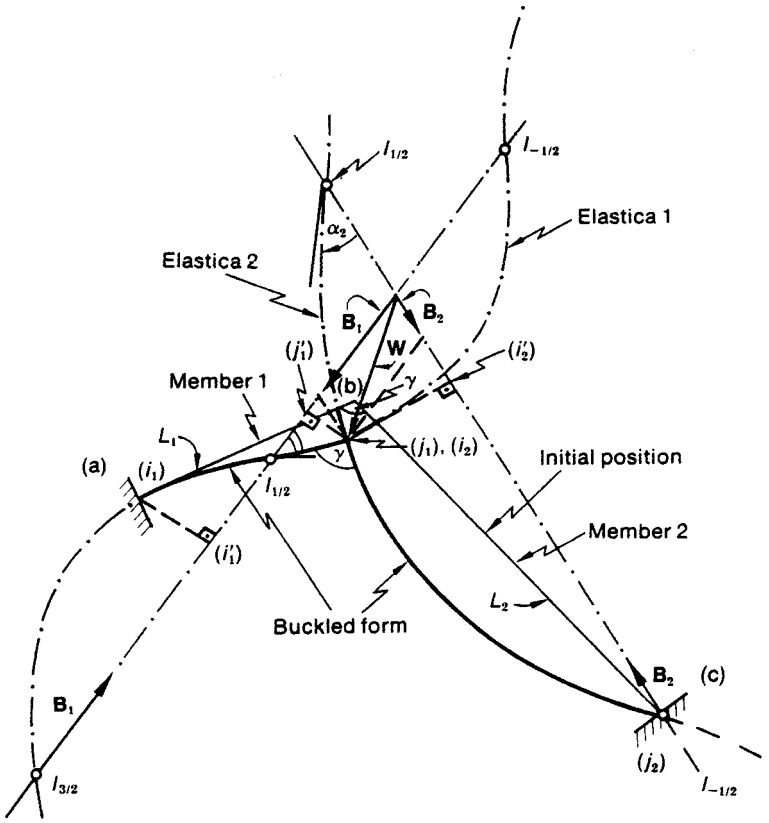

Figure (1-1.c) Buckled frame referred to tow inflectional elastic curve

By introducing the following assumptions we shall have the simplified or approximate theory which is known as small deflection theory:-

***Assumption I*:** Plane section remains plane after deformations.

***Assumption II*:** Fibers remain normal to the deflected axes after deformation, i.e., shear deformations are neglected.

Assumption III*:** The deflection is small and the slope angle ***Δ in radian is negligible

Compared to unity, so eq.(1-4) becomes:-

$$\theta << 1, \sin\theta \approx \theta, \cos\theta \approx 1, \tan\theta \approx \theta \ \& \ dx \approx ds \quad \text{..... (1-13)}$$

***Assumption VI*:** The influence of stress in x-direction (σx) on strain on z-direction

(ε_z) by ***Poisson***'s ratio is disregarded, which leads to ***Hook***'s Law to be:-

$$\sigma_x = E\varepsilon_x = \frac{E}{R_z} \quad \text{..... (1-14)}$$

So, eq.(1-12) becomes in the most known beam-column 2-D form:-

$$\phi = \frac{1}{R} = -w'' = -\frac{d^2w}{dx^2} \quad \text{..... (1-15)}$$

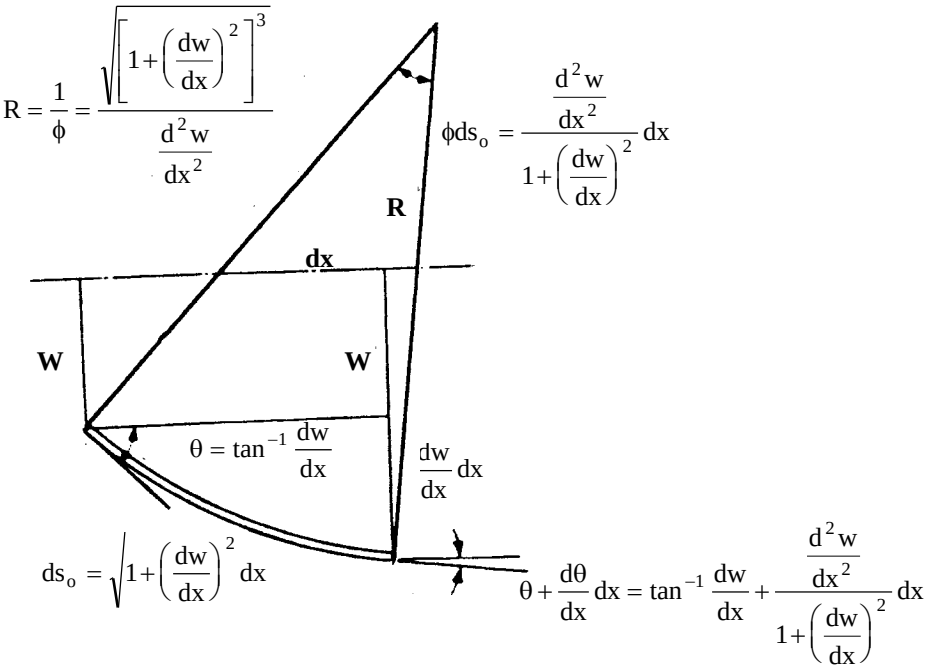

Figure (1-2) The effect of non-linear 2-D beam-column equation.

In 3-D beam-column theory the problem is more complicated; figure (1-3.a. and b). shows the 3-D beam-column equilibrium in space, while figure (1-3.c) shows the three types of twisting effects (***Snt. Vt.***, ***Warping***, and ***Wagner***), where the effect of the Z-directions i.e. the torsion, torsion-flexure and axial-torsion combinations must be taken into account, and after making the following additional assumptions:-

Assumption V:- Long prismatic members **(D/L, B/L<0.1)**

Assumption IV:- Thin-walled cross sections **(t/D, t/B<0.1)**

Assumption IIV:-No distortion is produced by the longitudinal bending stress and/or shear stress.

Assumption IIIV:- Elastic homogeneous material.

And after a long derivations, the most fundamental equations of it are:-

$$EI_x v'' + vP + M_{x0} + \theta M_{y0} = 0 \quad \text{..... (1-16)}$$

$$EI_y u'' + uP + M_{y0} + \theta M_{x0} = 0 \quad \text{..... (1-17)}$$

$$EI_w \theta''' + \left(GK_T + K\right)\theta' + u'M_{x0} + v'M_{y0} = 0 \quad \text{..... (1-18)}$$

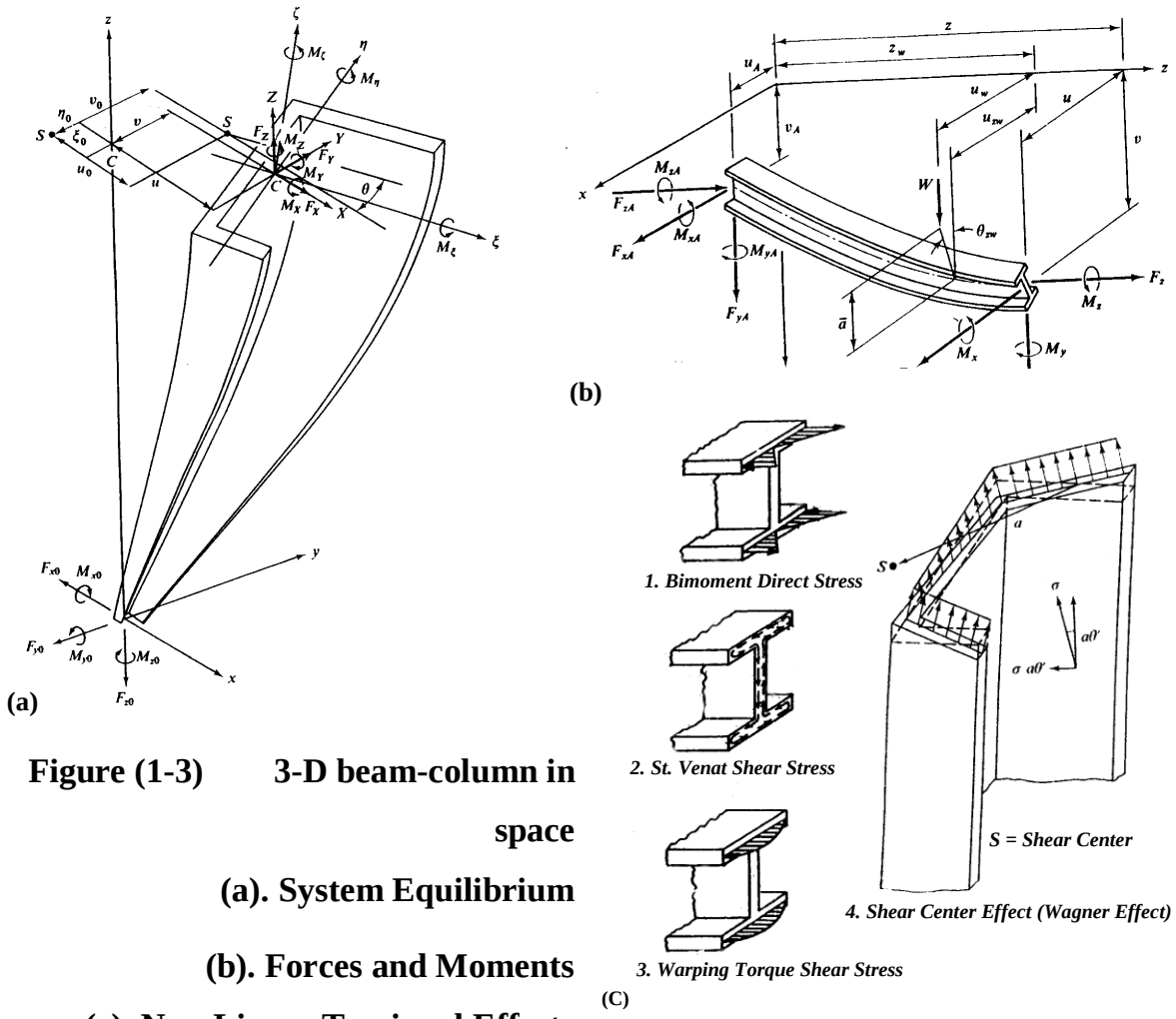

Figure (1-3) 3-D beam-column in space

(a). System Equilibrium

(b). Forces and Moments

(c). Non-Linear Torsional Effects

These equations are derived after introducing a number of simplifications:-

- Canceling the high non-linear terms of eight orders or even higher.
- Double symmetrical sections are proposed, so the shear center coincides with the centroid.
- Load applied symmetrically at both ends, so:-

$Mx = Mx_0, My = My_0, Mz_0 = 0, M'x = M'y = 0$, and the boundary conditions for the above equations are:-

Displacement u, v (=0 if supported)

Slope u', v' (=0 if fixed)

Bending moment EI_x v"= M_{xo} + Δ M_{yo} (=0 if simple support)

EI_x u"=M_{yo}+ Δ M_{xo}

Shear force EI_x v"' = -V_y- Δ V_x (=0 for free end)

EI_x u"' = -V_x-θV_y

Rotation angle θ (=0 if restrained)

Twist θ' (=0 if warping restrained)

Warping moment EI_w Δ " = M_w (=0 if warping free)

Twisting moment EI_w "' -(GKT +K) Δ '=M_z (=0 for free end)

The solution can be found by elliptical integral which is very lengthy, crude and impractical solution. So, the above assumptions simplify the solution of beam-column problem, but on the other hand many cases cannot be solved by the small deflection theory because of the divergence with the actual behavior of the structures.

In spite of the above simplifications, the problem is still very complex especially when dealing with the practical complicated structures, so alternative strategies must be adopted, the matter that has forced the investigators and researchers to find and then add the most significant effects that govern the divergence of the structures behavior from the linear small deflection path, these effects actually are **the non-linear effects.**

Small relative deformations are considered with large joint displacement using either ***Lagrangian*** (total or stationary) coordinates or ***Eulerian*** (Updating ***Lagrangian***) coordinates which is preferable than the ***langragian*** specially if large rotations and translations occurred. Equilibrium conditions are then satisfied in the last configuration of the member. The well-known direct stiffness method is used with updating stiffness matrix in each stage of loading to ensure the updating coordination caused by large displacements of joints, two types of structures are classified in terms of the change in the stiffness of structures, softening and hardening. In the hardening, the higher the load the higher the stiffness, which is rarely occurs. In the softening property, however, the common type of structures which gives stiffness to be decreased with load increasing, the zero

stiffness condition is called ***elastic critical load.*** However the large deflection theory breaks down at large deflections just as the small deflection theory does [20&21].

1.3 Non-linear Analysis:-

Various behaviors are called "**Non linear**" (the term states only what a behavior is not). Stress-strain relations may be non-linear in either a time-dependent or a time-independent way. Displacements may cause loads to alter their distribution or magnitude. Mating parts may stick or slip, gaps may open or close. Non linearity may be mild or sever, the problem may be static or dynamic. Many solutions have been proposed, and it is no surprise that no one is best for all problems[25].

As ***Koiter*** says :"the problem of elastic stability belongs inherently to the domain of the *non-linear theory of elasticity* " although satisfactory results may be obtained from the linearized analysis in many important practical cases. ***Kirchhoff***`'s uniqueness theorem which has a central role in the classical linear theory of elasticity is no longer valid. In fact, the simplest form of loss of instability manifests itself in the appearance of more than one solution. In other words, many structures which have a dimension much smaller than others-such as bars, thin plates & shells-are liable to exhibit more than one equilibrium configuration under a given external loading, thus evading ***Kerchief***'s Law. Such structures can undergo marked changes in the character of their deformation that is not associated with the failure of the material but rather respects a loss of stability of the original equilibrium configuration. This sort of behavior can no longer be described with sufficient accuracy by the linearized strain-displacement and stress-strain equations, so the theory of elastic stability emerges as an important branch of the non-linear theory of elasticity and, in a broader sense, applied mechanics. In the sequel, the words linear and non-linear may be used under different, though well-defined, circumstances, and it is important to bear in mined that while a procedure of analysis can be described as linear, the stress-strain relationships, for example, are always non-linear in structural instability problems. The principle of super position and the principle of proportionality which are fundamental in linear mechanics are no longer valid[42].

Problems of the theory of elastic stability are concerned mainly with two classes of systems depending on the equilibrium differential equation, namely, **conservatives** and **non-conservatives**, and they could be classified into[42]:-

- **Linear autonomous problems:-(e.g. distributed axial load).**

- **Linear non-autonomous problems :-(heteronomous systems -e.g. rod subjected to pulsing compressive force-).**
- **Non-linear problems :-(where the differential equations of equilibrium for the displacement together with its derivative(s) are exhibited).**
- **Stochastic problem :-(where stochastic quantities are governing the differential equation of equilibrium).**

So far the two causes of non linearity in structures have been attributed to the effects of:-

1.3.1 Geometrical Non-linearity.

1.3.2 Material Non-linearity (the material σ-ε relation).

All other factors that play an important part in aggravating the non linearity of real structures can be categorized into the two main divisions. These factors include **the effect of shape factor not being unity, the Strain-Hardening effect, the effect of uneven and non-linear behavior of foundation, the influence of the non-linear behavior of the cladding, the infilles and plates on the frames** [61], and **the connection non linearity**.

What we concerned with in our present study is **the geometrical non-linear problem** The geometrical non-linear effects may include all the large deformation effects such as rotational and translational changes in geometry, flexural bowing effect, initial geometry and axial forces and deformation effect or sometimes some of them, the geometric effects due to the axial load can be decomposed into two types, the first one is due to sway action or shear action or as it is widely used the (**P-Δ** effect), the second one is the axial effect on stability and bowing functions. In comparison with linear problems which have a constant stiffness matrix, the stiffness matrix of the geometrically non-linear problems contains terms that are non-linear functions of the deformations of the structure, this matrix is called the tangent stiffness matrix, **T.S.M.,** so this type of non-linearity can be subdivided into:-

1.3.1.1 Stability non-linearity:-

which is mainly due to the coupling effect of the axial force and flexural moment, solution of this problem is by introducing stability functions which depend on the axial force parameter only ***(P/PEuler)***.So the well known slope-deflection equations for linear analysis are no longer valid since the axial load parameter is greater or smaller than zero which leads to the stiffness factor ***(S or C_1)*** not to be equal to ***4*** and the stiffness-carry over factor ***(SC or C_2)*** not to be equal to (2). Force-deformation relations are based on beam-column approach, changes in member

chord length are caused by axial strain, and flexural bowing effect (i.e. the bowing functions), where the bowing means the shortening in the member due to flexural moments as illustrated in figure (1-4)**.** and it has the mathematical expression of[81]:-

$$\delta b = \int_0^L ds - dx = \frac{1}{2}\int_0^L \left(\frac{dy}{dx}\right)^2 dx \quad \text{..... (1-19)}$$

However, **the effect of shear slope** on curvature of element and consequently on the stability and bowing functions and factors has a variable influence depending on type of member. This effect is analyzed by two approaches:-

-The first approach is the total slope approach:- which is based on the assumption that the shear component of the axial load is calculated from the total slope which consists of bending and shear slope(this method is denoted in the present work as **Meth.-1-**).

-The second approach is the bending slope approach:- in this approach the shear component of the axial load is calculated from the bending slope only (this method is denoted in the present work as **Meth.-2-**).

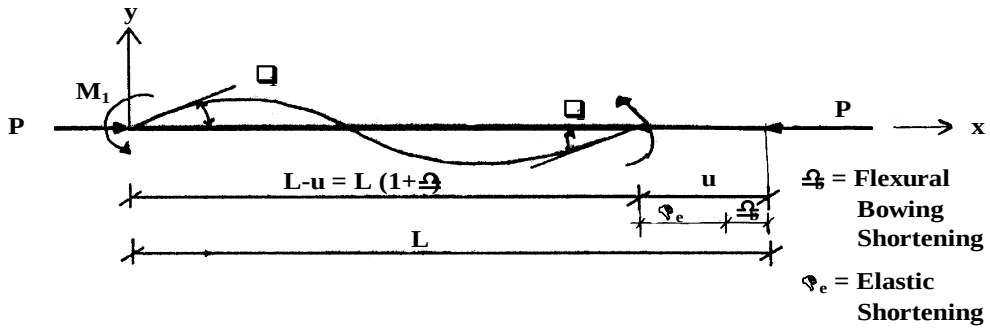

Figure (1-4) Bowing Effect

Shear effects vary with the magnitude of the axial force, rigidity of the web system, and the slenderness ratio of the span. In the absence of beam-column action, neglecting shear effects usually gives conservative results, but where beam-column action is applicable and the web system is flexible, neglect of shear effects leads to computed shears and bending moments which are low relative to those based on assumption of rigid web system. The discrepancy may be negligible in the case of very slender towers with long spans, light guy systems, and low gravity loads, particularly if arbitrary minimum size limitations largely control the design of the web system. Where conditions are less favorable, additional amplification of shears and bending moments due

to shear effects can be significant, and the designer may need to approximately estimate the importance of the additional amplification at the outset and account for it in the design[104].

The X-braced, Prate, How, Warren, Vierendeel and Three-legged pin-jointed trusses are usually used as compression members in applications ranging from laced columns in buildings and bridges to the latticed structures of radio and television towers. In such cases the design is often controlled by the elastic stability of overall system as opposed to local member buckling.

In the 3-D problems another factor is introduced that affects the stability non-linearity which is **the 3-D twisting effect** or the effect of twisting moments on the axial deformations of members **(a brand new effect formulated from a brand new theory of torsion derived in this study)**, in addition to the well-known ***Snt.Vt.*, Warping,** and ***Wagner* effects (ordinary lateral buckling effects).**

So, the stability geometrical non linearity can be subdivided into:-

* **Axial effect (the stability effect) .**
* **The sway effect (the P-Δ effect).**
* **The transverse loading effect (the fixed end action F.E.A. effect).**
* **The effect of shear slope on stability functions.**
* **The combined shear-flexural bowing effects (bowing functions including shear).**
* **The 3-D twisting effect.**

where the last two effects are the major originality of this work.

1.3.1.2 Change in geometry non-linearity:-

of which the non linearity occurs when the deformations become large enough to cause significant changes in the geometry of the structure, so that the equations of equilibrium must be formulated for the deformed equation.

1.3.1.3 Special effect of non linearity:-

Such as the temperature, the initial axial, shear, flexural, and torsional industrial imperfections, the lack of fit, the support yielding, and any other effects that cause initial tensile, compressive, shear & flexure stresses in the members. These effects can be treated either as F.E.A. or as initial geometry.

Geometrical non-linear problems are sometimes referred to as large displacement problems, but actually whenever the first axial effect is taken into account the structure undergoes a so-

called non-linear small deflection analysis, the actual large displacements must include all the effects mentioned above or at least the first two ones where the effect of change in geometry pushes the solution hardly towards the **Elastica**. Such problems do not necessarily differ from the small displacement or linear ones, not because large displacements latterly occur, but rather because axial forces exist which in the presence of lateral displacement exert a significant influence on and play a dominant rule in the stiffness of the member.

There are mainly two approaches of treating the geometrical non-linear problems:-

***The finite element approach (F.E.M.).**

***The beam-column approach (B-C), (where some of the F.E.M. supporters consider it belongs to them!).**

The first one has a relatively simple basic idea but a large number of elements is often needed for satisfactory accuracy, while in the second one fewer elements are needed but more complex analysis (actually it's very close to the closed-form solution). In both approaches, it is customary to use either ***Lagrangian*** or ***Eularian*** coordinates systems in developing the **T.S.M.** of the element.

In the first approach, the effect of geometrical non-linearity is accounted for by including the higher order terms in the strain-displacement relations, where for the 2-D analysis we have:-

$$\varepsilon_{xx} = \frac{du}{dx} + \frac{1}{2}\left(\left(\frac{du}{dx}\right)^2 + \left(\frac{dv}{dx}\right)^2\right) \quad \text{.....(1-20)}$$

and the non-linear behavior of the element can be represented by augmenting the linear stiffness matrix by geometrical stiffness matrix (initial stress and strain matrix) or by the use of incremental **T.S.M.**.

$$\left[K_t\right] = \left[K_E\right] + \left[K_p\right]$$
$$\left[K_t\right] = \left[K_E\right] + \left[K_p\right] + \frac{AE}{2}\left[K_{G1}\right] + \frac{AE}{3}\left[K_{G2}\right] \quad \text{.....(1-21)}$$

where:-

$\mathbf{K_E}$= the conventional linear elastic stiffness matrix.

$\mathbf{K_P}$ = the initial stress matrix.

$\mathbf{K_{G1}}$**&**$\mathbf{K_{G2}}$ = the non-linear stiffness matrices consisting respectively of terms that are linear and quadratic functions of the incremental element displacements.

In the second approach, which this work adopts, the effect of geometrical non linearity is accounted for by coordinate translation, the non-linear behavior of the element is presented by the incremental or tangent stiffness matrices **T.S.M.,** this matrix has different forms and shapes depending on the symbols and variables the author uses, but all these forms have the same physical and mathematical meanings.

Although the shear effect induced due to the bending moments of the elements has been included by many authors of both approaches, no one of the authors used either **F.E.M.** or the **B-C** has included **the effect of the bowing induced by this shear contribution.**

The most important point is that no one ever has introduced the effect of member shortening due to the twisting moments (***Snt.Vt.*** or **Warping**), simply because this effect was not taken into account even in the applied mechanics text books or any updated researches.

This effect which has been mentioned, derived and approved in this work is named the (***SS***) (***Siddeek-Al-Sarraf***) effect; this effect enables the author to derive the **coupled T.S.M.** which evaluates **the coupled axial-shear-flexural-torsional effects of the beam-column elements.** Again to our knowledge this matrix has never been introduced before by any other author for both approaches, this means:-

A brand new theoretical approach has been put forward both in applied mechanics and in the conventional beam-column theory.

In addition to **a new formulae of the F.E.A. including shear effect** by both **Meth.-1-** and **Meth.-2-.** In this work the author has introduced about ***80 new derived equations*** concerning all the above mentioned effects**.**

1.4 The cable element behavior:-

In the cable-frame interaction structures, the geometrical non-linearity arises because of nature of such structures. Additional non-linear effects are to be taken into consideration associating **the catenary action** (cable hanged under its own weight in the shape of catenary).

Many techniques have been suggested to handle such effect, however, **the tangent-secant equivalent cable modulus of elasticity ($E_{eq.}$)** seems to be the most efficient technique among them, and it is updated in the present work. However, the computational technique used in the present work for such structures doesn't appear to be used elsewhere.

1.5 The computational techniques and the numerical methods:-

Many numerical methods and computational techniques are adopted in the present formulation of **the new coupled T.S.M.** for the beam-column element plus the cable element in space, ***Cholisky factorization*** solving technique and the widely known **Newton-Raphson** incremental, iterative, and incremental-iterative mixed methods are used in this work.

1.6 The multi-purpose computer program *NASCFI*:-

This program ***NASCFI*** (Non-linear Analysis of Space Cable-Frame Interaction structures) introduces many services since it's capable to handle many types of analysis starting from the linear first order up to the non-linear analysis with all the non linearities mentioned above.

1.7 Objective of the study:-

The main objectives of the study can be classified as follows:-

1.7.1 Theoretical original contributions: - which are subdivided into:-

- Deriving *new bowing factors and functions including shear deformations* to be used in both 2-D and 3-D large deformation stability analysis of the structures using two approaches (Meth.-1- and Meth.-2-).
- Deriving new transverse effect (F.E.A.) functions including shear effect by both methods.
- Using *the new* (***SS*** effect), Deriving *new twisting factors and functions including shear deformations* to be used in both 2-D and 3-D large deformation stability analysis of the structures using two approaches (Meth.-1- and Meth.-2-).
- Deriving *new 3-D coupled tangent stiffness matrix (**T.S.M.**)* in global co-ordinates which includes the effect of axial-shear-flexural-torsional deformations by introducing stability, bowing, and twisting functions using both approaches mentioned above.
- Including *the special effects* of temperature, lack of fit, initial imperfections, and support yielding as an initial geometry into the 3-D large deformation shear effect stability analysis.

1.7.2 Application objective:-

Applying the above analysis to cable-frame structures with and without sags and including the effect of cable element on **T.S.M.**, also the effect of cable pretension and temperature effect are included.

1.7.3 Numerical objective:-

Introducing the well known efficient ***Cholisky*** factorization technique in order to solve the homogeneous equations of the problem.

1.7.4 Computer program NACSFI:-

A computer program (NACSFI) is created for testing the efficiency and the accuracy of the theory by making 30 different case studies.

1.7.5 Parametric study:-

A parametric study is made on different types of structures using the present theory to determine the effects of several influencing parameter on behavior of cable-frame interaction as well as ordinary structures.

1.8 Scope of the study:-

In the view of the objective, this study is presented in eight chapters.

- ***Chapter One*** introduces the problem and the aim of the study.
- ***Chapter Two*** views a historical background and brief review of earlier studies up to the most recent and updated researches with an interpretation of results where possible.
- ***Chapter Three*** introduces the detailed derivations of the new bowing and twisting factors and functions in addition to the conventional **coupled T.S.M.** in local and global coordinates of 3-D elastic stability B-C problems.
- ***Chapter four*** introduces **the tangent and secant methods** of calculating the modified modulus of elasticity "$\mathbf{E_c}$", which is the most recent and efficient non-linear approach of evaluating P-👎 behavior of cable-frame interaction structures.
- ***Chapter Five*** presents a description of the different numerical techniques used in solving non-linear homogeneous simultaneous equations, and the most widely used solvers. A brief description about the modified ***Newton-Raphson*** iteration used in both beam-column element and cable element is also given in this chapter, in addition to a description of the instability condition of the structure and the methods used for detecting it. Finally, a brief description of the convergence criteria used in the iterative analyses has been presented.

These techniques are then used in the computer program ***NASCFI*** coded in this study using ***FORTRAN77*** language applied on ***LEIHE*** compiler which enables the RAM to be fully used instead of the only 64KB, other languages can made. The program is also coded using ***Quick Basic 4.5*** language for simplicity.

- ***Chapter Six*** introduces the testing of the present theory programmed in ***NASCFI*** on more than 30 case studies with results to be discussed in this chapter also.
- ***Chapter Seven*** presents parametric studies on a (5) chosen structures to study the effect of different variables.
- ***Chapter Eight*** summarizes the most important conclusions of the study and the recommendations for future studies in the same field.
- Finally, several appendices associated with the present study are introduced in the final part of the study.

CHAPTER TWO

REVIEW OF LITERATURE

2.1 Introduction:-

Interest in the non-linear analysis of space frames has increased during the last decade. Several analytical procedures for predicting the large deformation response of such structures have been suggested. However, member deformations due to shear and axial force or in other word shear effect on stability usually are not considered in the analysis and design of frames made up of structural members of solid sections, this is due to the fact that the shear deformation in such members is resisted by a continuous web or webs, and the distortion caused by shear is relatively small except for short members, but in members with lattice, laced or batten built-up cross-sections the contribution of shear deformation to the total deflection may be appreciable, also other special effects such as thermal, industrial, constructional or any natural or man-made effects on the behavior of the structure have taken a big interest in the recent studies and researches. On the other hand the effect of flexural bowing coupled with shear effect on stability criteria has taken a very little interest in the updated papers.

The transmission towers, cable stayed or suspension bridges or any cable-frame interaction structures of the same type are highly non-linear structural systems because of many geometrical reasons associated with cable, beam or beam-column element. A large amount of interests has been focused on such systems since the sixties of this century.

From the theoretical viewpoint, the most important difference between the large deformation analysis of space frames and that of plane frames stems from the fact that large rotations cannot be treated as vectorial quantities in 3-D problems. However, its preferable to match the review of literature of 2-D from those of 3-D in both frames and cable-frame interaction structures.

2.2 Historical Background:-

Originating in ***Euler***'s classic investigation of an axially compressed column in (1744), the theory of elastic stability has become a very well-developed branch of Applied Mechanics. Most of the significant achievements, however, have been realized rather recently, two and a half centuries after ***Euler***'s pioneering work. The foundations of general theory of elastic stability were laid by ***Poincaré*** (1885) in his classical paper

on the stability of rotating liquid masses, which is developed by ***Bryan*** (1888), he based the analysis on energy criteria as a postulate generalized directly from the well-known ***Langrange***'s Theorem for discrete mechanical system. The subsequent studies, mainly by: ***Sowthwell*** (1913), ***Reissner*** (1925), ***Biezeno*** and ***Hencky*** (1929), ***Trefftz*** (1930 and 1933), ***Maraguerre*** (1938), ***Kappus*** (1939), and ***Biot*** (1938 & 1940). ***Koiter*** (1944) up to (1966), made a very important series of developments on the theory.

Studies into shear effects on the theory may be cited:- ***Engesser*** (1891 & 1909), ***Muller-Breslau*** (1910), ***Amstuts*** and ***Stussi*** (1941), ***Pippard*** (1948 & 1960), ***Takekasu*** (1951), ***Bleich*** (1952), ***Jones*** (1952), ***Timoshenko*** and ***Gere*** (1961), ***Koenigsberg*** and ***Moshin*** (1964 & 1965), and last but never least ***Tomayo*** (1965). These investigations have determined the critical loads and frame behavior of built-up members as affected by shear [(55)].

The cable-frame interaction systems such as stayed bridges or guyed towers have also an ancient history dating back to Egyptian sailing boats with rope-stayed sail beam up to the more recent applications of:- ***Verantius*** (1617) timber deck bridge, ***Loscher*** (1784) timber bridge, ***Redpath*** & ***Brown*** (1817), ***Poit*** (1821), ***Motly*** (1837), ***Clive*** (1843) original cable-stayed bridge, up to ***Joseph*** bridge(1868) and ***Albert*** bridge(1873)[(95)], up to the well-known stayed bridges of this century when the first modern cable-stayed bridge was built in Sweden in (1955), and finally the high technology bridges and towers of the last three decades of this century. Theory of this field was founded in the nineteenth century but the most important and efficient developments associated with cable-frame interaction theory were established in the fifties and sixties of this century.

A number of authors studied the non-linear cable-tower interaction methods for static analysis (***Walmsley*** (1924), ***Scoth et al***.(1956), ***Cohen*** & ***Perrin*** (1957), ***Fiesenheiser*** (1957), ***Rowe*** (1958), ***Davenport*** (1959), ***Dean*** (1961), ***Poskitt*** & ***livesley*** (1963), ***Davenport*** & ***Steels*** (1965), ***Goldberg*** & ***Meyers*** (1965), ***Odley*** (1966), ***Williamson et al***.(1966), ***Skop*** & ***O'Hara*** (1970 & 1972), ***Livesler*** (1970), ***Richert et al***.(1971), ***King*** (1972), ***Skop*** (1979), and ***Truax*** (1980)), dynamic analysis (***Hartmann*** & ***Davenport*** (1966), ***McCaffrey*** (1972), and ***Hartmann*** (1972)), stability (***Hull*** (1962), ***Goldberg*** & ***Gaunt*** (1973), and ***Chajes*** & ***Chen*** (1979)), and optimization (***Bill*** & ***Brown*** (1976)) [(55)].

2.3 Books Review:-

Many important books have been published in this field of structural engineering. However, the most widely known books that this study rely on are by the others:-

Kinney (1957)***, Timoshenko*** & ***Gere*** (1961)***, Gere*** & ***Weaver*** (1965)***, Marchent*** (1965)***, Poppov*** (1968)***, Majid*** (1972)***, Britvec*** (1973)***, Cook*** (1974), ***Huseyin*** (1975)***, Troitsky*** (1977)***, Chen*** & ***Atsuta*** (1977- Vol. (I & II)), ***Hinton*** & ***Owen*** (1977), ***Leipholz*** (1980), ***Smith*** & ***Griffiths*** (1982), and ***Kolousek, Pirner, Fischer*** & ***Naprstek*** (1984). These books are stated as references for this study.

2.4 More Recent Review of Literature:-

Since the fifth decade of this century the researches have taken more accurate paths and directions to formulate as accurate possible as the theories that can give the actual behavior of the systems, so, in order to take the problem gradually, the following classification of the literature shall be taken:-

2.4.1 Basic Theory Literature:-

A considerable amount of literature on the elastic analysis of steel framed structures has been undertaken and many researches, papers and books have been published to determine the real behavior of the structures by establishing the load-deflection response.

Livesly [58&59] (1956), published a paper on the non-linear behavior of framed structures, he developed a program for analyzing 2-D frames comprised prismatic linear elastic members subjected to in-plane loading applied on joints only, he neglected the effect of flexural bowing and chord rotation on the member shortening and assumed no change in geometry i.e., he was closer to the small deflection theory than to the exact theory.

Renton [78] (1962), studied the stability of 3-D frames, he formed the stiffness matrices of a certain type of cross-sections making allowance for the effect of relatively rigid gusset plates with different end conditions, he include the effect of torsional stiffness (see equations 1-18 to 1-20), a computer program was made in him and tested by an experimental work.

Saffan [81] (1963), presented a non-linear formulation for 2-D frames, he considered the effects of axial force, bowing and finite deflections with development of

a computer program for this purpose, his solution procedure involves iteration on the displacement of the kind of ***N-R*** method with one-load step, he concluded that:-

1. The stability and bowing functions may play an important part in the estimation of the theoretical carrying capacity of structural frames because the analysis was carried out to a latest stage of loading.
2. The classical phenomenon of the elastic critical loads needs to be considered.

He illustrated that end shortening due to flexure may be of the same order of magnitude as linear extensional term, ***Williams*** (1964)***, Merchant*** & ***Brotten*** (1964), ***Miller Brotten*** & ***Merchant*** (1966) reached the same conclusion.

In (1964), ***Argyris*** [9] employed an incremental techniques to determine the approximate non-linear load-deflection behavior of rigid jointed frames, he assumes linear behavior in each increment and changed the geometry after each load step, so, he used the **T.S.M.** evaluated at the end of each load step, the effect of axial force on member stiffness has been neglected in his **T.S.M.** derivation.

Conner et.al.[24](1968), established a non-linear formulation for rigid jointed frames comprised prismatic linear elastic members subjected to load applied to joints only, they concluded that the effect of axial force on the member stiffness is quite significant and that ***N-R*** method is very efficient for low convergence tolerance.

Also in (1968), ***Jennings*** [44] proposed a non-linear method for taking the effect of the change in geometry on load-deflection behavior of frames, member axial shortening due to inclination in no-large or rather small displacements was considered in his work. He concluded that accurate displacement transformation can be adopted in extremely large deformations cases.

Four years later, in the year (1972), ***Haisler, Stricklin,*** & ***Stebbins*** [37] presented a solution technique that is applicable to the non-linear differential equations characterizing geometrically non-linear behavior. Their results indicated that a new self correcting initial value formulation has possibilities as a powerful tool for non-linear analysis.

In the year (1973), ***Cenap Oran*** [71] derived a tangent stiffness matrix **T.S.M.** for linear elastic 2-D prismatic member according to the conventional beam-column theory; he included the effect of flexural bowing of deformed member and made no restriction on the displacement of the frame. Although large displacements were

assumed, relative member deformations were assumed to be small enough to justify the beam-column theory, loads were assumed to act on joints in his derivations.

Later in the same year ***Oran*** [72] used the same approach to derive the linear elastic 3-D prismatic **T.S.M.**

In the next year**,** ***Vinnakota*** & ***Aysto***[100] (1974), studied the 3-D inelastic special stability of restrained beam-column, they applied their work to closed circular sections, they took the coupled effect of the differential equations in space eq.(1-18 , 1-20), they developed a mathematical model governing the inelastic deformational response of restrained beam-column under bi-axial bending and torsion. The assumptions they suggested made their work closer to the small deflection theory.

In (1976), ***Cenap Oran*** & ***Islam Kassimali*** [70] suggested a method for the analysis of large deformations and stability of elastic framed structures using the general beam-column type method previously developed by ***Oran*** in (1973)**.** They mixed both the incremental and the iteration techniques in the solution they proposed, for incremental one they applied the loads in small increments, then they determined the corresponding configuration changes of the structure from the sequence of linearized analysis, so updating the **T.S.M.** in each load level must be made. For the second technique, any desired load level must have an approximate solution at first, then by ***N-R*** method a step-by-step iteration they improved the solution until the joint equilibrium equation are satisfied within a prescribed tolerance. Both ***Lagrangian*** (for initial geometry)and ***Eulerian*** (or updated ***Lagrangian*** for the updated configuration of the member) coordinates were used. They concluded that the possibility of reducing the required computational work for plane frames could be achieved by introducing some approximations such as using ***Lagrangian*** coordinates, neglecting the bowing effect so the **T.S.M.** would be a function of axial force only and using undeformed member length in the equilibrium equation of the member. They applied their work to many case studies and their results were the closest to the exact solutions.

In (1977), ***Wood*** & ***Zienkiewicz*** [109] presented a continuum approach for the geometrically non-linear analysis of oriented bodies e.g. beams, frames, arches in a total ***Lagrangian*** coordinate system using finite element method, they solved their non-linear equilibrium equations by ***N-R*** method for which a number of examples were given.

Epstein, Nixon & ***Murray*** [31] in (1978), presented a large displacement inelastic analysis of beam-column, they extended the formulation of a 2-D and 3-D large deformation analysis of thin walled beams previously presented by the authors in (1976) to include the solution of nontrivial inelastic member instability problems for the prediction of maximum load carrying capacity. A technique was suggested for discretizing the functional, evaluating residuals and forming the ***jacobian***, which is suitable for ***N-R*** solution of inelastic beam-column problems. Results for inelastic bi-axial bending of beam-column are compared with experimental results of other researchers and the results were very close.

Bridge & ***Aust*** [13] in (1979), described a numerical method for a second-order, 2-D analysis of portal steel frames accounting for both non-linear geometrical and material responses, they used a chain calculations and total ***Lagrangian*** coordinates in their work, the accuracy of the method has been confirmed by comparison with results of tested frames. The same method can be used to determine the elastic critical buckling loads for the frames. As large deformations are accounted for, the post-buckling behavior of frames can also be established. The method has been shown to be suitable for determining the influence of instability on the collapse loads for portal frames. Factors such as non-linear material properties, varying cross section properties, geometrical imperfection, temperature change and gradient, lack of fit, strain hardening and varying base restraints can be accounted for, the method is well suited to minicomputer applications.

Also in the same year (1979), ***Ricks*** [79] presented an incremental approach to the solution of snapping and buckling problems, he discussed the instability conditions of frames under conservative loads, he used the incremental approach for the computation of non-linear equilibrium paths of some problems with continuation through limit points and bifurcation points.

Effect of bowing on rectangular plane frames has been studied by ***Korn*** [51]in (1981), he concluded that the higher the structure the higher the axial force effect and also the more dominant the effect of bowing.

The pre-twist effect on the columns buckling load was studied by ***Tebedge*** [92]in (1982), large deformation finite element formulation is developed for the stability analysis of pre-twisted columns. Numerical examples and experimental results for various angles of pre-twist and different ratios of principle moment of inertia have been

checked and a good convergence and satisfactory accuracy are observed using few elements. He included the effect of warping and ***Snt. Vt.*** torsional moments only.

In the next year (1983), ***Fujii*** [34] presented a mixed variational formulation for Elastica problems of beams and frames. The bending moments and discontinuities in tangential slope of bi-linear SP-line functions respectively, these interpolations enable the energy terms in the mixed functional to disappear or to be linearized, whereas only the load potentials become non-linear and need to be estimated by a kinematics approach. The author then solved the resulting simultaneous non-linear equations by an iterative method.

In the same year**,** ***Islam Kassimali*** [47] presented a numerical procedure for the large deformation analysis of elastic-plastic frames, he based his work on ***Eulerian*** formulation, which was developed initially for elastic systems by ***Oran*** & ***Kassimali,*** and extended herein to include the elastic-plastic effects. The **T.S.M.** of elastic-plastic behavior of beam-column element has been established and tested by a computer program with numerical examples, the results were excellent.

Also in (1983), ***El-Zanaty et.al.***[30] presented a general geometrically non-linear formulation for the analysis of 2-D multistory frames using finite element method based on the simple geometric approximation which permits the virtual work equations to be derived in a manner consistent with full nonlinear strain displacement equations without introducing further approximations.

Z. Waszczyszyn [102] in the same year, presented a study on numerical problems of non-linear stability analysis of elastic structures, different stability criteria for the computation of critical points were discussed.

In the year (1984), ***Wen*** & ***Rahimzadeh*** [103] studied the 2-D and 3-D nonlinear elastic frame analysis using the finite element approach, large deformations and changes in geometry of the chord were considered, the longitudinal and transverse displacements were respectively interpolated by linear and cubic functions and the axial strain because the transverse displacement is averaged over the element length. The incremental stiffness matrices are derived in ***Langrangian*** coordinates for small displacements and ***Eularian*** coordinates for large displacements. Numerical examples were checked and comparison with other methods indicates that their method is competitive.

Two years later, in (1986)***, T. See*** & ***R. E. McConnel*** [84] studied the large displacement elastic buckling of 3-D structures, a non-linear stiffness matrix based computer program was used to investigate the stability of elastic space structures whose likely failure modes were determinated by examining the **T.S.M.** of the structures near its collapse load. Where the exact initial geometry was unknown, the addition of a suitable set of imperfections produced results in agreement with the experiments.

In (1986) also, ***Yang*** & ***McGuire*** [110], studied both non uniform torsion and the effect of joint rotations which are essential to the formulation of a consistent finite element model for elastic thin-walled beam-column element, they derived a new stiffness matrix for the analysis of 3-D thin-walled beam-column element. Starting from the principle of virtual displacements, they developed a modified ***Lagrangian*** procedure for non-linear analysis.

In the next year (1987), ***K.M.Hsiao*** & ***F.Y.Hou*** [41] presented a very simple and effective formulation and numerical procedure to remove the restriction of small rotations between two successive increments for the geometrically non-linear finite element analysis of 2-D frames, body attached coordinates (***Eularian*** coordinates) were used in the work and an incremental iterative method based on ***N-R*** method combined with a constant arc length control method was employed for the solution of the non-linear equilibrium equations. In order to improve convergence properties of the equilibrium iteration a two-cycle iteration scheme was introduced and nine numerical examples were presented to demonstrate the efficiency of their work.

In the same year (1987), ***A. Chajes*** & ***J.E. Churchill*** [17] presented the basic concepts involved in the construction of load-deflection curves for geometrically non-linear systems by finite element method, they used three procedures in solving the non-linear problem and they derived the governing equation for each method and the procedure was used to plot the load-deflection curve.

Kam [46] (1988), presented a general method for the large deflection analysis of inelastic 2-D frames, the large deflection analysis is based on ***Eularian*** formulation, he derived the **T.S.M.** using the exact differential equation and the moment-thrust-curvature relations of a member subjected to a large relative deflection, also the **T.S.M.** of W-shaped sections of elastic-plastic material was constructed as an example and its application to the large deflection analysis of inelastic frames was demonstrated with several examples. A simple form of the member **T.S.M.** was deduced from the exact

formulation using the assumptions of small member relative deflections, then he had shown that the simple one can yield excellent results compared with the exact one. Hence, it is reasonable to adopt the assumption of small member relative deformations in the large deflection analysis of inelastic frame structures which is the same conclusion previously adopted by ***Oran*** & ***Kassimali*****.**

In (1988), ***Panayotounakos*** & ***Theocaris*** [73] presented an analysis of the strongly non-linear differential equations governing the elastica configuration of a flexible straight bar due to a longitudinal compressive force continuously distributed along its length. They used for this derivation of a straightforward closed-form solution of this complicated problem several functional transformations and a quantitative analysis was adopted yielding reliable results in conformity with the physical problem, their transformations are simple, original and useful in solving, problems of non-linear elasticity without the use of numerical procedures.

In the same year (1988), ***Mendis*** & ***Darvall*** [61] introduced a second-order stability analysis of softening frames using their ***SOAPS*** computer program which is (Second-Order Analysis with Plasticity and Softening). Elastic-plastic softening characteristics, incorporating stability functions and the P-Δ effect were used, then they tested their work on three numerical examples and the results were sufficient.

In (1989), ***J.Meek*** & ***S.Loganathan*** [63&64] published two papers, the first one was on the non-linear behavior of 3-D frame structures concerning the methods of non-linear static analysis of space structures, they used the well known and efficient arc length method suggested by ***Riks*** & ***Crisfield*** within each increment of loading together with the ***N-R*** method as the iteration strategy. They applied their work to numerical examples. The second one was on geometrical and material non-linear behavior of 3-D beam-column element comprising thin-walled circular and square hollow sections. A simple and efficient formulation of beam-column elements for the large deflection analysis of elasto-plastic frame structures was presented; they used the same numerical technique of the first paper.

Borri & ***Chiostrini*** [12] in (1989), presented a non-linear approach to the stability analysis of space beam structures, they reviewed a special beam element recently introduced by several authors for application to a perturbative approach of post buckling analysis of 3-D beam, girders, and frames.

Fertis & ***Pallaki*** [32] in (1989), introduced an efficient pseudo linear and equivalent systems for large deflections of members, they used the second order non-linear differential equation of the elastic curve to prove their method. Their method simplifies a great deal the mathematical complexity of the non-linear problems especially when the initial problem has continuously varying stiffness (EI) along its length. For convenience, a very accurate approximate method was introduced.

Al-Bermani & ***Kitiporncha i***[2] in (1990), presented the derivation of a deformation stiffness matrix for an asymmetric thin-walled beam-column element, they coupled the axial stretching and the lateral and torsional deformations. Their work may be used together with the linear and geometrical stiffness matrices for thin-walled beam-column elements to analyze large deflection behavior of 3-D comprising members in which the influence of sectional warping in the section can be neglected. Their method is applicable in transmission towers in non-linear large deflections analysis.

In the same year, (1990) ***M.B Wong*** & ***F. Tin-Loi*** [108] developed a method for the elastic non-linear analysis of framed structures depending on the finite element method. They described the main forms of ***Langrangian*** coordinates systems and their relative merits are also discussed.

Also in (1990), ***Chandra, Trikha*** & ***Krishna*** [19] presented a second-order incremental iterative procedure based on displacement approach to carry out non-linear elastic analysis of 3-D frames considering the effect of geometrical non-linearities such as axial force effect on member stiffness matrix and flexural bowing, both secant and tangent stiffness matrices were used. Later, in the same year they improved the procedure to deal with elastic-plastic analysis of 3-D frames.

K.F.Sideek [85] (1990), presented an experimental investigation on eight portal frames studying the elasto-plastic behavior of rigid-ended steel frames, he tested a theoretical approach to large deflection based on step by step small deflection incremental procedure previously suggested by ***Al-Rifaie*** & ***Trikha*** in (1986) and developed by ***Masser*** in (1989), which was extended by ***Sideek*** in this study to include the effect of connection rigidity, he neglected the bowing effect and change in orientation and geometry of element.

In the year (1991), ***Goto, Suzuku*** & ***Chen*** [36] studied the bowing effect on elastic stability of frames under primary bending moments, a refined method of analysis for

the elastic stability of rigid frames considering the pre buckling deformations due to the primary bending moment is proposed, it differs from the method presented originally by ***Chwalla*** and later by ***Mansur et.al.*** and ***Lu,*** in that the proposed method considers precisely the bowing effect in the determination of all displacements and leads to a symmetric **T.S.M.** which is ignored by ***Chwalla.***

Also in (1991), ***Kassimali*** & ***Abbasnia*** [48] published a very important paper on the large deflection analysis of 3-D frames, he presented a method based on an ***Eulerian*** formulation, which takes into account the effect of large joint translations and rotations, the changes in member chord lengths caused by axial strain and flexure bowing, and the effect of axial force on member torsional stiffness, local member force-deformation relations are based on beam-column approach. Numerical solutions are presented for four structures, which indicate that the method they suggested is highly accurate in predicting large deformation responses of structures.

In (1992), ***R. Kouhia*** [53] published a paper on the solution of non-linear finite element equations which deals with basic requirements in the construction of a reliable continuation procedure.

In the year (1994)**,** ***Al-Sadder***[4] presented a general geometrical, material, and connection non-linearities of multistory steel structures, he adopted the method previously suggested by ***Oran*** & ***Kassimali*** as the geometrical non-linearities concerns and the conventional beam-column approach using ***Eulerian*** formulation which was also adopted. He suggested a new design formula to calculate the failure load of semi-rigid steel frames and they tested their work on number of case studies which gave excellent results.

In the year (1996)**,** ***Al-Raunduzy*** [3] presented an investigation into theoretical analysis for estimating the 2-D large displacement elastic stability behavior of steel frames subjected to either proportional or non-proportional increasing static and dynamic load applied at joints only. He adopted the beam-column approach based on ***Eulerian*** formulation allowing for the axial force on bending stiffness, change in member length due to axial strain and flexural bowing in addition to the change in member orientation is taken into account, they tested their work on many case studies.

Also in March of the same year (1996), ***R. M. Sully*** & ***G. J .Hancock*** [89] published a paper which describes a test program conducted on the behavior of cold-formed, compact square hollow section pin-ended beam-column. Load-deflection,

moment-curvature, local buckling, and moment capacity behavior were studied, curves were drawn. They included both material and geometrical non-linearities in their elastic-plastic finite-element theoretical analysis which gave a great deal of accuracy to their test results.

2.4.2. Shear Deformations of Lattice, Batten, and Laced Elements:-

In general the researches and studies have raised a significant interest in this field since the great efforts of ***Timoshenko*** & ***Gere*** [94].

Williamson & ***Margolin*** [104] (1966), introduced a very important study on shear deformations in 2-D open-web system of guyed towers, conventional beam-column theory was adopted. Since only axial thrust was considered, eccentric moments due to guy reaction, lateral deflection at each guy level were taken into account and neither change in geometry nor flexural bowing effect were considered, then their work may be underlined as a small deflection theory analysis, total curvature was assumed in their stability functions due to shear effect of open-web element. They examined one-level guy and multilevel guy.

In (1970), ***Lin, Glauser*** & ***Hon*** [56] presented a very important report, they introduced a non-dimensional shear flexibility parameter to characterize the shear flexibility of batten and laced members, this parameter takes into account the effect of axial force, local eccentric joint connections, local connection flexibility, and effect of rigid stay plates at the end of structural members, generalized slop-deflection or stability constants(stiffness & carry-over factors), fixed-end moments, and critical loads for built-up structural members were evaluated in terms of graphical charts, the fundamental linear second-order differential equation for the deflection curve of the member which includes the effect of shear deformation had been derived, and elastic buckling loads for the structural members have been evaluated for various boundary conditions. Finally, a numerical examples of frame analysis was presented to provide a comparison with the ordinary (no shear) small deflection theory.

J.D. Renton [77] in (1973), studied the buckling in long, regular pin-jointed trusses due to the axial force using finite deference method, small deflection theory were used, exact solutions were found, and approximate formulae were derived which may compared with the critical loads for analogous columns buckling due to bending and shear. He concludes that results taken from his formulae are identical to those from ***Timoshenko*** & ***Gere*** [94]**.**

A.K.Noor [67] in (1974), presented a mixed method between force and displacement methods to analyze the geometric and material non-linear pin-jointed 3-D trusses, the proposed method was examined using a computer program. For convenience, the constitutive relations were assumed to in the form of ***Ramberg-Osgood*** polynomials and the individual members of the truss were assumed to remain straight and stable under loading, i.e. no change in lengths (axial & bowing effects) were taken into account, so, he adopts the beam theory rather than the beam-column theory. He examined two-bar truss, two bay plane truss, and transmission tower case studies to check his method.

Lindgren [57] in (1979), made some developments on shear flexibility parameters of lattice or laced 2-D beam-column with various end conditions previously suggested by ***Timoshenko*** & ***Gere*** [94]**.**

In (1981), ***A.K.Noor*** & ***L.S.Weisstein*** [68] presented a very simple and efficient procedure of predicting the buckling load of 3-D beam like lattice trusses which are simply based on replacing the original lattice truss by an equivalent continuum beam model and then obtaining analytic solutions for the beam model which in turn accounts for warping and shear deformations in the plane cross section and is characterized by its strain energy and potential energy due to initial stresses from which the governing differential equations were derived. The accuracy of this method was demonstrated by means of numerical examples.

Svensson & ***Kragerup*** [90] in (1982), investigated the imperfection sensitivity of laced columns, this imperfection consisting of both a local and an overall geometric imperfections, they presented a simple numerical method for solving both elastic and elastic-ideally plastic problem and the collapse load was finally predicted.

In (1983) also, ***Gelu Onu*** [69] studied the shear effect in beam stiffness matrix, he adopted the beam theory using the energy method and so he formalized the stiffness, the geometric stiffness, and the consistent mass matrix for the four D.O.F. beam element including shear effect by coupling the transverse displacement field and the shear angular displacement field.

In (1986), ***Elyada*** & ***Babckok*** [29] presented a closed-form theoretical investigation of the non-linear structural behavior of idealized imperfect three-legged truss column, they examined equilateral-triangular cross sections columns formed by three longerons held by equally spaced battens. The columns were simply supported,

axially loaded, and locally as well as globally, geometrical imperfections were admitted. Closed-form expressions were obtained for local and global buckling, post buckling, imperfection sensitivities, non-linear response, and limit loads. Local-global mode interaction was accounted for fully and comparisons were made with numerical results.

S.Z.AL-Sarraf [5] in (1986), studied the shear effect on the elastic stability of frames**,** modified small deflection stability functions for prismatic beam-column having any solid cross-sectional shapes, laced or battened built-up sections were developed in terms of shear flexibility and axial load parameter which make possible the rapid prediction of the elastic critical load of structures taking into consideration the effect of the shear force in the members using a hand computing method. The modified stability functions were related to existing tabulated stability functions of ***Livesley*** & ***Chandler.*** The approximate formulae predict the accurate elastic critical load to within **1%**.

About two years later (1988), both ***F.Y. Cheng*** & ***C.P. Pantelides*** [22] used two approaches to derive differential equations, stiffness coefficients, and fixed-end forces for the small deflection analysis of structural systems composed of ***Timoshenko*** beam-columns that maybe supported by an elastic foundation. These two approaches differ in terms of the assumed shear component of the static axial load on the cross section. The first one is the total slope (bending and shear slope), and the second one calculates the shear component only form the bending slope. Numerical examples ensured the applications of both methods.

Also in (1988), ***S.H. Stoman*** [88] studied the stability criteria for the X-bracing systems using the energy method, he generated the curves for the effective length factor as a function of the ratios of the axial load in both tension and compression brace.

In (1989), ***Ekhande et.al.*** [28] presented a 3-D beam-column stability functions, including shear deformations, they derived an explicit expression for stability functions for 3-D beam-column, in terms of member length, cross-sectional properties, axial force and the end moments. The effect of flexural on axial stiffness i.e. bowing effect, the effect of axial force on flexural stiffness and stiffnesses against translation are considered, the effect of axial force on torsional stiffness and the effect of torsional moment on axial force are neglected. The non-linear stiffness matrix of 3-D beam-column element using stability functions was presented by modifying the linear elastic stiffness matrix for a beam-column which includes the effect of shear deformations

available in the literature. A numerical example showing the calculation of stability functions for a given beam-column was also presented.

In the year (1991), ***R .R .Avent, R .R . A.Issa,*** & ***M.L.Chow*** [11] used the techniques of discrete field analysis to investigate the critical buckling loads for various 2-D X-braced truss configurations and geometry. An explicit formula was developed for determining loads having a form of independent of the number of panels. The study indicates that the modified ***Euler*** critical load may vary up to **85%** of loads obtained by discrete field analysis.

Also in (1991),***Z.Y.Shen*** & ***K.Ding*** [86] presented a new theory of thin-walled beams involved the effect of shear deformations which can be applied to the analysis of capacity of such load-carrying beams under combined compression, bending, torsion, and initial imperfection. The accuracy and high speed in calculations compared with exact theory and experiments made the new theory very efficient.

In the year (1992), ***V. Paramasivam, T.R .Gowda,*** & ***D.M .Raj*** [74] published a technical note on the ***Timoshenko*** beam finite element with four D.O.F. and convergence of O (h^4), they stated that when transverse shear deformations and rotary inertia in beams are important, elements based on the ***Timoshenko*** beam theory are useful, and they are completely free of locking and perform equally efficiently in thick as well as in thin beam range.

In (1995), ***N. A. H. Alwash*** [6] studied the non-linear behavior of reinforced concrete Vierendeel trusses, in his work he included the effect of shear deformation using the bending slope approach only (and not the total slope approach), and derived the stability functions for this approach in such structures, he neglect the bowing effect, and the change in geometry in the chord and took only the effect of axial force in the geometrical non-linear stiffness matrix, so his work was closest to the approximate theory (small deflection theory) rather than the exact large deflection one.

In March of the year (1996), ***M.J.Alam*** & ***A .R . Santhakumar*** [1] published a paper on the new generation reliability analysis of a transmission tower. Their work itself doesn't concern our line of work, but the tower they analyzed and its loading taken from ***ASCE Manual 52*** & ***74*** does interest the present work as a parametric study.

2.4.3 Cable-Frame interaction literature:-

Over the years, significant time and effort have been spent on the study of guyed towers.

S.A.Saafan [82] in (1970), studied the structural behavior of suspension roofs under the action of non uniform or concentrated loads, he derived the stiffness matrix of a pre stressed cable element, and also he presented the finite deflection theory analysis of special system of nets on the basis of non-linear theory and a more accurate representation of the material's stress-strain relationship.

Also in ***G.R. .Buchanan*** [15] in (1970), derived and solved the equilibrium equations for the 2-D cable under both vertical and inclined loads, numerical results have been presented for non dimensional cable parameters that depended on cable tension and sag, applied load, and cable properties.

In the year (1974), ***D. E. Urelius*** & ***D. W. Fowler*** [98] made an investigation into the geometrical non-linear behavior of pre-stressed cable truss structures, solutions were obtained from a variety of cable truss configurations having both rigid and flexible supports and subjected to both symmetrical and unsymmetrical loading conditions. The influence of such parameters as sag-to-span ratio, cable size, tie spacing, and pre-stressing forces upon the behavior of the total structure was illustrated.

In (1976), ***K.H. Chu*** & ***D.C.C.Ma*** [23] presented a very important study on the non-linear cable-frame interaction, they presented two different approaches for analyzing the cable elements, the first one was the modified ($\mathbf{E_c}$ method), and the second one was the iteration method. For the mast element they adopted the ordinary beam theory with axial force effect to be included and neither bowing effect nor geometrical changes were taken into account in the geometrical stiffness matrix. They suggested a parabolic cable shape rather than catenary one and proposed a very efficient method for finding the correct root of cable equation concerning the first approach ($\mathbf{E_c}$ method), they tested their approaches on three different numerical examples and they concluded that:-

1. The secondary deflections due to axial force may be obtained by dividing the member into a number of finite divisions and applying the useful stiffness method.
2. The modified "$\mathbf{E_c}$" method with dividing the structural members(masts or columns) will give correct results in such members but not in cables, the sags and tensions in cables or cable tension components can obtained by the equations they proposed based on parabolic cables, those equations are incorrect for cables with very low tensions and large sags.

Chain calculation were used in (1976), by ***H. B. Harrison*** [38] for interactive non-linear structural analysis, he adopted the chain calculation for both masts and cables assuming cable subdivisions as link elements and loads concentrated on joints only, his method is very economical for computer applications since it needs a few numbers of iterations to insure the equilibrium and accuracy.

Buckling in cable-stayed girder bridges was investigated by ***M.C. Tang*** [91] also in (1976), he derived a procedure for estimating the critical load of such structures using energy method and developed a computer program to calculate the buckling load of four bridges with different types of cable configurations.

The buckling of stayed columns was also investigated in (1977) by ***Temple*** [95], he investigated the double cross-arm stays by two methods, the first one was based on the finite element method while the second one was an exact solution using stability functions, he presented some numerical examples to improve a solution procedure for determining the buckling load of stayed columns and not to optimize the stayed column configuration for maximum load-carrying capacity.

Wilson & ***Wheen*** [105] in (1977), published a paper on the inclined cable under load, the direct design expressions for taut cables is presented to include the case of inclined taut cables in which can also be used to solve the problem of larger sag cables under self-weight, concentrated loads, and uniform loading distributed part way across the span. Accuracy was improved by dividing the cable into a number of inclined segments.

In (1978), a non-linear cable behavior study was presented by ***Judd*** & ***Wheen*** [45] using a trial and error search procedure in which the initial value of the cable horizontal tension was calculated and then for increasing values of horizontal tension the magnitude of the corresponding applied load in the desired configuration was deduced. This procedure calculates a correct equilibrium cable profile for every loop in the computer analysis. Several examples were accurately checked.

Also in (1978), ***Russell, Morgen*** & ***Henghold*** [80] studied the cable equilibrium and stability in a steady wind, a finite element model for such case was presented. This study results in non-symmetric stiffness matrices and thus admits the possibility of both static and dynamic instabilities, so, they proved that a single-span cable with aerodynamics characteristics they presented is satirically and dynamically stable.

Hathout.I.A., M.C.Temple & ***J.S.Ellis*** [39] in (1979), studied the effect of the initial pretension in the stays on the buckling load of both 2-D and 3-D single-cross arm stayed columns. Experimental results were presented for the buckling load obtained by varying the initial pretension in the stays, and finally the expressions obtained were applied to numerical examples to demonstrate the influence of various stayed column parameters on the minimum effective and optimum pretensions as well as the maximum buckling load, both the experimental and theoretical results indicated the great influence of the initial pretension on the buckling load of the column.

Later in the same year, ***J. F. Fleming*** [33] presented a non-linear 2-D static analysis of cable-stayed bridges of both types (the stayed type which is subdivided into:-radiating, harp, fan, and star and also the suspended type) considering the effect of initial cable tensions, member dead weights, and distributed and concentrated live loads. A general computer program for this purpose was listed and detailed.

Also in (1979), ***Wang*** & ***Stiller*** [106] used the **T.S.M.** for the bifurcation analysis of cable-stayed frames including the cross-arms types; they removed the assumption of inextensible members and took into account the geometrical changes of members. The key assumption is that stresses and strains are proportional up to any stress level without limit, but they assumed ***Langrangian*** formulation. The computer program they presented has generality and can be easily applied to complex, irregular, and real structures with cable-stayed and rigid joints.

In (1981), ***A.Chajes*** & ***D.Ling*** [16] studied the post-buckling analysis of guyed towers using the theorem of stationary of potential energy, the axial shortening of the mast due to the bending and axial stresses and also the changes in slope and length of the cables were taken into account while the cable sag was neglected, they concluded that:-

1. The critical loads of hinged and fixed base towers with small cable pretensions are very close to those of hinged-hinged and hinged-fixed columns, respectively, with the exception of the systems of extremely small cable to mast stiffness ratios.
2. Towers with small cable pretension forces have unstable post-buckling curves.

3. The presence of sizable cable pretension forces decreases the load at which buckling begins by an amount equal to the sum of the vertical components of the cable forces.
4. The presence of the horizontal load results in a significant decrease in the capacity of tower to resist vertical loads.

In (1982), ***K.C.Wong*** & ***M.C.Temple*** [107] studied using the finite element method the effect of initial imperfection of single cross-arm stayed columns on the buckling strength of such structures. From experimental results and numerical examples they concluded that the presence of an initial out-of-straightness or imperfections changes the deflection rate and can significantly reduce the buckling load.

Schrefler, Otorizzi & ***Woods*** [83], presented in (1983) a unified formulation for the geometrically non-linear analysis of 2-D beam and line elements using a total ***Langrangian*** approach. The continuum approach used considers the same nodal displacements for elements with and without flexural stiffness and allows for a straightforward analysis of combined structures. The prescribed displacement technique is used extensively to overcome the initial mechanism which cable structures usually display, this requires the use of temporary constraints which are eliminated once the stress state due to cable pretension is established. Several examples show the capability of this approach, a number of which relate to real structures.

In (1984), ***Temple, Prakash*** & ***Ellis*** [96] presented a very important experimental and theoretical investigation of failure criteria for stayed columns, the theoretical load was predicted using a finite element method in conjunction with an iterative-incremental procedure. Good agreement between experimental and theoretical results was obtained when the initial pretension was less than the optimum pretension.

Raman, Kumar & ***Rao*** [76] in (1988) presented a 3-D large displacement analysis of guyed towers using finite element method. Beam-column element for masts and truss element for cables were adopted in this study and the solution technique essentially consists of solving guys and masts separately and alternately forcing the compatibility of displacements at the guy support points until the final equilibrium configuration is obtained and the given external loads are applied in one step. From the two numerical examples tested the authors found that the strains in cables and masts were observed to be substantially higher than the corresponding yield strains as the external loads approach the buckling loads.

In (1990), ***Nazmy*** & ***Abdel-Ghaffar*** [66] formulated the non-linear static analysis of 3-D long span cable stayed bridges under the effect of their own dead weight and a set of initial cable tensions, non-linearities due to sags, axial-bending moment interaction in the decks and towers, and change in bridge geometry due to large displacements were taken into accounts in this study. The results showed that these flexible structures are highly non-linear under dead load, especially for long span bridges.

In the year (1991), ***Issa*** & ***Avent*** [43] presented a methodology for analyzing three-legged guyed towers, and the process results in an exact analysis in the classical since. Three configurations were considered:-Warren, X-braced, and Vierendeel and the non-linear effects of guy-tower interaction were considered. Since discrete field analysis procedures were used, the numerical computations were not sensitive to the number of joints in the system. A 700 feet (213.41 m.) multi-guys tower was used to evaluate various tower sections configurations.

As it is obvious from the literature review no one (as far as the author knows) has introduced the coupled effect of shear plus flexural bowing in the large deflection theory (i.e. Large Deformation Bowing Functions Including Shear effect) both in plane or space, static or dynamic, elastic or elastic-plastic, analysis, therefore it is very important to fill this empty space of the large deflection theory of stability. The most important thing is that no one has ever introduced the effect of torsion on axial displacement, i.e. the (***SS*** effect) and the coupled **T. S .M.**

CHAPTER THREE

SHEAR AND 3-D EFFECTS OF BEAM-COLUMN ELEMENT BASIC THEORY AND DERIVATIONS

3.1 Introduction

This chapter presents the complete philosophy, physical phenomena and mathematical derivatives of the new so-called ***SS (Siddeek-Al-Sarraf)*** effect and the derivation of the new coupled 3-D element **T.S.M.** in both local and global coordinates

In the first section of this chapter the basic theory of the shear effect and the bowing effect are presented and then the full derivation of the new combined shear-flexural bowing functions are derived with the effect of fixed end action.

In the second section the (***SS*** effect) and the coupled **T.S.M.** are derived in detail.

In the third section, the special effects of non-linearities (temperature, lack of fit, initial imperfections and support yielding) are treated.

3.2 The shear effect on the non-linearity:-

The shear contribution in the entire deflection of a beam element as treated in the ordinary small deflection elastic theory is very simple as detailed in **App.F**. In the other hand the exact shear effect takes different path of behavior as it will be detailed below.

3.2.1 The effect of shearing force on the critical load:-

When the bulking load occurs, however, there will be shearing force acting on the cross sections of the bar as figure (3-1) shows, the shearing force "V" acting on the element of the length dx, between two cross sections (a-a) and (b-b), has the magnitude of:-

$$V = P\frac{dy}{dx} \quad \text{.....(3-1)}$$

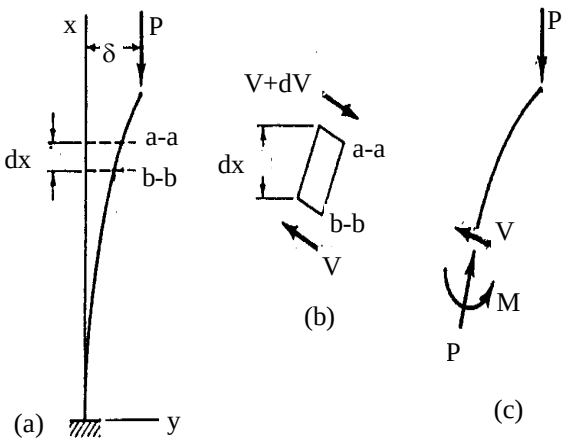

Figure (3-1) Shear force of beam-column element

The change in slope of the deflection curve produced by the shearing force is (nV/AG), where (A) is the total cross sectional area of the column, (G) is the shear modulus, and (n) is the numerical factor depending on the shape of the cross section therefore it's called the shape factor, whose its values are given in table (3-1).

Table 3-1: The Shape Factor Typical Values.

No.	***Type of Section***	***Shape Factor* (n)**
1	Rectangular Cross Section	1.20
2	Circular Cross Section	1.11
3	I-Sections Bent About Minor Axis	$\cong 1.2\ A/A_f$ (1.4-2.8)
4	I-Sections Bent About Major Axis	$\cong A/A_w$ (2-6)
A_f:-Area of The 2- Flanges.-A_w:-Area of The Web.		

So, the rate of change of slope produced by the shearing force "V" represents the additional curvature due to shear and it's equal to[(94)]:-

$$\frac{n}{AG}\frac{dV}{dx} = \frac{nP}{AG}\frac{dy^2}{dx^2} \quad \text{.....(3-2)}$$

Actually there are two approaches developed in formulating the axial load effect when shear effect is included as shown in figure (3-2):

3.1.1 The total shear angle effect (see figure 3-2.b)

3.1.2 The flexural shear angle effect (see figure 3-2.c)

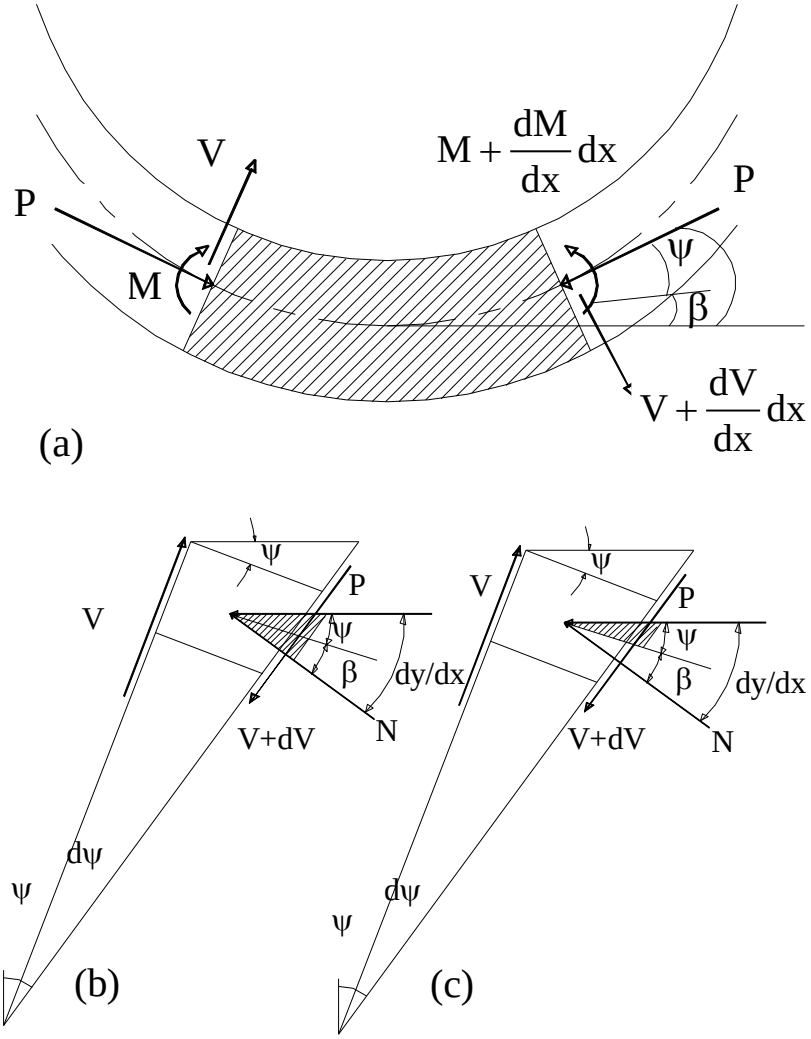

Figure (3-2) (a) Shear contribution of flexural curvature; (b) First approach; (c) Second approach.

In the first approach, the shear component of the axial load is assumed to act perpendicular to the tangent line of the total slope, which consists of the bending and shear slope, while in the second approach, the shear component of the axial load is acting perpendicular to the tangent line of the bending slope only. Though the differential equations for the two approaches are respectively as follows:-

$$\frac{dy}{dx} = \psi + \beta = -\frac{dy_m}{dx} + \frac{nV_x}{AG} \quad \text{.....(3-3)}$$

$$\frac{dy}{dx} = \psi\left(1 + \frac{n}{AG}P\right) + \beta = -\frac{dy_m}{dx}\left(1 + \frac{n}{AG}P\right) + \frac{nV_x}{AG} \quad \text{.....(3-4)}$$

where:-

$\psi = \frac{dy_m}{dx}$ = flexural slope

β= Shear slope

Timoshinko and ***Gere*** [94] named the second approach the modified shear equation.

The critical load of the two approaches is:-

I. For first approach, the modified critical load of a column fixed at one end and free of the other end is

$$P_{cr} = \frac{P_c}{1 + n\,P_c/AG} \quad \text{.....(3-5)}$$

II. For second approach

$$P_{cr} = \frac{\sqrt{1 + 4nP_c/AG} - 1}{2n/AG} \quad \text{.....(3-6)}$$

where:-

$$P_c = \frac{\pi^2 EI}{4L^2} \quad \text{.....(3-6.a)}$$

3.2.2 The equivalent shear parameter technique:-

The ratio of eq.(3-5) and (3-6) is very nearly equal to unity for solid cross sections or a column of (I) section. Hence in these cases the effect of shearing force can usually be neglected, while for built up columns consisting of struts connected by lacing bars or batten plates (i.e. the open web structures), the shear effect may become of practical importance and is considered dominant since the critical load for these types of columns is always less than that for a solid column having the same area (A) and the same slenderness ratio (L/r), this decrease in the critical load is due primarily to the fact that the effect of shear on deflections is much greater for laced column than for a solid bar, the actual value of the critical load depends upon the detailed arrangement and dimensions of the lacing bars[94].

So introducing a shear parameter or shear flexibility factor (u) enables us to replace any section type (whether solid or lattice) by a fictitious equivalent solid section with the same shear parameter (u) values[104]. This technique is called the equivalent shear parameter technique, table (3-2) illustrates the governing equation of the shear parameter (u) assuming hinged ends:-

Table 3-2 The shear parameter (u) governing equations

No.	*Type of Section*	*Shear Parameter* **(u)**	*Equation No.*
1	Solid Cross Section	$nP_e/AG = \frac{2n(1+\nu)\pi^2}{(L/r)^2}$	(3-7)
2	Pratt-Bracing	$\frac{EI\pi^2}{L^2}\left(\frac{1}{A_d\,E.\sin\alpha\cos^2\alpha}+\frac{b}{a.A_h.E}\right)$	(3-8)
3	Howe-Bracing	$\frac{EI\pi^2}{L^2}\left(\frac{1}{A_d.E.\sin\alpha\cos^2\alpha}+\frac{b}{a.A_h.E}\right)$	(3-9)
4	X- Bracing	$\frac{EI\pi^2}{L^2}\left(\frac{1}{A_d.E.\sin\alpha\cos^2\alpha}\right)$	(3-10)
5	Warren-Bracing	$\frac{EI\pi^2}{L^2}\left(\frac{1}{A_d.E.\sin\alpha\cos^2\alpha}\right)$	(3-11)
6	Vierendeel or Batten Lacing	$\frac{EI\pi^2}{L^2}\left(\frac{a.b}{12.E.I_h}+\frac{a^2}{24.E.I_l}+\frac{n.a}{b.A_h.G}\right)$	(3-12)

The typical types of the lattice columns are shown in figure (3-3) and the sub symbols:

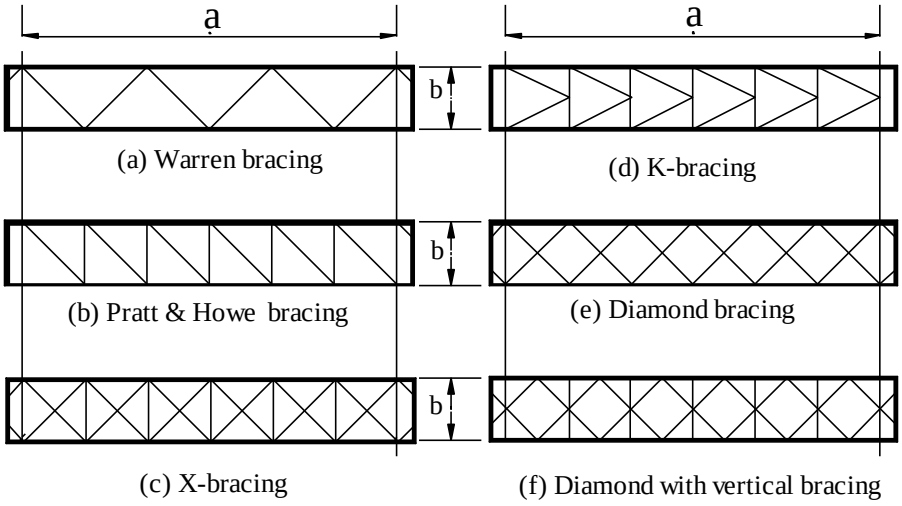

Figure (3-3) Types of lacing

l: longitudinal bars.

h: horizontal or batten bars.

d: diagonal or inclined bars.

while:-

ν: Poisson's ratio

E: modulus of elasticity

L: total length of the member.

a: height of one panel c/c.

b: width of the lattice column c/c.

n: The shape factor (see table 3-1)

P_e: ***Euler*** buckling load for pin-pin column = $EI\frac{\pi^2}{L^2}$

I: The second moment of area about the section centroid.

r: Radius of gyration $\sqrt{I/A}$

α: The angle of the lattice inclination = $\tan^{-1}$ a/b.

Its important here to refer to the great works of ***Renton*** [77], and ***Noor et al*** [68] where the detailed deviations of the buckling load of all types of lacing are introduced and then they concluded that ***Timoshinko*** and ***Gere*** [94] formulas the equations of table (3-2) depend on are sufficient. Also ***Avent et al*** [11], proved by the discrete field mechanics the validity of ***Timoshinko***s equations. These equivalent members have an effective thickness (t_e) calculated by:-

$$t_e = \frac{Lb}{\frac{G_i}{E_i}\sum\frac{l_i}{A_i}^3} = \frac{2L.b.(1+\nu)}{\sum\frac{l_i}{A_i}^3} \quad \text{.....(3-13)}$$

i: any type of web member (either d or h)

The effect of number of lacing panels has also a considerable effect on the (p_{cr}), briefly speaking if number of panels > 6[94] then the assumption that the chords or legs are continuos and only the diagonals are attached by hinges is correct and that the additional rigidity can be calculated from the assumption of continuity of the member so that the equation of the p_{cr} and then the shear parameters derived from it i.e. table 3-2 are always correct.

This equivalent flexible web or shear parameter method was first suggested by ***Niles*** and ***Newell*** (1935) and (1943) [104].

3.2.3 Shear effect on the elastic stability of frames:-

Many researchers applied both approaches in their pre-buckling, post buckling or stability analysis among those are the work of ***Lin*** and ***Glauser*** [56] (who studied the second method), ***Al-Sarraf*** [5] (studied both), ***Cheng*** and ***Pantelides*** [22] (studied both), and ***AlWash*** [6] (studied the

second method). The present work, however shall adopt the stability functions of the shear effect introduced by ***Al-Sarraf*** [5], and these two approaches shall be identified as Method-1 (Meth.-1-) and Method-2- (Meth.-2-), respectively.

The full derivation made by ***Al- Sarraf*** for evaluating the stability functions ($\overline{C}_1$), and ($\overline{C}_2$) for the shear effect are detailed in **App.A.**, what we are concerned with here is the final formulation of the stability functions ($\overline{C}_1$) & ($\overline{C}_2$). They are:-

3.2.3.1 Method -1- at $\rho > 0$ (compressive axial force)

$$\overline{C}_1 = \frac{\overline{\alpha}\left(1-2\left(1-u\rho\right)\overline{\alpha}\cot 2\overline{\alpha}\right)}{\tan\overline{\alpha}-\overline{\alpha}\left(1-u\rho\right)} \quad \text{.....(3-14)}$$

$$\overline{C}_2 = \frac{\left(2\left(1-u\rho\right)\overline{\alpha}-\sin 2\overline{\alpha}\right)\left(\overline{\alpha}\left(1-2\left(1-u\rho\right)\overline{\alpha}\cot 2\overline{\alpha}\right)\right)}{\left(\tan\overline{\alpha}-\overline{\alpha}\left(1-u\rho\right)\right)\left(\sin 2\overline{\alpha}-2\left(1-u\rho\right)\overline{\alpha}\cos 2\overline{\alpha}\right)} \quad \text{.....(3-15)}$$

3.2.3.2 Method -1- at $\rho < 0$ (tensile axial force)

$$\overline{C}_1 = \frac{\left(1-2\left(1+u\rho\right)\overline{\alpha}\coth 2\overline{\alpha}\right)}{\tanh\overline{\alpha}-\overline{\alpha}\left(1+u\rho\right)} \quad \text{.....(3-16)}$$

$$\overline{C}_2 = \frac{\left(2\left(1+u\rho\right)\overline{\alpha}-\sinh 2\overline{\alpha}\right)\left(\overline{\alpha}\left(1-2\left(1+u\rho\right)\overline{\alpha}\coth 2\overline{\alpha}\right)\right)}{\left(\sinh 2\overline{\alpha}-2\left(1+u\rho\right)\overline{\alpha}\cosh 2\overline{\alpha}\right)\left(\tanh\overline{\alpha}-\overline{\alpha}\left(1+u\rho\right)\right)} \quad \text{.....(3-17)}$$

where:-$\left[\overline{\alpha}=\frac{\pi}{2}\left(\overline{\rho}\right)^{1/2},\ \overline{\rho}=\frac{\rho}{1+u\rho},\ \rho=\oplus\right]$

3.2.2.3 Method-1- at ρ=0 (no axial force)

$$\overline{C}_1 \approx 4-\frac{2}{15}\pi^2\rho_1-\frac{11}{6300}\pi^4{\rho_1}^2-\frac{1}{27000}\pi^6{\rho_1}^3 \quad \text{.....(3-18)}$$

$$\overline{C}_2 \approx 2+\frac{1}{30}\pi^2\rho_1+\frac{13}{12600}\pi^4{\rho_1}^2+\frac{11}{378000}\pi^6{\rho_1}^3 \quad \text{.....(3-19)}$$

where:-(ρ_1) can be taken from eq.(3-48-a)

3.2.3.4 Method-2- at $\rho > 0$ (compressive axial force)

$$\overline{C}_1 = \frac{\overline{\alpha}\left[\left(1+u\rho\right)-2\overline{\alpha}\cot 2\overline{\alpha}\right]}{\left(1+u\rho\right)\tan\overline{\alpha}-\overline{\alpha}} \quad \text{.....(3-20)}$$

$$\overline{C}_2 = \frac{\left(2\overline{\alpha} - (1+u\rho)\sin 2\overline{\alpha}\right)\left(\overline{\alpha}(1+u\rho) - 2\overline{\alpha}^2 \cot 2\overline{\alpha}\right)}{\left((1+u\rho)\sin 2\overline{\alpha} - 2\overline{\alpha}\cos 2\overline{\alpha}\right)\left((1+u\rho)\tan\overline{\alpha} - \overline{\alpha}\right)} \quad \text{.....(3-21)}$$

where:-$\left[\overline{\alpha} = \frac{\pi}{2}\left(\overline{\rho}\right)^{1/2}, \overline{\rho} = \rho(1+u\rho)\right]$

3.2.3.5 Method-2- at $\rho < 0$ (tensile axial force)

$$\overline{C}_1 = \frac{\overline{\alpha}\left[(1-u\rho) - 2\overline{\alpha}\coth 2\overline{\alpha}\right]}{(1-u\rho)\tanh\overline{\alpha} - \overline{\alpha}} \quad \text{.....(3-22)}$$

$$\overline{C}_2 = \frac{\left(2\overline{\alpha} - (1-u\rho)\sinh 2\overline{\alpha}\right)\left(\overline{\alpha}(1-u\rho) - 2\overline{\alpha}^2 \coth 2\overline{\alpha}\right)}{\left((1-u\rho)\sinh 2\overline{\alpha} - 2\overline{\alpha}\cosh 2\overline{\alpha}\right)\left((1-u\rho)\tanh\overline{\alpha} - \overline{\alpha}\right)} \quad \text{.....(3-23)}$$

where:-$\left[\overline{\alpha} = \frac{\pi}{2}\left(\overline{\rho}\right)^{1/2}, \overline{\rho} = \rho(1-u\rho), \rho = \oplus\right]$

3.2.3.6 Method-2- at ρ=0 (no axial force)

$$\overline{C}_1 \approx 4 - \frac{2}{15}\pi^2\rho_2 - \frac{11}{6300}\pi^4{\rho_2}^2 - \frac{1}{27000}\pi^6{\rho_2}^3 \quad \text{.....(3-24)}$$

$$\overline{C}_2 \approx 2 + \frac{1}{30}\pi^2\rho_2 + \frac{13}{12600}\pi^4{\rho_2}^2 + \frac{11}{378000}\pi^6{\rho_2}^3 \quad \text{.....(3-25)}$$

where ρ_2 can be taken from eq.(3-48.b)

The graphs of these functions for u=0.1, 1.0, 5.0 and 10.0 are shown in figures (3-4, 3-5, 3-6 and 3-7), respectively.

The reason of chosing ***Al-Sarraf*** approach is summarized in table (3-3) which gives a comparison of the (P_{cr}-u) relation between different authors, which leads to the fact that ***Al-Sarraf***'s both approaches are very suitable.

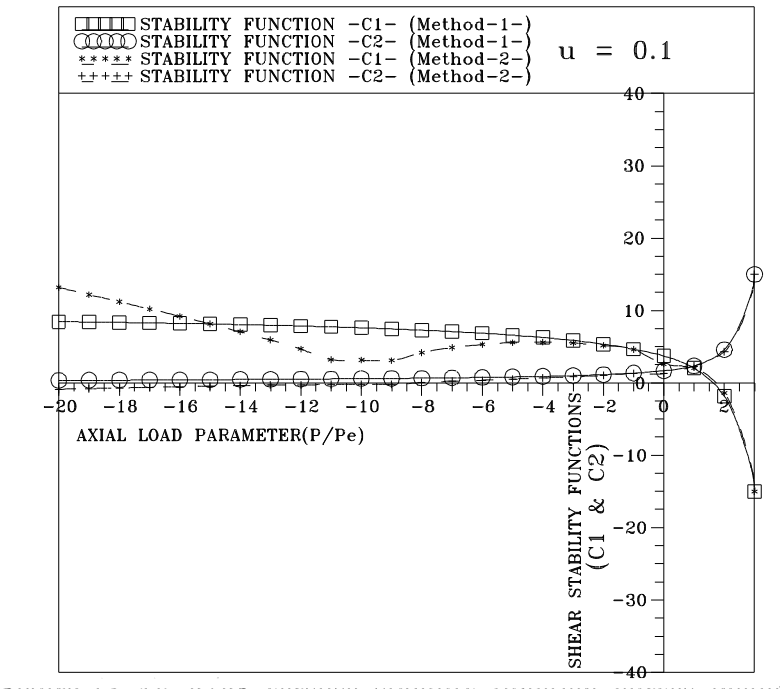
STABILITY FUNCTION -C1- (Method-1-)
STABILITY FUNCTION -C2- (Method-1-)
STABILITY FUNCTION -C1- (Method-2-)
STABILITY FUNCTION -C2- (Method-2-)
u = 0.1
AXIAL LOAD PARAMETER(P/Pe)
SHEAR STABILITY FUNCTIONS (C1 & C2)

Figure (3-4) **P/P_e versus stability function curves including shear effect by both methods (u=0.1)**

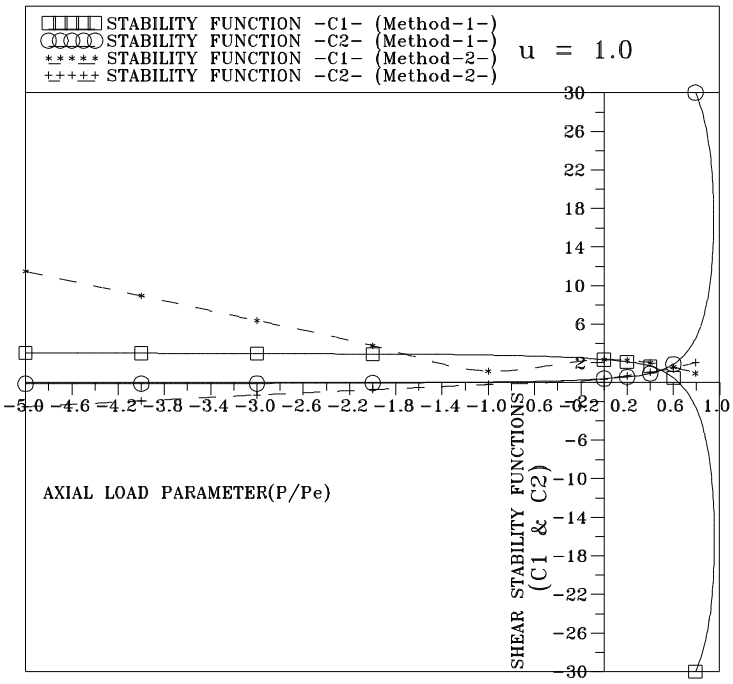
STABILITY FUNCTION -C1- (Method-1-)
STABILITY FUNCTION -C2- (Method-1-)
STABILITY FUNCTION -C1- (Method-2-)
STABILITY FUNCTION -C2- (Method-2-)
u = 1.0
AXIAL LOAD PARAMETER(P/Pe)
SHEAR STABILITY FUNCTIONS (C1 & C2)

Figure (3-5) **P/P_e versus stability function curves including shear effect by both methods (u=1.0)**

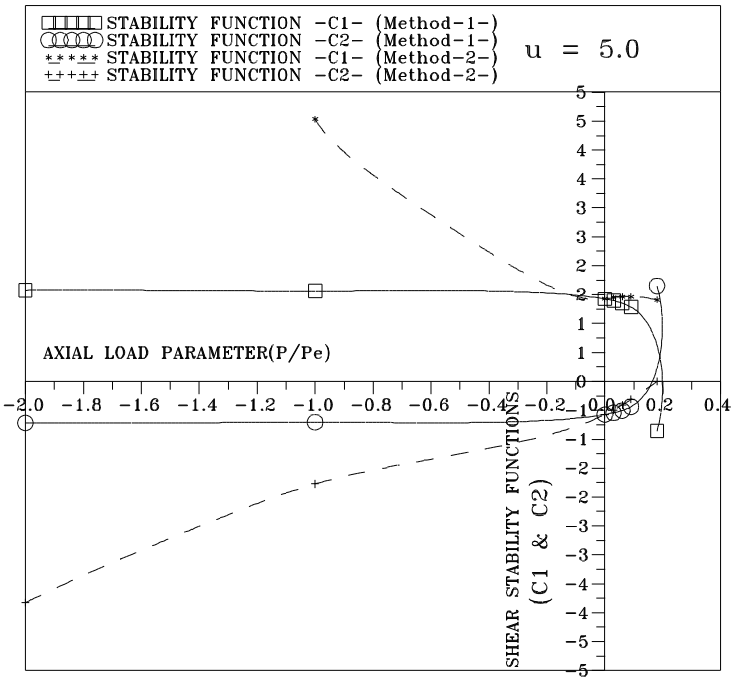
STABILITY FUNCTION -C1- (Method-1-)
STABILITY FUNCTION -C2- (Method-1-)
STABILITY FUNCTION -C1- (Method-2-)
STABILITY FUNCTION -C2- (Method-2-)
u = 5.0
AXIAL LOAD PARAMETER(P/Pe)
SHEAR STABILITY FUNCTIONS (C1 & C2)

Figure (3-6) **P/P_e versus stability function curves including shear effect by both methods (u=5.0)**

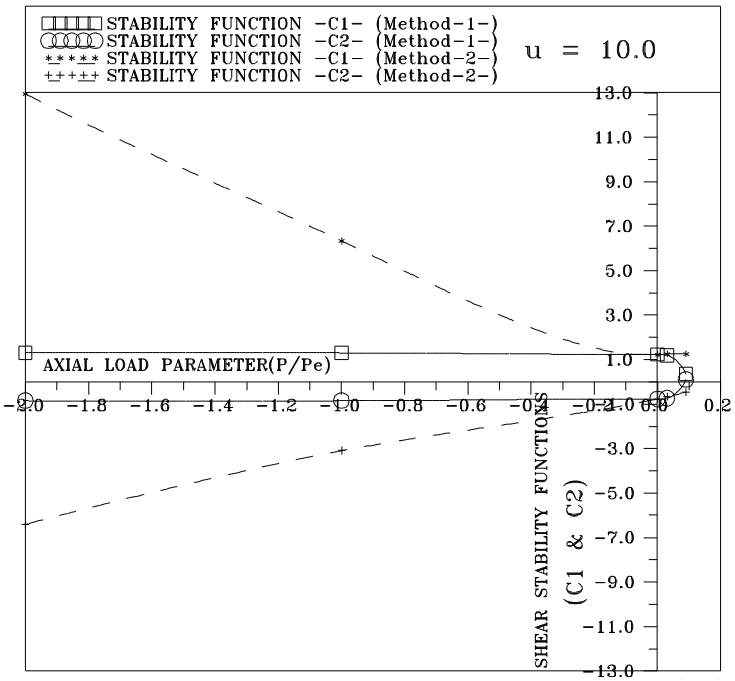
STABILITY FUNCTION -C1- (Method-1-)
STABILITY FUNCTION -C2- (Method-1-)
STABILITY FUNCTION -C1- (Method-2-)
STABILITY FUNCTION -C2- (Method-2-)
u = 10.0
AXIAL LOAD PARAMETER(P/Pe)
SHEAR STABILITY FUNCTIONS (C1 & C2)

Figure (3-7) **P/P_e versus stability function curves including shear effect by both methods (u=10.0)**

Table 3-3: Various methods for comparison of shear parameter (u) versus load parameter (P/P_e).

		Method -1- (dy/dx)			*Method-2- (dym/dx)*				
Cyc No.	***Shear Prmt. (u)***	***Temo. &Gere (1961)***	***Al-Sarraf (1986)***	***Cheng (1988)***	***Temo. &Gere (1961)***	***Al-Sarraf (unpblsh)***	***Cheng (1988)***	***Lin (1970)***	***Alwash (1995)***
1	0.00	1.0010	1.0010	1.0010	1.0010	1.0010	1.0010	1.0010	1.0010
2	0.10	0.9091	0.9091	0.9093	0.9114	0.9113	0.9117	0.9112	0.9112
3	0.20	0.8334	0.8341	0.8347	0.8556	0.8555	0.8559	0.8555	0.8555
4	0.30	0.7692	0.7699	0.7708	0.8063	0.8062	0.8069	0.8062	0.8062
5	0.40	0.7143	0.7146	0.7152	0.7671	0.7669	0.7677	0.7669	0.7669
6	0.50	0.6667	0.6713	0.6718	0.7336	0.7335	0.7339	0.7335	0.7335
7	0.60	0.6250	0.6280	0.6289	0.7062	0.7059	0.7070	0.7057	0.7057
8	0.70	0.5882	0.5881	0.5888	0.6791	0.6791	0.6800	0.6790	0.6790
9	0.80	0.5556	0.5557	0.5599	0.6560	0.6560	0.6576	0.6558	0.6558
10	0.90	0.5263	0.5261	0.5427	0.6361	0.6360	0.6368	0.6359	0.6359
11	1.00	0.5000	0.5000	0.5190	0.6193	0.6190	0.6199	0.6189	0.6189

3.2.4 The shear effect on the flexural bowing:-

As indicated in chapter one the flexural bowing effect is defined by:-

$$\delta_b = \frac{1}{2}\int_0^{L_c}\left(\frac{dy}{dx}\right)^2 dx \quad \text{.....(3-26)}$$

The bowing functions for the non-shear prismatic sections established by ***Saafan***[81] are detailed in **App.B.**.

Since the physical meaning of the bowing phenomenon is shortening in the member due to the combination of axial load and the bending moments, the shearing force has a significant role in this operation especially in the open web structures as mentioned earlier. Thus the modified bowing formula ($\overline{C}_b$) and the modified bowing functions ($\overline{b}_1$) and ($\overline{b}_2$) including the shear effect represented by the shear parameter or the shear flexibility indicator (u) must be introduced for both methods (Method-1- and Method-2-).

The original derivations of the bowing functions including the effect of shear is detailed below for both methods.

3.2.4.1 Modified Bowing formula and functions using Method-1-

Using the original definition of the bowing effect eq.(3-25) and setting up the elastic curve slope including the shear effect -dy/dx- (see **App.A.**) we can put the eq.(3-25) into a new form, keeping in mined that (M_1 and M_2) are the member end moments, (ω) is equal to $\left(\frac{\pi}{L}\sqrt{\bar{\rho}}\right)$, and (P) is the axial force.

$$\bar{C}_b = \frac{1}{2}\int_o^{L_c}\left(\frac{\overline{dy}}{dx}\right)^2 dx \quad \text{.....(3-27)}$$

where:-

($\overline{dy}/dx$) is the slope of the elastic curve including the shear effect (for method-1-)

$$\bar{y}\big)_1 = -\left(\frac{M_1}{P}\cot\omega L + \frac{M_2}{P}\csc\omega L\right)\sin\omega x + \frac{M_1}{P}\cos\omega x + \frac{M_1}{P}\left(\frac{x}{L}-1\right) + \frac{M_2}{P}\left(\frac{x}{L}\right) \quad \text{.....(3-28)}$$

$$\therefore \left(\frac{\overline{dy}}{dx}\right)_1 = \left(-\frac{M_1}{P}\cot\omega L - \frac{M_2}{P}\csc\omega L\right)\omega\cos\omega x - \frac{M_1}{P}\omega\sin\omega x + \frac{M_1}{PL} + \frac{M_2}{PL} \quad \text{.....(3-29.a)}$$

by squaring eq.(3-29.a):

$$\left(\frac{\overline{dy}}{dx}\right)^2 = \frac{\omega^2}{P^2}\Bigg[M_1^2\cot^2\omega L\cos^2\omega x + 2M_1M_2\frac{\cos\omega L}{\sin^2\omega L}\cos^2\omega x + M_2^2\frac{\cos^2\omega x}{\sin^2\omega L} +$$

$$2M_1^2\cot\omega L\cos\omega x\sin\omega x + 2M_1M_2\frac{\sin\omega x\cos\omega x}{\sin\omega L} + M_1^2\sin^2\omega x\Bigg] -$$

$$\frac{2\omega}{P^2L}\Bigg[M_1^2\cot\omega L\cos\omega x + M_1M_2\frac{\cos\omega x}{\sin\omega L} + M_1M_2\cot\omega L\cos\omega x + M_2^2\frac{\cos\omega x}{\sin\omega L} +$$

$$M_1^2\sin\omega x + M_1M_2\sin\omega x\Bigg] + \frac{1}{P^2L^2}\left[M_1^2 + 2M_1M_2 + M_2^2\right] \quad \text{.....(3-29.b)}$$

Substituting eq.(3-29.b) into eq.(3-27) and after a very long and crude operations and simplifications the new modified shear-bowing formula can be introduced:-

$$\bar{C}_{b_1} = \frac{\omega^2 L}{4P^2}\csc^2\omega L\left(M_1^2 + 2M_1M_2\cos\omega L + M_2^2\right) +$$

$$\frac{\omega}{4P^2}\cot\omega L\left(M_1^2+2M_1M_2\cos\omega L+M_2^2\right)-\frac{\left(M_1+M_2\right)^2}{2P^2L} \quad \text{.....(3-30)}$$

where $\omega=\frac{\pi}{2}\sqrt{\bar{\rho}_1}=\frac{2\bar{\alpha}}{L}, \bar{\alpha}=\frac{\pi}{2}\sqrt{\bar{\rho}_1}$ (for Meth.-1-)

since $M_1=K\bar{C}_1\theta_1+K\bar{C}_2\theta_2$

and $M_2=K\bar{C}_2\theta_1+K\bar{C}_1\theta_2$ .....(3-31)

where (K) is the stiffness of the member $=\frac{EI}{L}$

$\bar{C}_1 \& \bar{C}_2 =$ The stability functions including shear effect

$\theta_1 \& \theta_2 =$ end rotations due to shear flexural slope.

Equation (3-30) can be put into a form that introduces new modified shear bowing functions $\bar{b}_1 \& \bar{b}_2$

$$\bar{C}_{b_1}=\bar{b}_1\left(\theta_1+\theta_2\right)^2+\bar{b}_2\left(\theta_1-\theta_2\right)^2 \quad \text{.....(3-32)}$$

In order to find the values of the new bowing functions($\bar{b}_1$)and ($\bar{b}_2$) there must be a boundary conditions so that:-

- To find ($\bar{b}_1$) then M_1=M_2=M and θ_1= θ_2= θ
- To find ($\bar{b}_2$) then M_1=-M_2=M and θ_1=- θ_2=θ

Then from eq.(3-32) and for ($\bar{b}_1$) case:-

$M=K\bar{C}_1\theta+K\bar{C}_2\theta$ .....(3-33)

$$\therefore \bar{C}_{b_1}=4\bar{b}_1\theta^2=4\theta^2\left[\frac{\left(\bar{C}_1+\bar{C}_2\right)^2}{16\bar{\alpha}_1{}^2\sin^2 2\bar{\alpha}_1}\left(1+\frac{\sin 2\bar{\alpha}_1\cos 2\bar{\alpha}_1}{2\bar{\alpha}_1}-\frac{\left(\bar{C}_1+\bar{C}_2\right)^2}{32\bar{\alpha}_1{}^4}+\right.\right.$$

$$\left.\left.\frac{\left(\left(\bar{C}_1+\bar{C}_2\right)^2\left(\cos 2\bar{\alpha}_1-1\right)\left(2\bar{\alpha}_1-\sin 2\bar{\alpha}_1\right)\right)}{64\bar{\alpha}_1{}^3\sin^2 2\bar{\alpha}_1}\right)\right] \quad \text{.....(3-34)}$$

so, ($\bar{b}_1$) for Meth-1- can be put in a general form of:-

$$\bar{b}_1 = \frac{\left(\bar{C}_1 + \bar{C}_2\right)^2}{4\pi^4\rho^2}\left[\frac{2\bar{\alpha}_1}{\sin^2 2\bar{\alpha}_1}\left(2\bar{\alpha}_1 + \sin 2\bar{\alpha}_1 \cos 2\bar{\alpha}_1\right) - 2 + \frac{\left(\bar{\alpha}_1 \cos 2\bar{\alpha}_1 - \bar{\alpha}_1\right)\left(2\bar{\alpha}_1 - \sin 2\bar{\alpha}_1\right)}{\sin^2 2\bar{\alpha}_1}\right] \quad \text{.....(3-35)}$$

where:

- $\bar{\alpha}_1 = \frac{\pi}{2}\sqrt{\bar{\rho}_1} = \frac{\pi}{2}\left(\frac{\rho}{1-u\rho}\right)^{1/2}$ $\qquad u\rho \neq 1$
- $\rho = \frac{P}{P_e} = \frac{PL^2}{EI\pi^2}$ (positive value)
- u: is the shear parameter.

again from eq.(3.32) and for the ($\bar{b}_2$)case:-

$$M = K\bar{C}_1\theta - K\bar{C}_2\theta$$

$$\therefore \bar{C}_{b_2} = 4\bar{b}_2\theta^2 = 4\theta^2\left[-\frac{\left(\bar{C}_1 + \bar{C}_2\right)^2(\cos 2\bar{\alpha} - 1)\left(2\bar{\alpha} - \sin^2\bar{\alpha}\right)}{64\bar{\alpha}^3 \sin 2\bar{\alpha}^2}\right] \quad \text{.....(3-36)}$$

Then ($\bar{b}_2$) for Meth.-1- can be put into a general form of:-

$$\bar{b}_2 = \frac{\left(\bar{C}_1 + \bar{C}_2\right)^2}{8\pi^4\rho^2}\left[\frac{\left(2\bar{\alpha}_1 - 2\bar{\alpha}_1 \cos 2\bar{\alpha}_1\right)\left(2\bar{\alpha}_1 - \sin 2\bar{\alpha}_1\right)}{\sin^2 2\bar{\alpha}_1}\right] \quad \text{.....(3-37)}$$

again $\bar{\alpha}_1 = \frac{\pi}{2}\sqrt{\bar{\rho}_1} = \frac{\pi}{2}\left(\frac{\rho}{1-u\rho}\right)^{1/2}$, $u\rho \neq 1$

$\rho = \frac{P}{P_e} = \frac{PL^2}{EI\pi^2}$ (positive value) and "u" is the shear parameter

In the tensile axial force and using the same procedure, the modified bowing function, for Meth.-1- is:-

$$\bar{b}_1 = \frac{\left(\bar{C}_1 + \bar{C}_2\right)^2}{4\pi^4 \rho^2}\left[\frac{2\bar{\alpha}_1\left(2\bar{\alpha}_1 + \sinh 2\bar{\alpha}_1 \cosh 2\bar{\alpha}_1\right)}{\sinh^2 2\bar{\alpha}_1}\right] - 2 +$$

$$\frac{\left(\bar{\alpha}_1 \cosh 2\bar{\alpha}_1 - \bar{\alpha}_1\right)\left(2\bar{\alpha}_1 - \sinh 2\bar{\alpha}_1\right)}{\sinh^2 2\bar{\alpha}_1} \quad \text{.....(3-38)}$$

$$\bar{b}_2 = \frac{\bar{C}_1 + \bar{C}_2}{8\pi^4 \rho^2}\left[\frac{\left(2\bar{\alpha}_1 - 2\bar{\alpha}_1 \cosh 2\bar{\alpha}_1\right)\left(2\bar{\alpha}_1 - \sinh 2\bar{\alpha}_1\right)}{\sinh^2 2\bar{\alpha}_1}\right] \quad \text{.....(3-39)}$$

where: $\bar{\alpha}_1 = \frac{\pi}{2}\sqrt{\bar{\rho}_1} = \frac{\pi}{2}\left(\frac{\rho}{1+u\rho}\right)^{1/2}$

$\rho = \frac{P}{P_e} = \frac{PL^2}{EI\pi^2}\rho$ (positive value)

u: shear parameter

3.2.4.2 Modified bowing formula and functions using Meth.-2-.

The deflection equation of Meth.-2- is

$$\bar{y}_2 = \frac{M_1}{P}\cos\omega x - \frac{M_1}{P}\cot\omega L \sin\omega x - \frac{M_2}{P}\frac{\sin\omega x}{\sin\omega L} + \frac{M_1 + M_2}{PL}x - \frac{M_1}{P} \quad \text{.....(3-40)}$$

$$\therefore \left(\frac{\overline{dy}}{dx}\right)_2 = -\frac{M_1}{P}\omega\sin\omega x - \frac{M_1\omega}{P}\cot\omega L\cos\omega x - \frac{M_2}{P}\omega\csc\omega L\cos\omega x + \frac{M_1 + M_2}{PL} \quad \text{.....(3.41)}$$

By a long way of squaring, Integrating and simplifying of eq.(3-27) we have the final form of the modified shear-bowing formula of Meth.-2-

$$\bar{C}_{b_2} = \frac{\omega^2 L}{4P^2}\csc^2\omega L\left(M_1^2 + 2M_1 + M_2\cos\omega L + M_2^2\right) +$$

$$\frac{\omega}{4P^2}\cot\omega L\left(M_1^2 + 2M_1M_2\cos\omega L + M_2^2\right) - \frac{\left(M_1 + M_2\right)^2}{2P^2 L} \quad \text{.....(3-42)}$$

where: $\omega = \frac{\pi}{L}\sqrt{\bar{\rho}_2} = \frac{2\bar{\alpha}_2}{L} = \frac{\pi}{2}\sqrt{\bar{\rho}_2}$ (for Meth.-2-)

And by the same procedure used in Meth.-1-, we can introduce the modified shear bowing functions for Meth.-2-:-

For compressive axial force($\rho > 0$)

$$\bar{b}_1 = \frac{\left(\bar{C}_1 + \bar{C}_2\right)^2}{4\pi^4\rho^2}\left[\frac{2\bar{\alpha}_2\left(2\bar{\alpha}_2 + \sin 2\bar{\alpha}_2 \cos 2\bar{\alpha}_2\right)}{\sin^2 2\bar{\alpha}_2} - 2 + \frac{\left(\bar{\alpha}_2 \cos 2\bar{\alpha}_2 - \bar{\alpha}_2\right)\left(2\bar{\alpha}_2 - \sin \bar{\alpha}_2\right)}{\sin^2 2\bar{\alpha}_2}\right] \quad \text{.....(3-43)}$$

$$\bar{b}_2 = \frac{\left(\bar{C}_1 + \bar{C}_2\right)^2}{8\pi^4\rho^2}\left[\frac{\left(2\bar{\alpha}_2 - 2\bar{\alpha}_2 \cos 2\bar{\alpha}_2\right)\left(2\bar{\alpha}_2 - \sin 2\bar{\alpha}_2\right)}{\sin^2 2\bar{\alpha}_2}\right] \quad \text{.....(3-44)}$$

where: $\bar{\alpha}_2 = \frac{\pi}{2}\sqrt{\bar{\rho}_2} = \frac{\pi}{2}\left(\rho(1+u\rho)\right)^{1/2}$

$$\rho = \frac{P}{P_e} = \frac{PL^2}{\pi^2 EI} \text{ (positive value)}$$

For tensile axial force ($\rho<0$)

$$\bar{b}_1 = \frac{\left(\bar{C}_1 + \bar{C}_2\right)^2}{4\pi^4\rho^2}\left[\frac{2\bar{\alpha}_2\left(2\bar{\alpha}_2 + \sinh 2\bar{\alpha}_2 \cosh 2\bar{\alpha}_2\right)}{\sinh^2 2\bar{\alpha}_2} - 2 + \frac{\left(\bar{\alpha}_2 \cosh 2\bar{\alpha}_2 - \bar{\alpha}_2\right)\left(2\bar{\alpha}_2 - \sinh 2\bar{\alpha}_2\right)}{\sinh^2 2\bar{\alpha}_2}\right] \quad \text{.....(3-45)}$$

and

$$\bar{b}_2 = \frac{\left(\bar{C} + \bar{C}_2\right)}{8\pi^4\rho^2}\left[\frac{\left(2\bar{\alpha}_2 - 2\bar{\alpha}_2 \cosh 2\bar{\alpha}_2\right)\left(2\bar{\alpha}_2 - \sinh 2\bar{\alpha}\right)}{\sinh^2 2\bar{\alpha}_2}\right] \quad \text{.....(3-46)}$$

where: $\bar{\alpha}_2 = \frac{\pi}{2}\sqrt{\bar{\rho}_2} = \frac{\pi}{2}\left(\rho(1-u\rho)\right)^{1/2}$

$$\rho = \frac{P}{P_e} = \frac{PL^2}{\pi^2 EI} \text{ (positive value)}$$

The bowing functions ($\bar{b}_1$) and ($\bar{b}_2$) for both methods are shown in figures (3-8, 3-9, 3-10 and 3-11), respectively.

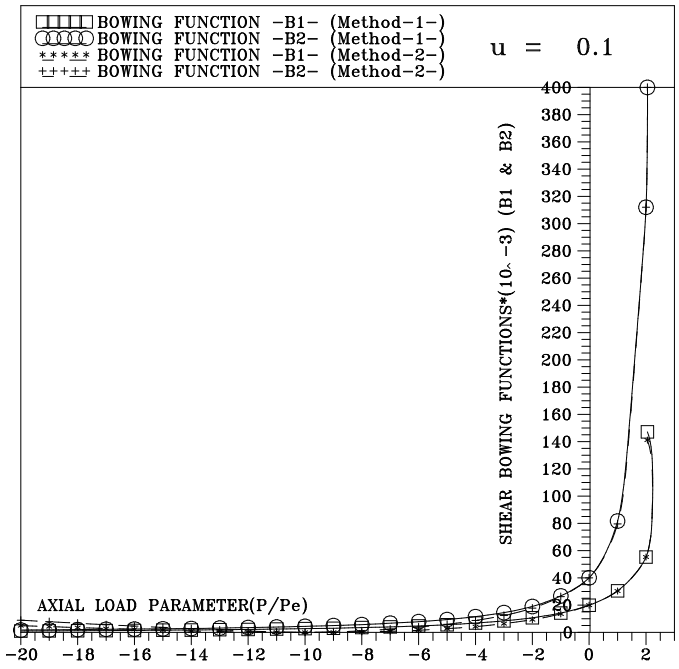
BOWING FUNCTION -B1- (Method-1-)
BOWING FUNCTION -B2- (Method-1-)
BOWING FUNCTION -B1- (Method-2-)
BOWING FUNCTION -B2- (Method-2-)
u = 0.1
SHEAR BOWING FUNCTIONS*(10^-3) (B1 & B2)
AXIAL LOAD PARAMETER(P/Pe)

Figure (3-8) **P/P_e versus bowing function curves including shear effect by both methods (u=0.1)**

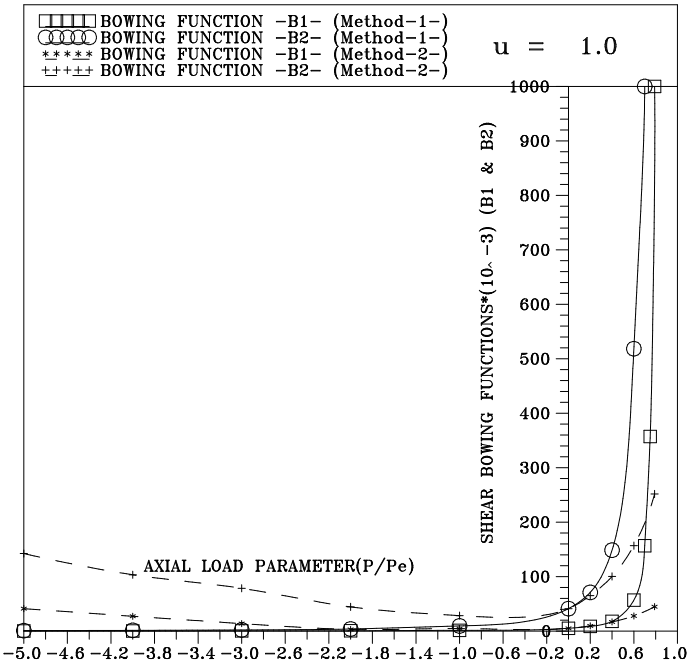
BOWING FUNCTION -B1- (Method-1-)
BOWING FUNCTION -B2- (Method-1-)
BOWING FUNCTION -B1- (Method-2-)
BOWING FUNCTION -B2- (Method-2-)
u = 1.0
SHEAR BOWING FUNCTIONS*(10^-3) (B1 & B2)
AXIAL LOAD PARAMETER(P/Pe)

Figure (3-9) **P/P_e versus bowing function curves including shear effect by both methods (u=1.0)**

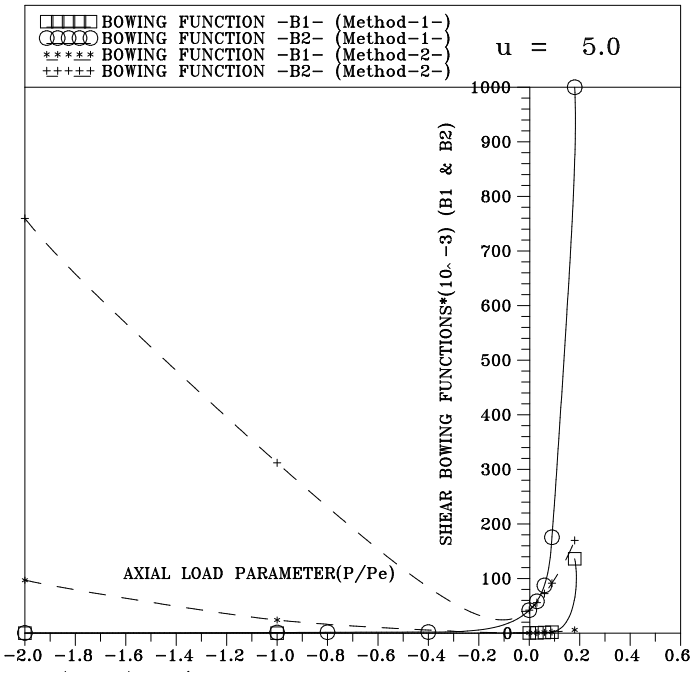
BOWING FUNCTION -B1- (Method-1-)
BOWING FUNCTION -B2- (Method-1-)
BOWING FUNCTION -B1- (Method-2-)
BOWING FUNCTION -B2- (Method-2-)
u = 5.0
SHEAR BOWING FUNCTIONS*(10.-3) (B1 & B2)
AXIAL LOAD PARAMETER(P/Pe)

Figure (3-10) **P/P_e versus bowing function curves including shear effect by both methods (u=5.0)**

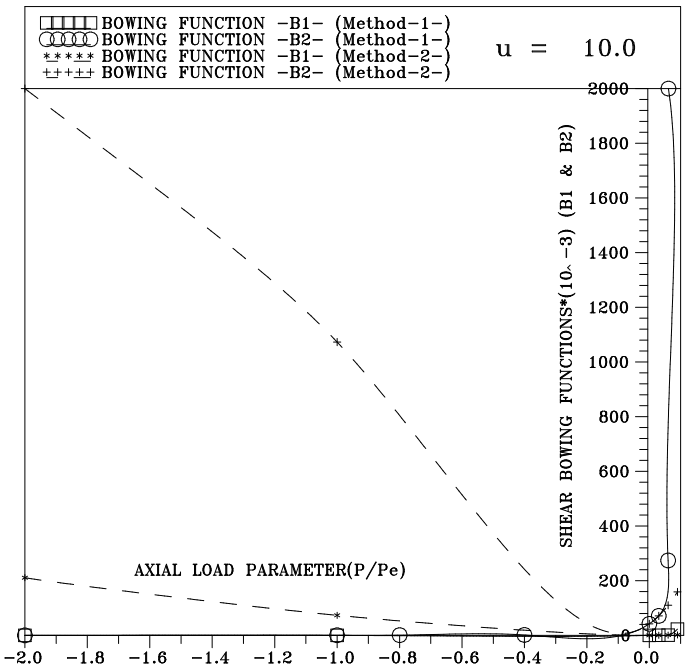
BOWING FUNCTION -B1- (Method-1-)
BOWING FUNCTION -B2- (Method-1-)
BOWING FUNCTION -B1- (Method-2-)
BOWING FUNCTION -B2- (Method-2-)
u = 10.0
SHEAR BOWING FUNCTIONS*(10.-3) (B1 & B2)
AXIAL LOAD PARAMETER(P/Pe)

Figure (3-11) **P/P_e versus bowing function curves including shear effect by both methods (u=10.0)**

3.2.4.3 Checking and testing the new modified bowing functions

In order to check the validity, accuracy and convergence of the bowing function derived, in this work we must do the following points:

- Check the new functions with the previously derived (b_1) and (b_2) functions of no shear effect (i.e. u=0) for both methods.
- Check convergence at ($\bar{\rho}$ =0) and ($\bar{\rho}$ >4)
- Check convergence with each other.
- Check the validity of the no shear stability bowing functions relations derived by ***Saafan***[81].
- Check the accuracy using the finite difference method.(F.D.M.)

For this purpose a special program ***CHECK*** is made.

3.2.4.3.1 Checking the new function with **Saafan**:-

By observing the formula derived by ***Saafan*** (see **App.B.**) for the bowing formula and comparing it with eq.(3-30) for Meth.-1- and eq.(3-42) for Meth.-2- we can easily find that they have the same equation, the only difference is that of the value of ($\bar{\alpha}$) which in ***Safaan***'s formula has the value of:

$$\bar{\alpha}_{\text{Saffan}} = \frac{\pi}{2}\sqrt{\rho}$$

while

$$\bar{\alpha}_1 = \frac{\pi}{2}\sqrt{\bar{\rho}_1} \qquad \text{.....(3-47)}$$

$$\bar{\alpha}_2 = \frac{\pi}{2}\sqrt{\bar{\rho}_2}$$

and ($\bar{\rho}_1$) and ($\bar{\rho}_2$) are the modified axial force parameters including shear deformation represented by the shear parameter (u) so that when u=0 the new bowing formula is translated automatically to ***Safaan***'s formula and also ($\bar{b}_1$) and ($\bar{b}_2$) in both methods return to their corresponding values of ***Safaan***'s no shear bowing functions. (b_1 and b_2).

3.2.4.3.2 Check the convergence of the functions at $\bar{\rho} = 0$ and $\bar{\rho} > 4$

The values of ($\bar{b}_1$) and ($\bar{b}_2$) in both methods are convergence near ($\bar{\rho} = 0$) even when ($\bar{\rho} = 0.001$) the function shows a great deal of continuity as it is obvious from the figures (3-8 to 3-11) obtained by ***CHECK***.

When ($\bar{\rho}$) is reaches the value of (4), ($\bar{b}_2$) goes to (∞) while ($\bar{b}_1$) increases rapidly so that ($\bar{\rho}$) must not be more than (4). When ($\bar{\rho}$) reaches zero, the stability and bowing functions of shear effect can be found from the same series presented by ***Kassimali*** [47], (see **App.B.**) but by substituting the values (ρ_1) and (ρ_2) for Meth.-1- and -2- respectively instead of (ρ) we get:-

$$\rho_1 = 0.0016/(1+u\times 0.0016) \quad \text{.....(3-48.a)}$$

$$\rho_2 = \left[-1+(1+0.064\times u)^{1/2}\right]/24 \quad \text{.....(3-48.b)}$$

The above behavior is exactly the same as the no shear behavior (i.e. at u=0) which indicates the fact of functions is valid.

Only one point must be settled since:-

$\rho = \bar{\rho}/(1+u\bar{\rho})$ for Meth.-1-

$\rho = \bar{\rho}(1-u\bar{\rho})$ for Meth.-2-

and $\bar{\rho} \le 4$ then:-

$$\rho \le \frac{4}{(1+4u)} \text{ for Meth.}-1-$$
$$\rho \le \frac{-1+\sqrt{1+16u}}{2u} \text{ for Meth.}-2- \quad \text{.....(3-48.c)}$$

Then it is considered as no axial force indicator (i.e. ρ=0), then we shall use the series mathematical approach.

3.2.4.3.3 Check the convergence of the functions with each other.

When (u=0) both methods show complete convergence with the no shear bowing function of ***Saafan***.

When (u) rises till we have (u≈1.0) there is a good agreement between both methods as figures (3-8) and (3-9) indicate for (u=0.1) and (u= 1).0 respectively.

When (u) continues to rise there is a divergence between methods functions as it is obvious from figures (3-10 and 3-11) for (u= 5.0) and (u=10.0) respectively.

These observations lead to the fact that when we have a very open-web structure (especially when batten elements have high (u) values are used) there will be misleading results of the methods either Meth.-1- or Meth.-2-. The question can be answered by the case studies testing (see **chapter-6-**).

3.2.4.3.4 Check the validity of relations of the no shear stability bowing functions derived by **Saafan**:-

Kassimali [47] stated that the no shear bowing functions are related to the no shear stability functions by equation:-

$$b_1 = \frac{(C_1 + C_2)(C_2 - 2)}{8\pi^2 \rho} = \frac{(C_1' + C_2')}{4\pi^2} \quad \text{.....(3-49.a)}$$

$$b_2 = \frac{C_2}{8(C_1 + C_2)} = \frac{C_1' - C_2'}{4\pi^2} \quad \text{.....(3-49.b)}$$

which means that the no shear bowing functions (b_1 & b_2) can be calculated from the stability function (C_1 & C_2) and also from their derivatives (C_1' & C_2').

CHECK proved that the new modified shear bowing functions ($\bar{b}_1 \& \bar{b}_2$) cannot be found from the shear stability functions ($\bar{C}_1 \& \bar{C}_2$), however, it can be calculated from their derivatives ($\bar{C}_1'$ & $\bar{C}_2'$) or:-

$$\bar{b}_1 = \frac{\bar{C}_1' + \bar{C}_2'}{4\pi^2} \quad \text{.....(3-50.a)}$$

$$\bar{b}_2 = \frac{\bar{C}_1' + \bar{C}_2'}{4\pi^2} \quad \text{.....(3-50.b)}$$

3.2.4.3.5 Check the accuracy by using the finite difference method (F.D.M.).

It is common knowledge to say that the F.D.M. is a very efficient method to check the new functions with.

It's known that any value (a) in a function f(a) can be found from the widely known central F.D.M. by:-

$$f(a) = \frac{f'_{(a+0.001)} - f'_{(a-0.001)}}{0.002} \quad \text{.....(3-51.a)}$$

so, the bowing function can be checked using this technique, let:-

$\overline{bb}_i$ = the bowing functions obtained from the F.D.M..

i= the function indicator either (1) or (2).

j= the method indicator either (1) or (2)

so:-

$$\overline{bb}_1(\rho) = \frac{\bar{b}'_{1(\rho+0.001)} - b'_{1(\rho-0.001)}}{0.002} \quad \text{.....(3-51.b)}$$

$$\overline{bb}_2(\rho) = \frac{\bar{b}'_{2(\rho+0.001)} - b'_{2(\rho-0.001)}}{0.002} \quad \text{.....(3-51.c)}$$

for both methods.

$\bar{b}_i'$: is the new bowing function derivative

for method-1-:-

$$\begin{aligned}\bar{b}_1' &= A_1B_1 + C_1 \\ \bar{b}_2' &= D_1 + E_1F_1\end{aligned} \quad \text{.....(3-52)}$$

For method -2-

$$\begin{aligned}\bar{b}_1{}' &= A_2B_2 + C_2 \\ \bar{b}_2{}' &= D_2 + E_2F_2\end{aligned} \quad \text{.....(3-53)}$$

where:-

$$A_{ji} = \frac{\left(\bar{C}_{j1} + \bar{C}_{j2}\right)}{4\pi^4\rho^2} \quad \text{.....(3-54.a)}$$

$$D_{ji} = \frac{2\bar{b}_{j2}}{\left(\bar{C}_{j1} - \bar{C}_{j2}\right)}\left(\bar{C}_{j1}' - \bar{C}_{j2}'\right) - \frac{2\bar{b}_{j2}}{\rho} \quad \text{.....(3-54.b)}$$

$$C_{ji} = 2\left(\bar{C}_{j1}' + \bar{C}_{j2}'\right)\frac{\bar{b}_1}{\left(\bar{C}_{j1} + \bar{C}_{j2}\right)} - \frac{2\bar{b}_{j1}}{\rho} \quad \text{.....(3-54.c)}$$

$$E_{ji} = \frac{\left(\bar{C}_{j1} - \bar{C}_{j2}\right)}{8\pi^4\rho^2} \quad \text{.....(3-54.d)}$$

$$B_{ji} = \csc^2 2\bar{\alpha}_1 \times \pi\rho^{-1/2}R_{ji}^{-3/2}\Big[4\bar{\alpha}_{ji} + 2\bar{\alpha}_{ji}\left(\cos^2 2\bar{\alpha}_{ij} - \sin^2 2\bar{\alpha}_{ji}\right) -$$

$$7\sin 2\bar{\alpha}_{ji}\cos 2\bar{\alpha}_{ji} + 6\bar{\alpha}_{ji}\cos 2\bar{\alpha}_{ji} + \sin 2\bar{\alpha}_{ji}4\bar{\alpha}_{ji}\sin 2\bar{\alpha}_{ji}\Big] +$$

$$\pi\rho^{-1/2}R_{ji}^{-3/2}\cot 2\bar{\alpha}_{ji}\csc^2 2\bar{\alpha}_{ji}\Big[\csc^2 2\bar{\alpha}_{ji}\left(2\bar{\alpha}_{ji}^2 + \bar{\alpha}_{ji}\sin 2\bar{\alpha}_{ji}\cos 2\bar{\alpha}_{ji} -\right.$$

$$\left.2\sin^2 2\bar{\alpha}_{ji} + 2\bar{\alpha}_{ji}^2\cos 2\bar{\alpha}_{ji} + \bar{\alpha}_{ji}\sin 2\bar{\alpha}_{ji}\right)\Big] \quad \text{.....(3-54.e)}$$

$$F_{ji} = -\pi\rho^{-1/2}R_{ji}^{-3/2}\Big[\Big(8\bar{\alpha}_{ji} - 8\bar{\alpha}_{ji}\cos 2\bar{\alpha}_{ji} + 8\bar{\alpha}_{ji}^2 2\bar{\alpha}_{ji}^2 - 2\sin 2\bar{\alpha}_{ji} -$$

$$4\bar{\alpha}_{ji}\cos 2\bar{\alpha}_{ji} - 4\bar{\alpha}_{ji}\sin^2 2\bar{\alpha}_{ji} + 2\sin 2\bar{\alpha}_{ji}\cos 2\bar{\alpha}_{ji} + 4\bar{\alpha}_{ji}\cos^2 2\bar{\alpha}_{ji}\Big)\times$$

$$\csc^2 2\bar{\alpha}_{ij} - 4\cot 2\bar{\alpha}_{ji} \csc^2 2\bar{\alpha}_{ji}\left(4\bar{\alpha}_{ji}^2 - 4\bar{\alpha}_{ji}^2 \cos 2\bar{\alpha}_{ji} - 2\bar{\alpha}_{ji} \sin^2 \bar{\alpha}_{ji} + \right.$$

$$\left. 2\bar{\alpha}_{ji} \sin 2\bar{\alpha}_{ji} \cos 2\bar{\alpha}_{ji}\right)\Big] \quad \text{.....(3-54.f)}$$

It's obvious that when (ρ < 0) then the hyperbolic function are used instead of the trigonometric functions and that:-

($\bar{\alpha}_{ji}$) depends on the method and the function (see the previous section)

(R_{ji}) = The ρ shear multiplier depends on the method and the function (either (1-uρ), (1+uρ) , (1/(1-uρ)), or (1/(1+uρ)).

Table (3-4) shows the convergence of the new functions with F.D.M. for (u=1).

Table (3-4): validity of new functions at u=1.

		Method -1- (dy/dx)				***Method-2- (dym/dx)***			
No.	$\rho = P/P_e$	$\bar{b}_1$	$\bar{b}_2$	$\bar{\bar{b}}\bar{b}_1$	$\bar{\bar{b}}\bar{b}_2$	$\bar{b}_1$	$\bar{b}_2$	$\bar{\bar{b}}\bar{b}_1$	$\bar{\bar{b}}\bar{b}_2$
1	-2.00	0.0005	0.0038	0.0005	0.0038	0.0030	0.0258	0.0030	0.0258
2	-1.00	0.0013	0.0180	0.0013	0.0180	0.0045	0.0330	0.0045	0.0330
3	0.00	0.0049	0.0420	0.0049	0.0420	0.0049	0.0420	0.0049	0.0420
4	0.20	0.0086	0.0710	0.0086	0.0710	0.0096	0.0652	0.0096	0.0652
5	0.40	0.0178	0.1487	0.0178	0.1487	0.0168	0.1003	0.0168	0.1003
6	0.60	0.0567	0.5185	0.0567	0.5185	0.0279	0.1569	0.0279	0.1569
7	0.79	1.0479	162.59	1.0479	162.59	0.0447	0.2519	0.0447	0.2519

where:-

$\bar{b}_i$ = the bowing function calculated from the new derivations.

$\bar{\bar{b}}\bar{b}_i$ = the bowing function calculated from the F.D.M. (eq.3.51.a and 3.51.b)

3.3 The effect of transverse loading on the non-linearity (fixed end action F.E.A.):-

It is obvious that the effect of transverse loading has a significant effect on predicting and evaluating the critical load and the entire stability non linearity of the element, this effect is what is known as the fixed end action.

Figure (3-12) shows two sets of the same structure member where the effect of (F.E.A.) can be noticed, so this effect must be taken into account in the stability problem most of the structure has a member loading at least its own weight:-

From ***Lin*** [56] (1970), we have this simple relation:-

$$Mf_1 = -F\frac{y}{\theta_a} \quad \text{.....(3-55)}$$

where "F" is the concentrated load at any distance (x) along the span, and (y) is the deflection of the elastic curve defined previously in eq.(3-28) for Meth.-1- and eq.(3-40) for Meth.-2-, also from eq.(3-31), we have:-

$$M_1 = K\overline{C}_1\theta_1 + K\overline{C}_2\theta_2$$
$$M_2 = K\overline{C}_2\theta_1 + K\overline{C}_1\theta_2$$

If we try to find each value of the end moments M_1 and M_2 for this action, first we have to take the right end as fixed joint (i.e. θ_2=0), and then the left one (i.e. θ_1=0) respectively, hence eq.(3-31) becomes:-

$$\begin{aligned} M_1 &= M_a = K\overline{C}_1\theta_1 \\ M_2 &= M_b = K\overline{C}_1\theta_2 \end{aligned} \quad \text{.....(3-56)}$$

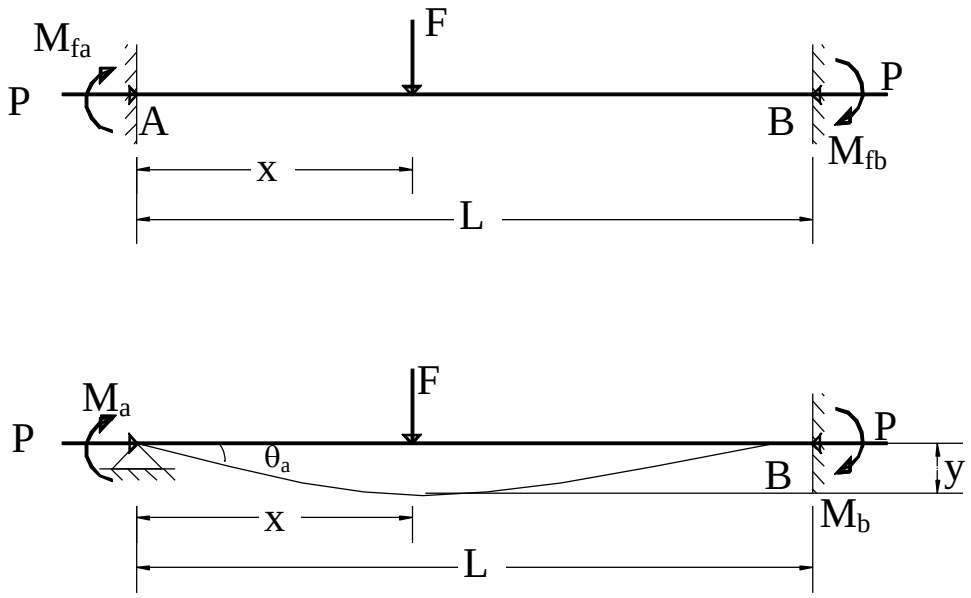

Figure (3-12) Fixed End Action: Tow Sets of force systems acting on same structural member

Substituting this equation into eq.(3-28 and 3-40) for both methods respectively and then into eq.(3-55), yields:-

$$Mf_1 = F\frac{K}{P}\left[\overline{C}_1\left(-\cot\omega L\sin\omega x+\cos\omega x+\frac{x}{L}-1\right)+\overline{C}_2\left(-\csc\omega L\sin\omega x+\frac{x}{L}\right)\right] \quad \text{.....(3-57)}$$

$$\text{Since: } \frac{K}{P}=\frac{EI/L}{\rho.\frac{\pi^2 EI}{L^2}}=\frac{L}{\rho\pi^2},\ \omega=\frac{2\overline{\alpha}}{L} \quad \text{.....(3-58)}$$

and introducing (i) as method indicator.

$$\therefore Mf_1=\frac{FL}{\rho\pi^2}\left[\overline{C}_1\left(-\cot 2\overline{\alpha}_i\sin\frac{2\overline{\alpha}_i}{L}x+\cos 2\overline{\alpha}_i\frac{x}{L}+\frac{x}{L}-1\right)+\right.$$

$$\left.\overline{C}_2\left(-\csc 2\overline{\alpha}_i\sin 2\overline{\alpha}_i\frac{x}{L}+\frac{x}{L}\right)\right] \quad \text{.....(3-59)}$$

This equation is due to a single concentrated force, any portion along the element has a uniformly distributed loading, the fixed end action can be determined by integrating eq.(3-59) along the required portion.

So, speaking of fully loading case:-

- For compressive axial force ($\rho>0$)

$$Mf_1=\frac{wL}{\rho\pi^2}\int_0^L\left[\overline{C}_1\left(-\cot 2\overline{\alpha}_i\sin\frac{2\overline{\alpha}_i}{L}+\cos 2\overline{\alpha}_i\frac{x}{L}+\frac{x}{L}-1\right)+\right.$$

$$\left.\overline{C}_2\left(-\csc 2\overline{\alpha}_i\sin 2\overline{\alpha}_i\frac{x}{L}+\frac{x}{L}\right)\right]dx \quad \text{.....(3-60)}$$

$$Mf_1=\frac{wL^2}{2\rho\pi^2\overline{\alpha}_i}\left[\overline{C}_{1i}\left(\cot 2\overline{\alpha}_i\left(\cos 2\overline{\alpha}_i-1\right)+\sin 2\overline{\alpha}_i-\overline{\alpha}_i\right)+\right.$$

$$\left.\overline{C}_{2i}\left(\cot 2\overline{\alpha}_i-\csc 2\overline{\alpha}_i+\overline{\alpha}_i\right)\right] \quad \text{.....(3-61)}$$

This equation is applicable to both end fixed end action moments (i.e.: $Mf_1=Mf_2$).

- For tensile axial force ($\rho<0$)

Using the same procedure, but putting the tensile relations for $\left(y_i,\theta_i,\overline{C}_{1i},\text{and}\overline{C}_{2i}\right)$, we have

$$Mf_1 = \frac{wL^2}{2\rho\pi^2\bar{\alpha}_i}\left[\bar{C}_{1i}\left(-\coth 2\bar{\alpha}_i\left(\cosh 2\bar{\alpha}_i - 1\right) + \sinh 2\bar{\alpha}_i - \bar{\alpha}_i\right) + \right.$$

$$\left.\bar{C}_{2i}\left(-\coth 2\bar{\alpha}_i + \operatorname{csch} 2\bar{\alpha}_i + \bar{\alpha}_i\right)\right] \quad \text{.....(3-62)}$$

where: (ρ) is taken positive, and (w) in both equations is the load per unit length.

❖ For no axial force (ρ=0):-

In this case a ***Taylor*** expansion can be used, using the same ($a = \bar{\alpha} = \frac{\pi}{50}$) and only for first term of the series (the function is rapidly converge) that ignoring second and further terms makes a negligible difference, although more accuracy can be achieved by taking more terms.

Since: $\bar{\alpha}_i = \frac{\pi}{50} = .0628$, and $\bar{\alpha}_i = \frac{\pi}{2}\sqrt{\bar{\rho}_i}$ .....(3-63)

$\therefore \bar{\rho}_i = .0016$, by using eq.(3-48.a and b):

$$Mf_0 = \frac{wL^2}{8} \times \frac{(1 + 0.0016u)}{(0.002)} \approx wL^2 \frac{(1 + 0.0016u)}{0.016} \text{ for Meth.-1- .....(3-64)}$$

$$Mf_0 = \frac{wL^2}{8} \times \left(\frac{2u}{1.24\left[-1 + (1 + 0.064u)^{1/2}\right]} \right) \approx \frac{wL^2}{5} \times \frac{u}{\left[-1 + (1 + 0.064u)^{1/2}\right]} \text{ for Meth.-2- ....(3-65)}$$

These functions are illustrated in figure (3-13) for different values of (u), where the values for Meth.-2- are completely equal to ***Lin***'s values.

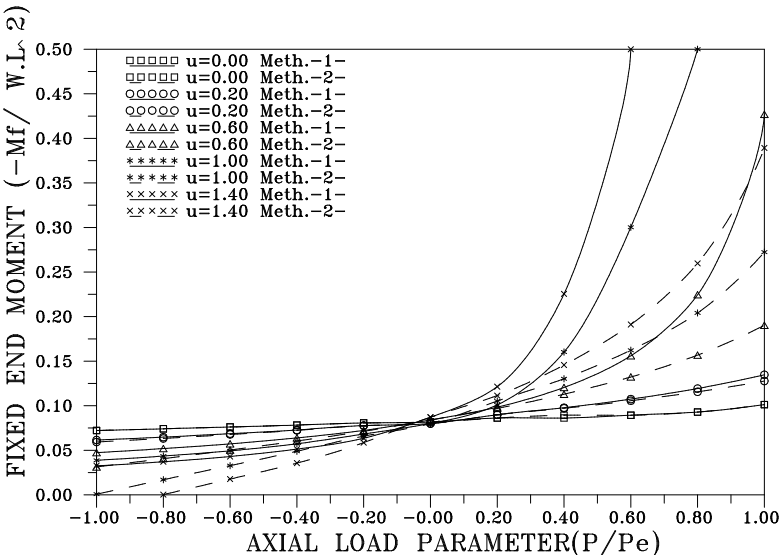

Figure (3-13) U.D.L. over full length P/P_e versus fixed-end moment including shear effect for various shear parameter (u) using both methods

3.4 The 3-D effect on the non-linearity

As mentioned in chapter one the original most familiar governing differential equation of the beam-column in space includes the combined action of torsional-flexural effects in which the torsion mainly consists of:

1-***Snt Vnt*** twisting effect (GJ).....(3-66)

2- The wrapping effect (C_w).....(3-67)

3- ***Wagner*** effect (i.e. the contribution of torsion about the shear center which is identified as

$$\overline{K} = P\frac{I_o}{A} \quad \text{.....(3-68)}$$

The torsion basic equation can be written in a simplified form:-

$$(GJ + \overline{K})\phi' - C_w\phi''' = M_t \quad \text{.....(3-69)}$$

where:-

ϕ : is the angle of twist.

M_t : is the torsion or the moment around the axial axis (-z- axis which can be any variable (constant or function of (z) and (ϕ) depending on the problem).

The derivations in the basic torsion theory neglect the effect of shear deformations since they adopt right angled deformations, what actually happened is that this assumption makes the behavior of the non-linear stability analysis shift from the actual elastica, our idea in this study is to break

this assumption and deeply enter the actual behavior and then build upon it a new physical phenomenon and new theory associated with member response to torsion and compiled axial-flexural-torsional systems. So let's enter the problem and see what really happening.

3.4.1 Basic phenomenon:-

If we take any member and try to twist it, the actual behavior that has never been studied before (depending on the no shear deformation assumption), is:-

When the member is twisted it shortens accordingly

Figure (3-14.a) shows a twisted rectangular solid section member with horizontal and vertical dividing lines to represent the outside fibers response. If this member is held in position from one of its ends these lines take a helical path which means that the final position of the lines ends has a horizontal distance less than the actual one as shown in figure (3-14.b).

This behavior means that there is an additional axial shortening caused by the twisting moments which obviously affect the entire behavior of the element and change the element **T.S.M.** This effect is going to be identified as the (***SS*** effect) or (***Siddeek - Al-Sarraf***) effect.

Depending on the basic phenomenon the brand new theory of the coupled **T.S.M.** shall be introduced starting from the differential equation derivation up to the final assemblage of the 3-D element coupled **T.S.M.**

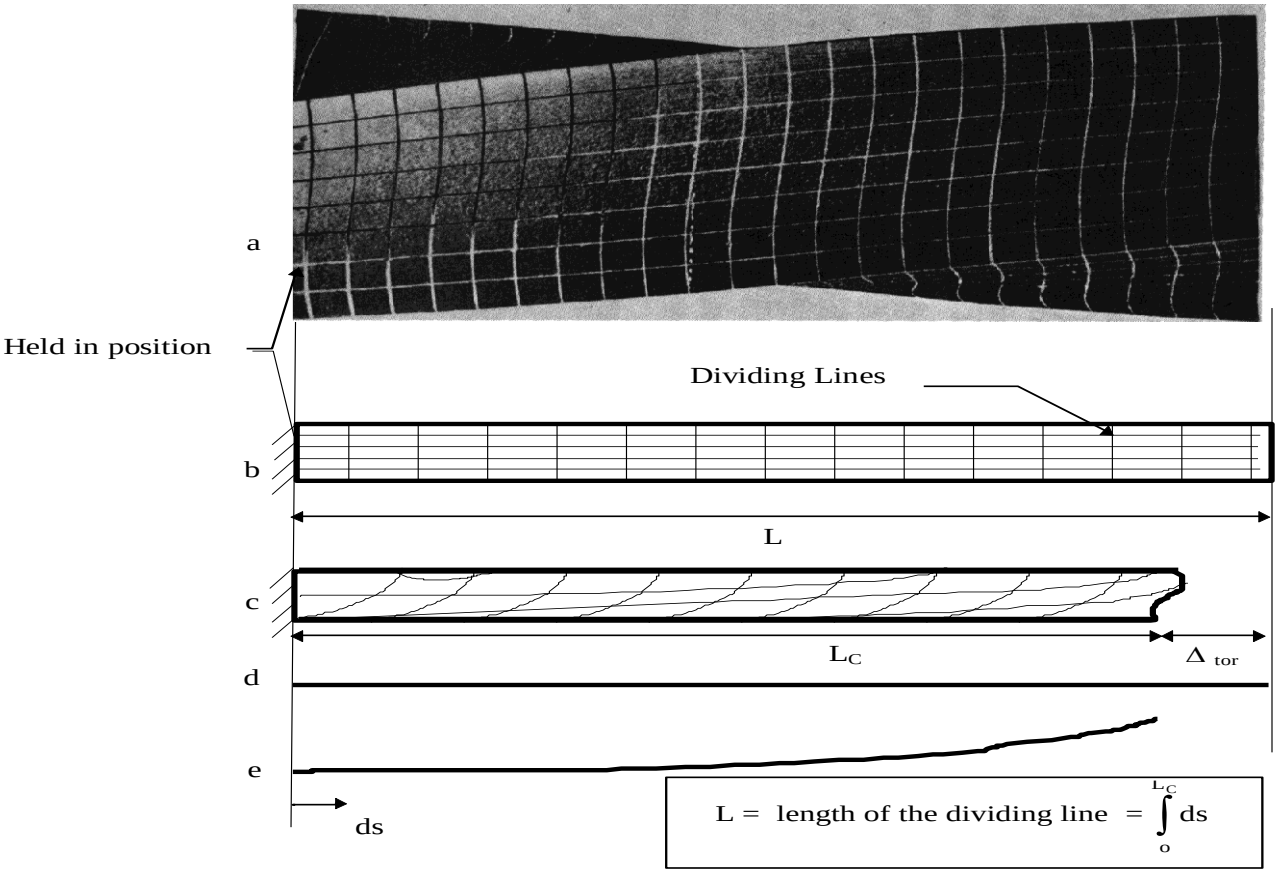

Figure (3-14)

a: Actual twisted bar b: Idealized undeformed bar.

c: Idealized twisted bar. d: Original dividing line.

e: Line after twisting.

3.4.2 The basic differential equation

In figure (3-15) all the symbols are identified

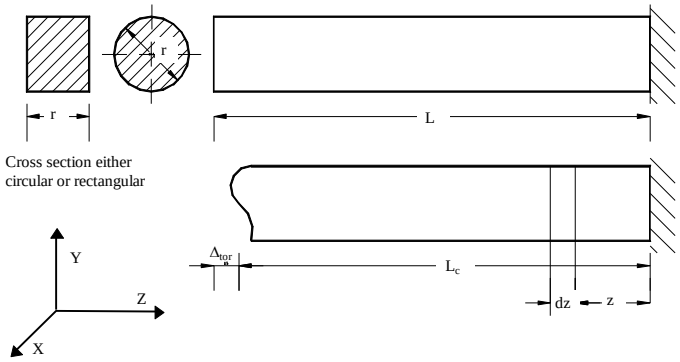

Figure (3-15) The twisted member

At any section a distance (z) from the member localized end one can take the section and observe what happens, the matter that is illustrated in figure (3-16.a).

From the figure above it can be noticed that the movement of point (a) to the new position (a') caused by the shear deformation induced by the twisting moments applied to the member is the axial displacement of the (***SS*** effect).

The basic differential equation of the (***SS*** effect) can be derived as follows:-

Since: $ds = r_{ave.} d\alpha$ .....(3-70)

and: $r_{ave.} = \frac{1}{2}\left[r\phi + (r + dr)(\phi + d\phi)\right]$ .....(3-71)

$$\therefore ds = r_{ave.}\, d\alpha = \frac{1}{2}\left(2r\phi + rd\phi + \phi dr + drd\phi\right)d\alpha \quad \text{.....(3-72)}$$

Ignoring the higher orders we find that eq.(3-72) becomes:

$ds = r\phi\, d\alpha$ .....(3-73)

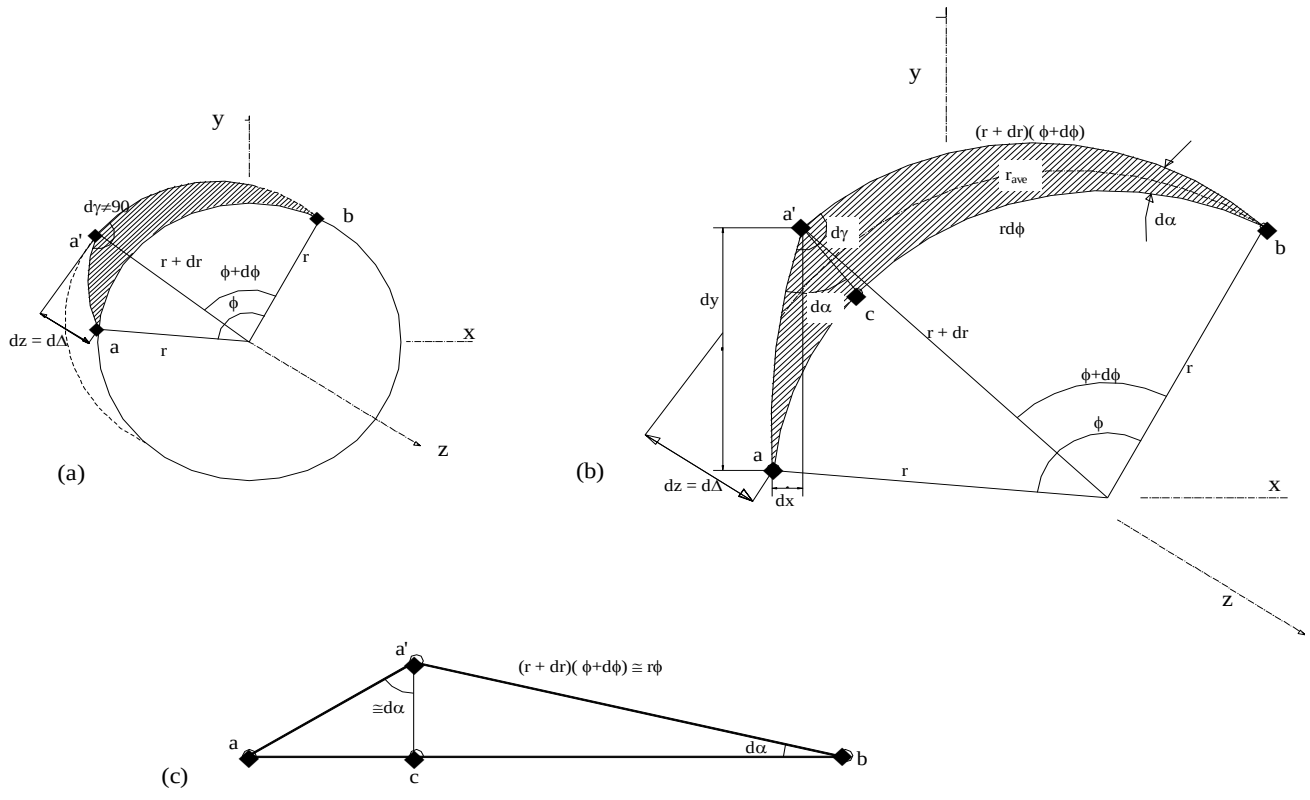

Figure (3-16) (a): Cross section behavior after twisting. Point -a- moves in a 3-D path to make a shear deformation dα in addition to the dx, dy, dz displacements. (b): The detailed section. (c): The approximate top view of the triangle (a-a'-b).

Since:-

$d\gamma \neq 90$

$aa' = ds = \sqrt{dx^2 + dy^2 + dz^2}$

$a'c = \sqrt{dy'^2 + dz^2}$ .....(3-74)

$ac = \sqrt{dx'^2 + dz'^2}$

$d\alpha = \tan^{-1} \frac{aC}{dC}$

Using small deflection assumption:

$\tan\alpha = \alpha = \sin\alpha$
$\cos\alpha = 1$ .....(3-75)

we find that:

$d\alpha = \frac{\sqrt{dx^2 + dz^2}}{\sqrt{dy^2 + dz^2}}$ .....(3-76)

By separating the contribution of each plane from each other we have:-

$dy \to 0$ x_1 plane
$dx \to 0$ x_3 plane .....(3-77)

And neglecting higher order terms eq.(3-76) becomes:-

$$d\alpha)_{1-\text{plane}} \approx \frac{dx}{dz} \left(\text{which is the elastic curve slope in } x_1 - \text{direction}\right)$$

$$d\alpha)_{3-\text{plane}} \approx \frac{dy}{dz} \left(\text{which is the elastic curve slope in } x_3 - \text{direction}\right)$$

where ($\frac{dx}{dz}$ and $\frac{dy}{dz}$) are taken from eq.(3-29) for Meth.-1- and eq.(3-41) for Meth.-2-

Since:-

$ds \cos d\alpha \approx d\Delta$, then:-

$ds \approx d\Delta$

So:-

$$d\Delta_1 = r\phi\, d\alpha_1 \approx r\,\phi\,\frac{dx}{dz}$$
$$d\Delta_3 = r\,\phi\, d\alpha_3 \approx r\,\phi\,\frac{dy}{dz} \quad \text{.....(3-79)}$$

This equation is the basic differential equation of the axial displacement which occurs in the B-C element caused by the twisting moment (M_t) in both planes.

The angle of twist depends on the type of section (weather its symmetric or not), the type of twisting moment function (weather it's constant, or function of (z)), two main cases can be exhibited:-

3.4.2.1 The constant torsion- no warping case (mono-symmetric sections with zero warping stiffness).

3.4.2.2 The variable torsion-warping case (skew or bi-symmetrical sections)

Both cases must be checked.

3.4.2.1 The constant torsion-no warping case (Closed and mono-symmetric sections with no warping stiffness)

This is the simplest and most widely used case since all symmetrical solid or hollow sections (circular or rectangular) are included.

In such case the warping is free, so (c_w=0), then (eq.3.69) becomes:-

$$\left(GJ + \overline{K}\right)\phi' = M_t \quad \text{.....(3-80)}$$

and since M_t is a constant moment all over the lengths of the member then by integrating we find that:-

$$\phi = \frac{M_t}{\left(GJ + \overline{K}\right)}\left(z + \phi_o\right) \quad \text{.....(3-81)}$$

where "ϕ_o" is the integration constant and it can be ignored herein and added to the initial conditions of the element as a (F.E.A.) as we shall see in the special effects section (section 3.5), so eq.(3-81) becomes:-

$$\phi = \frac{M_t}{\left(GJ + \overline{K}\right)}\, z \quad \text{.....(3-82)}$$

Substitute this equation in eq.(3-79), the axial shortening of the element can be introduced for this case:-

$$d\Delta = \frac{r\ M_t}{(GJ + \overline{K})} z \frac{dy}{dz} \quad \text{.....(3-83)}$$

In order to have the total shorting in the member we can integrate eq.(3-83) along the length (L_c), this shortening is defined as (C_T)

$$\Delta_z = C_T = \frac{r\,M_t}{(GJ + \overline{K})} \int_0^{L_c} z \frac{dy}{dz} dz \quad \text{.....(3-84)}$$

$\because \frac{dy}{dz}$ are taken from eq.(3-29) and eq.(3-41) for Meth.-1- and Meth.-2- respectively and by integrating and simplifying we have:

$$C_T = \frac{r\,M_t}{(GJ + \overline{K})} \left[\frac{-M_2}{P\omega} (\cot \omega L - \csc \omega L + \omega L) - \frac{M_1}{P\omega} (\csc \omega L - \cot \omega L) + \frac{L}{2P} (M_1 + M_2) \right] \quad \text{.....(3-85)}$$

introducing:

$$\omega = \frac{2\overline{\alpha}}{L}, K = \frac{EI}{L}, P_e = \frac{EI\pi^2}{L^2} \text{ and } \rho = \frac{P}{P_e} \quad \text{.....(3-86)}$$

and that:-

$$\begin{aligned} M_1 &= K\overline{C}_1(\theta_1 + \psi) + K\ \overline{C}_2(\theta_2 + \psi) \\ M_2 &= K\overline{C}_2(\theta_1 + \psi) + K\ \overline{C}_1(\theta_2 + \psi) \end{aligned} \quad \text{.....(3-87)}$$

where (ψ) represents the sway angle and introducing the method indicator (i), we have:

$$\frac{C_T}{L} = \frac{r\,M_t}{2\pi^2 (GJ + \overline{K})\rho} \left[-\left(\frac{\cot 2\overline{\alpha} - \csc 2\overline{\alpha} + 2\overline{\alpha}}{\overline{\alpha}} \right) \left(\overline{C}_2(\theta_1 + \psi) + \overline{C}_1(\theta_2 + \psi) \right) - \left(\frac{\csc 2\overline{\alpha} - \cot 2\overline{\alpha}}{\overline{\alpha}} \right) \left(\overline{C}_1(\theta_1 + \psi) + \overline{C}_2(\theta_2 + \psi) \right) + \left(\overline{C}_1 + \overline{C}_2 \right) (\theta_1 + 2\psi + \theta_2) \right] \quad \text{.....(3-88)}$$

In the rectangular sections the section dimension (a/2) is used instead of (r).

3.4.2.1.1 The twisting functions of the B-C element.

From eq.(3-88) it can be observed that the axial displacement due to the shear deformation caused by the twisting moment (C_T) can be written using a new function ($\bar{t}_1$) and ($\bar{t}_2$) called the twisting functions similar as the stability and bowing functions:-

$$\frac{C_T}{L}\Big)x_1 = \frac{r\,M_t}{\left(GJ+\overline{K}\right)}\left(\bar{t}_1\left(\theta_1+\psi\right)+\bar{t}_2\left(\theta_2+\psi\right)\right)_1 \quad \text{.....(3-89.a)}$$

$$\frac{C_T}{L}\Big)x_3 = \frac{r\,M_t}{\left(GJ+\overline{K}\right)}\left(\bar{t}_1\left(\theta_1+\psi\right)+\bar{t}_2\left(\theta_2+\psi\right)\right)_3 \quad \text{.....(3-89.b)}$$

- If $\rho>0$ (compressive axial force):-

$$\bar{t}_{1i} = \gamma_{1i}\,\overline{C}_{2i} + \gamma_{2i}\,\overline{C}_{1i} + \frac{\overline{C}_{1i}+\overline{C}_{2i}}{2\pi^2\rho} \quad \text{.....(3-90.a)}$$

$$\bar{t}_{2i} = \gamma_{1i}\,\overline{C}_{1i} + \gamma_{2i}\,\overline{C}_{2i} + \frac{\overline{C}_{1i}+\overline{C}_{2i}}{2\pi^2\rho} \quad \text{.....(3-90.b)}$$

where:-

$$\gamma_{1i} = \frac{-\left(\cot 2\overline{\alpha}_i - \csc 2\overline{\alpha}_i + 2\overline{\alpha}_i\right)}{2\overline{\alpha}_i\,\pi^2\rho} \quad \text{.....(3-91.a)}$$

$$\gamma_{2i} = \frac{-\left(\csc 2\overline{\alpha}_i - \cot 2\overline{\alpha}_i\right)}{2\overline{\alpha}_i\,\pi^2\rho} \quad \text{.....(3-91.b)}$$

$$\overline{\alpha}_i = \frac{\pi}{2}\sqrt{\overline{\rho}_i} \quad \text{.....(3-91.c)}$$

$\overline{\rho}_i =$ Axial load parameter including shear effect.

$\overline{C}_{1i}\,\&\,\overline{C}_{2i} =$ the stability functions including shear effect when $\rho>0$ (see section 3.2.3)

i= is the method indicator.

- If $\rho<0$ (tensile axial force):-

$$\bar{t}_{1i} = \gamma_{1i}\,\overline{C}_{2i} + \gamma_{2i}\,\overline{C}_{1i} + \frac{\overline{C}_{1i}+\overline{C}_{2i}}{2\pi^2\rho} \quad \text{.....(3-92.a)}$$

$$\bar{t}_{2i} = \gamma_{1i}\,\overline{C}_{1i} + \gamma_{2i}\,\overline{C}_{2i} + \frac{\overline{C}_{1i}+\overline{C}_{2i}}{2\pi^2\rho} \quad \text{.....(3-92.b)}$$

where:-

$$\gamma_{1i} = \frac{\left(\coth 2\overline{\alpha}_i - \operatorname{csch} 2\overline{\alpha}_i + 2\overline{\alpha}_i\right)}{2\overline{\alpha}_i\,\pi^2\rho} \quad \text{.....(3-93.a)}$$

$$\gamma_{2i} = \frac{\left(\operatorname{csch} 2\bar{\alpha}_i - \coth 2\bar{\alpha}_i\right)}{2\bar{\alpha}_i \pi^2 \rho} \quad \text{.....(3-93.b)}$$

$$\bar{\alpha}_i = \frac{\pi}{2}\sqrt{\bar{\rho}_i} \quad \text{.....(3-93.c)}$$

$\bar{\rho}_i$ = axial load parameter including shear effect.

$\bar{C}_{1i}$ & $\bar{C}_{2i}$ = the stability functions including shear effect when $\rho<0$ (see section 3.2.3)

i= is the method indicator.

- If $\rho=0$ (no axial force):-

when $\rho=0$ and (u=0) the twisting functions can be found using ***Taylor*** expansion by taking ($\bar{\alpha}_i = \frac{\pi}{10}$)as it will be discussed in the next section.

$$\begin{aligned} \bar{t}_{1i} &\approx -0.0815 \\ \bar{t}_{2i} &\approx \ \ 0.0815 \end{aligned} \quad \text{.....(3-94.a)}$$

when u>0, the same procedure of ***Taylor*** expansion can be used with $\bar{\alpha}_i = \frac{\pi}{10}$.

$$\begin{aligned} \bar{t}_1 &= (-1+0.04u)\left[-2.5109\bar{C}_2 + 0.022\bar{C}_1 + \frac{\bar{C}_1+\bar{C}_2}{2\pi^2}\right] \\ \bar{t}_2 &= (-1+0.04u)\left[-2.5109\bar{C}_1 + 0.022\bar{C}_2 + \frac{\bar{C}_1+\bar{C}_2}{2\pi^2}\right] \end{aligned} \quad \text{for Meth.-1-.....(3-94.b)}$$

$$\begin{aligned} \bar{t}_1 &= \frac{2u}{\left(-1+(1+0.16u)^{1/2}\right)}\left[-0.100436\bar{C}_2 + 8.84\times10^{-4}\bar{C}_1 + \frac{\bar{C}_1+\bar{C}_2}{2\pi^2}\right] \\ \bar{t}_2 &= \frac{2u}{\left(-1+(1+0.16u)^{1/2}\right)}\left[-0.100436\bar{C}_1 + 8.84\times10^{-4}\bar{C}_2 + \frac{\bar{C}_1+\bar{C}_2}{2\pi^2}\right] \end{aligned} \quad \text{for Meth.-2-.....(3-94.c)}$$

The function behavior is shown in figures (3-17) to (3-21) for u=0, 0.1,1.0,5.0 and 10.0 respectively.

3.4.2.1.2 Checking and testing the twisting functions:-

Since no one before has given a corresponding function, and though we have no other results to compare with. Meanwhile we can check the behavior of the function by:-

3.4.2.1.2.1 Check the behavior near $\rho=0$

When $\rho\rightarrow 0$ the functions rapidly increase so we must handle this situation using the well known ***Taylor*** expansion.

$$f(x)=f(a)+f'(a)(x-a)+\frac{(x-a)^2}{2!}f''(a)+\frac{(x-a)^3}{3!}f'''(a)+\ldots+\frac{(x-a)^n}{n!}f^n(a)+\ldots+R_n(x,a) \quad \ldots\ldots(3\text{-}95)$$

Kassimali [47] in (1983), presented the ***Taylor*** Expansions for the no shear effect stability and bowing functions (see **App.C.**). He used ($a=\pi/50$) for finding the no shear effect stability function (C_1) and (C_2) and ($a=\pi/20$) when finding the no shear effect bowing functions (b_1 & b_2), (the same Appendix).

For ($\bar{t}_1$) and ($\bar{t}_2$), if (ρ) approaches zero the same equations (eq.3.94.a, b, c) can be used with a very small error which can be neglected, so:-

When $|\rho \le 0.01|$ then eq.(3-94.a to c) can handle the problem of divergence and govern the twisting functions, however it may be refined using higher order terms of ***Taylor*** Expansion.

3.4.2.1.2.2 Check with the F.D.M.

Using the same check used in the modified shear bowing functions ($\bar{b}_1 \& \bar{b}_2$), we see that the twisting function ($\bar{t}_1 \& \bar{t}_2$) shows the same values as those shown by the finite difference method functions (tt_1 & tt_2), where:

$$tt_1=\frac{t_1'(\rho+0.001)-t_1'(\rho-0.001)}{0.002}$$
$$tt_2=\frac{t_2'(\rho+0.001)-t_2'(\rho-0.001)}{0.002} \quad \ldots\ldots(3\text{-}96)$$

This means that the derivation is correct and that ($\bar{t}_1 \& \bar{t}_2$) shown in figures (3-17) to (3-21) are valid for the no warping and constant torsion case.

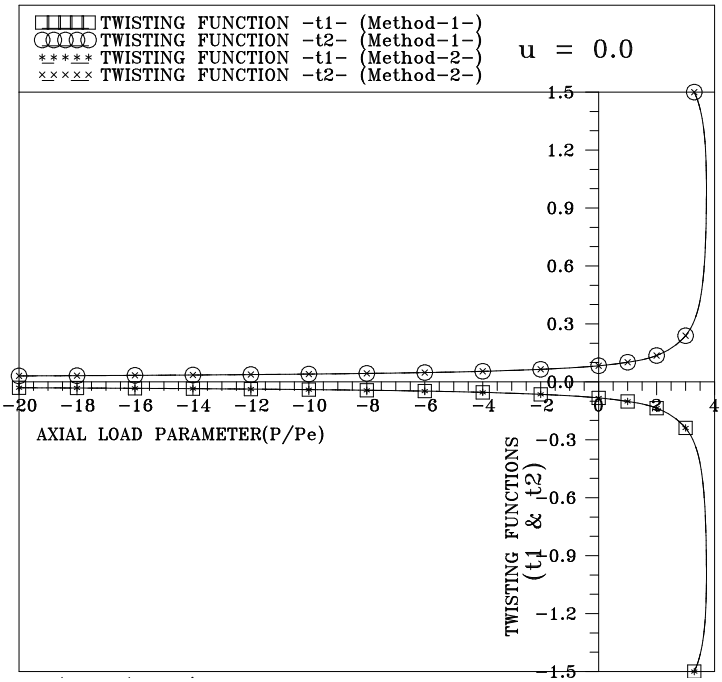

Figure (3-17) **P/P_e versus twisting function curves without shear effect by both methods (u=0.0)**

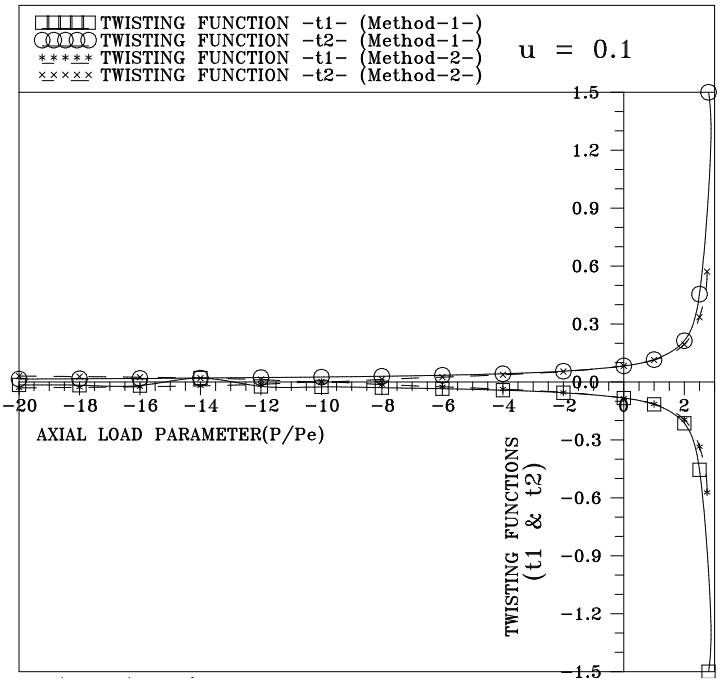

Figure (3-18) **P/P_e versus twisting function curves including shear effect by both methods (u=0.1)**

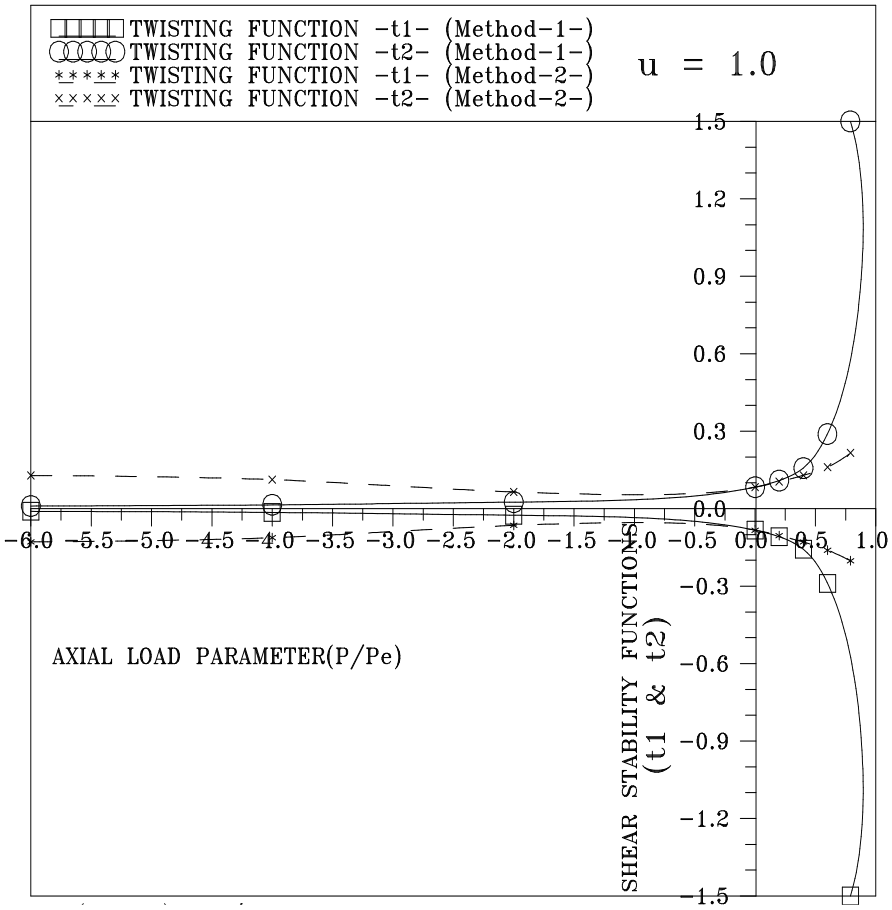

Figure (3-19) P/P_e versus twisting function curves including shear effect by both methods (u=1.0)

3.4.2.1.2.3 Check the values of ($\bar{t}_1$ & $\bar{t}_2$) with each other for different values of (u).

It can be noticed from the figures that ($\bar{t}_1$ & $\bar{t}_2$) are equal and opposite for every value of (ρ) and (u) which means when we have equal values of (θ) the axial shortening due to (***SS*** effect) vanishes which is true since the (dy/dz) used in the equation is the flexural slope of the elastic curve; however, this case rarely occurs.

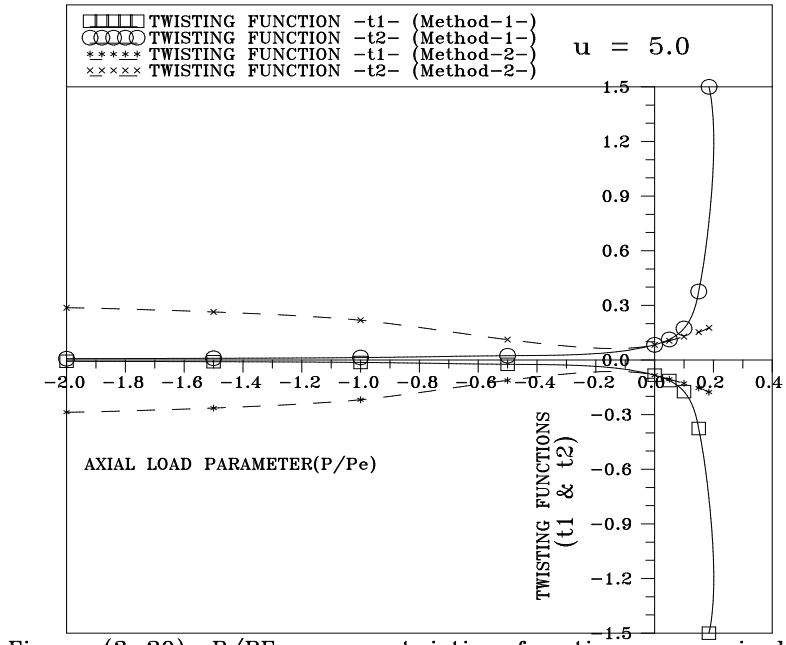

Figure (3−20):−P/PE versuse twisting function curves including sl
by both methods (u=5.0)

Figure (3-20) P/P_e versus twisting function curves including shear effect by both methods (u=5.0)

When (u) value arises, the difference between Meth.-1- and Meth.-2- arises till a high range of differences can be observed when (u=5) and (u=10) as figures (3-20) and (3-21) indicate respectively.

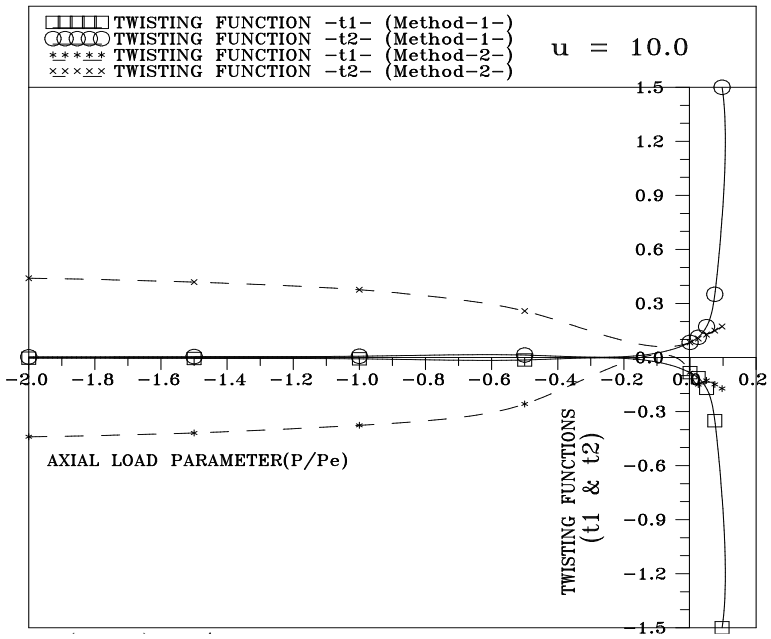

Figure (3-21) P/P_e versus twisting function curves including shear effect by both methods (u=10.0)

3.4.2.2 The variable torsion-warping case (open skew or bi-symmetric sections)

This is the most widely general case of the torsion problem, where eq.(3-69) must be completely solved, since ($C_w \neq 0$) and (M_t) is not constant (M_t is a function of (ϕ, z).

So, (eq.3-69) becomes:-

$$C_w \phi''' - (GJ + \overline{K})\phi'' - M_t(W, z, \phi) = 0 \quad \text{.....(3-97)}$$

where (W) is a concentrated or distributed load.

In solving this equation a method of infinite (trigonometric or exponential) series is used because its a very complex form of differential equation [94].

Timoshinko and ***Gere*** [94], suggested the following trigonometric expression keeping in mind the constraint conditions shown in figure (3-22) :-

$$\phi = a_1 \cos\frac{\pi z}{l} + a_2 \cos\frac{3\pi z}{l} + \ldots \quad \text{.....(3-98)}$$

and they prove that using more than two terms gives no larger than 0.1% difference in results while using the first term only shows 0.5% difference from accurate integration results.

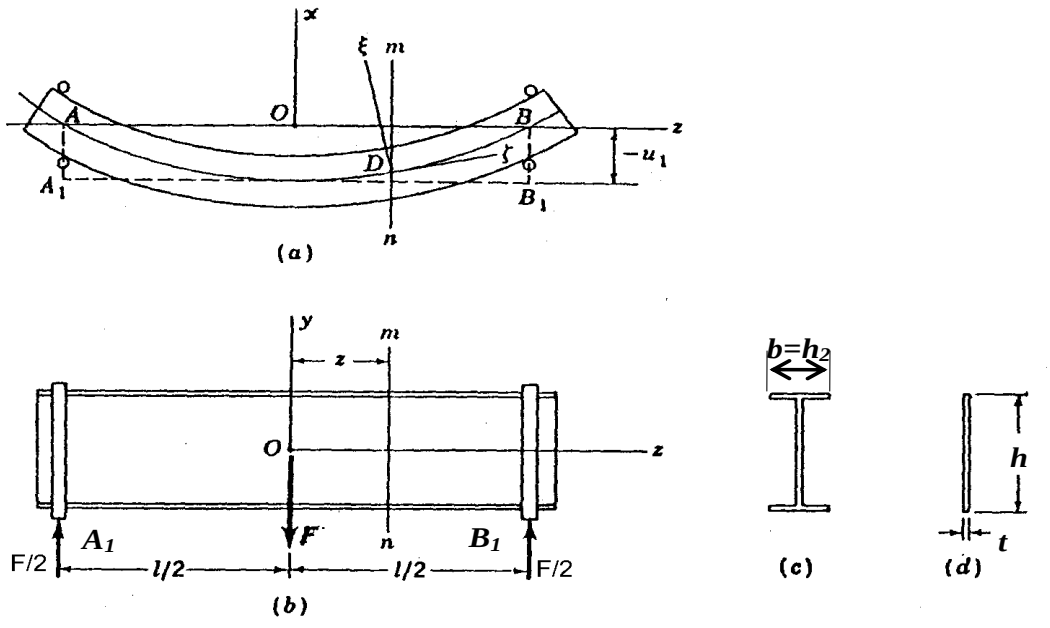

Figure (3-22): (a) B-C view. (b) B-C after lateral- buckling. "Notice the constraints at -A- and -B- ($\phi_A = \phi_B = 0$)". (c) & (d) cross sections

From the constraint conditions we have:-

$$\phi = a\left(\cos\frac{\pi z}{l} + \cos\frac{3\pi z}{l}\right) = a\cos\frac{\pi z}{l} \quad \text{.....(3-99)}$$

Substituting into eq.(3-80), and having known that (r) in this case is equal to half of the height (h/2) in X_1 plane and (b/2) in X_3 plane, we have:

$$d\Delta)_{x1} = \frac{h}{2}\, a\cos\frac{\pi z}{l}\,\frac{dy}{dz}$$
$$d\Delta)_{x3} = \frac{b}{2}\, a\cos\frac{\pi z}{l}\,\frac{dx}{dz} \quad \text{.....(3-100)}$$

it can be noticed that: $\cos\frac{\pi z}{l} = \cos\frac{w}{\sqrt{\bar{\rho}}}z$

$(\frac{dy}{dz}\text{and}\frac{dx}{dz})$ represent the elastic-curve slope of the B-C element, then:

$$C_T)_{x_1} = \frac{h}{2}a\int_0^{L_c}[SS]_{x_1}dz$$
$$C_T)_{x3} = \frac{b}{2}a\int_0^{L_c}[SS]_{x_2}dz \quad \text{.....(3-101)}$$

$$[SS] = \left[\left(-\frac{M_2}{P}\csc\omega L - \frac{M_1}{P}\cot\omega L\right)\omega\cos\omega Z\cos\frac{\omega}{\sqrt{\bar{\rho}}}Z - \right.$$

$$\left.\frac{M_1}{P}\omega\sin\omega Z\omega S\frac{\omega}{\sqrt{\bar{\rho}}}Z + \left(\frac{M_1}{PL} + \frac{M_2}{PL}\right)\omega S\frac{\omega}{\sqrt{\bar{\rho}}}Z\right] \quad \text{.....(3-102)}$$

since $\omega^2 \neq \frac{\omega^2}{\bar{\rho}}$ and letting (b = h_2) and $\left(\frac{\sqrt{\bar{\rho}}-1}{\sqrt{\bar{\rho}}} = k_1\right)$ $\left(\frac{\sqrt{\bar{\rho}}+1}{\sqrt{\bar{\rho}}} = k_2\right)$

Then by integration we have:

$$C_T)_{x_1} = \frac{h_i}{2}a\left[\left(-\frac{M_2}{P}\csc\omega L - \frac{M_1}{P}\cot\omega L\right)\omega\left(\frac{\sin\left(\omega - \frac{\omega}{\sqrt{\bar{\rho}}}\right)Z}{2\left(\omega - \frac{\omega}{\sqrt{\bar{\rho}}}\right)} + \frac{\sin\left(\omega + \frac{\omega}{\sqrt{\bar{\rho}}}\right)Z}{2\left(\omega + \frac{\omega}{\sqrt{\bar{\rho}}}\right)}\right) + \right.$$

$$\frac{M_1}{P}\omega\left(\frac{\cos\left(\omega+\frac{\omega}{\sqrt{\bar{\rho}}}\right)Z}{2\left(\omega+\frac{\omega}{\sqrt{\bar{\rho}}}\right)}+\frac{\cos\left(\omega-\frac{\omega}{\sqrt{\bar{\rho}}}\right)Z}{2\left(\omega-\frac{\omega}{\sqrt{\bar{\rho}}}\right)}\right)+\left(\frac{M_1+M_2}{PL}\right)\left(\frac{\sqrt{\bar{\rho}}}{\omega}\sin\frac{\omega}{\sqrt{\bar{\rho}}}Z\right)\Bigg]_0^{L_c} \quad \text{.....(3-103)}$$

$$C_T\Big)_{x_i}=\frac{h_i}{2}a\left[\left(\frac{-M_2}{P}\csc\omega L-\frac{M_1}{P}\cot\omega L\right)\frac{1}{2}\left(\frac{\sin k_1\omega L}{k_1}-\frac{\sin k_2\omega L}{k_2}\right)+\right.$$
$$\left.\frac{M_1}{2P}\left(\frac{\cos\omega k_1 L}{k_1}+\frac{\cos\omega k_2 L}{k_2}-\frac{1}{k_1}-\frac{1}{k_2}\right)\right] \quad \text{.....(3-104)}$$

Renton [78] (1962), however presented a stiffness matrix of space frames for these types of sections, but he neglected the bowing effect and adopted the well-known ***Snt. Vt*** no shear deformation assumption.

The equations of 3-D buckling (lateral buckling) are:-

$$\begin{aligned}
&EI_y u_o'''' + P\left(u_o'' + y_o\phi''\right) = 0\\
&EI_x v_o'''' + P\left(v_o + y_o\phi''\right) = 0\\
&GJ\phi'' - C_w\phi'''' - P\left(y_o u_o'' - x_o v_o'' + v_o^2\right) = 0
\end{aligned} \quad \text{.....(3-105)}$$

The general solution of these equations is:-

$$u_o = A_1\cos\mu_y Z + A_2\sin\mu_y Z + \alpha_1 Z + \alpha_o$$

$$\begin{aligned}
&x_o = B_1\cos\mu_x z + B_2\sin\mu_x t + B_1 z + B_0\\
&\text{and } \phi_0 = C_1\cosh\mu_z z + C_2\sinh\mu_z + \gamma_1 z + \gamma_0
\end{aligned} \quad \text{.....(3-106)}$$

$$\text{where: } \mu_x = \frac{p}{EI_x},\quad \mu_y = \frac{p}{EI_y},\quad \mu_z = \frac{(GJ-\bar{K})}{Cw} \quad \text{.....(3.107)}$$

A_1, A_2, B_1, B_2, C_1, C_2, α_1, α_2, β_1, β_2, ,γ_1 and γ_0 are integration constants. The matrix he presented although the coupled axial-torsional-flexural effect is included with the effect of rigid gusset plates, there is no sign of taking the (***SS*** effect) into consideration, just the way we've treated it.

Although ***Renton***'s approach of solving the coupled problem differs from ours the closed form solution he introduced for the three equations of lateral buckling supports the present formulation of treating the (dx/dz and dy/dz) as the flexural slope eq.(3-29 and 3-41) for both methods respectively.

This eq.(3-104) is the most general equation of the warping-variable twisting moment case which actually has no application in our study since we adopted the equivalent shear-parameter technique which allows any open section of a warping case to be idealized as a solid cross section with equivalent (u) value, that means we are dealing with no warping case so the twisting functions of this case (which actually of no big deal) shall be ignored.

3.4.2.3 The effect of torsion on bowing:-

The twisting moments have no effect on the flexural bowing and here is the proof:-

From eq.(3-26) we have:-

(for 2-D effect): $$C_b = \frac{1}{2}\int_0^{L_c} ds - dz = \frac{1}{2}\int_0^{L_c}\left(\frac{dy}{dz}\right)^2 dz \quad \text{..... (3-108.a)}$$

In the 3-D problems the equation becomes:-

$$C_b = \frac{1}{2}\int_0^{L_c}\left(\left(\frac{dy}{dz}\right)^2 + \left(\frac{dx}{dz}\right)^2\right)dz \quad \text{..... (3-108.b)}$$

In other words the (dϕ/dz) effect in the above equation is equal to zero which means that the angle of twist slope has no contribution in the existing flexural bowing equation.

This means that either eq. (3-26) must be changed to include the new shortening in the member due to torsion or both bowing effect and 3-D effect can be taken separately.

3.5 The special effects on non-linearity

The special effects of:-

* Temperature

* Lack of fit

* Initial imperfection (axial, flexural)

* Initial angle of twist

* Support yielding (in all D. O. F.)

shall be treated as F.E.A. to be added to the member local forces vector in the corresponding direction and D.O.F. of each effect. This means that each effect has its own contribution in the non-linear analytical operation during each incremental-iterational loop.

For this purpose **App. D.** illustrates all the F.E.A. of the special effects mentioned above.

These actions are put in a vector and added to the applied load vector of the element so equilibrium equation of the beam-column element can be written as:-

$$F = t.u \quad \text{..... (3-109.a)}$$

where "F" is the force vector of the element in local coordinates.

$$F = \begin{bmatrix} F_1 \\ F_2 \\ F_3 \\ . \\ . \\ . \\ F_{11} \\ F_{12} \end{bmatrix} \quad \text{..... (3-109.b)}$$

where:-

$F_i = F_{ia} + F_{is}$

F_{ia}= Applied load F.E.A. of the element+eq.(3-61, 3-62, 3-64 and 3-65)

F_{is}= Special effects F.E.A. of the element (see **App.D.**) ..... (3-109.c)

3.6 Full derivation of the new 3-D coupled T.S.M.:

App.C. gives the derivation of the uncoupled **T.S.M.** in space for the technique proposed by ***Oran*** (71& 72), ***Oran*** and ***Kassimali*** (70), and ***Kassimali***, and ***Abbassnia*** (48).

In our new theory a complete interaction between ϕ and (θ_1 & θ_2) occurs, so the coupled **T.S.M.** can be now built up:

since:-

$$t_{ij} = \frac{\partial s_i}{\partial u_j} + \frac{\partial s_i}{\partial q}\frac{\partial \rho}{\partial u_j} \quad \text{for (i, j = 1 to 6)} \quad \text{..... (3-110.a)}$$

Where:-

$$\begin{bmatrix} S_1 = M_{13} \\ S_2 = M_{23} \\ S_3 = M_{12} \\ S_4 = M_{22} \\ S_5 = M_t \\ S_6 = QL \end{bmatrix} = (\text{force vector}), \begin{bmatrix} u_1 = \theta_{13} \\ u_2 = \theta_{23} \\ u_3 = \theta_{12} \\ u_4 = \theta_{22} \\ u_5 = \phi \\ u_6 = \frac{\mu}{L} \end{bmatrix} = (\text{displacement vector}) \quad \text{..... (3-110.b)}$$

We must derive all the values of t_{ij}:

$$t_{11} = \frac{\partial S_1}{\partial u_1} + \frac{\partial S_1}{\partial \rho}\frac{\partial \rho}{\partial u_1} \quad \text{..... (3-111.a)}$$

$$\frac{\partial S_1}{\partial u_1} = \frac{\partial S_1}{\partial \theta_{13}} = \frac{EI_3}{L}\overline{C}_{13} \quad \text{..... (3-111.b)}$$

$$\frac{\partial S_1}{\partial \rho} = \frac{EI_3}{L}\left(\overline{C}'_{13}\overline{\theta}_{13} + \overline{C}'_{23}\theta_{23}\right) \quad \text{..... (3-111.c)}$$

where:- $\overline{C}' = \dfrac{\partial \overline{C}}{\partial \rho}$

and ρ = the axial force parameter $\left(\rho\right) = \dfrac{\lambda^2}{\pi^2}\left(\mu - C_{b3} - C_{b2} - C_{T3} - C_{T2}\right)$, $\lambda^2 = L^2/(I/A)$ ..... (3-111.d)

$$\frac{\partial \rho}{\partial u_1} = \frac{\partial \rho}{\partial \theta_{13}} = \frac{-\lambda^2}{\pi^2}\left(2\overline{b}_{13}\left(\theta_{13} + \theta_{23}\right) + \left(\theta_{13} + \theta_{23}\right)^2 \frac{\partial \overline{b}_{13}}{\partial \rho}\frac{\partial \rho}{\partial \theta_{13}} + 2\overline{b}_{23}\left(\theta_{13} - \theta_{23}\right) + \right.$$

$$\left.\left(\theta_{13} - \theta_{23}\right)^2 \frac{\partial \overline{b}_{23}}{\partial \rho}\frac{\partial \rho}{\partial \theta_{13}} + \frac{r}{L}\phi\,\overline{t}_{13} + \frac{r}{L}\phi\frac{\partial \overline{t}_{13}}{\partial \rho}\frac{\partial \rho}{\partial \theta_{13}}\right) \quad \text{..... (3-111.e)}$$

$$\frac{\partial \rho}{\partial \theta_{13}} = 1 + \frac{\lambda^2}{\pi^2}\left[\overline{b}'_{13}\left(\theta_{13} + \theta_{23}\right)^2 + \overline{b}'_{23}\left(\theta_{13} - \theta_{23}\right)^2 + \frac{r}{L}\phi\,\overline{t}'_{13}\right] \quad \text{.....(3-111.f)}$$

By the same procedure described above and by introducing some new symbols in order to simplify the element 3-D compiled **T.S.M.** in local coordinates, one can have:-

$$t_{11} = \frac{EI_3}{L}\left(\overline{C}_{13} + \frac{\overline{G}_{13}\overline{GN}_{13}}{\overline{H}_{13}}\right) \quad \text{..... (3-112.a)}$$

$$t_{12} = \frac{EI_3}{L}\left(\overline{C}_{23} + \frac{\overline{G}_{23}\overline{G}N_{13}}{\overline{\overline{H}}_{23}}\right) = t_{21} \quad \text{(3-112.b)}$$

$$t_{13} = \frac{EI_3}{L}\left(\frac{\overline{G}N_{13}\overline{G}_{12}}{\overline{\overline{H}}_{12}}\right) = t_{31} \quad \text{(3-112.c)}$$

$$t_{14} = \frac{EI_3}{L}\left(\frac{\overline{G}N_{13}\overline{G}_{22}}{\overline{\overline{H}}_{22}}\right) = t_{41} \quad \text{(3-112.d)}$$

$$t_{15} = \frac{EI_3}{L}\left(\overline{G}N_{13}\,SS\right) = t_{51} \quad \text{(3-112.e)}$$

$$t_{16} = \frac{EI_3}{L}\frac{\overline{G}N_{13}}{\overline{\overline{H}}} = t_{61} \quad \text{(3-112.f)}$$

$$t_{22} = \frac{EI_3}{L}\left(\overline{G}N_{13}\frac{\overline{G}_{12}}{\overline{\overline{H}}_{12}}\right) \quad \text{(3-113.a)}$$

$$t_{23} = \frac{EI_3}{L}\left(\overline{G}N_{23}\frac{\overline{G}_{12}}{\overline{\overline{H}}_{12}}\right) = t_{32} \quad \text{(3-113.b)}$$

$$t_{24} = \frac{EI_3}{L}\left(\overline{G}N_{23}\frac{\overline{G}_{22}}{\overline{\overline{H}}_{22}}\right) = t_{42} \quad \text{(3-113.c)}$$

$$t_{25} = \frac{EI_3}{L}\left(\overline{G}N_{23}\,SS\right) = t_{52} \quad \text{(3-113.d)}$$

$$t_{26} = \frac{EI_3}{L}\frac{\overline{G}N_{23}}{\overline{\overline{H}}} = t_{62} \quad \text{(3-113.e)}$$

$$t_{33} = \frac{EI_2}{L}\left(\overline{C}_{13} + \frac{\overline{G}N_{12}\overline{G}_{12}}{\overline{\overline{H}}_{12}}\right) \quad \text{(3-114.a)}$$

$$t_{34} = \frac{EI_2}{L}\left(\overline{C}_{22} + \frac{\overline{G}N_{12}\overline{G}_{22}}{\overline{\overline{H}}_{22}}\right) = t_{43} \quad \text{(3-114.b)}$$

$$t_{35} = \frac{EI_2}{L}\left(\overline{G}N_{12}\,SS\right) = t_{53} \quad \text{(3-114.c)}$$

$$t_{36} = \frac{EI_2}{L}\frac{\overline{G}N_{12}}{\overline{\overline{H}}} = t_{63} \quad \text{(3-114.d)}$$

$$t_{44} = \frac{EI_2}{L}\left(\overline{C}_{12} + \frac{\overline{G}N_{22}\overline{G}_{22}}{\overline{\overline{H}}_{22}}\right) \quad \text{(3-115.a).}$$

$$t_{45} = \frac{EI_2}{L}\left(\overline{G}N_{22}\,SS\right) = t_{54} \quad \text{(3-115.b)}$$

$$t_{46} = \frac{EI_2}{L}\frac{\overline{G}N_{22}}{\overline{H}} = t_{64} \quad \text{.....(3-115.c)}$$

$$t_{55} = \frac{Ct}{L} + SS^2\frac{EI}{L} \quad \text{.....(3-116.a)}$$

$$t_{56} = \frac{SS}{\overline{H}}\frac{EI}{L} = t_{65} \quad \text{.....(3-116.b)}$$

$$t_{66} = \frac{\pi^2}{\overline{H}} \quad \text{.....(3-117)}$$

$$\left(\overline{G}_{13} = 2\bar{b}_{13}\left(\theta_{13}+\theta_{23}\right) + 2\bar{b}_{23}\left(\theta_{13}-\theta_{23}\right) + \frac{r}{L}\phi\bar{t}_{13} = \frac{\partial s_6}{\partial u_1}\Big/EAL\right) \quad \text{.....(3-118.a)}$$

$$\left(\overline{G}_{23} = 2\bar{b}_{23}\left(\theta_{13}+\theta_{23}\right) + 2\bar{b}_{13}\left(\theta_{13}-\theta_{23}\right) + \frac{r}{L}\phi\bar{t}_{23} = \frac{\partial s_6}{\partial u_2}\Big/EAL\right) \quad \text{.....(3-118.b)}$$

$$\left(\overline{G}_{12} = 2\bar{b}_{12}\left(\theta_{12}+\theta_{22}\right) + 2\bar{b}_{22}\left(\theta_{12}-\theta_{22}\right) + \frac{r}{L}\phi\bar{t}_{12} = \frac{\partial s_6}{\partial u_3}\Big/EAL\right) \quad \text{.....(3-118.c)}$$

$$\left(\overline{G}_{22} = 2\bar{b}_{22}\left(\theta_{12}+\theta_{22}\right) + 2\bar{b}_{12}\left(\theta_{12}-\theta_{22}\right) + \frac{r}{L}\phi\bar{t}_{22} = \frac{\partial s_6}{\partial u_4}\Big/EAL\right) \quad \text{.....(3-118.d)}$$

$$\frac{\partial S_6}{\partial\rho} = \frac{\partial\mu}{\partial\rho} = \overline{H} = \frac{\pi^2}{\lambda^2} + \frac{1}{\zeta^2}\left(\overline{b}'_{13}\left(\theta_{13}+\theta_{23}\right)^2 + \overline{b}'_{23}\left(\theta_{13}-\theta_{23}\right)^2 + \frac{r\phi}{L}\left(\overline{t}'_{13}\theta_{13} + \overline{t}'_{23}\theta_{23}\right)\right) + \frac{1}{\zeta^2}\left(\overline{b}'_{12}\left(\theta_{12}+\theta_{22}\right)^2 + \overline{b}'_{22}\left(\theta_{12}-\theta_{22}\right)^2 + \frac{r\phi}{L}\left(\overline{t}'_{12}\theta_{12} + \overline{t}'_{22}\theta_{22}\right)\right) \quad \text{.....(3-118.e)}$$

$\therefore$ eq.(3-118.e) becomes:-

$$\frac{\partial S_6}{\partial\rho} = -EAL\left(H - \frac{\pi^2}{\lambda^2}\zeta_2\zeta_3\right) \quad \text{.....(3-118.f)}$$

$$\frac{\partial S_6}{\partial u_5} = \frac{\partial S_6}{\partial\phi} = -EAL\left\{-\frac{r}{L}\left(\bar{t}_{13}\theta_{13} + \bar{t}_{23}\theta_{23} + \bar{t}_{12}\theta_{12} + \bar{t}_{22}\theta_{22}\right)\right\} \quad \text{.....(3-118.g)}$$

$$\frac{\partial S_6}{\partial u_6} = \frac{\partial S_6}{\partial\mu} = EAL \quad \text{.....(3-118.h)}$$

$$\left(\overline{G}N_{13} = \overline{C}_{13}\theta_{13} + \overline{C}_{23}\theta_{23}\right) \quad \text{.....(3-118.i)}$$

$$\left(\overline{G}N_{23} = \overline{C}_{23}\theta_{13} + \overline{C}_{13}\theta_{23}\right) \quad \text{.....(3-118.j)}$$

$$\left(\overline{G}N_{12} = \overline{C}_{12}\theta_{12} + \overline{C}_{22}\theta_{22}\right) \quad \text{.....(3-118.k)}$$

$$\left(\overline{G}N_{22} = \overline{C}_{22}\theta_{12} + \overline{C}_{12}\theta_{22}\right) \quad \text{.....(3-118.l)}$$

$$\overline{H}_{13} = \frac{\pi^2}{\lambda^2} + \frac{1}{\zeta_3}\left[\bar{b}'_{13}\left(\theta_{13}+\theta_{23}\right)^2 + \bar{b}'_{23}\left(\theta_{13}-\theta_{23}\right)^2 + \frac{r}{L}\phi\,\bar{t}'_{13}\right] \quad \text{.....(3-118.m)}$$

$$\overline{H}_{23} = \frac{\pi^2}{\lambda^2} + \frac{1}{\zeta_3}\left[\bar{b}'_{13}\left(\theta_{13}+\theta_{23}\right)^2 + \bar{b}'_{23}\left(\theta_{13}-\theta_{23}\right)^2 + \frac{r}{L}\phi\,\bar{t}'_{23}\right] \quad \text{.....(3-118.n)}$$

$$\overline{H}_{12} = \frac{\pi^2}{\lambda^2} + \frac{1}{\zeta_2}\left[\bar{b}'_{12}\left(\theta_{12}+\theta_{22}\right)^2 + \bar{b}'_{22}\left(\theta_{12}-\theta_{22}\right)^2 + \frac{r}{L}\phi\,\bar{t}'_{12}\right] \quad \text{.....(3-118.o)}$$

$$\overline{H}_{22} = \frac{\pi^2}{\lambda^2} + \frac{1}{\zeta_2}\left[\bar{b}'_{12}\left(\theta_{12}+\theta_{22}\right)^2 + \bar{b}'_{22}\left(\theta_{12}-\theta_{22}\right)^2 + \frac{r}{L}\phi\,\bar{t}'_{22}\right] \quad \text{.....(3-118.p)}$$

$$\left(\text{SS} = \text{New factor} = -\frac{r}{L}\left(\bar{t}_{13}\theta_{13} + \bar{t}_{23}\theta_{23} + \bar{t}_{12}\theta_{12} + \bar{t}_{22}\theta_{22}\right)\frac{\pi^2}{\lambda^2}\right) \quad \text{.....(3-118.q)}$$

$$\left(\zeta_3 = I_3/I, \zeta_2 = I_2/I\right)$$
$$\left(\lambda = L/\sqrt{I/A}\right) \quad \text{.....(3-118.r)}$$

$\left(\overline{C}_{12}, \overline{C}_{22}, \overline{C}_{13}, \overline{C}_{23}: \text{Stability functions including shear deformation}\right)$
$\left(\bar{b}_{12}, \bar{b}_{22}, \bar{b}_{13}, \bar{b}_{23}: \text{New bowing functions including shear deformation}\right)$
$\left(\bar{t}_{12}, \bar{t}_{22}, \bar{t}_{13}, \bar{t}_{23}: \text{New twisting functions including shear deformation}\right)$

C_t: is the effect of axial force on torsional stiffness

1. for $C_w \neq 0$ and $\left(GJ - \overline{K}\right) > 0$

$$\therefore C_t = \frac{GJ - \overline{K}}{\left(1 - \frac{2}{KL}\tanh\frac{KL}{2}\right)} \quad \text{.....(3-119.a)}$$

$$K = \sqrt{\frac{1}{EC_w}\left(GJ - \overline{K}\right)} \quad \text{.....(3-119.b)}$$

2. for $C_w \neq 0$ and $\left(GJ - \overline{K}\right) < 0$

$$\therefore C_t = \frac{GJ - \overline{K}}{\left(1 - \frac{2}{KL}\tan\frac{KL}{2}\right)} \quad \text{.....(3.119.c)}$$

$$K = \sqrt{\frac{1}{EC_w}\left(\overline{K} - GJ\right)} \quad \text{.....(3-119.d)}$$

3. for $C_w = 0$

$$\therefore C_t = GJ - \overline{\overline{K}} \quad \text{.....(3-119.e)}$$

where:-

$\overline{\overline{K}} = \text{Wagner Effect} = Pr_o$

$P = \text{axial force}$

$r_o = \text{Polar Radius of gyration}$

So, the final 3-D **T.S.M.** of B-C element in local coordinates is:

$$t = \frac{EI}{L}\begin{bmatrix} \zeta_3\overline{C}_{13} + \frac{\overline{G}_{13}\overline{G}N_{13}}{\overline{\overline{H}}_{13}} & \zeta_3\overline{C}_{23} + \frac{\overline{G}N_{13}\overline{G}_{23}}{\overline{\overline{H}}_{23}} & \frac{\overline{G}N_{13}\overline{G}_{12}}{\overline{\overline{H}}_{12}} & \frac{\overline{G}N_{13}\overline{G}_{22}}{\overline{\overline{H}}_{22}} & SS\overline{G}N_{13} & \frac{\overline{G}N_{13}}{\overline{\overline{H}}} \\ \zeta_3\overline{C}_{23} + \overline{G}N_{13}\frac{\overline{G}_{23}}{\overline{\overline{H}}_{23}} & \zeta_3\overline{C}_{13} + \overline{G}N_{23}\frac{\overline{G}_{23}}{\overline{\overline{H}}_{23}} & \frac{\overline{G}N_{23}\overline{G}_{12}}{\overline{\overline{H}}_{12}} & \frac{\overline{G}N_{23}\overline{G}_{22}}{\overline{\overline{H}}_{22}} & SS\overline{G}N_{23} & \frac{\overline{G}N_{23}}{\overline{\overline{H}}} \\ \frac{\overline{G}N_{13}\overline{G}_{12}}{\overline{\overline{H}}_{12}} & \frac{\overline{G}N_{23}\overline{G}_{12}}{\overline{\overline{H}}_{12}} & \zeta_2\overline{C}_{12} + \overline{G}N_{12}\frac{\overline{G}_{12}}{\overline{\overline{H}}_{12}} & \zeta_2\overline{C}_{22} + \overline{G}N_{12}\frac{\overline{G}_{22}}{\overline{\overline{H}}_{22}} & SS\overline{G}N_{12} & \frac{\overline{G}N_{12}}{\overline{\overline{H}}} \\ \frac{\overline{G}N_{13}\overline{G}_{22}}{\overline{\overline{H}}_{22}} & \frac{\overline{G}N_{23}\overline{G}_{22}}{\overline{\overline{H}}_{22}} & \zeta_2\overline{C}_{22} + \frac{\overline{G}N_{12}\overline{G}_{22}}{\overline{\overline{H}}_{22}} & \zeta_2\overline{C}_{12} + \overline{G}N_{22}\frac{\overline{G}_{22}}{\overline{\overline{H}}_{22}} & SS\overline{G}N_{22} & \frac{\overline{G}N_{22}}{\overline{\overline{H}}} \\ SS\overline{G}N_{13} & SS\overline{G}N_{23} & SS\overline{G}N_{12} & SS\overline{G}N_{22} & \frac{C_t}{EI} + SS^2 & \frac{SS}{\overline{\overline{H}}} \\ \frac{\overline{G}N_{13}}{\overline{\overline{H}}} & \frac{\overline{G}N_{23}}{\overline{\overline{H}}} & \frac{\overline{G}N_{12}}{\overline{\overline{H}}} & \frac{\overline{G}N_{22}}{\overline{\overline{H}}} & \frac{SS}{\overline{\overline{H}}} & \frac{\pi^2}{\overline{\overline{H}}} \end{bmatrix} \quad \text{.....(3-120)}$$

while the uncoupled **T.S.M.** in space ***Kassimali*** & ***Abbasnia***[48]

$$t = \frac{EI}{L}\begin{bmatrix} \zeta_3 C_{13} + \frac{G_{13}^2}{\pi^2 H} & \zeta_3 C_{23} + \frac{G_{13}G_{23}}{\pi^2 H} & \frac{G_{13}G_{12}}{\pi^2 H} & \frac{G_{13}G_{22}}{\pi^2 H} & 0 & \frac{G_{13}}{\overline{\overline{H}}} \\ \zeta_3 C_{23} + G_{13}\frac{\overline{G}_{23}}{\pi^2 H} & \zeta_3 C_{13} + \frac{G_{23}^2}{\pi^2 H} & \frac{G_{23}G_{12}}{\pi^2 H} & \frac{G_{23}G_{22}}{\pi^2 H} & 0 & \frac{G_{23}}{H} \\ \frac{G_{13}G_{12}}{\pi^2 H} & \frac{G_{23}G_{12}}{\pi^2 H} & \zeta_2 C_{12} + \frac{G_{12}^2}{\pi^2 H} & \zeta_2 C_{22} + \frac{G_{12}G_{22}}{\pi^2 H} & 0 & \frac{G_{12}}{H} \\ \frac{G_{13}G_{22}}{\pi^2 H} & \frac{G_{23}G_{22}}{\pi^2 H} & \zeta_2 C_{22} + \frac{G_{12}G_{22}}{\pi^2 H} & \zeta_2 C_{12} + \frac{G_{22}^2}{\pi^2 H} & 0 & \frac{G_{22}}{H} \\ 0 & 0 & 0 & 0 & \frac{C_t}{EI} & 0 \\ \frac{G_{13}}{H} & \frac{G_{23}}{H} & \frac{G_{12}}{H} & \frac{G_{22}}{H} & 0 & \frac{\pi^2}{H} \end{bmatrix} \quad \text{.....(3-121)}$$

$$\begin{aligned} G_{13} &= C'_{13}\theta_{13} + C'_{23}\theta_{23} \\ G_{23} &= C'_{23}\theta_{13} + C'_{13}\theta_{23} \end{aligned} \quad \text{.....(3-122)}$$

$$\begin{aligned} G_{12} &= C'_{12}\theta_{12} + C'_{22}\theta_{22} \\ G_{22} &= C'_{22}\theta_{12} + C'_{12}\theta_{22} \end{aligned} \quad \text{.....(3-123)}$$

$$H = \frac{\pi^2}{\lambda^2} + \sum_{j=1,2}\frac{1}{\zeta_j}\left[b'_{1j}\left(\theta_{1j} + \theta_{2j}\right)^2 + b'_{2j}\left(\theta_{1j} - \theta_{2j}\right)^2 \right] \quad \text{.....(3-124)}$$

$C_1 =$
$C_2 =$ Stability function (u=0)

The **T.S.M.** in global coordinates is given by ***Oran*** [72]:

$$T.S.M = R\overline{B}\,t\,\overline{B}^{T}\,R^{T} + \sum_{K=1}^{6} \overline{S}_{K}\,R\,\overline{g}^{(K)}\,R^{T} \quad \text{.....(3-125)}$$

All these values are identified in **App.C.** (in addition to the complete derivation of the uncoupled **T.S.M.**)

CHAPTER FOUR

CABLE ELEMENT BASIC THEORY AND DERIVATION

4.1 Introduction

In this chapter the cable element used in the cable frame interaction structures such as bridges and towers of all types and purposes shall be discussed from all aspects concerning the material, the arrangement and structural details.

The catenary and parabolic representation of cables shall be introduced with the original derivation of temperature contribution in cable axial displacement. The flexural and shear effects shall be explained. All types of guy analysis shall be discussed (i.e. the preliminary and non-linear analysis).

4.2 Types, physical properties, and behavior of cables:-

4.2.1 Types, material and composition of cables:-

A cable may be composed of one or more structural ropes, structural strands, locked coil strands or parallel wire strands.

A **strand**, with the exception of a parallel wire strand, is an assembly of wires formed helically around a centre wire in one or more symmetrical layers and is produced in accordance with the ***ASTM standards A-586 specifications*** [10]. A strand may be used either as an individual load-carrying member, where the radius of curvature is not a major requirement, or as a component in the manufacture of structural rope.

A **rope** is composed of a plurality of strands helically laid around a core and is covered by ***ASTMA-603 standard specifications*** [10], in contrast to the strand, a rope provides increased curvature capability and is used where curvature of the cable becomes an important consideration.

The significant differences between a strand and a rope are:-

a. At equal sizes, a strand has a greater breaking strength than a rope.

b. The modulus of elasticity of a strand is higher than that of a rope.

c. A strand has less curvature capability than a rope.

d. The wires in a strand are larger than those in a rope of the same diameter. Consequently, strand of a given class of coating is more corrosion resistant because of the thicker zinc coating on the larger diameter wires required by the governing ***ASTM*** specifications [97].

For these reasons the structural strand is generally preferred to rope for cable-stayed bridges, and towers, while ropes are suitable in cable-suspended bridges and highly-sagged towers.

The three types of strand configuration are:

a. *The helically-wound strand.*

b. *The parallel wire strand, and*

c. *The locked coil strand.*

The first two types are composed of round wires and the differences lies in their construction. In the first, the wires are formed helically around a centre wire in one or more layers; and in the second all wires are parallel. The normal size range of helical structural strands produced in the USA are of 1/2- 4 in (12-100 mm) diameter with a range of breaking strengths of (15-925) tons for class-A-. Zinc coating. It should be noted that with structural design, it is important to choose the strand so as to obtain the correct modulus of elasticity for the cables.

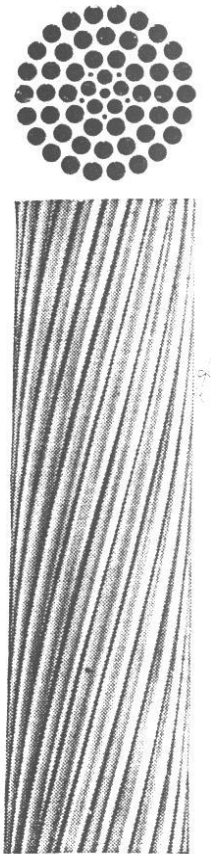

Figure (4-1)

Strand of Twisted Wires

Figure (4-1) shows a typical **strand of twisted wires** whose modulus of elasticity depends on the elasticity of the wires, the internal deformation of the cable, the sag of the cable, or on a combination of these three factors. Hence, the modulus of elasticity is constant but is a function of the force acting on the cable.

On the other hand, figure (4-2), shows the types of the **rope of twisted strands** which are a further step towards economy in the construction of inclined cable bridges and towers. The value of modulus of elasticity for these cables closely approaches that of the plain wire, and this fact has a favourable influence on the deformations because of the live load. The reduction of the value of the modulus of elasticity due to cable sag, however, produces the same percentage of figures as for the locked coil cables. But as there are no

plastic elongations, as in cables, the erection deformations can be accurately calculated in advance. It will be therefore possible to allow for the fatigue strength between 28500 psi and 42600 psi (19.65×10^4 and 29.37×10^4 kN/m^2) provided that anchorages and curves do not impose any reduction.

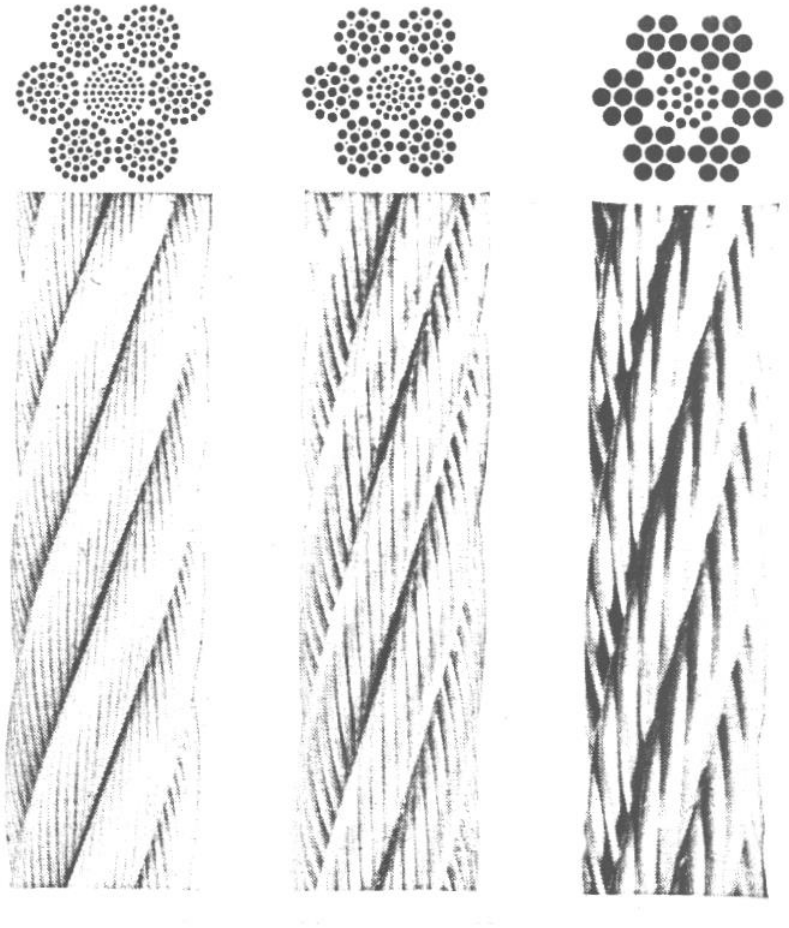

Figure (4-2) Rope of Twisted Strands

The majority of cable-stayed towers use the strand of twisted wires illustrated in figure (4-1) and the three types of rope of twisted strand illustrated in figure (4-2) are used when we have high tensions and low sags.

The majority of the existing cable-stayed bridges use **pre-formed, pre-stretched, galvanized locked-coil wire rope** shown in figure (4-3), this type exhibits more effective protection against corrosion as well as more favorable properties compared with those of a conventional spiral rope manufactured from round wires, so it introduces higher density of the material with higher modulus of elasticity which is almost exactly half-way between the value of the spiral cable and the solid structural steel. The flexibility required at curves is maintained in spite of the above properties because of its spiral construction; moreover,

locked-coil cables are largely insensitive to bearing pressure because the individual layers of profile wires support each other through their face and not just by point contact as in spiral cables [97].

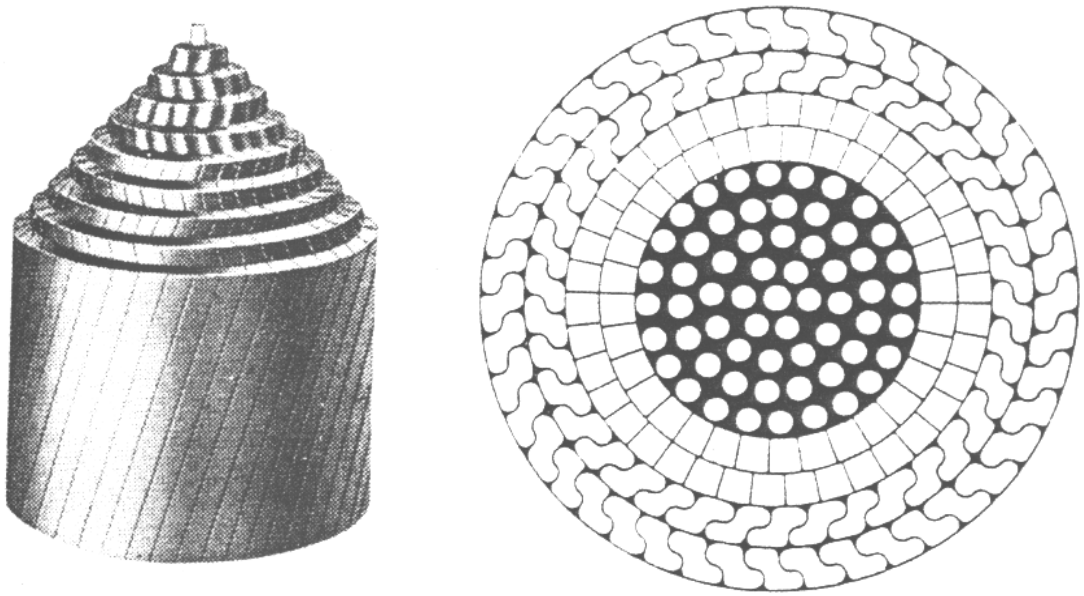

Figure (4-3) Typical Licked-coil wire rope

4.2.2 Pre-stretching

The total elongation or stretch of a structural strand is the result of several component deformations such as those due to its own weight, temperature, and industrial imperfections, however, the pre-stretching meant here is the one called constructional stretch which is caused by the lengthening of the strand lay (pitch length of the wire helix) due to subsequent adjustment of the wires in a strand into a denser cross section under load, this type of stretch is permanent. According to ***ASTM A-586*** the total pre-stretch load should not exceed **55%** of the rated breaking strength of the strand [97].

4.2.3 Modulus of elasticity of the cable

According to ***ASTM A-586*** specifications, the elongation readings for computing the modulus of elastic, they are taken when the strand or rope is stressed to not less than **10%** of the minimum rated breaking strength or more than **90%** of the pre-stretching load. The modulus of elasticity shall not be less than 24×10^6 psi (16.59×10^7 kN/m^2) for 1/2 - 29/16 in (12.7-65.1 mm) nominal diameter strand and 23×10^6 psi (15.86×10^7 kN/321) for 25/8 in (66.6 mm) and larger nominal diameter strands, these values are for normal pre-stretched

helical types strands. For a parallel-wire strand the modulus of elasticity is in the range of 28×10^6 -28.5×10^6 psi (19.30×10^7 - 19.65×10^7 kN/m^2).

The modulus of elasticity of the rope is low for low loads and increases as the load is increased into the normal working range. Creep may occur for sustained loads.

The stiffness of the cable-frame structure depends largely upon the tensile stiffness of the stay cables, the apparent modulus of elasticity "E_f" may be expressed as:-

$$E_f = \sigma / \varepsilon_f \quad \text{.....(4-1)}$$

while the ideal modulus of elasticity of the cable "E_I" under an axial load with its own weight to be considered and a sag "f" is introduced:-

$$E_i = \frac{\sigma}{\varepsilon_f + \varepsilon_e} \quad \text{..... (4-2.a)}$$

but:-

$$\varepsilon_f = \sigma / E_f$$
$$\varepsilon_e = \sigma / E_e \quad \text{.....(4-2.b)}$$

So, eq.(4-2.a) becomes:-

$$E_i = \frac{E_f E_e}{E_f + E_e} \quad \text{.....(4-3)}$$

To find "Δl" and "E_i", one of the analytical approaches must be adopted:-

a. The catenary behavior.

b. The parabolic behavior.

The comparison between the catenary and parabola indicates negligible difference [97]. Therefore, the catenary may be satisfactorily approximated over this length by a parabola, however, both approaches shall be detailed later in this chapter. So, eq.(4-3) becomes after some derivational effort:-

$$E_i = \frac{E_e}{1 + \left[\left(\gamma L_h \right)^2 / 12\sigma^3 \right] E_e} \quad \text{.....(4-4)}$$

If we assume a straight locked-coil steel wire rope eq.(4-4) becomes:-

$$E_i = \frac{10800}{1+\left(2.42\times10^{-3}\right)L_h^2/\sigma^3} \quad \left(\text{ton}/\text{in}^2\right) \qquad \text{.....(4-5)}$$

"L" in ft. and "σ" is in ton/in^2

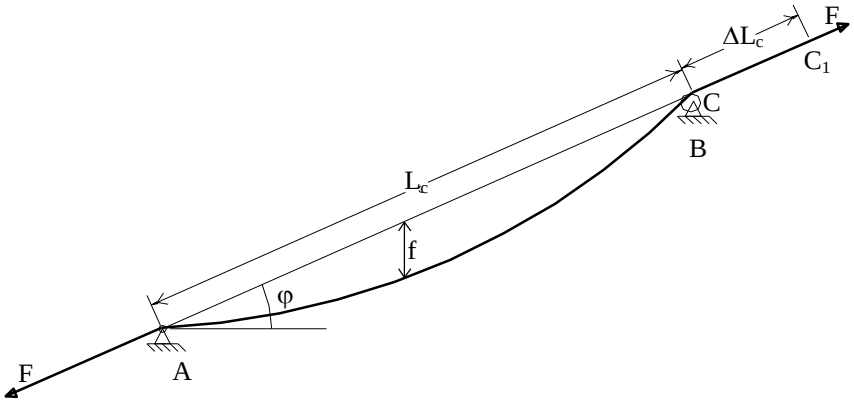

Figure (4-4.a) the Inclined Cable Arrangement

In the above equations:-

L_c : the chord length of cable.

L : the arc length of cable.

L_h : the horizontal length = L_c; cos φ = l

φ : the cable inclination

σ : tensile stress in the cable = F/A

F : tensile axial force

A : cable cross-sectional area

γ : specific gravity of the cable

E_e : the straight cable modulus of elasticity

E_i : the sagged cable modulus of= elasticity

ε_f : Δl -Δl1/ L_c

Δl : L - L_c , Δl_1 = L - L_{c1}

The above equations are illustrated in figure (4-4.a, b).

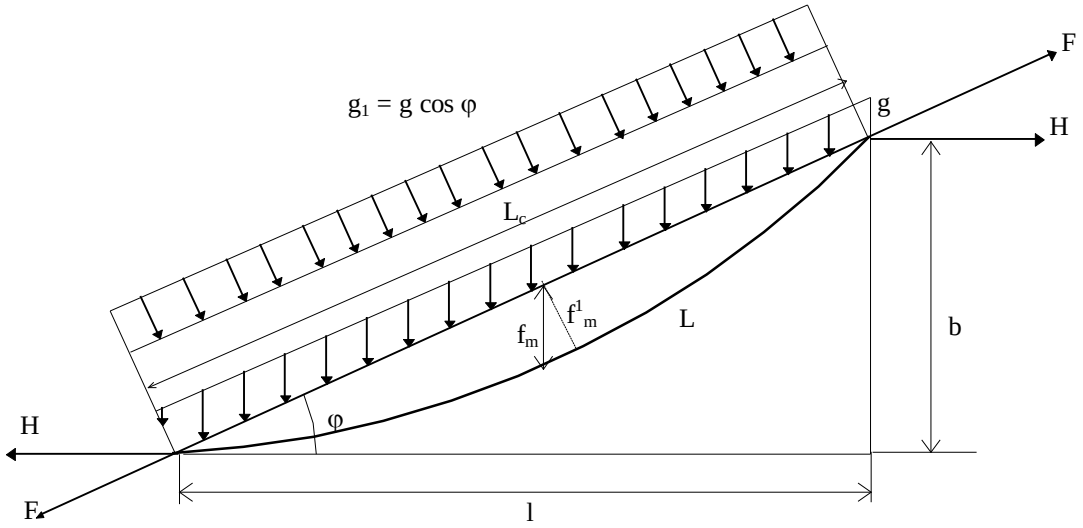

Figure (4-4.b) Uniformly Loaded Cable

Assuming numerical values for span "L" and stresses "σ", ***M.S. Trotisky***[97] formulated eq.(4-5) to illustrate the (E_i-L-σ) cable behavior, this behavior is shown in figure (4-5).

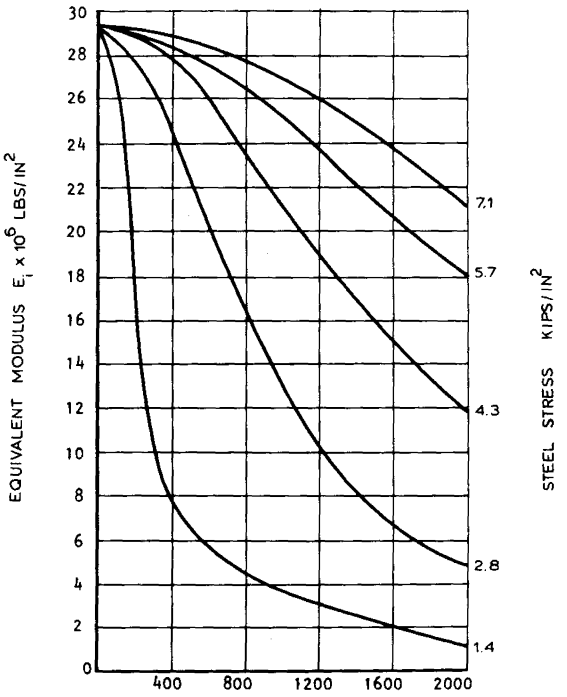

Figure (4.5) Variation of Ideal Modulus with Span Length

4.2.4 Permissible strength of the cables:-

The general factor of safety of the cable may be taken as K1 = 2.5 following practice in USA and Europe. This coefficient represents the reserve of the strength of the cable with respect to the loading. The calculated strength of the cable may be expressed as:-

$$R = R_{a11} \cdot K \cdot m_1 m_2 \quad \text{.....(4.6)}$$

where $m_1 = 0.8$ is the coefficient of the performance of material in structure.

$$m_2 = \frac{1}{K_{m_1} K_{res}} = 0.78$$ (some authors take it as 0.74)

$K_{res} \approx 2$

4.2.5. Flexural and shear behavior of bent cable:-

Under longitudinal tension applied to a spirally wound rope, transverse forces are developed between the individual wires. This reduces the ultimate capacity below the sum of the capacities of the individual wires for two reasons:-

a) A combined stress system exists at the contact areas.

b) plastic flow at the contact areas causes necking of the wires and results in reduction in their cross-sectional areas.

When rope is bent over a saddle, two additional effects are present:-

c) bending stresses are set up, and

d) transverse radial forces are applied to the rope.

For single wire of diameter "d" bent to a diameter "D" at its centerline, the bending stress is calculated (see figure.4-6) as follows:-

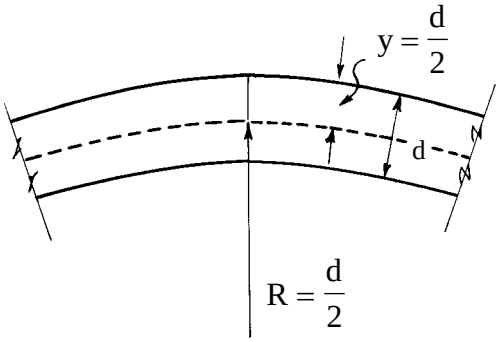

Figure (4.6) Bending stress of wire.

After substituting into the formula f = My/I the value M = EI/R, we have:

$$f = E\frac{y}{R} = E\frac{d}{D} \quad \text{.....(4.7)}$$

where "E" is the modulus of elasticity of the wire.

For a spirally wound rope, over a saddle of a moderate length, it appears probable that shear movement can occur between adjacent wires, and that the bending stress approaches the value given in (eq.4-7), with "d" equal to the diameter of the rope.

Considering that each wire in the strand makes one complete turn around the core of a strand, each wire takes either the upper or lower position and the corresponding stresses change their signs. This results in the equalizing of the stresses in the wires, in addition, because of the friction effect under transverse compression, there is a certain redistribution of the stresses among the separate wires in the cross-section of the cable. Because of these factors the bending of the cables over a saddle is disregarded in the analysis and the cable is not represented as a beam-column element, so the flexural rigidity and the shear rigidity are ignored. However the "I" and the "u" values shall be calculated and included in the case studies of this work to illustrate how small they are.

In spite of a small value of the shear parameter "u" of the cable, there is a small notation here. It must be considered that the shape factor "n" of cable cannot be calculated as ($n = 1.11$) for the corresponding solid circular section but as it is obvious from figures (4-1, 4-2 and 4-3) the cable cross section consists of a number of ropes and wires and since the actual shape factor definition is:-

$$n = \frac{A}{A_w} \quad \text{.....(4.8)}$$

A_w: is the web area that is nearly associated with shear flow, so (eq.4.8) becomes:-

$$n = \frac{d_c}{n_r d_r^2} \quad \text{.....(4.9)}$$

where:

d_c: is the diameter of the cable.

d_r: is the diameter of the rope.

n_r: number of ropes the cable consisting of as it is illustrated in figure (4-7).

Although, the "n" value makes no sense since the small effect of shear in the contribution of the cable element stiffness but it obviously differ from the (1.11) value of (eq.4.8-a), again this equation has an originality.

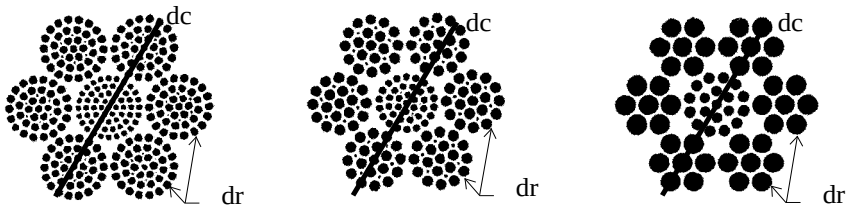

Figure (4-7) Rope diameter and cable diameter

More important is the effect of the transverse compression of the cables, which results in bi-axial stress of different sign in the wires, which leads to reduced bearing capacity of the material [97].

The above argument means that there is no bowing effect to be added to the axial displacement. The torsional effect however dose affect the axial displacement since the same (***SS*** effect) is applied in this case but the technique used in the cable-tower interaction joints does not permit the cable to twist since it transmits the twisting moments applied on the cables due to joint movements of rockers connected to the point of interaction between cable and mast.

4.3 Cable-structure interaction and methods of connecting:-

4.3.1 Idealized interaction:-

In the analysis or design of cable-stayed towers or bridges, different combinations are possible between supports for the towers and cable attachment to them, as shown in table (4-1). The actual interaction is detailed in the next section.

The tower base, generally is either fixed (as in short span cable-stayed and cable-suspended bridges, and some types of guy towers) or pin (as in most guy towers and long-span stay bridges).

The pin-connections are subjected to very heavy bearing stresses in addition to their complicated erection, rocker-towers, pin bearing at the base, afford the most economic and scientific design for bridges of longer span, they eliminate the stresses from unbalanced cable forces without requiring movable saddle construction, if rocker tower are adopted, they must be secured against tipping during erection. In addition this type of connection

prevents the cable shortening owing to the 3-D effect (***SS*** effect) caused by twisting moments induced by the lateral movement of the connected joints.

Table (4-1): Types of cable - tower interaction

BASE	LEGEND: FIXED SADDLE ROLLER OR ROCKER SADDLE			
FIXED	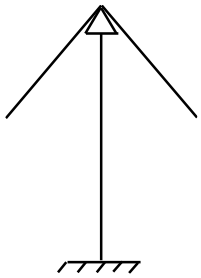	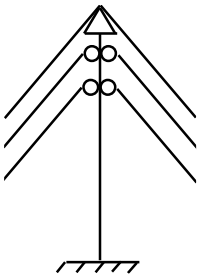	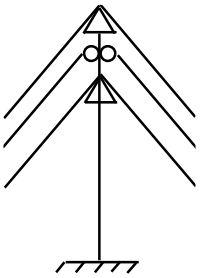	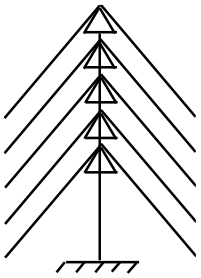
PIN-BEARING	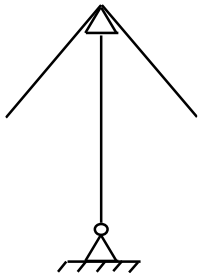	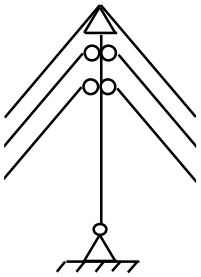	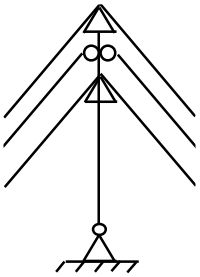	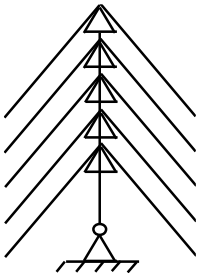

When fixed base is used then the tower is firmly anchored at the base of the tower pedestals, it is free to deflect longitudinally under the deformations of the cables when they are fixed to tower.

The cables are generally continuous over saddles located inside the towers, saddles are either bolted to the supports or provided with rollers, when fixed saddles are used, the resultant unbalanced horizontal forces must be calculated and allowed in the design of the tower, unless it is of the rocker type.

If the saddles are movable, the eccentricity of the vertical reaction under various loading conditions must be accounted for. The roller support for the saddle permits its horizontal movement. The resultant tensions of the cable should pass through the middle of the roller nest to give an even distribution of stress. The friction of the rollers is so small that the angle of inclination of the resultant reaction is negligible.

Instead of circular rollers, rockers may be used so as to furnish a greater diameter thereby reducing friction and roller bearing stress. Rockers, however, must be secured against excessive motion liable to cause overturning. Rollers, meanwhile serve to reduce the

bending stresses in the towers due to an unbalanced horizontal cable pull resulting from special loading conditions and temperature. On the other hand, they are expensive, add erection complications, increase maintenance, and merely substitute eccentric vertical loading for the unbalanced horizontal pull. On, the whole, fixed saddles provide a simple and safer solution [97]. But this type increases the possibility of cable shortening due to twisting movements induced by lateral joint movements (***SS*** effect).

4.3.2 Actual interaction

The fixed and pin saddles described earlier give an idealized picture of the field fixed or movable cable supports, a typical arrangement of these supports differs from one structure to another, they are usually provided at the top of the tower as well as at intermediate locations along the tower, depending on the number of the cables used. These supports are either:-

- Fixed to the tower by means of welding or riveting.
- Movable supports by means of rocker or roller devices.

There are other effects that must be taken into considerations such as anchoraging cables to pedestals, cable numbers and cable spacing and arrangement.

4.4 The Guy Analysis:

The guy analysis is divided in a way which depends on the behaviour of inclined cable under its own weight, this follows two approaches:

* The exact catenary approach.
* The approximate parabola approach.

When the required data of cables (such as dimensions, and initial tensions) for the certain structure (towers or bridges) are unknown, a type of analysis called the **preliminary** analysis must be used in order to evaluate the initial values of cable tensions in order to include it in the next stage of analysis of the structure which is the non-linear analysis.

4.4.1 The exact catenary approach:-

The differential equation of the equilibrium curve shown in figure (4-8), is:-

$$\frac{d^2y}{dx^2} = \frac{-w\sec\varphi}{-H} \qquad \text{.....(4.10)}$$

where:

φ is the inclination of the cable to the horizontal at any distance "x" since

$\tan\phi = \frac{dy}{dx}$, so (eq.4.10) may be written as:-

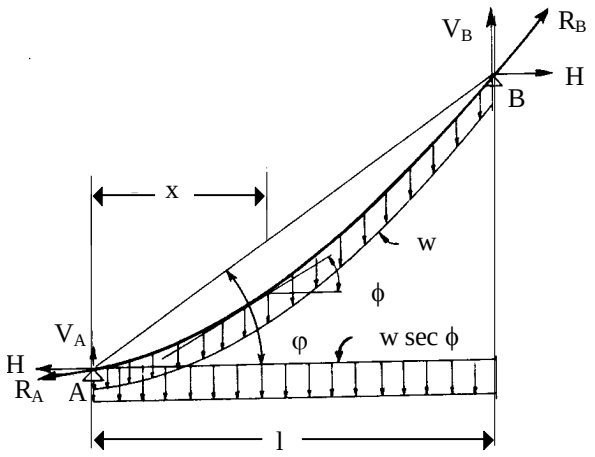

Figure (4-8): Inclined cable under its own weight

$$\frac{d^2y}{dx^2} = -\frac{w}{H}\left[1+\left(\frac{dy}{dx}\right)^2\right]^{\frac{1}{2}} \quad \text{.....(4.11)}$$

by integrating and organizing, we have:-

$$y = \frac{1}{2\frac{w}{H}}\left(e^{w/h\cdot x} + e^{-w/h\cdot x} - 2\right) \quad \text{.....(4.12)}$$

This equation is called **the catenary equation**; therefore, a cable under its own weight hangs in a catenary.

When the stay is taken to be a straight bar then the elastic stretch or elongation is:-

$$\Delta L_s = \frac{\left(F_1 - F_0\right)}{EA\cos\varphi_0^2} l \quad \text{.....(4.13)}$$

Where:

F_1: the tensile axial force after first stage of loading.

F_o: the initial tensile axial force after first stage of loading.

l: the horizontal chord length = $L_c \cos\varphi_o$

φ_0 the initial cable inclination.

E: the modulus of elasticity of cable.

A: the cross sectional area of cable.

w: the load intensity (weight of the cable (force/area).

H: the horizontal component of the cable tensile force.

f: the sag of cable.

4.4.2 The approximate parabolic approach:-

If the sag ratio $\eta = f / l$ is small, all the formula for the catenary may be replaced, with sufficient accuracy, by the formula for parabolic cables, this means that the cable is subjected to uniform vertical load only. Although parabola is only an approximation to the exact catenary analysis, the parabolic equation is familiar to most practicing engineers[23]. The elastic stretch or shortening in the cable is:-

$$\Delta L_s = \frac{HL_c}{AE\cos\varphi_o} \quad \text{.....(4.14)}$$

4.4.3 The preliminary analysis:-

The first step to non-linear analysis is to obtain an approximate set of reactions at the guy level. The tower is assumed to behave as a continuos beam over rigid supports, with the supports located at each guy level. A standard linear analysis is utilized in which the tower segments between supports are treated as beam-column elements using the ordinary (4) and (2) stability functions at $\rho=0$, so the tower is treated as an ordinary structure (with no cables) having either solid section or lattice section depending on the type of tower, the reactions of the rigid supports then represents the initial guy reactions which are ready to enter the non-linear analysis. The initial tensions are calculated in the cables by the following means [23]:-

- Measuring accurately the position of the end joints and control the sag of the cable.
- Controlling accurately the zero stress length and final length of the cable due to initial tensions.
- If cable is attached to eye bar links at the end initial tension can be controlled by measuring the stress in the eye bar.

4.4.4 The non-linear cable analysis:-

In spite of the fact that the behavior of the material of the structural elements in cable-stayed structures is linear-elastic, the overall load displacement relationship for the structure is non-linear under normal design loads [66], the overall non-linear behavior originates from four primary sources:-

1. The non-linear axial force-elongation relationship for the inclined cable stays due to sag caused by their own weight.
2. The non-linear axial force and bending movement deformation relation for the towers and masts (i.e. the stability non-linearity including the bowing and 3-D effect (***SS*** effect).
3. The geometrical changes caused by large displacement under normal design loads.
4. Special effects of non-linearity (such as, temperature, industrial imperfections, support yields, etc.) both in mast and cables.

The second, third and fourth effects are detailed earlier in **chapter 3,** .the first effect plus the special effects of the cable must be handled in order to establish the **T.S.M.** of the cable element.

The bowing and (***SS*** effects) cannot be taken into account in the cable elements since they cannot be treated as a flexural element or beam-column element, this means no flexural rigidity, though no application of stability, bowing and twisting functions.

The non-linear behavior of the cable is treated by many procedures but the most important one is **the equivalent modulus of elasticity technique**.

As mean showed earlier in this chapter that the "E" value of the cable is a function of many variables (see eq.4.4-4.5) when the cable tension increases , the sag decreases (see figure 4-8), and the apparent axial stiffness of the inclined cable increases. A convenient method to account for this variation in the cable axial stiffness is to consider an equivalent straight chord member "L" with an equivalent modulus of elasticity. This combines both the effect of material and geometrical deformations such that the axial stiffness of the equivalent chord member becomes equal to the apparent axial stiffness of the actual curved cable, this concept was first introduced by ***Ernst***, and has been verified by several additional investigators.

This "Equivalent" of the cable is given by two approaches

a. The tangent "$E_{eq.}$"

b. The secant "$E_{eq.}$"

$$\tan E_{eq.} = \frac{E_e}{1 + \frac{(wl)^2 AE_e}{12F_i}} \quad \text{.....(4.15)}$$

Notice that this equation is another form of (eq.4.4), while:-

$$\sec E_{eq.} = \frac{E_e}{1 + \frac{(wl)^2 (F_i + F_f) AE_e}{24F_i^2 F_f^2}} \quad \text{.....(4.16)}$$

in which:-

$E_{eq.}$: The equivalent modulus of elasticity of the cables.

E_e: The effective modulus of elasticity of the cables (or the straight cable modulus of elasticity).

l: The horizontal projection of the cable chord length.

A: The cross sectional area of the cable.

F_i, F_f: The initial and final cable tensions respectively.

w: Weight per unit length of the cable.

Equation (4.15) gives the tangential or instantaneous value of the equivalent modulus when the tension in the cable equals "F_i" or when the cable tensile stress is equal to "σ" as shown in figure (4-9), if the cable changes from "F_i" to "F_f" during the application of a certain load increment (which is equivalent to a change in cable stress from "σ_I" to "σ_f" as shown in figure (4-9), then the secant value of the equivalent modulus of elasticity over the load increases.

Let us now see what happens in the non-linear analysis of the cable-frame interaction, and especially as far as the cable is concerned:-

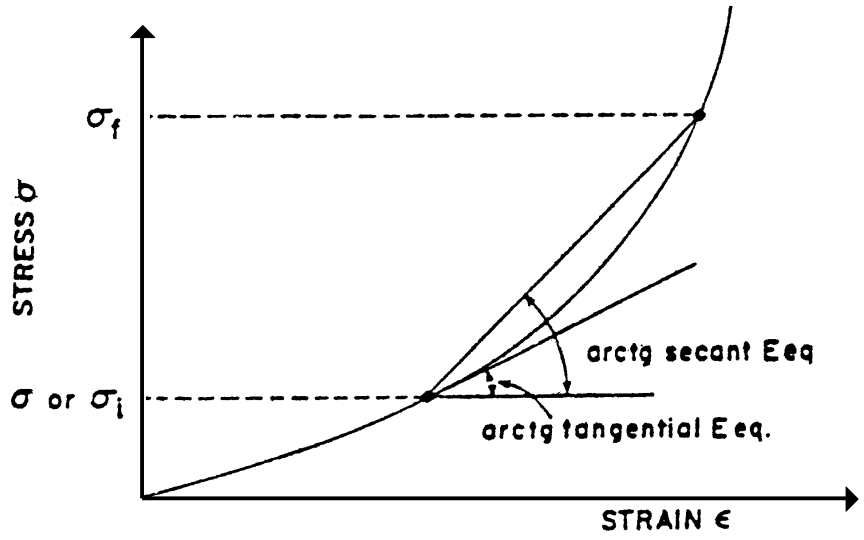

Figure (4-9): Non-linear stress-strain relationship for a cable stay

In the non-linear analysis, all cables are treated as straight members and represented geometrically by their chords, the actual shape, however, of a cable hanging freely under its own weight, tensioned from both ends is a catenary as it is mentioned earlier in this chapter. It can be replaced by parabola to avoid tedious calculations and especially when sags are smaller or tensions are higher than true length of the curved cable (arc length "L") which can be expressed by a series:-

$$L = L_c\left(1+\frac{W^2\cos^4\varphi_o}{24H^2}-\frac{W^2\cos^4\varphi_o}{640H^4}+\cdots\right) \quad \text{.....(4.17)}$$

where: "W" is the total weight of the cable, the third and subsequent terms inside the bracket are very small compared to the first and second terms, so they can be neglected, then the differentiation of (eq.4.17) yields:-

$$ds=\left(1+\frac{W^2\cos^4\varphi_o}{24H^2}\right)\Delta L-\left(\frac{L_cW^2\cos^4\varphi_o}{12H^3}\right)dH \quad \text{.....(4.18)}$$

which can be transformed to the elongation of the cable due to the change in "H":-

$$\frac{ds}{dH}\approx\frac{S}{EA\cos\varphi_o} \quad \text{.....(4.19)}$$

where "S" equal to "L".

Therefore, the axial deformation of the chord due to the change in "H" is:-

$$\frac{dL_c}{dH} = \frac{S}{EA\cos\varphi_o} + \frac{L_c W^2 \cos^4\varphi}{12H^3} = \frac{HL_c}{AE\cos\varphi_o}\left(1 + \frac{w^2 l^2}{12H^2}\right) \quad \text{.....(4.20)}$$

On the right hand side of this equation, the first term, is linear representation of the elastic stretch of the cable (i.e eq.4.13 or 4.14), while the second term, is non-linear and inversely proportional to "H^3". If a parabola cable shape is adopted, a modified stiffness of cable should be used in the analysis, so:-

$$EA)_{mod.} = r(AE) \quad \text{.....(4.21-a)}$$

where:

$$r = \frac{1}{1 + \dfrac{w^2 \cos^5\varphi_o EA}{12H^3}} \quad \text{.....(4.21-b)}$$

However, "r" varies as "H" varies as "H" increases from "H_1" to "H_2", an average cable stiffness should be used so that:-

$$EA)_{mod.} = r_1(EA) \quad \text{.....(4.21-c)}$$

where:

$$r_1 = \frac{1}{1 + \dfrac{w^2 \cos^5\varphi_o EA\left(H_1 + H_2\right)}{12H_1^2 H_2^2}} \quad \text{.....(4.21-d)}$$

Which means an iterational technique of solution must be adopted and that the cable stiffness is adjusted in every iteration, however, the non-linear effect can be compensated by applying a pair of imaginary forces "K" at the ends of each cable, instead of changing the cable matrices in each step.

So, for the "h^{th}" iteration, the condition of equilibrium gives:-

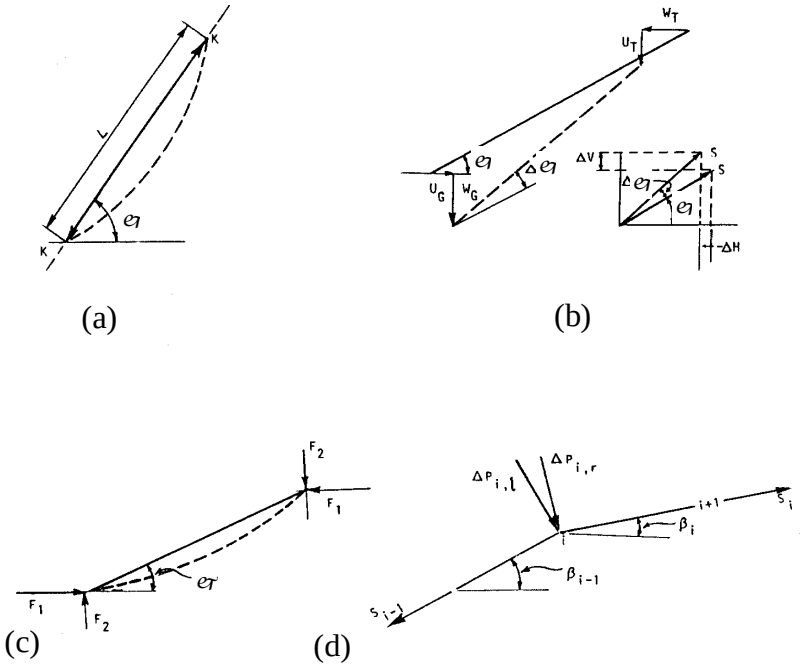

Figure (4-10): Geometrical non-linearity of cable element (a) imaginary forces "K" (b) the formed cable (c) total imaginary loads of cable (d) imaginary loads of tower.

$$K = \frac{EA)_o - EA)_h}{EA)_o} F_{(n-1)} \quad \text{.....(4.22)}$$

The second non-linear effect of cables is caused by the change of the angle "φ" due to displacement at both ends, this change in slope, or the rotation of the chord, is small compared with the original slope, therefore the change in vertical and horizontal components of the cable forces are approximately:-

$$\Delta H = -F \sin\varphi \Delta\varphi$$
$$\Delta V = S \cos\varphi \Delta\varphi \quad \text{.....(4.23-a)}$$

where:

$$\Delta\varphi = \frac{\left(u_G + w_T\right)\sin\varphi + \left(w_G - u_T\right)\cos\varphi}{L_c} \quad \text{.....(4.23-b)}$$

Summing up both non linear effects of cables and the imaginary forces which have to be applied at the end of the cables after "n^{th}" iteration is shown in figure (4-10):-

$$F_1 = F_n \sin\varphi\Delta\varphi - K_n \cos\varphi$$
$$F_2 = F_n \cos\varphi\Delta\varphi - K_n \sin\varphi \quad \text{.....(4.24)}$$

The above detailed non-linear behavior can be replaced by the equivalent modulus of elasticity of cable (eq.4.15-4.16) to include all the above geometrical non-linear effects in addition to any material with non-linear behavior, so introducing an additional effect of temperature:-

$$\Delta L_{temp.} \approx \varphi t^0 \times L = \varphi t^0 \times L_c\left(1+\frac{w^2 l^2 \cos^2 \varphi_o}{24H^2}\right) \quad \text{.....(4.25)}$$

And rearranging all the effects of parabolic equation we have what we called the cable non-linear equation:-

$$f(H) = \frac{L_c}{AE_e} H^3 - H^2\left[\Delta L_c + \frac{H_o L_{c_O}}{AE_e \cos\varphi_o}\left(1+\frac{w_o^2 l^2}{12H_o}\right) - \frac{L_{c_o}}{24} w_o^2 l^2 \frac{\cos^2 \varphi_o}{H_o^2} - \varphi t_c^o L_c\right] +$$

$$H\frac{w^2 l^2 L_c}{12AE_e} - \frac{L_c w^2 l^2 \cos^2 \varphi}{24}\left(1-\varphi t^0\right) = 0 \quad \text{.....(4.26)}$$

Knowing the initial and final geometry (i.e. $\Delta L_c = L_c - L_{c_o}$), the change of temperature and the change of vertical load, if any, a new value of "H" can be solved. This equation is of a third order that may have three roots. The correct root was found to be always larger than the largest value of "H" "e.g.H_2" which will cause either a maximum or minimum f(H). The value of "H_2" was found by solving the quadratic equation for "H" obtained by using $\partial f/\partial H = 0$ and using the positive sign before the square root quantity for the standard solution of the quadratic equation. The correct root of "H" is then found by half interval search between "H_2" and an arbitrary higher value, "H_3", i.e.[23]:-

1. Set $H_4 = \frac{H_2 + H_3}{2}$, then
2. Set $H_2 = H_4$ if $f(H_4) \times f(H_2) > 0$
3. Set $H_3 = H_4$ if $f(H_4) \times f(H_2) < 0$
4. Repeat this process till "H_4" is elevated, then
5. $H = H_{correct} = H_4$

The principle of this method for solving f(H) is shown in figure (4-11).

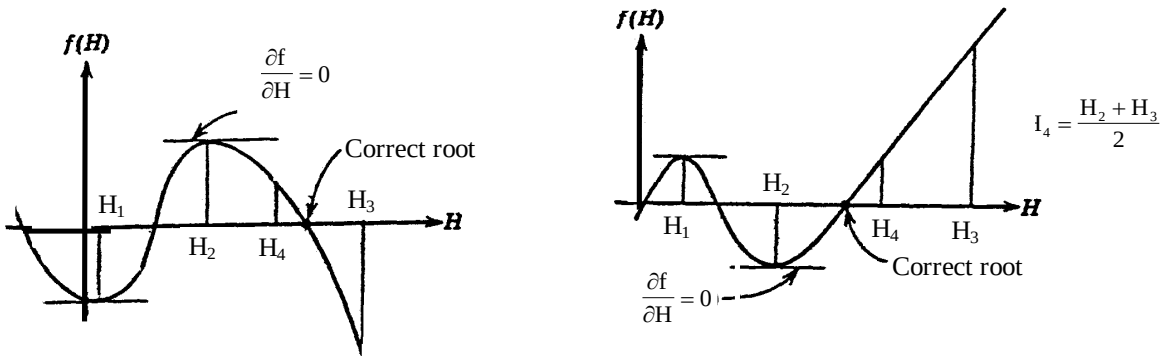

Figure (4-11): Method of finding correct root of cable equation

After this long operation and having solved the value of "H", the value of "ΔH" can be easily determined:-

$$\Delta H = H - H_o \quad \text{.....(4.27)}$$

Then the modified "E" value is :-

$$\overline{E} = E_{mod.} = \frac{\Delta H}{\Delta L_c} \frac{L_{c_o}}{A \cos\varphi} \quad \text{.....(4.28)}$$

This modified "E" value is shown in figure (4-12)

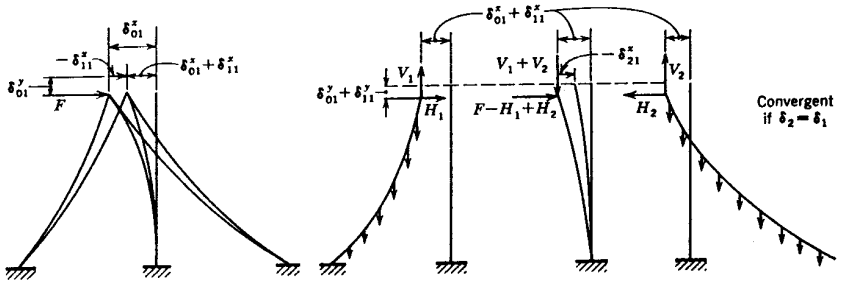

Figure (4-12): Principle of iterational technique in cable structure

For more exact iterational modified "E" method, (eq.4.15) shall be adopted as an initial value of "$E_{eq.}$" then (eq.4.16) shall be adopted as the governing equation of the method of equivalent modulus of elasticity of cables in the rest of "n^{th}" iterations. The algorithm of this technique shall be detailed in the next chapter.

4.5 The T.S.M. of the cable element in space:-

Two approaches are available to analyse cable structure non-linearly:-

a. The finite element approach.

b. The beam-column approach.

In the first approach to alternatives are available. A truss element representation of cable is used with (sag=0) and an increased number of elements is used to decrease the error with "E" value equal to "E_e", hence there is no need for the equivalent "E" value or it may be analysed using one parabolic cable element with the "E" value to be taken from (eq.4.15-4.16) having one D.O.F/each end). In this approach, the **T.S.M.** of cable in local coordinates is:-

$$[\text{T.S.M}] = \left[K_T\right] = \left[K_E\right] + \left[K_G\right] = \frac{AE_{eq}}{L_c}\begin{bmatrix} 1 & -1 \\ -1 & 1 \end{bmatrix} + \begin{bmatrix} G & -G \\ -G & G \end{bmatrix} \quad \text{.....(4.29-a)}$$

where the sub-matrices:

$$[G] = \frac{F}{L_c}\begin{bmatrix} 0 & 0 & 0 \\ 0 & 1 & 0 \\ 0 & 0 & 1 \end{bmatrix} \quad \text{.....(4.29-b)}$$

and $E_{eq.}$ are taken from (eq.4.15-4.16).

In the second approach, which is the approach adopted in the present work, the **T.S.M.** can be determined by the following procedure first adopted by ***Saafan*** [82] (1970):-

The basic idea is based on the original truss element in space and since the finite deflection theory is responsible for obtaining a solution tangent to the actual non-linear force-deflection curve at any intermediate stage, then the elements of this **T.S.M.** "t_{ij}" are obtained as partial derivations of the force vector [Q] with respect to each one of the displacements. Thus:-

$$\text{T.S.M.} = \left[\frac{\partial Q}{\partial U}\right] = \begin{bmatrix} \frac{\partial Q_1}{\partial U_1} & \cdots & \frac{\partial Q_1}{\partial U_6} \\ \vdots & & \vdots \\ \frac{\partial Q_o}{\partial U_1} & \cdots & \frac{\partial Q_6}{\partial U_6} \end{bmatrix}$$

$$= \begin{bmatrix} t_{11} & \cdots & t_{16} \\ \vdots & & \vdots \\ t_{61} & \cdots & t_{66} \end{bmatrix}$$

$$= \frac{E_{eq}A}{L_c}\begin{bmatrix} (l^2+\varepsilon) & lm & ln & -(l^2+\varepsilon) & -lm & -ln \\ ml & m^2+\varepsilon & mn & -ml & -(m^2+\varepsilon) & -mn \\ nl & nm & n^2+\varepsilon & -nl & -nm & -(n^2+\varepsilon) \\ -(l^2+\varepsilon) & -lm & -ln & l^2+\varepsilon & lm & ln \\ -ml & -(m^2+\varepsilon) & -mn & ml & m^2+\varepsilon & mn \\ -nl & -nm & -(n^2+\varepsilon) & nl & nm & n^2+\varepsilon \end{bmatrix}_{(1-\varepsilon)} \quad \text{..... (4.30)}$$

Where:

ε = the axial strain $= \left(\Delta_e \frac{L_c}{L} - \Delta_{temp.}\right)$

Δ_e = (eq.4.14)

$\Delta_{temp.}$ = (eq.4.25)

$Q = [T]^{-1}[P]=[T]^{-1}[N][T][U]=[K][U]$

$[T]^{-1}$: The orthogonal matrix inverse.

[T]: The orthogonal matrix.

[Q]: The stress resultant related to the number of loads {P}

{u}: The column vector of the displacements in member axis

{p}: The column vector of the forces in the member axis =[N]{u}

[N]: The stiffness matrix of the truss element $= E_eA \Big/ L_c \begin{bmatrix} 1 & -1 \\ -1 & 1 \end{bmatrix}$

[U]: The column vector of the displacement in the common axis.

[K]: is the stiffness matrix corresponding to the$[Q]=[T]^{-1}[N][T]$

[T]: is the orthogonal transformation matrix.

$$= \begin{bmatrix} l^2 & lm & ln & -l^2 & -lm & -ln \\ ml & m^2 & mn & -ml & -m^2 & -mn \\ nl & nm & n^2 & -nl & -nm & -n^2 \\ -l^2 & -lm & -ln & l^2 & lm & ln \\ -ml & -m^2 & -mn & ml & m^2 & nm \\ -nl & -nm & -n^2 & nl & nm & n^2 \end{bmatrix} \quad \text{..... 4-31}$$

$E_{eq.}$ is the value of equivalent "E" taken from (eq.4.15, 4.16)

l, m, n: the direction cosines of the member center line.

The member and common coordinates are shown in figure (4.13).

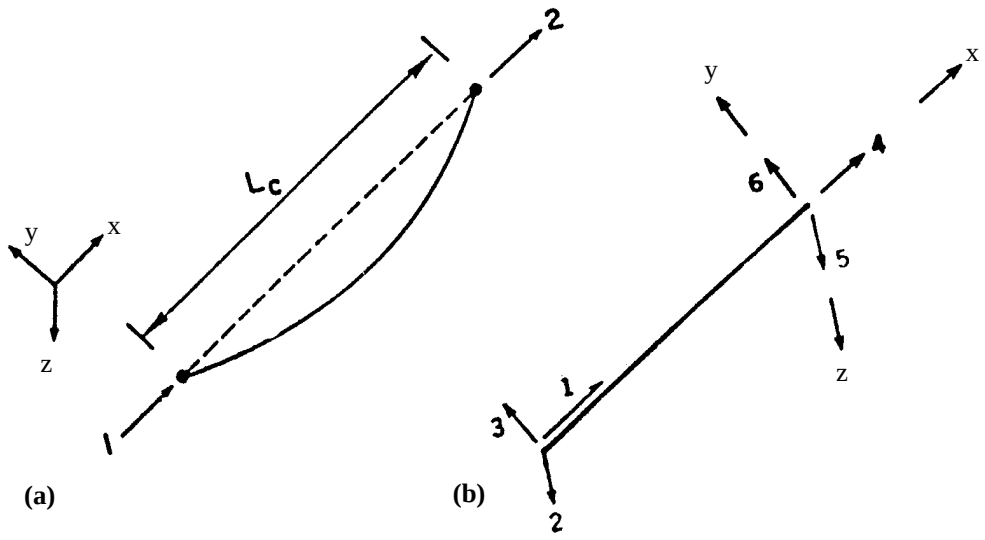

Figure (4-13) typical cable element in local co-ordinates (a) actual element with sag≠0, (b) idealization and D.O.F.

So, (eq.4.30) is the final **T.S.M.** in global coordinates adopted in the work concerning the cable element in space.

CHAPTER FIVE

COMPUTATIONAL TECHNIQUES AND NUMERICAL SOLUTIONS

5.1 Introduction

This chapter presents a description of the different numerical techniques used in tracing the equilibrium path for non-liner stability problems. Then the ***Newton-Raphson*** method used in this work is completely within detail, in addition to brief details about the modifications performed on the conventional ***N-R*** method (***N-R*** iterational technique), to reduce computer time (accelerating convergence) both in beam-column element and cable element.

A brief description of the types of convergence criteria usually used in the computer program is also presented in this chapter.

This chapter also introduces the instability condition of the elastic plane and space steel frames. Further more; the chapter presents different methods for the detection of instability and the calculation of the elastic critical loads.

This chapter finally introduces the primary strategy underlying the development of the multipurpose computer program ***NASCFI*** coded in the present formulation, its description algorithm, and flowchart.

5.2 Tracing the equilibrium path in the non-linear stability problems

Three techniques are commonly used in solving non-linear problems (***Chaies*** and ***Churchill***) [17]:-

5.2.1 Linear incremental method (*LIM*).

5.2.2 Non-Linear incremental method (*NLIM*).

5.2.3 Direct or secant method (*DM*).

5.2.1 Linear incremental method (LIM):

In this method (see figure 5.1) the load is applied in a series of small increments and for each of these increments, the change in deformation is determined using a linear analysis. A so called tangent stiffness matrix {$[K_T]$ or $[\tau]$}, based on geometry and internal forces existing at the beginning of any step (beginning of load increment) is constructed. The total displacement and internal forces existing at the end of any step are obtained by summing the incremental changes in displacements and internal forces up to that point.

At the end of the "n^{th}" increment, the total applied load is given by:-

$$\{P\}_n = \sum_{i=1}^{n} \{\Delta P\}_i \quad \text{.....(5-1)}$$

where $\{\Delta P\}_i$ is the "i^{th}" applied load incremental vector.

Similarly, the displacement at the end of the "n^{th}" increment is:

$$\{X\}_n = \sum_{i=1}^{n} \{\Delta X\}_i \quad \text{.....(5-2)}$$

The tangent stiffness for the "i^{th}" increment is formed for the conditions existing at the end of the previous (i-1) th increment. The linearized simultaneous equations to be solved in each increment are given by:-

$$[\tau]_{i-1}\{\Delta X\}_i = \{\Delta P\}_i \quad \text{.....(5-3)}$$

in which:-

$$[\tau]_{i-1} = \left[\tau\left(\{F\}_{i-1}\ ,\ \{X\}_{i-1}\right)\right] = \left[K_T\right]_{i-1} \quad \text{.....(5-4)}$$

$\{F\}_{i-1}$ is the vector of element nodal forces at the end of the previous load increment. The stiffness matrix is non-linear in terms of internal forces of the members and the updated configurations of the structure from the previous load increment. However, a more calibrate method is used herein which the axial force in the members is extrapolated within the load interval according to the load increment value in order to predict a closer estimate for a particular load increment. This method maybe defined to be the procedure obtained from ***N-R*** method but without any iteration, i.e. without any check on convergence, the two types of ***N-R*** modification associated with this method are the ***N-R*** iteration in a single step without equilibrium correction and the ***N-R*** iteration in a single step with equilibrium correction [(4)].

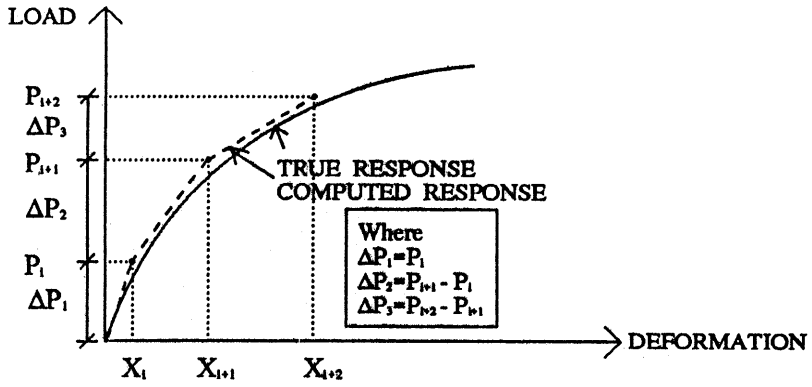

Figure (5-1) Linear Incremental Method.

5.2.2 Non-Linear incremental method (NLIM):

This method is similar to (*LIM*) in both applying load in small increments and then calculating the change in displacement caused by each load increment. The difference between the two methods is in the way of determining incremental displacement. The (*LIM*) employs a **T.S.M.** based on internal forces and deformation existing at the beginning of the load step. A single calculation suffices to give the incremental displacement for that load step. By comparison, the (*NLIM*) is an iterative technique. For any desired load level, an approximate solution is first assumed or calculated; it is then improved step by step via a ***N-R*** type of iteration until joint equilibrium equations ($f_i(x_1, x_2, x_3, \ldots, x_n) = p_i$, for i= 1, 2, 3, …, n) are satisfied within a prescribed tolerance.

The manner in which each of the two incremental methods approximate the actual load-deformation curve is shown in figure (5-1) and figure (5-2).

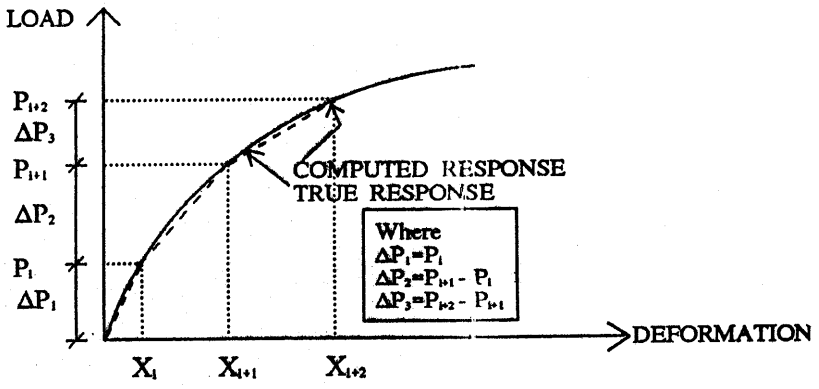

Figure.(5-2) Non-Linear Incremental Method.

It's shown that for (*LIM*), numerical solution tends to drift from the exact solution. This method requires smaller load increments than those needed when using (*NLIM*)

Five types of ***N-R*** modification are used in conjunction with *NLIM* method:

1. Conventional ***N-R*** method.
2. Modified ***N-R*** method.
3. Combined Conventional and Modified ***N-R*** method.
4. ***N-R*** iteration in a single step with equilibrium correction.
5. ***N-R*** iteration in a single step without equilibrium correction.

5.2.3 Direct or Secant method (DM):-

In this method, the deformation corresponding to any load along load-deformation curve is obtained by applying the entire load in a single step. This method thus deals with total deformations and total loads as compared to the incremental method which deals with incremental deformation and incremental loads. The DM can be used to obtain the deformation corresponding to a single value of the load and thus be used to plot the entire load deflection as shown in figure (5-3).

In this method, the desired deformation is related to the applied load by so-called Secant Stiffness Matrix, i.e.:

$$\left[K_s\right]\{X\} = \{P\} \quad \text{.....(5-5)}$$

Since $[K_s]$ depends on internal forces and deformation that exist when the total load is acting, and since thies cuantities are not known at the begining of calculations, the terms in $[K_s]$ must be determined by iteration. In this aspect the method resembles the *NLIM*[4].

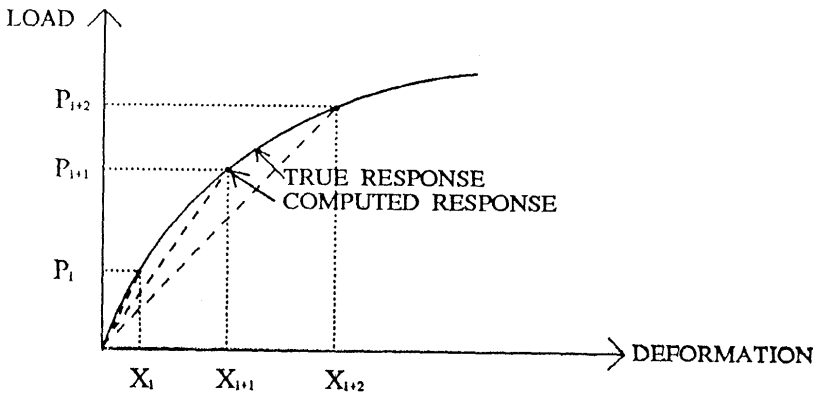

Figure (5-3) Direct Method

5.3 Iterative-Incremental methods of tracing equilibrium path

The literature on the numerical solution of the governing non-linear equations is voluminous, however, the need to treat non-monotone equilibrium paths originated a very large number of iterative methods, which, as briefed below, adopted many strategies, and the use of such strategies allows the tracing of any path in 2-D and 3-D stability problems, even if very twisted.

It is also noted that suitable iterative algorithm replaces the necessity for adopting a displacement control analysis. This kind of analysis is in fact very effective; but it has less physical meaning than the load control one, and it requires very difficult choices in the case of large numbers of degrees of freedom. Also the numerical non-linear stability analysis, especially when coupled to a perturbative method, has necessarily to be connected with an incremental iterative procedure so as to evaluate the stability properties of the structure in the actual vicinity of the critical point.

In view of' the above consideration, to perform a non-linear stability analysis, it is necessary to prevent the possibility of analyzing decreasing equilibrium paths and indefinite or negative-definite stiffness matrix

Just for these reasons, in application to the stability analysis, it is generally inappropriate to adopt a linear equation algorithm which needs a positive-definite matrix (e.g. ***Cholesky*** method). It is recommended to provide an; appropriate iterative method, excluding, for example, the simple and well-known ***Newton-Raphson*** method and its derivatives (with the exception of the ***Tesar*** method as treated below).

5.3.1 Newton Raphson Methods and Its Derivatives (Tesar Method)

The well-known ***Newton-Raphson*** method is adopted in this work for its general application in the non-linear analysis problems. This procedure is still employed today in some cases in stability. When this choice is made, it is necessary to abandon attempts to detect the post-buckling paths, and information on the post-critical behavior in this case is obtained only from the stiffness tangent matrix eigenvectors.

To overcome the well known limits of ***Newton-Raphson*** methods, ***Tesar*** method, the equilibrium iterations suppressing method, control displacements methods and ***Riks/Wempner*** method have been proposed.

The ***Tesar*** method in particular involves of a useful implementation of the classical ***Newton-Raphson*** formulation. The method still remains a load control procedure but, through an effective idea, it becomes capable of overtaking limit points on the equilibrium path. The single steps may be described in the following manner:-

a. a load increment $\{\Delta P_{i+1}\}$ is applied to the system and the corresponding displacements increment $\{\Delta X_{i+1}\}$ are evaluated.

b. the tangent stiffness matrix determinant is calculated at the level of step (a).

c. if the determinant is negative, it means that the limit point has been surpassed. In this case the next point is determined by this procedure if the $\{\Delta P\}$ and $\{\Delta X\}$ sign is reversed, another point on the path tangent but on the opposite part respect to the point of step (a) is detected

d. to avoid an excessive solution drifting in the limit point vicinity, an appropriate reduction of the distance between the two points is imposed:

$$\left\|\left\{\Delta X_{i+1}\right\}\right\| < e \quad \text{.....(5-6)}$$

where "e" is the maximum prescribed tolerance value for the admissible displacements. Another point is obtained in this way. Intersection between the equilibrium path and the new control surface is then detected by iteration.

e. to securely surpass the limit point, it can sometimes be convenient to perform a further step without any equilibrium iteration. Once the critical point is surpassed, the load parameter is varied by a negative increment so as to determine all the decreasing parts of the equilibrium path [12].

5.3.2 Riks-Wempner Method (The modified constant Arc-Length method)

The two main strategies used to define an iterative method -load control or displacement control- identify each new equilibrium state by the intersection of the equilibrium path with the control surface defined by imposing the control parameter constancy. As known, this is the cause of the failure of the methods in proximity of the

respective limit points, i.e. load limit point for load control methods and displacements limit points for displacement control ones.

In any case, the failure of the method is pre-announced by an increase of the number of iterations reaching the convergence with the equilibrium path. It is easy to note that the above phenomenon is connected with the corresponding decrease in the quality of the intersection between the equilibrium path and the adopted control surface measured by the ($\overline{\alpha}$) angle between the equilibrium path and the normal in the control surface.

Following these considerations, the ideal control surface family to be adopted in an iterative method would be orthogonal to the equilibrium path in each of the points to be determined. It is also clear that such a surface-family cannot be constructed because the equilibrium path is not known in advance. To construct an optimal control surface family, however, it is not absolutely necessary to reach the full condition ($\overline{\alpha}$ =0). To "protect" the procedure from failure, it is in fact sufficient to determine a "minor" condition, such as ($\overline{\alpha} < \pi/2$), for the above surface family.

In the above spirit the well known ***Riks/Wempner*** method was constructed separately by each of the two authors, adopting the cited minor condition. This approach uses the plane (or hyper-plane) normal to the tangent to the equilibrium path in the last known point as a control surface.

The classical formulation of the method has been considerably improved by some implementations as described below [12].

5.3.3 Wessels Modified Version of the Riks-Wempner Method

To apply the ***Riks/Wempner*** method in its classical formulation, inversion of the tangent stiffness matrix is required. In order to avoid this, ***Wessels*** introduced an alternative two-step procedure similar to the one adopted by ***Batoz*** and ***Dhatt*** for their displacement control algorithm.

The proposed procedure imposes the following decomposition of the "k^{th}" increment of the current position in the load configuration space (Δr_k).

$$\left\{\Delta r_k\right\} = \left\{\Delta r_{k1}\right\} + \left\{\Delta r_{k11}\right\} \quad \text{.....(5-7)}$$

where:-

$$\{\Delta r_k\} = \begin{bmatrix} \Delta X_k \\ \Delta \lambda_k \end{bmatrix} = \Delta \lambda_k \begin{bmatrix} \Delta X_{k1} \\ 1 \end{bmatrix} + \begin{bmatrix} \Delta X_{k11} \\ 0 \end{bmatrix} \quad \text{.....(5-8)}$$

Updating the current coordinates takes place by following the expressions:-

$$\begin{aligned} \{\Delta X_k\} &= \Delta \lambda_k \{\Delta X_{k1}\} + \{\Delta X_{k11}\} \\ \lambda_{k1} &= \lambda_k + \Delta \lambda_k \end{aligned} \quad \text{.....(5-9)}$$

while the two increment rates are evaluated by solving the following two linear systems:

$$\begin{aligned} [k_{Tk}]\{\Delta X_{k1}\} &= \{P^*\} \\ [k_{Tk}]\{\Delta X_{k11}\} &= \{P_{res}\} \end{aligned} \quad \text{.....(5-10)}$$

The coefficient matrix is the same for the two systems of eq.(5-10) In order to solve the two systems, it is sufficient to execute the matrix factorization once thereby when the first system is solved, the solution of the second one needs only a minimum effort. Once the two systems are solved, load parameter increment is obtained by the condition of othogonality:-

$$\{T_0\}\{\Delta r_k\} = 0 \quad \text{.....(5-11)}$$

where:-

$$\{T_0\} = \{\Delta r_0\} = \begin{bmatrix} \Delta X_0 \\ \Delta \lambda_0 \end{bmatrix} \quad \text{.....(5-12)}$$

The condition of orthogonality leads, therefore, to the following form:-

$$\Delta \lambda_k = -\left(\Delta X_0 \, \Delta X_{k11}\right) / \left(\Delta X_0 \, \Delta X_{k1} + \Delta \lambda_0\right) \quad \text{.....(13-5)}$$

which makes it possible to define the load parameter increment expression.

Wessels proposal is a "simple" and useful computational arrangement, without any new conceptual meaning, but it suggests other implementations [(12)].

5.3.4 Ramm Method

Ramm's method also involves in a further modification of the ***Riks/Wempner*** method. The idea is to update the condition of orthogonality expressed in the ***Riks/Wempner*** method at each iteration. By means of this technique it is in fact possible to increase the cited quality of the intersection between the equilibrium path and the control surfaces. The implementation is performed by introducing the information obtained in the last performed iteration into the procedure equations.

In the formal expression of the method, during the iterations for determining the "m^{th}" point on the equilibrium path, the quantities (ΔX_0) and ($\Delta\lambda_0$) change at each step. In the original ***Riks/Wempner*** method, on the contrary, these quantities refer to the preceding step "$(m-1)^{th}$" and are maintained constant for all iterations. In the method formulation it is also recommended to adopt the ***Wessels*** decomposition introduced in eqs.(5-7 and 5-8).

Once the displacement increments (ΔX_{k1} and (ΔX_{k11}) are obtained, the load parameter increment ($\Delta\lambda_k$) is calculated following the ***Wessels*** formulation in order to construct the $[\Delta r_k]$ vector; the next increment $[\Delta r_{k+1}]$ is then evaluated by imposing:

$$\begin{aligned}\Delta\lambda_0 &= \Delta\lambda_0 + \Delta\lambda_k \\ \Delta X_0 &= \Delta X_0 + \Delta X_k\end{aligned} \quad \text{.....(5-14)}$$

Also for the ***Ramm*** method it is possible to proceed by updating the global tangent stiffness matrix once for each step. In this manner, a modified ***Ramm*** method is defined. Advantages of performing one of the two possibilities are to be evaluated with respect to the case.

It's noted that the ***Ramm*** implementation does not require an analytical image with respect to the ***Riks/Wempner*** method and it improves the procedure reliability. For this reason it is always useful to adopt the implementation.

To demonstrate the ***Ramm*** method performance, some comparisons between ***Ramm*** and ***Riks/Wempner*** method have been made. A fictitious parabolic equilibrium path is adopted.

When the control parameter step amplitude is smaller than the one which surpasses the apex of the equilibrium path, the two methods show very similar performances. On the contrary, when the control parameter step amplitude is larger than the preceding value, the ***Ramm*** implementation becomes decisive in maintaining the procedure reliability. In this case, in fact, the ***Riks/Wempner*** method cannot determine other points on the equilibrium path while the ***Ramm*** method reaches a further equilibrium state in any case [12].

5.3.5 Crisfield Method

Crisfield method can also be considered as a modification to the classical ***Riks/Wempner*** method. This implementation provides for adopting a sphere with center in the last known point as the method control surface. Analytically, the method is

expressed by substituting the constancy of the distance between the last known point and the next to be determined (see figure 5-4) for the orthogonality condition. ***Crisfield*** also recommends updating the tangent stiffness matrix once in each step [12].

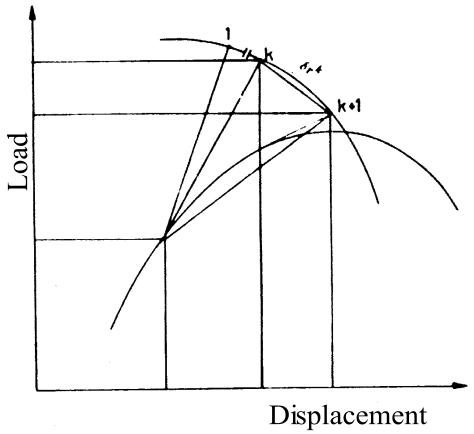

Figure (5-4) Crisfield Method

5.4 Non-linear stability analysis and perturative methods to trace equilibrium paths

In the present section some strategies for obtaining information about the critical and post critical behavior of space structures are introduced (see figure 5-5). Particular arrangements for adapting the perturbative analysis to the finite-element approach are discussed in order to obtain the required information without referring to high (third and fourth) order derivatives of the total potential energy.

Although the present study adopts the B-C approach it seems beneficial to get on with this stability criteria of 3-D frame.

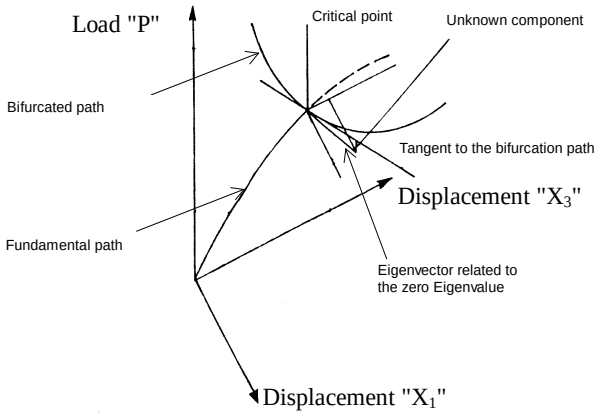

Figure (5-5) 3-D Tracing Equilibrium Path

5.4.1 Buckling of a Discrete N-dimensional System.

The well known ***Thompson*** and ***Hunt*** classification of discrete critical points is briefly referred to in order to introduce some considerations concerning the implementation aspects of a perturbative procedure in a finite element analysis.

Given a discrete n-dimensional structure, let the "n" function "u" be the system ***Langrangean*** coordinates and "λ" the assumed load parameter, the total potential energy "ϕ" in the vicinity of a discrete critical equilibrium state "c" can be expressed by:-

$$\overline{\phi} = \overline{\phi}\left(q_i . \lambda\right) = \overline{\phi}\left(q_{c_i} + [A]\{u\}. \lambda\right) \quad \text{.....(5-15)}$$

where "q_{c_i}"defines the configuration at the discrete critical point "c" and [A] is a non-singular linear operator that diagonalizes the quadratic form:

$$\overline{\phi}^2 = \left\{u_i\right\}^T \left[\overline{\phi}_{ij}\right] \left\{u_j\right\} \quad \text{.....(5-16)}$$

The discrete critical point "c" is characterized by a single zero stability coefficient. Without loss of generality it can be assumed that:-

$$\overline{\phi}_{c_{11}} = 0$$
$$\overline{\phi}_{c_{rr}} \neq 0, r = 2,3,...,n \quad \text{.....(5-17)}$$

The derivative with respect to "u" of the "i^{th}" equilibrium equation on the path also yields:

$$\left[\overline{\phi}_{ij}\right] \left\{u_{j,1}\right\} + \left\{\overline{\phi}'_i\right\}. \lambda_1 = 0 \quad \text{.....(5-18)}$$

where the apex indicates the derivation with respect to the load parameter."λ" In the above hypothesis, the important coefficient which differentiates limit point from bifurcation behavior is "$\overline{\phi}'_{c1}$".

As known, if ($\overline{\phi}'_{c1} \neq 0$), it follows that the condition for a load extremum at the critical point i.e. obtaining ($\lambda_{c_{11}} \neq 0$)is:-

$$\overline{\phi}_{c_{111}} \neq 0 \quad \text{.....(5-19)}$$

In this way, the above situation implies a limit point.

On the contrary, if the critical point is subject to the condition ($\overline{\phi}'_1 = 0$) i.e. the critical point is a bifurcation point, a further differentiation of eq.(5-18) gives, after

various manipulations the following condition, which reflects the situation of the slopes of the equilibrium paths passing through the critical point:

$$\left(\overline{\phi}'_1+\frac{\overline{\phi}_{1kr}\,\overline{\phi}'_r\,\overline{\phi}'_k}{\overline{\phi}_{rr}\,\overline{\phi}_{kk}}-2\frac{\overline{\phi}_{1r}\,\overline{\phi}'_r}{\overline{\phi}_{rr}}\right)\lambda_1{}^2+\left(2\overline{\phi}'_{11}-2\frac{\overline{\phi}_{11r}\,\overline{\phi}'_r}{\overline{\phi}_{rr}}\right)\lambda_1+\overline{\phi}_{111}=0 \quad \text{.....(5-20)}$$

Assuming that the above equation could admit two distinct roots, the condition for an asymmetric bifurcation point is ($\overline{\phi}_{c_{111}}\neq 0$). On the other hand ($\overline{\phi}_{c_{111}}=0$) furnishes the condition for a symmetric bifurcation point.

In this second case, the distinction between the stable and the unstable symmetric bifurcation points is to be imposed on the fourth derivative of the total potential energy "$\overline{\phi}$":-

$$\left.\begin{array}{l}\overline{\overline{\phi}}_{c_{1111}}>0 \;\; \text{stabel symmetric}\\ \overline{\overline{\phi}}_{c_{1111}}<0 \;\; \text{unstabel symmetric}\end{array}\right\} \text{ Bifurcation} \quad \text{.....(5-21)}$$

where:-

$$\overline{\overline{\phi}}_{c_{1111}}=\left(\overline{\phi}_{c_{1111}}-3\frac{\overline{\phi}^2_{c_{r11}}}{\overline{\phi}_{c_{rr}}}\right) \quad \text{.....(5-22)}$$

Equation (5-20) clearly shows that the slope of the equilibrium paths at a critical point depends on the third derivative of "$\overline{\phi}$".

When a tangent stiffness matrix approach is adopted (for instance in a finite element approach) only the second derivative of "$\overline{\phi}$" is calculated and higher order derivatives are not available. This is the reason for the difficulties involved in a perturbative analysis of equilibrium paths encountered by a finite element approach; moreover, the way of resolving the above stated problems is of great interest considering the large diffusion and reliability of such approaches [12].

5.4.2 Linear Stability Analysis

Linear stability represents the most common approach for obtaining important information concerning the stability behavior of a given structure, such as the existence or the type of critical equilibrium states and the corresponding load levels.

Assuming that the geometrical stiffness matrix depends linearly on the internal stresses of the elements, it is possible to hypothesize:

$$\left[K_G\right] = \lambda \left[K_G^*\right] \quad \text{(5-23)}$$

where $[K_G]$ represents the geometric stiffness matrix evaluated for the "λ" value of the local parameter and ($\left[K_G^*\right]$) is the same quantity evaluated for λ=1.

- While the $[K_G]$ matrix also depends on the system geometry, large displacements which can alter the referring situation (λ=1) are excluded.
- Linearity of the relation between the load parameter "λ" and the elements internal stresses level is presumed;
- Initial displacements are neglected.

By adopting the same hypothesis, the elastic stiffness matrix $[K_E]$ can be assumed as constant.

With the above positions, the incremental equation at a given load parameter value can be expressed as:

$$\left(\left[K_E\right] + \lambda\left[K_G^*\right]\right)\{\Delta X\} = \Delta\lambda\left\{P^*\right\} \quad \text{(5-24)}$$

where $[\Delta X]$ represents the displacements increment corresponding to the load variation $\Delta\lambda\{P^*\}$, with $\{P^*\}$ a fixed reference vector. Thus $\{\Delta X\}$ can be obtained by the expression:

$$\{\Delta X\} = \left(\left[K_E\right] + \lambda\left[K_G^*\right]\right)^{-1} \Delta\lambda\left\{P^*\right\} \quad \text{(5-25)}$$

and it is easy to recognize that the displacement increment becomes undetermined if:-

$$\det\left(\left[K_E\right] + \lambda\left[K_G^*\right]\right) = 0 \quad \text{(5-26)}$$

The load parameter levels corresponding to the critical states are thereby obtained by solving eq.(5-26) with respect to "λ" .

This solution is related to the above-stated hypothesis. When a non-linear structure is treated, the results obtained by eq.(5-26) are only an approximation of the actual critical load parameter level, and sometimes completely wrong solutions can be obtained in this way.

A modified version of the classical stability analysis can be usefully performed also for non-linear structures. In the proposed approach a "generalized" eigenvalue problem is solved in the form:

$$\left[K_E\right][V] = -\left[K_G^*\right][V][\lambda] \quad \text{.....(5-27)}$$

where the unknown quantities are the two matrices [V]and [λ].

[V] represents a matrix whose columns are the generalized eigenvectors of the given structure, while [λ] is a diagonal matrix which contains the corresponding generalized eigenvalues.

It is easy to recognize that eq. (5-27) originates (n) equations of the following form:

$$\left(\left[K_E\right] + \lambda\left[K_G^*\right]\right)\{v\} = 0 \quad \text{.....(5-28)}$$

where vectors {v} represent the matrix [V] columns. Thus, {v} being a non-zero vector, eq.(5-28) also implicates eq.(5-26).

The smallest value of the diagonal of {λ} represents the first critical load level estimate, while the corresponding column of [V] represents the related critical mode.

All the experiments which have been performed assure that the computed estimate of the critical modes {v} is generally correct, even when the corresponding eigenvalue represents the worst approximation of the actual critical load level. Moreover, knowing the critical modes of deformation before performing an effective non-linear analysis represents a very important effort to the best preparation of the approach possibilities (for instance, information about the imperfection sensitivity can be obtained). Limit points or bifurcation points can also be recognized by an examination of the determined critical mode and the most appropriate tools can be activated without a much more expensive non-linear analysis [(12)].

5.4.3 Non-linear Stability Analysis

Determination of the exact load level corresponding to all critical points, like snap-through or bifurcation, is an essential condition for a complete and accurate analysis of buckling and post buckling behavior.

In the case of the systems with pronounced non-linear behavior, the linear estimate can usually produce only some useful information without determining a reliable approximation of the real critical load levels. Non-linear stability analysis becomes necessary therefore especially for determining the equilibrium paths in the post-buckling domain.

Rewriting now the condition for the critical equilibrium at a point:-

$$\left[K_T\right]\{v\} = 0 \quad \text{(5-29)}$$

Therefore, for non-zero {v}, results the conditioning equation for the determinant of the global tangent stiffness matrix:

$$\det\left[K_T\right] = 0 \quad \text{(5-30)}$$

Developing this last condition in a power series, the mathematical expression of (eq.5.30) becomes the known non-linear eigenvalue problem:

$$\left([A] + \lambda[B] + \lambda^2[C] + \cdots\right)\{v\} = 0 \quad \text{(5-31)}$$

[A], [B] and [C] being appropriate independent matrices and {v} the eigenvector related to the critical state being sought (eq.5.31) shows the correct formulation of the non-linear stability analysis and is, in general, to be solved only by means of the iterative approach.

Since the work of ***Mallet*** and ***Marcal,*** several authors have formulated a non-linear approach to the stability analysis in the form of a quadratic eigenvalue problem. Firstly, the critical state refers to the current configuration introducing an appropriate coefficient "λ^*":

$$\{u\}_c = \lambda^*\{u\} \quad \text{(5-32)}$$

where the vector {u} represents the initial displacement (i.e. the difference between the current configuration and the initial undeformed one) of the system, and $\{u\}_c$ describes the critical state. Assumption eq.(5-32) obviously represents an approximation for all cases of non-linear pre-critical behavior.

Equation (5-30) with the position of eq.(5-32) leads to the following quadrate eigenvalue problem:

$$\left(\left[K_E\right] + \lambda^*\left[K_{G1}\right] + \lambda^{*^2}\left[K_{G2}\right]\right)\{v\} = 0 \quad \text{(5-33)}$$

in which $[K_{G1}]$ and $[K_{G2}]$ are, respectively, first and second order terms of the initial displacements and geometric matrices. eq.(5-33) involves the hypothesis of linearity between loads and displacements.

In the above hypothesis, the relationship between the load parameter "λ" and "λ^*" the coefficient is furnished by the equality at the critical state:

$$\{P\}_c = \lambda_c\{P^*\} = \lambda\lambda^*\{P^*\} \quad \text{(5-34)}$$

From eq.(5-34) it follows that the critical condition is reached for unitary values of the λ^* coefficient. eq. (5-32) shows that if $\lambda^*=1$, the current and critical configurations coincide.

A possible solution strategy for eq.(5-34) is to linearize stepwise the eigenvalue problem writing:

$$\left\{\left[K_E\right]+\lambda^*\left(\left[K_1\right]+\left[K_2\right]\right)\right\}\{v\}=0 \quad \text{.....(5-35)}$$

The path of the resulting "λ^*" values obtained during the solution is obviously incorrect, with the exception of the case "$\lambda^*=1$", which only verifies linear and non-linear formulations of the eigenvalue problem as coincident.

Determination of the critical equilibrium states is therefore transformed in the updating eq. (5-35) during the stepwise procedure until a unit load parameter "λ^*" is reached. The technique discussed above has been successfully developed in the recent past with applications to reticulated shells.

One of the most interesting tools provided by a non-linear analysis method is the ability to detect and construct the secondary paths in the case of a bifurcation point. In fact, in the preceding argument, it has been demonstrated how the properties of the bifurcation paths (e.g. the paths slope) depend on the higher order derivatives of the total potential energy.

To construct secondary paths following the tangent stiffness matrix approach, useful arrangements to avoid the necessity of referring to these quantities are therefore required [12].

5.5 Newton-Raphson (N-R) Methods

One of the oldest and best known methods is the ***Newton-Raphson*** (***N-R***) method. To show the resemblance in a simple way, consider now a single D.O.F system. Consider a load level {P}; and assume that the corresponding deformed configuration of the system, which may be devoted symbolically by {X}, is known (see figure 5-6).

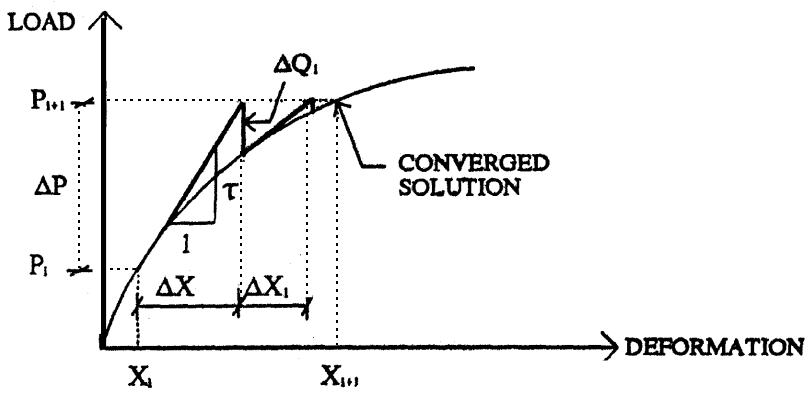

Figure (5-6) Conventional N-R Method

It is now desired to determine the configuration $\{X\}_{I+1}$ corresponding to the load level $\{P\}_{I+1}=\{P\}_i +\{\Delta P\}$, in which $\{\Delta P\}$ represents a small load increment using a linearized analysis; the change in configuration $\{\Delta X\}$, is first computed from:-

$$\{\Delta P\} = [\tau]\{\Delta X\} \quad \text{.....(5-36)}$$

By simply evaluating system tangent matrix $[\tau]=[K\text{-}1]$ at the beginning of the loading interval; i.e. at load level $\{P\}_i$ the solution $\{X\}_i+\{\Delta X\}$ thus obtained represents an approximate configuration in the sense that joint equilibrium equations are not necessarily satisfied at the load level $\{P\}_{i+1}$. This approximate solution is then corrected by a ***N-R*** type of iteration until equilibrium equations ($f(X1,X2,X3,\ldots Xn)=P_i$, for i= 1,2,3...n) are satisfied within prescribed tolerance. In our analysis, the subscript (j) is used to refer to the "j^{th}" iteration cycle while $\{P\}$ is kept constant at $\{P\}_{I+1}$

From ($f(X_1, X_2, X_3,...Xn) =P_i$ for i=1,2,3...n) the unbalanced joint forces can be calculated as:

$$\{\Delta Q\}_j = \{P\} - \{F(X)\}_j \quad \text{.....(5-37)}$$

in which $\{F(X)\}_j$ represents internal joint forces corresponding to configuration $\{X\}_j$. The unbalanced joint forces are then treated as a load increment and the correction vector, $\{\Delta X\}_j$ is then obtained from incremental relationship:

$$\{\Delta Q\}_j = \{\tau\}_j\{\Delta X\}_j \quad \text{.....(5-38)}$$

A new approximate condition $\{X\}_{j+1} = \{X\}_j + \{\Delta X\}_j$, is thus obtained, and the process continues until the latest correction vector is sufficiently small.

The ***N-R*** method requires that the tangent stiffness be formed and then triangulated in each step. This is expensive if the problem has many D.O.F. accordingly; various modifications have been proposed [(4)].

5.5.1 N-R methods modification:

5.5.1.1 Conventional N-R Method:

This method has been discussed briefly in the previous section (section 5.3), and is illustrated in figure (5-6)

5.5.1.2 Modified N-R Method: Constant Stiffness Iteration

A modified iterative scheme is illustrated [(25)] in figure (5-7)

The tangent stiffness [τ] is used in all iterations in one increment. As compared with figure (5-6), figure (5-7) requires more steps for convergence, but each step is done much more quickly (only requires forward and backward substitution when using ***Cholesky*** method for solving simultaneous linear equations).

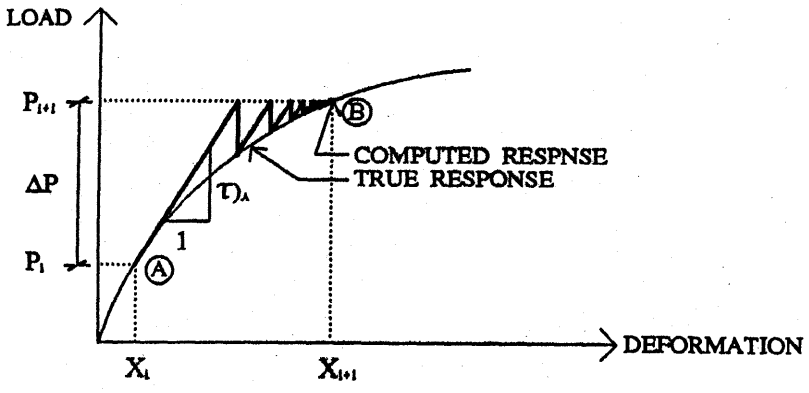

Figure (5-7) Modified* N-R *Method

5.5.1.3 Combined Conventional and Modified N-R Method:

In this method (see figure 5-8) the stiffness is held constant for several iterations or load levels and is updated only when the rate of convergence begins to deteriorate (Number of iterations exceeds maximum limit) [(4)].

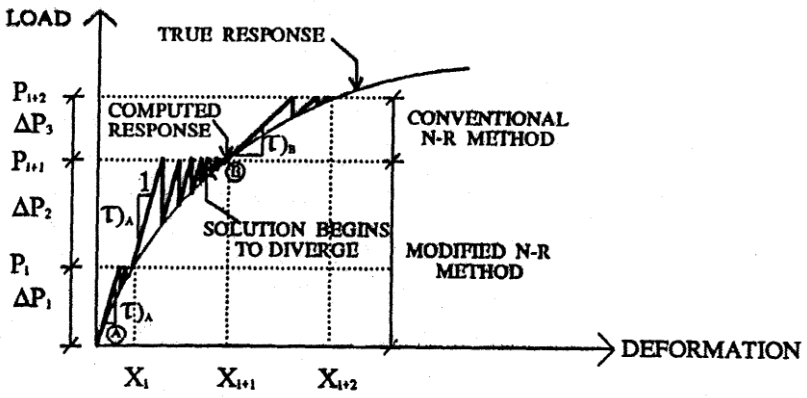

Figure (5-8) Combined Conventional and Modified **N-R** *Method*

5.5.1.4 N-R Iteration in a single step without Equilibrium Correction (step by step without Equilibrium Correction):

In this method of (***Mondkar*** and ***Pwell***) only a single iteration is performed on each load increment. The solution proceeds as shown by the dash lined tangents in figure (5-9), where points on computed curve are indicated by dots. This procedure might also be described as incremental, as successive displacement increment $\Delta X)_1$, $\Delta X)_2$, …etc., are produced by successive load increments $\Delta P_1=P_i$, $\Delta P_2=P_{i+1}- P_i$, and $\Delta P_3=P_{i+2}- P_{i+1}$.

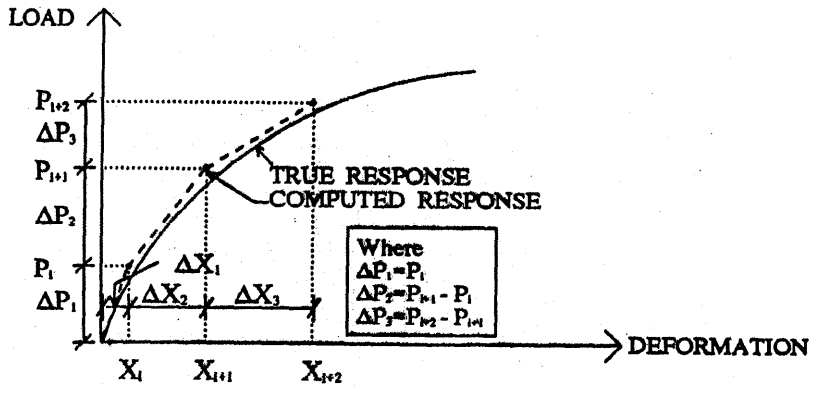

Figure (5-9) **N-R** *in a Single Step without Equilibrium Correction*

5.5.1.5 N-R Iteration in a single step with equilibrium correction (step by step with equilibrium correction):

This method (see figure 5-10) is similar to the previous one, but by adding "ΔP_{c2}"to "ΔP_2"and "ΔP_{c3}" to "ΔP_3" etc., the computed displacement increments are larger and more nearly correct. In other words the addition

of the force unbalance "ΔP_{ci}" to the load increment "ΔP_i" prevents large drift from the correct curve (True response). This method is usually called "Incremental in a single step ***N-R*** correction"[4].

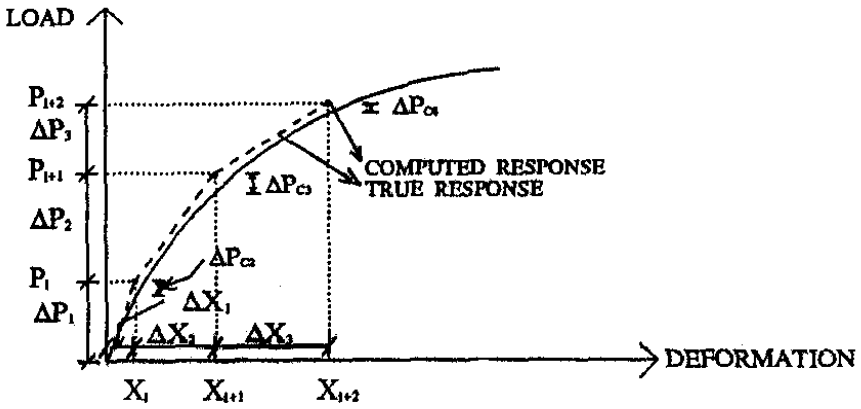

Figure (5-10) **N-R** ***in a single step with equilibrium correction***

5.6 Convergence Criterion:

A termination criterion for an iterative process should be used to stop iteration when sufficient accuracy is achieved (i.e. when no further iterations are necessary).

5.6.1 Displacement Criterion:

This criterion depends on comparison between incremental change in the displacement vector {ΔX} and cumulative displacement vector {X}. In applying this criterion, translations and rotations of the joint should be treated as separate groups, and convergence is assumed to have occurred when the inequality.

$$\left[\frac{\sum_{i=1}^{n}(\Delta X)_i^2}{\sum_{i=1}^{n}(X)_i^2}\right]^{1/2} \leq \text{tol.} \qquad (5\text{-}39)$$

is satisfied simultaneously and independently for each group. In eq.(5-39) the dimensionless quantity, "tol.", represents a prescribed tolerance [3].

5.6.2 Force Criterion:

This method depends on comparison between the internal force vector {f} and the applied load vector {P} in other words, seeking a vector called unbalanced force vector to be small within prescribed tolerance. Like the displacement criterion, in applying this

criterion the resultant force and moment vector of the joints are treated as separate groups and the convergence is assumed to have occurred when the inequality.

$$\left[\frac{\sum_{i=1}^{n}\left(\{P\}_i-\{f\}_i\right)^2}{\sum_{i=1}^{n}\left(\{P\}_i\right)^2}\right]^{1/2} \le \text{tol.} \quad \text{(5-40)}$$

is satisfied simultaneously and independently for each group.

5.6.3 Work Done Criterion:

This criterion uses a comparison between the work done by the external forces and the work done by the internal forces and convergence occurs when the inequality

$$\left|\frac{W_e - W_i}{W_i}\right| \le \text{tol.} \quad \text{(5-41)}$$

is satisfied where

W_e is the work done by the external forces.

W_i is the work done by the internal forces.

The prescribed tolerance, "tol.", in the inequalities eq. (5-41) is chosen to balance accuracy requirements against machine precision. Possible choices are "tol. $=10^{-5}$" in 64-bit arithmetic and "tol. $=10^{-3}$" in 32-bit arithmetic [25].

5.7 Detection of Instability:

As long as the structure remains in stable equilibrium there is only one available path for the load deflection curve that satisfies the equilibrium condition. In other words for any load level there is only one available set of deflection and the determinant of the stiffness matrix is positive.

During the analysis most structures lose their stiffness (softening) until the determinant of the stiffness matrix becomes zero. The zero stiffness point has two categories, the first, which is the *bifurcation point*, behind which there are two possible paths which satisfy equilibrium conditions. This means that there are two configurations, buckled and reference configurations are both possible equilibrium configurations. The first path refers to the reference configuration and it is called the primary path, while the other one is called the secondary path which is followed by most structures.

The buckling theory presumes the existence of a bifurcation point. So the buckling represents the bifurcation point. Actually, a bifurcation point exists if the column is perfectly straight, perfectly

uniform, perfectly free of end moments and lateral loads and forces are perfectly centered and perfectly axial [22]. In reality there are always imperfections. If there is any imperfection, the column displays no bifurcation point and structures in general, displays the second category of zero stiffness point *limit points.*

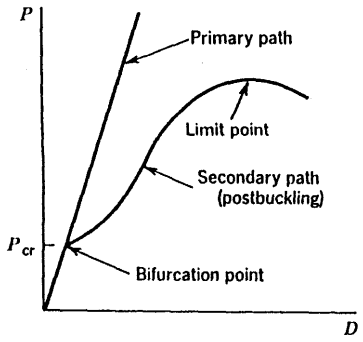

Figure (5-11) Imperfect Structure

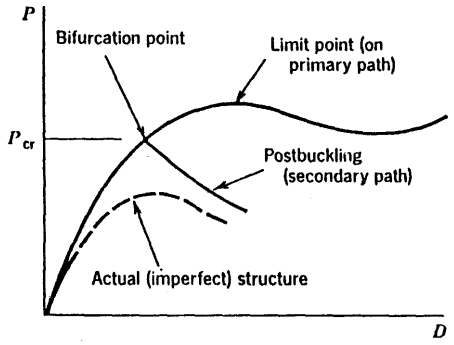

Figure (5-12) Imperfect Sensitive Structure in 2-D problems

A real structure may collapse at a load quite different from that predicted by a linear bifurcation buckling analysis, figures (5-11 and 5-12) illustrate some of the ways structure may behave. In figure (5-11), the *primary* or *pre-buckling* path happens to be linear. At bifurcation, either of two adjacent and infinitesimally close equilibrium positions are possible. Therefore for "$P>P_{cr}$" a real (imperfect) structure follows the secondary path. The *secondary* or *post buckling* path rises, which means that the structure has post buckling strengths. This structure finally collapses at a limit point, which is defined as a relatively maximum load versus displacement curve for which there is no adjacent equilibrium position. Another type of behavior is depicted in figure (5-12). Here the perfect (idealised) structure has a non-linear primary path. The post-buckling path falls, so there is no post-buckling strength. If the primary path is close to a falling secondary path, the structure is called imperfection sensitive, which means that the collapse load of the actual structure is strongly

affected by small changes in direction of loads, manner of support, or changes in geometry [25]. A real structure, which has imperfections, displays a limit point rather than bifurcation as shown by the dashed line.

In this study the post-critical behavior of the structure is not considered because the analysis at such a stage considers a negative stiffness matrix and a special procedure must be used to determine the behavior of the structure at that stage. So the analysis always stops at the first limit point (some structures have even more than one limit point) and that stage of load will be considered as the critical load.

In a problem with post-critical behavior as this in figure (5-13) one can provide displacement increments rather than load increments, i.e., using *displacement control* rather than *load control*. However, in a typical problem one does not know in advance how the displacement for each degree of freedom will be related to the others, so the appropriate increments are unknown.

In figure (5-13) displacement control yields the entire curve of load versus deflection. Under load control, the physical structure will experience a sudden *snap* from "A" to "B" when the limit point at "A" is reached. Even the displacement control method may not give the actual load-deflection curve [3].

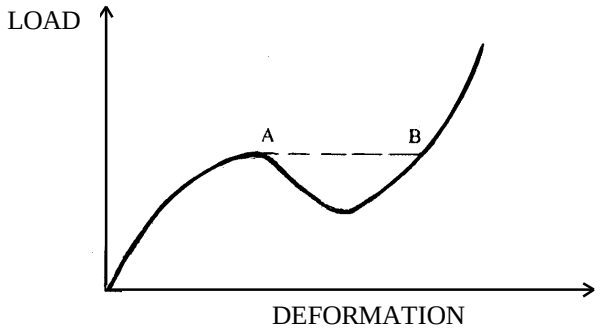

Figure (5-13) Load versus Displacement Plot Showing Limit Point at "A"

If a structure has a load deflection curve as in figure (5-14), then another method may be used. The modified arc-length method which is briefly described in section (5.3.2) looks to be the most effective method for determining the post critical behavior of the structure.

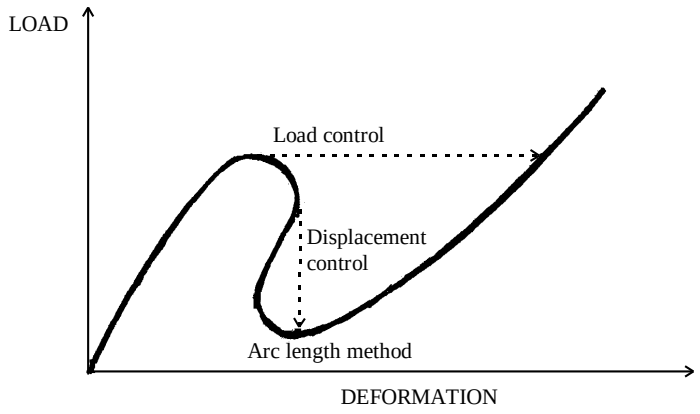

Figure (5-14) a Typical Load Displacement Plot with the Solution Obtained by Different Methods

There are many methods for the detection of the elastic instability condition, i.e. zero stiffness of plane steel frames. Some of these methods will be discussed here and a reduced modified arc-length method which is an extension for the modified arc-length method can be found in many references this work depend upon[3 & 108].

5.7.1 Detection of Convergence Criterion:

Many researchers view a lack of convergence in the iteration process as an indication of collapse and elastic instability [70]. This reasoning while it is clearly justified from the theoretical point of view appears to be unreliable as a practical criterion.

5.7.2 Extrapolation Method [102]:

The most conventional failure criterion is obtained by plotting the determinant of the tangent stiffness matrix against the load parameter and making an extrapolation process for the last two values to obtain an approximate value for the load factor at zero stiffness. Figure (5-15) shows the extrapolation procedure, and the approximate elastic critical load factor may be obtained by:

$$\lambda_{cr_i} = \lambda_i + \frac{\lambda_i - \lambda_{i-1}}{D_i - D_{i-1}} D_i \quad \text{.....(5-42)}$$

in which:-

- λ_{cr_i} = the approximate value for the elastic critical load factor at the i^{th} load step, and

- $\lambda_i, D_i =$ are the load factor and the determinant of the tangent stiffness matrix at i^{th} load step.

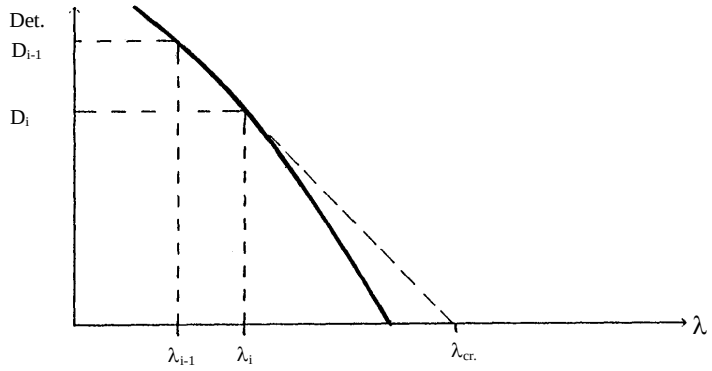

Figure (5-15) Determinant versus Load Factor Curve

It may be seen from the figure (5-15) that as long as the analysis is continued a better estimation for "λ_{cr}" is obtained. By monitoring the determinant of the tangent stiffness matrix and the approximate critical load factor we can apply a small load increment at final stages to obtain "λ_{cr}." The elastic critical load then may be detected when the approximate critical load is approximately equal to the applied load.

The efficiency of the method depends on the behavior of the structure. Figures (5-16 and 5-17) show the determinant vs., load factor parameter for a typical limit and bifurcation points respectively. It may be seen that the limit point is characterised by a vertical tangent and the bifurcation point by a finite angle of intersection. In the presence of small imperfection the bifurcation point may transform into a limit point indicating that the system is imperfection-sensitive, or it may disappear completely indicating that the imperfect system will have a post buckling strength. The method looks to be perfect for system with bifurcation points because the approximate buckling load parameter obtained after the first load increment will be exactly the actual buckling load (see figure 5-17). But in the case of imperfection sensitive structures, the approximate buckling load obtained from eq.(5-42) will give a wrong estimation for "$\lambda_{cr.}$" at the first steps of loads and then is modified with additional applied load increment. At the final increments of load, the method will give a good approximation to the buckling load as shown in curve "A" in figure (5-16), curve "B" in figure (5-16) shows that in some cases even at final load steps the method gives a wrong estimation for the buckling load.

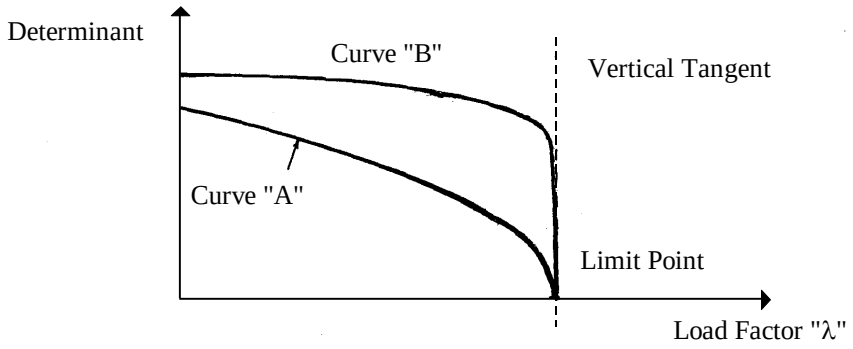

Figure (5-16) Typical Limit Point

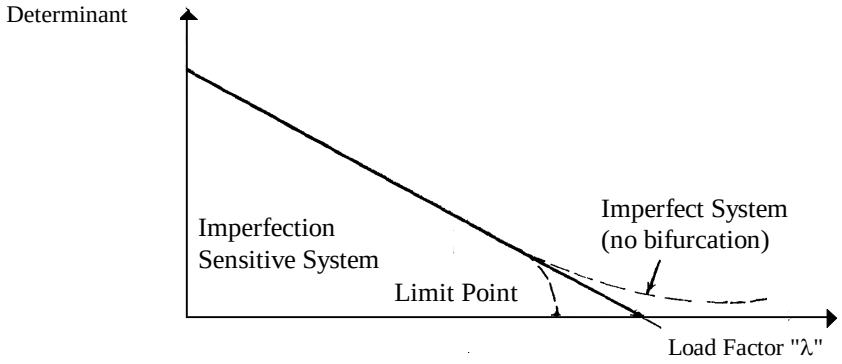

Figure (5-17) Typical Bifurcation Point

However, the determinant of the stiffness matrix is usually large, and may overflow. In some cases the determinant may be very small and may under flow. So the determinant is replaced by the natural logarithm of the determinant log (determinant) [25]. It may be noted that for big structures with multi-D.O.F. the log (determinant) vs. load factor will even give a better representation for the reduction in the stiffness of the structure.

5.7.3 Fundamental Eigenvalue Criterion:

In structures in which the effect of geometrical non-linearity is too small, prediction by the eigenvalue problem looks to be the best method for computing the elastic buckling load. Using the principles of strain energy method the stiffness matrix [K] for a system with constant axial force (P) may be given by:

$$[K] = [K_E] + P[K_G] \quad \text{.....(5-43)}$$

in which:-

$[K_E]$ is the conventional linear elastic stiffness matrix, and $[K_G]$ is the geometrical non-linearity matrix, which depends non-linearity on the axial force, but it can be approxiamted by considering the coefficients to be linearly axial force dependent only.

Now to find the buckling load we shall search for zero stiffness condition by solving the eigenvalue problem.

$$\left(\left[K_E\right] + P\left[K_G\right]\right)\{\Delta X\} = 0 \quad \text{.....(5-44)}$$

Solving eq.(5-44) for the lowest eigenvalue, we will approximate value for the buckling load. The accuracy of the elastic critical load is improved by increasing the number of elements per each member in the frame.

The method is very effective in shell analysis because most of the applications have constant axial forces. For problems with large displacements, the method is not effective because the stiffness matrix given in eq. (5-43) is no more representing the stiffness characteristics of the system [3].

5.8 Available procedures for non-linear analysis of cable stayed structures:-

The same iterative-incremental ***N-R*** technique can be adopted in the non-linear cable-stayed structure solutions, however ***Nazmy*** and ***Abdel-Ghaffar*** [54] (1989) introduced an efficient technique for such problems which is:

5.8.1 The proposed method of analysis

To simplify the non-linear static analysis the following assumptions and approximations were made:

1) All stresses in the structure components remain within the elastic limit.
2) All cables are fixed to the tower and to the support at their points of attachment.
3) All cable stays are of uniform section and are assumed to be straight chord links between the towers and the supports. An equivalent axial stiffness is assigned to these links to compensate for the sag effect.
4) The cables are assumed to be perfectly flexible, that the flexural stiffness of the cables can be neglected.

The mixed incremental iterative procedure mentioned previously is used in the present investigation for the non-linear static analysis of cable stayed structures. It was found that this technique results in faster convergence.

The first load increment is applied using the tangent stiffness matrix of the undeformed structure $[K_E]$ and the joint displacements $\{X_1\}_i$ are then computed using (P=K.X) with $\{P\}=1/3\{p\}$. The tangent stiffness matrix $[K_T\{X_1\}_i]$ that corresponds to the displaced shape of the structure is then computed and used to compute the incremental joint displacements due to the second load increment. These incremental displacements are then added to the previously computed joint displacements $\{X_1\}_i$ to obtain $\{X_2\}_i$, which correspond to point "B" in figure (5-18). The process is repeated for the last load increment until point "C" is reached, which represents the end of the first cycle. The computed displacements at the end of the cycle $\{X_3\}_I$ (or simply $\{X\}_i$) actually corresponds to loads on the true load displacement curve, namely point "E". The unbalanced loads at the end of the first cycle, $\{P\}_i$ represented by line "CE" are then computed and applied as a new set of joint loads during the second cycle of iteration using the tangent stiffness $[K_T\{X\}_i]$ represented by line "EF". The incremental displacements are then computed from:

$$\left[K_T(X)_i\right]\{\Delta X\}_i = \{P\}_i \quad \text{.....(5-45)}$$

where $\{P\}_i$ is the out of balance force vector computed from:

$$\{P\}_i = \{P\} - \left[K_S(X)_i\right]\{X\}_i \quad \text{.....(5-46)}$$

in which $[K_S(X)_I]$ is the secant stiffness matrix of the structure when the joint displacements are $\{X\}_i$. The new displacements are then computed from:

$$\{X\}_{i+1} = \{X\}_i + \{\Delta X\}_i \quad \text{.....(5-47)}$$

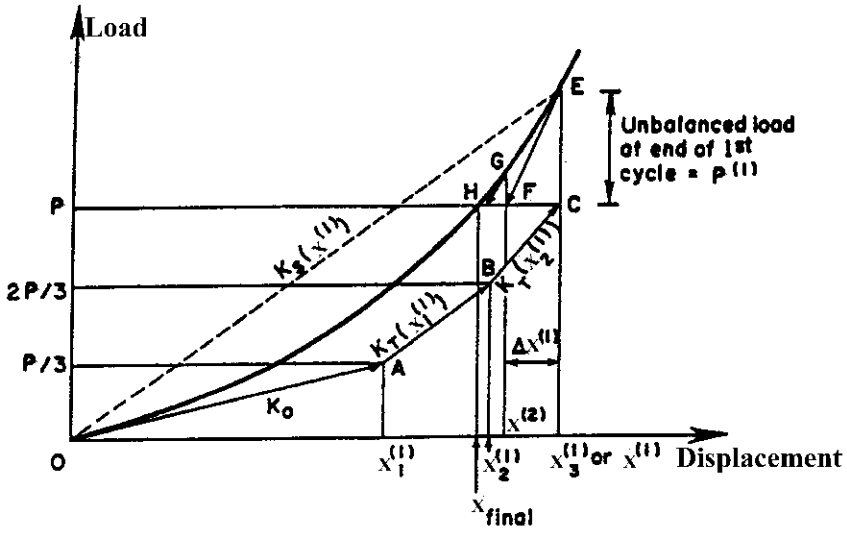

Figure (5-18) Mixed procedure used for non-linear structure analysis

The iteration process continues and the unbalanced loads at the end of each iteration cycle are computed. If the unbalanced loads, measured in some vector where the maximum norm is usually used, are not less than a certain acceptable tolerance, another iteration cycle is required. This process continues until convergence to the correct displacements represented by point "H" is obtained.

In eqs.(5-45 and 5-46) the global tangent stiffness or secant stiffness of the structure is obtained by the standard assembly procedure, from the individual element stiffness matrices. The formulation of both tangent and secant stiffness matrices for cable as well as bending elements were described in **chapter-4-&-3**-respectively, where the element stiffness matrix $\{K_e\}$ will be given in the member local coordinates. A transformation of the element stiffness matrix from local to global coordinates is performed, before assembling the global stiffness matrix, by using the standard transformation formula:

$$[K] = [r_e]^T [K_e][r_e] \quad \text{.....(5-48)}$$

in which [K] is the member stiffness matrix in global coordinates, and $[r_e]$ is its rotation matrix given by:

$$[r_e] = \begin{bmatrix} [r] & 0 & 0 & 0 \\ 0 & [r] & 0 & 0 \\ 0 & 0 & [r] & 0 \\ 0 & 0 & 0 & [r] \end{bmatrix} \quad \text{.....(5-49)}$$

where [r] is a sub-matrix of order three, which gives the direction cosines of the member local axes with respect to the global axes. Due to large displacements that occur in cable-stayed structures under normal design loads, the joint coordinates used in computing these direction cosines are based on the new geometry of the structure in its deformed state after applying the external loads.

The algorithm for the above described procedure is given later in this chapter and a flow chart of the computer program is listed in **App.E.** This algorithm is efficient for performing a non-linear static analysis of three dimensional cable-stayed structures subjected to their own dead loads and a set of initial cable tensions. These initial cable tensions are specified such that the deformations in the structures are minimised under dead loads.

5.9 The equilibrium equation solver techniques

After the assembly of the stiffness matrix the equilibrium equation must be solved. There are many types of solvers that can handle the solution of equilibrium equation depending on the numerical technique they adopt ranging from the iterative methods such as the ***Gauss-Seedel*** or ***Gauss-Jordan*** techniques to the direct ***Gaussian*** elimination algorithms.

When we deal with simple structures, there is no significant difference whether we use the simple inverse technique or ***Choliskey*** or any other technique, but when the structure becomes more complicated and space analysis is adopted it means that the D.O.F are doubled for single node, and since the global system D.O.F is very large, a large amount of memory storage must be on duty by the computer. Hence, the need for new techniques of solving the equations arises.

There are two main features in handling the stiffness matrix of the structural analysis problems:-

- The symmetry of the global stiffness matrix.
- The banded nature of the global stiffness matrix.

Anyway, the main strategies used in the solvers are:-

- Band solutions.
- Front solutions.
- Sky lining [87].

These strategies are illustrated in figure (5-19).

This work adopts the ***Cholesky*** *Factorisation Method* for solving simultaneous linear equations, which solves banded form assembled systems.

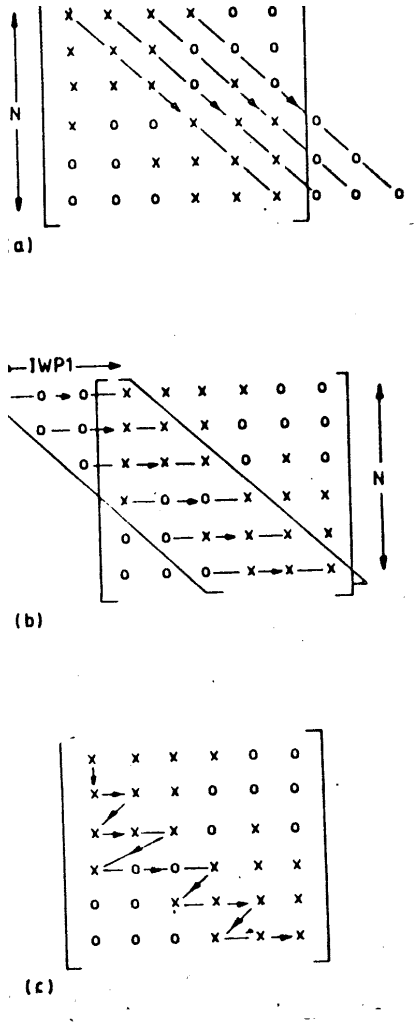

Figure (5-19) the most widely known solver strategies

5.10 The multipurpose computer program NASCFI

5.10.1 Program description and facilities:-

A multi-purpose computer program (***NASCFI***) is developed in the present study to carry out the large displacement elastic stability static analysis of 2-D and 3-D cable-frame interaction structures as well as of ordinary structures.

The program consists of several subroutines as described in tables of **App.E.** which complete the solution of the problem.

This program is a multi-purpose computer program which can introduce the following types of elastic static analysis:-

1. Neglecting all types of non-linearities (i.e. first order stability analysis)
2. S.D. geometrical non-linear analysis without axial effect (second order analysis).
3. L.D. geometrical non-linear analysis (axial and change in geometry)
4. L.D. geometrical non-linear analysis with bowing effect excluding the shear and (***SS*** effects).
5. L.D geometrical non-linear analysis including the coupled actions of both bowing and (***SS*** effects) and excluding the shear effects.
6. L.D geometrical non-linear analysis including the coupled actions of both bowing and (***SS*** effects) plus 2 methods of shear effect (the total angle shear effect and the flexural-angle shear effect).

Moreover, it has the following addition characteristics:-

* Both 2-D and 3-D problems can be handled by ***NASCF1***.
* ***NASCF1*** can handle the geometrical non-linear buckling analysis (the pre and post buckling critical loads adopting the arc length technique and convergence criterion described earlier).
* Both cable-frame as well as ordinary structures can be analysed by ***NASCF1***.

5.10.2 Program algorithm

Since this program deal with interaction between cable elements and beam column elements, the types of computational techniques mentioned earlier in this chapter (***N-R***, iterative, incremental and mixed) must be taken into account to satisfy the equilibrium equations, in addition, the tolerance must be achieved for the unbalanced load induced by these techniques at each load level. Based on the L.D. analysis detailed in **App.D.** and the **T.S.M.** for both B-C element and cable element and described in **chapter-3-**and **-4-** respectively, ***NASCF1*** follows the following algorithm path:-

1. Read the input data.

a. read the nature of structure (either cable-frame or ordinary structure)

b. Read nature of analysis

I. 2-D or 3-D

II. Type of geometrical non linearity.

III. Including shear method indicator included (either Meth.-0-,Meth.-1- or Meth.-2-)

IV. L.D. or S.D.

2. Using the latest available values for all geometric and static quantities determine the "t" matrix of all elements (**chapter-3- and -4-**).

a. Read the structural data (properties, geometry and F.E.A. with their "ΔP")and initial cable tensions, assume tolerance ≤ 0.01

b. Set all $\bar{C}_1, \bar{C}_2, \bar{b}_1, \bar{b}_2, \bar{t}_1 \& \bar{t}_2$ values at load parameter (ρ = 0).

c. Find "E_{eq}" from (eq.4.15).

3. Compute "τ for global coordinates, then assemble the system "**T.S.M.** thus obtained to establish the incremental equations of equilibrium.

4. Solve the equilibrium equations, by substituting "τ" and "ΔP" and solve for "ΔX", using the ***Cholesky*** factorisation method.

5. Determine the new geometric configuration of the structure.

a. Determine the new joint locations (coordinates) from:-

$$\{X\}_{i+1} = \{X\}_i + \{\Delta X\}_i \quad \text{.....(5.50)}$$

Note that the translation components of $\{X\}_{i+1}$ determine the new locations of all joints the joints of the system while the rotation components $\{X\}_{i+1}$ do not have a well defined physical significance, for example cumulative values are calculated exclusively for use in the convergence criteria described subsequently.

b. Determine the new joint orientation matrix for each joint:-

I. For each member, determine:-

$$\{\Delta\bar{v}\} = [R]^T\{\Delta v\}, \{\Delta u\} = [\bar{B}]^T\{\Delta\bar{v}\} \quad \text{.....(5-51)}$$

$$\{u + \Delta u\} \quad \text{.....(5-52)}$$

$$\{S + \Delta S\} = [t]\{u + \Delta u\} \quad \text{.....(5-53)}$$

$$\{\Delta r\} = [r]\left[\Delta\bar{\gamma}\right] \quad \text{.....(5-54)}$$

$$[r + \Delta r] \quad \text{.....(5-55)}$$

in which $[\Delta\bar{\gamma}]$ is the incremental rotation matrix for the member

in member coordinates and its equal to:-

$$\left[\Delta\bar{\gamma}\right] = \begin{bmatrix} 0 & -\Delta\bar{\gamma}_3 & \Delta\bar{\gamma}_2 \\ \Delta\bar{\gamma}_3 & 0 & -\Delta\bar{\gamma}_1 \\ -\Delta\bar{\gamma}_2 & \Delta\bar{\gamma}_1 & 0 \end{bmatrix} \quad \text{.....(5-56)}$$

$$\Delta\bar{\gamma}_1 = \frac{1}{2}\left(\Delta\bar{v}_4 + \Delta\bar{v}_{10}\right) \quad \text{.....(5-57.a)}$$

$$\Delta\bar{\gamma}_2 = \Delta\bar{v}_3 - \Delta\bar{v}_9 \quad \text{.....(5-57.b)}$$

$$\Delta\bar{\gamma}_3 = -\Delta\bar{v}_2 + \Delta\bar{v}_8 \quad \text{.....(5-57.c)}$$

II. for each member determine:-

$$[\Delta\alpha] = [\Delta W][\alpha] \quad \text{.....(5-58)}$$

$$[\alpha + \Delta\alpha] \quad \text{.....(5-59)}$$

in which [ΔW] is the incremental rotation matrix for the member

in global coordinates

and it is equal to:

$$[\Delta W] = \begin{bmatrix} 0 & -\Delta W_3 & \Delta W_2 \\ \Delta W_3 & 0 & -\Delta W_1 \\ -\Delta W_2 & \Delta W_1 & 0 \end{bmatrix} \quad \text{.....(5-60)}$$

and:

$$\Delta W_1 = \begin{bmatrix} \text{either } \Delta v_4 \\ \text{or} \quad \Delta v_{10} \end{bmatrix} \quad \text{.....(5-61.a)}$$

$$\Delta W_2 = \begin{bmatrix} \text{either } \Delta v_5 \\ \text{or} \quad \Delta v_{11} \end{bmatrix} \quad \text{.....(5-61.b)}$$

$$\Delta W_3 = \begin{bmatrix} \text{either } \Delta v_6 \\ \text{or} \quad \Delta v_{12} \end{bmatrix} \quad \text{.....(5-61.c)}$$

depending on the particular joint under consideration, all other quantities are defined in **App. C.**

6. Determine member end forces: for each member determined first the end forces "$\bar{S}$", and then the end forces in global coordinates ($\bar{F} = R\bar{B}\bar{S}$). In this step the computational difficulty of the axial force is induced from the relative member deformations (see remark B).

7. The solution obtained thus far represents an approximate configuration in the sense that the system equilibrium equations are not necessarily satisfied at the load level "P_{i+1}" This approximate solution is corrected by a ***N-R*** types detailed earlier until the equilibrium equations are satisfied within a prescribed tolerance. In the following, the subscript "j" refers to the "j^{th}" iteration cycle, while "P" is kept constant at "P_{i+1}". The unbalanced joint forces, "ΔQ" are determined from (ΔQ_j = P-f (F_j)).

8. Using latest available values of all geometric and static quantities determine "t" in local coordinates, then for each member **T.S.M.** in global coordinates, and then assemble the system **T.S.M.**

   For the cable element use eq.(4-16) to determine the secant equivalent modulus of elasticity, and then use it in calculating the new "t" matrix of this element, then establish its **T.S.M** (τ) using eq.(4-30).

9. Treating the unbalanced joint forces as a load increment determine the correction factor, "ΔX" from the incremental relationship:

   $[\tau]_j \{\Delta X\}_j = \{\Delta Q\}j$ (5-62)

10. If the correction displacement vector is not small enough, determine the new joint locations:-

    a. $\{X\}_{j+1} = \{X\}_j + \{\Delta X\}_j$ .....(5-63)

    b. New joint orientation matrix

   then repeat steps from "5" to "10" until the "ΔX" value is sufficiently small according to a prescribed criterion (see *remark A*).

11. Consider a new load increment, "ΔP", and return to step "2".

Remark A: The specific displacement convergence criterion used herein is given by:

$$\left[\frac{\sum_{1}(\Delta X)_i^2}{\sum_{1}(X)_i^2}\right] \le e \quad \text{.....(5-64)}$$

"e" is a prescribed tolerance, in applying this criteria, translation and rotation components of-X- are treated as separate groups, and convergence is assumed to have occurred when eq.(5-64) is satisfied simultaneously and independently for each group. However, "e" is taken equal to (10^{-5}).

Remark B: In step "6" the difficulty of the axial force from relative member deformation in determining $\bar{S}$ from "$\bar{u}$". This is because the expression for member axial force, "Q" as given:-

$$Q = EA\left(\frac{u}{L} - C_{b_3} - C_{b_2} - C_{T_3} - C_{T_2}\right) \quad \text{.....(5-65)}$$

Involves bowing and twisting functions ($\bar{b}_{1_j}, \bar{b}_{2_j}, \bar{t}_{1_j} \& \bar{t}_{2_j}$) which in turn are functions of *axial* force parameter "ρ", this problem can be solved using an iterational technique of [49]:

$$K(\rho) = \frac{\pi^2}{\lambda^2}\rho - \frac{u}{L} + C_{b_3} + C_{b_2} + C_{T_3} + C_{T_2} = 0 \quad \text{.....(5-66)}$$

Let ρ_i be an approximate solution of this equation. By using a first order ***Taylor*** series expansion eq. (5-66) becomes [47]:

$$K(\rho_i + \Delta\rho_i) = K(\rho_i) + K'(\rho_i)\Delta\rho_i = 0 \quad \text{.....(5-67)}$$

in which a prime superscript denotes a differentiation with respect to ρ, and:-

$$K'(\rho) = \frac{\pi^2}{\lambda^2} + C'_b + C'_T \quad \text{.....(5-68)}$$

An approximate solution, (ρ_i) of eq. (5-67) is initially assumed, and is modified successively by using relationship:-

$$\rho_{i+1} = \rho_i + \Delta\rho_i = \rho_i - \frac{K(\rho_i)}{K'(\rho_i)} \quad \text{.....(5-69)}$$

where:

$$K'(\rho_i) = \frac{dK(\rho)}{d\rho} = \overline{H} \quad \text{.....(5-70)}$$

" $\overline{H}$ " is taken from eq.(3-116)

This iteration continues till "$\Delta\rho$<e", where "e" is taken as a prescribed tolerance equal to (0.001).

$$C'_b = b'_1(\theta_1+\theta_2)^2 + b'_2(\theta_1-\theta_2)^2 + 2b_1(\theta_1+\theta_2)(\theta'_1+\theta'_2) + 2b_2(\theta_1-\theta_2)(\theta'_1-\theta'_2)$$
$$C'_T = \frac{rM_t}{(GJ+\overline{K})}(\bar{t}'_1\theta_1 + \bar{t}'_2\theta_2 + \bar{t}_1\theta'_1 + \bar{t}_2\theta'_2) \quad \text{.....(5-71)}$$

the prime superscript of the angle (θ) can be classified into two groups:-

* The rigidly connected joints, where the rotation at such rigid ends are defined by the global joint displacement and remain constant during this iteration process.

$$\theta'_i = 0 \quad \text{.....(5-72)}$$

* The pinned connected joints, the values of the angles (θi) and their derivatives (θ'i) as follows:-

- End-1- is hinged:-

$$\theta_1 = \frac{C_2}{C_1}\theta_2 \quad \text{.....(5-73)}$$

$$\theta'_1 = \frac{\theta_2}{C_1^2}(C'_1C_2 - C_1C'_2) \quad \text{.....(5-74)}$$

- End-2- is hinged:-

$$\theta_2 = \frac{C_2}{C_1}\theta_1 \quad \text{.....(5-75)}$$

$$\theta'_2 = \frac{\theta_1}{C_1^2}(C'_1C_2 - C_1C'_2) \quad \text{.....(5-76)}$$

- Both ends are hinged:-

$\theta_1 = -\theta_2$ for first buckling mode .....(5-77)

$\theta_1 = \theta_2$ for second buckling mode .....(5-78)

After determining the axial force, "Q", by the iterative procedure, member end moments are then computed from:

$$M_{1j} = \frac{EI_j}{L}\left(\overline{C}_{1_j}\,\theta_{1_j} + \overline{C}_{2_j}\,\theta_{2_j}\right) \quad \text{.....(5-79)}$$

$$M_{2j} = \frac{EI_j}{L}\left(\overline{C}_{2_j}\,\theta_{1_j} + \overline{C}_{1_j}\,\theta_{2_j}\right) \quad \text{.....(5-80)}$$

$$M_t = \frac{C_t}{L}\phi_t \quad \text{.....(5-81)}$$

$$Q = EA\left(\frac{u}{L} - C_{b_3} - C_{b_2} - C_{T_3} - C_{T_2}\right) \quad \text{.....(5-82)}$$

where j=2, 3.

However, this technique has never been used for the cable-stayed structures before.

This program is coded using both ***BASIC4.5*** language for the Quick basic compiler and ***FORTRAN77*** using ***LEIHE*** compiler on an IBM-PC computer.

All the subroutines used in the ***NASCF1*** program with the program flow chart are tabulated in **App.E**.

CHAPTER SIX

CASE STUDIES AND COMPUTER PROGRAM TESTING

6.1 Introduction:-

In an effort to asses the computational merits and limitations of the proposed large deflection including shear effect analysis this chapter presents a wide range testing of the computer program **(*NASCFI*)** based on the original theoretical developments made in this study.

As it is defined in **chapter-3-, the new shear bowing effect** can be ignored both in small and large deflection theories when we are dealing with solid or closed-web cross sections (only flexural bowing and change in length is considered), while it begins to be more dominant when lattice, trussed or open-web cross sections are used. **The new 3-D (*SS* effect)** in turn has no sign to be included elsewhere. Accordingly, "**30**" case studies representing different types of structures are tested in this chapter and can be classified into 3 major parts:-

- **Basic theory case studies:** in which the first main contributional goal of this study is achieved and the basic linearized-step conventional beam-column theory is tested including the(***SS*** effect**)** (for the 3-D problems) by analyzing "**15**" numerically various case studies in both 2-D and 3-D fields of analysis. Much attention is paid to the program validity, applicability and accuracy when applied to the most widely known structural stability problems. All the "**15**" problems are summarized in table (6-1.a)
- **Shear effect case studies:** in **which** the second main contributional goal of this study is achieved when **"5"** problems are studied to check the shear and the shear bowing effects on the large displacement stability analysis of structures. Table (6-1.b) summarizes these case studies.
- **Cable-Structure interaction case studies: where** "**10**" problems of different types of 2-D & 3-D cable stayed or suspended structures are analyzed using the (***NASCFI***) multi-purpose computer program. Table (6-1.c) illustrates these "**10**" case studies.

For the **30** case studies mentioned earlier, the following points will be observed:-

1. The agreement of the **P-Δ** behavior with other researchers results using the ratios of the methods **Meth.-0-, Meth.-1-,** and **Meth.-2-** to others.
2. The **shear effect** ratio using **Meth.-1- / Meth.-0-** and **Meth.-2- / Meth.-0-** results.
3. The **bowing and change in length effects** using **L.D. / S.D.** ratios, where the **S.D.** herein represent the non-linear bowing-change in length excluding analysis while **L.D.** represents those effects to be included.
4. The **3-D (*SS* effect)** i.e., the coupled torsional-shear-flexural effect for the 3-D problems using the ratio of **SS/SS0** (e.g., including the ***SS*** effect to ignore it).
5. Other points like $\mathbf{P_{cr}}$, hence the pre-buckling and post-buckling paths, the load-**T.S.M.** determent curves are made for some of them to check the first mode buckling load, and the relationship between the cable sags, and pretensions in cables.

6.2 Basic theory case studies:-

Table (6-1.a) illustrates the "**15**" case studies with their researchers names, publishing years, type of analytical method used, the values of each case study shear parameter "**u**" which are as much as zero (i.e. the effect of shear can be negligible in such cases), and their sketches.

Table (6-1.a): Basic Theory Case Studies

Case No.	***Notation***	***Reference***	***Year***	***Type of Analysis***	***Shear Parameter.(u)***
1	2-D Cantilever Beam	Oran &Kassimali[70]	1976	Exact Solution	$3.55*10^{-5}$
2	2-D Two-Member Cantilever Beam	Oran& Kassimali[70]	1976	Exact Solution	0.0000108 - 0.0000115
3	3-D Angle Cantilever Column	Al-Bermani & Kitipornchai[2]	1990	Theoretical	u_{x1}= 0.01387 u_{x3}= 0.00744
4	3-D Init.Imprf.Circular. Ring Pin-End.B-C. "with Variable L/r"	Meek & Loganathan[63]	1989	Theoretical	0.00128 -0.00513 (all directions)
5	3-D Init.Imprf.S.H.S Pin - End. B- C.	-Meek & Loganathan[63]	1989 -	Theoretical & Experimental	0.00388 -0.01516 (all directions)

	"with Variable L/r"	-Sully &Hancock[89]	1996		
6	3-D Circular.Ring Fixed-Ended B-C. "with Variable L/r "	Meek& Loganathan[63]	1989	Theoretical & Experimental	u_1 = 0.00634 u_2= 0.04190 (all directions)
7	2-D Two-Bar Shallow Truss	Oran & Kassimali[70]	1976	Exact Solution	$3.60*10^{-13}$
8	2-D One-Story Bent Frame	Oran & Kassimali[70]	1976	Theoretical	Girder = 0.065 Column = 0.065
9	2-D William Toggle Frame	Wong & Tin Loi [108]	1990	Theoretical & Experimental.	0.00104
10	2-D Rigid-End.Portal "H/V=Var.1/2-1/4"	Siddeek K.F[85].	1990	Theoretical & Experimental.	Beam = 0.026 Column = 0.0367
11	2-D Clamped-Hinged Arch	Hsiao & Hou[41]	1987	Theoretical	0.00146
12	3-D Bent Joint Cantilever	Kassimali & Abbasania[48]	1991	Theoretical	u_{x1}=0.0013-0.045 u_{x3}=0.0006-0.022
13	3-D Pretilt.&Pretwis. Pyramide Shaped	See & McConnel[84]	1986	Theoretical & Experimental	0.0038 (all directions)
14	3-D Arch Frame	Wen & Rahimzadeh[103]	1983	Theoretical	u_{x1}= 0.0044-0.018 u_{x3}= 0.0015-0.018
15	3-D Framed Dome	Kassimali & Abbasania[48]	1991	Theoretical	u_{x1}=0.0105- 0.105 u_{x3}=0.107-0.0411

Table (6-1.b): Effect of Shear Case Studies

Case No.	*Notation*	*Reference*	*Year*	*Type of Analysis*	*Shear Parameter (u)*
1	2-D Simple-Suprt.Beam with L/D " 5,10,15 & 20"	J.S.Kinney[49]	1957	Theoretical	u_1=1.42,u_2=0.35 u_3=0.158,u_4=0.0887
2	2-D Four-Story Frame H/V Varies:- ".1,.24 & .5"	T.Y.Kam[46]	1988	Theoretical	Girder=0.026 Bottom Col.=0.184

					Other Col.=0.13
3	2-D, X-Bracing Cantilever Truss	A.K.Noor[67]	1974	Theoretical	0.2506
4	3-D, X-Bracing Transmission Tower	A.K.Noor[67]	1974	Theoretical	u_{x1}= 1.24-2.48 u_{x3}=0.0031-2.48
5	2-D,2-Bay Lattice Frame "3 different loading cases"	Lin &Glauser[56]	1970	Theoretical	Outer Col.=0.8863 Inner Col.=3.86 Girder=0.1115

Table (6-1.c): Guy Towers Case Studies

Case No.	*Notation*	*Reference*	*Year*	*Type of Analysis*	*Shear Parameter (u)*
1	2-D Stay Col. "with Initial Imperfect. & Pretension"	Temple, Parkash& Ellis[95]	1984	Theoretical & Experimental	u_1= 0.0112 u_2= 0.3204
2	2-D Simple Guy Tower	• Chu & Ma[23] Schreffler et.al.[83]	1976 1983	Theoretical	$6.4*10^{-4}$
3	3-D Single-Level Guyed-Tower "W.L."	Ramman et al.[76]	1988	Theoretical	u_{xi} =0.00314(all dir.)
4	3-D Multiple Guyed-Tower "W.L."	Ramman et al.[76]	1988	Theoretical	u_{xi} (Varies from:-) 0.0009-0.0046 (all directions)
5	2-D Bow-String Girder	Schreffler et al.[83]	1983	Theoretical	Bow Arch=0.002 Girder =0.081
6	2-D Simple-Span Lattice Tower	Williamson & Margolin[104]	1966	Theoretical	u_1 = 0.1334 u_2 = 2.1338
7	2-D Multi-Span Lattice Tower	Williamson & Margolin [104]	1966	Theoretical	u_i = 0.072,0.061, 0.052,0.048,11.15
8	3-D, R.C. Tower Cable-Stay Bridge "Model I"	Nazmy & Abdel Ghaffar[66	1990	Theoretical	u_{xi} (Varies From:-) $7.18*10^{-8}$ -$2.39*10^{-7}$

9	3-D, R.C. Tower Cable-Stay Bridge "Model II"	Nazmy & Abdel Ghaffar[66]	1990	Theoretical	u_{xi} (Varies From:-) $6.15*10^{-8}$ -$3.59*10^{-7}$
10	2-D Continuos Lattice Tower Suspension Bridge	Schrefler et al[83]	1983	Theoretical	3.3405

In all the mentioned studies we tried the wide range of different structures to be fully equipped.

6.2.1 Case study no. 1(cantilever beam):-

The elliptical integral exact solution of this problem is made by ***Bisshopp*** & ***Drucker*** (1945) by assuming that the beam is perfectly inextensible, a relatively large area is assumed in the present analysis in order to approximate a similar condition of inextensibility. Table (6-2.a) summarizes the properties of this problem where its obvious that the cantilever is analyzed using one beam-column element, its also obvious that the effect of shear in this problem is equal to zero since the value of the shear parameter **"u"** reaches zero value.

Table (6-2.a): Cantilever Beam Properties

Elm. "(i)"	*Length "L_i (mm)"*	*Area "A_i (mm^2)"*	*Elastic Modulus "E_i (Mpa)"*	*Moment of Inertia "I_i (mm^4)"*	*Shear Prmtr. "u_i"*	*Joint Load "P12 (kN)"*
1	2540	64516	68.95	416231.43	3.553*10-5	1.78*10-3

Many researchers studied this problem where no instability occurred, some of them analyzed it linearly or using **S.D.** theory while others took the effects of axial, change in length, or flexural bowing, i.e. **L.D.** effects into considerations, table (6-2.b) summarizes the efforts of many investigators as a comparison of **P-Δ** results. Also figure (6-1) illustrates the **P-Δ** behavior of this case study by analyzing it by putting **u = 0** which represents **(Meth.-0-)** and the shear parameter value **u = 3.553E-5** to be considered as shear effect analysis which represents **(Meth.-1-&Meth.-2-)** both in **S.D. non-linear analysis (no bowing and no change in length)** which is denoted in dashed lines, and in **L.D.** analysis denoted in solid lines. Both horizontal and vertical displacements of point "**B**" are drawn.

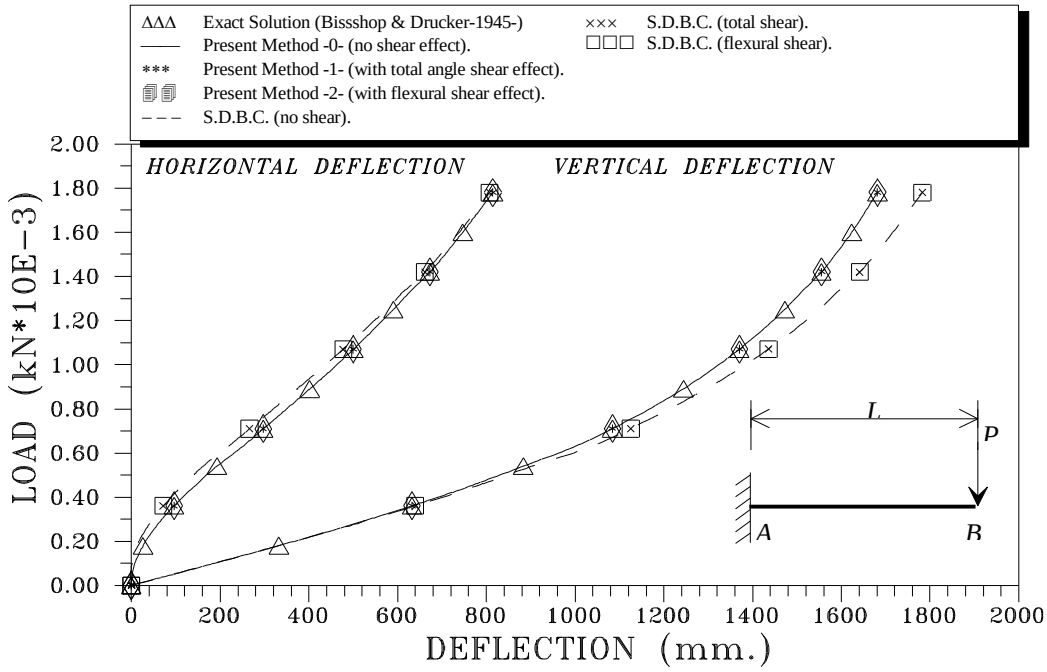

Figure (6-1) Load-Deflection Curve For cantilever Beam

It can be seen that all **Meth.-0-, Meth.-1-,** and **Meth.-2-**are in excellent agreement with the exact solution, this is because of the very small value of "**u**" which means no significant role of shear in this solid section problem. ***Langrangian*** and ***Eulurian*** iterative solutions of ***Oran*** and ***Kassimali*** [70](1976) have also a good agreement with the exact solution as it can be noticed from table (6-2.b) while ignoring **the bowing effect** shifted the results away by about **11.325%.**

From figure (6-1) it can be noticed that the shear effect in both **S.D.** and **L.D.** gives no difference in horizontal and vertical deflections, the final displacements occur at **1.78E-3 kN** have **-5.84%** and **0.12%** difference between **S.D.** and **L.D.** analysis for vertical and horizontal deflections respectively.

6.2.2 Case study no. 2(two-member cantilever):-

This case study was solved exactly by ***Frisch-Fay*** (1961) using elliptical integral, also it was examined by many investigators as it obviously noticeable in table (6-3.b)**,** table (6-3.a) in turn gives the detailed properties of this problem where it can easily be seen that the **"u"** value is so small that the shear effect has no influence on its stability analysis.

Table (6-2.b): Compression of Solutions for Cantilever Beam

No.	*Method*	*Type of Analysis*	*No. of Element*	*No. of Increment*	*Vertical Deflection (mm)*
1	Elastica	Exact Solution	1		1682.55
2	Linear	Beam-Column S.D.	1	20	3444.24
3	Oran & Kassimali (1976)	Beam-Col.L.D. Incremental Eularian (with no bowing)	1	20	2004.82
4	Oran & Kassimali (1976)	Beam-Column L.D. Incremental Eularian	1	20	1777.77
5	Oran & Kassimali (1976)	Beam-Column L.D. Iterative Lagrangian	1	20	1725.19
6	Oran & Kassimali (1976)	Beam-Column L.D. Iterative Eularian	1	20	1682.55
7	Present Method "0"	Beam-Column L.D. "No Shear"	1	20	1682.55
8	Present Method "1"	Beam-Column L.D. "with Shear"	1	20	1682.55
9	Present Method "2"	Beam-Column L.D. "with Shear"	1	20	1682.55

Table (6-3.a): Two-Member Cantilever Beam Properties

Element "(i)"	*Length "L_i (mm)"*	*Area "A_i (mm^2)"*	*Elastic Modulus "E_i (Mpa)"*	*Mom.of Inertia "I_i (mm^4)"*	*Shear Prmtr. "u_i"*	*Joint Load "P_{i2} (kN)"*
1	1328.42	129.03	200000	69.37	$1.083*10^{-5}$	0.004450
2	1288.54	129.03	200000	69.37	$1.151*10^{-5}$	0.007076

Table (6-3.b): Compression of Solutions for Two-Member Cantilever Beam

No.	*Method*	*Type of Analysis*	*No. of Element*	*No. of Increment*	*Uc/L Horizontal*	*Vc/L Vertical*
1	Elastica	Exact Solution	-	-	0.3081	0.6551
2-a	Argyris (1964)	Finite Element (L.D.)	2	20	0.3521	0.7314
2-b	Argyris (1964)	Finite Element (L.D.)	20	100	0.3403	0.6884
3-a	Martin (1965)	Finite Element (L.D.)	2	20	0.3505	0.7219
3-b	Martin (1965)	Finite Element (L.D.)	20	100	0.3345	0.6872
4	Mallet&Marcal(1968)	Finite Element (L.D.)	2	20	0.0002	0.0172
5-a	Jennings-NR (1968)	Finite Element (L.D.)	2	20	0.2980	0.6479
5-b	Jennings-SI (1968)	Finite Element (L.D.)	2	20	0.0052	0.1096
5-c	Jennings-SI (1968)	Finite Element (L.D.)	20	100	0.2989	0.6557
6-a	Powel-NR (1969)	Finite Element (L.D.)	10	20	0.0765	0.3436
6-b	Powel-SI (1969)	Finite Element (L.D.)	2	20	0.0002	0.0602
6-c	Powel-SI (1969)	Finite Element (L.D.)	20	100	0.1112	0.4330
7	Oran (1973)	Beam-Column (L.D.)	2	20	0.3081	0.6491
8	Oran&Kassimali(1976)	Beam-Column (L.D.)	2	20	0.2928	0.6686
9-a	Wen&Rahimzadeh(1983)	F.E.M.(L.D."Lagrng.")	2	20	0.7679	1.1414
9-b	Wen&Rahimzadeh(1983)	F.E.M.(L.D."Eulrn. ")	2	20	0.3496	0.711
10	Present Method "0"	B.C.(L.D."No Shear")	2	20	0.2996	0.6515
11	Present Method "1"	B.C.(L.D."withShear")	2	20	0.2997	0.6515
12	Present Method "2"	B.C.(L.D."withShear")	2	20	0.2997	0.6515

It's clear from table (6-3.b) and figure (6-2) that the present analytical solution, although it uses only two elements and 20 load increments, is as accurate as, if not more so than the other investigators, solutions obtained by using sometimes more than 2 elements. The **V/L** ratio for the present solution gives **99.45%** accuracy with the exact solution, while the **H/L** ratio gives **97.274%**. The shear effect has no role in this case since the "**u**" value is very small, so **Meth.-0-, -1-, & -2-** again coincide with each other. Also its noticeable from figure (6-2) that the **L.D./S.D.** (both non-linear) ratio is about **28.57%** for the vertical deflection of point "C" at last stage of loading.

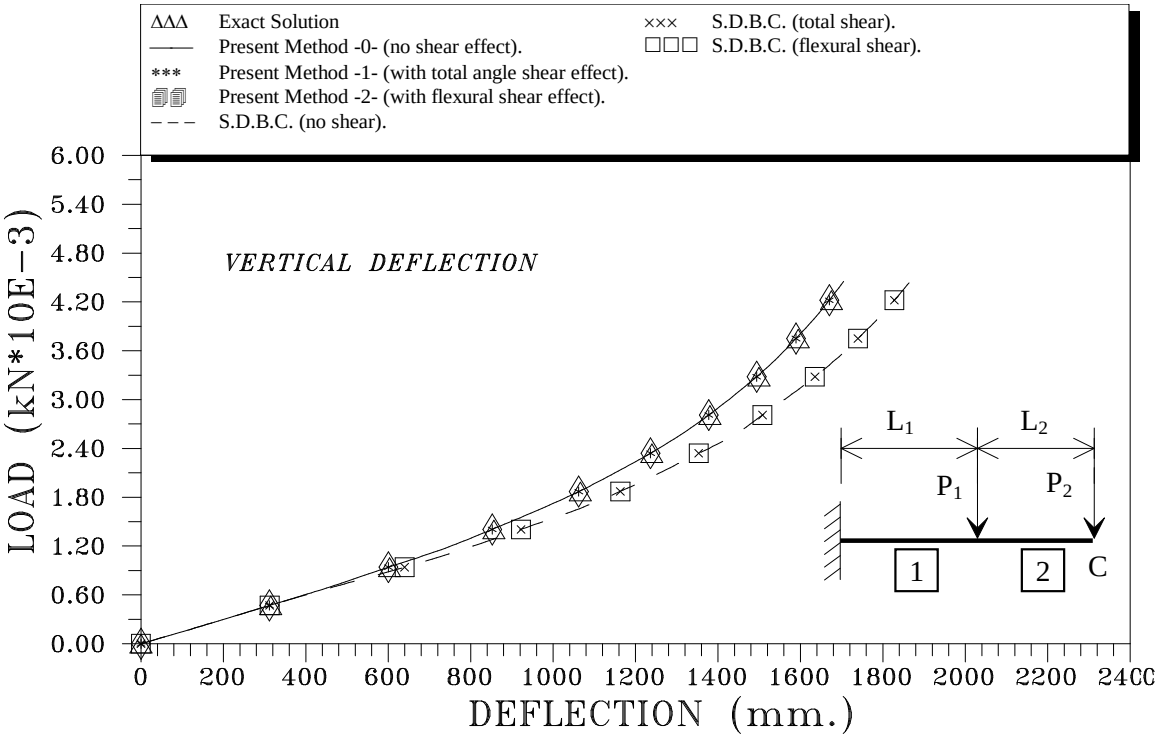

Figure (6-2) Load-deflection curve for the two-member cantilever

6.2.3. Case study no. 3(3-D angle cantilever beam-column):-

As it known that the beam-column differs from the beam element in the dominant role of axial force on the stiffness matrix of the element, although this case has no exact solution, some researchers tried to analyze it either by **F.E.M.** or by ordinary stiffness method or even by beam-column technique. Table (6-4.a) summarizes this case properties and table (6-4.b) summarizes the different investigators analytical results. In this problem an angle cross section of the properties detailed above with a ***Poisson***'s ratio **ν = 0.5** to be constant in all directions leads to shear parameter **"u"** as shown in the table subjected to gravity load along the shear center axis at the free end and has been analyzed for 3-D large deflection by present analytical procedure using one element in modeling the structure.

Table (6-4.a):3-D Angle Cantilever Column Properties

Element ***(i)***	***Element Section***	***Length*** ***"L_i(mm)"***	***Elastic Modulus*** ***"E_i (Mpa)"***	***Area*** ***"A_i (mm^2)"***	***Web Area*** ***"A_w(mm^2)"***	***Shape Factor*** ***"n=A/A_w"***	***Moment. of Inertia*** ***"Ix_i (mm^4)"***	***L/r***	***Shear Parameter*** ***"u"***	***Joint Axial Load*** ***"P_{12} (kN)"***
1	L76*51*6.5	1400	200000	767.74	X_1= 494.0 X_3= 331.5	X_1= 1.554 X_3 = 2.316	X_1=453692.25 X_3=163162.71	X_1= 57.59 X_3= 96.03	X_1= 0.01387 X_3=0.00744	20

The effect of unsymmetry of the cross section leads to the horizontal

displacement in both directions -X_1-and -X_3- as it is obviously seen in figure (6-3) The excellent agreement in the 3-directions deflection results in comparison with others leads to the conclusion of the applicability and accuracy of **(*NASCFI*).** Meanwhile figure (6-3) and table (6-4.b) illustrate the negligible role of the shear stiffness in the overall tangent stiffness matrix **(T.S.M.)** of the structure since we have a closed web element. Also excellent agreement in the **P-Δ** results using **S.D. analysis** has been introduced between shear and no shear effect analysis. In comparison with the first two case studies we can notice that there is some amount of difference between **Meth.-0-** and both **Meth.-1- & Meth.-2-** results and this is because the value of "**u**" increases about **2000** times than case-1- and about **6500** over case-2-.

Table (6-4.b):-Various Methods Compression for 3-D Angle Cantilever Deflections

					Deflections in 3-Directions (mm.)		
No.	***Method***	***Type of Analysis***	***No.of Element***	***No.of Increment***	***Axial Shortening(u)***	***Lateral Deflection(w)***	***Lateral Deflection(v)***
1	Al-Bermani& Kitipornchai (1990)	Beam-Column L.D.	1	20	20	26.57	22.23
2	Chan & Kitipornchai (1987)	Beam-Column L.D.	6	20	20.19	26.57	22.23
3	Present Method "0"	Beam-Column L.D."No Shear"	1	20	20.21	26.60	22.22
4	Present Method "1"	Beam-Column L.D."with Shear"	1	20	20.23	26.60	22.22
5	Present Method "2"	Beam-Column L.D."with Shear"	1	20	20.23	26.60	22.22

The (***SS*** effect) can be measured by the ratio **SS/SS0,** which is **2.68%** decrement for -X_1- and **4.38%** increment and -X_3- respectively for both methods.

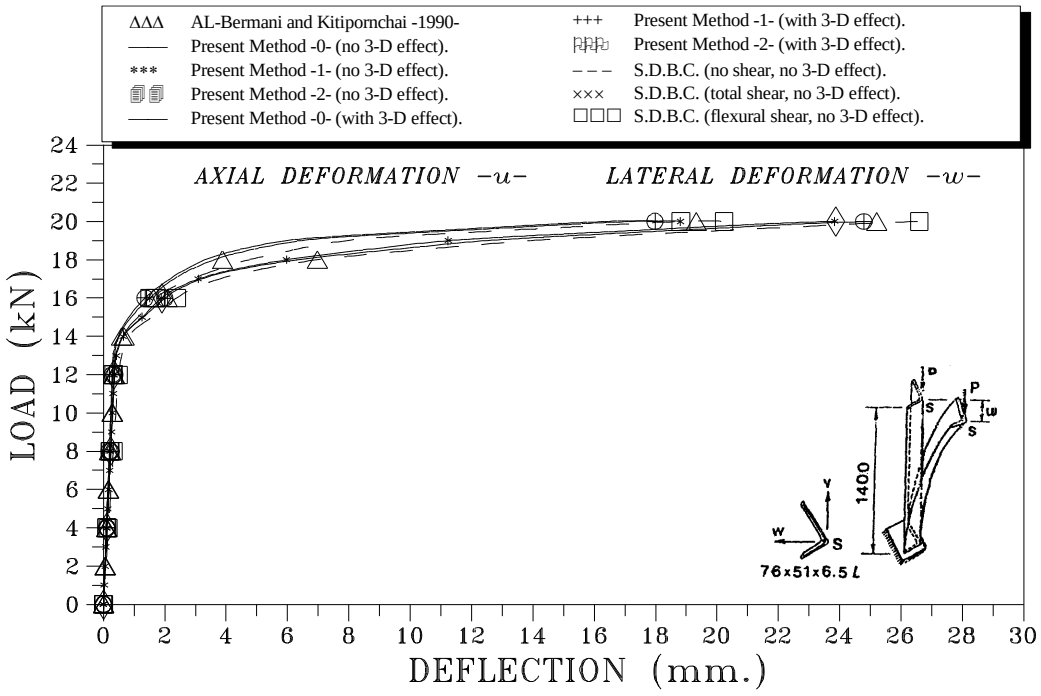
ΔΔΔ AL-Bermani and Kitipornchai -1990-
Present Method -0- (no 3-D effect).
*** Present Method -1- (no 3-D effect).
Present Method -2- (no 3-D effect).
Present Method -0- (with 3-D effect).
+++ Present Method -1- (with 3-D effect).
Present Method -2- (with 3-D effect).
S.D.B.C. (no shear, no 3-D effect).
××× S.D.B.C. (total shear, no 3-D effect).
S.D.B.C. (flexural shear, no 3-D effect).
AXIAL DEFORMATION -u-
LATERAL DEFORMATION -w-
LOAD (kN)
DEFLECTION (mm.)
1400
76×51×6.5 L

Figure (6-3) Load-deflection curve for the 3-D angle cantilever beam-column

6.2.4 Case study no.4 3-D initial imperfect circular ring pin-ended beam-column):-

This problem was analyzed by many investigators using elastic-plastic analysis as it is shown in table (6-5.b) Three cases are studied for this problem (**L/r =80, 120, & 160,** respectively), the properties of all cases are detailed in table (6-5.a).

Table (6-5.a):3-D Initial Imperfection Circular Ring Pin-Ended Beam-Column Properties

Case	*Element Section D*t(mm.)*	*L/r*	*Leng. "L(mm)"*	*Area "A(mm²)"*	*Moment of Inrtia. "I(mm⁴)"*	*Elastic Modulus "Ei(Mpa)"*	*Initial Imperfect. "e₀/L"*	*Shear Prmt."u"* (all directions)	*Axial Load "P(kN)"*
1	114.3*2.38	80	4318	807.095	2351416.2	199955	0.001	0.00513	170.0
2	114.3*2.38	120	6477	807.095	2351416.2	199955	0.001	0.00282	100.0
3	114.3*2.38	160	8636	807.095	2351416.2	199955	0.001	0.00128	57.75

This problem was analyzed non-linearly covering both material and geometry in elastic and elastic-plastic behavior and the usual technique used in analysis of this problem was the finite segment method assuming the generalized cyclic stress-strain relationship for the material non-linearity and an automatic load-control technique as ***Han*** & ***Chen*** or ***Sugimoto*** & ***Chen*** did, an initial central deflection of **(0.001 L)** was assumed.

Table (6-5.b) illustrates all the previous attempts in the analyzing of this problem, in addition to the present three methods **(Meth.-0-,-1-, &-2-)**. Although the work done before was elastic-plastic, the portion concerning our work deals with pre-buckling stability analysis which is actually elastic analysis, so the comparison is done in this portion only with a recommendation that an elastic-plastic development on our study is be done in the future. The "**u**" value is taken constant in both horizontal directions since the same Poisson's ratio "**ν= 0.5**", and shape factor "**n**" for circular section are used.

Table (6-5.b): Results & Comparison of 3-D Initial Imperfection Circular Ring Pin-Ended Beam-Column

					Central Deflection "(mm.)"		
No.	***Method***	***Type of Analysis***	***No.of Element***	***No.of Increment***	***Case 1***	***Case 2***	***Case 3***
1	Sugimoto & Chen (1985)	E-P ,F.S.M. L.D.	26	10	16.784 at169.1 kN	15.082 at 70.0 kN	37.341 at 45.336 kN
2	Chan& Kitipornchai(1988)	E-P ,F.S.M. L.D.	12	16	16.513 at 169.1 kN	15.243 at 70.0 kN	36.953 at 45.336 kN
3	Meek& Loganathan(1989)	E-P ,F.S.M. L.D.	12	16	16.979 at169.1 kN	15.973 at 70.0 kN	37.342 at 45.336 kN
4	Present Method "0"	Beam-Col. L.D."No Shear"	1	10	17.308 at 169.1 kN	15.330 at 70.0 kN	35.531 at 45.336 kN
5	Present Method "1"	Beam-Col. L.D."withShear"	1	10	17.309 at 169.1 kN	15.330 at 70.0 kN	35.531 at 45.336 kN
6	Present Method "2"	Beam-Col. L.D."withShear"	1	10	17.308 at 169.1 kN	15.330 at 70.0 kN	35.530 at 45.336 kN

In figures (6-4.a, 6-4.b, and 6-4.c)**,** it can be observed clearly that the shear effect in all the three cases is negligible in both **S.D.** and **L.D.** analysis. Nevertheless, the higher **L/r** the lower difference between **Meth.-0-** and shear including methods **Meth.-1-.&Meth.-2-**, this because the simple fact that the "**u**" value depends on the **L/r** value as it is obvious from the definition of the shear parameter "**u**" (see table 3-2).

Furthermore, the larger the **L/r** value the higher divergence between **S.D.** and **L.D.** results and this is simply because of the reason that whenever the member or the element get longer or less slender the **L.D.** effects will be more considerable and effective.

The critical load of the three cases of this problem are **(169.1 kN, 70 kN, and 45.4 kN)** respectively, as it seen from both the graph and the table and a good agreement is also noticed between the present formulation and the other researchers elastic results.

The higher **L/r** the higher (***SS*** effect) observed as the **SS/SS0** ratio for the three cases indicate which they are **2.83%, 3.46%,** and **5.58%** increment respectively for both methods.

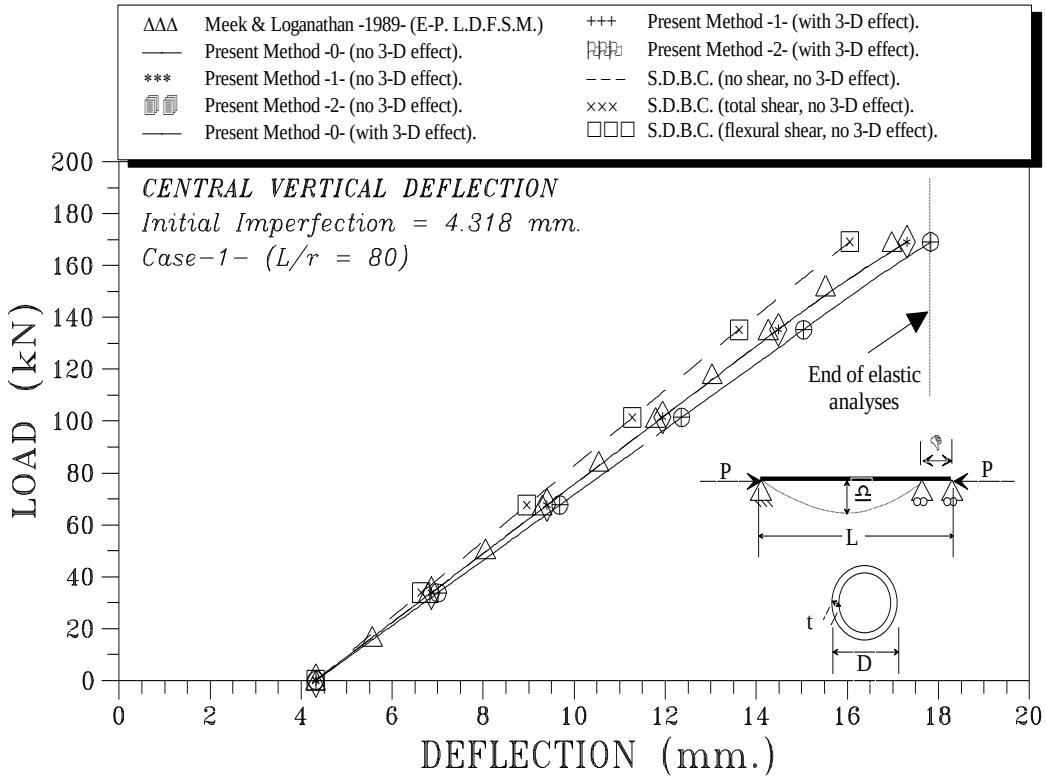

Figure (6-4.a) Load-deflection curve for the 3-D initial imperfection pin-ended circular ring for L/r =80

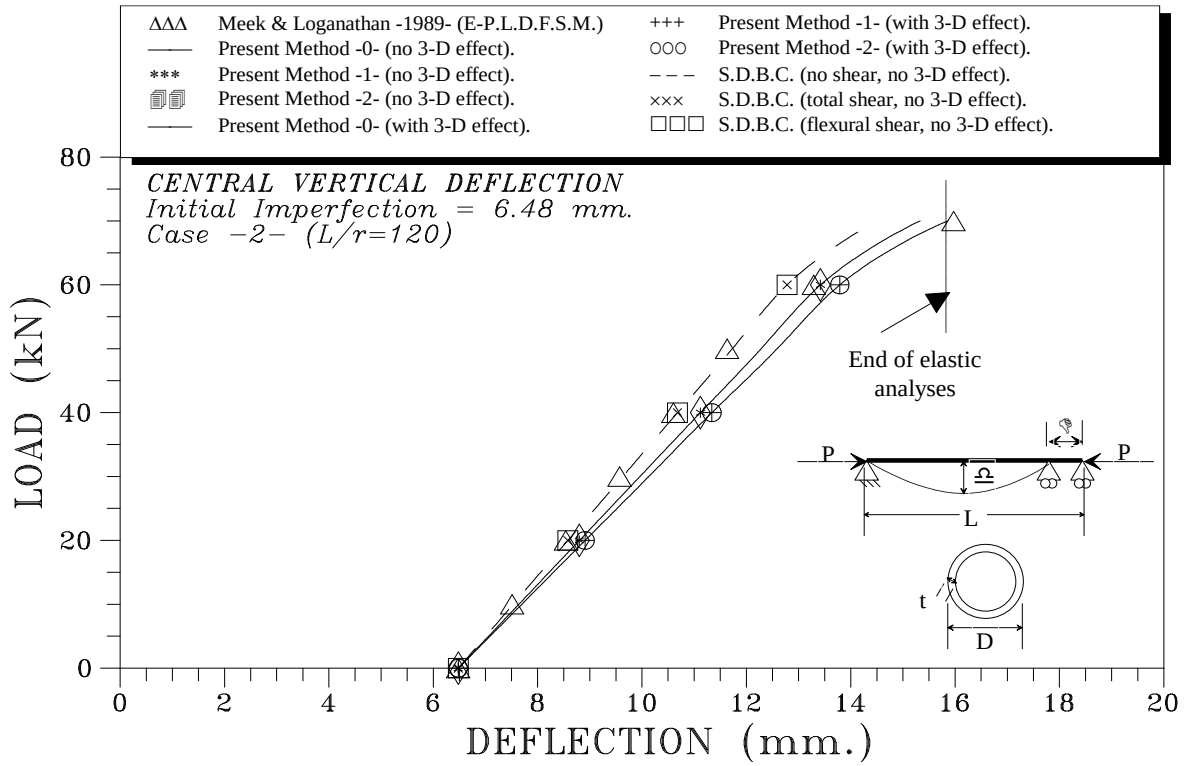

Figure (6-4.b) Load-Deflection curve for the 3-D initial imperfection pin-ended circular ring for L/r =120

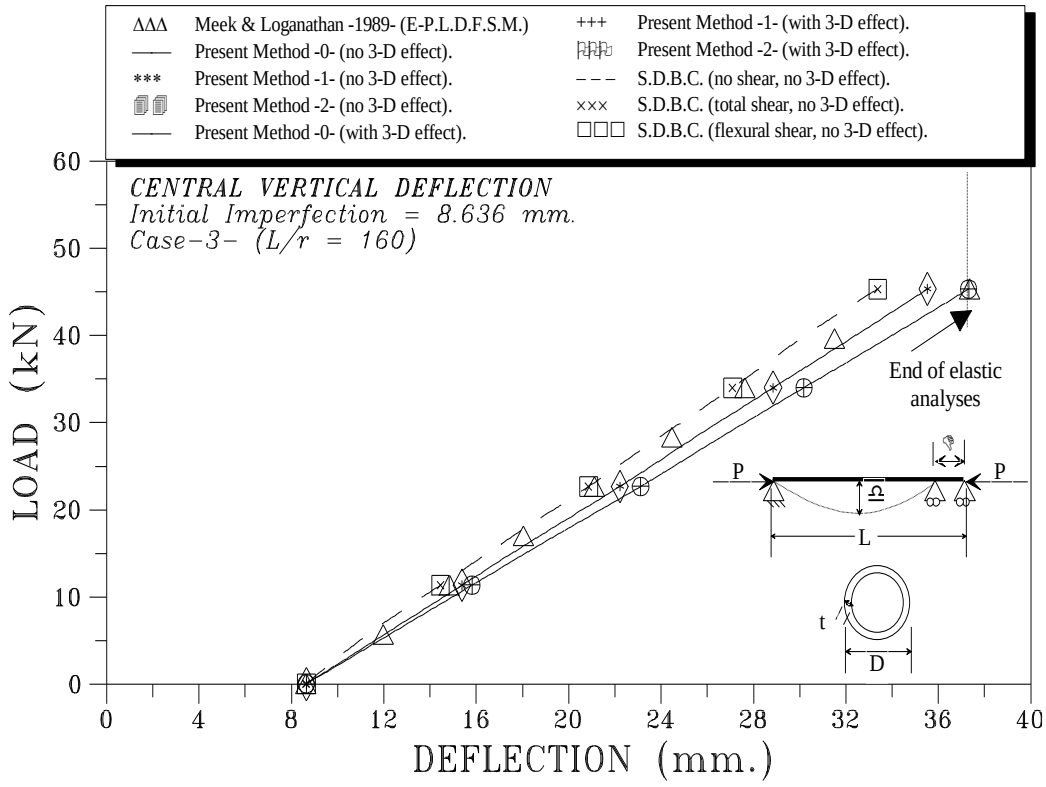

Figure (6-4.c) Load-Deflection curve for the 3-D initial imperfection pin-ended circular ring for L/r =160

6.2.5 Case study no.5 (3-D initial imperfection S.H.S. pin-ended beam-column):-

In table (6-6.a)**,** the properties of the three cases of different **L/r** ratio of this problem and the initial central imperfection ratio ($\frac{\delta_0}{L}$ **)** are mentioned with constant "**u**" value in X_1 and X_3 directions since double symmetry exists, although the present work deals with the elastic stability analysis while others are elastic-plastic analysis, the comparison can be made on the elastic zone only.

The first two cases of L/r=65.7 and 95.7 were examined experimentally by ***Key*** and ***Hancock*** (according to ***Meek*** and ***Loganathen*** [63]) in (1985), while the third case of L/r equal to 62.5 and properties different from the first two cases a sit is detailed in table (6-6.a) was experimentally examined by ***Sully*** and ***Hancock*** [89] in (1996).

Table (6-6.a): 3-D Cold-Formed Initial Imperfection S.H.S Pin-Ended Beam-Column Properties

Case	*Element Section "D×t"mm.*	*L/r*	*Length "L_i(mm)"*	*Area "A_i(mm^2)"*	*Moment of Inertia "I_i(mm^4)"*	*Elastic Modulus "E_i(Mpa)"*	*Initial Imperfect "e_0/L"*	*Shear Parametrt"u" (all directions)*	*Axial Load "P_i(kN)"*
1	203*203*6.3 SHS	65.7	5270.75	4956.84	$3.196*10^7$	208000	0.001	0.00823	1600
2	203*203*6.3 SHS	95.7	7684.45	4956.84	$3.196*10^7$	208000	0.001	0.00388	515
3	125*125*6.0 SHS	62.5	3000.00	2730.00	$6.290*10^6$	208000	0.000	0.01516	1150

Table (6-6.b) summarizes the attempts of some investigators who analyzed this type of structures by elastic-plastic analysis, and again our concern here is with the elastic zone of behavior and a very good agreement of the present **Meth.-0-, Meth.-1-,** and **Meth.-2-** with the others results. Of course shear effect is still far away from getting significantly effective on the stability behavior of this problem since the values of "**u**" are as can be seen from the table above. However, its obvious that the 3 rd case has a specifically higher shear effect than the other two cases since its "**u**" value is the highest and accordingly its **L/r** value is the lowest.

From figures (6.5.a, b, and c), its also can be observed that the divergence between the **S.D.** theory results and the **L.D.** results get higher when the **L/r** ratio gets higher, since this greatly affects the **L.D**. formulations. $\mathbf{P_{cr}}$ of the three cases occurred at **(1529.96 kN, 508.53 kN,** and **750.03 kN)** respectively. Another notation can be concluded from the figures that in case -3- the axial displacements are very small in comparison with case-1- and -2-, and this is because of :-

- No initial imperfection in case-3-
- Case-3- is more slender than the first two cases.

The **SS/SS0** for the three cases are **2.56%, 3.26%,** and **1.43%** increment respectively for both methods and the results are closer to the experimental *which gives a great support to our new theory*.

Table (6-6.b):-Results & Comparison of 3-D Cold-Formed Initial Imperfection S.H.S Pin-Ended Beam-Column

					Axial Displacement "mm."		
No.	***Method***	***Type of Analysis***	***No. of Element***	***No. of Increment***	***Case 1***	***Case 2***	***Case 3***
1	Key et al.(1985)	Experimental	1	15	13.782 at 1476 kN	15.075 at 434 kN	-
2	Kitipornchai et. al. (1988)	E-P , F.S.M. L.D.	12	15	13.716 at 1482 kN	15.394 at 435 kN	-
3	Meek&Log-anathan(1989)	E-P , F.S.M. L.D.	12	20	13.752 at 1475 kN	15.394 at 435 kN	-
4	Sully&Hancock (1996)	Experimental	1	20	-	-	0.981 at 750 kN
5	Clarke (1993)	E-P,F.E.M. L.D. "Tot.Lagr.2-Nod., Curv.& Istr.B.Elm."	64 at Corner 128 at Flat	20	-	-	0.953 at 750 kN
6	Present Method "0"	Beam-Column L.D."No Shear"	1	10	13.815 at 1530 kN	15.441 at 508.53 kN	0.890 at 750 kN
7	Present Method "1"	Beam-Column L.D. "with Shear"	1	10	13.815 at 1530 kN	15.442 at 508.53 kN	0.892 at 750 kN
8	Present Method "2"	Beam-Column L.D. "with Shear"	1	10	13.813 at 1530 kN	15.441 at 508.53 kN	0.891 at 750 kN

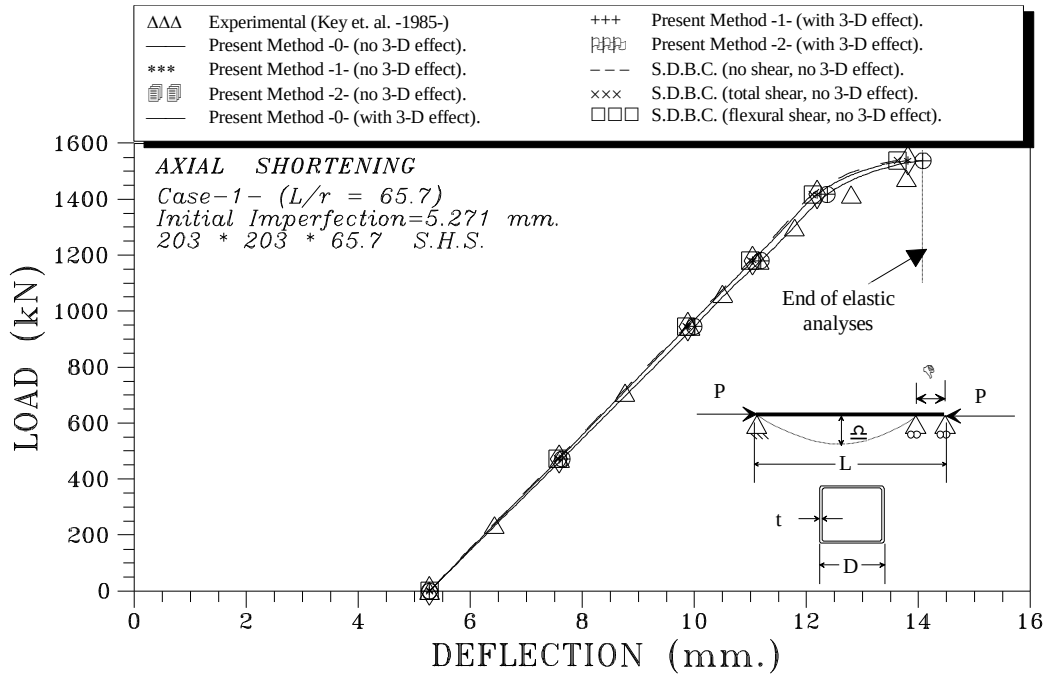
ΔΔΔ Experimental (Key et. al. -1985-)
Present Method -0- (no 3-D effect).
*** Present Method -1- (no 3-D effect).
Present Method -2- (no 3-D effect).
Present Method -0- (with 3-D effect).
+++ Present Method -1- (with 3-D effect).
Present Method -2- (with 3-D effect).
S.D.B.C. (no shear, no 3-D effect).
××× S.D.B.C. (total shear, no 3-D effect).
S.D.B.C. (flexural shear, no 3-D effect).
AXIAL SHORTENING
Case-1- (L/r = 65.7)
Initial Imperfection=5.271 mm.
203 * 203 * 65.7 S.H.S.
End of elastic analyses
P
P
L
t
D
LOAD (kN)
DEFLECTION (mm.)

Figure (6-5.a) Load-deflection curve for the 3-D initial imperfection square hollow section S.H.S. (L/r=65.7, e_{imp}=5.271 mm.)

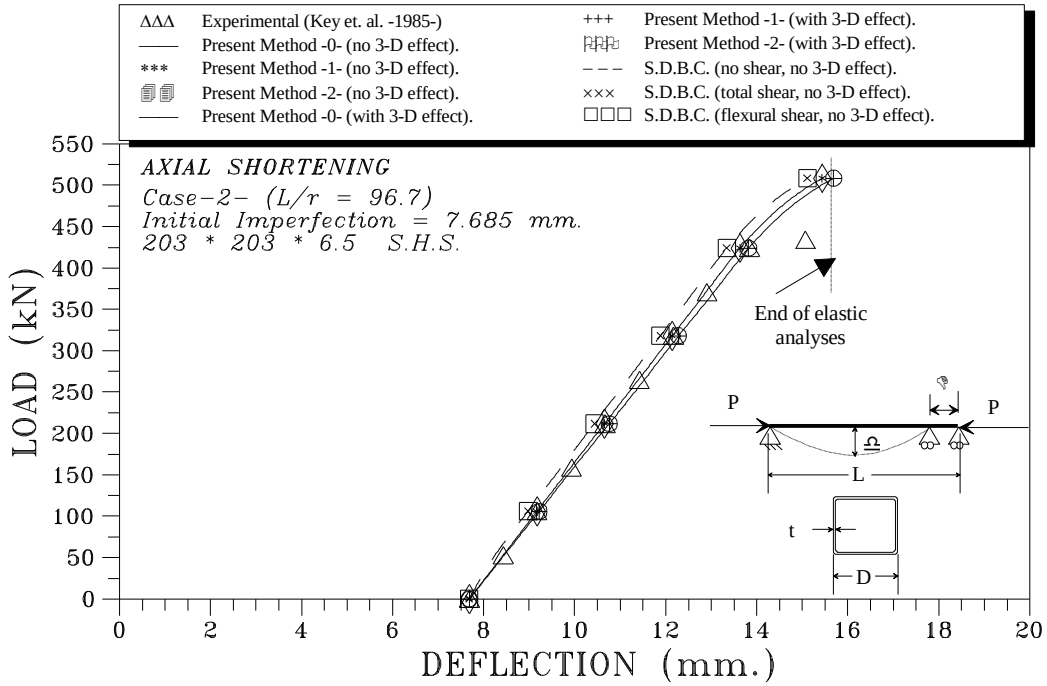
ΔΔΔ Experimental (Key et. al. -1985-)
Present Method -0- (no 3-D effect).
*** Present Method -1- (no 3-D effect).
Present Method -2- (no 3-D effect).
Present Method -0- (with 3-D effect).
+++ Present Method -1- (with 3-D effect).
Present Method -2- (with 3-D effect).
S.D.B.C. (no shear, no 3-D effect).
××× S.D.B.C. (total shear, no 3-D effect).
S.D.B.C. (flexural shear, no 3-D effect).
AXIAL SHORTENING
Case-2- (L/r = 96.7)
Initial Imperfection = 7.685 mm.
203 * 203 * 6.5 S.H.S.
End of elastic analyses
P
P
L
t
D
LOAD (kN)
DEFLECTION (mm.)

Figure (6-5.b) Load-deflection curve for the 3-D initial imperfection square hollow section S.H.S. (L/r =96.7, e_{imp}=7.685 mm.)

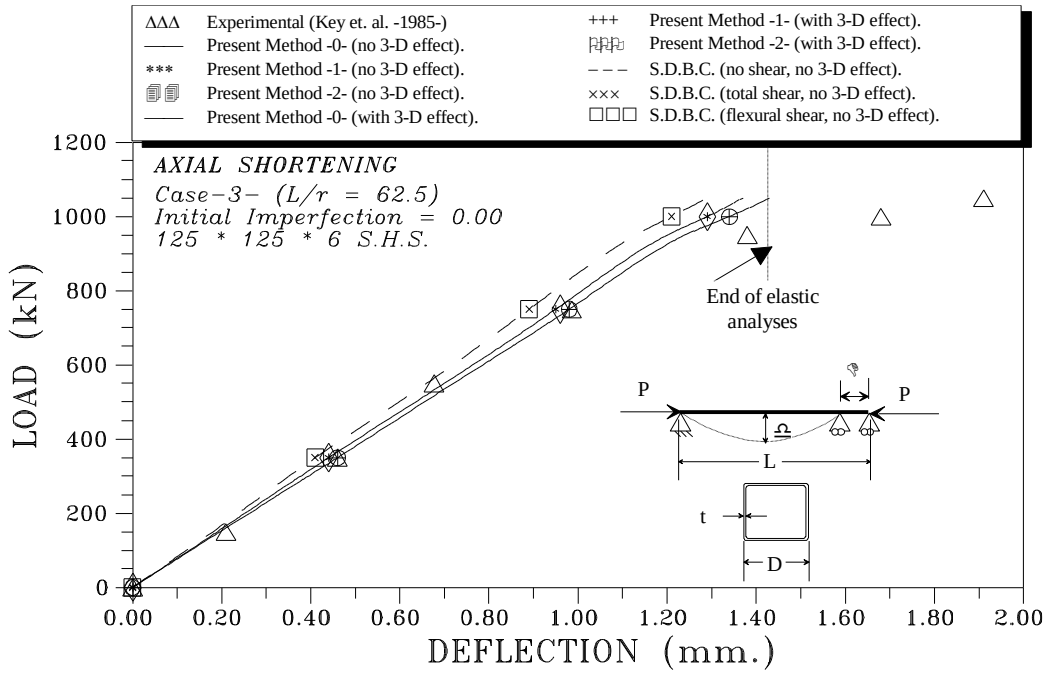

Figure (6-5.c) Load-Deflection curve for the 3-D initial imperfection square hollow section S.H.S. (L/r=62.5, e_{imp}=0 mm.)

6.2.6 Case study no.6 ((3-D initial imperfect. circular ring fixed-ended beam-column):-

Sherman investigated this problem experimentally in (1980) [63]**.** An effective slenderness ratio of **KL/r = 72** and **28**, constant "**u**" value in "X_1" and "X_3" directions, and initial central imperfection ratio $\frac{\delta_0}{L}$ of **0.001** are to be taken as 2 cases of analysis as its detailed in table (6-7.a).

Table (6-7.a): 3-D Circular Ring Fixed-Ended Beam-Column Properties

Case	*Element Section D*t(mm.)*	*KL/r*	*Length "L_i(mm)"*	*Area "A_i(mm^2)"*	*Mom.of Inertia "I_i (mm^4)"*	*Elastic Modulus "E_i(Mpa)"*	*Initial Imperfect "e_0/L"*	*Shear Parameter "u" (all directions)*	*Axial Load "P_i(kN)"*
1	114.3*2.38	72	5720	807.095	2351416.2	199955	0.001	0.00634	150.00
2	114.3*2.38	28	2270	807.095	2351416.2	199955	0.001	0.04190	200.25

As it's clear from table (6-7.b) that although one beam-column element is taken in the present study in comparison with large number of elements (26 and 12) taken by other researchers the accuracy of the present study is excellent.

Table (6-7.b): Results & Comparison of 3-D Circular Ring Fixed-Ended Beam-Column

					Central Deflection " (mm.)"	
No.	***Method***	***Type of Analysis***	***No.of Element***	***No.of Increment***	***Case 1***	***Case 2***
1	Sherman (1980)	Experimental	1	16	32.653 at 143.17 kN	8.151 at 200.25 kN
2	Chan & Kitipornchai(1988)	E-P ,F.S.M. L.D.	26	16	32.665 at 142.45 kN	-
3	Meek & Loganathan (1989)	E-P ,F.S.M. L.D.	12	16	32.654 at142.5 kN	8.148 at 200.25 kN
4	Present Method "0"	Beam-Col. L.D."No Shear"	1	10	24.261 at 154.38 kN	8.071 at 200.25 kN
5	Present Method "1"	Beam-Col. L.D."withShear"	1	10	24.262 at 154.38 kN	8.071 at 200.25 kN
6	Present Method "2"	Beam-Col. L.D."withShear"	1	10	24.261 at 154.38 kN	8.070 at 200.25 kN

Nearly the same observations (no shear effect, difference between **S.D.** and **L.D.**, relation between **L/r** or "**u**" vs. divergence between **Meth.-0-, Meth.-1-**, and **Meth.-2-**) of cases 3 and 4 can be concluded as it's shown in figure (6-6), in spite of the difference in end condition of this case. The buckling loads of the two cases are **(154.38 kN,** and **200.25 kN)** respectively, and the stability analysis beyond the elastic region is one of the improvements to be made on this formulation.

The **SS/SS0** ratio are **2.98%**, and **2.12%** increment respectively for both methods, and gain the results are pushed towards the experimental results which again push our new theory towards the exact elastica.

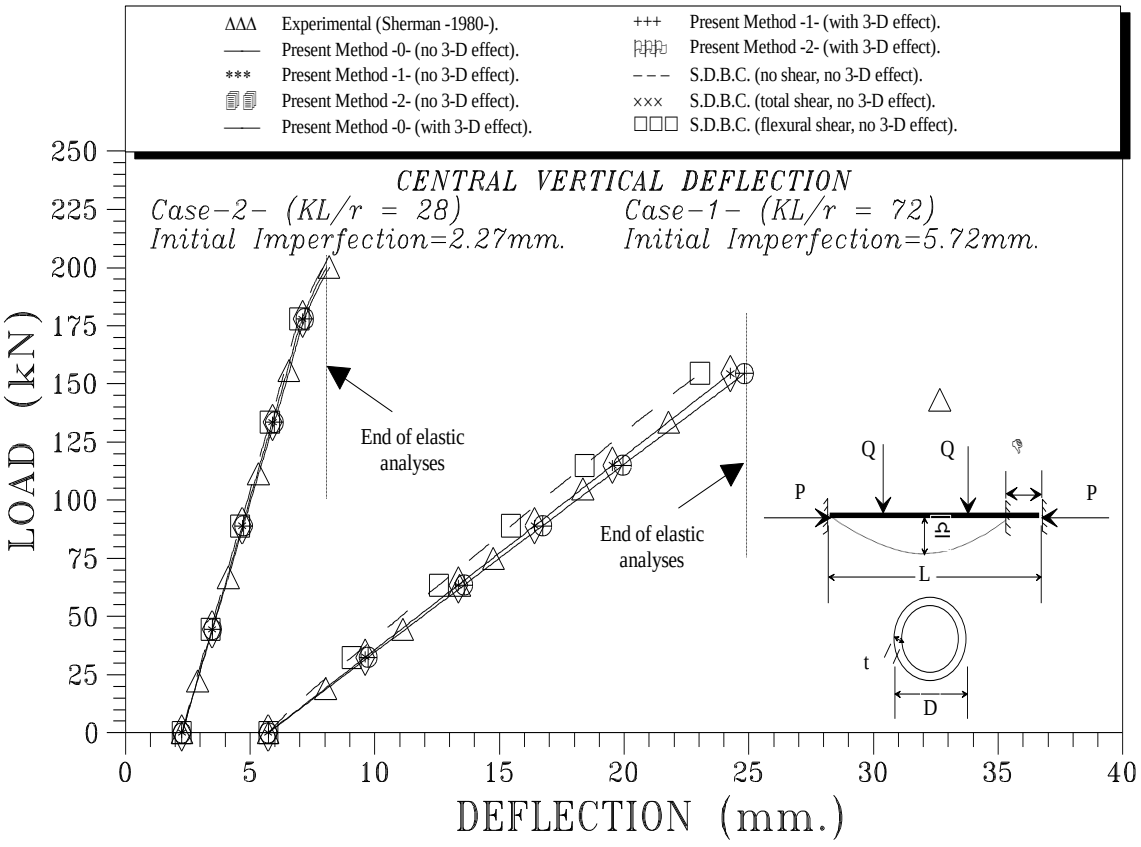

Figure (6-6) Load-deflection curve for the 3-D initial imperfection fixed-ended circular ring for various L/r

6.2.7 Case study no. 7 (Two bar shallow truss):-

This limit point snap through buckling case has an exact solution as it's shown in both figure (6-7) and table (6-8.b). Table (6-8.a) spotlights this problem's properties.

Table (6-8.a): Two-Bar Shallow Truss Properties

Element "(i)"	*Length "L_i (mm.)"*	*Area "$A_i(mm^2)$"*	*Elastic Modulus "E_i (Mpa)"*	*Shear Parameter "u_i"*	*Joint Load (kN)*
1	2540	645.16	200000	$3.6*10^{-13}$	7342.5
2	2540	645.16	200000	$3.6*10^{-13}$	7342.5

The excellent accuracy of the present formulation over the exact solution solved by the elliptical integral is very clear from observing figure (6-7) and table (6-8.b), in addition the shear effect still has no rule; the **S.D.** is about **86.6%** of the **L.D. P-Δ** results.

Table (6-8.b): Compression of Solutions For Two-Bar Shallow Truss

No.	*Method*	*Type of Analysis*	*No. of Element*	*No. of Increment*	*Vertical Deflection d(mm)*
1	Elastica	Exact Solution	2		574.548
2	Oran& Kassimali (1976)	Beam-Column L.D. "Incremental Eularian (no bowing)"	2	18	432.561
3	Oran&Kassimali (1976)	Beam-Column L.D. "Incremental Eularian"	2	18	434.596
4	Oran&Kassimali (1976)	Beam-Column L.D. "Iterative Lagrangian"	2	18	501.143
5	Oran& Kassimali (1976)	Beam-Column L.D. "Iterative Eularian"	2	18	574.548
6	Present Meth. -0-	Beam-Column L.D."no shear"	2	18	574.548
7	Present Meth. -1-	Beam-Column L.D. "with shear"	2	18	574.548
8	Present Meth. -2-	Beam-Column L.D. "with shear"	2	18	574.548

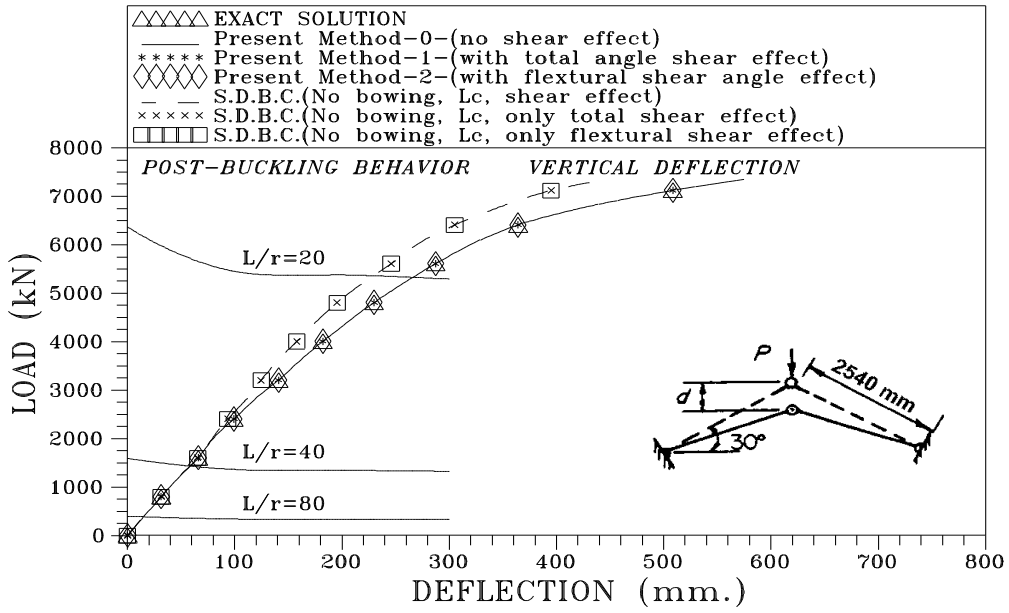

Figure (6-7) Pre-buckling and post-buckling load-deflection curve for the two-bar truss

Critical load $\mathbf{P_{cr}}$. is **7342.5 kN** as it is obvious from figure (6-8) or as it known as the load-**T.S.M.** determinant curve **(P vs. det. [λ])**, it can be shown that the solutions made by either the present formulation's **(Meth.-0-, Meth.-1- & Meth.-2-)** or the exact solution do exhibit the typical behavior of limit point.

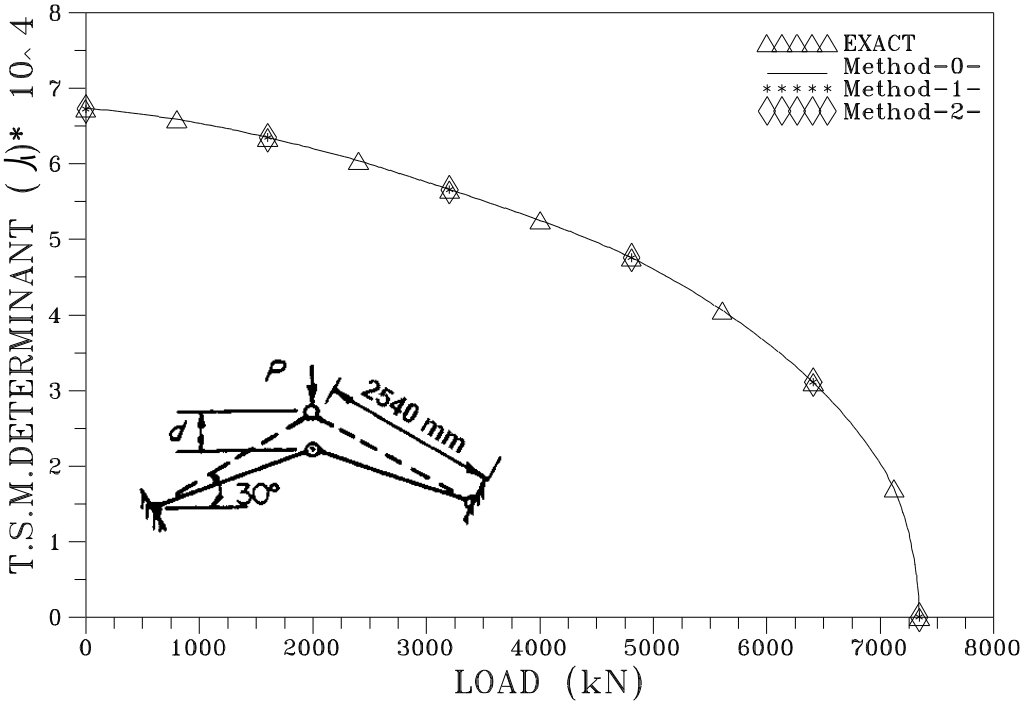

Figure (6-8) Load versus determinant curve for the two-bar truss

The post-buckling (secondary path) behavior is also depicted in figure (6-7) for different (L/r) ratios which they are (20, 40, and 80) respectively. The instability detection detailed in **chapter-5-** can be clearly observed in this imperfection sensitive structure where the pre-buckling path is close to falling secondary post buckling paths of different (L/r).

It can be noticed that the larger the (L/r) the smaller (P_e) which gives "d" equals to zero and the closer to a strait line. The (P_{cr}) of such systems are (5306.2 kN), (1483.29 kN), and (379.45 kN) respectively, which can be detected from the point of intersection between the primary and the secondary paths.

6.2.8 Case study no. 8 (one storey bent frame):-

Four cases of **H/V** (horizontal to vertical loading ratio) are tested in this problem as it's detailed in the properties table (6-9.a).

Table (6-9.a): One-Storey Bent Frame Properties

		Element Properties					
Case	***H/V Ratio***	***Length "L_i(mm.)"***	***Area "A_i(mm^2)"***	***Moment of Inertia "I_i (mm^4)"***	***Elastic Modulus "E_i(Mpa)"***	***Shear Parameter "u_i"***	***Joint Load (kN)***
1	1/2	3048	7593.534	129073365	200000	0.065	22250
2	1/10	3048	7593.534	129073365	200000	0.065	22250
3	1/100	3048	7593.534	129073365	200000	0.065	22250
4	1/1000	3048	7593.534	129073365	200000	0.065	22250

Many researchers examined this problem as table (6-9.b) illustrates, it is particularly important to note that no convergence difficulties happened up to, even beyond, the critical load of limiting case of the perfect bent in the present formulation as well as the **T.S.M.** iterative strategy made by ***Oran & Kassimali*** [70] (1976), it may be of interest to note, in this connection, that ***James's et. al.*** (1974) alternate iterative technique failed to have convergence at low load level.

The horizontal load is increased from **1/2** (case-1-) to **1/1000** (case-4-), the **P-Δ** behavior of all cases shown in figures (6-9.a. and 6-9.b.)

Table (6-9.b): Compression of Solutions for One-Story Bent Frame

					Horizontal deflection at point "B" for various cases in (mm.)			
No.	***Method***	***Type of analysis***	***No. of Element***	***No. of Increment***	***Case 1***	***Case 2***	***Case 3***	***Case 4***
1	James et. al.	Beam-Column L.D.	3	10	1148.84 at 13350 kN	683.84 at 17800 kN	-	-
2	Oran & Kassimali (1976)	Beam-Column L.D. "Iterative .Eularian (no bowing)"	3	10	2121.92 at18912.5 kN	1043.84 at18912.5 kN	-	-
3	Oran& Kassimali (1976)	Beam-Column L.D. "Iterative .Eularian"	3	10	2620.42 at 22250 kN	1772.46 at 22250 kN	1311.29 at 22250 kN	1241.65 at 22250 kN
4	Present	Beam-Column	3	10	2620.42 at 22250	1772.42 at 22250	1311.29 at 22250	1241.65 at 22250

	Meth.-0-	L.D. "no shear"			kN	kN	kN	kN
5	Present Meth.-1-	Beam-Column L.D. "with shear"	3	10	2620.44 at 22250 kN	1772.44 at 22250 kN	1311.30 at 22250 kN	1241.66 at 22250 kN
6	Present Meth.-2-	Beam-Column L.D. "with shear"	3	10	2620.44 at 22250 kN	1772.44 at 22250 kN	1311.30 at 22250kN	1241.66 at 22250kN

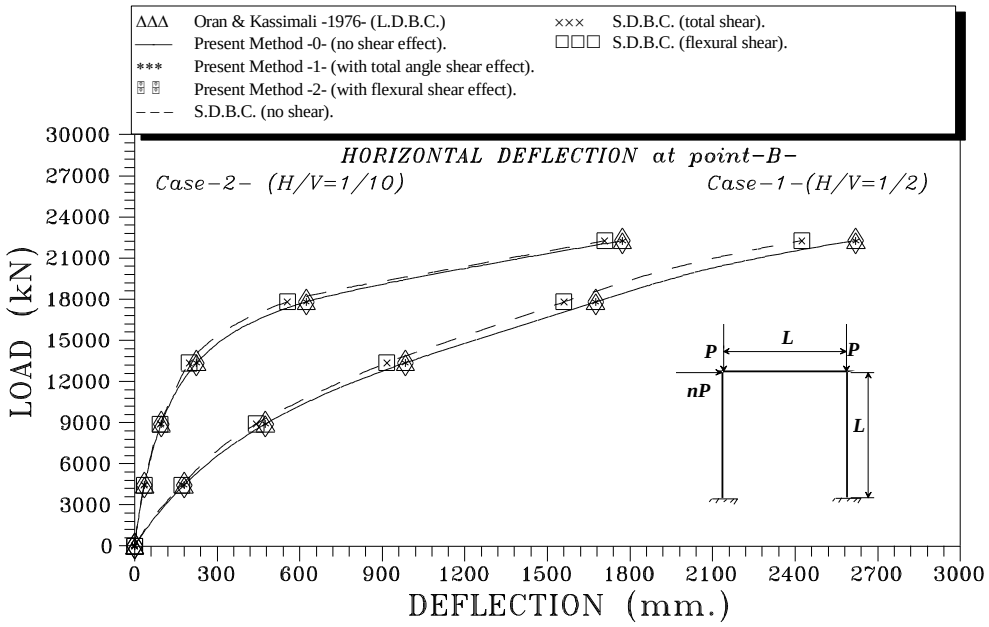

Figure (6-9.a) Load Deflection Curve for the one story bent frame (case 1 & 2)

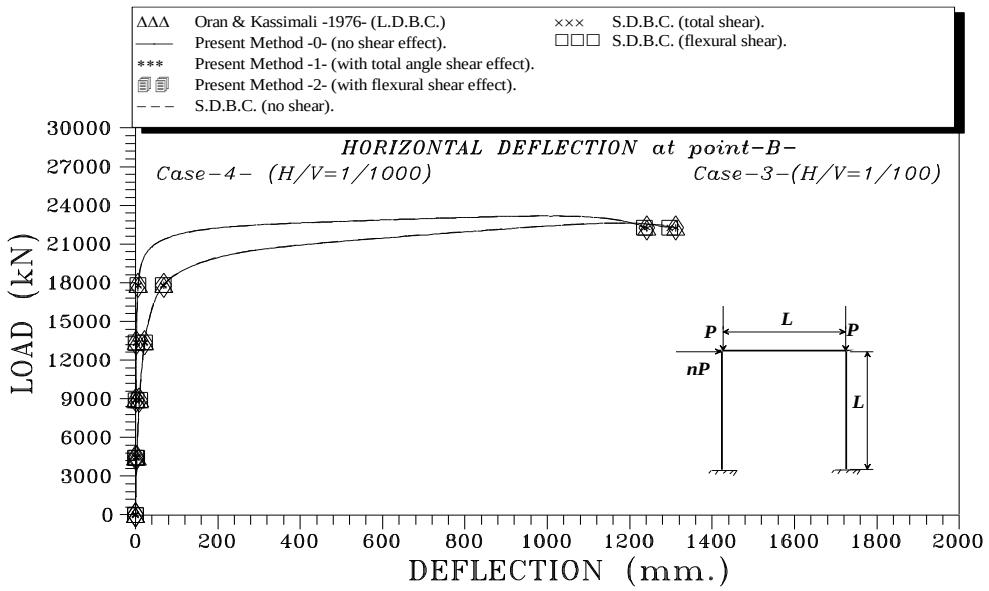

Figure (6-9.b) Load Deflection Curve for the one story bent frame (case 3 & 4)

The following notes can be noticed:-

- Good agreement between the present formulation and ***Oran*** - ***Kassimali***'s [70] (1976)**,** in all the four cases.
- **Meth.-0-** and shear including methods **(Meth.-1- & Meth.-2-)** coincides in results since **"u"** values are very small in spite of the **H/V** ratio difference.
- The higher the **H/V** ratio the higher the divergence between **S.D.** and **L.D.** results, this is simply because of the higher deformations at the joints which cause redistribution in the axial force. This is the reason that the axial force parameter **(ρ)** is dominantly affected by the horizontal force **(H)**. These percentage ratios of **(S.D./L.D.)** for the four cases are **(76.1%, 80.38%, 87.84%, and 93.86%)** respectively.

Figure (6-10) illustrates the **P-det.[λ]** curve of case-4-, it may be seen that the determinant of the structure decreases linearly with the applied load until the load reaches a value of **20.915 kN**, after this stage the value of the determinant deteriorates severely and after some load steps this deterioration becomes smaller. This behavior is due to the horizontal force which causes an imperfection in the structure.

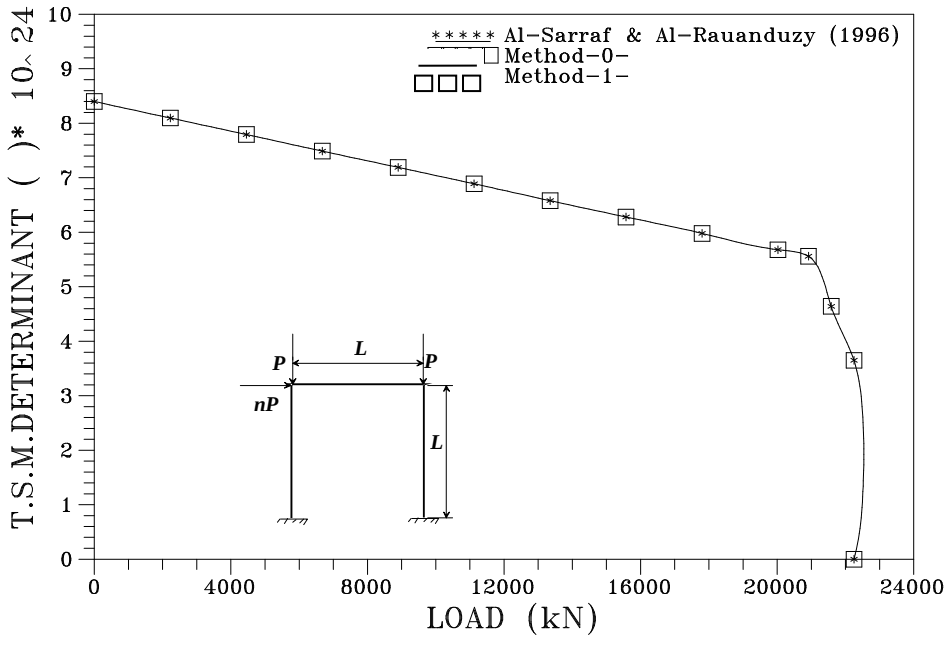

Figure (6-10) Load versus determinant curve of one-story bent frame (with n=1/1000)

6.2.9 Case study no. 9 (William Toggle frame):-

This case was first experimentally treated and solved by ***William*** (1964) [108], and has since been used as a benchmark to test new methods by various researchers as table (6-10.b) indicates. Table (6-10.a) on the other hand illustrates the properties and load condition of this problem.

Table (6-10.a): William-Toggle Frame Properties

Element"(i)"	*Length "L_i(mm)"*	*Area "A_i(mm^2)"*	*Elastic Modulus "E_i(MPa)"*	*Shear Parameter "u_i"*	*Joint Load (kN)*
1	328.722	118.00	70880.60	0.00104	0.2225
2	328.722	118.00	70880.60	0.00104	0.2225

This snap though buckling problem is highly non-linear just like the two bar shallow truss case study, so its one of the perfect solved examples to check and examine the reliability of the present formulation including the extrapolation method for evaluating the critical points.

Table (6-10.b): Compression of Solutions for William Toggle Frame

No.	*Method*	*Type of Analysis*	*No. of Element*	*No. of Increment*	*Vertical Deflection d(mm)*
1	William (1964)	Experimental	2	10	5.24 at .151 kN 16.77 at .22 kN
2	Wood & Zienkewich (1977)	Finite-Element L.D.	5/Mem.	20	5.28 at .151kN 13.28 at.178kN 17.40 at.303kN
3	Meek & Loganathan (1989)	Finite Element "using Arc Length Method"	2	28	5.21 at.151kN 13.48 at.178kN 16.64 at.303kN
4	Al-Bermani & Kitipornchai (1990)	Beam-Column L.D. "with bowing"	2	20	4.67 at.151kN 13.11 at.178kN 17.25 at.303kN
5	Wong & Tin-Loi (1990)	Beam-Column L.D.	2	10	5.24 at.151kN
6	Al-Raunduzy	Beam-Column	2	20	5.21 at.151 kN

	(1996)	L.D. "with bowing"			14.25 at.178kN
7	Present Meth.-0-	Beam-Column L.D. "no shear"	2	20	5.21 at.151kN 16.75 at.22kN
8	Present Meth.-1-	Beam-Column L.D. "with shear"	2	20	5.21 at.151kN 16.75 at.22kN
9	Present Meth.-2-	Beam-Column L.D. "with shear"	2	20	5.21 at.151kN 16.75 at.22kN

In his theoretical work, ***William*** (1964), adopted a beam-column model to describe the behavior of individual member of the frames, then by solving the differential equation for each member a corrected axial strain expression, including terms up to the second order, was obtained and used for his elastic stability finite deflection and flexural shortening analysis, results as shown in the figure (6-11) varying from a simple linear analysis to more highly complex non-linear analysis, formulated by including more and more terms in the governing equation [108].

The same excellent agreement of our work with others, and the coincidence of **Meth.-0-**with **Meth.-1-** & **Meth.-2-**(i.e. no shear effect) can be concluded from both figure (6-11) and table (6-10.b). The final post-buckling **S.D./L.D.** displacement ratio at **0.22 kN** is **(1.153)**.

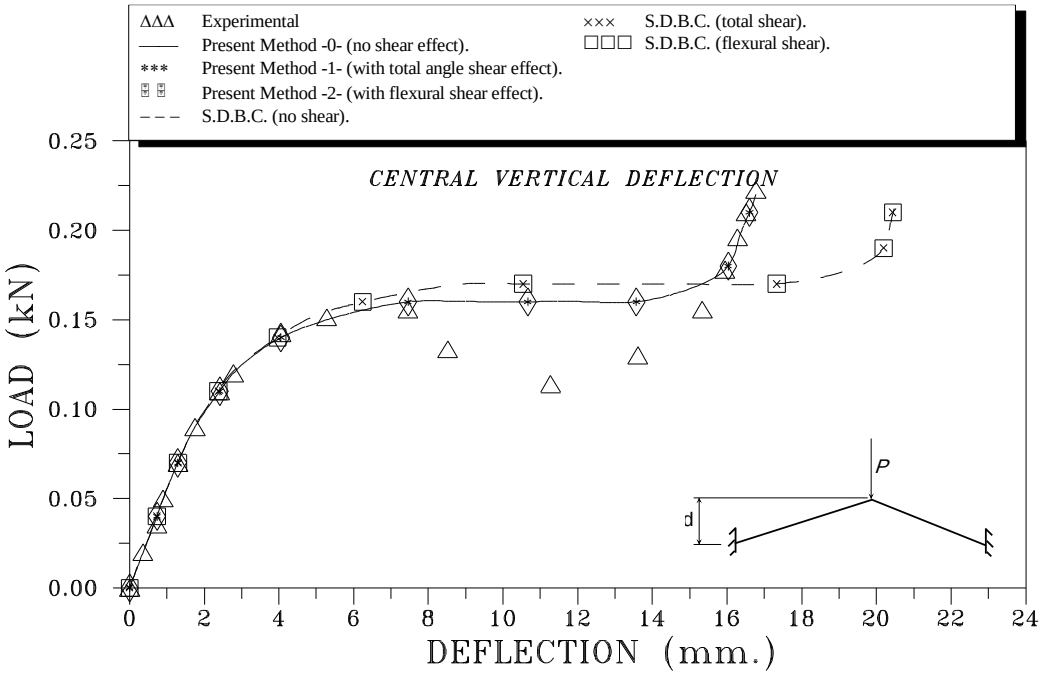

Figure (6-11) Load-deflection curve for the William Toggel frame

Because of the fact that our present formulation is an iterative load control technique and not a deflection control technique, there is a shift in the present curve with the actual behavior after first buckling occurred, as it can be noticed from figure (6-11). However, ***NASCFI*** is able to handle the post-buckling behavior of structures, in the imperfect sensitive problems only.

6.2.10 Case study no. 10 (rigid-ended portal frame):-

Sideek [85] (1990), experimentally examined full-scale portal frames with properties detailed in table (6-11.a) He drew the elastic-plastic behavior of this problem.

Table (6-11.a): Rigid-Ended Portal Frame Properties

Mem	*Section Type*	*Length "L(mm)"*	*Area "A(mm^2)"*	*Mom. of Inrt. "I (mm^4)"*	*Elastic Modul. "E(Mpa)"*	*Pos. Ratio "ν"*	*Shape Factor "n"*	*Shear Parameter "u"*	*3 Cases H/V:1/4, 1/3,1/2*
Gir.	IPE 140	3000	1640	5410000	200000	0.30	2.674	0.0260	
Col.	S 4*7.7	2000	1468	2555000	200000	0.30	3.324	0.0367	

Three cases are to be solved by the present stability analysis and checked with the solutions of other researchers as it's explained in table (6-11.b), and figure (6-12). Case-1-is for **H/V** ratio of **1/4**, case-2- for **1/3**, and case-3- represents **H/V** which equals **1/2**.

Table (6-11.b): Compression of Solutions for Rigid-Ended Portal Frame

					Horizontal Deflection at point "B" in (mm.) for various cases		
No.	*Method*	*Type of Analysis*	*No. of Element*	*No. of Increment*	*Case 1*	*Case 2*	*Case 3*
1	Siddeek (1990)	Experimental	3	30	22.04 at 14.95 kN	22.54 at 12 kN	20.93 at 10 kN
2	Al-Refaie & Trikha (1986)	Beam Theory E-P, L.D.	3	4 Plastic Hinges	22.68 at 15.0 kN	22.89 at 12 kN	20.68 at 10 kN
3	Present Meth.-0-	Beam-Column L.D."no shear"	3	12	20.25 at 14.95 kN	20.22 at 12 kN	22.47 at 10 kN
4	Present	Beam-Column	3	12	20.25	20.22	22.47

	Meth.-1-	L.D. "with shear"			at 14.95 kN	at 12 kN	at 10 kN
5	Present	Beam-Column	3	12	20.24	20.22	22.46
	Meth.-2-	L.D. "with shear"			at 14.95 kN	at 12 kN	at 10 kN

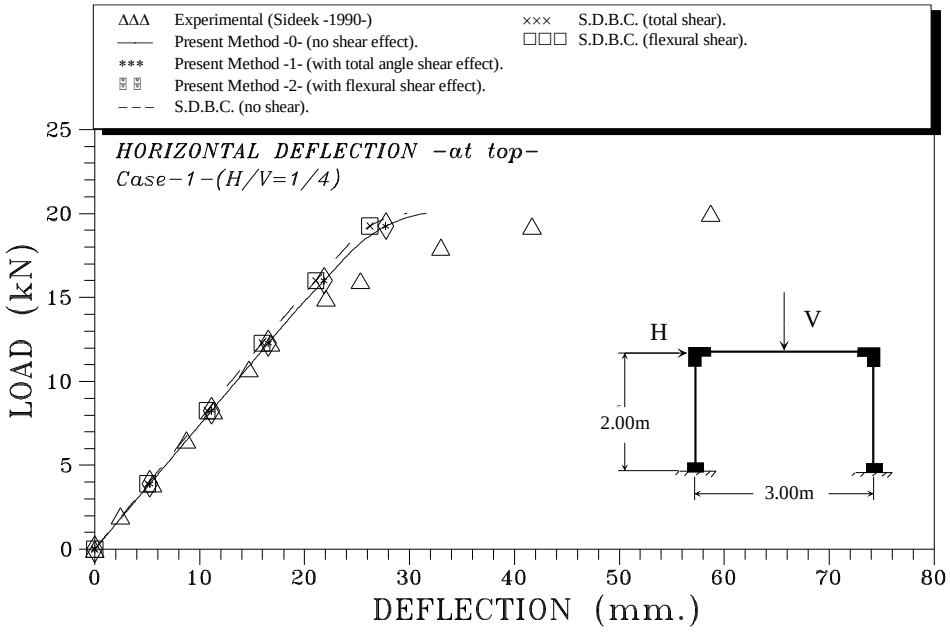

Figure (6-12.a) Load-Deflection curve for the Rigid-Ended portal frame

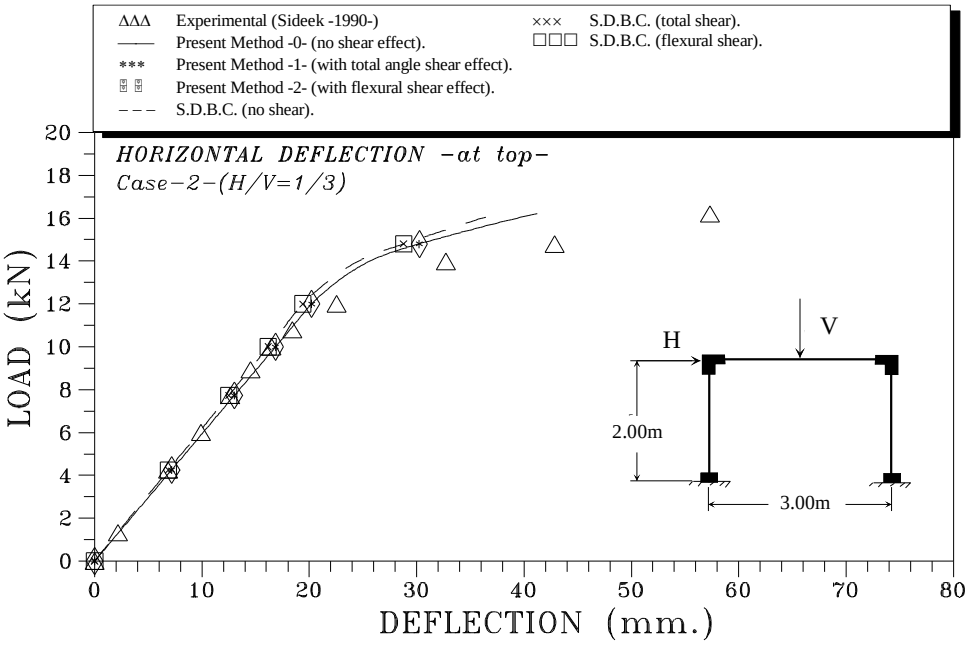

Figure (6-12.b) Load-Deflection curve for the Rigid-Ended portal frame

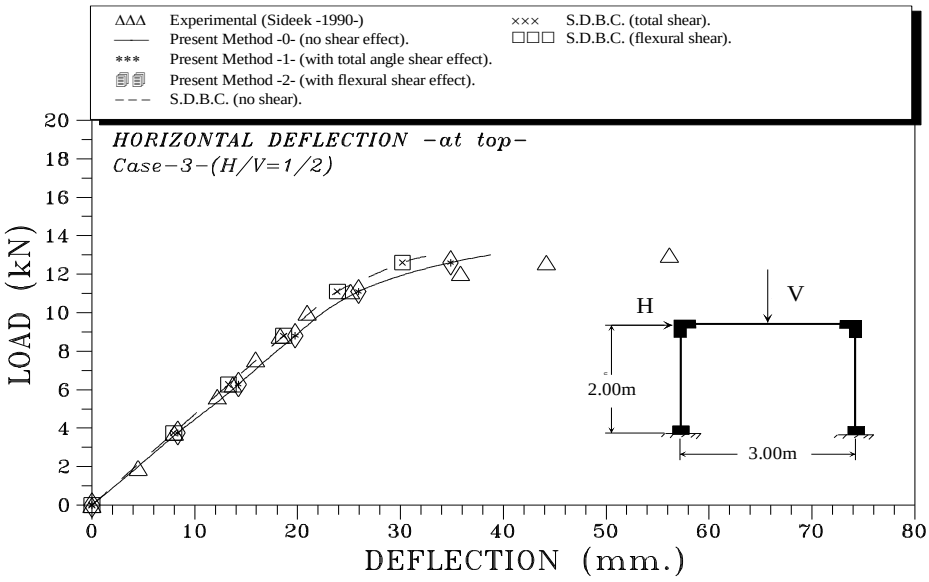

Figure (6-12.c) Load-Deflection curve for the Rigid-Ended portal frame

The shear effect in the three cases is negligible in spite of the value of shear parameter "**u**" which starts increasing over the previous cases, the divergence between **S.D.** and **L.D.** analysis increases when **H/V** increases, and the most important conclusion taken from the table and the graph is the agreement in results between the present formulation and the experimental in the elastic region.

It can be also noticed from table (6-11.a) that the shape factor "**n**" is rather more than expected because its taken by dividing the total area "**A**" over the web area "**Aw**" which in fact is the real definition of the shape factor "**n**" as it is referred to in **chapter-3-**. The buckling loads of the three cases are **(14.95 kN, 11.99 kN,** and **10.02 kN)** respectively.

6.2.11 Case no. 11 (clamped hinged deep arch):-

A highly non-linear imperfect problem is solved by many investigators as summarized in table (6-12.b), with properties detailed in table (6-12.a), and a point load at the crown level. The horizontal and vertical deflections of crown are graphed in figure (6-13) and their comparison with other investigators attempts are shown in both figure (6-13) and table (6-12.b) from which it can be observed that although only 10 elements of our attempt with 12 incremental steps and about seven to ten iteration per step in comparison with 30 elements of ***Hsiao*** & ***Hoa*** [41] (1986), the present work is closer to the work done by ***Deppo*** & ***Schmidt*** (1975) which represents the exact solution of this problem. The shear effect still has no role and **S.D./L.D.** ratio is **82.34 %** for vertical and **88.7%** for horizontal at **P = 0.0004 kN** load level.

Table (6-12.a): Clamped Hinged Arch Properties

Element "(i)"	*Length "L_i(mm)"*	*Thickness "t (mm.)"*	*Area "A_i (mm^2)"*	*Flexural Stiffness "EI($kN.m^2$)"*	*Shear Parameter "u_i"*	*Curvature of Arch "ϕ (rad.)"*	*Radius "R_i (mm)"*	*Load Parameter ($PR^2/EI)_i$*	*Load "P (kN)"*
1-10	953.117	25.40	506.71	113058.943	0.00146	3.75245	2540.00	10.00	$4.45*10^{-4}$

Table (6-12.b): Comparison of Solutions for Clamped-Hinged Arch

					Deflection Ratios at Crown U/R & V/R	
No.	*Method*	*Type of Analysis*	*No. of Element*	*No. of Increment*	*Vertical "V/R"*	*Horizontal "U/R"*
1	Deppo & Schmidt (1975)	Exact Solution	1	-	1.165 at L .Pr.= 9.1	0.59 at L .Pr.= 9.1
2	Oran &Kassimali (1976)	Beam-Column L.D. "with bowing"	10	12	1.165 at L .Pr.= 9.4	0.59 at L.Pr.= 9.4
3	Hsiao & Hoa (1986)	Finite Element L.D.	30	11	1.165 at L .Pr.= 9.0	0.59 at L .Pr.= 9.0
4	Present Meth.-0-	Beam-Column L.D. "no shear"	10	12	1.165 at L.Pr.=9.32	0.59 at L.Pr.=9.32
5	Present Meth.-1-	Beam-Column L.D. "with shear"	10	12	1.165 at L.Pr.=9.32	0.59 at L.Pr.=9.32
6	Present Meth.-2-	Beam-Column L.D. "with shear"	10	12	1.165 at L.Pr.=9.32	0.59 at L.Pr.=9.32

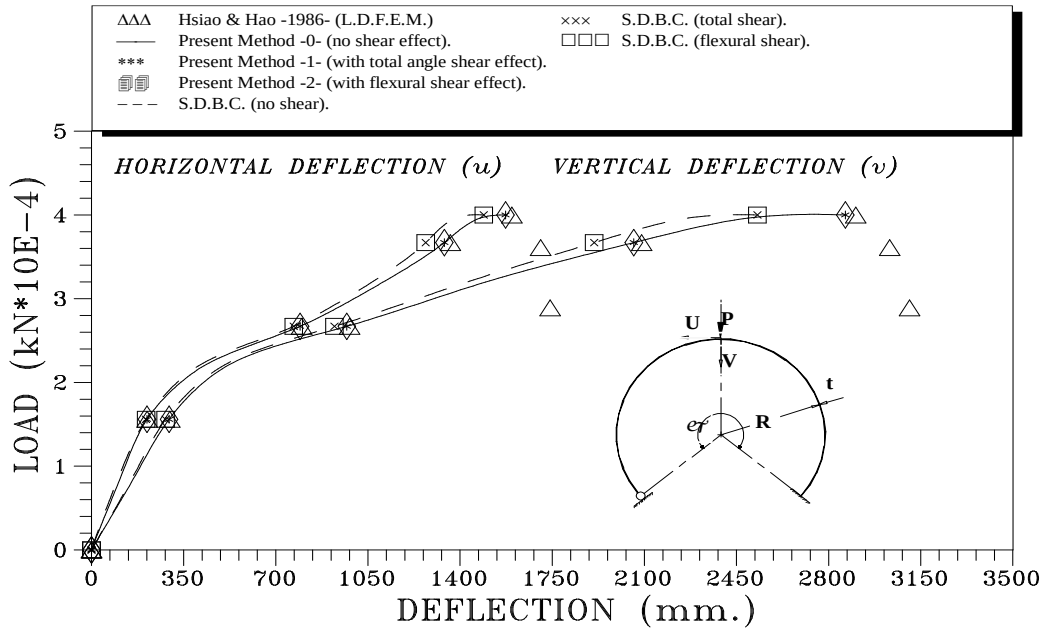

Figure (6-13) Load-deflection curve for the clamped hinged arch

6.2.12 Case no. 12 (3-D cantilever horizontal bent joint):-

It was shown by ***Kassimali*** and ***Abbassinia*** [49] (1991)**,** that the numerical results of this problem nearly coincide by taking **2** elements or **4** elements except for X_3-direction. The properties of this problem are given in table (6-13.a)**,** while table (6-13.b) summarizes the other researchers results and their comparison with the present analytical results, also figure (6-14) illustrates the **P-Δ** behavior of this problem in the directions $X_1$and X_3 where one can easily recognize the great deal of coincidence, between our work and ***Kassimali*** and ***Abbassionia*** (1991), it also can be noticed that **Meth.-0-& Meth.-1-** and **Meth.-2-** are having absolutely the same path i.e. no shear effect noticed.

Table (6-13.a): Two-Member Bent-Joint Frame Properties

					Moment of Inertia of 3-Directions					
Element "(i)"	***Length "L_i (mm)"***	***Area "A_i(mm^2)"***	***Shear Modulus "G_i(Mpa)"***	***Elastic Modulus "E_i (Mpa)"***	***In X_1-Direct "I_1 (mm.^{4})"***	***In X_2-Direct "I_2 (mm.^{4})"***	***In X_3-Direct "I_3 (mm.^{4})"***	***Polar Inertia "J (mm.^{4})"***	***Shear Parameter "u_{xi}"***	***Joint Load (kN)***
1	1524.00	511.3925	80000	200000	41623.14	20811.57	20811.57	41623.14	X_1=.00125 X_3=.00062	0.00
2	254.00	511.3925	80000	200000	41623.14	20811.57	20811.57	41623.14	X_1=.04483 X_3=.02241	8.90

Table (6-13.b):-Comparison of Solutions For Two-Member Bent-Joint Frame

					Deflections of Joint -C- in (mm.)		
No.	***Method***	***Type of Analysis***	***No. of Element***	***No. of Increment***	***Vertical Deflection "x_2"***	***Horizontal Deflection "x_1"***	***Horizontal Deflection "x_3"***
1	Oran (1973)	Beam-Column L.D.	2	10	1131.73	291.96	-76.225
2	Kassimali & Abbasnia(1990)	Beam-Column L.D. "with bowing"	2	10	1131.57	290.17	-158.75
3	Present Meth.-0-	Beam-Column L.D. "no shear"	2	10	1131.57	290.17	-158.75
4	Present Meth.-1-	Beam-Column L.D. "with shear"	2	10	1131.58	290.18	-158.75
5	Present Meth.-2-	Beam-Column L.D. "with shear"	2	10	1131.57	290.18	-158.75

The **S.D./L.D.** divergence at **8.9 kN** are **0.935** for X_1 direction, **1.141** for X_2 direction, and **0.913** in X_3 direction respectively. No instability has been noticed in this case study. When the bowing terms were neglected, convergence could not be achieved for the two elements modeled at the first load step **P=0.89 kN** states the study of ***Kassimali*** and ***Abbassinia*** [49].

The **SS/SS0** values are **5.896%** increment for X_1, and **5.619%** decrement for X_2 respectively for both methods, which confirms the validity of *our new theory.*

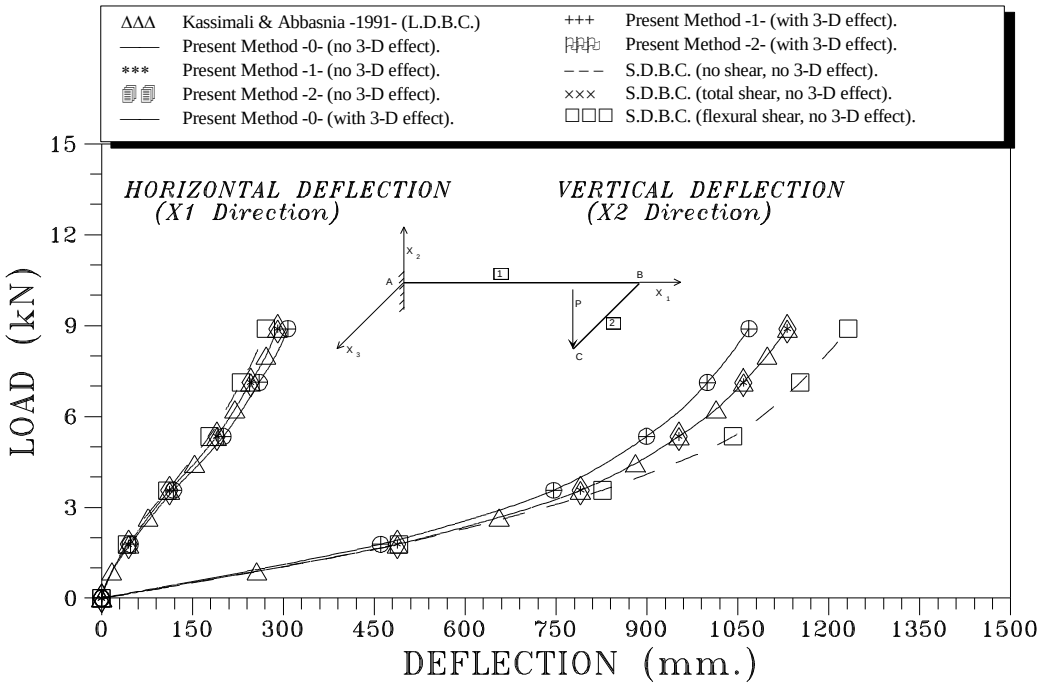

Figure (6-14) Load-Deflection curve for the 3-D Horizontal bent joint frame

6.2.13 Case no. 13(Pre-tilted, & pre-twisted, pyramid-shaped frame):-

A cyclic-symmetric pyramid-shaped four-member model structure with solid circular cross sections was designed to exhibit bifurcation behavior under single vertical load and two types of imperfections, as it is illustrated in figure (6-15.a):-

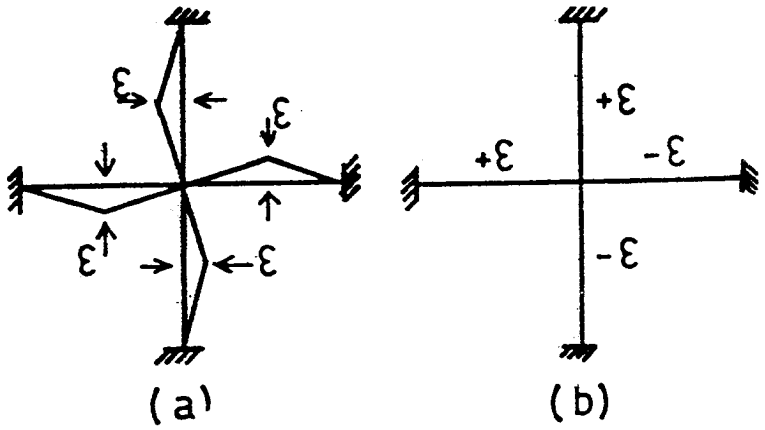

Figure (6-15.a) the pre-tilted and pre-twisted pyramid-shaped frame.

Table (6-14.a): Pretensioned, Pre-tilted, & Pre-twisted Pyramid-Shaped Four-Member with Crown Load Properties

							Initial Imperfections				
Element "(i)"	***L/r***	***Length "L_i(mm)"***	***Area "A_i(mm^2)"***	***Moments of Inertia "I_i (mm^4)"***	***Shear Parameter "u_i" (all directions)***	***Elastic Modulus "E_i (Mpa)"***	***Axial (mm.)***	***Pre-tilted (mm.)***	***Pre-twisted (mm.)***	***Load Parameter "P/P_e"***	***Load "kN*10^{-6}"***
1 to 4	96.54	556.785	11.62	386.52	0.00381	0.19540	1.00	1.00	1.00	1.00	2.405

- **1.00 mm.** twist imperfection.
- **1.00 mm.** tilt imperfection.

See and ***McConnel*** [84] (1986), tested this problem with properties as in table (6-14.a) experimentally and analytically using non-linear analysis as in table (6-14.b). By observing both figure (6-15.b) and table (6-14.b) for the vertical deflection at apex a good agreement can be noticed in addition to the inconsiderable shear effect with **91% S.D./L.D.** ratio or about **9%** divergence. The **SS/SS0** is **6.74%** decrement for both methods.

Table (6-14 .b): Comparison of Solutions For Pre-tensioned, Pre-tilted & Pre-twisted Pyramid-Shaped Four- Member with Crown Load

No.	***Method***	***Type of Analysis***	***No. of Element***	***No. of Increment***	***Crown vertical deflection (mm)***
1	See & McConnel (1986)	Experimental	4	10	0.84 at 2.28E-6 kN
2	See & McConnel (1986)	Beam-Column L.D.	4	10	0.72 at 2.28E-6 kN
3	Present Meth.-0-	Beam-Column L.D. "no shear"	4	10	0.72 at 2.28E-6 kN
4	Present Meth.-1-	Beam-Column L.D. "with shear"	4	10	0.72 at 2.28E-6kN
5	Present Meth.-2-	Beam-Column L.D. "with shear"	4	10	0.72 at 2.28E-6 kN

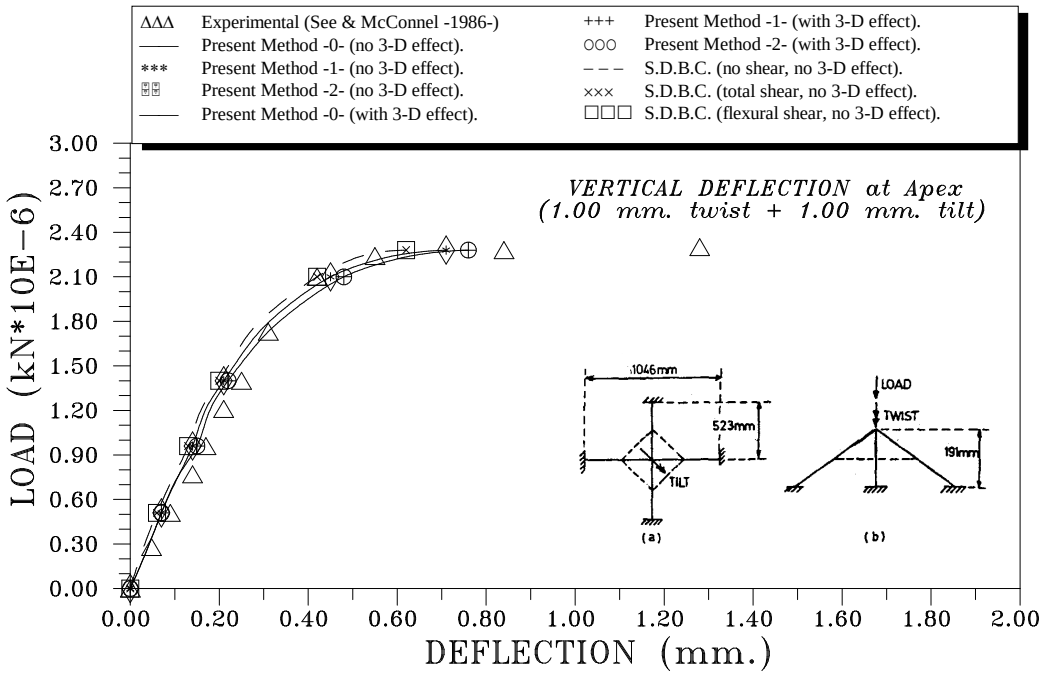

Figure (6-15.b) Load-deflection curve for 3-D pre-tilted, pre-twisted pre-tensioned member pyramid-shaped

6.2.14 Case no.14 (Space arch frame):-

The structure load system, system properties, the comparison among various investigators results, and the load-displacement curve for this are detailed in tables (6-15.a and 6-15.b) and figure (6-16) respectively.

Table (6-15.a): Space Arch Frame Properties

					Moment of Inertia of 3-Directions				
Element ***"(i)"***	***Length*** ***"L_i(mm)"***	***Area*** ***"A_i(mm^2) "***	***Torsional Stiffness*** ***"GJ_i(kN)"***	***Elastic Modulus*** ***"E_i (Mpa)"***	***X_1-Direction*** ***"I_1 (mm^4)"***	***X_3-Direction*** ***"I_3 (mm^4)"***	***X_2-Direction*** ***"I_2 (mm^4)"***	***Shear Parameter*** ***"u_{xi}"***	***Joint Load (kN)***
1-4	2031.95	322.58	1846750	29797259.59	166492.57	55358.7796	166492.57	X_1=0.00444 X_3=0.00148	V= 375 H=0.375
5 & 6	1560.576	322.58	1846750	29797259.59	166492.57	55358.7796	166492.57	X_1=0.00753 X_3=0.00250	
7 & 8	762.00	64.516	738700	29797259.59	20811.5713	20811.5713	20811.5713	X_1= 0.0197 X_3= 0.0197	

The ***NASCFI*** high accuracy can be readily concluded by observing both the table and the graph mentioned.

A considerable amount of increment occurred on the value of shear parameter "**u**" , especially for members **7** and **8** as its obvious from table (6-15.a) but a very small, rather negligible, shear effect has been noticed from results in table (6.15.b) and figure (6-16). Though **Meth.-0-** and both **Meth.-1-** & **Meth.-2-** are nearly coincide with each other. The **S.D./L.D.** ratio is about **92.87%**, and the **SS/SS0** is **4.84%** decrement for both methods.

Table (6-15.b): Comparison of Solutions For Space Arch Frame

No.	*Method*	*Type of Analysis*	*No. of Element*	*No. of Increment*	*Horizontal Deflection "x_3" in "mm."*
1	Wen & Rahimzadeh (1983)	F.E.M.L.D. "Lagrangian"	2	10	15.75 at 361.411 kN
2	Wen & Rahimzadeh(1983)	F.E.M. L.D. "Eularian"	2	10	15.75 at 358.54kN
3	Present Meth.-0-	Beam-Column L.D. "no shear"	2	10	15.75 at 355.75 kN
4	Present Meth.-1-	Beam-Column L.D. "with shear"	2	10	15.75 at 355.75 kN
5	Present Meth.-2-	Beam-Column L.D. "with shear"	2	10	15.75 at 355.75kN

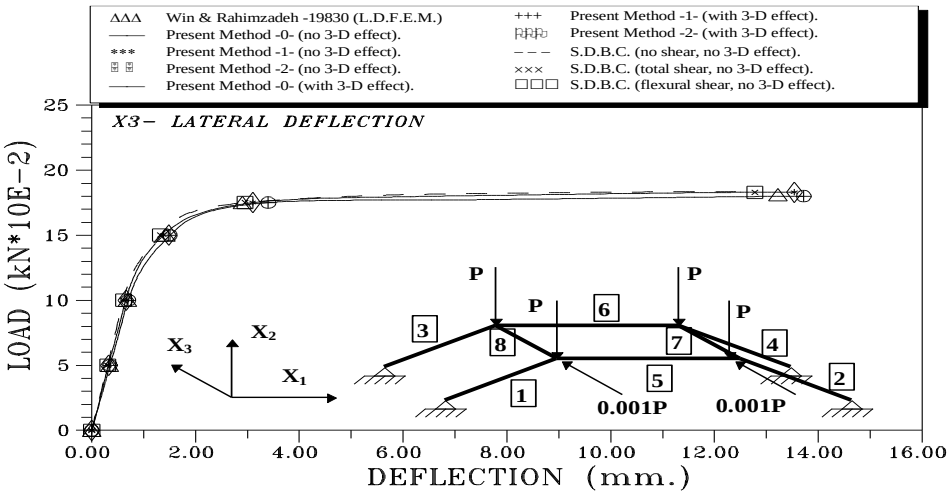

Figure (6-16) Load-Deflection curve for the 3-D arch frame

6.2.15 Case study no. 15 (Framed dome with vertical load):-

As another validational and important 3-D example, the imperfect sensitive 18-member frame dome shown in figure (6-17.a) was analyzed by many researchers as table (6-16.b) indicates. Table (6-16.a) states the properties and load condition of the problem. A single load is applied at the top joint or crown of the dome.

Table (6-16.a): Framed Dome with Crown Load Properties

Element "(i)"	*Length "L_i (mm)"*	*Area "A_i (mm^2)"*	*Typical Inertia "I_1(mm^4)"*	*Typical Inertia "I_3 (mm^4)"*	*Elastic Modulus "E_i (Mpa)"*	*Shear Modulus "G_i(Mpa)"*	*Shear Parameter "u_{xi}"*	*Equal Joint Load =8 9000 kN*
1 & 6	1084.20	6451.60	5550029.83	2167872.01	20685	1280	X_1=0.0260 X_3=0.0102	
2,3,4 & 5	620.93	6451.60	5550029.83	2167872.01	20685	1280	X_1=0.0793 X_3=0.0309	
7,9,10&12	1047.50	6451.60	5550029.83	2167872.01	20685	1280	X_1=0.0278 X_3=0.0109	
8 & 11	1047.50	6451.60	5550029.83	2167872.01	20685	1280	X_1=0.0278 X_3=0.0109	
14,15,17&18	539.50	6451.60	5550029.83	2167872.01	20685	1280	X_1=0.1050 X_3=0.0411	
13&16	1055.50	6451.60	5550029.83	2167872.01	20685	1280	X_1=0.0274 X_3=0.0107	

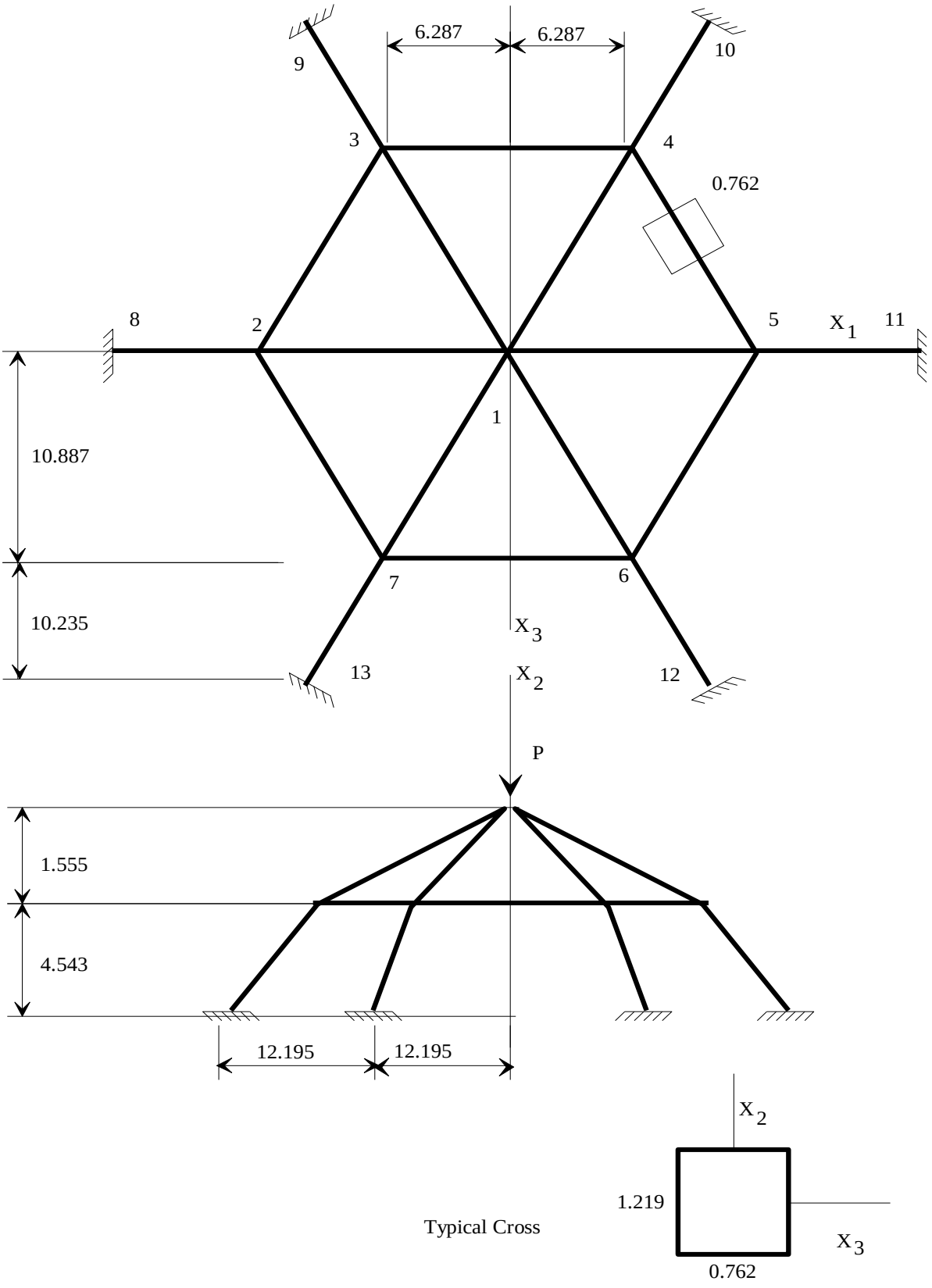

Figure (6-17.a) Frame dome with crown load details

Figure (6-17.b) shows the excellent convergence between the present formulation and the other efforts in both pre-buckling and post-buckling regions of the curve. Although the "**u**" value is increased in comparison with the earlier cases, we find that the shear effect still far from being effective in the stability analysis of the structures, and the **S.D./L.D.** divergence at **89 MN** is about **1.1208**, while the **SS/SS0** is **5.77%**.decrement.

Table (6-16.b): Comparison of Solutions For Framed Dome with Crown Load

No.	***Method***	***Type of Analysis***	***No. of Element***	***No. of Increment***	***Crown Vertical Deflection "mm."***
1	Oran (1973)	Beam-Column L.D.	18	22	2636.52 at 89 MN
2	Papadrakakis & Ghionis (1986)	Finit-Element L.D.	48	25	2650.10 at 89 MN
3	Al-Bermani& Kitipornchai (1990)	Beam-Column L.D.	18	25	2647.014 at 89 MN
4	Kassimali & Abbassnia (1990)	Beam-Column L.D. "with bowing"	18	22	2651.70 at 89 MN
5	Present Meth.-0-	Beam-Column L.D. "no shear"	18	22	2651.73 at 89 MN
6	Present Meth.-1-	Beam-Column L.D. "with shear"	18	22	2651.84 at 89 MN
7	Present Meth.-2-	Beam-Column L.D. "with shear"	18	22	2651.82 at 89 MN

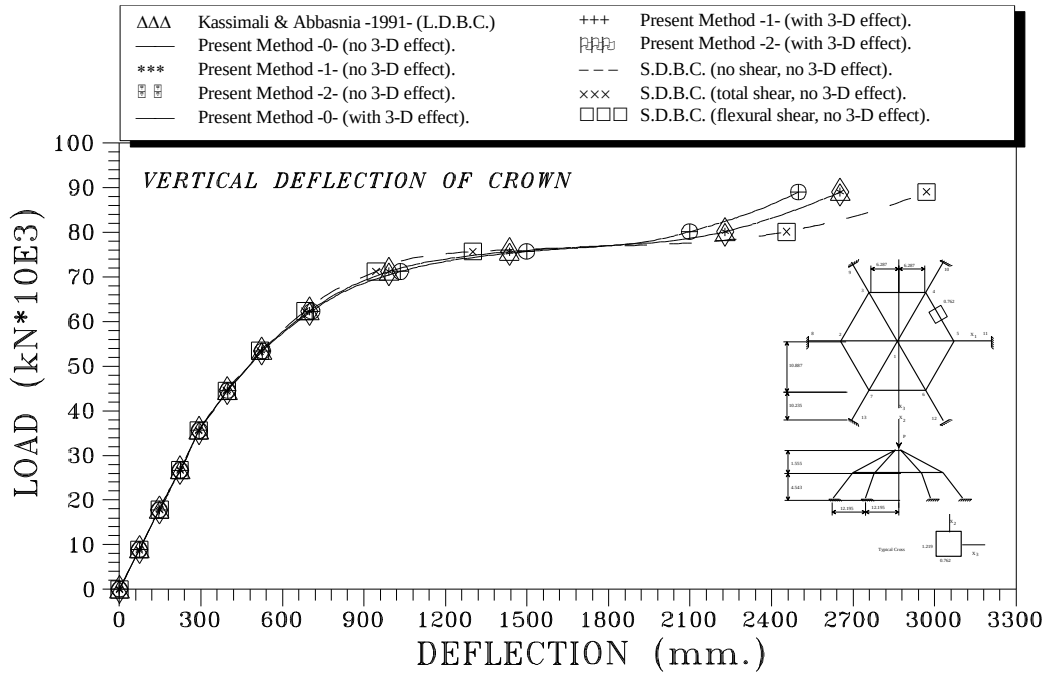

Figure (6-17.b) Load-deflection curve for the 3-D crown vertical load dome

In the previous 15 case studies the main aim has been achieved, that is (***NASCFI***) is accurately able to deal with the most widely known basic theory pre solved examples, besides, the (***SS*** effect) has a considerable influence on the 3-D problems behavior which supports *our new theory*.

6.3 Shear effect case studies:-

In the second stage of testing **(*NASCFI*),** the shear effect must be checked for structure having "**u**" values (i.e. open-web structures). From now on the structures will have more high values of the shear parameters "**u**", and hence we are dealing with more seriously linked and associative problems with our main aim, purpose, and goal of this study. As it is previously and briefly mentioned in table (6-1.b) in the beginning of this chapter, five case studies are to be tested herein in order to observe **the real effect of shear on the (P-Δ) behavior of structures.**

In **chapter-3-**, we mentioned the basic idea of the equivalent shear parameter approach the present study adopts in which any structure can be idealized as an equivalent solid structure with the value of the shear parameter "**u**" as indicated and that this "**u**" value is usually high in *the lattice, trussed or open-web structure.*

6.3.1 Case study no.16 (Simply-supported slender beam):-

The essential benefit from taking this example:-

- to show the effect of increasing the shear parameter "**u**" on the (P-Δ) behavior.

- to show that the present work is differ than the simple small deflection (S.D.) linear theory.

This simple case study was solved by ***Kenny*** [49] in (1957), by using the small deflection linear unit-load method technique to evaluate the shear and flexure deflections separately, he found that the shear to flexure deflection ratios for all the four cases of slenderness ratio **(L/D)** as detailed in table (6-17.b)

In the non-linear analysis either (S.D.) or (**L.D.)** it is neither practical nor actual behavior to separate the pure shear deflection from the pure flexure deflection because they both act simultaneously.

Table (6-17.a) summarizes the properties and the load condition of this problem and figure (6-18) and table (6-17.b) show this case results, it is clear that the beam is loaded in its middle span by a concentrated load (**P**) and that the four cases of different **L/D** ratios are taken to illustrate the effect of slenderness ratio on the value of shear parameter and accordingly the shear effect on the (**P- Δ)** behavior. By observing table (6-17.b) and figure (6-18), it can be seen that when **L/D** decreases or "**u**" increases, the divergence between **Meth.-0-**(no shear included) and the including shear methods **Meth.-1-** (total shear angle method) and **Meth.-2-** (flexural shear angle) increases as it is obvious from cases -1- (**u =1.419**) and -2- (**u = 0.3548**), meanwhile in cases-3 (**u =0.1577**) and -4- (**u = 0.0887**) the shear effect is getting closer to be vanished.

Another point can be settled from table (6-17.b), which is the shear contribution ratios ($(\delta_v/\delta_b)_1$=Meth.1-Meth.0/Meth.0) and ($(\delta_v/\delta_b)_2$=Meth. 2-Meth. 0/Meth. 0) are approximately equal in S.D. analysis to their corresponding values in L.D. analysis (even though the displacement values are different in both approaches), i.e., when the L.D. major effects (C_1, C_2, b_1, b_2, G_1 and G_2) are neglected the effect of shear contribution is as noticeable as when concluding these effects. Also noticed that Meth.-2- does not work when u = 1.419, this is because of the fact that at high "**u**" values (just like this case) the stability and bowing functions of **Meth.-2-** shift far away from their corresponding values of **Meth.-1-** especially at the high tension axial load parameters **(ρ<0)**, (see figures (3-7) to (3-12). At these load levels a different stability and bowing functions lead to a misleading stiffness and then no iteration tolerance is achieved which means an infinity loop of displacement iterations with no end preventing any

result from showing, if the tolerance increases more than ($\mathbf{10^{-5}}$) this method gives some results but it surely misleading.

Table (6-17.a): Properties of Simply-Supported Slender Beam

Case	*Element Section "(i)"*	*Length L_i(mm.)*	*Depth of Section D_i(mm.)*	*L/D*	*Area Ai(mm^2)*	*Moment of Inertia "$I_i(mm^4)$"*	*Section Modulus $S_i(mm^3)$*	*Elastic Modulus E_i(Mpa)*	*Shape Factor "n"*	*Shear Paramet. "u_i"*	*0.6Fy "Mpa"*	*P_{all} "Mpa"*	*Concent. Load "kN" at Mid-span*
1	12W27	1524	12.00	5	4896.7644	84911210.8	560437.6	200000	2.89	1.419	148.93	5093.47	2630.00
2	12W27	3048	12.00	10	4896.7644	84911210.8	560437.6	200000	2.89	0.3548	148.93	5093.47	2630.00
3	12W27	4572	12.00	15	4896.7644	84911210.8	560437.6	200000	2.89	0.1577	148.93	5093.47	2630.00
4	12W27	6096	12.00	20	4896.7644	84911210.8	560437.6	200000	2.89	0.0887	148.93	5093.47	2630.00

Table (6-17.b): Comparison of Simply-Supported Slender Beam Results

		Deflections (mm.)			*Max. Deflection Ratio "Shear/Flexure"*				
Case	*No. of Increments*	*Present Meth.-0-*	*Present Meth.-1-*	*Present Meth.-2-*	*$(\delta_v/\delta_b)_1$*		*$(\delta_v/\delta_b)_1$*		*Kinney (1957)*
					L.D.	*S.D.*	*L.D.*	*S.D.*	*S.D.*
1	10	13.829	14.327	14.164	0.4308	0.4314	D.N.W.	0.4261	0.60
2	10	86.314	86.624	86.478	0.1072	0.1078	0.1065	0.1064	0.15
3	10	196.543	196.567	196.552	0.0468	0.0479	0.0463	0.0475	0.07
4	10	311.854	311.859	311.856	0.02518	0.02698	0.02526	0.0266	0.04

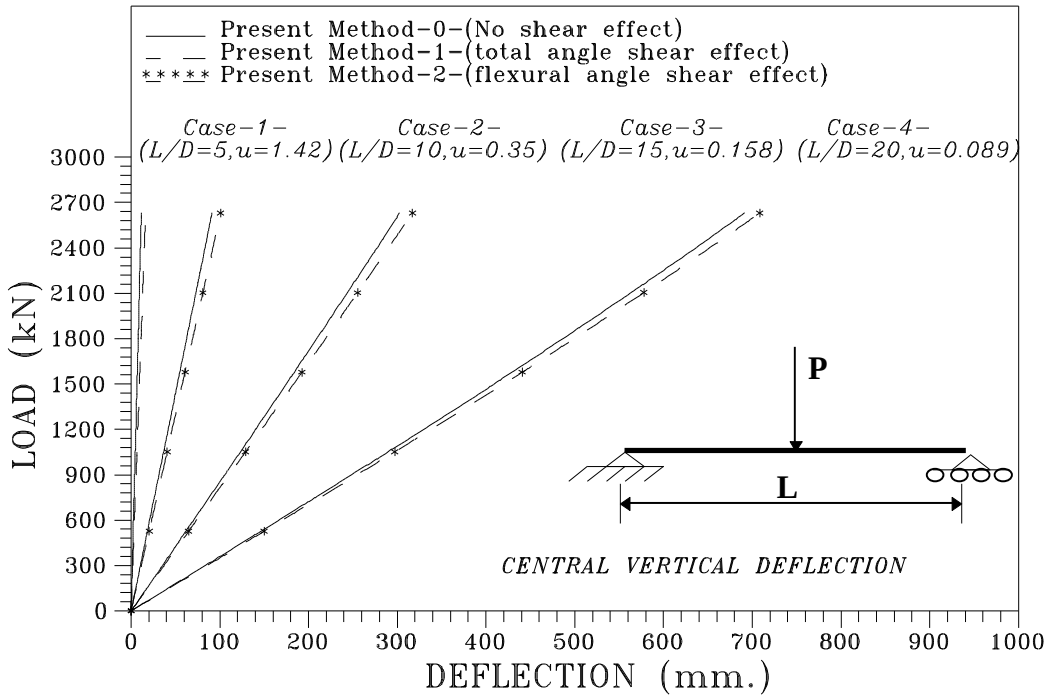

FiFigure (6-18) Load-Deflection Curve for the Simply Supported Slender Beam

6.3.2 Case study no.17 (Four storey frame):-

The properties and load condition of this example are detailed in table (6-18.a), its sketch and load vs. deflection behavior are illustrated in figure (6-19.a and b) respectively, and the comparison of results of various investigators are shown in table (6-18.b). The present elastic stability analysis is to be compared only with the elastic zone of elastic-plastic (**P-Δ)** curve established by many researchers as table (6-18.b) indicates.

Table (6-18.a): Four-Storey Frame Properties

Member	*Section Type*	*Area* "A(mm^2)"	*Moment of Inertia* "I(mm^4)"	*Radius of Jyration* "r(mm)"	*Elastic Modulus* "E(Mpa)"	*Poison Ratio* "ν"	*Shape Factor* "n=A/A_w"	*Shear Parameter* "u"	*3 Cases of H/V Ratio* *0.5,0.24,0.1*
Girders	W 16*40	7612.890	215607878.4	1684.02	201000	0.50	2.579	0.0259	
Bot. Col.	W 12*79	14967.712	275545203.7	1356.36	201000	0.50	4.525	0.1842	
Upp.Col.	W 10*60	11354.820	141934916.1	1115.06	201000	0.50	4.729	0.1302	

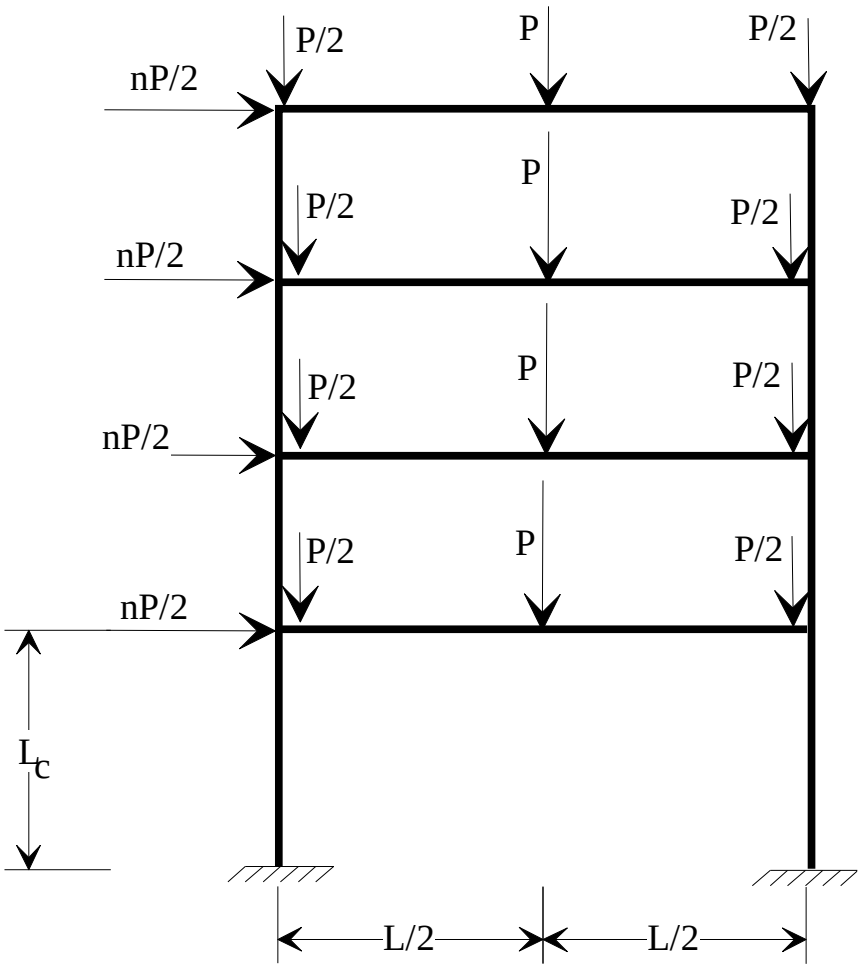

Figure (6-19.a) Four-Story Frame

Three cases of different **H/V** ratios of (**0.5, 0.24,** and **0.1**) which essentially affect the "**u**" value are tested and checked with other results. Good agreement is noticed between all the three present methods (**Meth.-0-,-1-,** and-**2-**) and the theoretical results taken from the previous researchers, but as it is clearly noticeable that the (shear) to (no shear) ratio of **Meth.-1-** or (**Meth.-1-/Meth.-0-**) results at **137.37 kN** is (**4.71%)** increment, at **176.6025 kN** is (**5.87%**) increment, and at **215.87 kN** is(**6.51%**) increment for cases 1, 2, and 3 respectively, while (**Meth.-2-/Meth.-0-**) results are (**4.43%, 5.43%,** and **6.19%**) for the three cases respectively and incrementally and at the same load stages for **Meth.-1-**, which shows how close the two methods are. From figure (6-19.b) its also obvious that the shear effect does exist when analyzed by the **S.D.** theory and it has nearly the same percentage ratios as the **L.D**. with an important remark the **S.D./L.D.** ratio increases with the **H/V** increase which is reasonable since the horizontal force dominantly affects the deformation and the axial force parameter

P/P_e which in turn governs the large deflection analysis. The shift noticed in the results of other researchers is due to elasto-plastic effects which are not included in the present work and can be added in the future, the work that actually no big deal.

Table (6-18.b): Comparison of Solutions for Four-Story Frame

					Horizontal Deflection at point "B" in (mm.) for Various cases		
No.	***Method***	***Type of Analysis***	***No. of Element***	***No. of Increment***	***Case 1***	***Case 2***	***Case 3***
1	Al-Zanaty & Murray(1983)	Finite Element L.D.	12	30	216.353 at 137.37 kN	140.97 at 176.62 kN	99.715 at 215.87 kN
2	Kam (1988)	E-P, F.E.M. S.D.	12	30	216.353 at 137.37 kN	140.37 at 176.62 kN	99.956 at 215.87 kN
3	Kam (1988)	E-P, F.E.M. L.D.	12	30	216.353 at 137.37 kN	140.38 at 176.62 kN	99.971 at 215.87 kN
4	Kassimali (1983)	Beam-Column L.D.E-P.stab.anal.	12	10	199.786 at 137.37 kN	124.89 at 176.62 kN	78.731 at 215.87 kN
5	Present Meth.-0-	Beam-Column L.D. "no shear"	12	10	165.122 at 137.37 kN	100.91 at 176.62 kN	56.475 at 215.87 kN
6	Present Meth.-1-	Beam-Column L.D. "with shear"	12	10	172.89 at 137.37 kN	106.91 at 176.62 kN	60.15 at 215.87 kN
7	Present Meth.-2-	Beam-Column L.D. "with shear"	12	10	172.45 at 137.37 kN	106.46 at 176.62 kN	59.97 at 215.87 kN

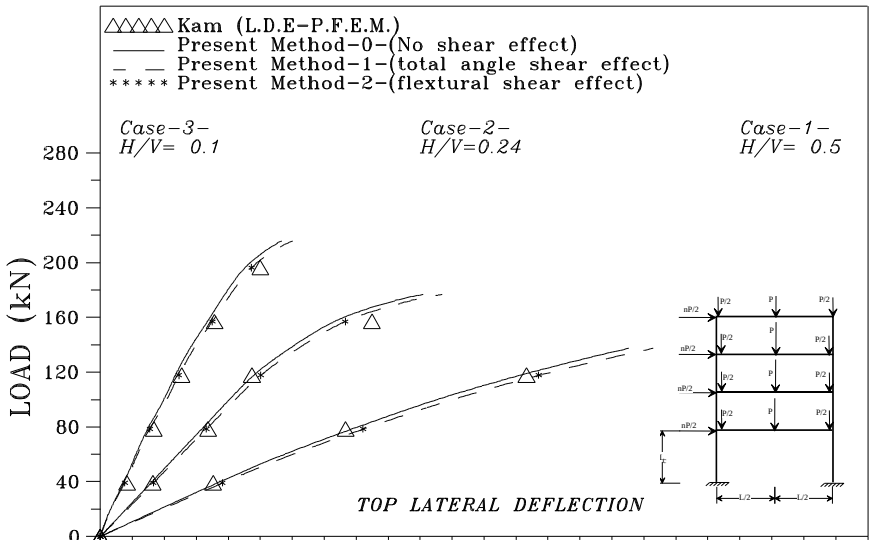

Figure (6-19.b) Load-Deflection curve for the four story portal frame

It seems important to mention that cases no.16 and 17 do exhibit shear effect even though they have solid closed-web cross sections. But since their "**u**" value forms a relatively valuable amount, we noticed a relatively movable divergence between the shear including effect and no shear values due to the high values of "**u**".

6.3.3 Case no. 18 (Truss cantilever):-

Although one of the most important conditions of the equivalent shear parameter method is that the panels must not be less than 5-6 in order to give an accurate "**u**" value calculated according to table (3-2), it might be a good task to take this case study and the one after to illustrate the shear effect in lattice sections.

As it was previously indicated in **chapter-3-** the lattice, trussed or open-web structures exhibit a relatively higher shear deformations than the solid and closed-web structures. Using the present formulations an equivalent members with solid cross sectional areas and shear parameter **"u"** are to replace the actual members or structures, their equivalent areas, inertia and lengths must be detailed according to the approach detailed in **chapter-3-**. In order to explain this, the case study of truss cantilever which studied by other researchers like ***A. Noor*** [67] (1974) is an absolutely perfect example to study. The actual and equivalent properties are detailed in tables (6-19.a and b) respectively, and their sketches are in figure (6-20.a), notice that "**u**" becomes more noticeable (**0.2506**) in comparison with the cases studied so far for the single members modeling represented by the present work.

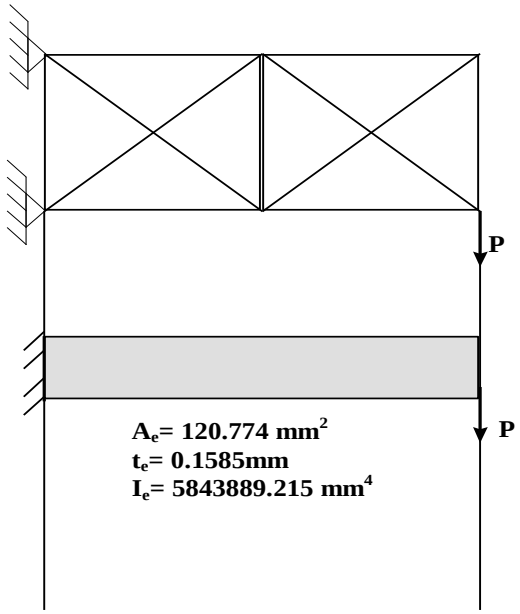

Figure (6-20.a) Actual and Equivalent elements of truss cantilever

Table (6-19.a): Truss Cantilever Actual Properties

Element "(i)"	*Length "L_i(mm)"*	*Area "A_i(mm^2)"*	*Moment of Inertia "I_i(mm^4)"*	*Elastic Modulus "E_i(Mpa)"*	*Shape Factor "n_i"*
Horizontal	762	161.29	83.25	68950	1.2
Vertical	1016	129.03	69.37	68950	1.2
Diagonal	1270	129.03	69.37	68950	1.2

Table (6-19.b): Truss Cantilever Equivalent Properties

Type of Bracing	*Bracing Angle "α"*	*Equivalent. Length "L_i(mm)"*	*Diagonal Area "Ad(mm^2)"*	*Equivalent Thickness "t_e(mm)"*	*Equivalent Area "A_e(mm^2)"*	*Equivalent Inertia "I_e(mm^4)"*	*Shear Parameter "u_i"*	*"u" Govern. Equivalent*	*Joint Load (kN)*
X-Bracing	36.869	1524	129.032	0.1585	120.774	5843889.215	0.2506	Eq. 3-7	-

From table (6.19.c) and figure (6.20.b) it can be noticed that **(Meth.-1-/Meth.-0-)** at **P= 53.4 kN** for the **L.D.** analysis gives an increase of **7.615%** while **Meth.-2-** exhibits **6.63%** increment which is purely the **effect of shear deflection** on the load-deflection behavior and indeed it means that both **Meth.-1-** and **Meth.-2-** introduce an enormous difference in the load-deflection behavior, and no response at all not even for just one load increment.

At the same load stage ***A. Noor***`s ten elements geometrical and material non-linearity mixed method of analysis gives a decrease of **8.02%** in the deflection value with **Meth.-0-** (no shear effect) analysis if we use "0.5E", while using "E" the results

are very close to ***Noor***'s. This is because his method did not included the geometrical non-linearity effect of **L.D.** very important parameters which are **the stability and the flexural bowing effects** which are included in **Meth.-0-**, although he included the important change in length parameter. Meanwhile **Meth.-1-** and **Meth.-2-**give a **16.22%** increment and **15.17%** increment respectively over ***A. Noor*** deflection result.

Table (6-19.c): Comparison of Solutions For Truss Cantilever

No.	*Method*	*Type of Analysis*	*No. of Element.*	*No. of Increment*	*Vertical Deflection at "E"(mm.)*
1	Richard & Goldberg(1963)	Beam Theory Linear S.D.	10	12	20.955
2	A.Noor (1974)	Beam Theory L.D. (G.N.L.)	10	12	25.005
3	A.Noor (1974)	Beam Theory L.D. (G&M.N.L.)	10	12	49.89
4	Present Method "0"	Beam-Column L.D.	2	12	26.95 -E- 53.89 -0.5E-
5	Present Method "1"	Beam-Column L.D. "with Shear"	2	12	28.994 -E- 57.98 -0.5E-
6	Present Method "2"	Beam-Column L.D. "with Shear"	2	-	28.73 -E- 57.46 -0.5E-

It must be noticed that there is some overestimation in **Meth.-1-** resulting from the fact that the number of panels are two which is less than 5 (the minimum number of panels required by the equivalent shear parameter method).

This case is analyzed also using different values of "E" in order to investigate it's effect on the (P-Δ) behavior, the conclusions of this variation indicate that no difference occurred neither in the shear parameter "u" and accordingly in the shear effect represented by (Meth.-1-,-2-/Meth.-0-), nor in the shape of the curve which is a straight line, but meanwhile this variation does affect the strength and deflection values, i.e. the higher the "E" values the less deflection of the structure.

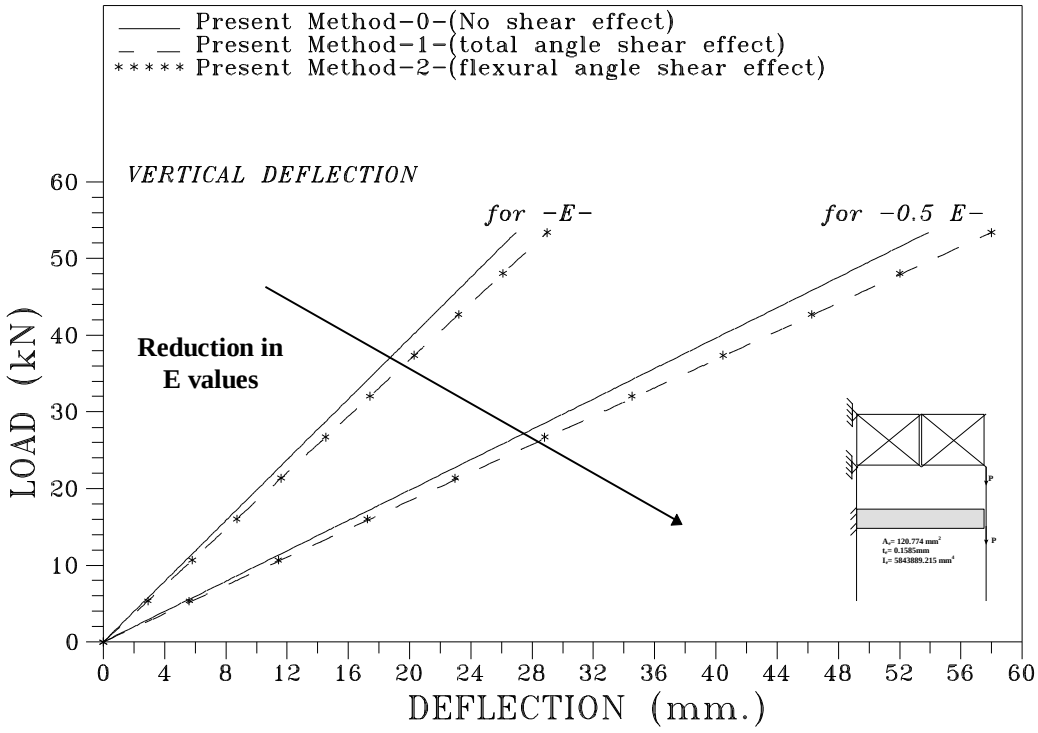

Figure (6-20.b) Load-Deflection curve for the truss cantilever

6.3.4 Case study no. 19 (3-D transmission tower):-

A very efficient example is one which shows the effects of both 3-D and shear effects on the load-displacement behavior of structures, since 3-D problems include the effect of torsional stiffness on axial force, axial stiffness on torsional rigidity, and the commutative effects of shear and flexural stiffnesses on torsion and visa versa, which all are included in our present formulation. Figure (6-21.a) shows the actual and equivalent sketches of the problem in question. Table (6-20.a) illustrates the equivalent properties, and figure (6.21.b) and table (6-20.b) illustrate the final (**P-Δ)** results of this problem.

Table (6-20.a): 3-D Transmission Tower Equivalent Properties

Elm. "(i)"	*Type of Bracing -X_1-*	*Bracing Angle "α"*	*Type of Bracing -X_3-*	*Bracing Angle "α_3"*	*Equivlnt. Length "L_i(mm)"*	*Equivlnt. Thick. t_e(mm)*	*Equivlnt. Area A_e(mm^2)*	*Equivlnt. Inertia I_{e1}(mm^4)*	*Equivlnt. Inertia I_{e3}(mm^4)*	*Shear Paramet. "u_{x1}"*	*Shear Paramet. "u_{x3}"*	*Joint Load (kN)*
1	Warren	26.565	Warren	26.565	1787.5	0.03678	162.045	262122809.8	262122809.8	2.4818	2.4818	-
2	Warren	53.130	Warren	53.130	712.5	0.0776	228.456	165007142.4	165007142.4	1.2421	1.2421	-
3	Warren	53.130	Vereindeel	53.130	1270.00	0.06165	139.61	59667501.2	39787.89	1.3702	0.0031	-
4	Warren	53.130	Vereindeel	53.130	1270.00	0.06165	139.61	59667501.2	39787.89	1.3702	0.0031	P_y= 53.4 P_z= 213.6

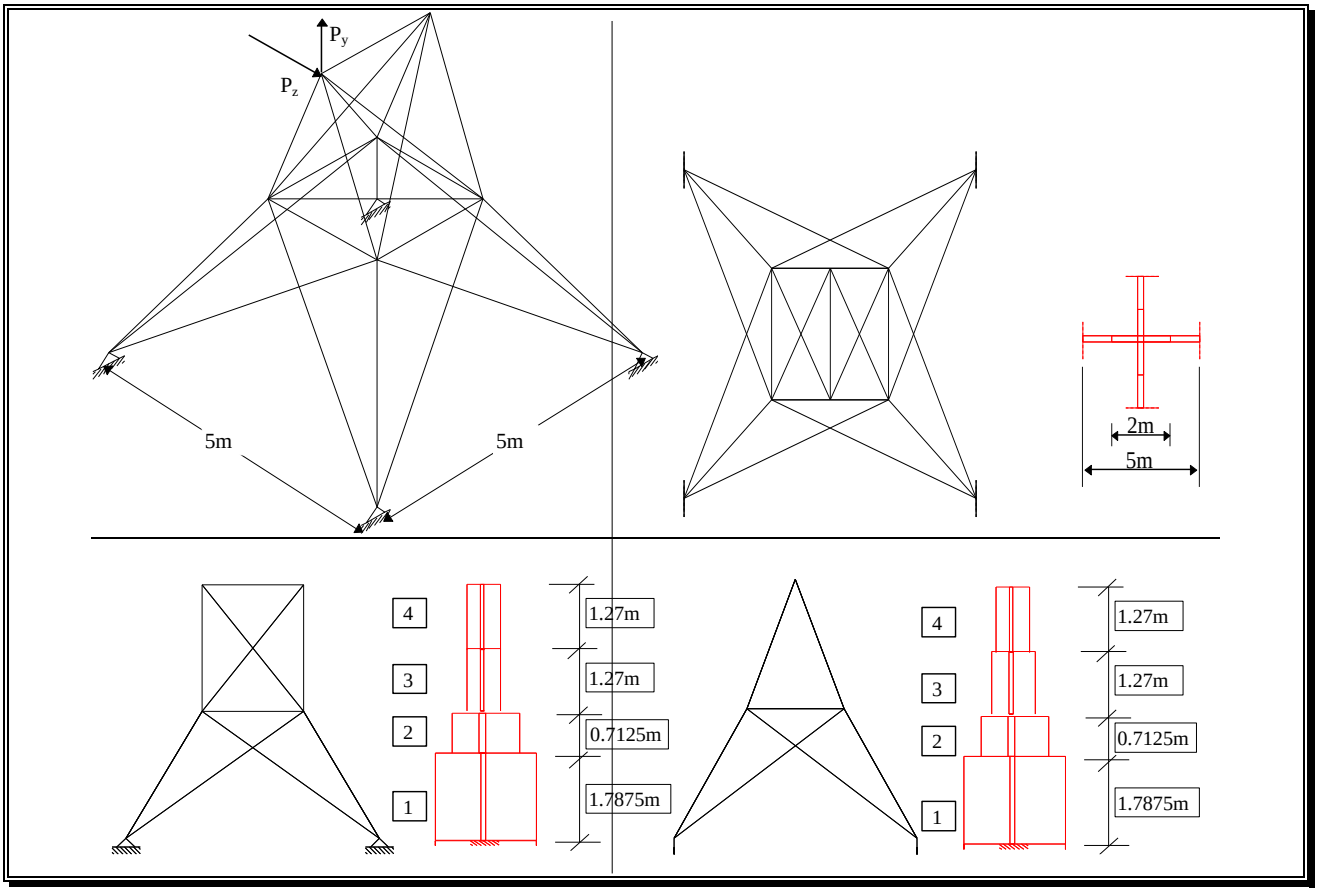

Figure (6-21.a) the actual and equivalent towers

The same ***A. Noor***[67] (1974) used the mixed method in the previous 2-D case study to solve this (25) truss element 3-D problem and again used by the author using

only 4 beam-column equivalent elements to check the validity of the present formulation.

It can be noticed that the shear parameter "**u**" has extremely high value for the four members that represent the equivalent idealization of the problem based on the present procedures indicated in table (6-20.a).

Table (6-20.b): Comparison of Solutions For 3-D Transmission Tower

				Deflections at Mid-Top End	
No.	***Method***	***Type of Analysis***	***No. of Element***	***X_1-Direction "mm."***	***X_2-Direction "mm."***
1	Linear	S.D. Beam Theory	25	30.752	62.765
2	A.Noor (1974)	L.D. Beam Theory	25	42.42	104.65
3	Present Meth.-0-	Beam-Column L.D. "no shear"	2	43.425	108.511
4	Present Meth.-1-	Beam-Column L.D. "with Shear"	2	50.641 (**SS**) 46.735 (**SS0**)	129.38 (**SS**) 118.33 (**SS0**)
5	Present Meth.-2-	Beam-Column L.D. "with Shear"	2	Did Not Work	Did Not Work

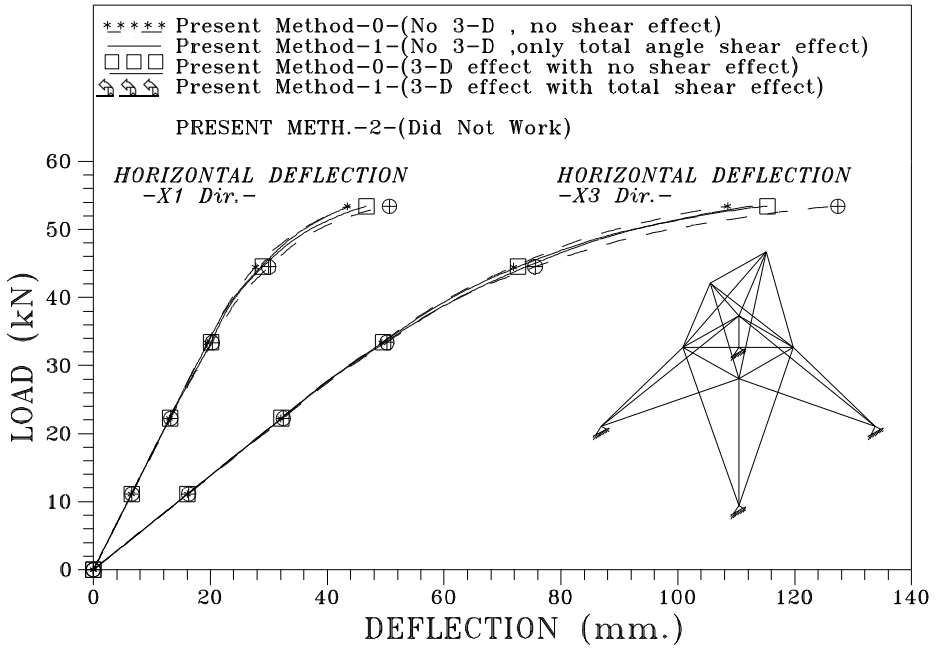

Figure (6-21.b) Load-Deflection curve fir the 3-D Transmission

For the X_1 direction (the opposite direction to the horizontal top concentrated force which is 4 times the vertical load), the **(Meth.-1-/Meth.-0-)** ratio at **(P= 53.4 kN)** is **7.62%** increment. In the other direction of the applied horizontal force (X_3 direction), the ratio is (**9.05%** increment), which means that **Meth.-1-** gives us a dominantly different load-deflection behavior from the no shear one. **Meth.-2-** again exhibits no response and fails to give at least one load increment for the same reason mentioned in case no.(16) keeping in mined that the present case is more non-linear and thus higher tension axial load parameters are expected.

At the same load stage and referring to ***A. Noor*** mixing method the ratios to the present **Meth.-0-**(no shear effect) are **2.36%** decrement and **3.69%** decrement in X_1 and X_3 directions respectively, while **Meth.-1- / *Noor*** ratio at the same final load level are **10.17%** increment and **13.07%** increment for X_1 and X_2 directions respectively and.

The (***SS*** effect) is **8.35%** increment**,** and **9.34%** increment for X_1- and X_2-directions respectively which is too high to be ignored, the matter that means that it is larger than for solid section which is logical since the larger "**u**" value the larger twisting functions. However, there is an error in the results since the warping contribution has been ignored. It must be added (using the modified eq.3-104).

Eight Warren-bracing idealized elements were also taken in this problem (2 members per each element of the 4 elements analysis) with an average ± **0.86%** divergence in the (4) element results.

The problem is also solved using only (2) equivalent beam-column elements with "**u**" value calculated from X-bracing $\mathbf{P_{cr}}$ control equation i.e.(eq.3-7) instead of (4) Warren bracing elements, **(u_1=3.005 ,u_2= 3.798)** respectively and the results were shifted by **28.4%**. Away from the 4 element analysis which means that there is a misleading in the results since in the 4 element case we must have at least 20 panels while in the 2 element case, 10 panels must be available at least.

Although it is not accurate to apply the present formulation that depends on the equivalent shear rigidity solid section unless we have at least 5-6 panels of lacing or bracing of any type as it is previously mentioned in **chapter-3-**. This specific problem has no other alternatives of idealization or representation, so there might be some inaccuracy in the results, besides, the non-prismatic sections of the tower and accordingly the equivalent (4) idealized elements may give some incorrect results

because the effect of **non-prismatic stability and bowing functions** are not included in the present formulation.

The above discussion dealing with this 3-D problem and the one before it dealing with the 2-D problem lead us to the following facts:-

1. **Shear effect plays a major role governing the P-Δ behavior of the open-web structure.**
2. **Because of the high values of "u", Meth.-2- behaves strangely and fails to give logical results associating shear effect.**
3. **In the absence of the axial load and the stability geometrical non-linearity, the material non-linearity becomes the dominant effect that governs the non-linear behavior and the geometrical non-linearity is linearly affects the curve, while in the presence of both actions the geometrical non-linearity becomes the dominant leaving the material non-linearity to behave linearly.**
4. **Changing the number of equivalent elements more than 1 element for the truss case and 2 elements for the tower case leads to misleading results.**
5. **Misestimated and erroneous results may be expected in the non-prismatic problems since this effect is not included in the present study, besides, the number of panels not being at least (5) leads to some overestimated results.**
6. **Changing the type of bracing system in the equivalent elements with the number of elements kept constant leads to a misleading result in the P-Δ behavior of the open-web structure.**
7. **There is an error in the 3-D effect (*SS* effect) analysis of the 3-D open-web problems owing to ignoring the warping contribution of the lateral buckling equations, which means that there must be a modification to the twisting functions equations (an alternate solution is by using equation 3-104 to include such effect), still the (*SS* effect) has a more influential role on the behavior of such structure than the corresponding solid sections.**

6.3.5 Case study no. 20 (2-bay lattice portal frame):-

Lin [56](1970), subjected this problem to an analytical large deflection procedure he derived using **the flexural shear angle** (i.e., **Meth.-2-**) in a very appreciable effort as mentioned in **chapter-3-**, he studied this problem under three load conditions as detailed in table (6-21.a), with its properties were included in the same table. figure (6-22) illustrates the actual and equivalent sketches of the problem.

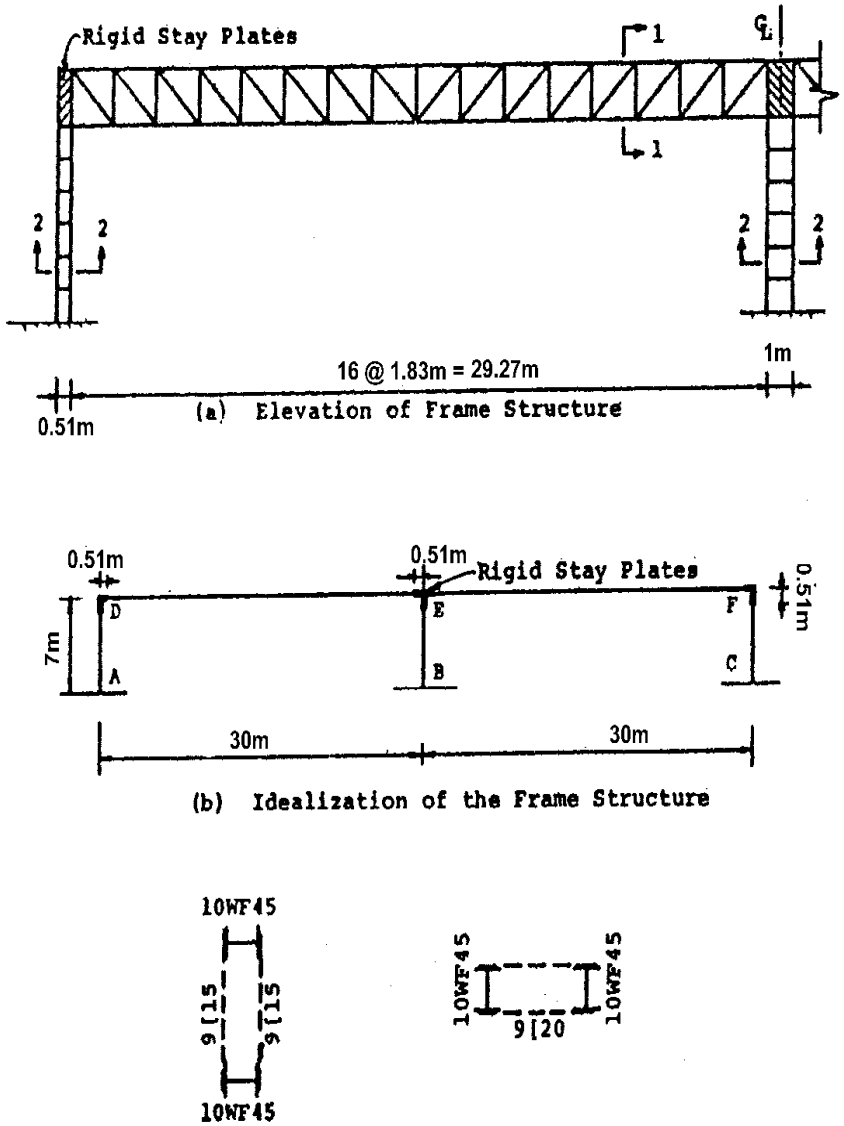

Figure (6-22) the actual and equivalent lattice frames.

The present work adopts the well known ***Cholisky*** *Factorization Technique* as an equation solver as mentioned in **chapter-5-** in an effort to reduce the computer storage

during execution although this subject does not form a major problem with the high advanced technology of computers nowadays. This technique exhibits a very efficient procedure in treating the prescribed deflection problems just like the one under test.

Even though the ***Lin***`s procedure differs from the present, keeping in mind that neither the change in length nor the bowing effects have been included in his work, as a matter of fact there are major aspects of coincidence between his way and the author's in treating some problems like the fixed end action (see **chapter-3-**), and the most important issue is that the same equivalent properties were adopted in both methods.

Since only the **B.M.D.** is shown by ***Lin,*** the comparison between the three cases of different load conditions is taken by compressing the **B.M.D.** of each case instead of the **P-Δ** curve as other cases were treated; this comparison is detailed in table (6-21.b)

It's noticeable that **Meth.-1-** results are very close to ***Lin*** methods with an average divergence of **3.54%**, **4.44%**, and **5.27%** for cases(1, 2, and 3) respectively, **Meth.-1- / Meth.-0-** ratio are **(2.29%, 2.86%, and 3.65%)** respectively, this difference belongs actually to **the combined summed effects of shear, change in length and flexural bowing parameters.**

Meth.-2- in turn gives results as close as (maybe sometimes closer than) **Meth.-1-** to ***Lin*** results with an average divergence of **25.86%** for case 1, but for cases 2 and 3 this method did not work.

The performance of **Meth.-2-** in this problem, (in cases 2 and 3), is just like the last two case studies and seems to be reasonable. The reason maybe due to the values of the shear parameter getting higher than **1**, **the stability and bowing functions** of this method ($\overline{C}_1, \overline{C}_2, \overline{b}_1 \& \overline{b}_2$) start to shift away from the same values obtained from **Meth.-1-, e**specially when **(ρ< 0)**as it can be seen in figures (3-6,7,10 and 11), while for the "**u**" values **<1**, these functions begin to converge to each other till they nearly coincide at (**u = 0**). In this particular problem the "**u**" values fluctuate from **0.115** at girders (where the axial force is small in comparison with columns), to **0.8863** at outer columns, to **3.859** at inner or middle batten column (where both axial and shear effects are high), and since the inner column really exhibits tension (ρ) in the three load cases (except maybe for case -1- in which the results of **Meth.-2-** are so close to **Meth.-1-**).

Table (6-21.a): Geometric Arrangements and Elements Properties of Two-Bay Lattice Frame Structure

Remarks		*a*b:Pannel Size.-n: Shape Factor. r :Radious of Jyration.*					*Longitudinal Elements*				*Batten Elements*				*Diagonal Elements*		*Shear Parameter "u"*
Member	*Section Type*	*No. of Panels.*	*A "mm"*	*b "mm"*	*L "mm"*	*I "mm⁴"*	*Size*	*A_c "mm²"*	*r_c "mm"*	*n_c*	*Size*	*A_b "mm²"*	*r_b "mm"*	*n_b*	*Size*	*A_d "mm²"*	
DE, EF	Pratt	16	1828.8	1828.8	30022.8	$1.44*10^{10}$	10W45	8541.92	-	-	9C15	7561.27	-	-	9C15	5664.5	0.1115
AD, CF	Batten	6	1016.0	508.0	7010.40	$1.15*10^{9}$	10W45	8541.92	50.80	1.32	9C15	7561.27	81.79	1.45	-	-	0.8863
BE	Batten	6	1016.0	1016.0	7010.40	$4.47*10^{9}$	10W45	8541.92	50.80	1.32	9C15	7561.27	81.79	1.45	-	-	3.8590

Table (6-21.b): Moments Calculated by Different Methods For The Two-Bay Lattice Frame Structure.

		Moments in (kN.m)										
Case of Loading	*Method of Analysis*	*A*	*B*	*C*	*D*		*E*			*F*		*Sketch*
Moment Results Comparasion Only		*AD*	*BE*	*CF*	*DA*	*DE*	*ED*	*EB*	*EF*	*FE*	*FC*	*Moment Diagrams*
1	1-Small Deflection	174.95	0	-174.95	349.90	-349.90	1881.79	0	-1881.79	349.90	-349.90	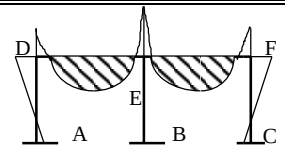
	2-Large Def.(***Lin***)	91.96	0	-91.96	357.83	-357.83	1924.07	0	-1924.07	357.83	-357.83	
	3-Present study:-											
"DL only"												
	Meth.-1-	94.903	0	-94.903	370.60	-370.60	1998.34	0	-1998.34	370.60	-370.60	
W_V = -18.245 kN/m	Meth.-2-	94.342	0	-94.342	366.35	-366.35	1977.37	0	-1977.37	366.35	-366.35	

2	1-Small Deflection	105.52	-114.07	244.37	338.23	-338.23	1923.09	82.59	-1840.5	-361.56	361.56	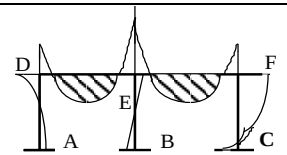
	2-Large Def.(***Lin***)	15.22	-82.11	168.96	335.74	-335.74	1960.12	77.89	-1882.21	-386.25	386.25	
"DL+WL"	3-Present study:-											
Wv = -18.245 kN/m	Meth.-1-	15.84	-85.48	176.17	349.81	-349.81	2044.61	82.22	-1962.39	-405.48	405.48	
Wh = 7.3 kN/m	Meth.-2-	-	-	-	-	-	-	-	-	-	-	
3	1-Small Deflection	1350.91	-808.95	475.77	702.27	-702.27	2006.09	542.33	-1463.77	-584.97	584.97	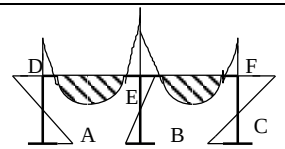
	2-Large Def.(***Lin***)	907.31	-351.09	358.01	421.18	-421.18	2030.05	350.30	-1679.75	-591.29	591.29	
"DL+Ft.Rot."	3-Present study:-											
Wv = -18.245 kN/m	Meth.-1-	939.70	-367.17	378.02	442.44	-442.44	2151.24	366.73	-1784.51	-628.25	628.25	
Rot.= 0.001 rad.	Meth.-2-	-	-	-	-	-	-	-	-	-	-	

We can notice that in cases 2 and 3 this method did not work, in the last two cases the axial tension force represents an essential weight in both case behaviors, the way just cases -2- and -3- of this example behave in, though **Meth.-2-** at examples no.**(16, 17, 18, & 19)** makes sense keeping in mind its stability and bowing performance at high values of "**u**", while in case-1- of this example **(20)** it does behave strangely**!.**

An interested notation can be observed from the previous cases that in some non-linear structures (e.g. case 6.3.1 and 6.3.3) although all the geometrical non-linearities are included in the present analysis, these cases exhibit a linear P-Δ behavior, this is because that the **T.S.M.** of such cases remains constants throughout the loading increments and though the critical load can not be reached.

6.4 Cable-frame interaction case studies:-

The third and last stage of the ***NASCFI*** testing is the cable-structure interaction case studies where the behavior, theory, derivations, and other details are explained in **chapter-4-**, the author tried as much as he could to include the most well known available experimental, theoretical, or actual existing structures that are summarized in table (6-1.c) which have been tested by other investigators in his testing survey of ***NASCFI*** applicability and accuracy. The survey begins from simple 2-D stayed solid section column and goes to include more complex structures like 3-D cable stayed towers and both suspension and stayed bridges with solid or open-web cross sections.

Generally, these types of structures are highly non-linear and this non-linearity arises according to many factors such as the geometrical and material properties for the cable and the structure, the load conditions, other special effects like temperature, lack of fit, imperfections, yield of support, etc. The structure stiffness increases with load increase, and the longer unsupported length (heights of towers and spans of bridges) increase the more flexibility and accordingly more susceptibility to non-linear behavior.

The non-linearity in these types of structures is geometrical and needs to be handled by the large deflection theory. The complex geometry of the tower or bridge configuration is adopted in design; the static behavior of these structures cannot be fully represented by a planner or 2-D analysis where neither **the pure torsional effects**, **the shear-flexural-torsional combination effects**, nor **the orthogonality or normal effects of the cross sections of masts and cables or the loading** are included. Though, the 3-D analysis seems to be very necessary to be adopted in dealing with complex non-linear behavior problems.

6.4.1 Case study no. 21 (simple stayed column):-

This simple cross-arm stayed column shown in figure (6-23.a) was first experimentally examined by ***Temple, Parkash,*** & ***Ellis*** [96] (1984), they tested the failure modes and behavior in addition to buckling modes of this column in five different initial tension of the stay or cable with constant initial centre core deflection equal to $\mathbf{y_0/1000}$, they stated two buckling modes with $\mathbf{P_{cr} = 40.05\ kN}$ and they distorted *the old criteria of stayed columns that stated that the buckling load is the load at which the tension in the stays on the concave side goes to zero.* They also stated that:-

- The maximum load was reached when the column became unstable and in turn caused the stays to yield.
- Approximately constant failure loads were concluded for all cases with rapid increasing after $\mathbf{T_0=150}$.

The same properties, loading condition, and imperfections detailed in table (6-22.a) are given to the problem to reanalyze it using the present formulation with 4 cable elements and 4 beam-column elements idealization. The value of shear parameter "**u**" of cross arm element is relatively higher than the steel central core since its a short member.

The elastic behavior only is comprised with the experimental results with the elastic-plastic behavior to be left for future developments.

Table (6-22.a): Properties of Simple Stayed Column

Element "(i)"	*Type of Element*	*Length "Li(mm.)"*	*Area "Ai(mm^2)"*	*Moment of Inertia "Ii(mm^4)"*	*Shear Parameter "ui"*	*Midhight Initial Deflection "y0=L/1000(0.8128mm.)"*
1	Stay	416.545	7.068	3.975422	0.0001065	
2	Steel Central Core	406.50	250.00	13020.83	0.0112	
3	Stay	416.545	7.068	3.975422	0.0001065	
4	Steel Crossarm	76.00	250.00	13020.83	0.3204	
5	Steel Crossarm	76.00	250.00	13020.83	0.3204	
6	Stay	416.545	7.068	3.975422	0.0001065	
7	Steel Central Core	406.50	250.00	13020.83	0.0112	
8	Stay	416.545	7.068	3.975422	0.0001065	

The mid height lateral deflection ratios of (Meth.-1- / Experimental) are (**0.67%**, **1.016%**, **-1.259%**, **1.0025%**, & **44.82%**) at loads of (18.9125 kN, 18.9125 kN, 22.25 kN, 22.25 kN, & 22.25 kN) respectively, while the same ratios for Meth.-2- are (**0.62%**, **1.009%**, **-1.27%**, & **44.77%**) for the five cases and for the same load levels respectively-see table (6-22.b) and figure (6.23.b).

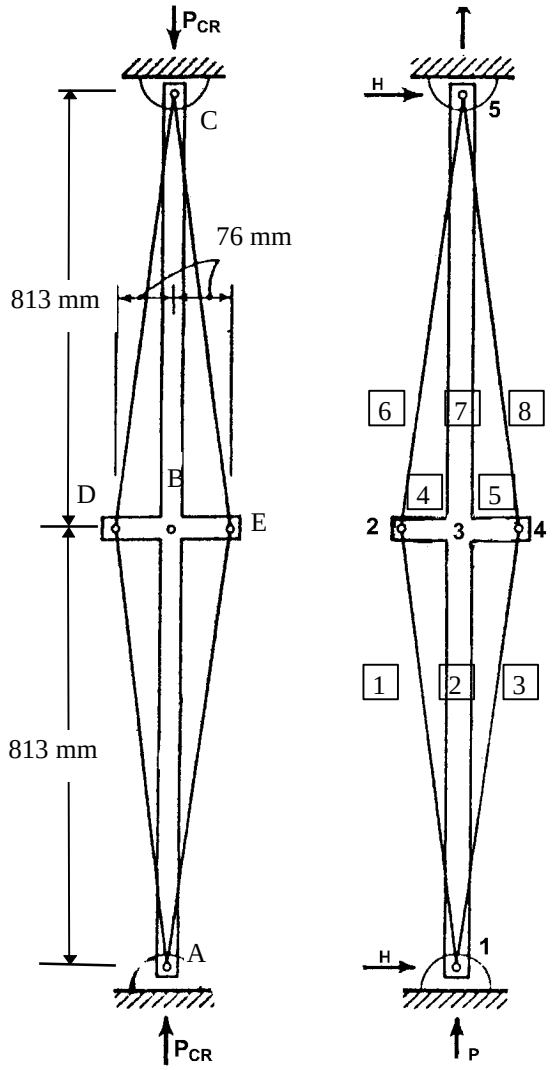

Figure (6-23.a) The Simple stay column tested by *Temple et.al.*[39]

Meanwhile the shear effect can be sensitively noticed for the five cases from both **Meth.-1- / Meth.-0-** ratios which are **(1.473%, 1.4057%, 1.2096%, 1.0311%, & 1.38%)**, and **Meth.-2- / Meth.-0-** ratios which they are **(1.1419%, 1.3989%, 1.1975%, 0.9981, & 1.28%)** for the same load levels above respectively which means that the lower the initial pretension the higher the shear effect noticed. This is logical since

more flexible structure we have whenever T_0 decreases then the tension axial load parameter rises which pushes the shear effect ahead.

As a general judgment, excellent agreement in results can be noticed in both figure (6.23.b) and table (6-22.b) between the experimental results and the present **L.D.** analytical procedure (with **Meth.-2-** sometimes closer to experimental results), this is true for all cases taken for initial pretension, while ***Wong*** and ***Temple*** (1982) theoretical analysis agreed exception for the last case when T_0 **= 1.33 kN,** in spite of using **E-P.L.D.F.E.M.** iterative-incremental mixed technique in their analysis, this is because :-

1. They neglect **the combined effect of both change in length and flexural bowing** in the stay column, the effects which are dominant in the structural behavior, though the accuracy of the present formulation compared with the experimental work of case-5- is better than the others.
2. **The effect of shear** in the column which actually has some influence as we noticed from the above argument has been ignored in their formulation.
3. They predict a mode that involves a type of triple curvature while the stayed column actually buckled in a double curvature.

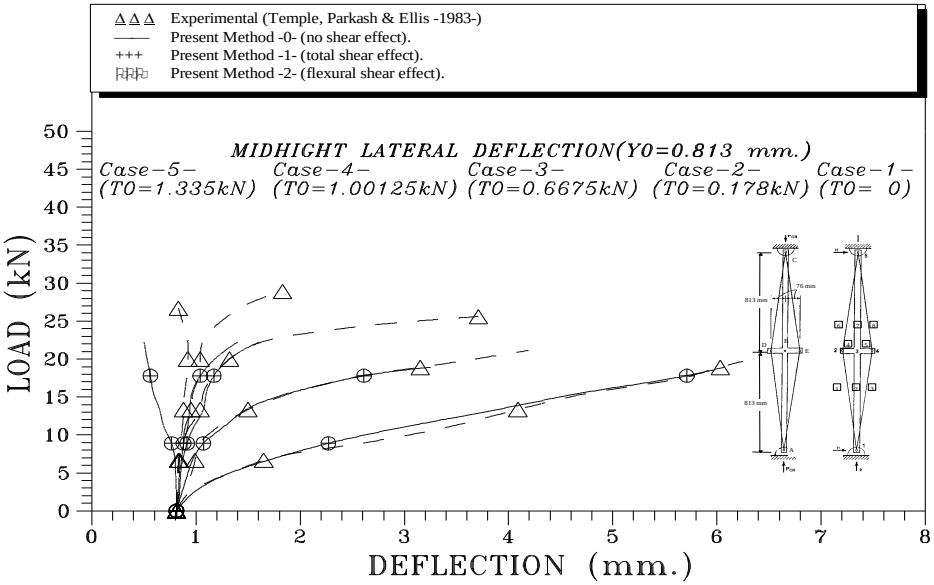

Figure (6-23.b) Load-deflection curve for the simple stayed column

One of the important causes that the experimental study referred to concerning the rapid increase in failure load after **200 kN** initial pretension is that "The tension in the stays on the concave side goes to zero before the maximum load is reached, thus only the stays in the convex side are effective to resist lateral deflections ". This behavior is actually more noticeably effective in ***Wong*** and ***Temple*** elastic-plastic analysis than the present elastic stability analysis.

Table (6-22.b): Results of Comparison of Mid-Height Lateral Deflections in Simple Stayed Columns

				Experiment	*E-P.L.D. F.E.M.*	*L.D.B-C. "No Shear"*	*L.D.B-C. "with Shear"*	*L.D.B-C. "with Shear"*
Case	*Initial Tension "T_0 (kN)"*	*Load "kN"*	*No. of Increment*	*Temple & Parkash (1983)*	*Wong & Temple (1982)*	*Present Study "Meth.0"*	*Present Study "Meth.1"*	*Present Study "Meth.2"*
1	0.00	18.9125	12	6.0362	-	5.9887	6.0769	6.0737
2	0.178	18.9125	12	3.1504	-	3.1383	3.1824	3.1822
3	0.6675	22.2500	14	1.6314	1.6284	1.5916	1.6109	1.6107
4	1.00125	22.2500	14	1.4146	-	1.4037	1.4182	1.4011
5	1.335	22.2500	14	0.9202	-0.0486	0.4067	0.4123	0.4119

6.4.2 Case study no. 22 (Simple guy tower):-

Figure (6.24.a) illustrates this case sketch while table (6-23.a) gives all what the mast and cables properties, and the related load conditions.

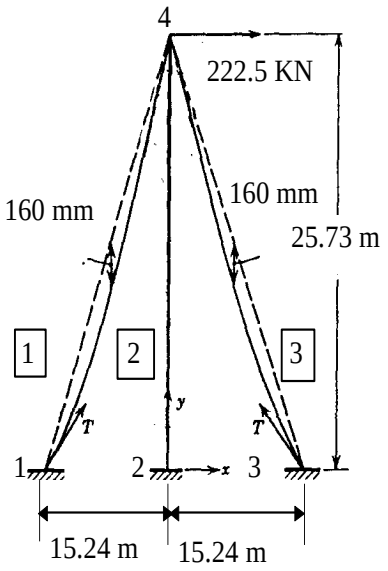

Figure (6-24.a) the simple guy column

The very efficient secant or equivalent $\mathbf{E_c}$ method previously detailed in **chapter-4-**, enables any parabolic or catenary cable to be analyzed as one element, the point that some researchers prefer to consider many truss, link, or even spring elements to the point cable element.

Table (6-23.a): Simple Guy Column Properties

Element "(i)"	*Type of Element*	*Length "L_i(mm.)"*	*Area "A_i(mm^2)"*	*Moment of Inertia "I_i(mm^4)"*	*Elastic Modulus "E_i(Mpa)"*	*Shear Parameter "ui"*	*Cable Sag "mm"*	*Joint Load & Cable Pre-tension "kN"*
1	Cable	L_v= 45720 L_h= 15240	1225.8	119571.966	151690	$1.38*10^{-6}$	160.02	P12= 850.00 T_0 = 44.50
2	Mast	45720	96774	$3.64*10^{9}$	199955	$6.40*10^{-4}$	-	P22= 850.00
3	Cable	L_v= 45720 L_h= 15240	1225.8	119571.966	151690	$1.38*10^{-6}$	160.02	P31= 850.00 T_0 = 22.50

As detailed in table (6-23.b) many researchers examined this problem, however ***NASCFI*** succeeds to show its strength as a powerful program to deal with such problems as figure (6-24.b) and table (6-23.b) both illustrate, where in spite of the (**7)** elements that ***Scherffler*** [83](1983) adopted in his **L.D.F.E.M**. analysis, the present method introduces a closer but rather more accurate results to ***Chu*** and ***Ma*** [23](1976) where **L.D.** stiffness method with parabolic cable analysis.

Table (6-23.b): Deflections at Free End for the Simple Guy Column by Different Methods

Load	**"kN"**	222.5
1. Chu & Ma (1976)	**X-Direction "mm."**	683.18
Modified E_c	**Y-Direction "mm."**	-13.995
L.D. Stiffness Method	**θ "rad."**	0.0232
2. Chu & Ma (1976)	**X-Direction "mm."**	681.48
Iterative E_c	**Y-Direction "mm."**	-3.894
L.D. Stiffness Method	**θ "rad."**	0.0231
3. Schreffler et.al. (1983)	**X-Direction "mm."**	668.26
L.D.F.E.M.	**Y-Direction "mm."**	-
	θ "rad."	-
4. Present Study	**X-Direction "mm."**	695.59
Without Shear	**Y-Direction "mm."**	-11.913
"Meth.-0-"	**θ "rad."**	0.037
L.D. Beam-Column Theory		
5. Present Study	**X-Direction "mm."**	695.59
With Shear	**Y-Direction "mm."**	-11.913
"Meth.-1-"	**θ "rad."**	0.037
L.D. Beam-Column Theory		
6. Present Study	**X-Direction "mm."**	695.59
With Shear	**Y-Direction "mm."**	-11.913
"Meth.-2-"	**θ "rad."**	0.037
L.D. Beam-Column Theory		

This problem exhibits no shear effect since it offers only **0.00064** for the shear parameter "**u**", the present **(Meth-0-) / (*Chu* & *Ma* -**iteration method**-)** ratio is only **2.07%** increment while ***Scherffler*/*Ma*** ratio is about **1.94%** decrement.

Chu and ***Ma*** introduced an iterational technique to control the convergence of left and right cables deflection configurations, the method that corrects the defaults made by their first modified $\mathbf{E_c}$ method. Although the high non-linearity introduced by this problem, is never be more non-linear than a simple cantilever mast or column with

same properties and loading conditions, because of the deflection resistance cables exhibit at the end of the guy level, the matter that reduces the structure flexibility and makes it more stiff, which in turn reduces the non-linear effects on the **T.S.M**. of the structure.

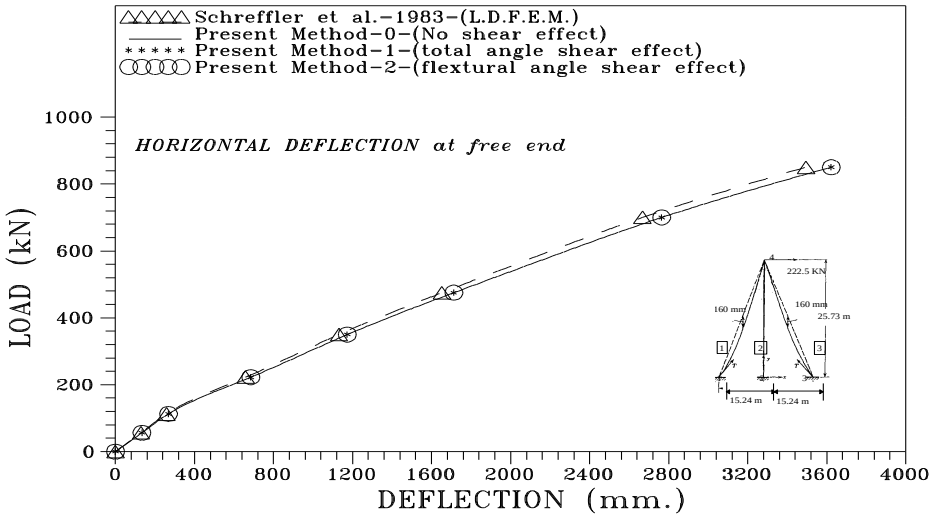

Figure (6-24.b) Load-deflection curve for the simple guy column

The (**P-Δ)** behavior is nearly bi-linear as figure (6-24.b) indicates, during the load increment next to **P=222.5 kN** one cable becomes slack necessitating a restart procedure to be implemented for the continuation of the analysis. Thereafter the slack cable is ignored and cause the tilt in the curve at this load stage which indicates that this load level is $\mathbf{P_{cr}}$.

6.4.3 Case study no. 23 (3-D 2-Pretensioned single level guy tower):-

In this case and the one after, a very important problem to study is taken which shows the effect of increasing wind velocities from **0 - 350 Km / h** evaluated according to ***ANSI A58*** [8](1972) on the 3-D pretensioned stayed cables solid shaft tower (i.e. no shear effect exists). Both 2-single and 3-multileveled cable stayed (see figure 6-25.a), in which guy-mast functions are previously detailed in **chapter-4-**. The properties and guys initial pretension of the single level case are detailed in table (6-24.a) and the wind loading stages are illustrated in table (6-24.b)**.** For both cases ***Raman et. al***. (1988), analyzed this problem using the **F.E.M.**, iterative incremental strategy for the load-displacement solution algorithm, and both elastic and tri-linear elastic-plastic cable

behavior in both **S.D.** and **L.D.** theories procedures. They used (4) beam-column elements for the mast and (8) truss elements for each cable. The variation in wind velocity (Vel) with height is assumed to follow the well known wind load equation as (psi units) ***ANSI A58*****(**1972) indicates:-

W.L.(lb.) = 0.00256 .Vel (mile / h.) .A (ft) .Cd ..... (6.1)

or, in **S.I.** units, by the substitution of **0.32** for $\mathbf{C_d}$ and **134.11m.** by **2.286m.** for the area **(A)** as:-

W.L.(kN/m^2.) = 1.0388×10^{-4}. Vel (Km / h.) ..... (6.2)

The wind load acting on each element is assumed to be uniform and is computed at mid height level of the element which means that **U.D.L.** acts on each element of the values detailed in the each case in the corresponding tables mentioned below. This load is transformed to equivalent nodal forces and **F.E.A.** moments the way just **App.-D-** indicates, this actually forms one of the major privileges of the present study on ***Raman***`s **F.E.M.** approach where only the equivalent nodal loads are taken and no moments are considered at the nodes, the wind velocities specified are at (**10 m**) above the ground level for both examples taken of this problem. The wind load direction is applicable to one of the horizontal plane directions either X_1-direction or X_3-direction. Neither **the change in length** nor **the 3-D** (***SS*** effects) were included in ***Raman***`s **F.E.M.** non-linear work where the most important privilege of the present study in addition to the nearly negligible **shear effect** is achieved.

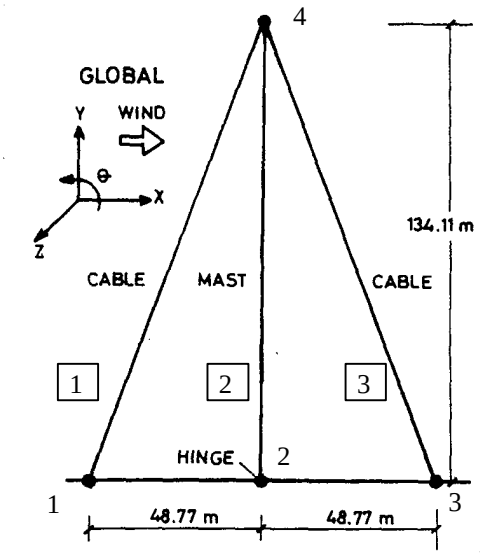

Figure (6-25.a) 3-D, 2-Pretensioned single-level guy tower.

For the first case taken herein is the 3-D, 2-pretensioned single level guy tower shown in figure (6-25.b), properties and initial pretension are illustrate in table (6-24.b)**.** The present formulation exhibits a very close path to ***Raman et. al.*** elastic-plastic cable behavior path even though the present study used only 2 beam-column element for mast

and 1 cable element per each cable, which gives another privilege to the present study.

Table (6-24.a): Two-Level Guy Tower Properties

Element "(i)"	*Type of Element*	*Length L_i"m"*	*Area A_i"mm^2"*	*Moment of Inertia I_i"mm^4"*	*Elastic Modulus E_i"Kpa"*	*Shear Parameter "u_i" (all directions)*	*Initial Tension "kN"*	*Breaking Tension "kN"*	*Weight "kN/m"*	*Drag Coefficient*	*Width "mm."*
1	Cable	L_h=48.77 L_v=134.11	948.3	71561.863	$165.48*10^6$	$1.2179*10^{-7}$	128.1	1334.4	0.07426	1.10	DIA
2	Mast	67.055	62400	$2.48*10^{10}$	$206.84*10^6$	0.00314	-	-	4.9033	0.32	2286
3	Mast	67.055	62400	$2.48*10^{10}$	$206.84*10^6$	0.00314	-	-	4.9033	0.32	2286
4	Cable	L_h=48.77 L_v=134.11	948.3	71561.863	$165.48*10^6$	$1.2179*10^{-7}$	128.1	1334.4	0.07426	1.10	DIA

The **SS/SS0** is **4.73%** increment and **Meth.-0-, -1-, and -2-** all coincide with each other which is so obvious since $\mathbf{u_{x_1} = u_{x_3} = 0.00314}$ (symmetrical section), in other word, no shear effect.

At wind velocity of **280 Km/h** or wind lateral load of **8.144 kN/m** the load at which approximately $\mathbf{P_{cr}}$. occurs, the lateral deflection obtained from the present method to ***Raman***`s elastic cable behavior method of analysis is **5.72%** increment while the **L.D/S.D.** ratio at the same load level is **33.46%** increment.

Table (6-24.b): Comparison of Results of Two-Level Guyed Tower

		Horizontal Deflection at Level of (67.055 m) in "mm"					
Wind Velocity "Km/h"	*Wind Load "kN/m"*	*S.D.T. Ramman et. al.*	*L.D.T. Ramman et al. with Elastic-Cable Analysis*	*L.D.T. Ramman et al. with Tri-linear E-P Cable Analysis*	*L.D.T. Present Study Meth.-0- "No. Shear"*	*L.D.T. Present Study Meth.-1- "with Shear"*	*L.D.T. Present Study Meth.-2- "with Shear"*
0.00	0.00	0.00	0.00	0.00	0.00	0.00	0.00
101.2	1.0639	880.13	880.87	880.08	878.34	878.34	878.34
143.11	2.1275	2540.42	2550.53	2550.75	2560.54	2560.54	2560.54
202.386	4.2549	3810.74	4120.83	4220.44	4190.96	4190.96	4190.96
247.87	6.3823	6970.05	8030.14	8590.61	8320.73	8320.73	8320.73
286.22	8.5101	11360.12	14340.94	-	15161.07	15161.07	15161.07
320	10.6373	18730.86	-	-	-	-	-

The load-deflection response is linear initially up to a wind velocity of **80 Km/h**, after this velocity the behavior becomes non-linear. Its interesting to note that for ***Raman***`s **S.D.** analysis and beyond **273 Km/h** wind velocity the deflection increases very rapidly. At the maximum deflection is about **1/14** of the span, which gives a very high and rather incorrect result indicating the need for the application of **L.D.** theory. However, at **320 Km/h** wind velocity very large deflection increments are observed even for a small increments in velocity. Such behavior is usually interpreted to signify the buckling load and the corresponding wind velocity may be referred to as critical velocity.

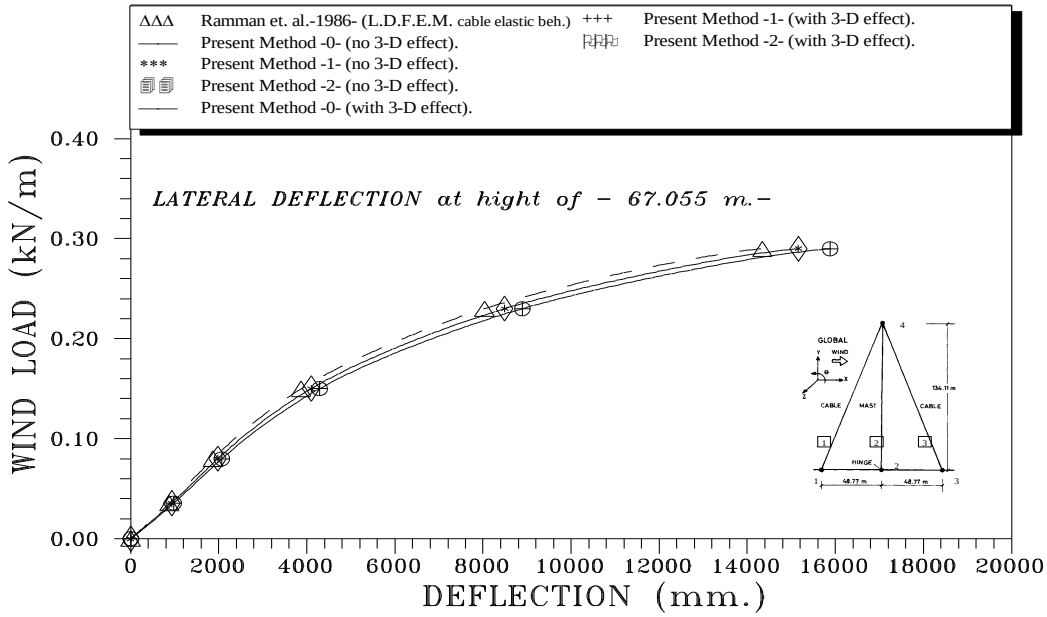

Figure (6-25.b) Load-deflection curve for the 3-D single-level guy tower

When large displacement effects on the mast are considered, it may be seen that the tower is more flexible, resulting in larger displacements as wind velocity exceeds **125 Km/h**, to about **280 Km/h** the **L.D./S.D.** ratio is about **33.46%** increment, beyond this speed, the incremental displacements are observed to increase enormously during successive iteration. The behavior that indicates that the wind velocity is close to the critical velocity and that the load level is reaching up the critical one which actually occurs at **286.22 Km/h** or **8.51 kN/m**, the load forms **96.69%** of ***Raman***`s tri-linear elasto-plastic cable analysis and about **4.08%** over his elastic cable analysis $\mathbf{P_{cr}}$ which occurred at **296 Km/h** and **275 Km/h** respectively, the matter that indicates a very good agreement with ***NASCFI***.

6.4.4 Case study no. 24 (3-D, 3-Pretensioned multilevel guy tower):-

This is the second case of ***Raman***`s problem which indeed is a very important case study as mentioned earlier, however this specified case is to be taken as parametric study in the next chapter to include the effect of varying the wind direction angle on the structures **3-D** behavior (cable geometry, shaft axial force and bending moments) as it will be detailed later.

For the time being, let us check what the wind direction **(α= 0)** case (see figure 6-26.a), keeping in mind what has been previously mentioned about all wind velocities and loading calculations, differences between ***Raman***`s and the present formulations. The properties, initial cables pretension and all associative are given in table (6-25.a).

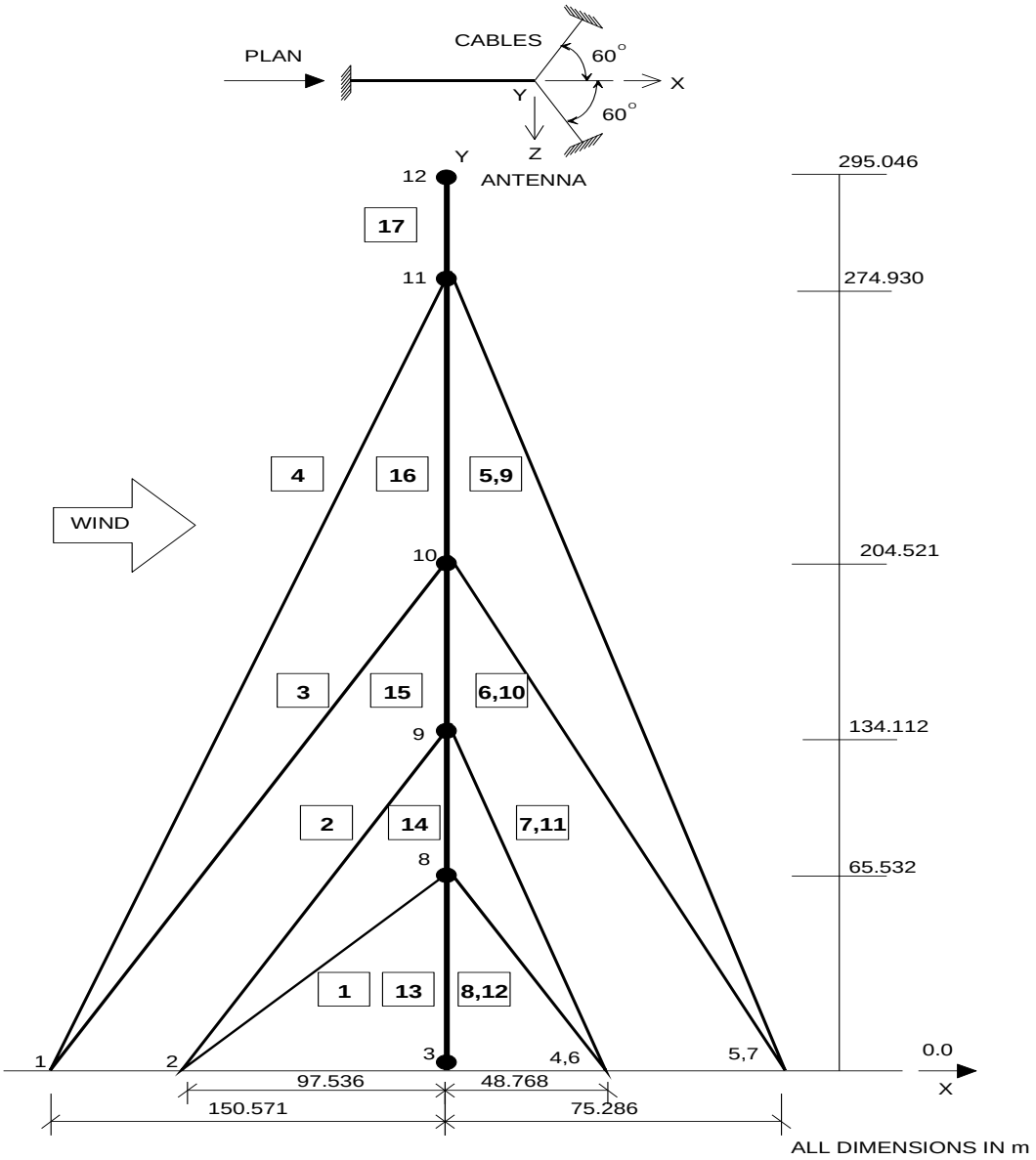

Figure (6-26.a) 3-D, Multi-level Pretensioned guy tower

Table (6-25.a): Multiple Guy Tower Properties

Element "(i)"	*Type of Element*	*Length L_i"m"*	*Area A_i"mm²"*	*Elastic Modulus E_i"Kpa"*	*Moment of Inertia I_i" mm⁴"*	*Shear parameter "u_{Xi}" (all directions)*	*Initial Tension "kN"*	*Breaking Tension "kN"*	*Weight. "kN/m"*	*Drag Coefficient*	*Width "mm."*
1,8,12	Cable	L_h=150.57 L_v=274.93	800	$165.47*10^6$	50929.582	$2.12939*10^{-8}$	91.6	1032	0.057	1.10	DIA
2, 7, 11	Cable	L_h=150.57 L_v=204.52	1361	$158.47*10^6$	147403.022	$5.51867*10^{-8}$	213.5	1922	0.107	1.10	DIA
3, 6, 10	Cable	L_h=97.536 L_v=134.11	948	$165.47*10^6$	71516.592	$9.01632*10^{-8}$	128.1	1334	0.074	1.1	DIA
4, 5, 9	Cable	L_h=97.536 L_v=65.532	729	$165.47*10^6$	42290.731	$1.38083*10^{-7}$	91.6	1032	0.057	1.1	DIA
13	Mast	65.532	82100	$206.84*10^6$	$4.57*10^{10}$	0.0046	-	-	6.45	0.32	2286
14	Mast	68.58	72700	$206.84*10^6$	$3.63*10^{10}$	0.0038	-	-	5.706	0.32	2286
15	Mast	70.409	62400	$206.84*10^6$	$2.98*10^{10}$	0.0034	-	-	4.903	0.32	2286
16	Mast	70.409	62400	$206.84*10^6$	$2.48*10^{10}$	0.0029	-	-	6.45	0.32	2286
17	Antenna	20.124	39000	$206.84*10^6$	$4.00*10^8$	$9*10^{-4}$	-	-	3.065	1.10	300

The "**u**" values of the (5) beam-column elements including the antenna member, (9 elements taken by ***Raman***) taken by the author are too small **(0.0009-0.0046)** to give any chance for the shear effect to show, though we notice that all methods **(Meth.-0-, -1-, & -2-)** give results which coincide with each other as it appears from observing table (6-25.b), which illustrates the displacements, axial forces, and **B.M.D.** in shafts up to **120 Km/h** wind velocity by various methods. Figure (6-26.b) goes beyond this velocity up to **350 Km/h**, furthermore this table indicates the fact that there is a large amount of divergence between the present results and ***Raman***`s, while it's so close to ***Shears***'s ***et. al.*** result. This is because of the major different in cable idealization taken by the present approach which is indeed close to ***Shears***'s ***et. al.*** with that one taken by ***Raman*** as mentioned earlier and as table (6-25.b) referred to. These differences can be summarized as follows:-

1. Maximum deflection ratios of the present approach to that of ***Raman*** **(Meth.-0-/*Raman*** are **(32.4%, 13.5%,** and **1.7%)** increment, while **Meth.-0-/Shears et al.** are **(1.2%** decrement**, 0.8%** increment**,** and **2.1%** increment**)** for X_1, X_2, and X_3 directions respectively.

2. Maximum axial force in shaft ratios of **Meth.-0-/*Raman*** are **(3.2%,** and **2.3%)** increment, while **Meth.-0-/Shears et al.** ar**e (0.7%**, and **0.4%)** increment for top and bottom members respectively.

3. The present maximum axial force ratio in the (8) cables is **4.3%** increment to ***Raman*** and **1.46%** increment to ***Shear et al.***

4. The maximum shaft bending moment ratios **Meth.-0-/*Raman*** are **(7.69%, 24.89%, 12.5%,** and **15.6%)** increment, while **Meth.-0-/Shears et al.** are **(7.14%, 2.5%, 2.6%,** and **3.33%)** increment at nodes **9, 8, 7,** and **6** respectively.

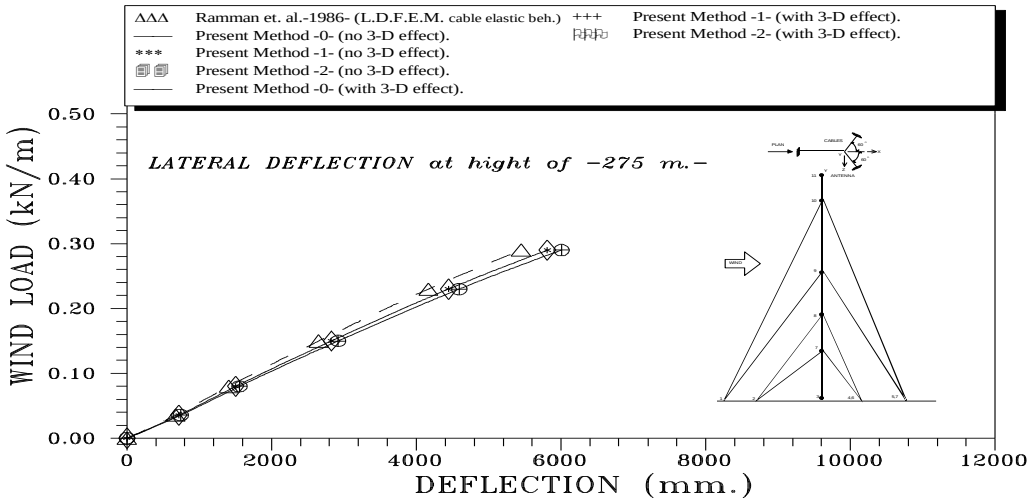

Figure (6-26.b) Load-deflection curve for the 3-D multi-level guy tower

The **SS/SS0** is **3.325%** increment for both methods. The present study as well as ***Raman***`s overcomes the difficulties that were already suffered in dealing with the leeward cables becoming slake leading to the higher velocities that act on the structure which would not be under control. Such difficulties were not encountered during the present study. In fact, tower responses to increasing winds up to **360 Km/h** can be obtained unless buckling occurs, which actually does occur herein as illustrated in figure (6-26.b) at **279.48 Km/h** wind velocity i.e., **8.075 kN/m**. loading giving a divergence ratio of **2.96%** decrement to ***Raman***`s elasto-plastic analysis in which **288 Km/h** is the critical wind velocity. The load versus deflection response appears to be bi-linear for the load velocities considered giving a **Meth.-0-/*Raman***`s elastic cable analysis deflection ratio of **33.83%** increment as its obvious from figure (6-26.b), further study will be made on this case in **chapter-7-**.

Table (6-25.b): Comparison of Results of Multilevel Guyed Tower

Results are approximated to the nearest integer value		***Wind Velocities at 10 m Level in (Km/h)***														
For further velocities see figure (6-26.b)		***Wind Load Using ANSI A58.1 1972 in (kN/m)***														
Function	***Details***	***Shears et al. (1968)***			***Ramman et al. (1986)***			***Present Method "0"***			***Present Method "1"***			***Present Method "2"***		
		40	80	120	40	80	120	40	80	120	40	80	120	40	80	120
		0.166	0.665	1.5	0.166	0.665	1.5	0.166	0.665	1.5	0.166	0.665	1.50	0.166	0.665	1.50
1-Horizontal	X_1	46	238	738	40	201	550	42	231	729	42	231	729	42	231	729
Displacement.in (mm.)	X_2	27	125	341	25	119	303	27	121	344	27	121	344	27	121	344
	X_3	18	73	183	16	70	176	17	74	179	17	74	179	17	74	179
2-Axial Force	2-1. Mast:-															
	Top Member	-551	-574	-676	-547	-552	-681	-553	-570	-677	-553	-570	-677	-553	-570	-677
	Bottom Member	-2966	-2998	-3194	-2962	-2962	-3109	-2963	-2989	-3181	-2963	-2989	-3181	-2963	-2989	-3181
	2-2. Cables:-															
	Elements 10,12	161	208	310	161	198	312	162	201	313	162	201	313	162	201	313
in (kN)	Elements 7 , 9	255	306	415	258	303	392	257	305	409	257	305	409	257	305	409
	Elements 4 , 6	141	173	233	145	174	233	143	174	234	143	174	235	143	174	235
	Elements 1 , 3	105	124	160	107	125	165	106	124	162	106	124	162	106	124	162

3-Shaft Bend. Moment in(kN.m)	At Levels:-															
	274.93m(node 9)	15	59	135	14	56	125	14	58	131	14	58	131	14	58	131
	204.52m(node 8)	68	322	866	62	306	691	64	314	836	64	314	836	64	314	836
	134.11m(node 7)	29	117	274	28	135	271	28	120	272	28	120	272	28	120	272
	65.532m(node 6)	38	155	371	39	142	395	38	150	379	38	150	379	38	150	379
4-Remarks	Cable Tensions Are Given For Windward Cables	-One Parabolic Cable Element - Sag > 0			- 8 Truss Cable Elements - Sag = 0			- One Parabolic Cable Element - Sag > 0			- One Parabolic Cable Element - Sag > 0			- One Parabolic Cable Element - Sag > 0		

The following general notes can be concluded from the past two cases (no. 23 and 24):-

1. The **3-D, bowing,** and **change in length effects** significantly alter the **L.D.** load-deformation behavior of guyed tower system, resulting in lower critical loads, which in turn enormously affect this behavior's defaults owing to the **S.D.** path.
2. **Shear effect** has no role at all in the solid shafts or closed-web masts guy towers as well as in the strands.

6.4.5 Case study no. 25 (2-D bow-string girder):-

Figure (6.27) and table (6-26.a) illustrate the properties and loading conditions of this highly non-linear problem, a problem that consists of an arch connected to a girder using a number of vertical hanger cables, a **U.D.L.** condition of **89.9 kN/m** both as dead plus live load is exhibited **(D.L.= 41.18 kN/m & L.L. = 48.72 kN/m)**.

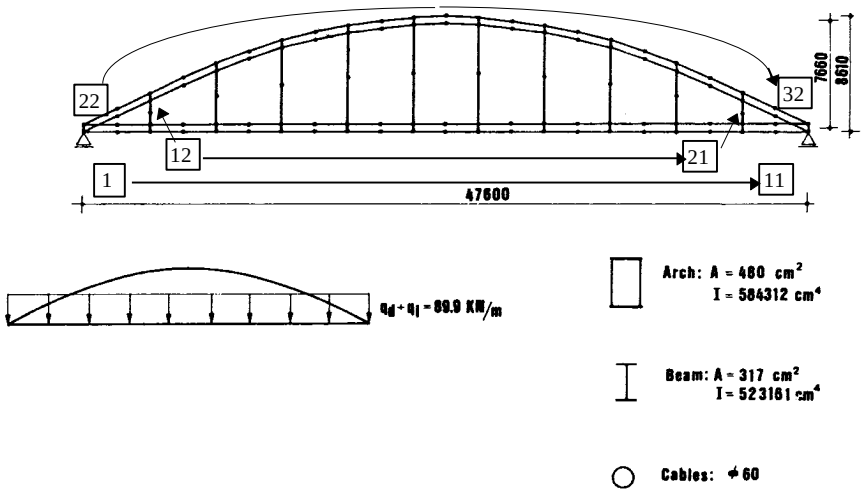

Figure (6-27) The Bow-String Girder properties and loading

Single parabolic cable elements were used in the present procedure approach of analyses as well as in ***Scherffler*** [83] -as table (6-26.b) indicates- to allow for the possibility of singular **T.S.M.** developing should a stringer becomes slack.

Table (6-26.a):2-D Bow-String Girder Properties

Element "(i)"	*Type of Element*	*Length L_i"m"*	*Area A_i"mm^2"*	*Elastic Modulus E_i"Kpa"*	*Moment of Inertia I_i"mm^4"*	*Shear Parameter "u_i"*	*Initial Tension "kN"*	*U.D.L. (L+D) "kN/m"*
1-11	Girder	53.273	31700	$206.84*10^6$	$5.23*10^9$	0.081	-	89.9
12-21	Cable	Varies From 27.216-81.65	2830	$156.913*10^6$	637328.01	$(1.115-9.992)*10^{-6}$	19.6	-
22-32	Arch	45.75	48000	$206.84*10^6$	$5.84*10^9$	0.0021	-	-

During the first load increment only the bottom nodes of the stringer were displaced vertically to produce a small initial pretension of about **20 kN**, the load is incremented until girder buckled as indicated by singularity of **T.S.M**. leading to the snap through buckling limit load of **33162.73 kN** (i.e. **14.3** times **L.L**), while ***Scherffler*** indicated **15** times **L.L**.

No **shear effect** was noticed leads to all the three methods **(Meth.-0-, -1-,** and **-2-)** to coincide with each other as its expected since **u = 0.0021** for the arch and **0.081** for the girder.

Just prior to the instability the total **L.D.** to linear **S.D.** theory displacement ratio at the apex of the arch was **88%** increment as ***Scherffler*** indicated, meanwhile the **Meth.-0-/*Scherffler*** vertical displacement ratio is **2.76%** increment again just prior to the instability, the matter that indicates good agreement with the present approach, as it's illustrated in table (6-26.b)

Table (6-26.b): In-Plane Bow-String Girder Results

	Arch Apex Vertical Displacement. Just Prior Instability in "mm."		
L.D.T. F.E.M. Schrefler et al.(1983)	*L.D.T. without Shear Present Study Meth.-0-*	*L.D.T. with Shear Present Study Meth.-1-*	*L.D.T. with Shear Present Study Meth.-2-*
169012	173670.75	173670.75	173670.75

6.4.6 Case study no. 26 (2-D single level single-sided lattice guy tower):-

As detailed in **chapter-3-**, when the axial load is negligible, the calculations of shears and bending moments follow straight forward, well-known procedures after the end moments and shears are evaluated, and need no further elaboration. In the absence of the axial thrust, a distribution needs to be made between **a shear acting normal to**

the chord line which for small deflections is essential acting normal to the undisplaced axis load and **a shear acting normal to the elastic curve**. However, this distribution can become so important in the presence of beam-column effects because of **the secondary shear caused by the thrust**. Furthermore when **the bowing** and **change in length effects** are included this distribution becomes more and more essential in predicting the **(P-Δ)** behavior of structure, this phenomenon is so clearly observed in lattice, trussed, or open-web structures, though the following two examples are identical for observing both **shear+bowing+change in length** and **stayed cables effects** on *the 2-D elastic stability behavior of open-web structures.*

The two cases (previously analyzed by ***Williamson***[(104)](1966) using the **L.D.** approach and excluding the **bowing** plus **change in length effect**)are shown in figures (6-28.a and 6-29.a), while table (6-27.a) illustrates the actual properties of both single and multi-span X-bracing single-sided lattice tower. The Sketch of the actual properties of both the lattice X-bracing tower and the designed cables are illustrated in figures (6-28.b. and 6-29.b), table (6-28.a and b), respectively.

For the single-span case, the cable element in ***Williamson***`s method of analysis was taken as a spring having a constant **K= 1750 kN/m.**, however, the present formulation must design cables in order to give the same characteristics as the spring idealization does, this is absolutely what **Preliminary Tower Analysis (P.T.A.)** and **Guy Analysis (G.A.)** associate, the matter that is detailed in **chapter-4-**.The spring constant actually means that **1750 kN** reaction force is generates when **(1 m)** displacement occurs, this assumption is adopted as an initial condition to evaluate the cable initial pretension.

As it shown in **chapter-4-**, the catenary exact analysis of cables helped us to put an equation describing the horizontal displacement of a support. The preliminary analysis is made on towers that have no initial conditions in order to find the guy reactions to be used in evaluating initial pretensions in cables. This **L.D.** non-linear elastic stability analysis is made assuming the tower to behave as a continuous beam over rigid supports, with the support located at each guy level. So, $\mathbf{F_0}$ and $\mathbf{F_i}$ can be evaluated by analyzing the structure preliminarily using only its own weight and final load (plus its own weight) respectively.

Table (6-27.a): Single &Multi-Span Lattice Guyed Tower actual properties (Mast properties)

Element "(i)"	*Type of Section*	*Length "L_i(mm)"*	*Area "A_i(mm^2)"*	*Moment of Inertia "I_i(mm^4)"*	*Shape Factor "$n_i=A/A_w$"*	*Elastic Modulus "E_i(Mpa)"*	*Shear Modulus "G_i(Mpa)"*
Ver.Leg	L 6*6*3/4	6096.00	5445.15	11737726.2	2.00	206850	82740
Hor.Batt.	2L 4*3*1/4	6096.00	2180.64	2305922.1	1.34	206850	82740
Diag.Strut	2L 4*3*1/4	8620.76	2180.64	2305922.1	1.34	206850	82740

The design operation (summarized in table 6-27.b) is made to find the cable reactions, after finding these reactions and using the above equation, with the simple geometry equation of the tangent of angle, and since **A** and **E** of cable can be evaluated using the ***(A.S.T.M. Standards A-586 Specifications)*** [10] by the simple definition of axial stress **($A = F_0/F_{all.}$)**, where $F_{all.}$ is taken as the allowable breaking axial tensile stress, and the initial tangent modulus of elasticity equations, keeping in mined that the minimum E_i is ranging between **(158.561-165.4556) E6 Kpa** (see **chapter-4-**)

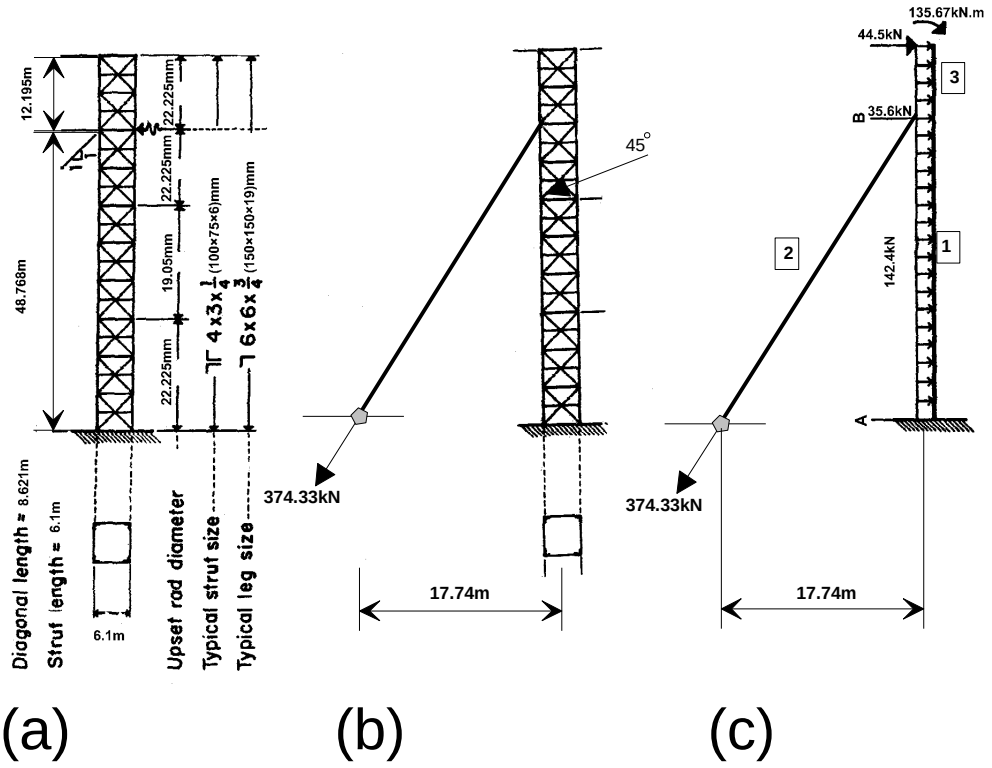

Figure (6-28) (a) spring idealization of the single-span single-sided guy tower. (b)The present designed single-span single-sided tower. (c)Equivalent cable stayed tower

Table (6-27.b): Single-Span Lattice Guyed Tower actual properties (Cable properties)

Element No. "(i)"	*Breaking Strength. "kN"*	*Initial Tension. "kN"*	*Length L_i"m"*	*Cable Specification*	*Properties A"mm^2" I"mm^4"*	*Shape Factor "n_i"*	*Shear Parameter "u_i"*	*Straight Cable Elastic Modulus E_e"Kpa"*	*Sagged Cable Elastic Modulus E_i"Kpa"*
2	708.00	374.33	Lh= 17.74 Lv = 48.78	Zinc-Coated Steel Structure. Strand-5wire Class-A- Coat.	A=489.7 I=19083.16	6.171	$2.643*10^{-6}$	$167.3146*10^{6}$	$167.217*10^{6}$

Now the above preliminary analysis is done by ***NASCFI***, and the design procedure made accordingly, finally enables us to analyze the tower, but for the time being using the complete cable properties and pre-tensioning, the choice that made on the **Zinc-Coated Steel Structural Strand, Class -A-Throughout coating (5 Wires Round Type)** is made according to **A.S.T.M. (A-586),** and because of the high initial tension exhibited in the preliminary design, however other options are open. Table (6-27.c) summarizes the equivalent properties of the problem using the shear parameter equivalent method mentioned earlier in **chapter-3-**, while table (6-27.d) summarizes comparisons of the final results with ***Williamson***`s analysis, with the following brief points to be stated:-

1) **Deflection comparison:-**

   The shear effect can be noticed by **Meth.-1-/Meth.-0-** and **Meth.-2-/Meth.-0-** ratios which they are (**11.22%** increment, and **9.93%**), respectively.

2) **The tower bending moment comparison**:-

   a) The shear effect ratios are **(14.03%** and **12.64%)** for both methods respectively.

   b) The agreement ratios are **(6.01% & 4.68%)** for **Meth.-1-/*Williamson*** and **Meth.-2-/ Williamson)** respectively, notice here that **Meth.-2-**is nearer to ***Williamson***`s **L.D.** than to **Meth.-1-**

   c) **The no shear large deflection combined (axial + bowing +change in length) effects** can be evaluated from the ratios **Meth.-0-/*Williamson*`s linear S.D.** which is **43.61%** increment.

Table (6-27.c): Comparison of Solutions for Single-Span Lattice Guyed Tower

No.	*Method*	*Remarks*	*B.M. at -A- "kN.m"*	*Deflection at-Free End- "mm."*
1	**Williamson (1966)**	**-Beam-Column , S.D.T. -No Bowing Effect. -No Shear Effect. -Cables were Represented by Springs -Fixed End Action included.**	-2185.66	-
2	**Williamson (1966)**	**-Beam-Column, L.D.T. -No Bowing Effect. -No Shear Effect. -Cables were Represented by Springs -Fixed End Action included.**	-3376.85	-
3	**Present Meth.-0-**	**-Beam-Column, L .D.T -Bowing Effect. -No Shear Effect. -Cable Sag &Geometrical Concederations -Fixed End Action included.**	-3138.96	576.4024
4	**Present Meth.-1-**	**-Beam-Column, L .D.T -Bowing Effect. -Total Shear Effect. -Cable Sag &Geometrical Concederrations -Fixed End Action included.**	-3579.47	641.099
5	**Present Meth.-2-**	**-Beam-Column, L .D.T -Bowing Effect. -Flexural Shear Effect. -Cable Sag &Geometrical .Concederations -Fixed End Action included.**	-3535.04	633.623

d) The shear large deflection combined effect (axial +shear) can be found from ***Williamson***`s **L.D. / linear S.D.** which is **54.51%** increment.

e) **The overall combined effects** of **(axial +shear +bowing +change in length)** can be established from the present work i.e.

Meth.-1- & Meth.-2-/*Williamson*`s linear S.D, they are **(63.77% & 61.74%)** increment respectively.

Although a good agreement is concluded from the above summarized results, the fact is that earlier mentioned procedure for designing the cables based on **(A.S.T.M. A-508)** has given an optimum design and gave reasonable results to compare with.

6.4.7 Case study no. 27 (Multi-span single-sided lattice guy tower):-

When we use the same design procedure of the previous example, this multi-span single-sided guy tower example shall be treated and designed.

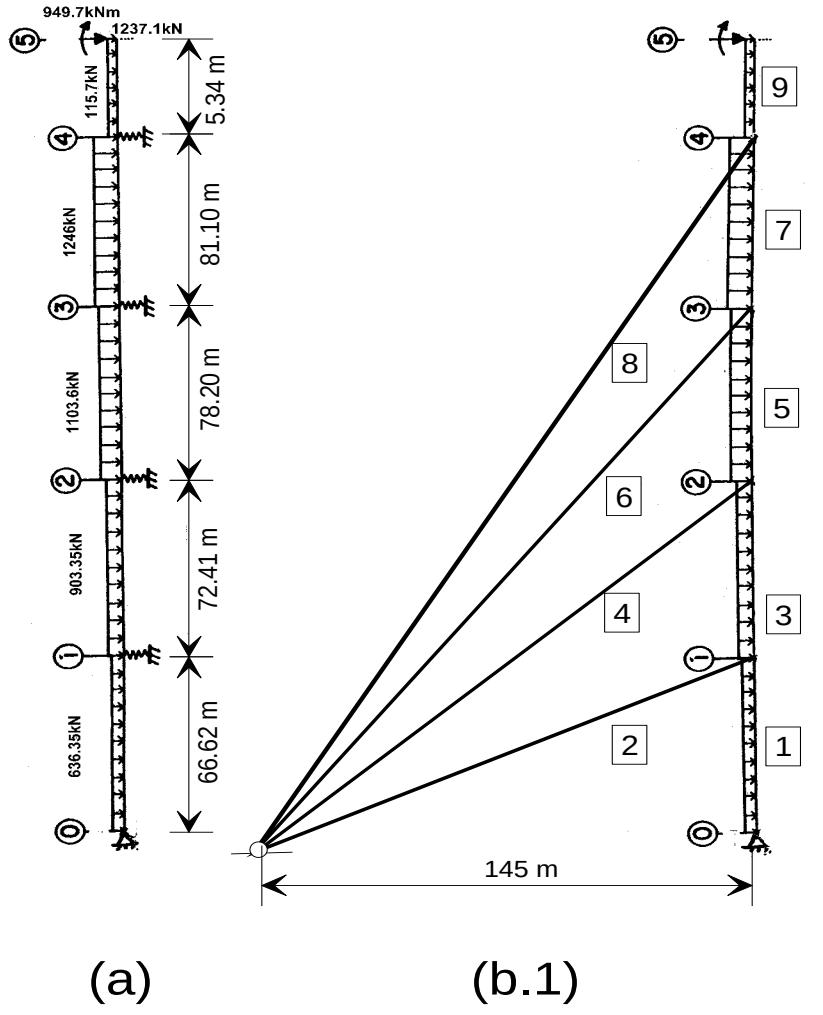

Figure (6-29) (a) Actual spring representation tower. (b.1) Designed cable stayed tower model -I-

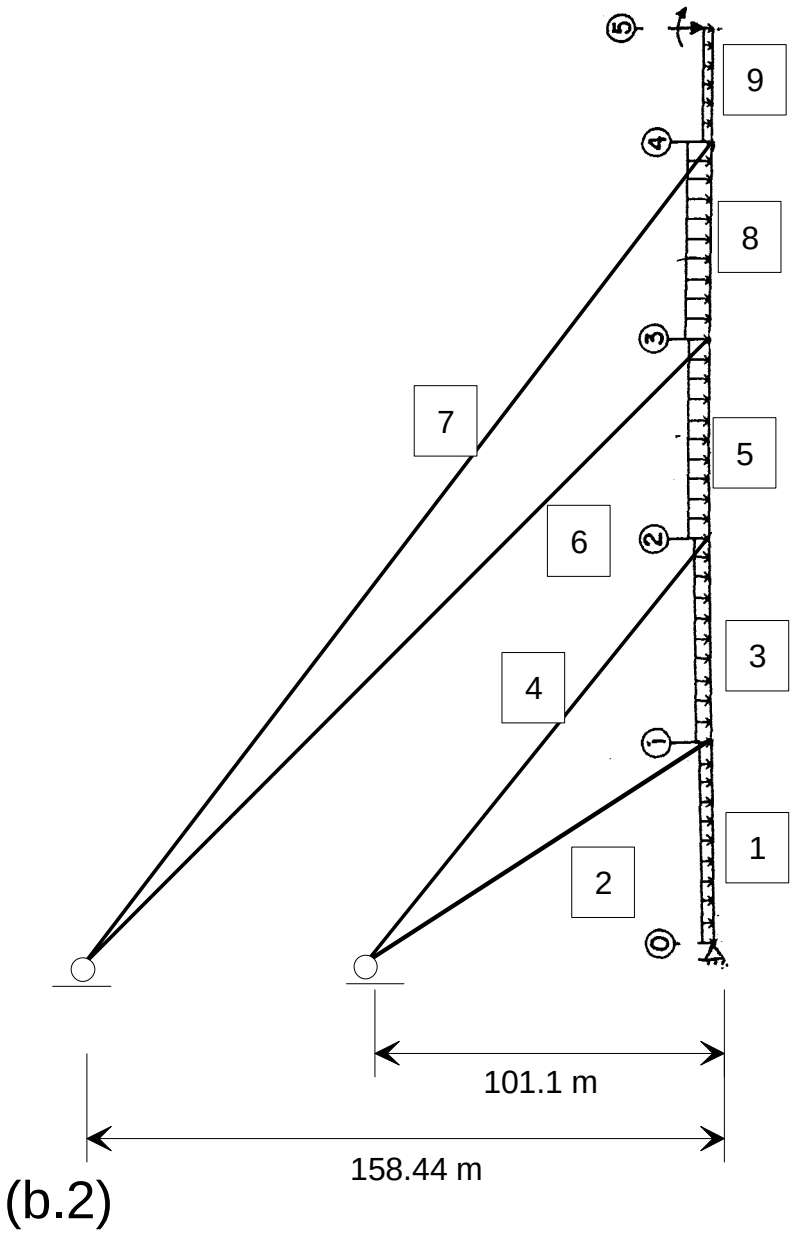

Figure (6-29.b2) Designed cable stayed tower Model-II-

The design operation is made to find the cable properties and initial tensioning condition that is identical to the spring condition idealized by ***Williamson*** which is summarized in table (6-28.b). There two types of four cables geometrical idealization in which either the four cables jointed together in one support at the point of pre-stretching (this type is preferable when double-sided cable is used) **-Model -I-** (figure 6-29.b1), or two supported pre-stretching points, two cables per each point -**Model -II- (**figure 6-29.b2), the second model shall be adopted herein.

Since the tower is single-sided which must exhibit higher cable pretensions than the double-sided, and since the **U.D.L.** of this example is rather high, hence, very high

initial tensile forces are expected to be induced in the cables, so the same **Zinc-Coated Steel Structural Strand, Class -A-Throughout coating** shall be used as table (6-28.a) specifies. Table (6-28.b) illustrates the equivalent properties of the tower.

Table (6-28.a): Multi-Span Lattice Guyed Tower actual properties (Cable properties)

Element No. "(i)"	*Break. Strength "kN"*	*Initial Tension "kN"*	*Length L_i"m"*	*Cable Specification*	*Properties A"mm^2" I"mm^4"*	*Shape Factor "n_i"*	*Shear Parameter "u_i"*	*Straight Cable Elastic Modulus E_e"Kpa"*	*Sagged Cable ElasticModulus E_i"Kpa"*
2	2368	1210.55	L_h=101.1 L_v =66.60	Zinc-Coated Steel Structural Strand, Class-A-(38 wire)	A=1645.2 I=215391	2.084	$5.519*10^{-7}$	$167.3146*10^6$	$166.721*10^6$
4	3783	1989.76	L_h=101.1 L_v=139.0	Zinc-Coated Steel structural Strand, Class-A-(65 wire)	A=2664.5 I=564965.1	1.972	$4.191*10^{-7}$	$167.3146*10^6$	$166.173*10^6$
6	4482	2443.47	L_h=158.44 L_v=217.17	Zinc-Coated Steel Structural Strand, Class-A-(87 wire)	A=3200 I=814873.3	1.771	$1.848*10^{-7}$	$167.3146*10^6$	$164.726*10^6$
8	4881	2617.96	L_h=158.44 L_v=298.40	Zinc-Coated Steel Structural Strand, Class-A-(101 wire)	A=3483.9 I=965876.3	1.660	$1.194*10^{-7}$	$167.3146*10^6$	$163.181*10^6$

Table (6-28.b): Multi-Span Lattice Guyed Tower Equivalent Properties

Equivalent Element "(i)"	*Type of Bracing*	*Bracing Angle "α"*	*Equivalent Length "L_i(mm)"*	*Equivalent Inertia "$I_i(mm^4)$"*	*Shear Parameter "u_i"*	*Member Load "kN/m"*	*Joint Load P (kN), M (kN.m)*
1	X-Bracing+Battens	45	66598.8	$9.911*10^{10}$	0.0715	2087.23	-
3	X-Bracing+Battens	45	72390.0	$9.911*10^{10}$	0.0605	2962.99	-
5	X-Bracing+Battens	45	78181.2	$9.911*10^{10}$	0.0519	3619.81	-
7	X-Bracing+Battens	45	81229.2	$9.911*10^{10}$	0.0482	4086.88	-
9	X-Bracing+Battens	45	5334.0	$9.911*10^{10}$	11.154	379.496	P=1237.1,M=949.695

The results of comparison with ***Williamson*** study is detailed in table (6-28.c), and the same results will be discussed in order to check the **(bowing+change in length)** effect, the (**shear** effect), the **(axial+shear)** effect, the **(axial+change in length+bowing)** effects, and the overall effects in both the lattice tower and the idealized cables. These effects are examined using **(Meth.-1-/*Williamson* L.D. & Meth.-2-/*Williamson* L.D., Meth.-1-/Meth-0- & Meth.-2-/Meth.-0-, *Williamson*`s S.D./L.D., Meth.-0-/*Williamson*`s S.D., and Meth.-1-/*Williamson*`s S.D. & Meth.-2-/*Williamson*`s S.D.)** respectively.

Table 6-28.c: Comparison of Results of Multi-Span Lattice Guyed Tower Model -I-

Function	*Details*	*Williamson*	*Williamson*	*Present Meth.-0-*	*Present Meth.-1-*	*Present Meth.-2-*
1-Guy Horizontal Reaction in (kN)	Joint -0- (Hinge)	298.174	328.913	313.125	349.953	344.322
	Joint -1-	804.339	859.758	816.083	915.818	903.404
	Joint -2-	991.732	1069.626	1021.599	1143.138	1131.217
	Joint -3-	1186.409	1284.043	1225.362	1372.035	1351.319
	Joint -4-	1769.455	1920.757	1827.043	2047.507	2021.974
	Free End	0.00	0.00	0.00	0.00	0.00
2-Joint or Guy Displacement in (mm.)	Joint -0- (Hinge)	-	0.00	0.00	0.00	0.00
	Joint -1-	-	440.466	403.165	463.965	458.235
	Joint -2-	-	976.671	899.507	1028.133	1019.072
	Joint -3-	-	1681.216	1549.371	1763.895	1758.017
	Joint -4-	-	2056.242	1894.445	2163.627	2151.788
	Free End	-	2059.779	1897.601	2166.216	2155.383
3-Remarks	**Tower is Single-Sided Cable-Stayed**	**-Small Deflection (No Axial Effect) -No(Bow.+Geo.Chng.) -No Shear Effect -Spring Cab.Rprsnt. -FEA included.**	**-Large Deflection -No Bowing Effect -No Shear Effect -Spring Cables Representation -FEA included.**	**-Large Deflection - Bowing+Geom.Chng -No Shear Effect -Cab.Geom.Concedr. -FEA included.**	**-Large Deflection - Bowing+Geom.Chng -Total Shear Effect -Cab.Geom.Concedr. -FEA included.**	**-Large Deflection -Bowing+Geom.Chng. -Flext. Shear Effect -Cab.Geom.Concedr. -FEA included.**

The above mentioned ratios are **6.56%** increment, **5.41%** increment, **11.9%** increment, **10.7%** increment, **9.46%** increment, **4.37%** decrement, **16.73** increment, and **15.57%** increment, for the guy reaction respectively, and **5.02%**, **4.65%**, **12.43%**, and **11.36%** increment, for the displacements respectively.

6.4.8 Case study no. 28 (3-D R.C. Tower cable-stay bridge, Model -I-):-

In the next two examples two models of 3-D, R.C tower deck cable-stay bridge are to be analyzed and checked with the great effort of ***S.Nazmy*** and ***A.M.Abdel-Ghaffar*** [66] where no **3-D** (***SS*** effect) and **shear bowing effects** were included. Cable secant elastic modulus 3-D large deformation analysis including geometrical changes in structure and cable sags analytical procedure was used. These two models are shown in figure (6-30.a).

The choice of the structural properties of the elements of the two analytical models was based on examining several proposed cable-stayed bridges in the eastern region of United States and Japan [66].

Although table (6-29.a) detailed all the problem properties, the next section gives a brief explanation of the bridge modeling.

Model -I- has a center-span length of **335.366 m**, and two side spans of **146 m** each. This model represents the present trend in the design of cable-stayed bridges. The general configurations of the tower and cables arrangement, the nodal points and deck elements of this model are shown in figure (6-30.a)

The practical considerations that the modeling process based on are taken from ***Nazmy*** and ***Abdel-Gaffar*** [66], and they can be detailed as follows:-

1. The non-linearity of such structures is caused by the **L.D.** of the system and the **B.M.-Axial-Torsional forces** interactions, and relations between stresses and strains at any cross-section are assumed to be linear.
2. The technique used consists of loading a structural model of a cable-stayed bridge with **D.L.+L.L.** applied accordingly to the configuration of influence lines, in order to get the most critical axial force in cables and bending moments or torsions in the stiffing girders and towers, the loads are applied in two steps. First, a fraction of a **D.L. +L.L.** is applied in a way to have linear behavior, and then the model is loaded with its full load to have the real behavior. In the two examples studied herein the **D.L. +L.L.** is to be taken as 5 times the **D.L**. and the first to second stages ratio is **1/5.**

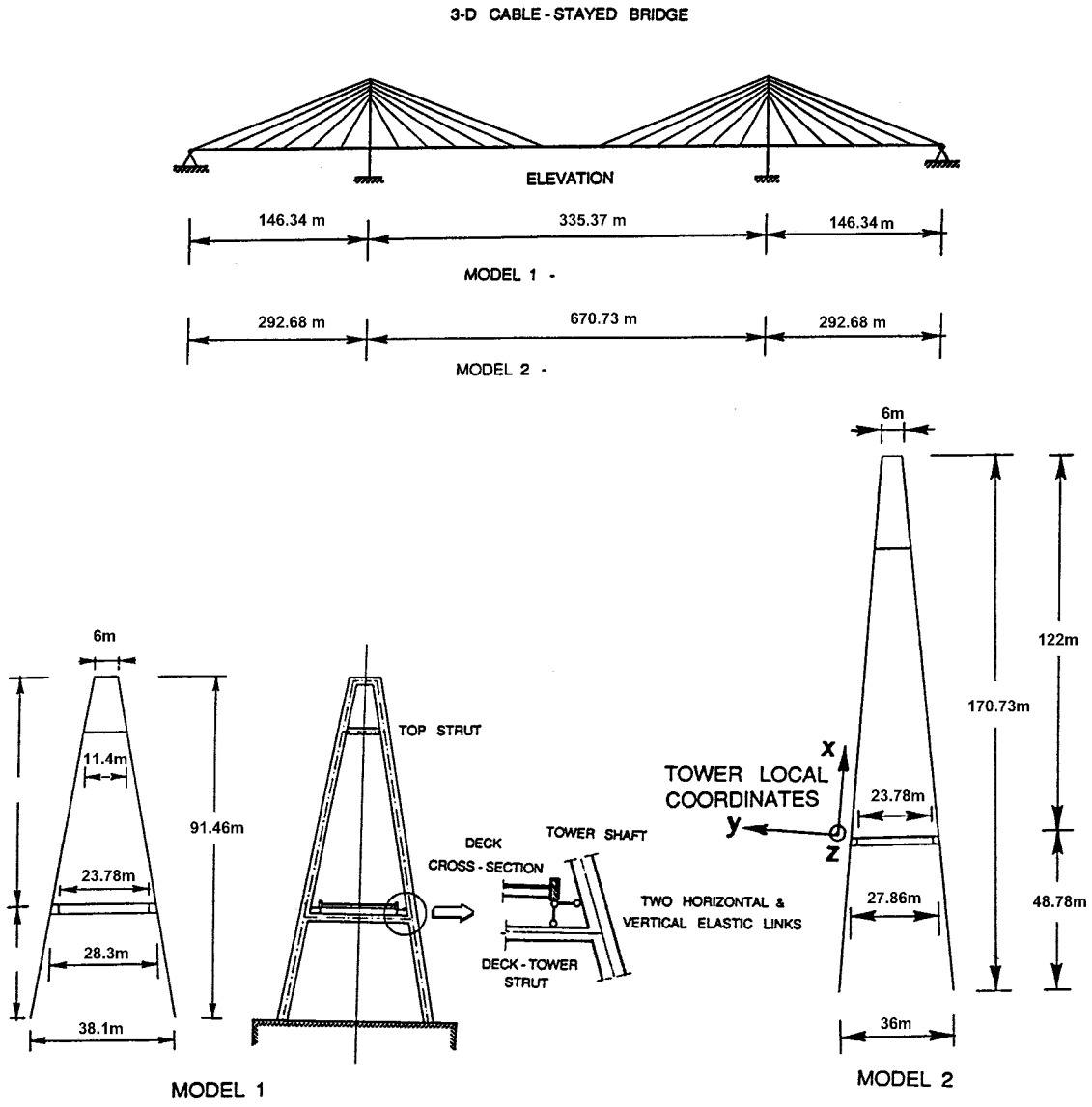

Figure (6-30.a) the two models of 3-D, R.C. tower deck cable-stayed bridge

3. The A-shape tower was adopted in the mathematical modeling to reduce the deformations that may occur in the bridge deck and towers especially under symmetrical loading, and to increase the overall stability of the structure, the A-shaped tower which has a very high torsional rigidity, is the most desirable one, so far, for the majority of long span cable stayed bridges.
4. The main girders were assumed to be simply supported and not to be fixed at the end piers or abutments in order to reduce the structural

redundancy, thus reducing the sectional forces induced by the environmental loads.

5. The towers were assumed to be rigidly fixed to the piers to reduce the overall structural deformations.
6. The bridge deck was assumed to be elastically connected to the towers rather than being fixed. In fact, the response of such structures to applied loads is highly dependent on the manner in which the bridge deck is connected to the towers. If the deck is swinging freely at the towers, the induced member forces due to wind, earthquake, and even water wave loads will be kept at minimum values, but the bridge may be flexible under service loads (e.g. D.L.& L.L.). On the other hand, a rigid connection between the deck and the towers will result in reduced movements under service loads but will attract much higher winds and seismic forces. Therefore it is very important to provide special devices at the deck-tower connections to control the bridge natural period of vibration in order to reduce the sizes of the towers and foundations and this was achieved by assuming that the bridge girder is connected to the tower by vertical and horizontal links whose elastic constants can be specified to reflect a wide band of practical construction options.
7. Horizontal strut near the top of the tower was added, to improve the tower behavior under the static and dynamic loads. It was noticed that the towers without top struts, in both models, experienced large bending deformations under vertical static loads due to the high comprehensive forces that come from the cables.

The full detailed results of **Model-I-** are illustrated in table (6-29.b) and figure (6-30.b), where the vertical displacement of node -30- (deck mid-span), and the horizontal displacement of node -60- (Top of left tower) are evaluated and checked with $\mathbf{E_{eq}}$.-secant modulus method-. From figure (6-30.b) and table (6-29.b), it can be concluded from noticing the displacements computed that even though an expected misestimation in results is due to the non-prismatic section effect, the results refer to good agreement.

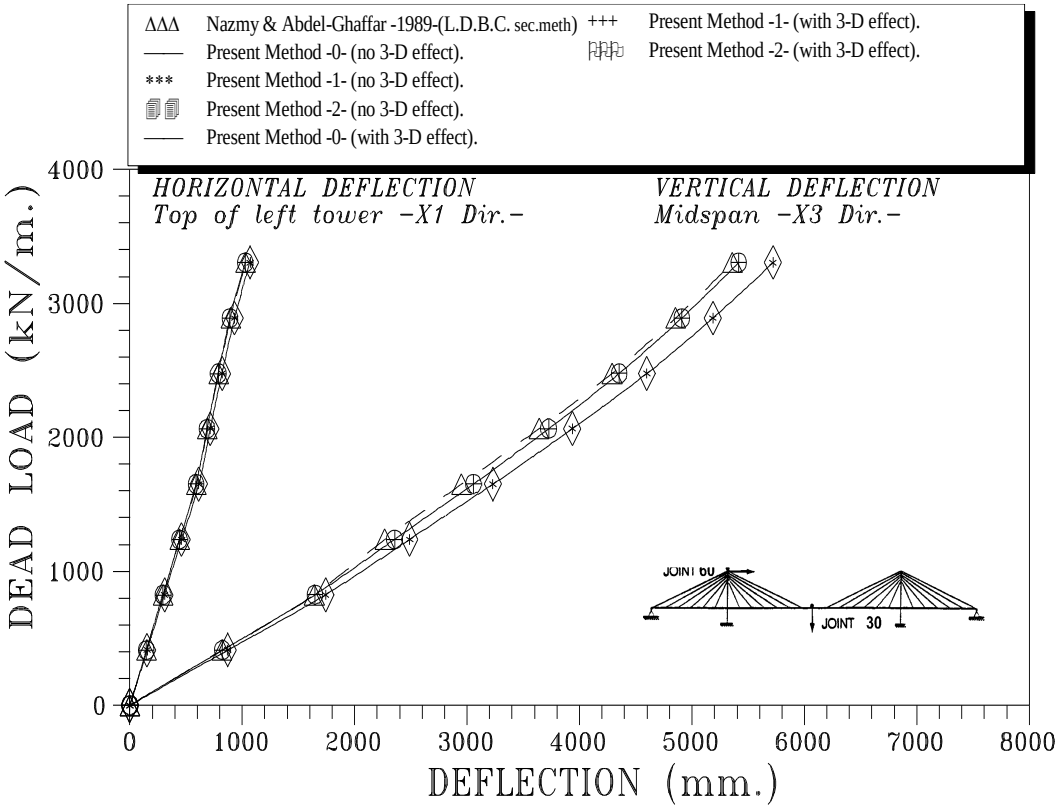

Figure (6-30.b) Load-deflection for the 3-D R.C. tower cable-stayed bridge (Model -I-)

As a matter of fact, the present formulation indicates rather better results since it includes the beam-column **3-D** (***SS*** effect) previously derived in **chapter-3-**, and not included in ***Nazmy*** and ***Abdel-Ghaffar*** analytical procedure, hence, the horizontal and the vertical displacements calculated by **Meth.-0-** are **3.82% & 6.76%** overruling the original **F.E.M.** analysis at **3305 kN/m.** (4 times the actual **D.L.** of the structure) which actually is very close to $\mathbf{P_{cr.}}$, and the **SS/SS0** for X_1- and X_3- directions are **4.15%** and **5.64%** respectively and incrementally for both methods. This supports the combined action effects.

Table (6-29.b): Deflections at Mid-span & Top of Left Tower for Model "I" By Different Methods

Load "4*D.L."	**"kN/m"**	**5508**
1. Nazmy & Abdel-Ghaffar (1989)	**X-Displacement (mm.) (Left Tower)**	**3137.41**
"Tangent $E_{eq.}$" F.E.L.D. Beam Theory	**Y-Displacement (mm.) (Mid-span)**	**-12192.0**
2. Nazmy & Abdel-Ghaffar (1989)	**X-Displacement (mm.) (Left Tower)**	**2401.06**
"Secant $E_{eq.}$" F.E.L.D. Beam Theory	**Y-Displacement (mm.) (Mid-span)**	**-11886.25**
3. Present Study Without Shear	**X-Displacement (mm.) (Left Tower)**	**2584.32**
"Meth.-0-" L.D. Beam-Column Theory	**Y-Displacement (mm.) (Mid-span)**	**-12510.29**
4. Present Study With Shear	**X-Displacement (mm.) (Left Tower)**	**2584.32**
"Meth.-1-" L.D. Beam-Column Theory	**Y-Displacement (mm.) (Mid-span)**	**-12510.29**
5. Present Study With Shear	**X-Displacement (mm.) (Left Tower)**	**2584.32**
"Meth.-2-" L.D. Beam-Column Theory	**Y-Displacement (mm.) (Mid-span)**	**-12510.29**

Table (6-29.a): 3-D, R.C. Cable-Stayed Bridge Model-I- Properties

No.	*Type of Element*	*Elements Number "i"*	*Length* L_i"mm"	*Area* A_i"mm^2"	*Elastic Modulus* E_i"Mpa"	*Shear Modulus* G_i"Mpa"	*Moment of Inertia* $I_{xi}mm^4*10^{10}$	*Moment of Inertia* $I_{yi}mm4*10^{10}$	*Moment of Inertia* $I_{zi}mm^4*10^{10}$	*Initial Tension "kN"*	*Weight "kN/m"*	*Shape Factor* n_i	*Shear Parameter* u_i
1	Steel Girder	1 - 6 &20-25 26-31&45-50 7-19 &32-44	24384.00 24384.00 23948.14	464515.20 464515.20 557418.24	199896.77	79958.707	8.63097	2157.74	12.496 12.496 64.732	-	87.576	1.2	1.2-1.44*10^{-7}
2	Steel Cross -Beam	51-56,58-69 &71-76,57&70	18288.00 18288.00	139354.56 325160.64	199896.77 199896.77	79958.707 79958.707	1.29465 8.63097	517.858	5.17858	-	21.894	1.2	2.05-4.79*10^{-7}
3	R.C. Tower "Above Deck Level"	77 & 78	60960.00	6503212.8	27782.59	11113.035	1726.195	1726.195	863.097	-	153.258	1.4	8.62* 10^{-8}
4	R.C. Tower "Below Deck Level"	79 & 80	30480.00	9290304.0	27782.59	11113.035	6473.231	4315.487	4315.487	-	218.940	1.667	7.18* 10^{-8}
5	R.C. Tower "Upp. Two Strut"	81 & 82	11430.00	4645152.0	27782.59	11113.035	129.465	776.788	129.465	-	109.470	1.11	9.56* 10^{-8}
6	R.C. Tower "Deck Level Strut"	83 & 84	28285.44	5574182.4	27782.59	11113.035	172.619	863.097	172.619	-	131.364	1.11	7.97* 10^{-8}
7	Tower Deck "Horz. Steel Links"	85,87,89&91	-	278709.12	199896.77	8013.1032	0.0008631	0.0008631	0.0008631	-	21.894	1.2	2.39* 10^{-7}
8	Tower Deck "Vert. Steel links"	86,88,90&92	-	278709.12	199896.77	8013.1032	0.0008631	5.17858	5.17858	-	21.894	1.2	2.39* 10^{-7}
9	Cable	93,104,105,116	158496.00	18580.608	199896.77	-	0.002747	0.002747	-	8900.00	2.043	1.11	1.93* 10^{-6}
10	Cable	94,103,106,115	135369.91	11612.88	199896.77	-	0.001073	0.001073	-	5562.50	1.277	1.11	1.66* 10^{-6}
11	Cable	95,102,107,114	112815.32	10219.334	199896.77	-	0.008310	0.008310	-	4895.00	1.124	1.11	2.10* 10^{-6}
12	Cable	96,101,108,113	91257.485	8825.789	199896.77	-	0.006198	0.006198	-	4227.50	0.971	1.11	2.77* 10^{-6}
13	Cable	97,100,109,112	71601.482	6967.728	199896.77	-	0.003863	0.003863	-	3337.50	0.766	1.11	3.55* 10^{-6}
14	Cable	98,99,110,111	55891.481	5667.085	199896.77	-	2555698.3	2555698.3	-	2714.50	0.623	1.11	4.75* 10^{-6}

Table (6-30.a): 3-D, R.C. Cable-Stayed Bridge Model-II- Properties

No.	*Type of Element*	*Elements Number "i"*	*Length L_i"mm"*	*Area A_i"mm^2"*	*Elastic Modulus E_i"Mpa"*	*Shear Modulus G_i"Mpa"*	*Moment of Inertia I_{xi}mm^4*10^{10}*	*Moment of Inertia I_{yi}mm^4*10^{10}*	*Moment of Inertia I_{zi}mm^4*10^{10}*	*Initial Tension "kN"*	*Weight "kN/m"*	*Shape Factor "n_i"*	*Shear Parameter "u_i"*
1	Steel Girder	1- 6 & 20-25 26-31&45-50 7-19 & 32-44	48768.00 48768.00 47896.27	696772.80 696772.80 836127.36	199896.77	79958.707	10.35717	10788.718	64.7323 64.7323 323.6616	-	105.821	1.2	$7.982\text{-}.578*10^{-8}$
2	Steel Cross Beam	51-56,58-69 &71-76,57&70	18288.00 18288.00	139354.56 325160.64	199896.77 199896.77	79958.707 79958.707	10.35717 8.630975	517.8585	5.1786	-	21.894	1.2	$2.05\text{-}4.79*10^{-7}$
3	R.C. Tower "Above Deck Level"	77 & 78	121920.00	13006425.6	27782.59	11113.035	3452.3899	8630.975	4315.487	-	306.516	2.00	$6.15*10^{-8}$
4	R.C. Tower "Below Deck Level"	79 & 80	48768.00	18580608	27782.59	11113.035	12946.462	21577.437	21577.437	-	437.88	2.50	$5.38*10^{-8}$
5	R.C. Tower "Upp.Two Struts"	81 & 82	11430.00	6503212.8	27782.59	11113.035	129.4646	776.788	129.4646	-	153.26	1.11	$6.83*10^{-8}$
6	R.C.Tower "Deck Level Strut"	83 & 84	72858.72	7432243.2	27782.59	11113.035	172.6195	863.0975	172.6195	-	175.15	1.11	$5.97*10^{-8}$
7	Tower Deck "Horzt. Steel Link"	85,87,89&91	-	278709.12	199896.77	8013.1032	0.0008631	0.0008631	0.0008631	-	21.894	1.2	$2.39*10^{-7}$
8	Tower Deck "Vert. Steel links"	86,88,90&92	-	278709.12	199896.77	8013.1032	0.0008631	5.178585	5.178585	-	21.894	1.2	$2.39*10^{-7}$
9	Cable	93,104,105,116	190445.14	39948.31	199896.77	-	126995081	126995081	-	20247.50	4.649	1.11	$2.881*10^{-6}$
10	Cable	94,103,106,115	172420.79	25083.82	199896.77	-	50069988	50069988	-	12015.00	2.759	1.11	$2.207*10^{-6}$
11	Cable	95,102,107,114	152356.11	22761.25	199896.77	-	41227059	41227059	-	10902.50	2.5032	1.11	$2.564*10^{-6}$
12	Cable	96,101,108,113	129854.86	19509.64	199896.77	-	30289259	30289259	-	9345.00	2.1456	1.11	$3.026*10^{-6}$
13	Cable	97,100,109,112	113431.62	16165.29	199896.77	-	20794914	20794914	-	7743.00	1.7778	1.11	$3.286*10^{-6}$
14	Cable	98,99,110,111	100537.67	12356.10	199896.77	-	12149348	12149348	-	5918.50	1.3589	1.11	$3.197*10^{-6}$

As expected, no shear effect is noticed since solid mast is used, so the three methods coincide with each other.

Nazmy and ***Abdel-Ghaffar*** indicated that **the tangent E_c** method is overruling **the secant E_c** at the same load level above by **4.26%** and **5.91%** in the vertical and horizontal directions respectively.

6.4.9 Case study no. 29 (3-D R.C. tower cable-stayed bridge, Model-II-):-

This model as shown in figure (6-30.a) has taller A-shaped tower, longer span and though is less slender than **Model -1-**, although of the same design considerations mentioned in **Model -I-** are adopted herein, with the full description of all the elements properties and loading conditions illustrated in table (6-30.a).

The center span and side spans of the second model have double the lengths of the first one (i.e. **670.73 m.** for center and **292.683 m.** for side span), however this model represents the future (or may be updating) trend of the cable-stayed bridges, as ***Nazmy*** and ***Abdel-Ghaffar*** stated. The 4 times **D.L.** loading is **5508 kN/m.**, which indeed is very close to the **P_{cr}.** of the system, and is divided into 10 loading increments.

Table (6-30.b): Deflections at Mid-span & Top of Left Tower for Model-II- By Different Methods

Load	**"kN"**	222.5
1. Chu & Ma (1976)	**X-Direction "mm."**	683.18
Modified E_c	**Y-Direction "mm."**	-13.995
L.D. Stiffness Method	**θ "radian"**	0.0232
2. Chu & Ma (1976)	**X-Direction "mm."**	681.48
Iterative E_c	**Y-Direction "mm."**	-3.894
L.D. Stiffness Method	**θ "radian"**	0.0231
3. Schreffler et.al. (1983)	**X-Direction "mm."**	668.26
L.D.F.E.M.	**Y-Direction "mm."**	-
	θ "radian"	-
4. Present Study	**X-Direction "mm."**	695.59
No Shear "Meth.-0-"	**Y-Direction "mm."**	-11.913
L.D. Beam-Column Theory	**θ "radian"**	0.037
5. Present Study	**X-Direction "mm."**	695.59
With Shear "Meth.-1-"	**Y-Direction "mm."**	-11.913

L.D. Beam-Column Theory	**θ "radian"**	0.037
6. Present Study	**X-Direction "mm."**	695.59
With Shear "Meth.-2-"	**Y-Direction "mm."**	-11.913
L.D. Beam-Column Theory	**θ "radian"**	0.037

From table (6-30.b) and figure (6-31), good agreement can be noticed although the tower has non-prismatic section, the effect that is not-included in the present formulation. **The 3-D beam-column effect** is not included in ***Nazmy*** and ***Abdel-Ghaffar*** **L.D. F.E.M.** analysis. These differences shifted the results away in the horizontal and vertical directions for node **-60-**and **-30-** respectively by a percentage ratios of **7.6%**, and **5.25%** respectively at the load level mentioned above, and again no shear effect has been noticed. The **SS/SS0** values are **6.23%** and **8.49%** for X_1 and X_3 directions respectively and incrementally for both methods. The last two cases hold the following conclusions:-

1. The cable-stayed bridge system is a hardened structural system in which the overall stiffness of the structure increases as the load increases.
2. The non-linearity is more pronounced in the taller tower-longer span model (Model-II-), this supports the fact that non-linearity in cable stayed bridges is of geometric nature.
3. As the span increases, larger deformations occur and strong non-linearity in the behavior of the bridge under loads takes place.
4. As complex geometry of the tower's configuration is adopted in design the static behavior of cable-stayed bridges cannot be fully represented by a planner analysis, so the 3-D models are essential in order to study the torsional behavior of the bridge under unsymmetrical loading, the behavior that does affect the overall behavior of the system.

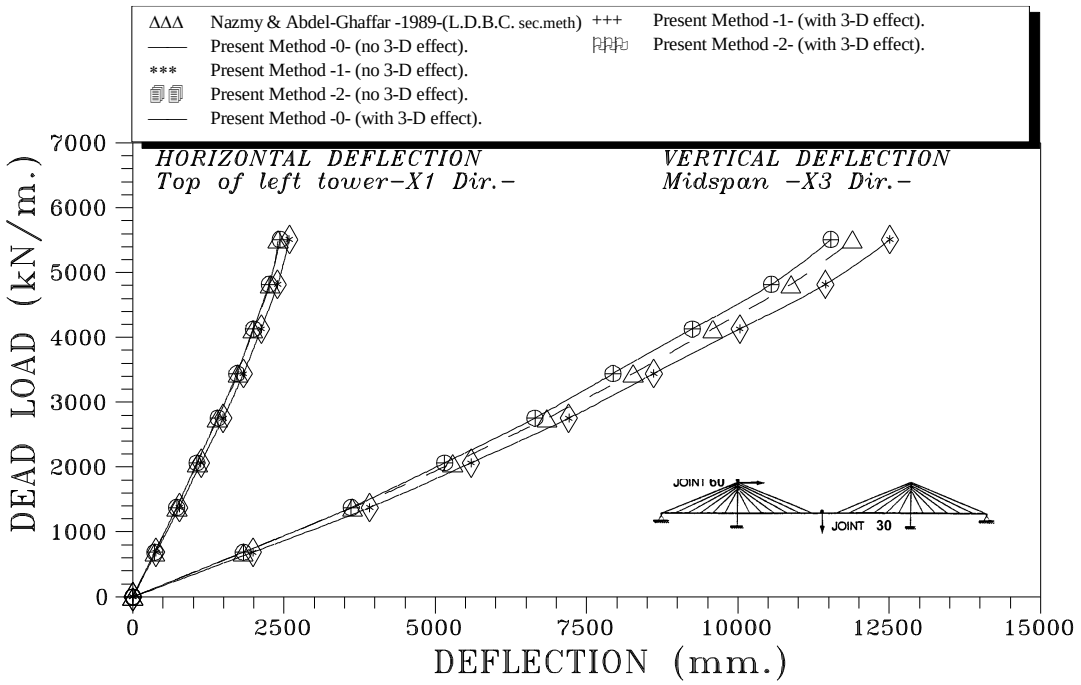

Figure (6-31) Load-deflection for the 3-D R.C. tower cable-stayed bridge (Model-II-)

6.4.10 Case study no. 30 (2-D, warren bracing tower, cable-suspended bridge):-

This structure has been constructed over the river ***Adige*** in Northern Italy**,** (see figure 6-32.a), and has been studied by ***Scherffler*** [83] many times throughout many papers in (1977, 1978, and 1983). He analyzed the structure using **2-D, L.D., F.E.M.** with line elements and parabolic elements as cables idealizations, the total structure consists of (41) elements with (76) nodes, he stated. Since the bridge is gas carrying, the piping is tested by filling it with water and the analysis is concerned with the resulting symmetrical and unsymmetrical loading, he made all the initial analysis based on catenary calculations to evaluate sags, initial pretensions, tower inclinations, etc., the vertical loading is **6.72 kN/m**.

Since the present formulation uses the parabolic cable analysis with all the possible non-linearities of such structures and the capabilities to handle both cable-stayed and cable-suspended structures, ***NASCFI*** used only (9) beam-column and cable elements with ***Scherffler*** initial calculations to be adopted for 2-D analysis. This structure is subjected to symmetrical vertical loading, the non-prismatic warren-bracing tower is considered as one prismatic equivalent shear parameter element with average width to get the "**u**" equal to **3.3405** calculated using (eq. 3-7), although an

overestimation in results is expected due to this effect. All the above details are summarized in table (6-31.a) and figure (6-32.b and c).

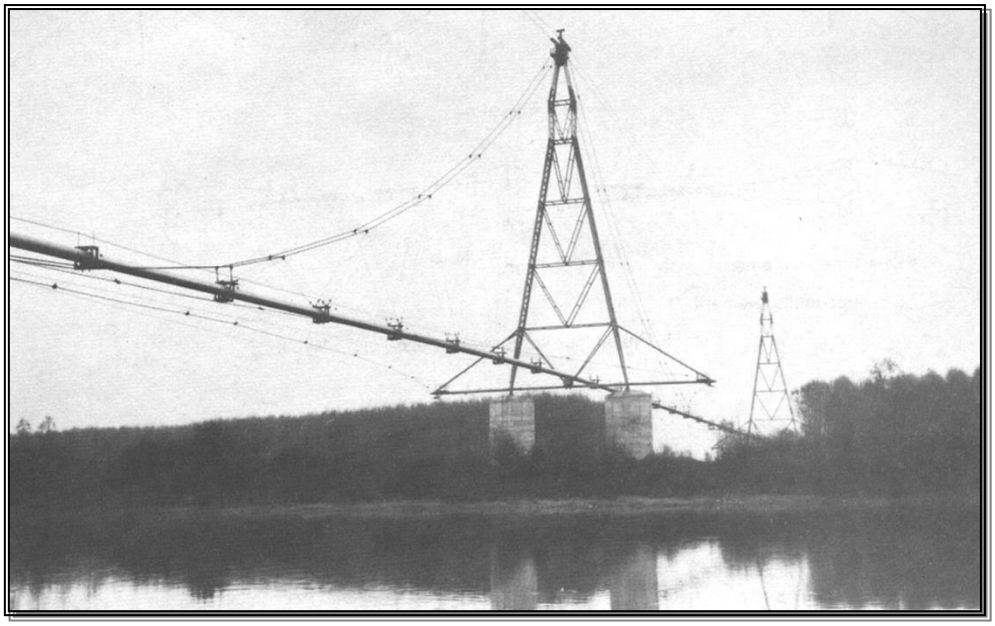

Figure (6-32.a) ***Adige River*** **cable-suspended bridge**

Table 6-31.a:2-D Continuous Cable-Suspension Bridge Properties

No.	***Type of Element***	***Elements Number "i"***	***Length*** L_i***"mm"***	***Area*** A_i***"mm²"***	***Moment of Inertia*** I_{xi}***"mm⁴"***	***Elastic Modulus*** E_i***"Mpa"***	***Shear Parameter*** u_i	***Initial Configuration***	***Vertical Dead Load=6.27"kN/m"***
1	Inclined Cable	1 & 7	121880	1963.5	306786.1576	150000	$3.457*10^{-7}$	Preten.=1847 kN Sag = 0.00	
2	Non-Prismatic Warren-Bracing Tower	2 ,4, & 6	56500	Ad= 7850 Al= 31400	Il= $4.91*10^{6}$ Id=$7.85*10^{7}$	200000	3.3405 "7 panels"	Outer Towers Inward Initial Inclination 0.46m	
3	Parabolic Cable	3 & 5	283319	3848.5	1178588.119	150000	$1.254*10^{-7}$	Preten.= 760 kN Sag = 2.2 m	
4	Horizontal Cable	8 & 9	249000	1963.5	306786.1576	150000	$0.828*10^{-7}$	Preten.= 775 kN Sag = 0.00	

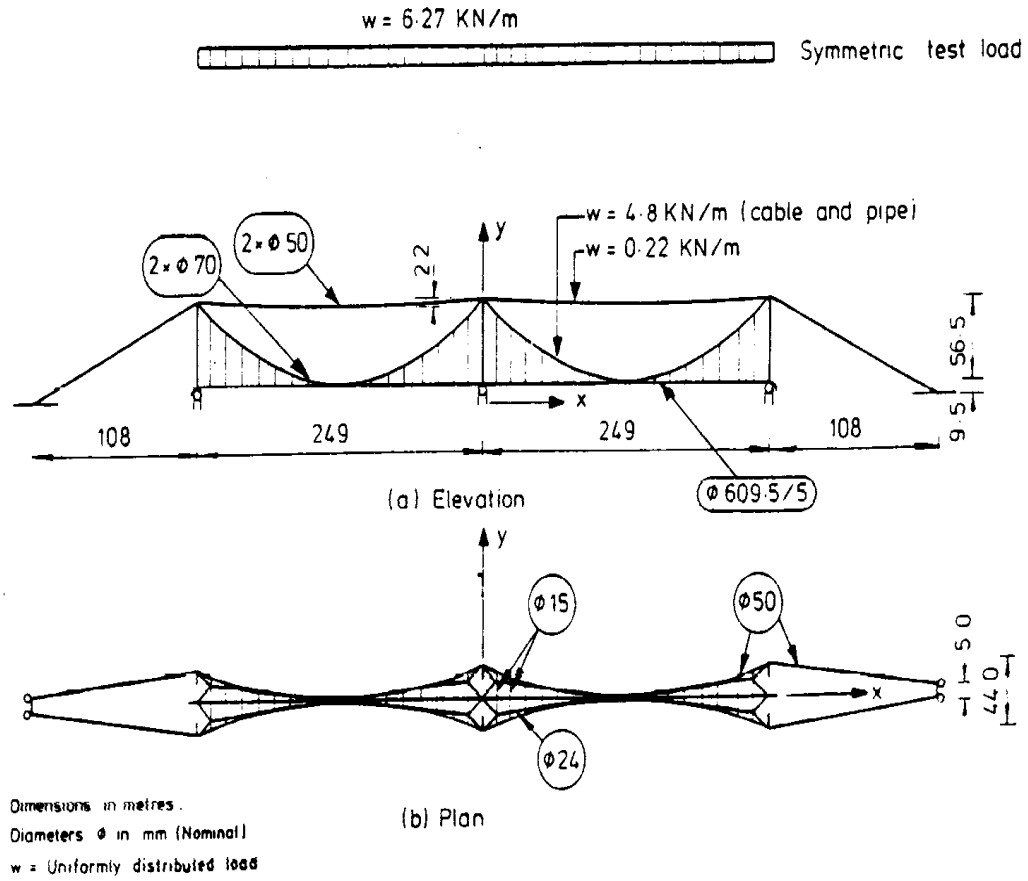

Continuous suspension bridge—layout and loading.

Figure (6-32.b) Idealization of the suspended bridge

The results shown in table (6-31.b) for the symmetrical vertical loading of the 2-D analysis of the bridge indicate neither vertical movement of the cable nor horizontal displacement of the tower under such loading circumstances, the matter that seems logical since the movement of the right part of the bridge cancels the left side one because of the symmetry. This zero displacement leads the cable forces to be nearly equal regardless of the method of analysis and they are so close to their initial values. ***Scherffler*** indicates **3.47%, 1.48%,** and **1.2%**, while the present approach exhibits **4.58%, 2.39%,** and **0.64%** as a divergence with the initial tensions values for the inclined, parabolic, and vertical cables respectively, which leads to the fact that excellent agreement is concluded from ***NASCFI***.

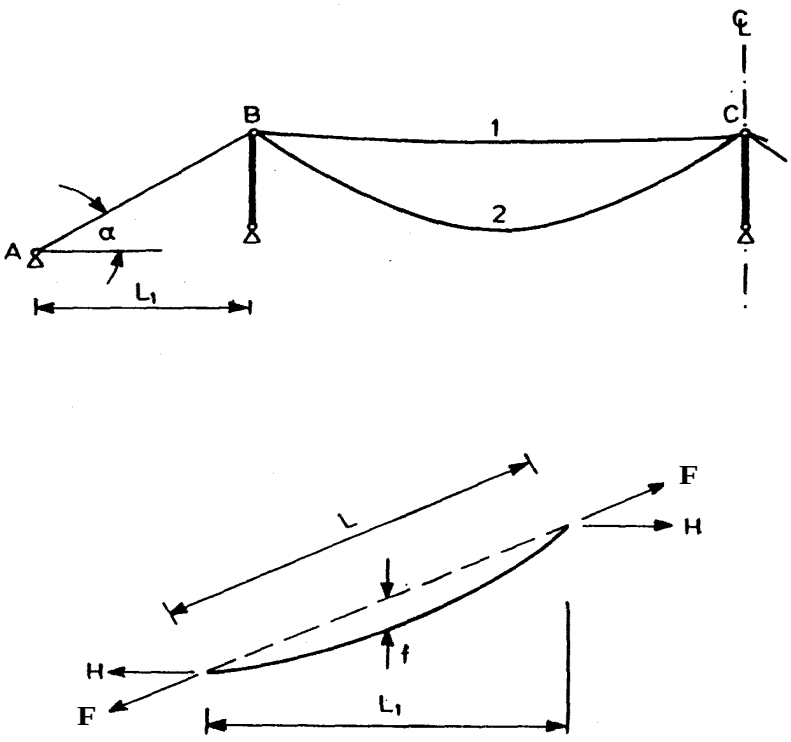

Figure (6-32.c) Continues suspension bridge-idealization and initial configuration

Table (6-31.b): 2-D Continuous Cable-Suspension Bridge Results

No.	*Method*	*Type of Analysis*	*Tower Display "mm"*		*Cable Display "mm"*		*Horizontal Component of Cable Tension "kN"*		
Comparison for Symmetric Vertical Loading Condition			*Outer Towers*	*Inside Tower*	*Horizontal Cables*	*Parabolic Cables*	*Inclined Cables*	*Horizontal Cables*	*Parabolic Cables*
1	Scheffler et al. (1983)	L.D., F.E.M. (Line&Parb.Cab) -No Bowing -No Shear.	0.00	0.00	0.00	0.00	1433.00	747.50	70
2	Present "Meth.-0-	L.D., B-C.A. -Bowg. Effect -No Shear.	0.00	0.00	0.00	0.00	1440.65	739.36	17
3	Present "Meth.-1-	L.D., B-C.A. -Bowg. Effect -Tot.Shear Eff.	0.00	0.00	0.00	0.00	1440.65	739.36	17
4	Present "Meth.-2-	L.D., B-C.A. -Bowg. Effect -Flx.Shear Eff.	*Did Not Work*:- Because of high value of "u" which leads to misleading stability and bowing functions						

As a final general conclusion for this chapter multi-purpose ***FORTRAN77 NASCFI*** program which depends on the present approach previously described exhibits a very good agreement with the 30 pre-examined case studies which represent numerical, experimental, and field or actual structures, and though it has a capability and flexibility to deal with:-

- Both (2-D) and (3-D) ordinary frames, trusses and other simple structures
- Both (2-D) and (3-D) ordinary open or closed web towers and frames.
- Both (2-D) and (3-D) cable-stayed and cable-suspended solid, lattice, and trussed towers and bridges.

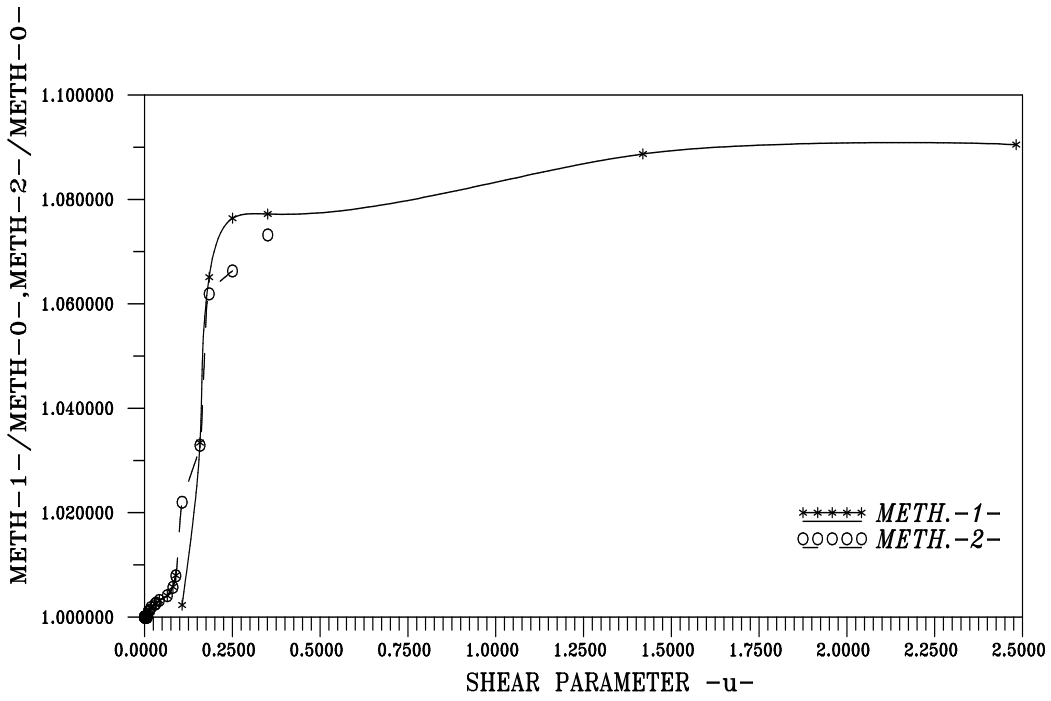

Figure (6-33) the effect of shear represented by Meth.-1 & 2-/Meth.-0- vs. shear parameter "u'

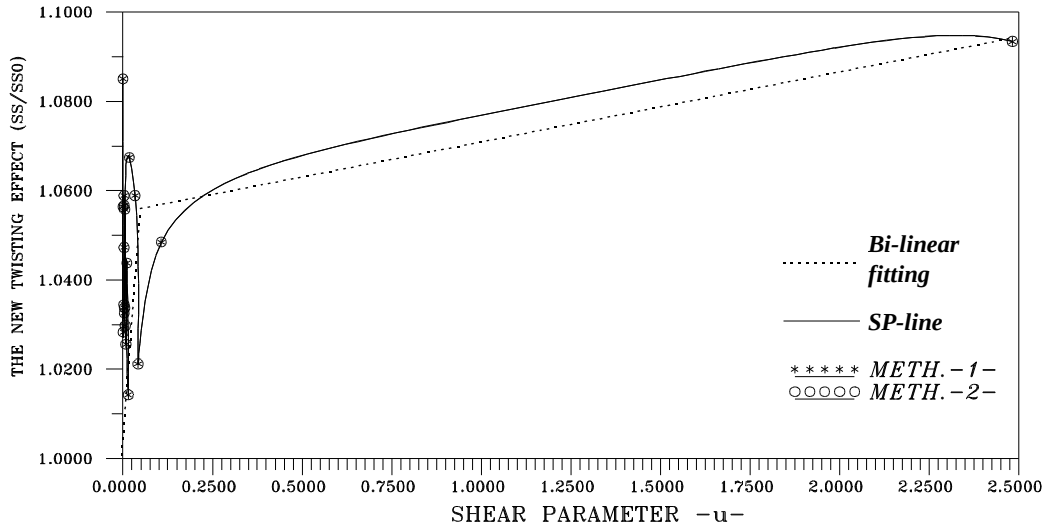

Figure (6-34) the new twisting effect (*SS* effect) represented by SS/SS0 vs. shear parameter "u"

Figures (6-33) and (6-34) illustrate the relation between the shear parameter "u" and the shear effect "δ_v" for both methods, represented by the ratios ($\frac{\text{Meth.}-1-}{\text{Meth.}-0-}, \frac{\text{Meth.}-2-}{\text{Meth.}-0-}$) and the new twisting effect (the ***SS*** effect) represented by the ratio ($\frac{SS}{SS_0}$) respectively, for almost the 30 cases studied in this chapter.

The values of "u" are takes in the applied load direction (either in 2-D or 3-D cases) and it's also takes as the maximum values for the multi-elements structures, this value is varied in a widely ranged manner from "3.5×10^{-13}" to approximately "2.5".

The values of ratios ($\frac{\text{Meth.}-1-}{\text{Meth.}-0-}, \frac{\text{Meth.}-2-}{\text{Meth.}-0-}$ and $\frac{SS}{SS_0}$ -for both methods-) are taken from the (P-Δ) relations of the cases.

It's obvious from figure (6-33) that the increasing of "**u**" values loads to the increasing of the shear effect for both methods .Meth.-2-, however, seems to behave as Meth.-1- in the lower values of "**u**", but when this value arises with Meth.-2- fail to give any results for the reason detailed in this chapter. It can be easily observed that the shear effect represented by both ratios is lightly increases from "1.0" to approximately "1.1".

In spite of a direct relation between the ***SS*** effect factor "C_T" and the shear parameter "u" as derived in **chapter-3-**, the statistical relation of figure (6-34) gives an idea of fluctuation behavior, which means that there is no rule governs the shear

deflection and the axial deflection, the matter that physically make no sense. However, if a more reliable fitting curve of a first degree (indicated as dashed line) is used instead of the SP-line (indicated as solid line), the relation would be a bi-linear which is more logically, i.e. the higher the "u" value the higher the ***SS*** effect.

CHAPTER SEVEN

PARAMETRIC STUDY AND APPLICATIONS

7.1 Introduction:-

In this chapter, the author tried to show the possible benefit ***NASCFI*** can offer**,** so there will be a parametric study on four types of different structures as table (7-1) illustrates.

The major points that are studied in this chapter are:-

1. The effect of changing the shear parameter "**u**" on the (e-Δ) behavior of the initial imperfection X-bracing lattice pin-ended 3-D beam-column structures, (only analysed using new coupled **T.S.M.**).
2. The effect of varying the eccentric wind load to dead load ratio on the P-Δ behaviour of 3-D free standing transmission tower, (only analysed using new coupled **T.S.M.**).
3. The effect of bracing type and section properties on the Deflection, B.M., and Axial forces behaviour of X-bracing 2-D cable-stayed towers, (no 3-D effect).
4. The effect of changing the wind velocities and directions on the cable tension, and the Mast B.M. and axial force behavior of multi-level solid mast 3-D towers, (only analysed using coupled T.S.M.).
5. The effect of studying the influence lines of the cable tensions and nodal displacement for the 2-D cable-stayed, solid-tower bridge.

These effects vs. behaviors taken are mainly the most important and practical issues that a researcher can deal with owing to the fact that they represent the most important researching fields in static structural applications both in analysis and design.

Table (7-1): Types of applications & parametric studies applied to (*NASCFI*)

Case No.	*Notation*	*Reference*	*Year*	*Type of Analysis*	*Shear Parameter (u)*	*Parameters*	*Cases*		*Behavior Study*
1	3-D, 3-Legged, X-bracing, Pin-Ended Truss Column	D.Elyada & C.D.Babcock[29]	1987	Closed-Form Solution	u_{xi} =Taken as Variable (i= 2,3)	Global Imperfections (e_{imp}.)	u(5 cases) (0.1,0.5, 1.0, 5.00, and 10.0)	e_{imp}(4 cases/u) 0.00, 500.00, 1000.00 and 2000.00)	Effect of changing (u) on the (e_{imp}.-Axial Displ.) curve
2	3-D, Free Standing Full-Scale Transmission Tower	M.J.Alam & A.R. Santhakumar[1]	1993 & 1996	Theoretical & Experiment	u_1=0.1063,u_2 = 0.1528 u_3=0.0159,u_4 =0.6927 (all directions)	W.L./D.L. (3 cases) Eccentricity (3 cases)	1-W/D=0.025:ec=0,.5,1m 2-W/D=0.150:ec=0,.5,1m 3-W/D=0.300:ec=0,.5,1m		Load-Deflection (P- Delta Curve) "Shear +Torsion"
3	2-D Cable-Stayed Transmission Tower	R.R.A. Issa & R.R. Avent[43]	1991	Theoretical	u(X.)=0.013-0.0925 u(W.)=0.0024-0.195 u(V.)=2.72-76.28	1-Type of Section 2-Type of Bracing	2 types(Const.&Varb.). 3types(X, Warren &Vierendeel).		1-Hight-Deflection. 2-Hight-Axial Forces. 3-Hight-B.Moment.
4	3-D Multilevel Guyed Tower	Raman et al[76].	1988	Theoretical	u=0.0009-0.0185 (all directions)	1- Wind Velocities 2- Wind Direction	8Veloct.(from0-296km/h). 6 Wind Directions:-o (0,30,60,90,120 & 150).		1-Cable Tension. 2-Axial Force. 3-Bending Moment.
5	2-D Cable-Stayed Bridge Model	Troitsky [97]	1977	Theoretical & Experiment	u=0.00647-0.0519	Influence lines	6 cables 5 nodes		1-Cable tensions 2-Nodal vertical displacement

7.2 Parametric study no.1 (3-D, 3-legged, X-bracing, pin-ended 40-bay truss column):-

This example was studied by ***D. Elyada*** and ***C. D. Babckock*** [29], they considered an idealised simply supported 3-legged truss column as shown in figure (7-1), loaded in pure axial compression. They assumed that the transverse shear is carried by an unspecified web of infinite rigidity that does not modify the longeron (legs) forces, these longerons were assumed discontinuous. Their segments between battens are pinned to each other as well as to the battens. Sine half-wave imperfections are assumed to occur in both longhorn and global lengths respectively. Sought is the complete non-linear behaviour of the general column. The closed form exact solution were obtained for locally and globally general imperfection case, hence all their values were normalized.

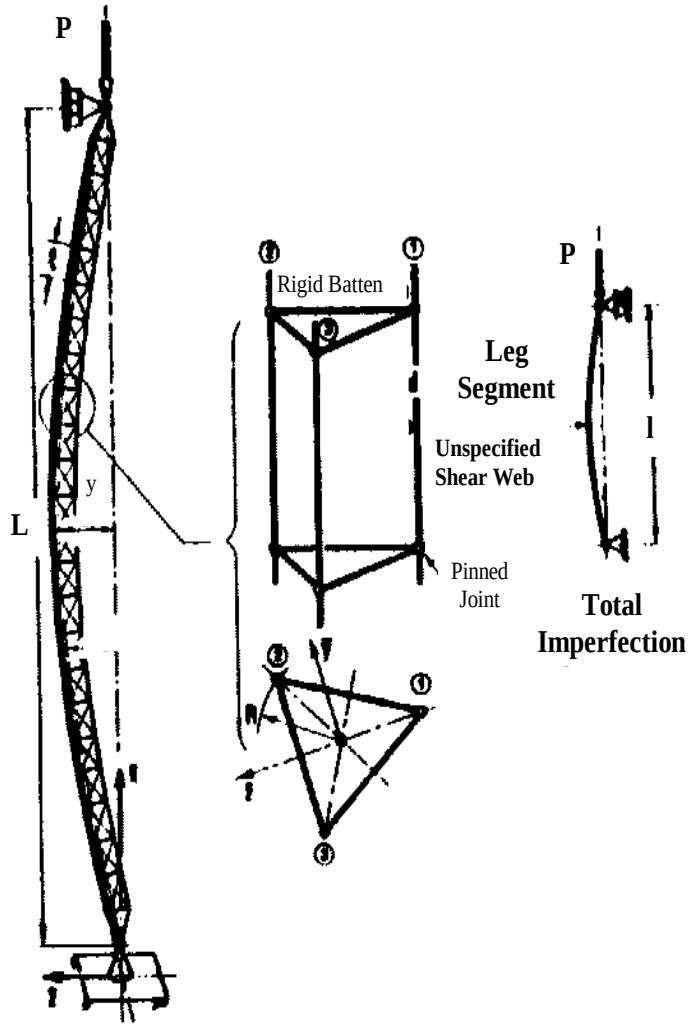

Figure (7-1) 3-D, 3-Legged, X-bracing pin-ended truss column

As it was detailed in **chapter -3-**, the initial imperfection effect is one of the special effects that the present formulation is associated with. This effect was treated (as the other special effects) as **F.E.A**. (see **App.D.**) where it is transferred to the element force vector, and then acts either as an axial force effect or a flexural bowing effect i.e. it's transferred to non-linear effect, besides the present procedure takes the exact shape of the curve and not the sine half-wave as ***Elyada*** and ***Babcock*** did. The design operation of the section properties and stiffnesses **(A, I)** is based on their normalized equations and the special cases they took, and with the help of the ***AISC Specifications*** [7]. The X-bracing governing "**u**" value equation below, all the design requirements are fulfilled, besides all the parametric values of the shear parameter "**u**", the global imperfection "**e**"**,** and the maximum axial load "**P**" which is taken as "**1.8 P_e**"**,** are summarized in table (7-2):-

$$u = \frac{I_{eq}.\pi^2}{2L^2 A_{br}.\sin\alpha\cos^2\alpha} \quad \text{.....(7-1)}$$

Table (7-2): 3-Legged, X-Bracing Truss column Properties

Element (I)	***Bracing Type -3 faces-***	***Bracing Angle (α)-3 faces-***	***Length "L(mm)"***	***Triangle Distance "R(mm)"***	***Global Section Area "A(mm^2)"***
1	X-Bracing	63.435	8000.00	750.00	206290.164
Type Leg Member (ϕ150) -Type Bracing Member (ϕ100) -Type Batten Member (ϕ50)					
Area (mm^2):-(A_d=2045.1572 A_l=3600.00 $A_{bt.}$=690.3212) Inertia (mm^4):-(I_d=3009353.207 I l=11696103.06 $I_{bt.}$=277210.1294)					
Design is Based on:- 1-***AISC Manual -ASD-*** (9/1989) 2-***Elyada*** and ***Babcock*** Normalized Formulae 3-Different "$\mathbf{e_{imp}}$" and "**u**" values (see table 7-3)					
E=200000Mpa-Loading Condition:-Axial Compression + Initial Imperfection					

The **combined flexure-shear bowing** with the **effect of shear on the axial rigidity** (represented by "**u**") herein, and the secondary effects caused by the axial force all have important role in the **P-Δ** behavior. The **3-D torsional effect** (i.e. the ***SS*** effect) has an influence in this example since torsion-flexure coupled action exists, though the major role of non-linearity in such case is taken by the **combined effects of axial + shear +3-D + imperfection**.

Table (7-3): 3-Legged, X-Bracing Truss column design requirements

Case	*Shear parameter (u)*	*Equivalent. Inertia (Ieq.-mm⁴-)*	*Initial Imperfect 4-Cases(e_{imp}-mm-)*	*Maximum Axial Load(P-kN-)*
1	0.10	474471950	0, 500, 1000, &2000	26.340
2	0.50	2372359840	0, 500, 1000, &2000	131.700
3	1.00	4744719500	0, 500, 1000, &2000	263.400
4	2.00	9489439200	0, 500, 1000, &2000	526.820
5	10.00	47447195000	0, 500, 1000, &2000	2634.000

The parametric designed values are summarized in table (7-3), and the parametric study of the "$\mathbf{e_{imp}}$-$\mathbf{\Delta}$" for deferent "**u**" and "$\mathbf{e_{imp}}$" values is illustrated in figure (7-2).

By examining figure (7-2), it's obvious that the higher the shear parameter (i.e. more open-web section) the higher axial displacement, besides increasing the initial imperfection per each shear parameter leads to an increase in the axial displacement which supports the fact that these types of structures are of stiffening nature and that the non-linearity type is geometrical in nature. However, the results indicate a good agreement with ***Elyada*** and ***Babcoock*** which leads to the fact that the sine half-wave imperfection they suggested was indeed a suitable selection and it's nothing but **2.438%** (taken as average) away from actual behavior of the elastic curve taken by the present formulation.

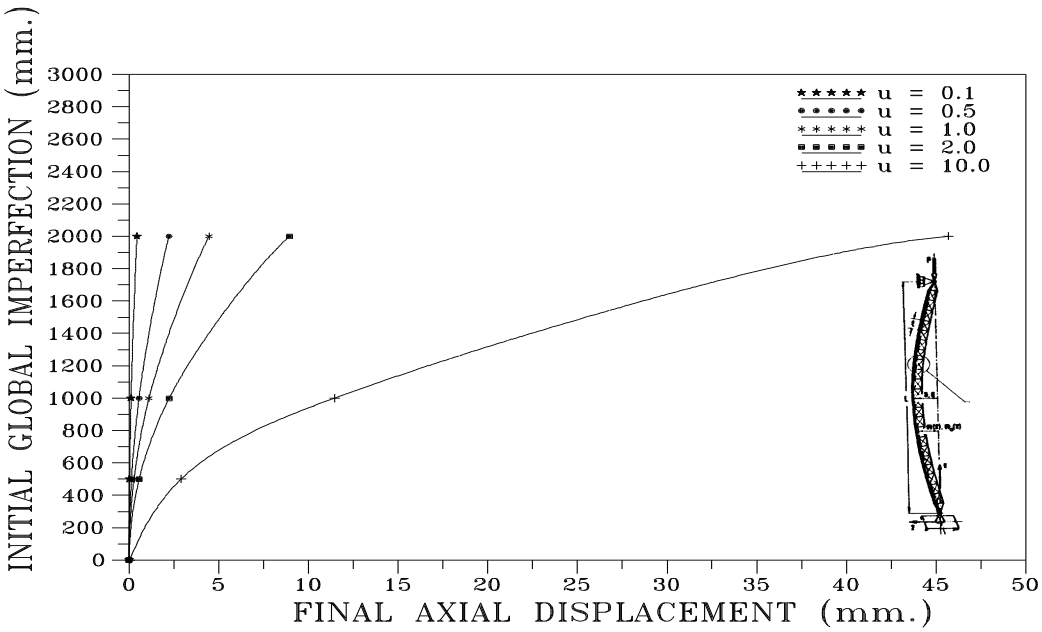

Figure (7-2) Meth.-1- (e_{imp}-Δ) curve for the 3-D initial imperfection pin-ended lattice column for various "u" values

7.3 Parametric study no. 2(3-D, Full-scale Free standing Transmission Tower):-

Although this full-scale free standing transmission tower with common structure illustrated in figure (7-3) was reliability analyzed by ***M. J. Alam*** and ***A. R. Santhakumar*** [1] (1993 & 1996), it is taken herein as a parametric study for the **P-Δ** for three different wind load to dead load ratios **W.L./D.L.** and three eccentricities to observe the effect of applied torsion induced thereby.

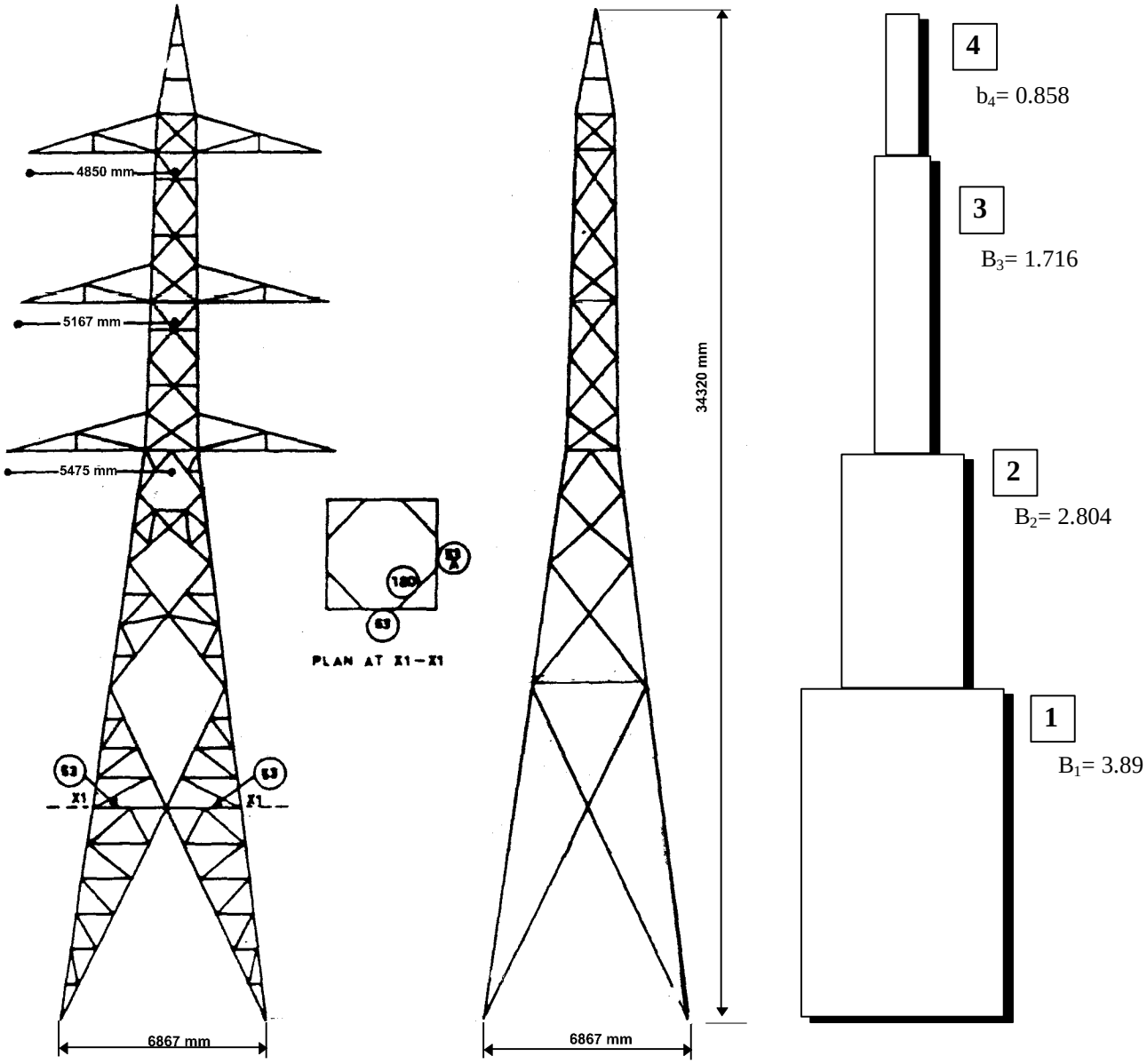

Figure (7-3) 3-D, Full scale, Free-standing, 220-kV Double-Circuit Tangent Transmission Tower

The same problems faced the author in the previous chapter when testing ***A. Noor*** space tower because of **the non-prismatic effect** not being considered and the number of panels is less than (4)

(in members 1 and 4), the matter that leads to expecting overestimated results facing us in this example, besides the cable holder arms of the tower are ignored in the equivalent member calculations. However this case is simpler to idealize in our equivalent shear parameter formulation than ***Noor***`s. Briefly, it's four equivalent member idealization with properties plus all the design considerations as shown in table (7-4).

Table (7-4): Free-Standing Full-Scale X-Bracing Transmission Tower Equivalent Properties

Element "(i)"	*Equivalent Length & Thickness*	*Equivalent Area "$A_e(mm^2)$"*	*Equivalent Inertia "$I_e(mm^4)$"*	*Shear Parameter "u_i"*	*Cases of U.D.L. (D.L+W.L) "kN/m"*	*Cases of Eccentricity E_c"mm"*	*Cases of Uniform Torsion "kNm/m"*
1	L_e = 11445.25mm t_e = 0.01491 mm	80.203	193391491.2	0.1003	D L = 26.6025 W/D=0.025,0.15&0.3	0, 500&1000	0- 0.0125,0.075, 0.15-0.025,0.15,0.30
2	L_e = 8011.50 mm t_e = 0.07448 mm.	208.842	136834968.4	0.1528	D L = 26.6025 W/D=0.025,0.15&0.3	0, 500&1000	0- 0.0125,0.075,0.15-0.025,0.15,0.30
3	L_e = 11445.25mm t_e = 0.09567 mm	164.2414	40338123.94	0.0159	D L = 26.6025 W/D=0.025,0.15&0.3	0, 500&1000	0- 0.0125,0.075,0.15-0.025,0.15,0.30
4	L_e = 3418.00 mm t_e = 2.6732 mm.	2293.606	140705822.7	0.6927	D L = 26.6025 W/D=0.025,0.15&0.3	0, 500&1000	0- 0.0125,0.075,0.15-0.025,0.15,0.30
Typical Leg Member:-(C150*150*12) -Typical Bracing Member.(C50*50*4), E=200000 Mpa							
Area (mm^2):-(Ad=384, Al=3556), Inertia(mm.4):-(Id=71593.5,I l= 6072934.5)							
Loads are Based on:- **1-*ASCE Manual* 74(1991).** **2-*LRFD Manual* &** **3-*IEC International. Electro-technical Commission* (1992).** **Wind Load on X_1-Direction or X_3-Direction only** **Cable Load = 0 (Free Stand. Tower)**							
Buckling Concederations are Based on:- **1-*ASCE Manual* 52 (1988) &** **2-*IS:802"Indian"*(1977,1992).**							

The parametric study in this example is to be taken for the effect of **W/D** on the **P-Δ** behavior of both horizontal X_1 and X_3 directions, the wind load is applied at **0, 0.5, & 1.00 m.** eccentricity to observe the effect of applied torsion induced by such eccentricity respectively, the eccentricity is due to imperfection or other special effects or even due to tornadoes so we have 3 cases of applied torsion per each case of **W/D** as table (7-4) indicates.

The eccentricity is defined as the distance between the **U.D.** wind load (otherwise a non-uniform torsion would be induced) application center and the center of equivalent thickness of the open-web member "$\mathbf{t_e}$" is evaluated by eq. (3-13).

It's obvious from figure (7-4), figure (7-5) and figure (7-6), that the torsion induced by the eccentric wind application dominantly affects the P-Δ behavior so the critical load decreases rapidly with increasing the eccentricity "e_c". Accordingly the applied torsion "**T**", and with the torsion

increasing continuously the structure becomes weaker and weaker till the case of tornado occurs (very high torsional and twisting moments induced by high wind velocities and eccentricities) when the P_{cr}. as well as the entire strength of the structure become so low.

The present approach of the coupled actions of total shear on the axial stiffness, the combined effects of **3-D torsional** (i.e. the ***SS*** effect) and **flexure-shear bowing** on the axial displacement are very significant in this practical example.

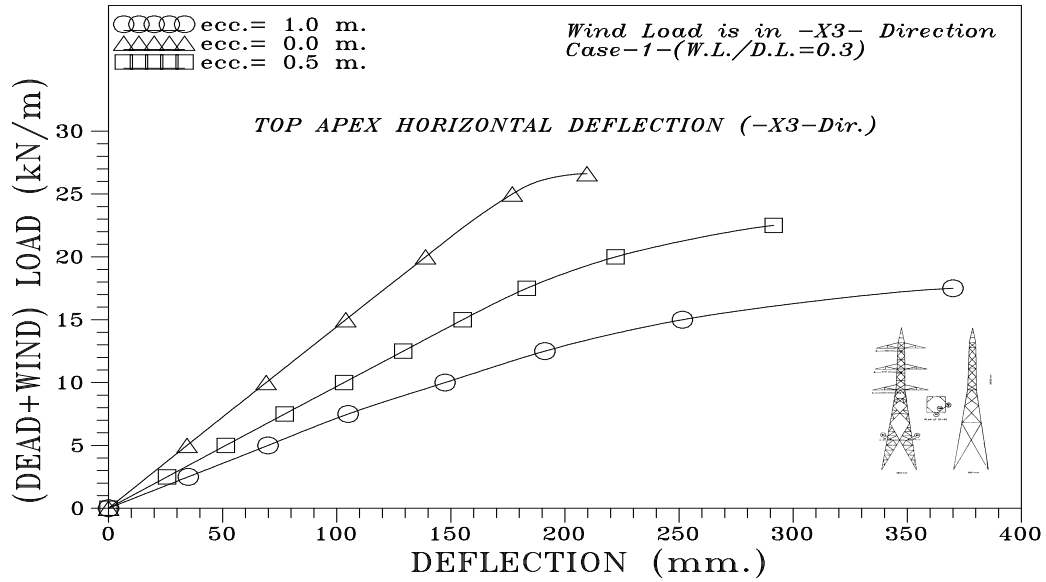

Figure (7-4) **3-D effect Meth.-1- load-deflection curve for the 3-D free standing full-scale transmission tower (case -1- with various eccentricities)**

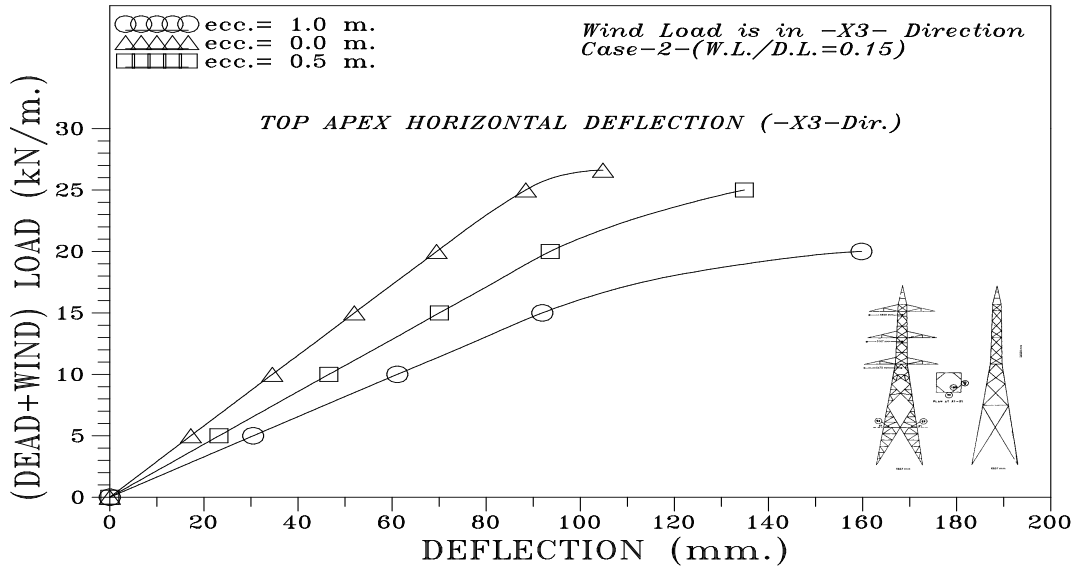

Figure (7-5) **3-D effect Meth.-1- load-deflection curve for the 3-D free standing full-scale transmission tower (case -2- with various eccentricities)**

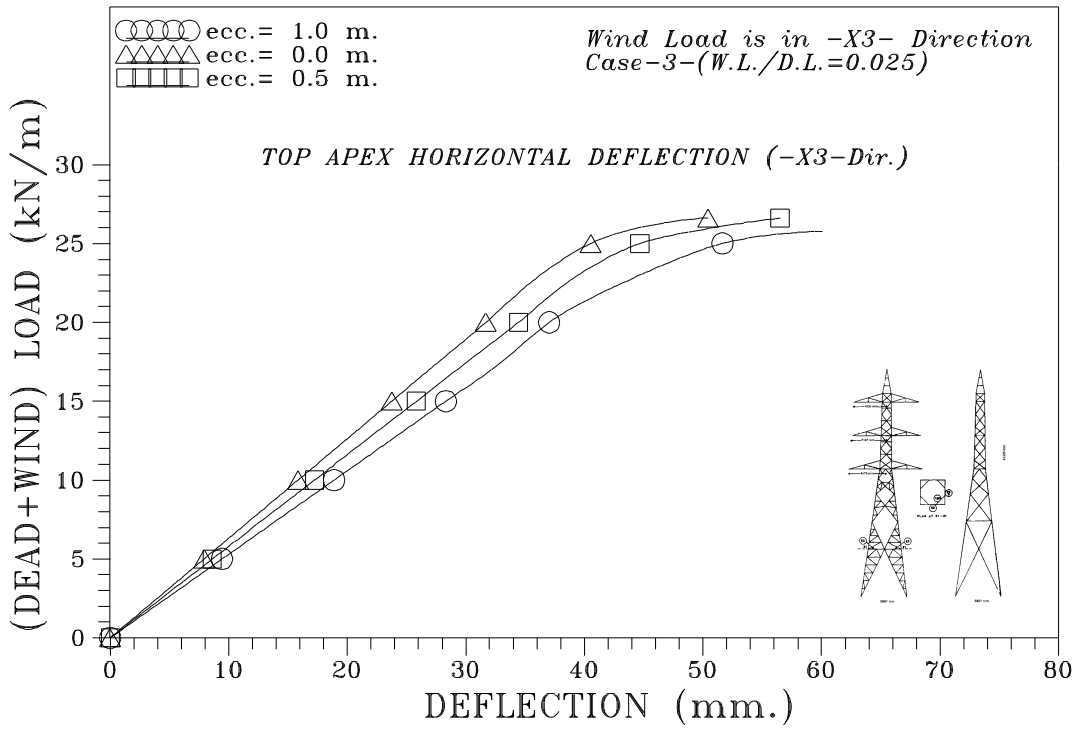

Figure (7-6) 3-D effect Meth.-1- load-deflection curve for the 3-D free standing full-scale transmission tower (case -3- with various eccentricities)

7.4 Parametric study no.3 (2-D lattice guyed tower):-

This case was analyzed by ***Issa*** and ***Avent*** [43]**,** using the discrete field analysis, the full detailed data of actual and equivalent properties, loading conditions, type of bracing, and type of sections are illustrated in tables (7-5.a , 7-5.b and 7-5.c), with the detailed sketch of the case in figure (7-7).

The work done by ***Issa*** and ***Avent*** [43] paved the way to other researchers since they put out all the required data for the tower, so instead of making the preliminary and guy analysis described earlier in order to introduce the initial geometry and cable forces, the tower already has a complete data as shown in table (7-5).

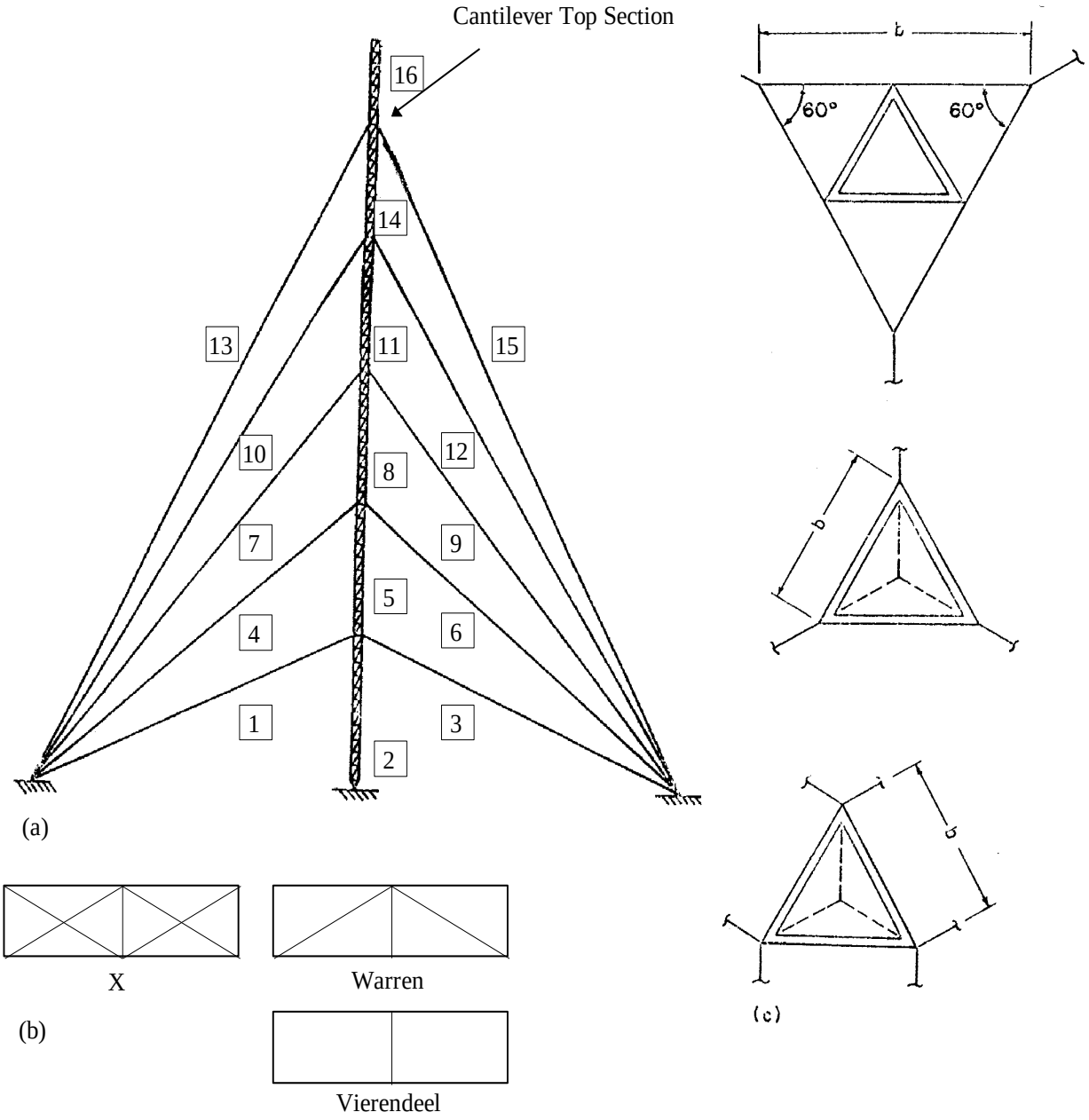

Figure (7-7) Lattice guyed transmission tower:-

a:-Typical guyed tower,

b:-Typical bar arrangements for space truss segment(X, Warren, & Vierendeel lacing),

c:-Typical cable support arrangement(starmount, 120 radial, and 60 radial)

Table (7-5.a): 3-D, 3-Legged, Constant & Variable Cross Sectional Area, Multi-Span Cable-Stayed Lattice Tower Actual Properties For Deferent Types of Bracing

Elment Data		***Actual Properties***															
No. "i"	***Type***	***Panel Size "m"***	***Length L_i"m"***	***Actual Area "mm^2"***			***Moment of Inertia Ix("$mm.^4$"*10^7)***			***Moment of Inertia Iy("$mm.^4$"*10^7)***			***Moment of Inertia Iz("$mm.^4$"*10^7)***			***Elastic Modulus E_i"Mpa"***	***Shear Modulus G_i"Mpa"***
				A_l	A_v	A_d	I_l	I_v	I_d	I_l	I_v	I_d	I_l	I_v	I_d	Same Cable Propert.For Both Cases "Const.&Varb." Cross Sec.	
1	Cable	-	113.31	-	-	-	-	-	-	-	--	-	-	-	-	165456	-
2	Tower	1.524 * 1.524	38.11	10387.08	a:2774.2 b:2774.2 c:3600.0	a:3941.93 b:3941.93 c:-	a:17.648 b:17.648 c:17.648	a:2.339 b:2.339 c:2.339	a:- b:- c:-	a:8.824 b:8.824 c:8.824	a:1.169 b:1.169 c:1.169	a:- b:- c:-	a:8.824 b:8.824 c:8.824	a:1.169 b:1.169 c:1.169	a:- b:- c:-	206820	79970.4
3	Cable	-	113.31	-	-	-	-	-	-	-	-	-	-	-	-	165456	-
4	Cable	-	135.71	-	-	-	-	-	-	-	-	-	-	-	-	165456	-
5	Tower	1.524 * 1.524	45.73	10387.08	a:2774.2 b:2774.2 c:3600.0	a:3941.93 b:3941.93 c:-	a:17.648 b:17.648 c:17.648	a:2.339 b:2.339 c:2.339	a:- b:- c:-	a:8.824 b:8.824 c:8.824	a:1.169 b:1.169 c:1.169	a:- b:- c:-	a:8.824 b:8.824 c:8.824	a:1.169 b:1.169 c:1.169	a:- b:- c:-	206456	79970.4
6	Cable	-	135.71	-	-	-	-	-	-	-	-	-	-	-	-	165456	-
7	Cable	-	162.05	-	-	-	-	-	-	-	-	-	-	-	-	165456	-
8	Tower	1.524 * 1.524	38.11	7677.40	a:2374.2 b:2374.2 c:3600.0	a:3600.0 b:3600.0 c:-	a:13.403 b:13.403 c:13.403	a:2.34 b:2.34 c:2.34	a:- b:- c:-	a:6.701 b:6.701 c:6.701	a:1.169 b:1.169 c:1.169	a:- b:- c:-	a:6.701 b:6.701 c:6.701	a:1.169 b:1.169 c:1.169	a:- b:- c:-	206820	79970.4
9	Cable	-	162.05	-	-	-	-	-	-	-	-	-	-	-	-	165456	-
10	Cable	-	198.76	-	-	-	-	-	-	-	-	-	-	-	-	165456	-
11	Tower	1.524 * 1.524	45.73	7677.40	a:2374.2 b:2374.2 c:3600.0	a:3600.0 b:3600.0 c:-	a:13.403 b:13.403 c:13.403	a:2.34 b:2.34 c:2.34	a:- b:- c:-	a:6.701 b:6.701 c:6.701	a:1.169 b:1.169 c:1.169	a:- b:- c:-	a:6.701 b:6.701 c:6.701	a:1.169 b:1.169 c:1.169	a:- b:- c:-	206820	79970.4
12	Cable	-	198.76	-	-	-	-	-	-	-	-	-	-	-	-	165456	-
13	Cable	-	231.81	-	-	-	-	-	-	-	-	-	-	-	-	165456	-
14	Tower	1.524 * 1.524	38.11	3600.00	a:1096.8 b:1096.8 c:3600.0	a:1729.03 b:1729.03 c:-	a:2.34 b:2.34 c:2.34	a:0.127 b:0.127 c:0.127	a:- b:- c:-	a:1.169 b:1.169 c:1.169	a:0.064 b:0.064 c:0.064	a:- b:- c:-	a:1.169 b:1.169 c:1.169	a:0.064 b:0.064 c:0.064	a:- b:- c:-	206820	79970.4
15	Cable	-	231.81	-	-	-	-	-	-	-	-	-	-	-	-	165456	-
16	Cant. Top Sact.	1.524 * 1.524	7.62	3600.00	a:1096.8 b:1096.8 c:3600.0	a:1729.03 b:1729.03 c:-	a:2.34 b:2.34 c:2.34	a:0.127 b:0.127 c:0.127	a:- b:- c:-	a:1.169 b:1.169 c:1.169	a:0.064 b:0.064 c:0.064	a:- b:- c:-	a:1.169 b:1.169 c:1.169	a:0.064 b:0.064 c:0.064	a:- b:- c:-	206820	79970.4
Remarks		**1-Type of Tower Configuration:- a: X-Bracing Tower, b: Warren Bracing Tower, c: Vierendeel or Batten Tower.**								**2-Case of Analysis (Cross Section Type):- Case "1":-Constant Cross Section(All tower members are same as member 8&11) , Case "2":-Variable Cross Section as mentioned in the table.**							

Table (7-5.b): 3-D, 3-Legged, Constant & Variable Cross Sectional Area, Multi-Span Cable-Stayed Lattice Tower Loading Data for Deferent Types of Bracing

Elm. Data		*Load Data*					
No.	*Type*	*WL "kN/m"*	*D.L. "kN/m"*	*Concent Moment M_o"kN/m"*	*Concent Force F_o"kN"*	*Cable Pretension "kN"*	
		For Cables Total Load is Recommended				*Case 1*	*Case 2*
1	Cable	-	0.0452	-	-	a:16.688 b:17.800 c:16.020	a:15.575 b:17.132 c:16.020
2	Tower	a:1.634 b:1.854 c:1.007	a:5.619 b:4.306 c:2.598	-	-	-	-
3	Cable	-	0.0452	-	-	a:16.688 b:17.800 c:16.020	a:15.575 b:17.132 c:16.020
4	Cable	-	0.0569	-	-	a:18.913 b:20.025 c:21.138	a:18.913 b:21.138 c:21.138
5	Tower	a:1.634 b:1.854 c:1.007	a:5.619 b:4.306 c:2.598	-	-	-	-
6	Cable	-	0.0569	-	-	a:18.913 b:20.025 c:21.138	a:18.913 b:21.138 c:21.138
7	Cable	-	0.0569	-	-	a:42.275 b:42.275 c:36.713	a:43.388 b:45.613 c:36.713
8	Tower	a:1.357 b:1.182 c:1.007	a:4.670 b:3.503 c:2.598	-	-	-	-
9	Cable	-	0.0569	-	-	a:42.275 b:42.275 c:36.713	a:43.388 b:45.613 c:36.713
10	Cable	-	0.0569	-	-	a:44.500 b:44.500 c:37.825	a:46.725 b:55.625 c:37.825
11	Tower	a:1.357 b:1.182 c:1.007	a:4.670 b:3.503 c:2.598	-	-	-	-
12	Cable	-	0.0569	-	-	a:44.500 b:44.500 c:37.825	a:46.725 b:55.625 c:37.825
13	Cable	-	0.0365	-	-	a:28.925 b:26.700 c:33.375	a:20.025 b:17.800 c:33.375
14	Tower	a:0.642	a:2.204	142.45	21.375	-	-

		b:0.555 c:1.007	b:1.649 c:2.598				
15	Cable	-	0.0365	-	-	a:28.925 b:26.700 c:33.375	a:20.025 b:17.800 c:33.375
16	Cantilever. Top Section	a:0.642 b:0.555 c:1.007	a:2.204 b:1.649 c:2.598	142.45	21.375	-	-

Table (7-5.c): 3-D, 3-Legged, Constant & Variable Cross Sectional Area, Multi-Span Cable-Stayed Lattice Tower equivalent Properties for Deferent Types of Bracing

Elm.	*No. of panels*	t_e *"mm."*	A_e $(t_e x b)$ *"mm.²"*	I_e *"mm.⁴"*	*u X-bracing*	*u warren*	*u Vierendeel*
2	25	2.378	3619.5	701431887.5	1.71×10^{-3}	3.42×10^{-3}	2.716
5	30	2.378	3619.5	701431887.5	1.19×10^{-3}	2.37×10^{-3}	3.910
8	25	2.378	3619.5	701431887.5	1.87×10^{-3}	3.75×10^{-3}	3.280
11	30	2.378	3619.5	701431887.5	1.30×10^{-3}	2.60×10^{-3}	4.723
14	25	2.378	3619.5	701431887.5	3.90×10^{-3}	7.80×10^{-3}	30.496
16	5	2.378	3619.5	701431887.5	0.0975	0.195	76.280

The shear parameter values are calculated using each type of bracing corresponding formulae (see table 3-2). It's assumed that the members are continuous after each guy level, so studying the **B.M.** parameter of each type of bracing system and for both constant and variable cross sections are shown in figures (7-8, 7-9**,** and 7-10) for the X, Warren, and Vierendeel bracing systems respectively.

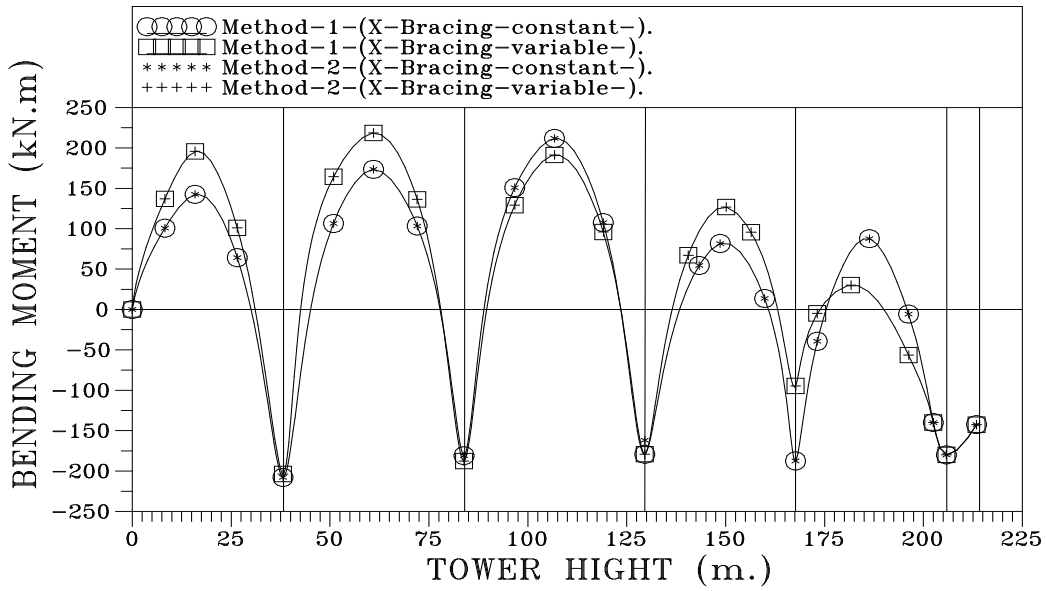

Figure (7-8) Height-bending moment curve for the 2-D, X-bracing type, constant and variable cross section cable stayed tower

Meth.-2- in the Vierendeel case did not work for the same reason of the bowing functions mentioned in chapter-6-, while in the other two types the difference between the methods is very small due to the small shear parameter we have. The shape and maximum moments of the X and Warren braced tower are very similar, while the Vierendeel maximum moments are significantly smaller. The other parameter to be studied is the deflected shape or the deflection vs. tower height which is shown in figures (7-11 and 7-12) for the constant and variable cross section respectively.

The flexibility of the Vierendeel tower is very obvious with respect to the X and Warren types, even though the maximum overall deflection is smaller. The new shear bowing effect derived in this study is one of the major causes that make ***Issa*** and ***Avent*** results away from the present approach by an average difference of **3.5%** .

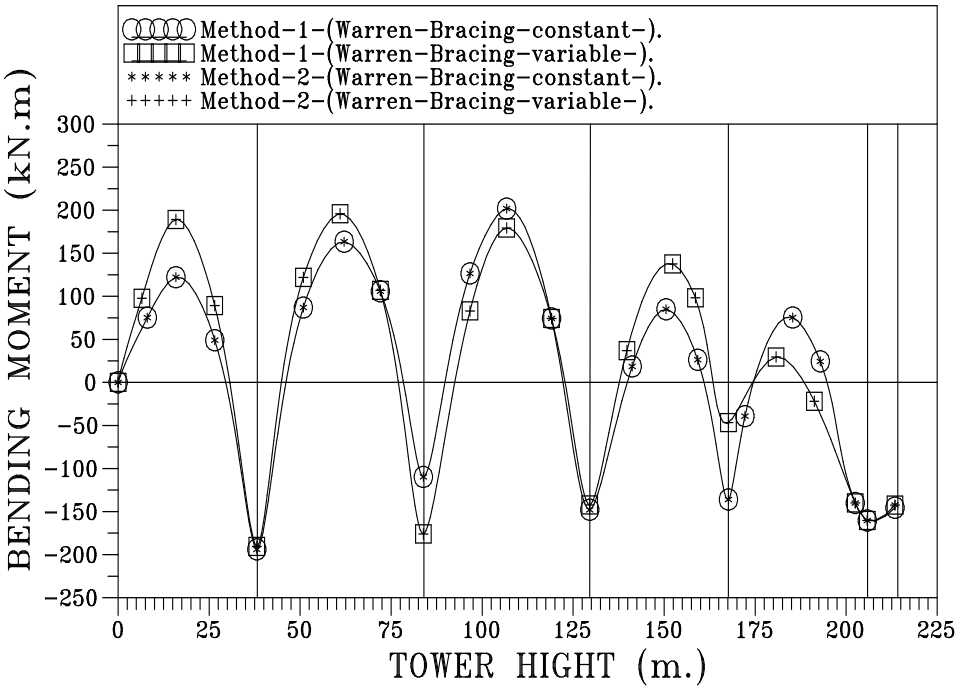

Figure (7-9) Height-bending moment curve for the 2-D, Warren-bracing type, constant and variable cross section cable stayed tower

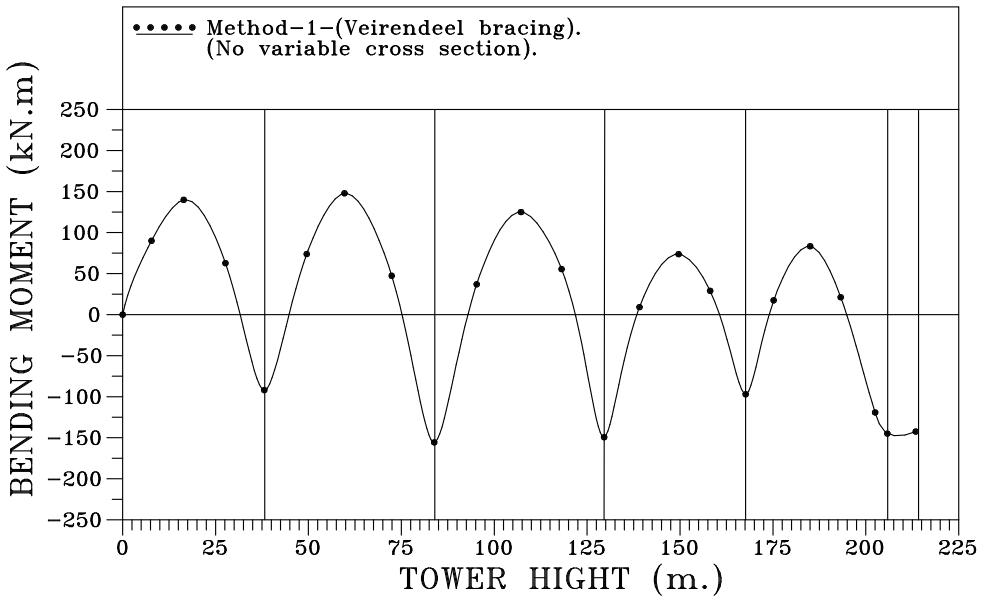

Figure (7-10) **Height-bending moment curve for the 2-D, Vierendeel-bracing type, constant and variable cross section cable stayed tower**

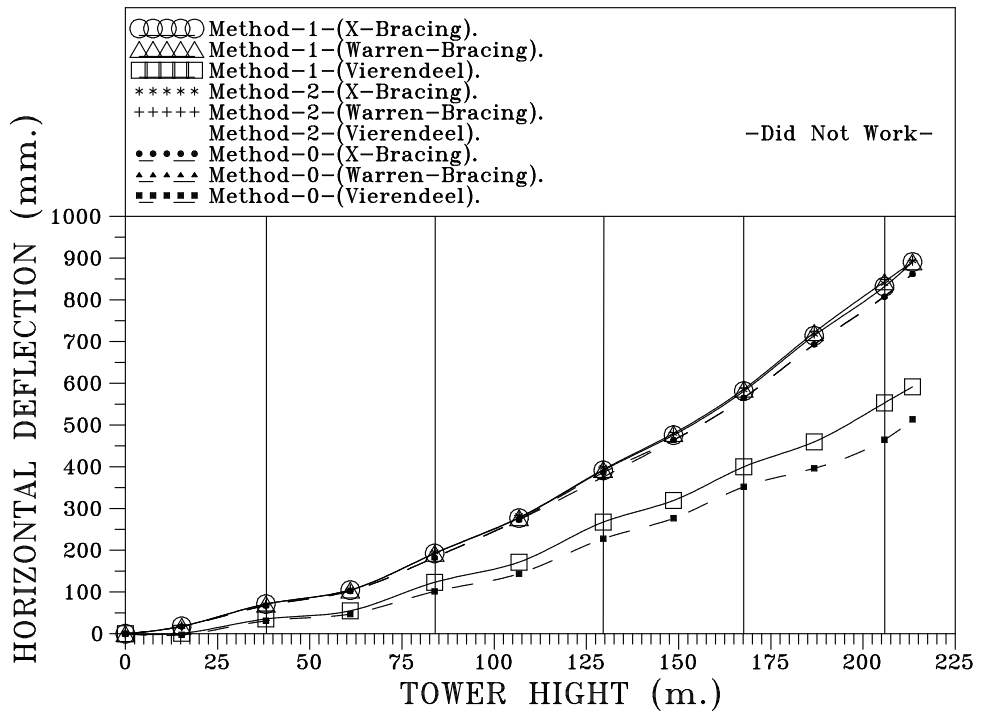

Figure (7-11) **Height-deflection curve for the 2-D, various bracing, constant cross section cable stayed tower.**

The last parametric study of this case is the axial force in the lattice mast, this parameter is illustrated in figures (7-13, 7-14, and 7-15) for the X, Warren and Vierendeel bracing systems respectively. The **D.L.** with the **W.L.** and the cable initial tensions significantly affect the axial force in the mast.

It can be obviously noticed that the guy reaction increases with the height increase which means that the high cables (which have more lengths) are more dominant for the behavior of the tower. Also it can be noticed that the light weight (i.e. the variable cross section) has less axial load.

Generally, the forces in Warren configuration are smaller than those in X-braced system, since the member sizes are identical for both systems and the Warren has only one diagonal in each panel instead of two, it appears that the Warren configuration is superior to X-braced. The Warren is approximately **30%** lighter and has smaller stresses. It's more difficult to make comparison with the Vierendeel configuration. While the axial forces are indeed significantly smaller, there are bending stresses that must also be considered.

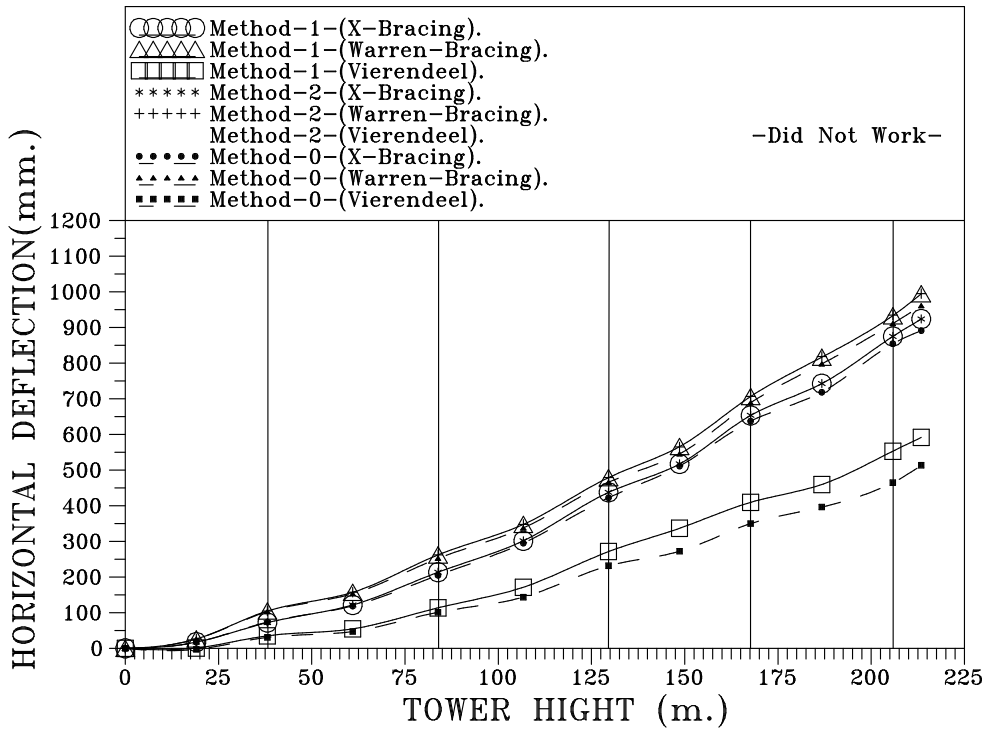

Figure (7-12) Height-deflection curve for the 2-D, various bracing, variable cross section cable stayed tower

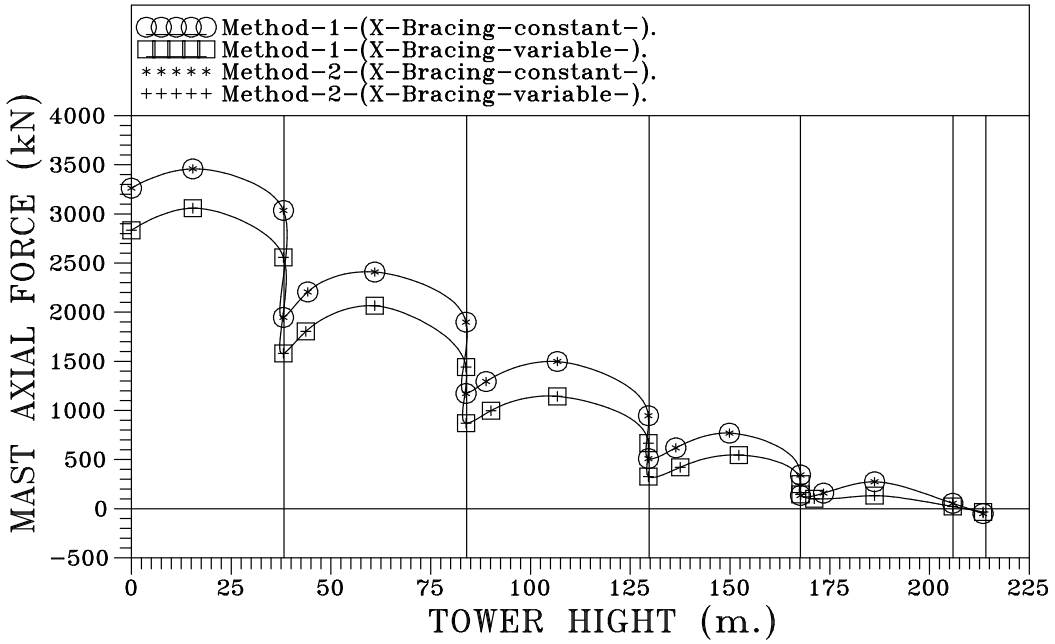

Figure (7-13) Height-axial force curve for the 2-D, X-bracing type, constant and variable cross section cable stayed tower

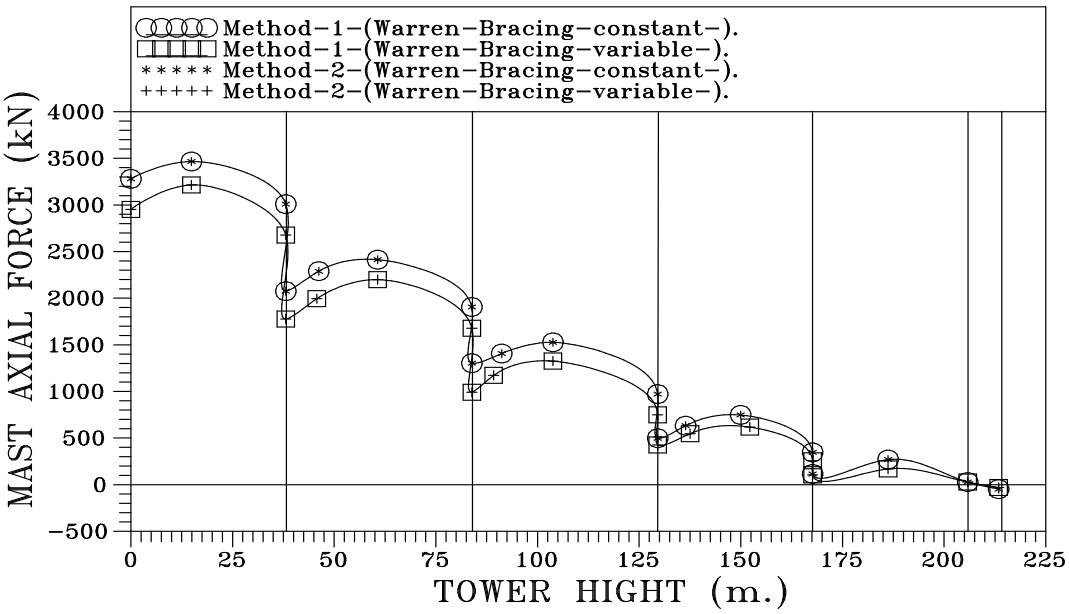

Figure (7-14) Height-axial force curve for the 2-D, Warren-bracing type, constant and variable cross section cable stayed tower

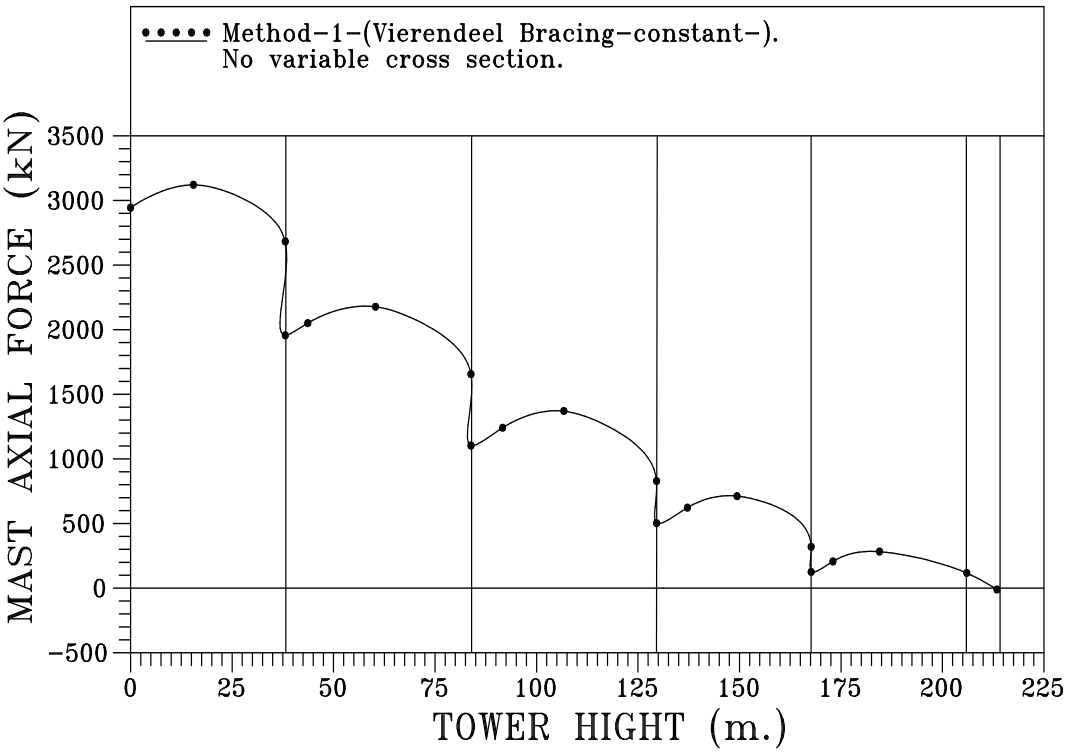

Figure (7-15) Height-axial force curve for the 2-D, Vierendeel-bracing type, constant and variable cross section cable stayed tower

7.5 Parametric study no.4 (3-D, Multilevel guyed tower):-

This example was taken as case study in the last chapter to check the validity of ***NASCFI*** based on the present new developed theoretical approach of the **T.S.M.**, but it's taken herein as a parametric study in order to observe the effect of increasing wind velocities and angle of directions on the mast axial force, the **B.M.** in the mast and each cable tension force.

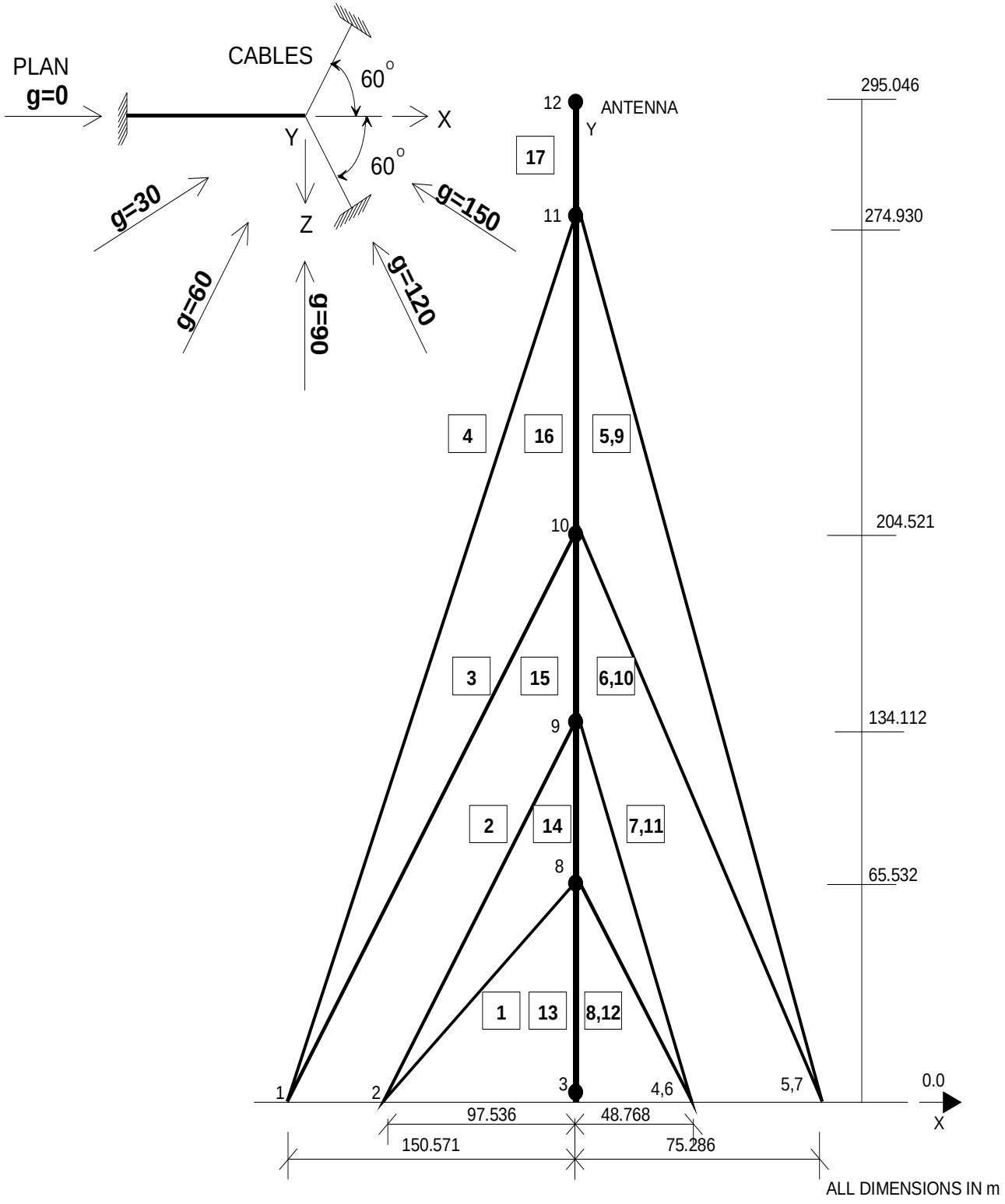

Figure (7-16) Multilevel solid mast guy tower:-

a: Top plan with wind directions (g), b: Side view.

All the properties, loading conditions and other data are detailed in the same table (6-25.a). The new variable parameter changes with the wind direction angle (α) increasingly with the horizontal from (**0**) to (**150**) as shown in the tower plan, figure (7-16).

The wind load vs. cable tensions of cable elements 4, 6, and 10 for all values of (**g**) are illustrated in figures (7-17, 7-18, and 7-19) respectively, while the wind loads vs. B.M. at node-9- are shown in figure (7-20), and the wind loads vs. the axial force in the bottom mast element-14- are shown in figure (7-21). The final observations concluded from the figures are:-

1. **The flexural shear effect has no role at all since solid sections are used.**
2. **The 3-D torsional effect (i.e. *SS* effect) has a considerable effect on the structure over all behavior.**

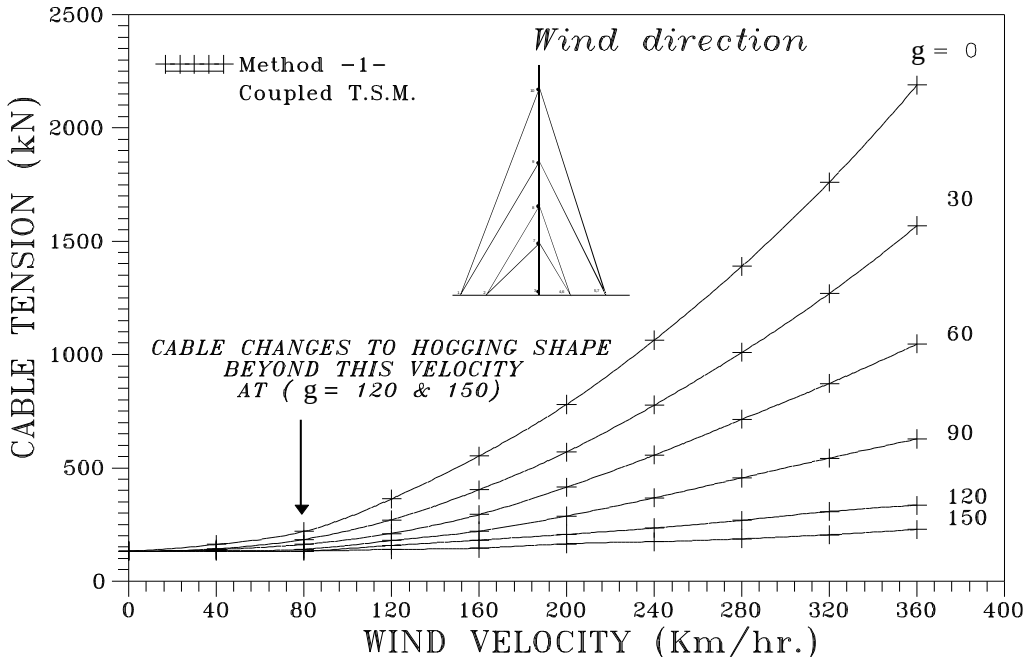

Figure (7-17) Wind velocity versus cable tension curve of cable -4- for the 3-D solid section cable stayed tower

3. **The tower failure is initiated by the yielding of windward guys at the velocity of about 288 Km/h. and the mast experiences a maximum strain at about 320 Km/h.**
4. **At velocity close to 350 Km/h the top windward cable element 2 reaches a maximum values of tensions very close to its breaking**

strength at g= 0, while at nearly the same velocity cable 3 exhibits a maximum tension at g=120, and for cable 4 at g=150.

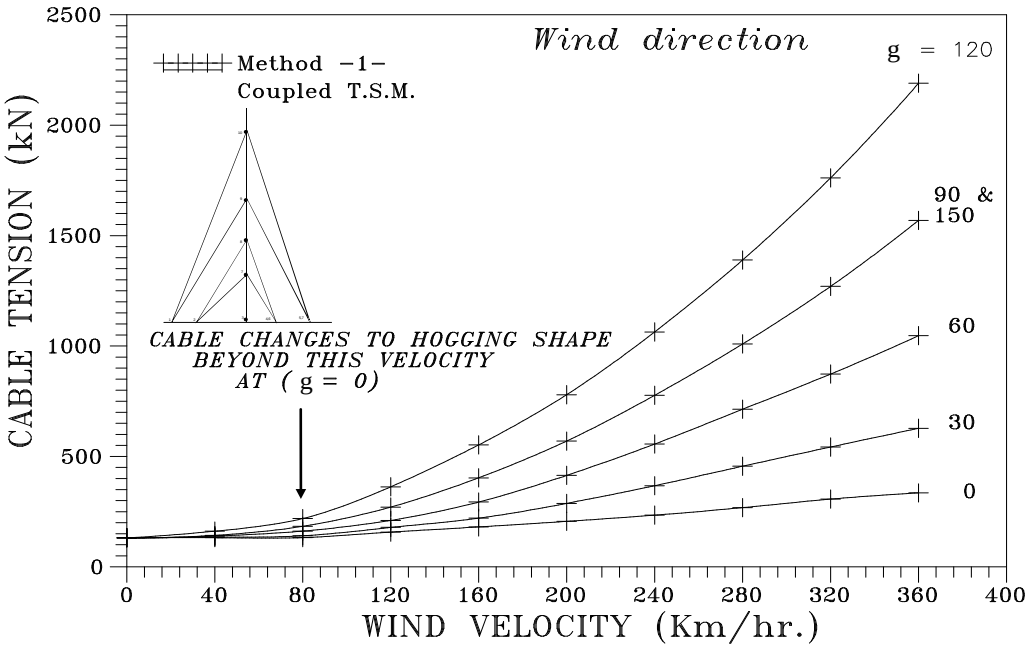

Figure (7-18) Wind velocity versus cable tension curve of cable -6- for the 3-D solid section cable stayed tower

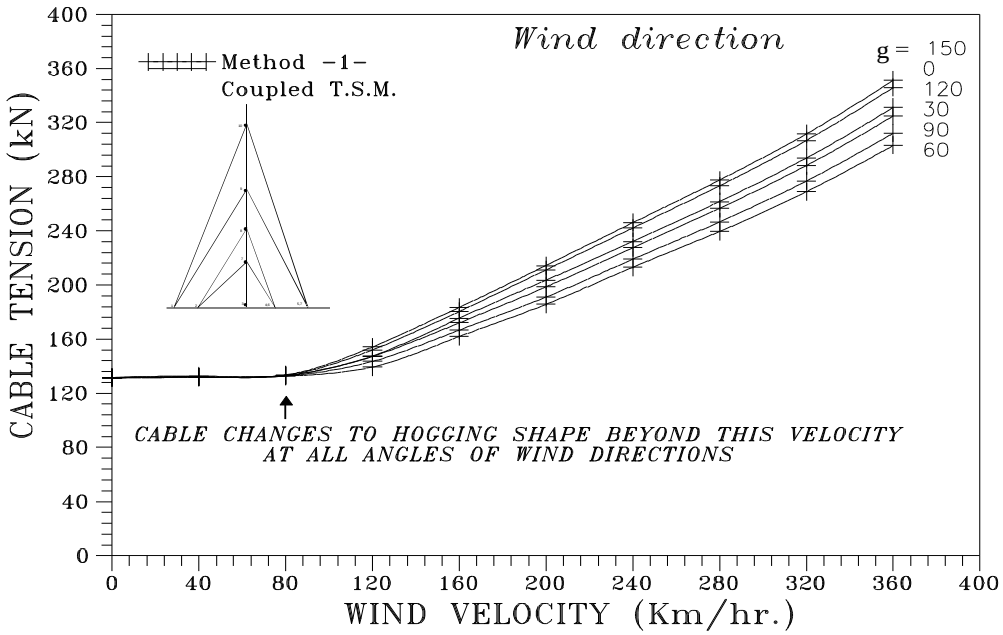

Figure (7-19) wind velocity versus cable tension curve of cable -10- for the 3-D solid section cable stayed tower

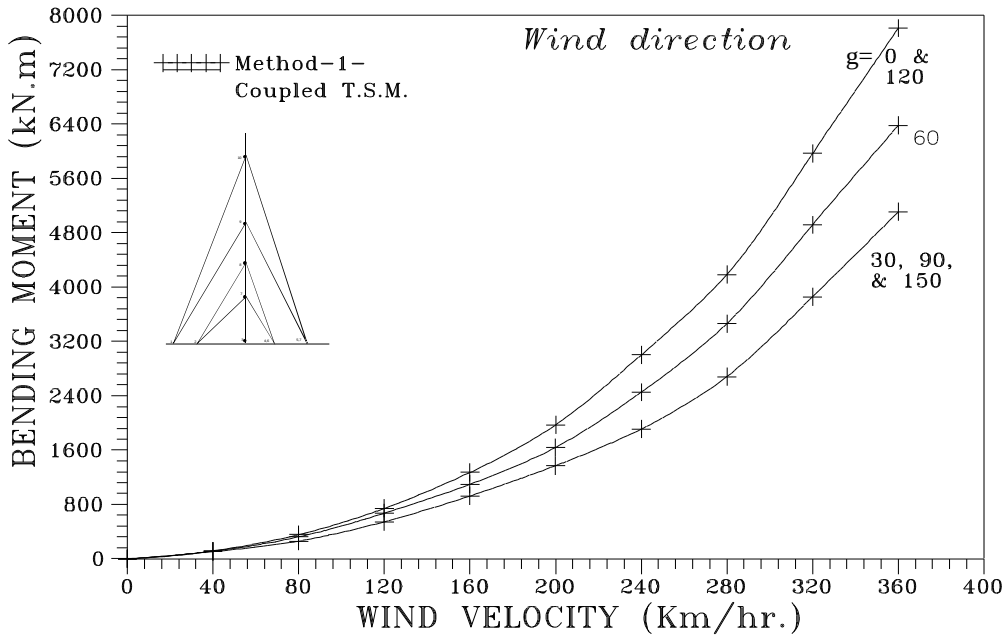

Figure (7-20) wind velocity versus bending moment curve of cable -2- of node -9- for the 3-D solid section cable stayed tower

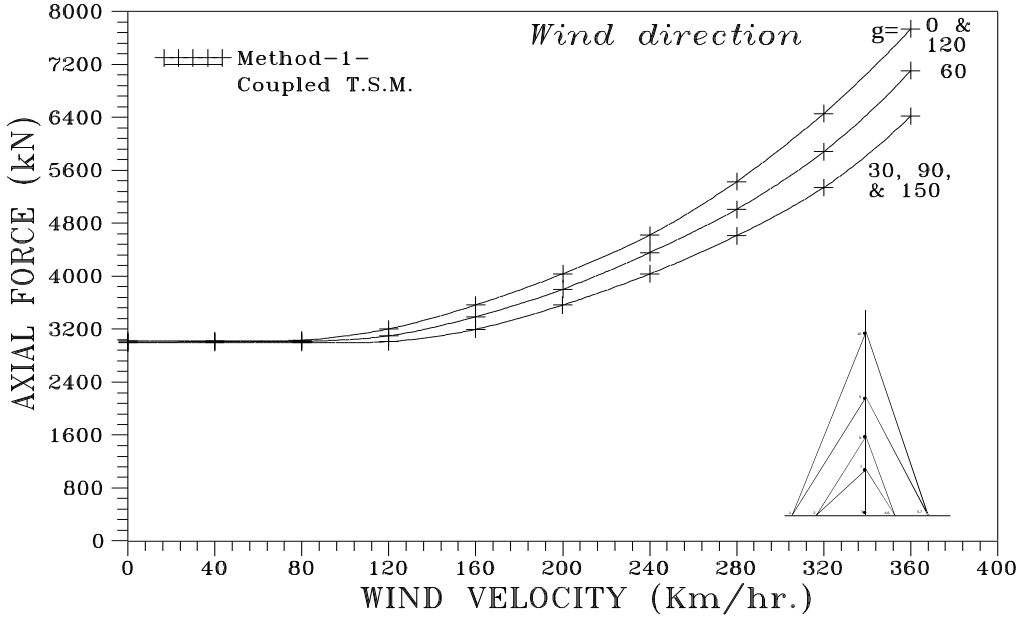

Figure (7-21) wind velocity versus axial force curve of cable -2- of bottom member for the 3-D solid section cable stayed tower

5. **At all wind directions the same hogging shape of cables starts at 80Km/h.**
6. **Cable 4 exhibits fluctuated W.L.-Tension behavior at different wind directions (g).**

7. **The present analysis indicates that the strains in cables and masts are substantially higher than the corresponding yield strains when external loads approach the magnitude of buckling loads, the matter that emphasizes the need to handle the problem by elasto-plastic approach.**

7.6 Parametric study no.5 (2-D, Cable-stayed bridge):-

In his book ***Troitsky*** [97], shows a laboratory test for a 2-D cable-stayed bridge where it's prototype, model, and test set-up are shown in figures (7-22.a, b and c).

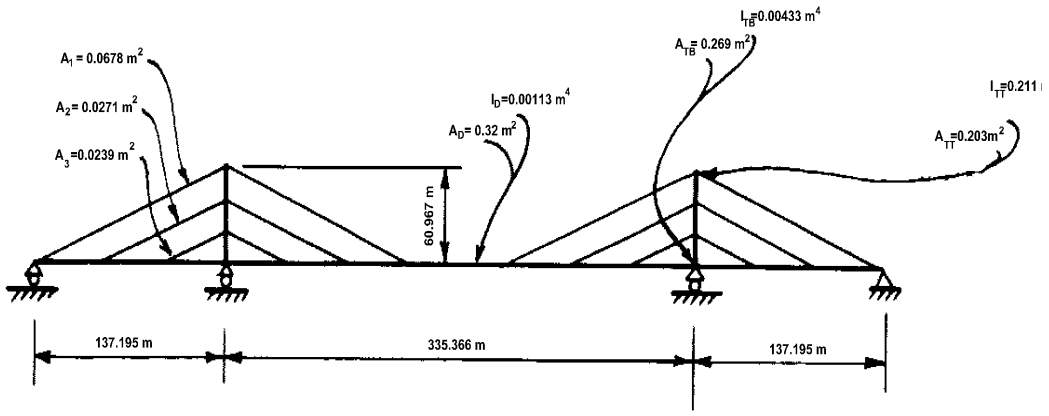

(a)

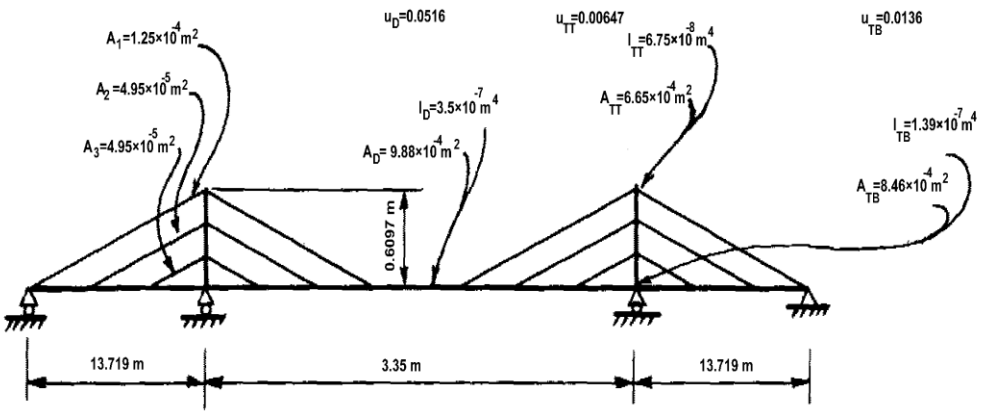

(b)

Figure (7-22: a-b) the 2-D cable stayed bridge: a: Geometry and sectional properties of bridge prototype. b: Dimensions and sectional properties of the bridge model.

(C) 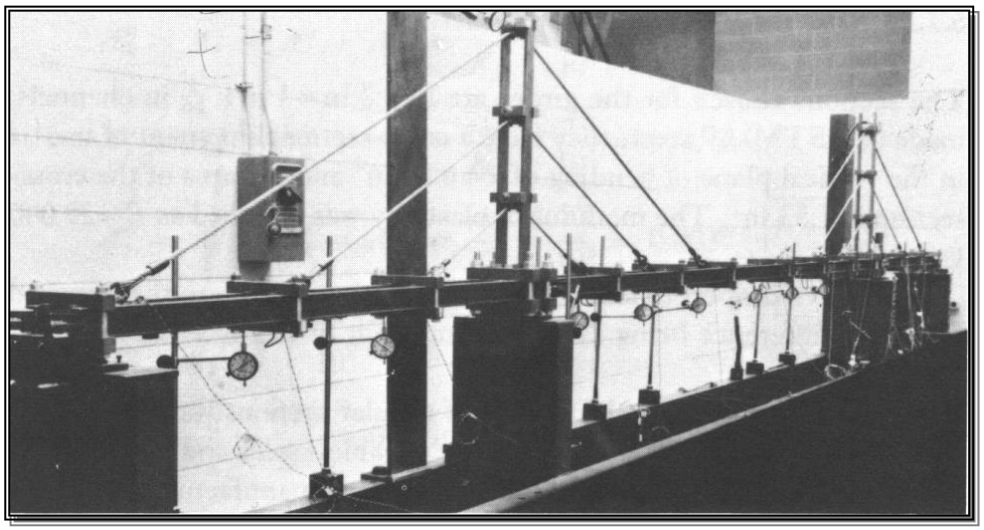

Figure (7-22) c: The bridge model test set-up.

The study of this case influence lines for the cable tensions and vertical nodal displacement are very important in the bridge design operation since it indicates the position of largest unit stress at the cross sections to be investigated and also the position of the load that gives the largest displacement occurred at nodes. Therefore a unit load (1kN) is applied vertically at each node at mid-span and between nodes as illustrated in figure (7-23).

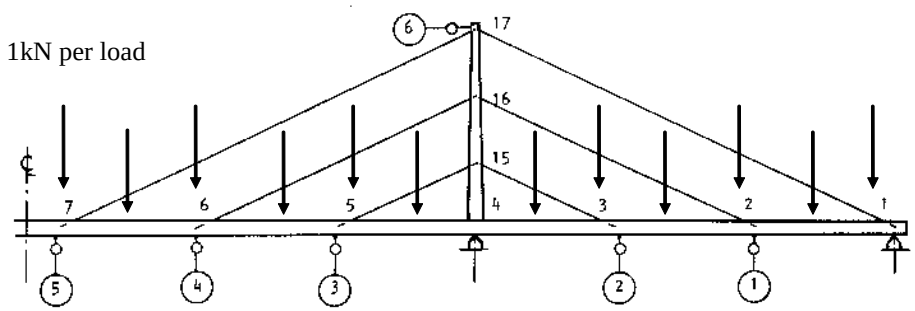

Figure (7-23) Bridge node numbering and load positions

The "u" values are relatively small indicated small shear contribution; however the model is analyzed using Meth.-1-. The 3-D effect (***SS*** effect) is absence here since 2-D analysis of the bridge is adopted.

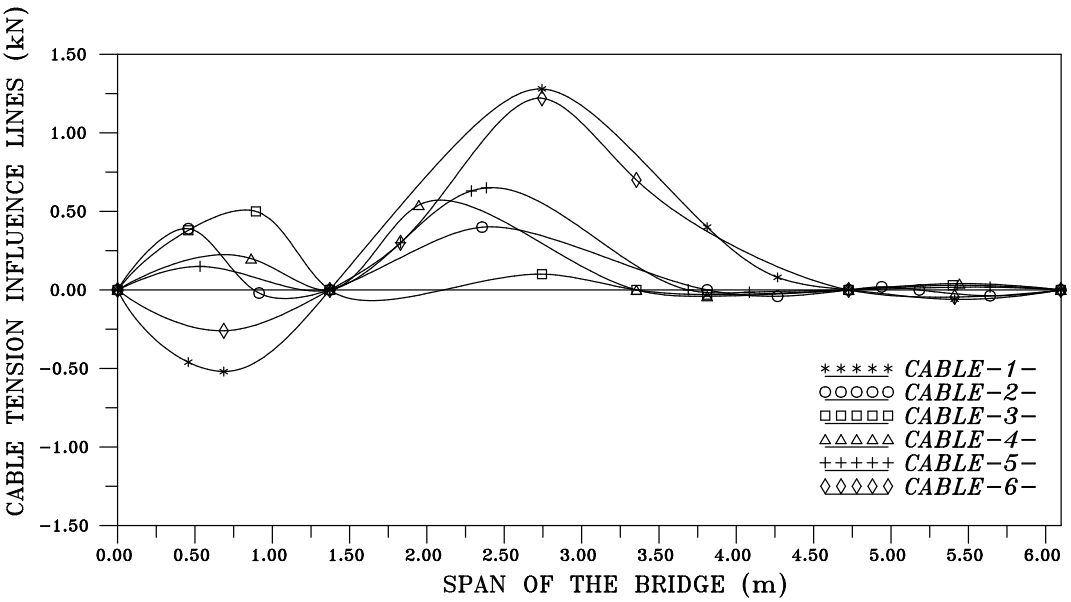

Figure (7-24) the influence lines for the cable tension

The results are shown in figures (7-24) and (7-25) for the influence lines of cable tension and nodal vertical deflection respectively, it can be noticed that:-

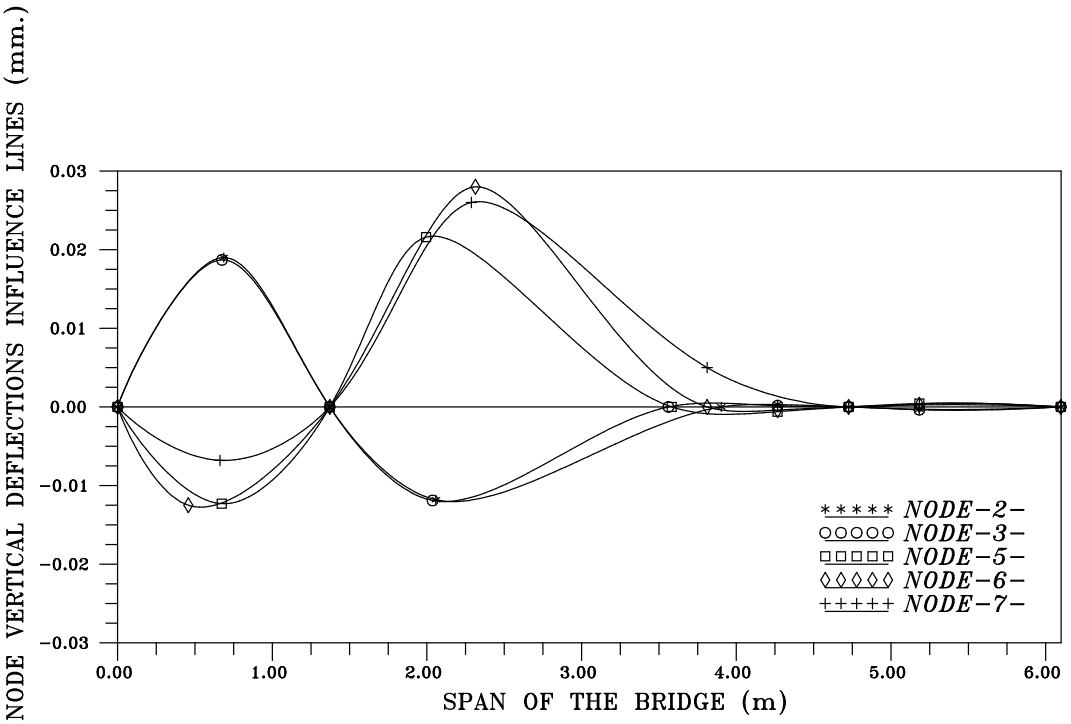

Figure (7-25) the influence lines for the nodal vertical displacement

The longer (outer) cables exhibit more tension forces than the inner cable and that the most critical position for cable tension are approximately at mid-span of the bridge.

For the deflection influence line node -6- and -7- which are approximately at mid-span represent the most critical nodes for the deflection behavior, in other word, the more outward the bridge we direct the less critical nodes we have , also the position of the load that create critical deflection is at mid-span. However, the present analysis gives a divergence with the experimental results not more than **3.42%** as a maximum value.

In this chapter and the one before, one of the most important conclusions can be established which is the equivalent shear parameter technique represents one of the most important and successfully applied procedure that can deal with analyzing all types of structures including the most complex structures that consist of a large number of elements. This technique exhibits an efficient time consumption treatment since it idealizes at least five lattice panels to only one equivalent element, the matter that leads to reduce all the time and efforts complications to very simple controlling structures.

CHAPTER EIGHT

CONCLUSIONS AND RECOMENDATIONS

8.1 Introduction:-

The new Flexural-Shear-Torsion coupled action 3-D T.S.M. described, derived, and approved in this work open the doors widely to a new idealisation of different types of structures that can easily reach the exact solutions of space beam-column theory.

The general conclusions and recommendations based on the present work can be summarised below.

8.2 Final Conclusions on the beam-column element:-

1. The basic theory of this work depends on the geometrical non-linear elastic 2-D and 3-D beam-column static theory.
2. The equivalent shear parameter, beam-column elements and the well-known T.S.M. approach both in 2-D and 3-D are adopted in this work.
3. The well-known total-shear slope and flexural-shear slope approaches are both adopted to include the effect of the shear deformations on the axial force **non-linear** effect, these two methods are indicated as **Meth.-1- and Meth.-2-** respectively while the non shear approach is denoted as **Meth.-0-.**
4. Accordingly, new **bowing functions** to include **the combined flexural-shear effect** on the **flexural bowing** action of **2-D and 3-D** beam-column elements are derived **and** checked for different values of shear parameter "**u**" by ***the author*.**
5. Also new **transverse effect (F.E.A.) functions** are derived for the shear effect using both methods**.**
6. In order to idealise the **Elastica,** both the non-linear small deflection theory and **the** large deflection theory (which actually is a small relative deflections using either ***Langrangian*** or ***Eularian*** coordinates), the well-known ***Snt.Vnt.*** and ***Wagner* effects** of uniform torsion for the non-warping sections assume no **shearing**

strain caused by **torsional moments** and hence no **axial shortening** of the beam-column member occurs since they adopted the well-known ***Snt.Vnt.*** **principles** of approximations. The new approach adopted in this work is that there is actually significant **axial displacement** formed during **the shear deformations** caused by ***Snt.Vnt.*** **uniform torsion,** and hence the complete derivations of the **axial deformations** developed thereby is achieved by ***the author,*** a point that leads ***the author*** to establish **the Flexural-Torsional coupled action effect** that the original **T.S.M.** ignored, so the other **effect of shear (the 3-D effect)** is evaluated and then we are as close as ever to **the exact Elastica. This new effect is called the "*SS* effect" and the new functions are called the "The Torsional Functions".**

7. All the special non-linearity effects of temperature, lack of fit, initial imperfections due to axial, shear, flexural moments and torsional moments, and support yielding for the beam-column elements are included in the present formulations as a Fixed End Action which also includes the applied load action.
8. About **20** case studies for different types of previously exact or theoretical solved or experimentally examined structures are taken to check the validity of the present approach.

8.3 Final Conclusions on the catenary cable element:

1. The basic theory adopted in this work is the elastic secant modulus of elasticity of catenary cables.
2. The special effects of **temperature, initial tensions,** and **sags,** for the catenary cable element are included in the present work.
3. About **10** cases some of them are field cases, others are experimental are taken as case studies to check the present formulation accuracy.

8.4 Final Conclusions on the numerical techniques:

1. The well-known ***Newton-Raphson*** incremental-iterative procedures are adopted in this work.

2. The work is uses load control convergence criteria rather than deflection control convergence criteria.
3. The well-known ***Cholisky Factorisation Technique*** is used in this work as an equation solver to deal with the high D.O.F. and effect of the prescribed displacements problems.

8.5 Final Conclusions on the multi-propose computer program (NASCFI):

1. A ***FORTRAN77***, ***LEIHY*** compiler multi-purpose program (***NASCFI***), is introduced by *the author* to handle the large deflection non-linear elastic stability static analysis of the 2-D and 3-D cable-frame interaction structures.
2. ***NASFI*** can deal with all types of structures starting from simple structures to the free standing electrical high-tension tangent tower, the cable-stayed transmission towers, and the cable-stayed and cable-suspended bridges.

8.6 Final conclusions on case and parametric study results:-

1. **The equivalent shear parameter technique represents one of the most important and successfully applied procedures that can deal with analyzing all types of structures including the most complex structures that consist of a large number of elements. This technique exhibits an efficient time consumption treatment since it idealizes at least five lattice panels to only one equivalent element, the matter that leads to reduce all the time and efforts complications to very simple controlling structures.**
2. **For the beam-column case studies, *NASCFI* show an excellent agreement of the new approach with exact large Elastica solved problems or with the experimental problems.**
3. **Shear effect plays a major role governing the P-Δ behavior of the open-web structure.**
4. **Including new effects of both (the flexural-shear bowing and the 3-D effect) the present work indicated a significant amount of**

difference with other researcher's results of the corresponding problems.

5. **Meth. -1- exhibits an excellent response in the cases solved regardless of the "u" value, while Meth. -2- failed in giving a logical response in the cases of high values of "u" i.e., the open-web structures, meanwhile it does give excellent results when "u" approximately < 1.**
6. **The results of the cable-frame interaction cases were excellent and sometimes closer to the experimental work done by others owing to the excellent convergence introduced by the new computational technique used in *NASCFI* (associating the cable-stayed problems).**
7. **In the absence of the axial load and the stability geometrical non-linearity, the material non-linearity becomes the dominant effect that governs the non-linear behavior and the geometrical non-linearity is linearly affects the curve, while in the presence of both actions the geometrical non-linearity becomes the dominant leaving the material non-linearity to behave linearly.**
8. **Changing the number of equivalent elements in the open web structures leads to misleading results.**
9. **Misestimated and erroneous results may be expected in the non-prismatic problems since this effect is not included in the present study, besides, the number of panels not being at least (5) leads to some overestimated results.**
10. **Changing the type of bracing system in the equivalent elements with the number of elements kept constant leads to a misleading result in the P-Δ behavior of the open-web structure.**
11. **There is an error in the 3-D effect (*SS* effect) analysis of the 3-D open-web problems owing to ignoring the warping contribution of the lateral buckling equations, which means that there must be a modification to the twisting functions equations (an alternate solution is by using equation 3-104 to include such**

effect), still the (*SS* effect) has a more influential role on the behavior of such structure than the corresponding solid sections.

12. **In some non-linear structures, although, all the geometrical non-linearities are included in the present analysis, these cases exhibit a linear P-Δ behavior, this is because that the T.S.M. of such cases remains constants throughout the loading increments and though the critical load can not be reached.**
13. **The new twisting effect (*SS* effect) has dominant role that relate the axial deformation with the shear effect acted transversely.**
14. **The variation of "E" value indicates that no difference occurred neither in the shear parameter "u" and accordingly in the shear effect represented by (Meth.-1-,-2-/Meth.-0-), nor in the shape of the curve which is a straight line, but meanwhile this variation does affect the strength and deflection values, i.e. the higher the "E" values the less deflection of the structure.**
15. **The cable-stayed bridge system is a hardened structural system in which the overall stiffness of the structure increases as the load increases.**
16. **The non-linearity is more pronounced in the taller tower-longer span model (Model-II-), this supports the fact that non-linearity in cable stayed bridges is of geometric nature.**
17. **As the span increases, larger deformations occur and strong non-linearity in the behavior of the bridge under loads takes place.**
18. **As complex geometry of the tower's configuration is adopted in design the static behavior of cable-stayed bridges cannot be fully represented by a planner analysis, so the 3-D models are essential in order to study the torsional behavior of the bridge under unsymmetrical loading, the behavior that does affect the overall behavior of the system.**
19. **The increase of the torsional rigidity decreases the (*SS* effect).**

20. **The higher the "u" values for the bridge deck and the tower the lower the strength of the bridge.**
21. **The higher the "u" the higher the (*SS* effect).**
22. **The longer (outer) cables exhibit more tension forces than the inner cable and that the most critical position for cable tension are approximately at mid-span of the bridge, and the more outward the bridge we direct the less critical nodes we have , also the position of the load that create critical deflection is at mid-span.**
23. **The higher the shear parameter (i.e. more open-web section) the higher axial displacement, besides increasing the initial imperfection per each shear parameter leads to an increase in the axial displacement which supports the fact that these types of structures are of stiffening nature and that the non-linearity type is geometrical in nature.**
24. **The higher the "H/V" ratio and the higher the eccentricity of the wind the higher the torsion induced by the eccentric wind. This increasing twisting moment affects the (P-Δ) behavior so the critical load decreases rapidly with increasing the eccentricity "e_c". Accordingly the applied torsion "T", and with the torsion increasing continuously the structure becomes weaker and weaker till the case of tornado occurs (very high torsional and twisting moments induced by high wind velocities and eccentricities) when the "P_{cr}" as well as the entire strength of the structure become so low.**
25. **Generally, the forces in Warren configuration are smaller than those in X-braced system, since the member sizes are identical for both systems and the Warren has only one diagonal in each panel instead of two, it appears that the Warren configuration is superior to X-braced. The Warren is approximately 30% lighter and has smaller stresses. It's more difficult to make comparison with the Vierendeel configuration. While the axial forces are indeed significantly smaller, there are bending**

stresses that must also be considered. The flexibility of the Vierendeel tower is very obvious with respect to the X and Warren types, even though the maximum overall deflection is smaller, and the guy reaction increases with the height increase which means that the high cables (which have more lengths) are more dominant for the behavior of the tower. Also it can be noticed that the light weight (i.e. the variable cross section) has less axial load.

26. **The change in wind speed and direction is highly affect the cable stayed bridges and towers behavior, however, at velocities approximately equal to 80 km/h and at all wind directions, the cables begin to hog for the symmetrical three cable stayed multi-level tower, but meanwhile for the symmetrical section cable stayed tower, the change in wind direction does not affect the 3-D (*SS* effect).**

8.7 Recommendations:-

The following extensions can be drowning from the present work:-

1. Although the effect of coupled flexural-warping torsion on axial stiffness of the open sections and non-uniform torsion has been mentioned in this work, further work must be continued and refined.
2. Work should make on:
   a. The effect of non-prismatic shear stability, bowing, and torsion functions.
   b. The effect of shear and 3-D on elastic-plastic behaviour functions.
   c. The dynamic 2-D and 3-D stability effects for the beam-column elements and the cable elements.
   d. The aerodynamic analysis of the towers and bridges i.e., the dynamic wind effects.
   e. The elastic foundations of the bridges.
   f. The seismic analysis of these structures.

g. The new (***SS*** effect) theory can be applied to more complicated structures that exhibit a significant amount of torsion such as aerospace structures

References

1. Alan, M.J. and A.R. Santhakumar, "Reliability Analysis and Full Scale Testing of Transmission Tower", Journal of Structural Engineering, ASCE, Vol. 122, No. 3, March 1996, pp. 338-343.
2. Al-Bermani, G.A. and S. Kitipornchai " Non-linear Analysis of Thin-walled Structures Using Least-Element Member", Journal of Structural Engineering, ASCE, Vol. 116, No. 1, January, 1990. pp. 215-234.
3. Al-Rawanduzy, A.A., "Large Displacement Elastic Stability Analysis of Plane Steel Frames and Dynamic Loads", Thesis presented to the University of Technology, Building and Construction Engineering Dept., January 1996, in partial fulfillment of the requirements for the Degree of Master of science.
4. Al-Sadder, S.Z.R., " Large Displacement Elastic-Plastic Stability Analysis of Plane Steel Frames with Non - Linear Connections", Thesis presented to the college of Engineering of the University of Baghdad, December 1994, in partial fulfillment of the degree of M.sc. in Structural Engineering.
5. Al-Sarraf, "Shear Effect on the Elastic Stability of Frames", The Structural Engineer Journal, Vol. 64B, No. 2, June 1986.
6. Alwash, N.A., "Non-linear Behavior and Optimal Design of Reinforced Concrete Vievendeel Truss", Thesis presented to the University of Technology; December, 1995, in partial fulfillment of the requirements for the degree of Doctor of Philosophy in Structural Engineering.
7. American Institute of Steel Construction AISC manual- ASD- (9/1989), USA
8. American National Standards ANSI, A-58-1, 1972.
9. Argyris, J.H., "Recent Advance in Matrix Methods of Structural Analysis", Pergamon press, London, 1964, pp. 115-145.
10. ASTM Standards, Annual Book, part-3 1972.
11. Avent, R.R., R.R.A. Issa, and M.L. Chow, " Discrete Field Stability Analysis of Planar Trusses", Journal of Structural Engineering, ASCE, Vol.117, No.2, February 1991, pp. 423-439.

12. Borri, C. and S. Chostrini, "Non-Linear Approach to the Stability Analysis of Space Beam Structures", International Journal of Space Structures, Vol. 4 No. 4, 1989, pp. 193.

13. Bridge, R.Q. and M.I.E. Aust, "Large Deflection Analysis of Portal Frames", Civil Engineering Transaction, 1979, pp. 75-79.

14. Britrec, S.J. "The Stability of Elastic Systems", Pergamon Press, Inc. 1973.

15. Buchanan, G.R.," Two-Dimensional Cable Analysis", Journal of Structural Division, ASCE, Vol. 96, No. ST7, July 1970, pp. 1581-1587.

16. Chajes, A. and D. Ling, "Post-Buckling Analysis of Guyed Towers", Journal of Structural Division, ASCE, Vol.107, No. ST12, December 1981, pp: 2313-2323.

17. Chajes, A. and J.E. Churchill, "Non-Linear Frame Analysis By Finite Element Methods", Journal of Structural Engineering, Vol.113, No.6, June 1987, pp. 1221-1235.

18. Chajes, A., "Post-Buckling Behavior", Journal of Structural Engineering ASCE, Vol. 109, No. 10, October 1983, pp. 2450-2460.

19. Chandra, R., D.N. Trikha, and P. Krishna, "Non-Linear Analysis of Steel Space Structures", Journal of Structural Engineering, ASCE., Vol.116, No. 4, April 1990, pp. 898-909.

20. Chen, W.F. and Atsuta, T. "Theory of Beam-Column", Vol.1 In Plane Behavior and Design, McGraw-Hill, Inc. New York 1976.

21. Chen, W.F. and Atsuta, T., "Theory of Beam-Column", Vol.2 In Space Behavior and Design, McGraw-Hill, Inc., New York 1976.

22. Cheng, F.Y., and C.P. Pantelides, "Static Timoshenko Beam-Column on Elastic Media", Journal of Structural Engineering, ASCE, Vol. 114, No.5 February 1987, pp. 1152-1172.

23. Chu, K.H., and D.C.C. Ma, "Non-Linear Cable and Frame Interaction", Journal of Structural Division ASCE, Vol. 102, No. ST3, March, 1976. pp 569-589.

24. Connor, J.J., Logcher, R.D. and Shing-Ching, C, "Non-Linear Analysis of Elastic Framed Structures", Journal of Structural Division, ASCE, Vol. 94, No. ST6, June, 1968, pp. 1525-1547.

25. Cook D.Cook, "Concepts and Applications of Finite Element Analysis", 2nd Edition, John Wiley and sons, Inc., New York, 1981.

26. Costello, G.A., and J.W. Phillips, "Post-Buckling Behavior of Guyed Towers", Journal of Structural Engineering, Vol.109.

27. Crisfield, M.A., "A fast Incremental/Iterative Solution Procedure That handles Snap-Through", International Journal of Computers and Structures, Vol.13, No. 1, January, 1981, pp.55-62.

28. Ekhands, S.G., M. Selvappalam, and M.K.S. Madugula, "Stability Functions for Three Dimensional Beam-Column", Journal of Structural Engineering, Vol. 115, No.2, February 1989, pp. 467.

29. Elyada, D. and C.D. Babcock, " Buckling and Non-Linear Response of Imperfect Three-Legged Truss Column, Journal of American Institute of Aeronautics and Astronautics, AIAA, Vol.25, No.2, 1986 pp. 324-330.

30. El-Zanaty, M.H. and Murray, D.W., "Non-Linear Finite Element Analysis of Steel Frames", Journal of Structural Engineering, ASCE, Vol.109, No.2, February 1983, pp. 353-368.

31. Epstien, M., D. Nixon, D.W. Murray, "Large Displacement in Elastic Analysis of Beam-Column", Journal of Structural Division, Vol. 104, No. STS, May 1978, pp. 841-853.

32. Fertis, D.G., and S. Pallak," Pseudolinear and Equivalent Systems for Large Deflections of Members", Journal of Engineering Mechanics ASCE, Vol.115, No.11, November 1989, pp. 2440-2459.

33. Fleming, J.F., "Non-Linear Static Analysis of Cable-Stayed Bridge Structures", International Journal of Computers and Structures, Vol. 10, 1979, pp. 621-635.

34. Fuji, F. "A Simple Mixed Formulation For Elastica Problems", International Journal of Computers and Structures, Vol. 15, No. 4, 1983, pp. 79-88.

35. Gere and Weaver, "Analysis of Framed Structures", D.Van Nostrand Company, 1963.

36. Guto, Y., S. Suzuki, and W. F. Chen, "Bowing Effect on Elastic Stability of Frames Under Primary Bending Moments" Journal of Structural Engineering, ASCE, Vol. 117, No. 1, January 1991, pp. 111-127.

37. Haisler, W.E., Stricklin, J.A. and Stebbins F.J., "Development and Evaluation of Solution Procedures for Geometrically Non-Linear Structural Analysis", AIAA Journal , Vol. 10, No. 3, 1972, pp. 264-272.

38. Harrison, B.H., "Interactive Non-linear Structural Analysis", Journal of Structural Divisions, ASCE, Vol. 102, No.ST7, July 1976, pp. 1353-1364.

39. Hathout, I.A., M.C. Temple, and J.S. Ellis, "Buckling of Space Stayed Columns", Journal of Structural Division, ASCE, Vol. 105, No. ST9, September 1979, pp. 1805-1821.

40. Hinton, E. and D.R.J. Owen, "Finite Element Programming" Academic Press, Inc. London 1977.

41. Hsiao, K.M. and F.Y. Hou, "Non-Linear Finite Element Analysis of Elastic Frames", International Journal of Computers and Structures, Vol. 26, No. 4, pp 693-701, 1987.

42. Huseyin, K. "Non-Linear Theory of Elastic Stability", Noordhoff International Publishing, Leyden, Netherlands, 1975.

43. Issa R.R.A. and R.R. Avent, "Microcomputer Analysis of Guyed Towers as Lattices", Journal of Structural Engineering ASCE, Vol. 117, No. 4 April 1991, pp. 1238-1256.

44. Jennings, A., "Frame Analysis Including Change of Geometry", Journal of Structural Division, ASCE, Vol. 94, No. ST3, March 1968, pp. 627-644.

45. Judd, B.J. and R.S. Wheen, "Non-Linear Cable Behavior ", Journal of Structural Division, ASCE, Vol. 104, No. ST3, March 1978, pp. 567-575.

46. Kam, T.Y., "Large Deflection Analysis of Inelastic Plane Frames", Journal of Structural Engineering, ASCE, Vol. 114, No.1, January, 1988. pp. 184-197.

47. Kassimali W.A. "Large Deformation Analysis of Elastic-Plastic Frames", Journal of Structural Engineering ASCE, Vol. 109, No.8, August 1983, pp. 1869-1887.

48. Kassimali W.A., and R. Abbasnia, "Large Deformation Analysis of Elastic Space Frames", Journal of Structural Engineering ASCE, Vol. 117, No. 7, July 1991, pp. 2069-2087.

49. Kinney, J.S. "Indeterminate Structural Analysis", Addison-Wesley Publishing Company, Beading, Massachusetts, USA, 1967.

50. Kolousek, V. et.al., "Wind Effects on Civil Engineering Structures", Elsevier, Amsterdam, 1984.

51. Korn, A.," Effect of Bowing in Rectangular Plane Frames", Journal of Structural Division, ASCE, Vol.107, No. ST3, March 1981, pp. 569-574.

52. Kouhia, R., "On the Solution of Non-linear Finite Element Equations", International Journal of Computer and structures, Vol.44, No.1/2, 1992,pp. 243-254.

53. Kounadis, A.N., "An Efficient Simplified Approach for the Non-Linear Buckling Analysis of Frames", Journal of American Institute of Aeronautics and Astronautics, AIAA, Vol.23, No. 8, 1984, pp. 1254-1259.

54. Lai, S.M.A., and J.G. MacGregor, "Geometric Non-Linearitics in Unbranched Multistory Frames", Journal of Structural Engineering ASCE, Vol.109, No. 11, November 1983, pp. 2520-2545.

55. Leiphon, H., "Stability of Elastic Systems", First Eddition, Sijthoff and Noordhoff, Netherlands, 1980

56. Lin, F.J., and E.C. Glauser, "Behavior of Laced and Battened Structural Members", Journal of Structural Division, ASCE, Vol. 96, No. ST7, July 1970, pp. 1377-1401.

57. Lindgren, S. "Shear Flexibility", Journal of Structural Division, ASCE, Vol. 105, No. ST10, October 1979, Technical Note, pp. 2117-2121.

58. Livesely, R.K., "The Applications of an Electronic Digital Computer to Some Problems of Structural Analysis", the Structural Engineer, Vol. 34, No.1, London, England, 1956, pp. 1-12.

59. Livesely, R.K., Chandler D.B., "Stability Functions For Structural Frameworks", Manchester University Press, Manchester, 1956.

60. Lothers, J.E.," Design in Structural Steel", 3rd Edition, Printice-Hall Inc., 1972, USA.

61. Majid, K.I.," Non-Linear Structures", First Edition, the Butterworth and Co., England, 1972.

62. Mendis, P.A. and Darvall, P.L., "Stability Analysis of Softening Frames", Journal of Structural Engineering, ASCE., Vol.14, No. 26, 1987. pp. 1057-1073.

63. Miek, J.K. and S. Loganathan, "Geometrically Non-Linear Behaviour of Space Frames Structures", International Journal of Computers and Structures, Vol.31, No. 1, 1989, pp. 35-45.

64. Miek, J.K. and S. Loganathan, "Geometrical and Material Non-Linear Behaviour of Beam-Column", International Journal of Computers and Structures, Vol.34, No. 1, 1990, pp. 87-100.

65. Nakashima, M., Nakamura Takeshi and M. Wakabayashi, "Post Bukling Instability of Steel Beam-Column", Journal of Structural Engineering, ASCE., Vol. 109, No. 6, June 1983, pp. 1414-1430.

66. Nazmy, A.S., and A.M. Abdel-Ghaffar, " Three Dimensional Non-Linear Static Analysis of Cable-Stayed Bridges", International Journal of Computers and Structures, Vol.34, No.2, 1990, pp.257-271.

67. Noor, A.K., "Non-Linear Analysis of Space Truss", Journal of Structural Division, ASCE., Vol. 100, No. ST3, March, 1974.

68. Noor, A.K., and L.S. Weisstein, " Stability of Beam like Lattice Trusses", Computer Methods in Applied Mechanics And Engineering, Vol. 25, 1981, pp. 179-193.

69. Onn, G., "Shear Effect of Beam Stiffness Matrix", Journal of Structural Engineering, ASCE, Vol.109, No.9, September, 1983, pp. 2216-2221.

70. Oran, C. and A. Kassimali, "Large Deformation of Framed Structures Under Static and Dynamic Loads:, International Journal of Computers and Structures, Vol.6, 1976, pp. 539-547.

71. Oran, C., "Tangent Stiffness in Plane Frames", Journal of Structural Division, ASCE., Vol. 99, No. ST6, June 1973, pp. 973-985.

72. Oran, C., "Tangent Stiffness in Space Frames", Journal of Structural Division, ASCE, Vol. 100, No. ST7, July 1974, pp. 1473-1487.

73. Panayatounakos, D.E. and Treocaris, P.S., "Large Deflections of Buckled Bars under Distributed Axial Load", International Journal of Solids Structures, Vol. 24, No. 12. 1988, pp. 1179-1192.

74. Paramaisvam, V., S.P.T.R. Gowda, and D.M. Raj, "Timoshenko Beam Finite Element with Four DOF and Convergence of $O(h^4)$", International Journal of Computers and Structures, Vol.43, 1992, pp. 1187-1189.

75. Popov, E.P. "Introduction to Mechanics of Solids" Printice Hall, Inc., New-Jersey, 1968.

76. Raman, N.V., G.V. Surya Kumar, and V.V. Sreedhara Rao, “Large Displacement Analysis of Gyed Towers", International Journal of Computers and Structures, Vol. 28, No. 1, 1988, pp. 93-104.

77. Renton, J.D., "Buckling of Long Regular Trusses", International Journal of Solid Structures, Vol. 9, 1973, pp. 1489-1500.

78. Renton, J.D., "Stability of Space Frames by Computer Analysis", Journal of Structural Division, ASCE, Vol. 88, No. ST4, August 1962, pp. 81-103.

79. Ricks, E., "An Incremental Approach to the Solution of Snapping and Buckling Problems", International Journal of Solids Structures, Vol.15, No.7, 1979, pp.529-551.

80. Russell, J.J., J.D. Morgan, and W.M. Henghold, "Cable Equilibrium and Stability In a Steady Wind", Journal of Structural Division, ASCE, Vol. 109, No. ST2, February 1978, pp. 301-311.

81. Saffan, S.A." Non-Linear Behavior of Structural Plane Frames", Journal of Structural Division, ASCE, Vol.89, No. ST4, August, 1963, pp. 557-579.

82. Saffan, S.A. "Theoretical Analysis of Suspension Roots", Journal of Structural Division, ASCE, Vol.969, No. ST2, February, 1970, pp. 393-405.

83. Schrefler, B.A. and S. Oborizzi, " A total Lagrangian Geometrically Non-Linear Analysis of Combined Beam and Cable Structures", International Journal of Computers and Structures, Vol. 17, No. 1, 1983, pp. 115-127.

84. See, T. and R.E. McConnel, "Large Displacement Elastic Buckling of Space Structures", Journal of Structural Engineering, ASCE, Vol.112, No.5, May, 1986, pp.1052-1069.

85. Sedeek. K.F. "Elastic-Plastic Behavior of Steel Frame Structures", Thesis, presented to the University of Technology, September-1990, in partial fulfillment of the requirements of the Degree of M.sc. in Structural Engineering.

86. Shen, Z.Y., and K. Ding, "A New- Theory of Thin Walled Beams Involved the Effects of Shear Deformations", Computational Mechanics, (Cheung, Lee and Leung (eds), 1991, Balkema, Kotterdam).

87. Smith, J.M. and D.V. Griffiths, "Programming the Finite Element Method, Second Eddition, John Wiley and Sons Ltd., 1988.

88. Stomans, S.H., "Stability Criteria for X-Bracing Systems", Journal of Engineering Mechanics, ASCE, Vol. 114, No.8, August 1988. pp. 1426-1434.

89. Sully, R.M. and G.J. Hancock, "Behavior of Cold-Formed SHS Beam-Column", Journal of Structural Engineering, ASCE, Vol. 122, No.3 March 1996, pp. 326-336.

90. Svensson, S.E., and J.Kragerup, "Collapse Loads of Laced Columns", Journal of Structural Division ASCE, Vol.108, No. ST6, June 1982, pp. 1367-1384.

91. Tang, M.C., "Buckling of Cable-Stayed Girder Bridge", Journal of Structural Division, ASCE, Vol.102, No. ST9, September, 1976, pp. 1675-1684.

92. Tebedge, N., "Buckling of Pretwites Columns", Journal of Structural Division, ASCE, Vol. 108, No. ST5, May 1982, pp. 1124-1139.

93. Timoshenko and Goodier, "Theory of Elasticity", McGraw-Hill 1970.

94. Timoshenko, S.P. and Gere, J.M., "Theory of Elastic Stability" Second Edition, McGraw-Hill Book Co., Inc., New York, 1961.

95. Temple, M.C., "Buckling of Stayed Columns ", Journal of Structural Division, ASCE, Vol. 103, No.ST4, April 1977, pp. 839-851.

96. Temple, M.C., M.V. Parkash, and J.S. Ellis," Failure Criteria for Stayed Columns", Journal of Structural Engineering, ASCE., Vol. 110, No.11, November 1984, pp. 2677-2689.

97. Troitsky, M.S. "Cable-Stayed Bridges-Theory and Design", Crosby Lockwood Staples, London 1977.

98. Urelius, D.E. and D.W. Fowler, "Behavior of Prestressed Cable Truss Structures" Journal of Structural Division, ASCE, Vol. 100, No. ST8, August 1974, pp. (1627-1641).

99. Varghese, P.C. and C.G. Chettiar, "Lateral Stability of Plane Open-Web Structures", Journal of Structural Division, ASCE, Vol. 100, No. ST11, November, 1974, pp. 2223-2233.

100. Vinnaketa, S. and P. Aysto, "Inelastic Spatial Stability of Restrained Beam-Column", Journal of Structural Division, ASCE, Vol. 100, No. ST11, November, 1974, pp. 2235-2254.

101. Wang, C.K., and J.K. Stiller, "Stability of Cable-Stayed Rigid Frames", Journal of Structural Division, ASCE, Vol. 105, No. ST11, November, 1979, pp. 2383-2398.

102. Waszczyszyn, Z. "Numerical Problems of Non-Linear Stability Analysis of Elastic Structures", International Journal of Computers and Structures, Vol. 17, No. 1, pp. 13-24, 1983.

103. Wen, R.K. and J. Rahim Zadeh, "Non-Linear Elastic Frame Analysis by Finite Element", Journal of Structural Engineering, ASCE., Vol. 109, No. 8, August, 1983, pp. 1952-1971.

104. Williamson, R.A., and M.N. Margolin, " Shear Effects in Design of Guyed Towers" Journal of Structural Division, ASCE., Vol. 92, No. ST5, October, 1966, pp. 213-235.

105. Wilson, A.J. and R.J. Wreen, "Inclined Cables Under Load-Design Expressions", Journal of Structural Division, ASCE, Vol. 103, No. ST5, May, 1977, pp. 1061-1078.

106. Wong, K.C. and M.C. Temple, "Stayed Column with Initial Imperfection", Journal of Structural Division, ASCE, Vol. 108, No. ST7, July, 1982, pp. 1623-1640.

107. Wong, M.B. and Tin-Loi, F., "Geometrically Non-Linear Analysis of Elastic Framed Structures", International Journal of Computers and Structures, Vol. 34, No. 4, 1990, pp. 633-640.

108. Wood, R.D. and Zienkiewicz, O.C., "Geometrically Non-Linear Finite Element Analysis of Beams, Frames Arches and Axissymmetric Shells", International Journal of Computers and Structures, Vol. 7, No. 5, 1979, pp. 725-735.

109. Yang, Y.B., and W.McGuire, "Joint Rotation and Geometric Non-Linear Analysis", Journal of Structural Engineering, Vol. 112, No. 4, April, 1986, pp. 879-905.

Appendix A

Total shear and flexural shear methods

In his paper [5], ***Al-Sarraf*** (1986) presented modified stability functions ($\overline{C}_1$) and ($\overline{C}_2$) including shear effect by using the total shear slope (identified in the present work as Meth.-1-). He also presented the modified stability functions including shear effect by using the flexural shear slope (identified in the present work as Meth.-2-) in a paper not published yet.

A-1 the total shear slope (Meth.-1-)

From figure (A-1), it is clear that the elastic stability of a prismatic strut taking into consideration the effect of shear force by Meth.-1- subjected to axial load (P) depend on the solution of the differential equations.

$$\frac{dy}{dx} = -\frac{dy_m}{dx} + \frac{nV_x}{AG} = \psi + \beta = \text{Flexural slope} + \text{Shear slope} \quad \text{.....(A-1)}$$

by differentiation with respect to (x):-

$$\frac{d^2y}{dx^2} - \frac{d^2y_m}{dx^2} + \frac{n}{AG}V'_x = -\frac{M_x}{EI} + \frac{n}{AG}V'_x \quad \text{.....(A-2)}$$

The bending moment (M_x) and the shear force (V_x) can be written as:-

$$M_x = \left(1 - \frac{x}{L}\right)M_1 - \frac{x}{L}M_2 + Py \quad \text{.....(A-3)}$$

$$V_x = -\frac{\left(M_1 + M_2\right)}{L} + P\frac{dy}{dx} \quad \text{.....(A-4)}$$

by substituting the expressions for (M_x) and (V_x) into (A-2) yields:-

$$\left(1 - \frac{n}{AG}P\right)\frac{d^2y}{dx^2} + \frac{P}{EI}y = \frac{1}{EI}\left(M_1\frac{x}{L} - 1\right) + M_2\frac{x}{L} \quad \text{.....(A-5)}$$

The general solution of such equation is:-

$$y = D_1 \sin \omega x + D_2 \cos \omega x + \frac{M_1}{P}\left(\frac{x}{L} - 1\right) + \frac{M_2}{P}\frac{x}{L} \quad \text{.....(A-6)}$$

where:-

$$\omega^2 = \frac{P}{EI}\left(\frac{1}{1-\frac{n}{AG}P}\right) = \frac{\pi^2}{L^2}\bar{\rho} \quad \text{.....(A-7)}$$

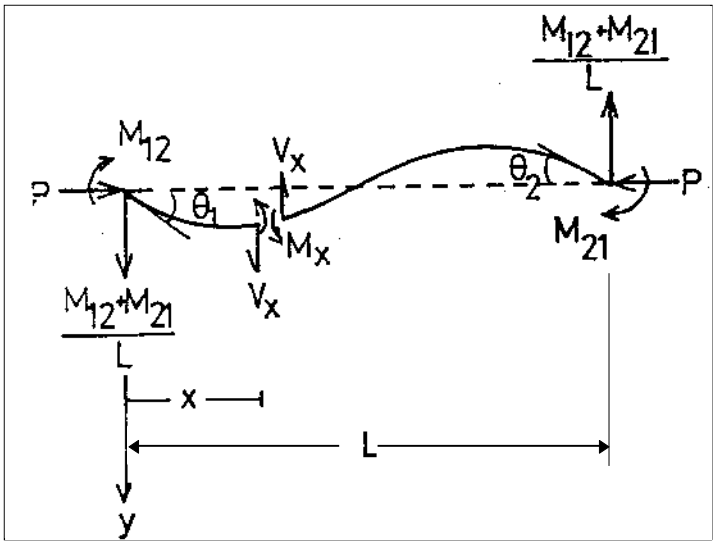

Figure (A-1) Force system of elastic beam-column

$$\bar{\rho} = \frac{\rho}{1-u\rho} \quad \text{.....(A-8)}$$

$$u = \frac{n}{AG}P_e = \frac{n}{AG}\frac{\pi^2}{L^2}EI \quad \text{.....(A-9)}$$

(D_1) and (D_2) are integration constants

At x=0, y=0)

$$D_2 = \frac{M_1}{P} \quad \text{.....(A-10)}$$

At x=L, y=0

$$D_1 = -\frac{M_2}{P}\csc\omega L - \frac{M_1}{P}\cot\omega L \quad \text{.....(A-11)}$$

So, by substituting (A-10) and (A-11) into (A-6), we have:-

$$y = \left(-\frac{M_2}{P}\csc\omega L - \frac{M_1}{P}\cot\omega L\right)\sin\omega x + \frac{M_1}{P}\cos\omega x + \frac{M_1}{P}\left(\frac{x}{L}-1\right) + \frac{M_2}{P}\frac{x}{L} \quad \text{.....(A-12)}$$

and since:-

$$\left.\frac{dy}{dx}\right)_{end1} = \frac{\theta_1 - \frac{n}{AG}\frac{\left(M_1 + M_2\right)}{L}}{1 - u\rho} \quad \text{.....(A-13)}$$

$$\left.\frac{dy}{dx}\right)_{end2} = \frac{\theta_2 - \frac{n}{AG}\frac{\left(M_1 + M_2\right)}{L}}{1 - u\rho} \quad \text{.....(A-14)}$$

Applying eq. (A-13 and A-14) into eq. (A-12), and introducing a stability functions ($\overline{C}_1$) and ($\overline{C}_2$):-

$$M_2 = K\overline{C}_1\theta_1 + K\overline{C}_2\theta_2 \quad \text{.....(A-15)}$$

$$M_2 = K\overline{C}_2\theta_1 + K\overline{C}_1\theta_2 \quad \text{.....(A-16)}$$

Where:-

$$\overline{C}_1 = \frac{\overline{\alpha}\left(1 - 2\left(1 - u\rho\right)\overline{\alpha}\cot\overline{\alpha}\right)}{\tan\overline{\alpha} - \overline{\alpha}\left(1 - u\rho\right)} \quad \text{.....(A-17)}$$

$$\overline{C}_2 = \frac{\left(2\left(1 - u\rho\right)\overline{\alpha} - \sin 2\overline{\alpha}\right)\left(\overline{\alpha}\left(1 - 2\left(1 - u\rho\right)\overline{\alpha}\cot 2\overline{\alpha}\right)\right)}{\left(\tan\overline{\alpha} - \overline{\alpha}\left(1 - u\rho\right)\right)\left(\sin 2\overline{\alpha} - 2\left(1 - u\rho\right)\overline{\alpha}\cos 2\overline{\alpha}\right)} \quad \text{.....(A-18)}$$

$$\overline{\alpha} = \frac{\pi}{2}\sqrt{\overline{\rho}} \ , \quad \text{where}\,(\rho)\,\text{is}\oplus\,\text{and}\,\overline{\rho} > 4 \quad \text{.....(A-19)}$$

when $\rho<0$ (tensile axial force)

$$\overline{C}_1 = \frac{\overline{\alpha}\left(1 - 2\left(1 + u\rho\right)\overline{\alpha}\coth\overline{\alpha}\right)}{\tanh\overline{\alpha} - \overline{\alpha}\left(1 + u\rho\right)} \quad \text{.....(A-20)}$$

$$\overline{C}_2 = \frac{\left(2\left(1 + u\rho\right)\overline{\alpha} - \sinh 2\overline{\alpha}\right)\left(\overline{\alpha}\left(1 - 2\left(1 + u\rho\right)\overline{\alpha}\coth 2\overline{\alpha}\right)\right)}{\left(\tanh\overline{\alpha} - \overline{\alpha}\left(1 + u\rho\right)\right)\left(\sinh 2\overline{\alpha} - 2\left(1 + u\rho\right)\overline{\alpha}\cosh 2\overline{\alpha}\right)} \quad \text{.....(A-21)}$$

$$\overline{\alpha} = \frac{\pi}{2}\sqrt{\overline{\rho}} \ , \quad \text{where}\,(\rho)\,\text{is}\oplus \quad \text{.....(A-22)}$$

A-2 The flexural shear slope (Meth.-2-)

The same procedure used in deriving Meth.-1- formula is used in this method:-

$$\frac{dy}{dx} = -\frac{dy_m}{dx}\left(1 + \frac{n}{AG}\rho\right) + \frac{nV_x}{AG} = \psi\left(1 + \frac{n}{AG}\rho\right) + \beta \quad \text{.....(A-23)}$$

by substituting (M_x), (V_x) and differentiate once with respect to (x):-

$$\frac{1}{1+\frac{n}{AG}P}\frac{d^2y}{dx^2}+\frac{P}{EI}y=\frac{1}{EI}\left(P\psi_x+\left(M_1+M_2\right)\frac{x}{L}-M_1\right) \quad \text{.....(A-24)}$$

where (ψ) is the sway angle of the member = $\frac{\Delta}{L}$

This means that when $\rho>0$ (Compressive axial force)

$$y=\frac{M_1}{P}\csc\omega x-\frac{M_1}{P}\cot\omega L\cos\omega x-\frac{M_2}{P}\csc\omega L\sin\omega x+\frac{M_1+M_2}{P}\frac{x}{L}+\psi_x \quad \text{.....(A-25)}$$

and

$$\overline{C}_1=\frac{\overline{\alpha}\left(\left(1+u\rho\right)-2\overline{\alpha}\cot 2\overline{\alpha}\right)}{\left(1+u\rho\right)\tan\overline{\alpha}-\overline{\alpha}} \quad \text{.....(A-26)}$$

$$\overline{C}_2=\frac{\left(2\overline{\alpha}-\left(1+u\rho\right)\sin 2\overline{\alpha}\right)\left(\overline{\alpha}\left(\left(1+u\rho\right)-2\overline{\alpha}\cot 2\overline{\alpha}\right)\right)}{\left(\left(1+u\rho\right)\tan\overline{\alpha}-\overline{\alpha}\right)\left(\left(1+u\rho\right)\sin 2\overline{\alpha}-2\overline{\alpha}\cos 2\overline{\alpha}\right)} \quad \text{.....(A-27)}$$

$$\overline{\alpha}=\frac{\pi}{2}\sqrt{\overline{\rho}}\text{ , wher}(\rho)\text{is}\oplus\text{and }\overline{\rho}<4 \quad \text{.....(A-28)}$$

when $\rho > 0$ (Compressive axial force)

$$y=\frac{M_1}{P}\csc h\omega x-\frac{M_1}{P}\coth\omega L\cosh\omega x-\frac{M_2}{P}\csc h\omega L\sinh\omega x+\frac{M_1+M_2}{P}\frac{x}{L}+\psi_x \quad \text{.....(A-29)}$$

$$\overline{C}_1=\frac{\overline{\alpha}\left(\left(1-u\rho\right)-2\overline{\alpha}\coth 2\overline{\alpha}\right)}{\left(1-u\rho\right)\tanh\overline{\alpha}-\overline{\alpha}} \quad \text{.....(A-30)}$$

$$\overline{C}_2=\frac{\left(2\overline{\alpha}-\left(1-u\rho\right)\sinh 2\overline{\alpha}\right)\left(\overline{\alpha}\left(\left(1-u\rho\right)-2\overline{\alpha}\coth 2\overline{\alpha}\right)\right)}{\left(\left(1-u\rho\right)\tanh\overline{\alpha}-\overline{\alpha}\right)\left(\left(1-u\rho\right)\sinh 2\overline{\alpha}-2\overline{\alpha}\cosh 2\overline{\alpha}\right)} \quad \text{.....(A-31)}$$

$$\overline{\alpha}=\frac{\pi}{2}\sqrt{\overline{\rho}}\text{ , where}(\rho)\text{is}\oplus \quad \text{.....(A-32)}$$

A-3 No axial force case (P=0):-

When u=0 and ρ=0, then for both methods:-

$$\overline{C}_1=4 \quad \text{.....(A-33)}$$

$$\overline{C}_2=2 \quad \text{.....(A-34)}$$

But when ρ=0 and u≠0, then the values of the modified functions ($\overline{C}_1$) and ($\overline{C}_2$) by both methods can be calculated by the ell known ***Taylor*** Expansion using $a = \alpha_1 = \frac{\pi}{50}$

$$\overline{C}_1 \approx 4 - \frac{2}{15}\pi^2\rho_i - \frac{11}{6300}\pi^4\rho_i^2 - \frac{1}{27000}\pi^6\rho_i^3 \quad \text{.....(A-35)}$$

$$\overline{C}_2 \approx 2 + \frac{1}{30}\pi^2\rho_i + \frac{13}{12600}\pi^4\rho_i^2 + \frac{11}{378000}\pi^6\rho_i^3 \quad \text{.....(A-36)}$$

where (i) is the method indicator (1 or 2)

$$\rho_1 = \frac{0.0016}{1 + 0.0016u} \quad \text{.....(A-37)}$$

$$\rho_2 = \frac{-1 + \sqrt{1 + 0.0064u}}{2u} \quad \text{.....(A-38)}$$

Appendix B

The conventional stability and bowing functions with their derivatives

B-1 Stability Functions [47]:-

Compressive Axial Force, ($\rho>0$):

$$C_1 = \frac{\phi(\sin\phi - \phi\cos\phi)}{2(1-\cos\phi) - \phi\sin\phi} \quad \text{.....(B-1)}$$

$$C_2 = \frac{\phi(\phi - \sin\phi)}{2(1-\cos\phi) - \phi\sin\phi} \quad \text{.....(B-2)}$$

In which:

$$\phi^2 = \frac{PL^2}{EI} = \pi^2\rho \quad \text{.....(B-3)}$$

- Zero Axial Force, ($\rho < 0$)

  $C_1 = 4$ .....(B-4)

  $C_2 = 2$ .....(B-5)

- Tensile Axial force, ($\rho<0$):

  $$C_1 = \frac{\psi(\psi\cosh\psi - \sinh\psi)}{2(1-\cosh\psi) + \psi\sinh\psi} \quad \text{.....(B-6)}$$

  $$C_2 = \frac{\psi(\sinh\psi - \psi)}{2(1-\cosh\psi) + \psi\sinh\psi} \quad \text{.....(B-7)}$$

  In which:

  $$\psi^2 = -\frac{PL^2}{EI} = -\pi^2\rho \quad \text{.....(B-8)}$$

B-2 Bowing Functions [47]:-

$$b_1 = \frac{(C_1 + C_2)(C_2 + 2)}{8\pi^2\rho} \quad \text{.....(B-9)}$$

$$b_2 = \frac{C_2}{8(C_1 + C_2)} \quad \text{.....(B-10)}$$

B-3 Derivatives with Respect to ρ [47]:-

$$C_1' = -2\pi^2\left(b_1 + b_2\right) \quad \text{(B-11)}$$

$$C_2' = -2\pi^2\left(b_1 + b_2\right) \quad \text{(B-12)}$$

$$b_1' = -\frac{\left(b_1 + b_2\right)\left(C_1 + C_2\right) + 2C_2 b_1}{4\rho} \quad \text{(B-13)}$$

$$b_2' = \frac{\pi^2\left(16 b_1 b_2 - b_1 + b_2\right)}{4\left(C_1 + C_2\right)} \quad \text{(B-14)}$$

B-4 Series Expressions [47]:-

$$C_1 \approx 4 - \frac{2}{15}\pi^2\rho - \frac{11}{6300}\pi^4\rho^2 - \frac{1}{27000}\pi^6\rho^3 \quad \text{(B-15)}$$

$$C_2 \approx 2 + \frac{1}{30}\pi^2\rho + \frac{13}{12600}\pi^4\rho^2 + \frac{11}{378000}\pi^6\rho^3 \quad \text{(B-16)}$$

$$b_1 \approx \frac{1}{40} + \frac{1}{2800}\pi^2\rho + \frac{1}{168000}\pi^4\rho^2 + \frac{37}{388080000}\pi^6\rho^3 \quad \text{(B-17)}$$

$$b_2 \approx \frac{1}{24} + \frac{1}{720}\pi^2\rho + \frac{1}{20160}\pi^4\rho^2 + \frac{1}{604800}\pi^6\rho^3 \quad \text{(B-18)}$$

$$C_1' \approx -\frac{2}{15}\pi^2 - \frac{11}{3150}\pi^4\rho - \frac{1}{9000}\pi^6\rho \quad \text{(B-19)}$$

$$C_2' \approx \frac{1}{30}\pi^2 + \frac{13}{6300}\pi^2\rho + \frac{11}{126000}\pi^6\rho^2 \quad \text{(B-20)}$$

$$b_1' \approx \frac{1}{2800}\pi^2 + \frac{1}{84000}\pi^4\rho + \frac{27}{129360000}\pi^6\rho^2 \quad \text{(B-21)}$$

$$b_2' \approx \frac{1}{720}\pi^2 + \frac{1}{10080}\pi^4\rho + \frac{1}{201600}\pi^6\rho^2 \quad \text{(B-22)}$$

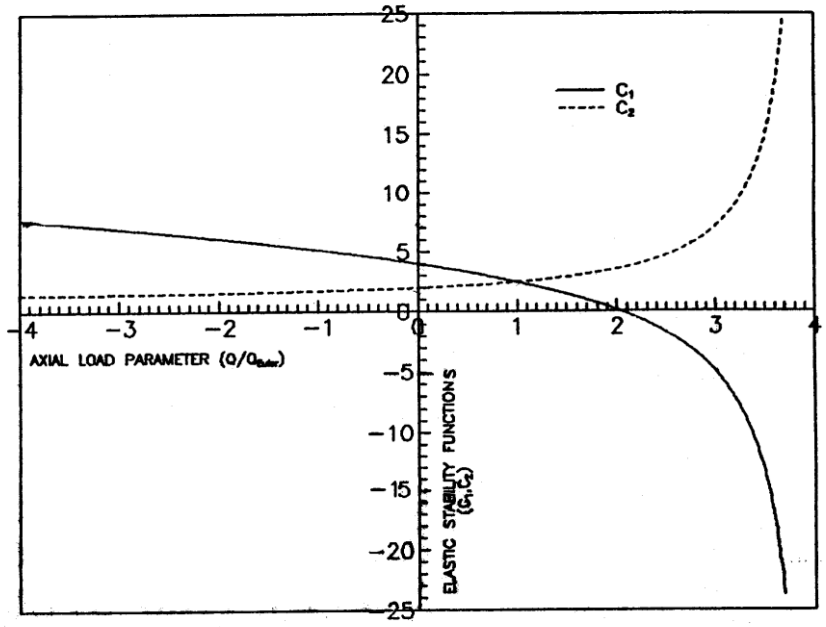

Figure (B-1) **No shear elastic stability functions (C_1 and C_2)**

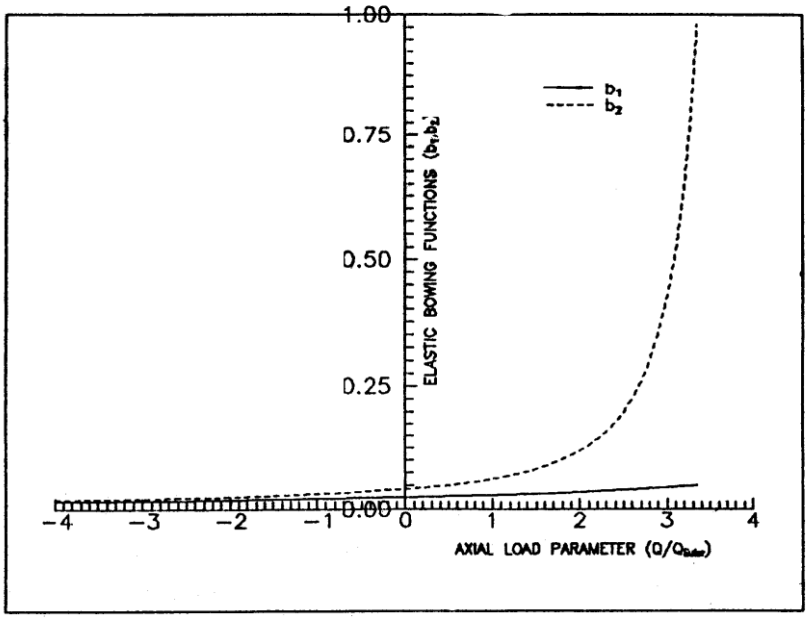

Figure (B-2) **No shear elastic bowing functions (b_1 and b_2)**

Appendix C

The Conventional Beam-Column Linearized-Incremental Large-Deformation Analysis

C-1 the Large Deformation Analysis:-

Saffan [81](1973), was the first how stated the analytical procedure of linearized incremental **T.S.M.** of conventional beam-column theory that this work adopts for analysis, then an updated development continued till ***Oran*** [71&72](1973), ***Oran*** and ***Kassimali*** [70](1976), ***Kassimali*** [47] (1983) and last but never least ***kassimali*** and ***Abbasnia*** [48](1991) made their progressive contribution on the 3-D **T.S.M.**

The new (***SS*** effect) presented in **chapter-3-** gives a new derivation of this procedure to include the coupled torsional-flexural action, the following items of this appendix holds a brief explanation of their work.

C-2 Original system equilibrium equation:-

The condition of equilibrium of a discrete elastic system subjected to prescribed external disturbance can generally be written as:-

$$f(x) = P \quad \text{.....(C-1)}$$

in which (P) refers to external forces and moments acting at the joints (indicating to a suitable global co-ordinate system); and (f) resultant internal forces.

In the special case of 2-D analysis (X) is represented by a set of generalized co-ordinates (X) which usually consist of translation and rotations of the joint. In the case of 3-D elements, however, the problem is complicated by the fact that large joint rotations cannot be treated as generalized coordinates.

For computational purposes, it proves useful to rewrite 3-110 into:-

$$\Delta P = \tau \Delta X \quad \text{.....(C-2)}$$

in which (ΔP) and (ΔX) denote incremental values of the external loads and joint displacement, respectively, and:-

$$\tau = \frac{\partial f_i}{\partial X_i} = \text{T.S.M.} \quad \text{.....(C-3)}$$

which is the system **T.S.M.,** it should be emphasized at this stage that, while "X" is not necessarily defined in space frames; the incremental vector (ΔX) is the new system configuration[47].

C-3 Joint rotation matrix:-

The deformed orientation of a space frame as ***Oran*** [69](1973) indicated can be represented by a joint orientation matrix "α", the column of which is the direct cosines, with respect to the fixed global coordinate axis of three mutually perpendicular lines that are assumed to be rigidly attached to, and moving with, the joint:-

$$\alpha = \begin{bmatrix} \alpha_{11} & \alpha_{12} & \alpha_{13} \\ \alpha_{21} & \alpha_{22} & \alpha_{23} \\ \alpha_{31} & \alpha_{32} & \alpha_{33} \end{bmatrix} \quad \text{.....(C-4)}$$

For convenience, these joint reference lines can be assumed to be parallel to the global co-ordinates axes in the initial undeformed configuration of the system.

In determining the response of a space frame by the idealized incremental approach, an important question that arises is that of how to update the orientation matrix of a joint as the deformed configuration of the structure changes. To that end, consider an arbitrary joint of a structure, and let "α" be the corresponding joint orientation matrix in a given configuration of the system. Assume now that the particular joint under consideration rotates in a finite angle ($\bar{\gamma}$) about an axis with direction cosines n_1, n_2, n_3. The orientation matrix of the joint, ($\bar{\alpha}$) in the new configuration, is given by:

$$\bar{\alpha} = W\alpha \quad \text{.....(C-5)}$$

In which (W) is the rotation matrix using the right-hand value to define the positive direction of the rotation, it can be shown that:-

$$W = \begin{bmatrix} \cos\bar{\gamma} + n_1^2(1-\cos\bar{\gamma}) & -n_3\sin\bar{\gamma} + n_1n_2(1-\cos\bar{\gamma}) & n_2\sin\bar{\gamma} + n_1n_3(1-\cos\bar{\gamma}) \\ n_3\sin\bar{\gamma} + n_1n_2(1-\cos\bar{\gamma}) & \cos\bar{\gamma} + n_2^2(1-\cos\bar{\gamma}) & -n_1\sin\bar{\gamma} + n_2n_3(1-\cos\bar{\gamma}) \\ -n_2\sin\bar{\gamma} + n_1n_3(1-\cos\bar{\gamma}) & n_1\sin\bar{\gamma} + n_2n_3(1-\cos\bar{\gamma}) & \cos\bar{\gamma} + n_3^2(1-\cos\bar{\gamma}) \end{bmatrix} \quad \text{.....(C-6)}$$

It should be realized that the last two equations are valid for arbitrarily large rotations, if " $\bar{\gamma}$ " is infinitely small, then the approximation is:

$$\cos\bar{\gamma} \approx 1, \quad \sin\bar{\gamma} \approx \bar{\gamma} \quad \text{.....(C-7)}$$

which reduces eq.(C-6) to:-

$$W \approx \begin{bmatrix} 1 & -\bar{\gamma}_3 & \bar{\gamma}_2 \\ \bar{\gamma}_3 & 1 & -\bar{\gamma}_1 \\ -\bar{\gamma}_2 & \bar{\gamma}_1 & 1 \end{bmatrix} \quad \text{.....(C-8)}$$

in whitch

$$\begin{aligned} \bar{\gamma}_1 &= \bar{\gamma}_{n1} \\ \bar{\gamma}_2 &= \bar{\gamma}_{n2} \\ \bar{\gamma}_3 &= \bar{\gamma}_{n3} \end{aligned} \quad \text{.....(C-9)}$$

and when "$\bar{\gamma}$" is assumed to be small, a vectorial representation "$\bar{\gamma}$" can be used for the rotation with rotation components "$\bar{\gamma}_1$","$\bar{\gamma}_2$","$\bar{\gamma}_3$".

The rotation matrix "W" as defined by eq.(C-6) can be used in interpreting the results of a linear analysis in the linearized incremental procedure as follows:

- Consider a load level (P_i) and assume that the corresponding deformed configuration of the system, (X_i), is known. It is now desired to determine the configuration ($X_{(i+1)}$), corresponding to a load level

  $$P_{i+1} = P_{(i)} + \Delta P \quad \text{.....(C-10)}$$

  where:- (ΔP) represents a finite but small load increment.

- Even in a space frame with large rotations (where the displacement vector (X) is not necessarily defined), the small changes that take place in the configuration of the system as a result of (ΔP) can be described by a vector (ΔX), the element of which represents finite but small translations and rotations of the joints of the structure with respect to the global coordinate system used. In the linearized incremental procedure:

- X is obtained from eq. (C-2) by simply evaluating (τ) at the beginning of the loading interval, i.e., at load level (P_i).

- Let($\Delta\bar{\gamma}_1, \Delta\bar{\gamma}_2$ and $\Delta\bar{\gamma}_3$) be the incremental rotation components for the joint of the structure, as exemplified by the incremental vector {ΔX}, from eq.(C-5), the new orientation matrix of that particular joint is given by:-

  $$\bar{\alpha}_{i+1} = \overline{W}\bar{\alpha}_i \quad \text{.....(C-11)}$$

  where:-

  $\overline{W} = W$ in eq.(C-6) but replacing $\Delta\bar{\gamma}$ instead of $\bar{\gamma}$

$$\Delta\gamma = \left(\Delta\bar{\gamma}_1^2 + \Delta\bar{\gamma}_2^2 + \Delta\bar{\gamma}_3^2\right)^{1/2}$$

$$n_1 = \frac{\Delta\bar{\gamma}_1}{\Delta\bar{\gamma}}, n_2 = \frac{\Delta\bar{\gamma}_2}{\Delta\bar{\gamma}}, n_3 = \frac{\Delta\bar{\gamma}_3}{\Delta\bar{\gamma}}, \quad \text{..... (C-12)}$$

Since $\Delta\bar{\gamma}_1, \Delta\bar{\gamma}_2$ and $\Delta\bar{\gamma}_3$ are small, again "$\overline{W}$" can be replaced by eq. (C-8) with "$\Delta\bar{\gamma}$" instead of "$\bar{\gamma}$". However, it should be noted that in the approximate form eq. (C-8), the column of "W" or "$\overline{W}$" are not exactly unit vectors and are not exactly orthogonal to each other.

The above description of "W" and "$\overline{W}$" rotation matrices can be replaced by simpler technique detailed in the algorithm of the ***NASCF1*** program.

C-4 Member geometry:-

To separate the large rigid body of a member from its relative deformations, which are assumed to be small, a moving ***Eulerian*** member coordinate system is used as shown in figure (C-1) and (C-2), and it is defined as follows:-

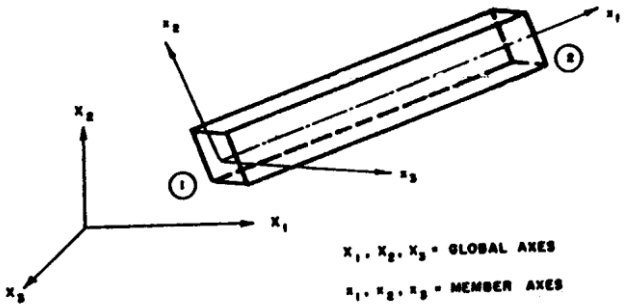

Figure (C-1) Member coordinates

For analytical convenience, the relative deformations of a member often refer to a moving coordinate system attached to the member itself. The particular member coordinate system used herein figure (C-1) is a right handed one, and is defined as follows. The (x) axis passes through the centroids of member end sections and the x_2 and x_3 axes are parallel to the principal directions of the cross section. Note that, on account of the relative deformations of the member, the principal directions will vary slightly from one cross section to another. The x_2 and x_3 axes are defined here in refer to an average cross section.

Let r_{1n}, r_{2n}, r_{3n}, denote the direction cosines of the member (x_n) -axis with respect to the global coordinates X_1, X2, X3. The member coordinate system is then completely defined by the orthogonal matrix

$$[r] = \begin{bmatrix} r_{11} & r_{12} & r_{13} \\ r_{21} & r_{22} & r_{23} \\ r_{31} & r_{32} & r_{33} \end{bmatrix} \quad \text{.....(C-13)}$$

which by analogy to eq. (C-4), may be referred to as the "member orientation matrix".

Small relative deformations of a typical frame member can be represented by end angles θ_{13}, θ_{23}, θ_{12}, θ_{22}, as shown in Figure (C-2), total twist ϕ_t, (i.e. relative rotation of member ends about the centroidal axis), and relative displacement u. Note that the first subscript on θ_{mn} refers to the point where the angle is measured (1 for left and 2 for right), while the second subscript indicates the particular member axis about which the rotation takes place.

- In the determination of the member deformation and orientation, an interesting and relevant question arises. Given the deformed positions and orientation of two adjacent joints, how are the relative deformations and deformed orientation of the member connecting the two joints determined?

  Let $\{X_{(1)}\}$ and $\{X_{(2)}\}$ be the joint coordinate vectors in the deformed configuration, and $\{\alpha_{(1)}\}$ and $\{\alpha_{(2)}\}$ the associated joint orientation matrices. Recalling that the two end sections will not generally be exactly parallel to each other let $\{P_{(1)}\}$ and $\{P_{(2)}\}$ be "end section orientation matrices" defined as follows.

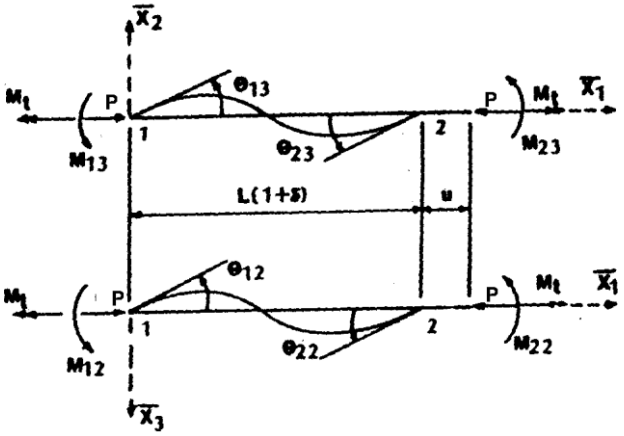

Figure (C-2) Relative member deformations and corresponding forces

The columns of each matrix represent the direction cosines of the normal and principal directions of the corresponding end section in as much as the member end sections are rigidly connected to the respective joints

$$\left[P_{(1)}\right]=\left[\alpha_{(1)}\right]\left[r_{(0)}\right] \quad \text{(C-14)}$$

$$\left[P_{(2)}\right]=\left[\alpha_{(2)}\right]\left[r_{(0)}\right] \quad \text{(C-15)}$$

in which $\{r_{(0)}\}$= member orientation matrix in the undeformed configuration.

The first column $\{r_1\}$, of the desired $\{r\}$ matrix, as well as the relative axial displacement, u are readily obtained from the coordinate vectors, $\{X_{(1)}\}$ and $\{X_{(2)}\}$. By virtue of the assumed smallness of the relative deformations the end angles, θ_{mn}, can be obtained as scalar products of $\{r_1\}$ with appropriate columns of $\{P_{(1)}\}$ and $\{P_{(2)}\}$. Thus, in compact notation

$$\left[P_{(1)}\right]^T\left\{r_1\right\}=\begin{Bmatrix}1\\-\theta_{13}\\\theta_{12}\end{Bmatrix} \quad \text{(C-16)}$$

$$\left[P_{(2)}\right]^T\left\{r_1\right\}=\begin{Bmatrix}1\\-\theta_{23}\\\theta_{22}\end{Bmatrix} \quad \text{(C-17)}$$

in which the superscript T denotes transpose. Similarly

$$\phi_1 \cong -\left\{P_2^{(1)}\right\}^T\left\{P_3^{(2)}\right\} \cong \left\{P_3^{(1)}\right\}^T\left\{P_2^{(2)}\right\} \quad \text{(C-18)}$$

To determine the second and third columns of [r], let

$$\left[e_{(1)}\right]=\begin{bmatrix}1 & \theta_{13} & -\theta_{12}\\-\theta_{13} & 1 & 0\\\theta_{12} & 0 & 1\end{bmatrix} \quad \text{(C-19)}$$

$$\left[e_{(2)}\right]=\begin{bmatrix}1 & \theta_{23} & -\theta_{22}\\-\theta_{23} & 1 & 0\\\theta_{22} & 0 & 1\end{bmatrix} \quad \text{(C-20)}$$

If the end sections are rotated slightly about their principal directions (but not about their normal) in such a way as to make them perpendicular to the member (x_1) axis, then the new end section orientation matrices would be given by the products $[P_{(1)}]\,[e_{(1)}]$ and $[P_{(2)}]\,[e_{(2)}]$, respectively. The (x_2) and (x_3) axes could then be defined (arbitrarily, but conveniently and accurately) as the principal directions of an average cross section, thus resulting in the following expression for the member orientation matrix:

$$[r] \cong \frac{1}{2}\left[P_{(1)}\right]\left[e_{(1)}\right] + \frac{1}{2}\left[P_{(2)}\right]\left[e_{(2)}\right] \quad \text{.....(C-21)}$$

- Assumptions Used in Member Analysis:-

  The term beam-column generally refers to an initially straight-structural member subjected to a prescribed combination of axial and lateral loads. In the "conventional beam-column theory" which as indicated constitutes the basis of the present analysis, the axial force is considered to be much larger than the effects associated with the flexural deformations of the member. From a mathematical viewpoint, this implies that the axial force is finite whereas the displacement rotations, curvatures, shears and bending moments are infinitesimal. Accordingly, the formulation used is essentially linear, i.e., the strains (curvatures) are expressed as linear functions of the displacements, and except for the contribution of the axial force, the equilibrium equations are written for the undeformed geometry of the member [(69)].

  In their work, the attention is confined to members with doubly symmetric cross sections, thus ruling out torsion-flexure coupling. Shear deformations, restraint against warping and self-straining (i.e. temperature effects, lack of fit, support settlements) are neglected; besides, the external loads are assumed to be configuration independent and applied at the joints only. All these effects are included in our work.

C-5 Basic Member Force-Deformation Relations

The basic member force-deformation relations, consistent with the conventional beam-column theory as outlined in the preceding sections are [(69)]:-

$$M_{1n} = \frac{EI_n}{L}\left(C_{1n}\theta_{1n} + C_{2n}\theta_{2n}\right); \text{for } n = 3,2 \quad \text{.....(C-22)}$$

$$M_{2n} = \frac{EI_n}{L}\left(C_{2n}\theta_{1n} + C_{1n}\theta_{2n}\right); \text{for } n = 3,2 \quad \text{.....(C-23)}$$

$$M_1 = \frac{GJ}{L}\phi_1 \quad \text{.....(C-24)}$$

$$Q = EA\left(\frac{u}{L} - C_{b1} - C_{b2}\right) \quad \text{.....(C-25)}$$

in which M_{mn} is the bending moment corresponding to θ_{mn}; M_t is the torque; Q is the axial force (positive when compression); A is the area of cross section, I_n is the moment of inertia about the x_n axis, E is the modulus of elasticity; GJ is the torsional rigidity; L is the undeformed length of

member; C_{1n} and C_{2n} are the stability functions associated with bending moments about the (x) axis and C_{bn} is the length correction factor resulting from flexural deformations about the (x) axis.

The coefficients, C_{1n} and C_{2n} are functions of the dimensionless quantity:

$$\rho_n = \frac{QL^2}{\pi^2 EI_n} \quad \text{.....(C-26)}$$

Similarly $C_{1n} = b_{1n}\left(\theta_{1n} + \theta_{2n}\right)^2 + b_{2n}\left(\theta_{1n} + \theta_{2n}\right)^2$ .....(C-27)

in which b_{1n}, b_{2n} =bowing function defined as [69]:

$$b_{1n} = \frac{\left(C_{1n} + C_{2n}\right)\left(C_{2n} - 2\right)}{8\pi^2 \rho_n} \quad \text{.....(C-28)}$$

$$b_{2n} = \frac{C_{2n}}{8\left(C_{1n} + C_{2n}\right)} \quad \text{.....(C-29)}$$

Let $\xi_n = \frac{I_2}{I}$ .....(C-30)

$$\eta = \frac{GJ}{EI} \quad \text{.....(C-31)}$$

in which I= reference moment of inertia and

$$\lambda = \frac{L}{\sqrt{\frac{I}{A}}} \quad \text{.....(C-32)}$$

$$\rho = \frac{QL^2}{\pi^2 EI} = \xi_n \rho_n \quad \text{.....(C-33)}$$

eq.(C-23) can now be rewritten as:-

$$\rho = \frac{\lambda^2}{\pi^2}\left(\mu - C_{b3} - C_{b2}\right) \quad \text{.....(C-34)}$$

with $\mu = \frac{u}{L}$ .....(C-35)

Note that via eq.(C-33), C_{mn} and b_{mn} are indirectly functions of the "dimensionless axial load parameter (ρ)".

C-6 Tangent Stiffness for Relative Deformations

For convenience, introduce the notation

$$u_1=\theta_{13};u_2=\theta_{23};u_3=\theta_{12};u_4=\theta_{22};u_5=\phi_t;u_6=\mu \quad \text{.....(C-36)}$$

and

$$S_1=M_{13};S_2=M_{23};S_3=M_{12};S_4=M_{22};S_5=M_t;S_6=QL \quad \text{.....(C-37)}$$

The relation between incremental vectors $\{\Delta s\}$ and $\{\Delta u\}$ can be written as

$$\{\Delta S\}=[t]\{\Delta u\} \quad \text{.....(C-38)}$$

in which [t]= tangent stiffness matrix for relative deformations with

$$t_{ij}=\frac{\partial S_i}{\partial u_j}+\frac{\partial S_i}{\partial q}\frac{\partial q}{\partial u_j},\text{for ij}=1,2,\ldots,6 \quad \text{.....(C-39)}$$

By using ***Saafan***[81] definition of (b_1)and (b_2):-

$$b_{1n}=-\frac{C'_{1n}+C'_{2n}}{4\pi^2} \quad \text{.....(C-40)}$$

$$b_{2n}=-\frac{C'_{1n}+C'_{2n}}{4\pi^2} \quad \text{.....(C-41)}$$

in which a prime superscript indicates one differentiation with respect to (ρ_n). Thus recalling eqs (C-27 and C-34):

$$\frac{\partial\rho}{\partial\theta_{mn}}=\frac{G_{mn}}{\pi^2 H};\frac{\partial\rho}{\partial\phi_n}=0;\frac{\partial\rho}{\partial\mu}=\frac{1}{H} \quad \text{.....(C-42)}$$

in which $G_{1n}=C'_{1n}\theta_{1n}+C'_{2n}\theta_{2n}$ .....(C-42.a)

$$G_{2n}=C'_{2n}\theta_{1n}+C'_{1n}\theta_{2n} \quad \text{.....(C-42.b)}$$

and:-

$$H=\frac{\pi^2}{\lambda^2}+\sum_{n-12}\frac{1}{\xi_n}\left[b'_{1n}\left(\theta_{1n}+\theta_{2n}\right)^2+b'_{2n}\left(\theta_{1n}+\theta_{2n}\right)^2\right] \quad \text{.....(C-42.c)}$$

In the case of hinged joints the tangent stiffness matrix in local coordinates, [t], can be developed by eliminating the released coordinates from eq.(5-79 to 5-82) and differentiating the resulting relations, term by term, with respect to the remaining coordinates:-

- For member with hinge at end-1-:-

$$t_{h22} = t_{22} - \frac{t_{12}^2}{t_{11}}, t_{h26} = t_{h62} = t_{26} - \frac{t_{12}t_{16}}{t_{11}}, t_{h66} = t_{66} - \frac{t_{16}^2}{t_{11}} - \frac{t_{36}^2}{t_{33}} \quad \text{.....(C-43.a)}$$

$$t_{h44} = t_{44} - \frac{t_{34}^2}{t_{33}}, t_{h46} = t_{h64} = t_{46} - \frac{t_{34}t_{36}}{t_{33}} \quad \text{..... (C-43.b)}$$

- For member with hinge at end-2-:-

$$t_{h11} = t_{11} - \frac{t_{12}^2}{t_{22}}, t_{h16} = t_{h61} = t_{16} - \frac{t_{12}t_{26}}{t_{22}}, t_{h66} = t_{66} - \frac{t_{26}^2}{t_{22}} - \frac{t_{46}^2}{t_{43}} \quad \text{.....(C-44.a)}$$

$$t_{h33} = t_{33} - \frac{t_{34}^2}{t_{44}}, t_{h36} = t_{h63} = t_{36} - \frac{t_{34}t_{46}}{t_{44}} \quad \text{..... (C-44.b)}$$

- For member with hinge at both ends:-

$$t_{h66} = \text{AEL} \quad \text{..... (C-45)}$$

where (i, j) represent the node D.O.F. (1-6), "t_{hij}" represents the tangent stiffness matrix in local coordinates of hinged end and "t_{ij}" represents the original tangent stiffness matrix in local coordinates of rigid ends detailed in **chapter-3-.**

It should be emphasized that a prime superscript on (C_{mn}) or (b_{mn}) indicates one differentiation with respect to ρ_n (not ρ). The actual process of differentiation is complicated by the fact that the explicit expressions for (C_{mn}) and (b_{mn}) depend on whether (g_n) is positive, zero or negative. As demonstrated elsewhere [69], the desired derivatives can alternatively be obtained from simple algebraic operations on C_{mn}. from eq. (C-39), by making use of eq. (C-40 to C-45).

C-7 Local Transformation

If $\{\overline{F}\}$ denotes a 12x1 vector representing member end forces in member coordinates as shown in figure.(C-3), then:-

$$\{\overline{F}\} = \{\overline{B}\}\{S\} \quad \text{.....(C-46)}$$

$$[\bar{B}] = \begin{bmatrix} 0 & 0 & 0 & 0 & 0 & 1 \\ 1 & 1 & 0 & 0 & 0 & 0 \\ 0 & 0 & -1 & -1 & 0 & 0 \\ 0 & 0 & 0 & 0 & -1 & 0 \\ 0 & 0 & 1 & 0 & 0 & 0 \\ 1 & 0 & 0 & 0 & 0 & 0 \\ 0 & 0 & 0 & 0 & 0 & -1 \\ -1 & -1 & 0 & 0 & 0 & 0 \\ 0 & 0 & 1 & 1 & 0 & 0 \\ 0 & 0 & 0 & 0 & 1 & 0 \\ 0 & 0 & 0 & 1 & 0 & 0 \\ 0 & 1 & 0 & 0 & 0 & 0 \end{bmatrix} \quad \text{.....(C-47)}$$

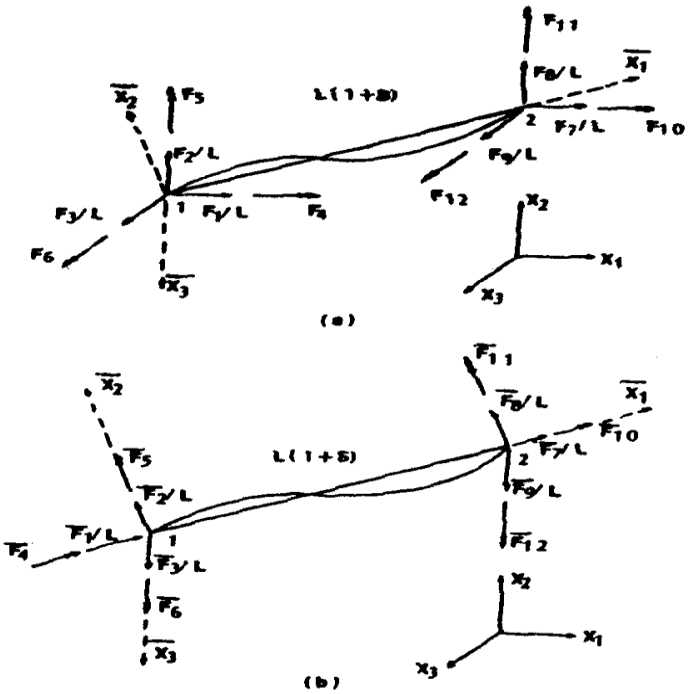

Figure (C-3) Member forces

Let now $\Delta\bar{v}$ denote a 12x1 vector of infinitesimal displacements of member end sections in member coordinates; ($\Delta\bar{v}_1$ to $\Delta\bar{v}_3$) and ($\Delta\bar{v}_7$ to $\Delta\bar{v}_9$) represent translations of the centroids (nondimensionalized via division by L) whereas ($\Delta\bar{v}_4$ to $\Delta\bar{v}_6$) and ($\Delta\bar{v}_{10}$ to $\Delta\bar{v}_{12}$) denote rotations of the respective cross sections. By analogy to eq.(C-46)

$$\{\Delta u\} = [\bar{B}]^T \{\Delta\bar{v}\} \quad \text{..... (C-48)}$$

in which as before, the superscript T denotes transpose

Rewriting eq.(C-46) in terms of differentials:

$$\{\Delta\bar{F}\} = [\bar{B}]\{\Delta S\} + [\Delta\bar{B}]\{S\} \quad \text{(C-49)}$$

in which $[\Delta\bar{B}]$ = change in $[\bar{B}]$ resulting from $\{\Delta\bar{v}\}$. Within the limitations of the beam-column theory as outlined in an earlier section (i.e. a theory which, except for the contribution of the axial force, is essentially linear), $[\Delta\bar{B}]$ is obtained as:-

$$[\Delta\bar{B}] = \begin{bmatrix} -\Delta\delta_2 & -\Delta\delta_2 & \Delta\delta_3 & \Delta\delta_3 & 0 & 0 \\ -\Delta\delta_1 & -\Delta\delta_1 & 0 & 0 & 0 & \Delta\delta_2 \\ 0 & 0 & \Delta\delta_1 & \Delta\delta_1 & 0 & \Delta\delta_3 \\ 0 & 0 & 0 & 0 & 0 & 0 \\ 0 & 0 & 0 & 0 & 0 & 0 \\ 0 & 0 & 0 & 0 & 0 & 0 \\ \Delta\delta_2 & \Delta\delta_2 & -\Delta\delta_3 & -\Delta\delta_3 & 0 & 0 \\ \Delta\delta_1 & \Delta\delta_1 & 0 & 0 & 0 & -\Delta\delta_2 \\ 0 & 0 & -\Delta\delta_1 & -\Delta\delta_1 & 0 & -\Delta\delta_3 \\ 0 & 0 & 0 & 0 & 0 & 0 \\ 0 & 0 & 0 & 0 & 0 & 0 \\ 0 & 0 & 0 & 0 & 0 & 0 \end{bmatrix} \quad \text{(C-50)}$$

in which $\Delta\delta_1 = -\Delta\bar{v}_1 + \Delta\bar{v}_7$ (C-51)

$\Delta\delta_2 = -\Delta\bar{v}_2 + \Delta\bar{v}_8$ (C-52)

$\Delta\delta_3 = -\Delta\bar{v}_3 + \Delta\bar{v}_9$ (C-53)

the kth column of [B] can be expressed as

$$\{\Delta\bar{B}^{(k)}\} = \{\bar{g}^{(k)}\}\{\Delta\bar{v}^{(k)}\} \quad \text{(C-54)}$$

thus introducing the following six symmetric 12 x12 matrices:

$$[\bar{g}^{(1)}] = [\bar{g}^{(2)}] = \begin{bmatrix} [f^{(1)}] & [-f^{(1)}] \\ [-f^{(2)}] & [f^{(2)}] \end{bmatrix} \quad \text{(C-55)}$$

$$[\bar{g}^{(3)}] = [\bar{g}^{(4)}] = \begin{bmatrix} [f^{(3)}] & [-f^{(3)}] \\ [-f^{(4)}] & [f^{(4)}] \end{bmatrix} \quad \text{(C-56)}$$

$$[\bar{g}^{(5)}] = [0] \quad \text{(C-57)}$$

$$[\bar{g}^{(6)}] = \begin{bmatrix} [f^{(6)}] & [-f^{(6)}] \\ [-f^{(6)}] & [f^{(6)}] \end{bmatrix} \quad \text{(C-58)}$$

in which $[f^{(1)}]$,$[f^{(3)}]$ and $[f^{(6)}]$ are 6 x 6 matrices defined by

$$f_{ij}^{(1)} = 0 \quad \text{except} \quad f_{12}^{(1)} = f_{21}^{(1)} = 1 \quad \text{.....(C-59)}$$

$$f_{ij}^{(3)} = 0 \quad \text{except} \quad f_{13}^{(3)} = f_{31}^{(3)} = -1 \quad \text{.....(C-60)}$$

$$\text{and} \quad f_{ij}^{(6)} = 0 \quad \text{except} \quad f_{22}^{(6)} = f_{33}^{(6)} = -1 \quad \text{.....(C-61)}$$

Recalling further eq.(C-47), eq.(C-49) can now be rewritten as:

$$\{\Delta\bar{F}\} = [\bar{T}]\{\Delta\bar{v}\} \quad \text{.....(C-62)}$$

in which

$$[\bar{T}] = [\bar{B}][t][\bar{B}]^T + \sum_{k=1}^{6} S_k[\bar{g}^{(k)}] \quad \text{.....(C-63)}$$

Note that $[\bar{T}]$ is symmetric.

C-8 Tangent Stiffness in Global Coordinates

Let [R] be a 12 x 12 orthogonal matrix defined by

$$[R] = \begin{bmatrix} [r] & 0 & 0 & 0 \\ 0 & [r] & 0 & 0 \\ 0 & 0 & [r] & 0 \\ 0 & 0 & 0 & [r] \end{bmatrix} \quad \text{.....(C-64)}$$

in which [r] = member orientation introduced in eq.(C-13). Let further {ΔF} and {Δv} denote increments of member end forces and end displacements, respectively, in global coordinates, then

$$\{\Delta F\} = [R]\{\Delta\bar{F}\} \quad \text{.....(C-65)}$$

$$\{\Delta\bar{v}\} = [R]^T\{\Delta v\} \quad \text{.....(C-66)}$$

in which $\{\Delta\bar{F}\}$ is as given in eq.(C-49) substituting into eq.(C-62)

$$\{\Delta F\} = [T]\{\Delta v\} \quad \text{.....(C-67)}$$

$$\text{in which} \quad [T] = [R][\bar{T}][R]^T \quad \text{.....(C-68)}$$

eq.(C-68) is the desired tangent stiffness matrix in global coordinates. Alternatively,

$$\text{in which} [T] = [R][\bar{B}][t][B]^T + \sum_{k=1}^{6} S_k[R][\bar{g}^{(k)}][R]^T \quad \text{.....(C-69)}$$

or:

$$[T] = [\bar{B}][t][B]^T + \sum_{k=1}^{6} S_k \left[\bar{g}^{(k)}\right] \quad \text{(C-70)}$$

$$[B] = [R][\bar{B}] \quad \text{(C-71)}$$

is the "instantaneous global static matrix" and

$$\left[g^{(k)}\right] = [R]\left[\bar{g}^{(k)}\right][R]^T \quad \text{(C-72)}$$

eq. (C-69) is formally identical with the corresponding result derived earlier.for plane frames[71]. Note that [T] is symmetric.

It should be emphasized at this stage that Δv_4 to Δv_6 and Δv_{10} to Δv_{12} which denote infinitesimal rotations of member ends, are not to be interpreted as increments of any generalized coordinates representing large joint rotations.

As examined in detail in a previous section, the deformed orientation of each joint is represented not by three rotations components, but by a joint orientation matrix $[\bar{\alpha}]$. However, Δv_1 to Δv_3 and Δv_7 to Δv_9 do denote increments of large joint translations (non-dimensionalization via division by L).

Appendix D

The fixed end actions (F.E.A)

The fixed end actions mentioned in **chapter-3-** for the transverse loading or for the special effects are tabulated in this appendix.

Figures D-1 to D-4, illustrate these actions: which are, respectively:-

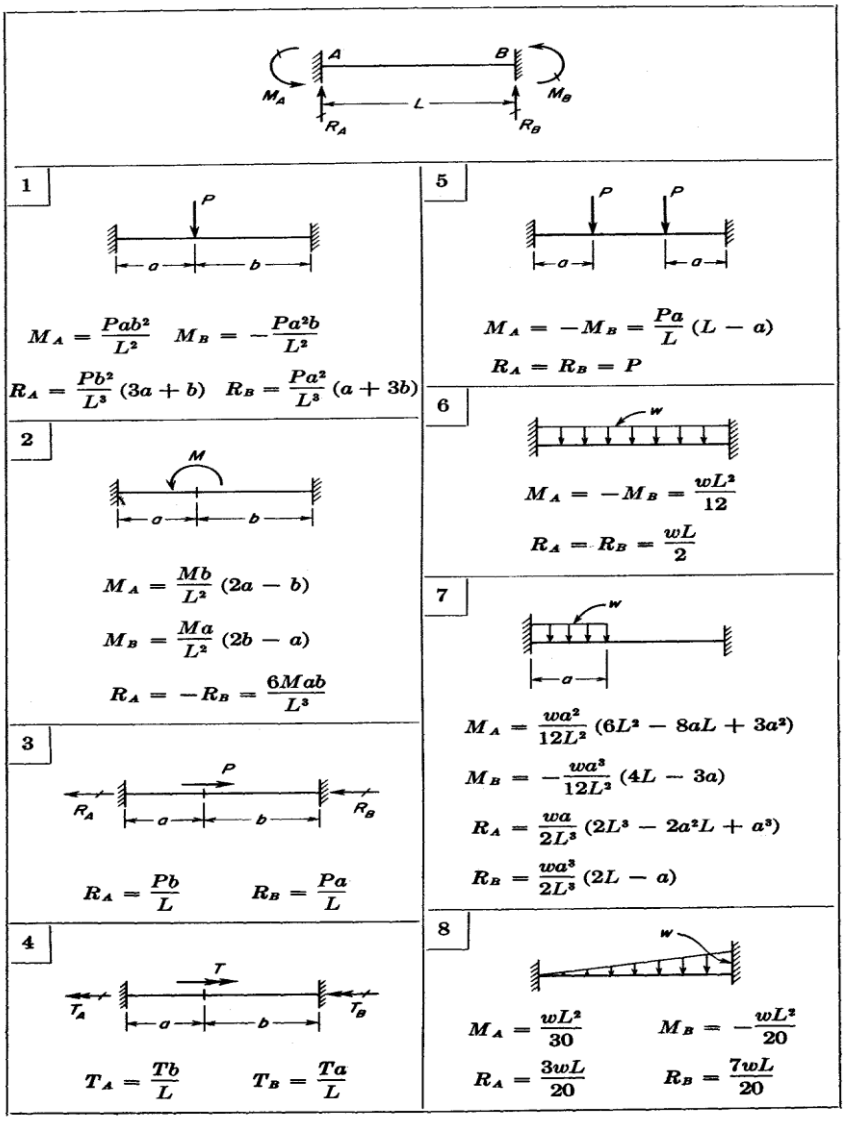

D-1.a the transverse load action for fixed ended elements.

1

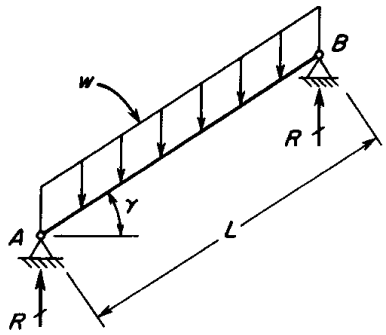

$$R = \frac{wL}{2}$$

2

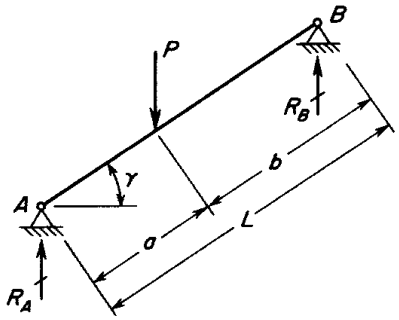

$$R_A = \frac{Pb}{L}$$

$$R_B = \frac{Pa}{L}$$

3

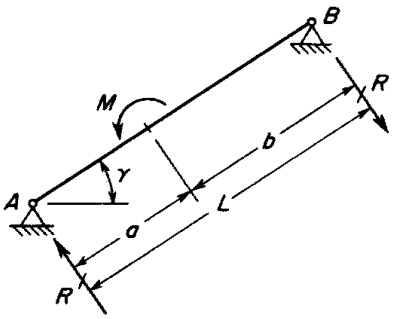

$$R = \frac{M}{L}$$

D-1.b **the transverse load action for hinged elements.**

1	Uniform increase in temperature	2	Temperature differential
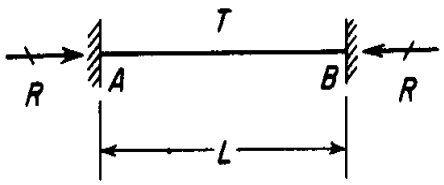		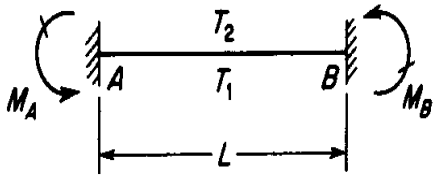	
$R = EA\alpha T$		$M_A = -M_B = \frac{\alpha EI(T_1 - T_2)}{d}$	
E = modulus of elasticity		I = moment of inertia	
A = cross-sectional area		T_1 = temperature at bottom of beam	
α = coefficient of thermal expansion		T_2 = temperature at top of beam	
T = temperature increase		d = depth of beam	

D-2 **the temperature action.**

1 Bar with excess length

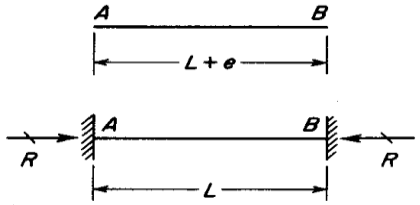

$$R = \frac{EAe}{L}$$

E = modulus of elasticity

A = cross-sectional area

e = excess length

2 Bar with a bend

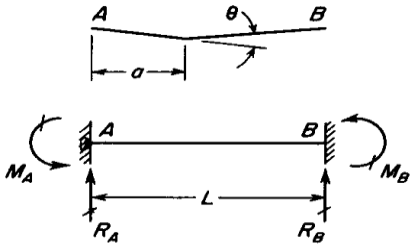

$$M_A = \frac{2EI\theta}{L^2}(2L - 3a)$$

$$M_B = \frac{2EI\theta}{L^2}(L - 3a)$$

$$R_A = -R_B = \frac{6EI\theta}{L^3}(L - 2a)$$

I = moment of inertia

θ = angle of bend

3 Initial circular curvature

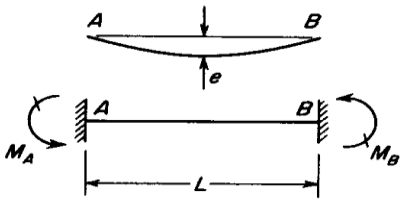

$$M_A = -M_B = \frac{8EIe}{L^2}$$

e = initial deflection at middle of bar

D-3 the pre-strains fixed end action

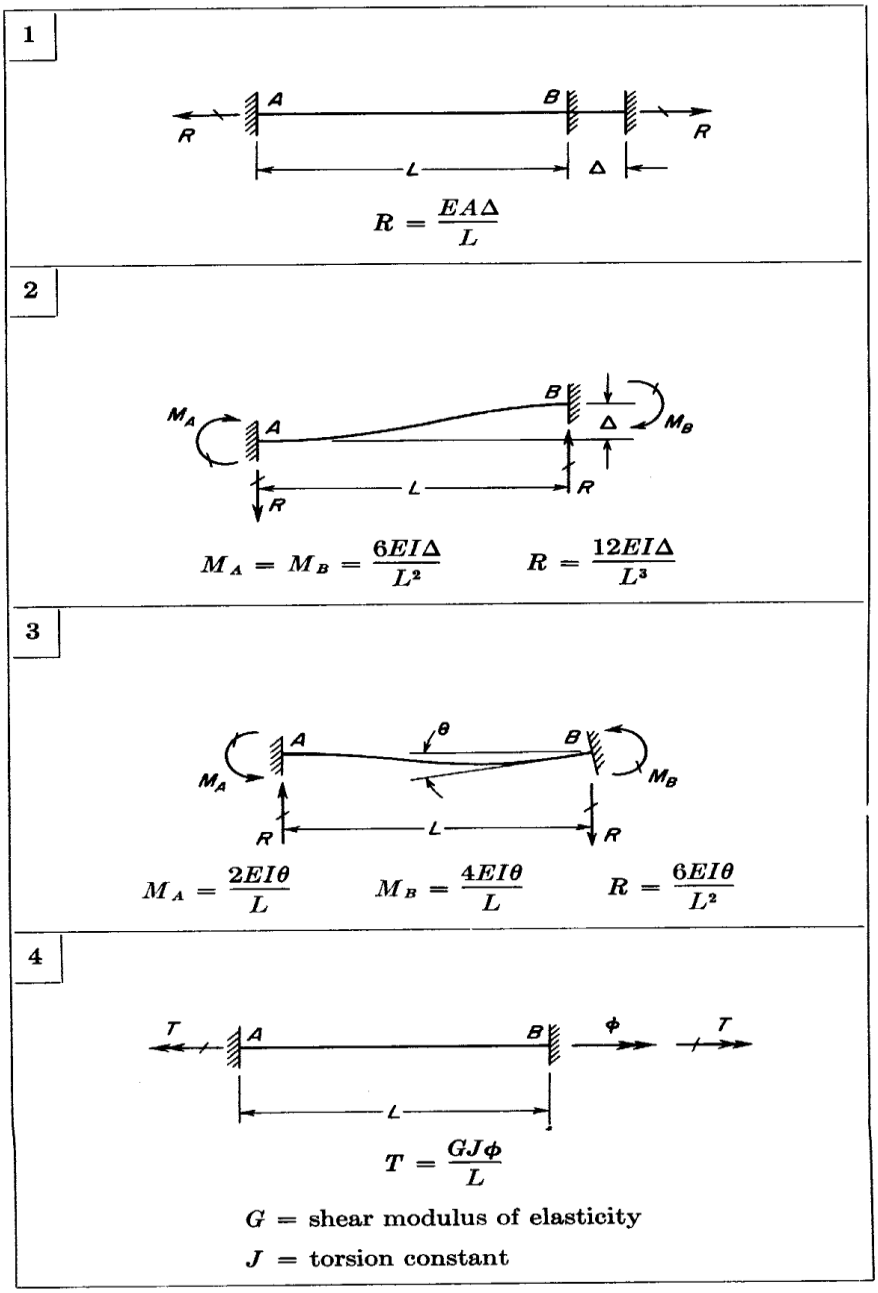

D-4 the end-displacement action:-

Axial displacement; Sway displacement; Flexural displacement; Twist displacement

Appendix E

"Program description and structure"

Table (E-1) describes the main subroutines and list of identifiers used in the computer program (***NASCFI***)

Table E-1-

Subroutine		***Description***
1	Globdat	Read the number of elements, nodes, loaded member, special effects member, loaded joints, supported joints and yielded supports.
2	Meth.	Indicates the method of analysis whether with no shear (Meth. -0-), total shear slope (Meth.-1-) or flexural shear slope.
3	TYDM	indicates if the analysis 2-D or 3-D 2 for 2-D 3 for 3-D
4	TYAN	Indicates if the analysis is: -0- S.D. Linear -1- S.D. non-linear (axial effect only) -2- L.D. CB=0, CT=0 -3- L.D. CB≠0, CT=0 -4- L.D. CB≠0, CT≠0
5	TYP	Indicates the type of element: 1-BC Beam-column 2-CBL Cable element
6	TYS	Indicates the type of section for the B_C: 1-SOL Solid section 2-XB X-bracing 3-WB Warren-bracing 4-PHB Pratt or how bracing 5-VB Veirndeel or batten bracing
7	TOL	Displacement convergence tolerance
8	TOLe	Axial load convergence tolerance
9	CCC	Load increment indicator -0- convergence not checked -1- convergence checked

10	IT	Displacement convergence indicator
11	ITT	Axial load unbalancing indicator -0- convergence not checked -1- convergence checked
12	DOF	Indicates the supported joint DOF: -0- fixed -1- free
13	ZZERO	Makes all the third-dimension properties equal to zero
14	NZERO	Makes the shear effect equal to zero
15	PROP	Reads the physical properties of the element (B-C or cable).
16	GEOM	Reads the geometrical properties (A, I, J, TYP, TYS, n, IN, JN)
17	COORD	Reads the joint co-ordinates (JN, I, X(I), Y(I), Z(I))
18	LATPROP	Reads the lattice member properties, (width and height of panel, angle of inclination)
19	FEVL	Applied load vector, reads all the fixed end actions of the applied load, the initial special effects and initial cable tension
20	ROTORIENT	Calculates the initial rotation and or orientation matrices
21	NN, NE, NR, NL, NLM. NSM	No. of : nodes, elements, restraint joints, loaded joints, load members, special effects members respectively
22	IN, JN	Lower and upper joint No.
23	INDICAT-K-	N-R iterative technique indicator of five types: -1- conventional N-R -2- modified N-R -3- combined N-R -4- no load corrections N-R -5- load correction N-R
24	TSME	Calculates the TSM in local co-ordinates
25	TSMG	Calculates the TSM in global co-ordinates
26	ASMB	Assembles the TSM in banded form
27	CHOLSVR	***Cholesky*** factorisation equation solver
28	CRITCAL	Determines the elastic critical load
29	DISP	Calculates the displacements in global co-ordinates
30	UPDAT	Updates the geometry of the structure by calculating the location and orientation of the joints (new chord length, direction cosines, orientation matrices, rotation matrices and new relative deformation).

31	MOM	Calculates the end rotations and moments
32	FORCE	Calculates the end forces of the member
33	STBWTW	Calculates the stability, bowing and twisting functions
34	NEWCAB	Calculates the cable element new tension and "$E_{eq.}$"
35	CHECKL	Checks axial load convergence criteria (ITT)
36	GLOBAL	Transverse the member forces from local to global co-ordinates
37	VECL	Incremental load vector: adds the increment of loads in each load increment
38	BALANCE	Calculates the unbalance force vector
39	CONVERGENCE	Checks displacement convergence criteria
40	EIGEN	Determines the firs fundamental Eigenvalue of the linear system
41	PRINT	Prints all the desired results

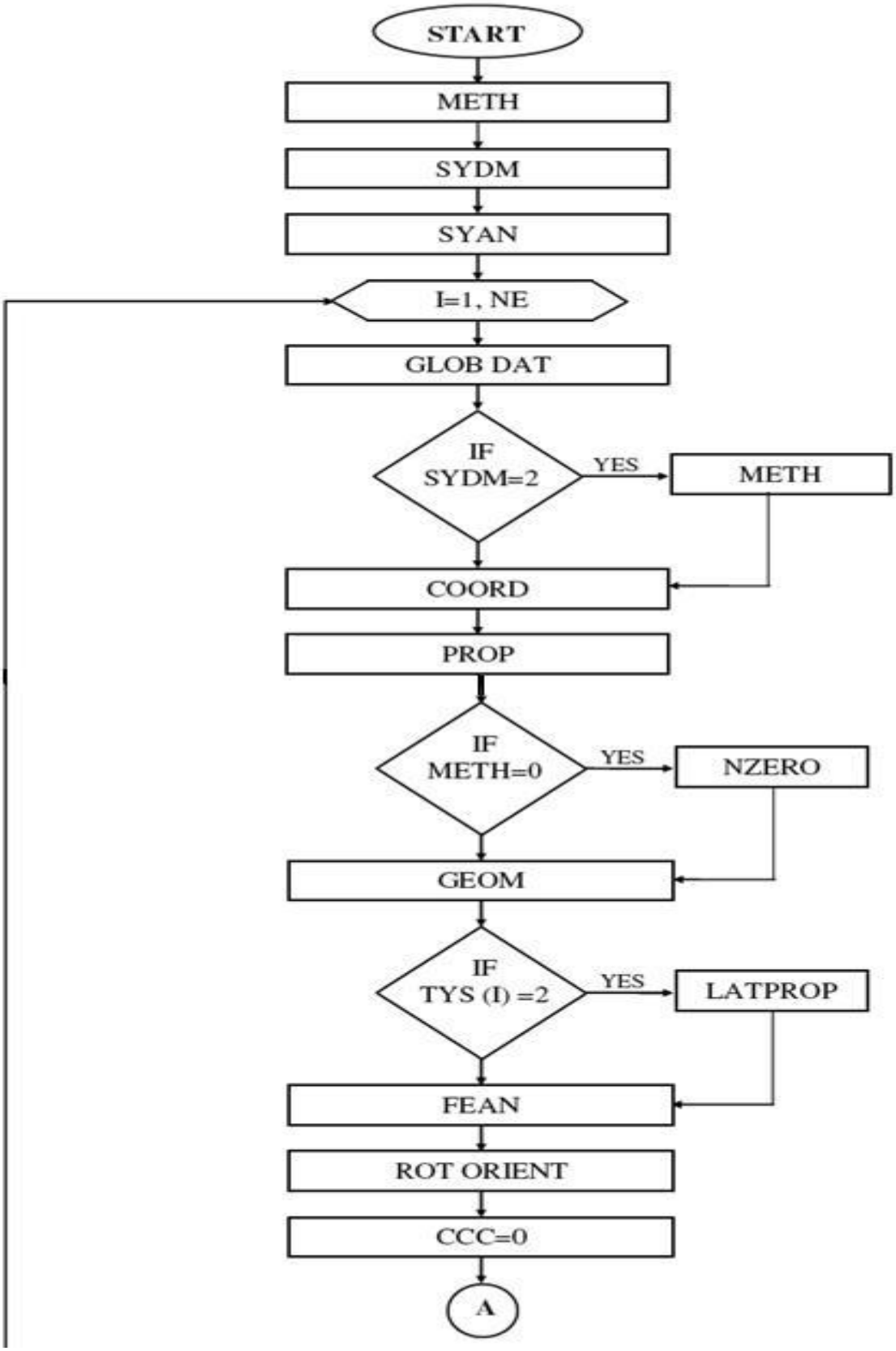
START
METH
SYDM
SYAN
I=1, NE
GLOB DAT
IF SYDM=2
YES
METH
COORD
PROP
IF METH=0
YES
NZERO
GEOM
IF TYS (I) =2
YES
LATPROP
FEAN
ROT ORIENT
CCC=0
A

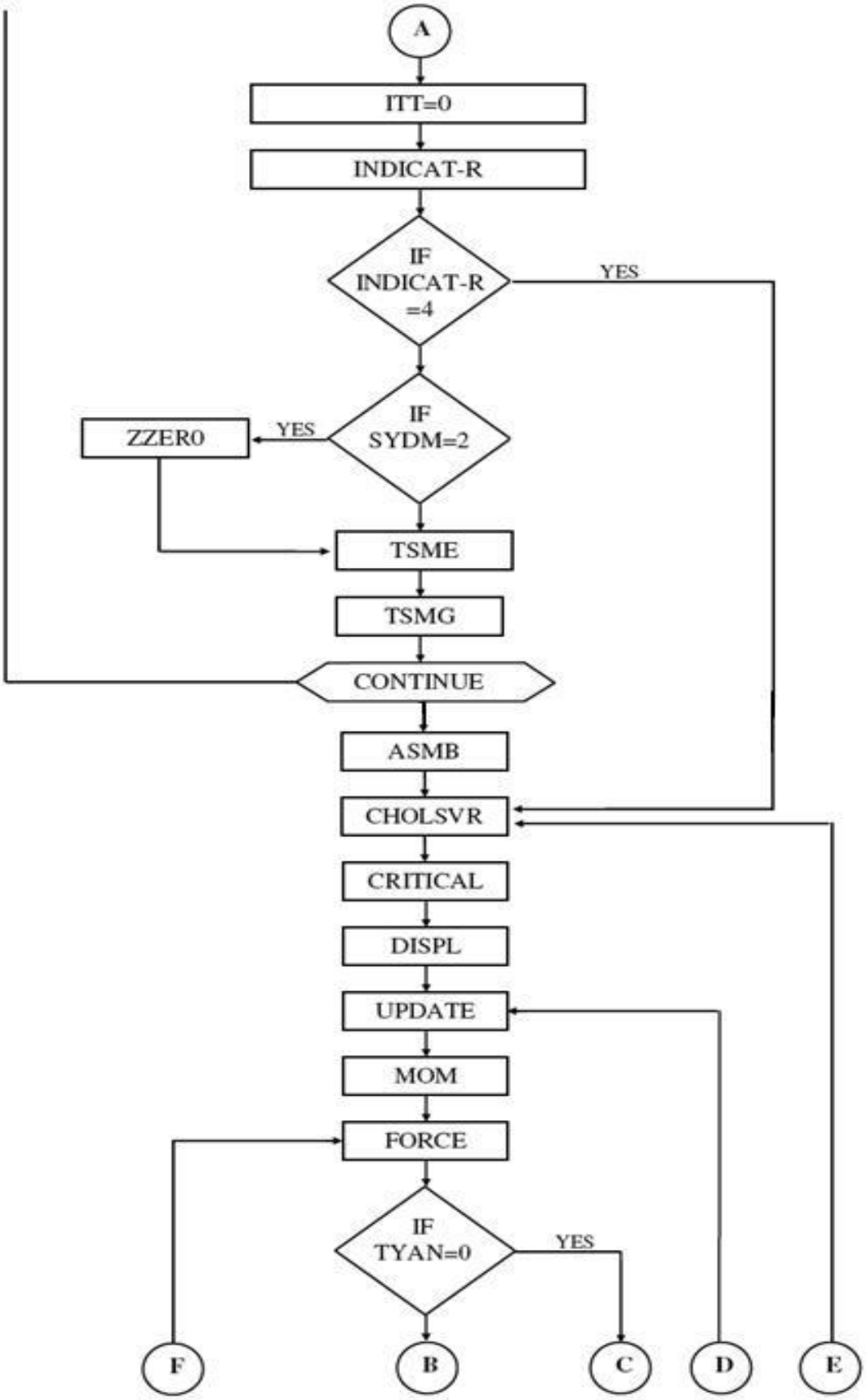
A
ITT=0
INDICAT-R
IF INDICAT-R =4
YES
IF SYDM=2
YES
ZZER0
TSME
TSMG
CONTINUE
ASMB
CHOLSVR
CRITICAL
DISPL
UPDATE
MOM
FORCE
IF TYAN=0
YES
F
B
C
D
E

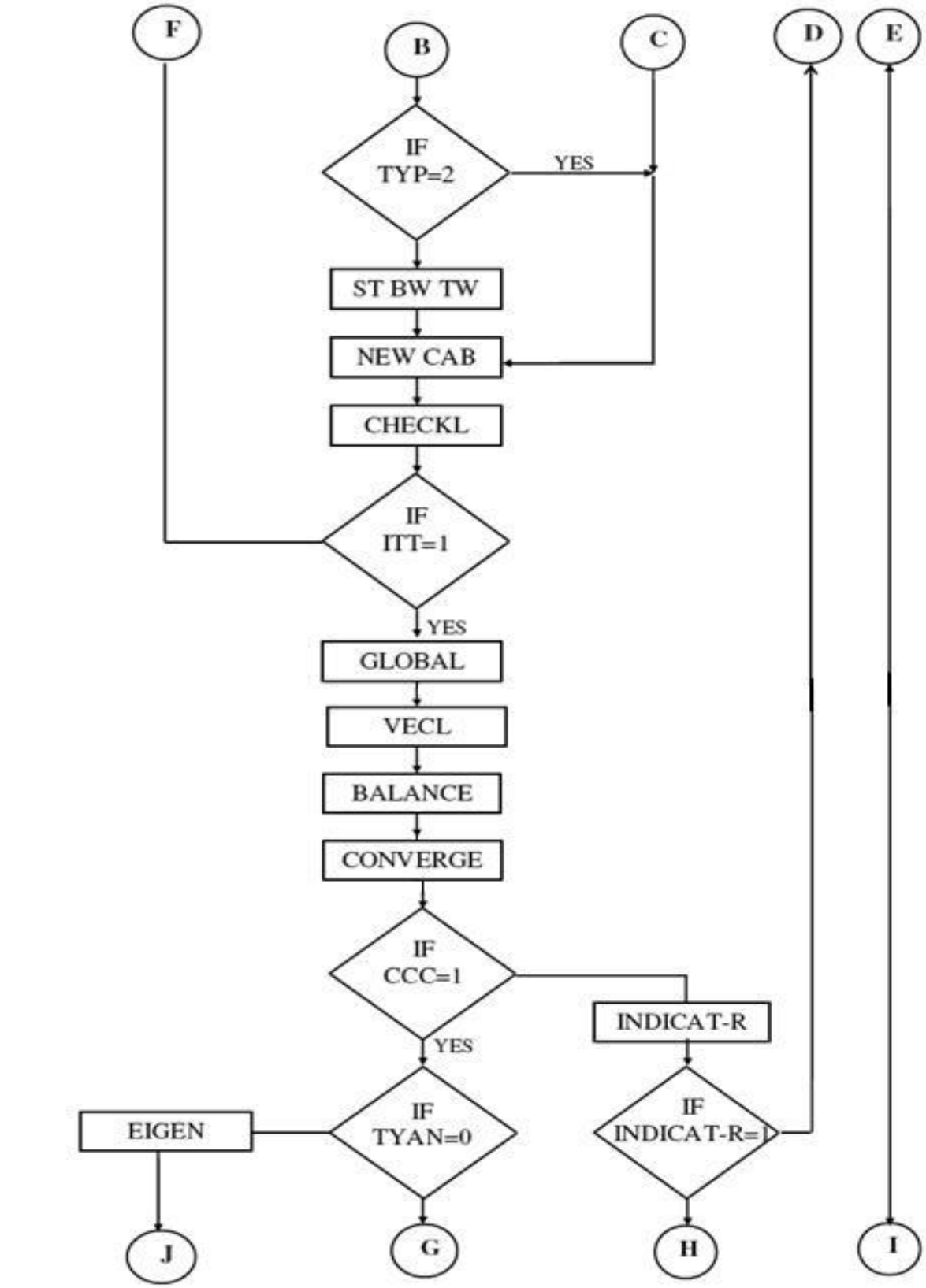
F
B
C
D
E
IF
TYP=2
YES
ST BW TW
NEW CAB
CHECKL
IF
ITT=1
YES
GLOBAL
VECL
BALANCE
CONVERGE
IF
CCC=1
INDICAT-R
YES
IF
TYAN=0
IF
INDICAT-R=1
EIGEN
J
G
H
I

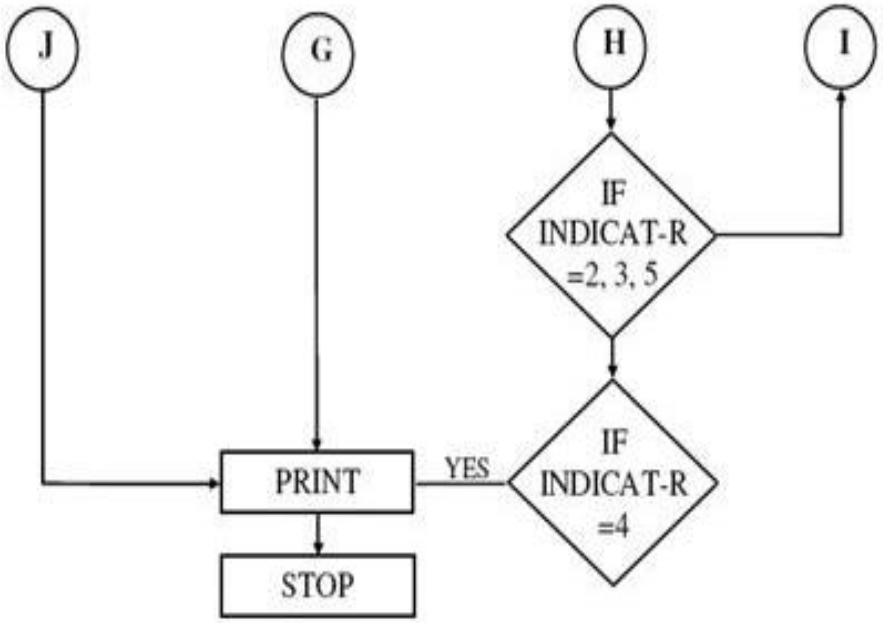

Figure (E-1) Program flowchart

Appendix F

Shear Deflection in Beams

F1- Nature of Shear Deflection

Shear stresses in a beam section cause a displacement or sliding action on a plane normal to the axis of the beam, as shown in the right hand view of figure (F-1). This is unlike the deflection resulting from bending in a beam, which is shown in the left hand view in the same figure.

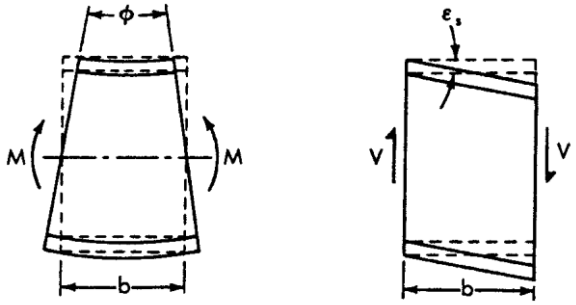

Figure (F-1) Deflection in beam caused by bending moment, left, and by shear, right

Normally deflection due to shear in the usual beam is ignored because it represent a very small percentage of the entire deflection. Figure(F-2) shows that the deflection due to shear increases linearly as the length of the beam increases, whereas the deflection due to bending increases very rapidly as a third power of the beam length. For this reason the deflection due to shear is not an important factor except for extremely short spans where deflection due to bending drops off to a very small value, also in the open-web (laced or batten) beams the shear deflection takes a significant contribution of the entire deflection.

The deflection due to the shear is dependent entirely on the shear distribution across the cross section of the member and also the value of the shear stress (τ_s). Figure (F-3) shows the shear stress-strain diagram which is similar to the usual stress-strain diagram, although the shear yield strength is much lower than the tensile yield strength of the same material. After the shear yield strength is reached, the shear strain (ε_s) increases rapidly and the shear strength increases because of strain hardening.

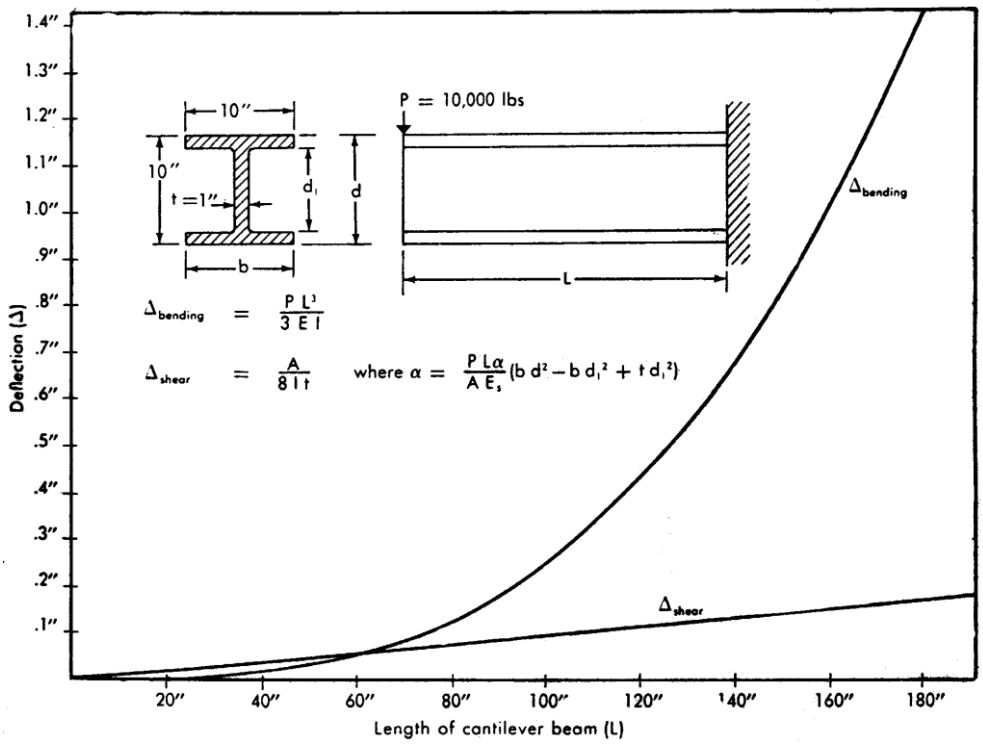

Figure (F-2) **Shear deflection and bending deflection of cantilever I-section**

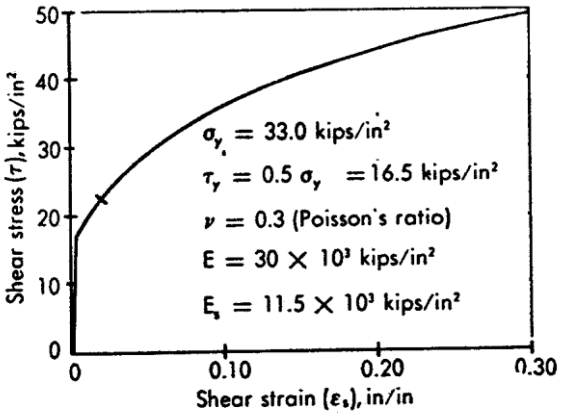

Figure (F-3) **Shear stress-strain diagram**

F2- Determining Shear Deflection

In the small deflection theory, the deflection caused by shear stress is rather simple. However, the actual determination of the shear stresses and their distribution across the beam section (which two factor cause the deflection) is more difficult i.e. the large deflection theory. In all cases, some kind of form factor (α) must be determined, and this is simply a matter of expressing the distribution of shear stress throughout the web of the section. Since there is practically no shear stress in the flange area, this particular area has negligible effect on the deflection due to the shear (Δ_s) except for the

case of the twisting moment is included. The following formulas are valid for several types of beams and loading:

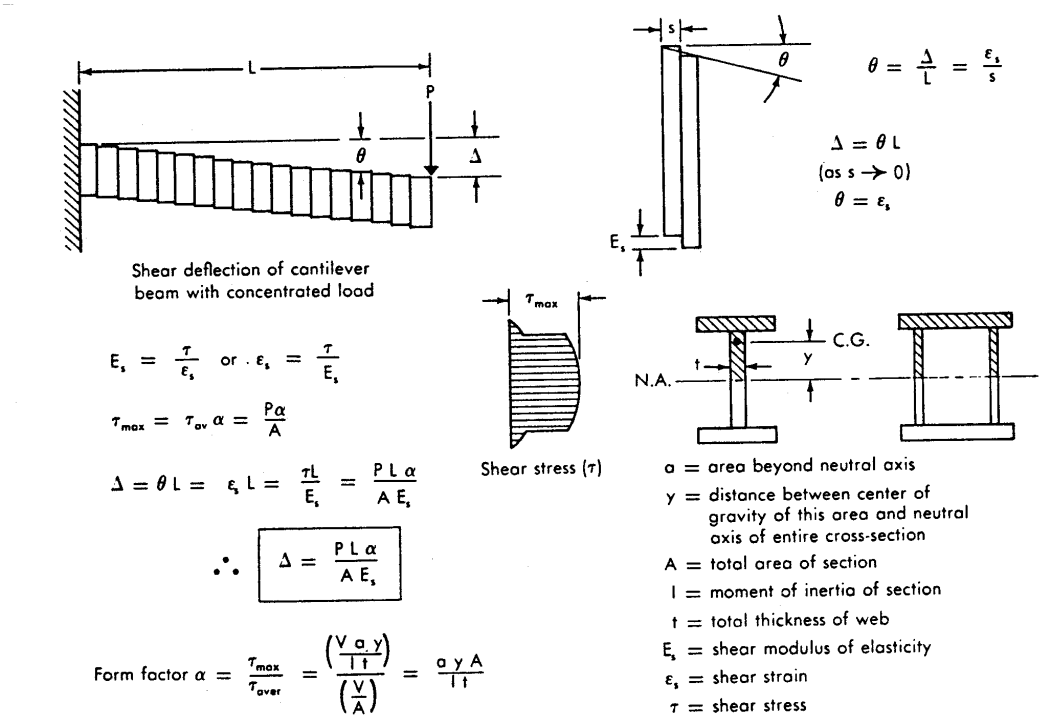
L
P
θ
Δ
Shear deflection of cantilever beam with concentrated load
s
θ
θ = Δ/L = ε_s/s
Δ = θ L
(as s → 0)
θ = ε_s
E_s
τ_max
Shear stress (τ)
C.G.
N.A.
t
y
E_s = τ/ε_s or ε_s = τ/E_s
τ_max = τ_av α = Pα/A
Δ = θ L = ε_s L = τL/E_s = P L α/A E_s
∴ Δ = P L α/A E_s
Form factor α = τ_max/τ_aver = (V a y/I t)/(V/A) = a y A/I t
a = area beyond neutral axis
y = distance between center of gravity of this area and neutral axis of entire cross-section
A = total area of section
I = moment of inertia of section
t = total thickness of web
E_s = shear modulus of elasticity
ε_s = shear strain
τ = shear stress

Figure (F-4) Form factor for shear deflection in built-up beams

- Simply supported beam; uniform load (w):

$$\Delta_s = \frac{wL^2\alpha}{8AE_s} \quad \text{.....(F-1)}$$

- Simply supported beam; concentrated load (P):

$$\Delta_s = \frac{PL\alpha}{4AE_s} \quad \text{.....(F-2)}$$

- Cantilever beam; uniform load (w):

$$\Delta_s = \frac{wL^2\alpha}{2AE_s} \quad \text{.....(F-3)}$$

- Cantilever beam; concentrated load (P):

$$\Delta_s = \frac{PL\alpha}{AE_s} \quad \text{.....(F-4)}$$

where:

P= total load, lbs.

A= area of entire section

E_s= modulus of elasticity in shear (12000 ksi for steel)

w= distributed load, lbs. Per linear inch

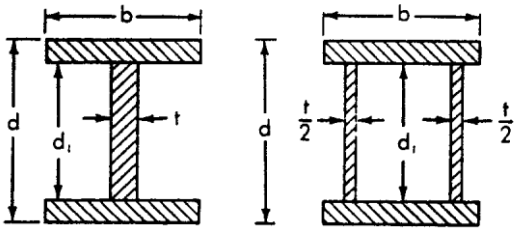

Figure (F-5) Beam sections for which eq.(F-5) applies

The slope of the deflection curve (θ) is equal at each cross section to the shearing strain (ε_s) at the centroid of the cross section. (α) is a factor with which the average shearing stress (τ_{av}) must be multiplied in order to obtain the shearing stress (τ_{max}) at the centroid of the cross sections.

On the spaces, the form factor (α) for an I-beam or box beam would be:

$$\alpha = \frac{A}{8It}\left(bd^2 - bd_1^2 + td_1^2\right) \quad \text{.....(F-5)}$$

where figure (F-5) applies. Don't compute area (A) in this formula because it will cancel out when used in the formulas for shear deflection.